Molybdenum (IV) Imido Silylamido and Hydride Complexes: Stoichiometric and Catalytic Reactivity, Mechanistic Aspects of Hydrosilation Reactions

Andrey Y. Khalimon
Dipl. Chem.

Chemistry

Thesis submitted to the Faculty of Graduate Studies
In the partial fulfillment of the requirements
For the Ph.D. degree in chemistry

Chemistry Department
Faculty of Mathematics and Science
Brock University
St. Catharines, Ontario

July, 2010

Dedicated to my parents

Manuscripts based on this work

1. Khalimon, A. Y.; Holland, J. P.; Kowalczyk, R. M.; McInnes, E. J. L.; Green, J. C.; Mountford, P.; Nikonov, G. I. "Synthesis and Molecular and Electronic Structure of an Unusual Paramagnetic Borohydride Complex $Mo(NAr)_2(PMe_3)_2(\eta^2\text{-}BH_4)$" *Inorg. Chem.* **2008**, *47*, 999-1006.
2. Khalimon, A. Y.; Simionescu, R.; Kuzmina, L. G.; Howard, J. A. K.; Nikonov, G. I. "Agostic NSi-H···Mo Complexes: From Curiosity to Catalysis" *Angew. Chem.* **2008**, *120*, 7815-7818; *Angew. Chem. Int. Ed.* **2008**, *47*, 7701-7704.
3. Peterson, E.; Khalimon, A. Y.; Simionescu, R.; Kuzmina, L. G.; Howard, J. A. K.; Nikonov, G. I. "Diversity of Catalysis by an Imido-Hydrido Complex of Molybdenum. Mechanism of Carbonyl Hydrosilylation and Silane Alcoholysis" *J. Am. Chem. Soc.* **2009**, *131*, 908-909.
4. Ignatov, S. K.; Khalimon, A. Y.; Rees, N. H.; Razuvaev, A. G.; Mountford, P.; Nikonov, G. I. "β-Agostic Silylamido and Silyl-Hydrido Compounds of Molybdenum and Tungsten" *Inorg. Chem.* **2009**, *48*, 9605-9622. Manuscript was placed on a *Front Cover*.

Abstract

This thesis describes the synthesis, structural studies, and stoichiometric and catalytic reactivity of novel Mo(IV) imido silylamide $(R^1N)Mo(R^2)(\eta^3\text{-}R^1N\text{-}SiR^3{}_2\text{-}H)(PMe_3)_n$ (**1**: R^1 = ^{t}Bu, Ar', Ar; R^2 = Cl; $R^3{}_2$ = Me_2, MePh, MeCl, Ph_2, HPh; n = 2; **2**: R^1 = Ar, R^2 = SiH_2Ph, n = 1) and hydride complexes $(ArN)Mo(H)(R)(PMe_3)_3$ (R = Cl (**3**), SiH_2Ph (**4**)). Compounds of type **1** were generated from $(R^1N)Mo(PMe_3)_n(L)$ (**5**: R^1 = ^{t}Bu, Ar', Ar; L = PMe_3, η^2- C_2H_4) and chlorohydrosilanes by the imido/silane coupling approach, recently discovered in our group. The mechanism of the reaction of **5** with $HSiCl_3$ to give $(ArN)MoCl_2(PMe_3)_3$ (**8**) was studied by VT NMR, which revealed the intermediacy of $(ArN)MCl_2(\eta^2\text{-}ArN{=}SiHCl)(PMe_3)_2$ (**9**). The imido/silyl coupling methodology was transferred to the reactions of **5** with chlorine-free hydrosilanes. This approach allowed for the isolation of a novel β-agostic compound $(ArN)Mo(SiH_2Ph)(\eta^3\text{-}NAr\text{-}SiHPh\text{-}H)(PMe_3)$ (**10**). The latter was found to be active in a variety of hydrosilation processes, including the rare monoaddition of $PhSiH_3$ to benzonitrile. Stoichiometric reactions of **11** with unsaturated compounds appear to proceed *via* the silanimine intermediate $(ArN)M(\eta^2\text{-}ArN{=}SiHPh)(PMe_3)$ (**12**) and, in the case of olefins and nitriles, give products of Si-C coupling, such as $(ArN)Mo(R)(\eta^3\text{-}NAr\text{-}SiHPh\text{-}CH{=}CHR')(PMe_3)$ (**13**: R = Et, R' = H; **14**: R = H, R' = Ph) and $(ArN)Mo(\eta^2\text{-}NAr\text{-}SiHPh\text{-}CHR{=}N)(PMe_3)$ (**15**). Compound **13** was also subjected to catalysis showing much improved activity in the hydrosilation of carbonyls and alkenes.

Hydride complexes **3** and **4** were prepared starting from $(ArN)MoCl_2(PMe_3)_3$ (**8**). Both hydride species catalyze a diversity of hydrosilation processes that proceed *via* initial substrate activation but not silane addition. The proposed mechanism is supported by

stoichiometric reactions of **3** and **4**, kinetic NMR studies, and DFT calculations for the hydrosilation of benzaldehyde and acetone mediated by **4**.

Acknowledgements

I am extremely grateful to a number of people who have helped to bring this PhD thesis to its culmination. I owe my gratitude to many individuals and sincerely apologize to those who are not explicitly mentioned; if you feel you should be, consider yourself added as of now.

First and foremost, I would like to acknowledge my supervisor Dr. Georgii Nikonov. It has in every respect been a privilege to work in Nikonov's group during the last 10 years. Dr. Nikonov's enthusiasm, guidance and dedication to chemistry have inspired me as a scientist, have always pushed me further and raised my academic standards. I am endlessly impressed by his creativity in chemistry and can only hope that I have acquired some of it during our collaboration. Thank you for sharing your philosophies and for being a great friend.

I would like to thank my graduate committee members at Brock University Prof. Ian Brindle and Dr. Melanie Pilkington, for their helpful suggestions. Dr. Martin Lemaire is thanked for his participation in my PhD candidacy examination. Dr. Heather Gordon and Prof. Stuart Rothstein spent their valuable time professionally navigating me through countless administrative obstacles and I thank them for this. The following people are also recognized for their technical support: John Vandenhoff, Jordan Vandenhoff (Glassblowing Shop), and Steve Crumb (Machine Shop). I would like to acknowledge Brock University and the Ontario Graduate Scholarship Program (OGS) for their financial support.

A particular gratitude is expressed to the following two people. First, I want to thank Prof. Lyudmila Kuzmina (Institute of General and Inorganic Chemistry RAS, Moscow, Russia) for her priceless work and providing us with X-ray data. I have been always impressed by her talent as crystallographer and her ability to make a "candy" from "garbage". I truly believe that she is one of the best in the field and have been lucky to collaborate with her. Also, I would like to acknowledge NMR technologist Razvan Simionescu (Brock University) for his personal interest in research in Nikonov's group and his valuable assistance with numerous nontrivial NMR experiments and NMR data analysis. Without Razvan, we would have a hard time finishing this research. Also, I

would like to thank Prof Stanislav Ignatov (Nizhnii Novgorod State University, Russia) for solving our mechanistic puzzles by DFT calculations.

I am also particularly grateful to a number of people I previously worked with at Moscow State University, in particularly: Prof. Dmitrii Lemenovskii and Dr. Galina Brusova for their constant advice and support during my study; former Nikonov's group members Dr. Konstantin Dorogov and Dr. Alexander Osipov for showing me *the way* of modern inorganic synthesis and being great collaborators and friends; Dr. Anastasia Selina for all the smiles and coffee breaks that diluted the stress of hard-working days.

Also, I would like to mention Prof. Philip Mountford from Oxford University (Oxford, UK) and the Royal Society of Chemistry (London, UK) for giving me an opportunity to work in one of the world's best inorganic chemistry laboratories, which greatly improved my synthetic skills; Prof. Christina Möberg from the Royal Institute of Technology (KTH, Stockholm, Sweden) and Swedish Institute (Stockholm, Sweden) for giving me an opportunity to learn modern organic chemistry and asymmetric catalysis techniques.

I want to thank all of the former and present Nikonov's group members, as I have been lucky to work with them at both Moscow State and Brock University, in particular: Dr. Konstantin Dorogov, Dr. Alexander Osipov, Dr. Somying Leelasubcharoen, Dmitry Gutsulyak, Oleg Shirobokov, Andrea Findlay, Erik Peterson, Nick McLeod, Philip Farha, and Sun-Hwa Lee for excellent collaboration and being good friends. Also, graduate studies at Brock University have brought me a lot of friends: Dr. Robert Carroll, Dr. Jonathan Collins, Dr. Hannes Leisch, Dr. Joshua Zaifman, Dr. Elisabeth Kloser, Patrizio Cassolato, Sarah Laronde, Shufen Xu, Melissa Drouin, Rachel Saxon, Kristina Whitbread, Candice Kerling, and Dylan Levac – thank you guys for just being who you are.

Finally, I am extremely grateful to my family, especially my parents and brother, for their endless support and understanding during all of these long years of my education.

Table of Contents

Manuscripts based on this work.....i
Abstract.....ii
Acknowledgements.....iv
Table of Contents.....vi
Abbreviations.....ix
List of Figures.....xiii
List of Schemes.....xviii
List of Tables.....xxvi
I. Introduction 1
II. Historical 6
II.1 Agostic Si-H···M interactions in transition metal complexes 6
II.1.1 Bonding aspects of Si-H···M agostic and silane σ-complexes 7
II.1.2 Structural features of Si-H···M agostic and silane σ-complexes 9
II.1.3 Spectroscopic features of Si-H···M agostic and silane σ-complexes 13
II.1.4 Recent advances in the chemistry of β-agostic NSi-H···M complexes 15
II.2 Homogeneous hydrosilation of unsaturated organic molecules 24
II.2.1 Mechanisms of TM catalyzed hydrosilation of alkenes 25
II.2.2 Mechanisms of TM catalyzed hydrosilation of alkynes 37
III.2.3 Mechanisms of TM catalyzed hydrosilation of C=X (X = O, N) bonds 44
II.2.3.1 Hydrosilation of carbonyl compounds 46
II.2.3.2 Hydrosilation of imines 64
II.2.4 Mechanisms of TM catalyzed hydrosilation of nitriles 68
II.2.5 Mechanisms of TM catalyzed silane alcoholysis and aminolysis 75
II.2.6 Early TM catalyzed hydrosilation reactions 85
II.2.6.1 Hydrosilation of alkenes 85
II.2.6.2 Hydrosilation of alkynes 88
II.2.6.3 Hydrosilation of carbon-heteroatom multiple bonds 89
II.2.6.4 Hydrolysis, alcoholysis and aminolysis of silanes 94
III. Results and Discussion 96

III.1 Introduction 96
III.2 Preparation of bis(imido) complexes of molybdenum and tungsten 98
III.3 Reactivity of $(RN)_2M(PR'_3)_n$ with chlorohydrosilanes 101
III.3.1 Reactions of $(RN)_2Mo(PR'_3)_n$ with mono- and dichlorosilanes 101
III.3.1 Reactions of $(RN)_2M(PR'_3)_{n-1}L$ with $HSiCl_3$ 107
III.4 Reactivity of $(RN)_2M(PR'_3)_{n-1}L$ towards hydrosilanes 113
III.4.1 Reactions of $(RN)_2M(PR'_3)_{n-1}L$ with $PhSiH_3$ 113
III.4.1.1 Reactions of Ar and Ar' complexes 113
III.4.1.2 Reactions of $(^tBuN)_2Mo(PMe_3)L$ 123
III.4.2 Reactions of $(RN)_2M(PR'_3)_{n-1}L$ with $PhMeSiH_2$ and $(EtO)_3SiH$ 129
III.5 Reactivity of $(ArN)Mo(SiH_2Ph)(\eta^3\text{-}NAr\text{-}SiHPh\text{-}H)(PMe_3)$ (**III-1**) 132
III.5.1 VT NMR study of complex **III-1** 133
III.5.2 Reactions of complex **III-1** with hydrosilanes 135
III.5.3 Catalytic reactivity of complex **III-1** 139
III.5.4 Stoichiometric reactivity of complex **III-1** 144
III.5.4.1 Reactions of complex **III-1** with alkenes 145
III.5.4.2 Reactions with ketones and aldehydes 150
III.5.4.3 Reactions with organic nitriles 153
III.6 Reactivity of $(ArN)Mo(Et)(\eta^3\text{-}NAr\text{-}SiHPh\text{-}CH{=}CH_2)(PMe_3)$ (**III-3**) 155
III.6.1 Reactions of **III-3** with hydrosilanes and H_2 156
III.6.2 Catalytic reactivity of complex **III-3** 162
III.6.3 Reactions of **III-3** and **III-112** with unsaturated organic molecules 166
III.7 Preparation and reactivity of molybdenum imido hydride complexes 172
III.7.1 Mono- and bis(imido) molybdenum borohydrides 172
III.7.2 Preparation and reactivity of imido hydride molybdenum complexes 183
III.7.2.1 Preparation of molybdenum imido hydride complexes 183
III.7.2.2 Catalytic activity of complexes **III-6** and **III-7** 186
III.7.2.3 Stoichiometric reactivity of **III-6** and the mechanism of hydrosilation of benzaldehyde and alcoholysis of $PhSiH_3$ 191
III.7.2.4 Stoichiometric reactivity of **III-7** and the mechanism of carbonyl hydrosilation 204

III.7.2.5 Reactions of **III-7** with EtOH and PhCN 218
IV. Conclusions and Future Work 220
V. Experimental 223
General methods and instrumentation 223
Preparation of starting materials and reagents 224
Reactions of $(RN)_2M(PR'_3)_{n-1}L$ with chlorohydrosilanes 231
Reactions of $(RN)_2M(PR'_3)_{n-1}L$ with hydrosilanes 244
Preparation of silylamide molybdenum complexes 256
Stoichiometric reactions of $(ArN)Mo(SiH_2Ph)(\eta^3\text{-}NAr\text{-}SiH_2Ph)(PMe_3)$ (**III-1**) 260
Reactions of $(RN)_2Mo(PMe_3)_{n-1}L$ with carbonyls 273
Stoichiometric reactivity of imido (vinylsilyl)amide complexes 277
Preparation and reactivity of mono(imido) complexes 292
Preparation and reactivity of molybdenum borohydride complexes 294
Preparation of $(ArN)Mo(H)(R)(PMe_3)_3$ (R = H, SiR'_3) 299
Stoichiometric reactivity of $(ArN)Mo(H)(Cl)(PMe_3)_3$ (**III-6**) 302
Stoichiometric reactions of $(ArN)Mo(H)(SiH_2Ph)(PMe_3)_3$ (**III-7**) 313
Catalytic studies 324
Kinetic NMR studies 328
Experimental details of EXSY NMR studies 331
Crystal structure determinations 332
DFT calculations 333
VI. Appendix 334
VII. References 357

Abbreviations

Å	Angström
acac	acetylacetonato
Ar'	2,6-dimethylphenyl, unless stated otherwise
Ar''	3,5-dimethylphenyl, unless stated otherwise
Ar	2,6-diisopropylphenyl, unless stated otherwise
Ar^{tBu}	3,5-di-*tert*-butylphenyl
atm	atmosphere (1 atm = 1 bar, 760 mm Hg, 101.3 kPa, 14.696 psi)
b	broad (NMR)
Bn	benzyl
^{n}Bu = Bu	butyl
^{t}Bu	*tert*-butyl
calcd	calculated
cat.	catalyst
Cat	catechol
°C	degrees Celcius
3c-2e	three center – two electron bonding
chapt.	chapter
COD	cyclooctadiene
Cp	η^5-C_5H_5, unless specified
Cp'	η^5-C_5H_4Me, unless specified
Cp*	η^5-C_5Me_5, unless specified
Cy	cyclohexyl
d	doublet (NMR)
DCD	Dewar-Chatt-Duncanson bonding model
DCM	dichloromethane
DFT	density functional theory
DIOP	2,3-*O*-isopropylidene-2,3-dihydroxy-1,4-bis(diphenylphosphino)butane
DMAP	4-dimethylaminopyridine
DME	1,2-dimethoxyethane

DMF	dimethylformamide
DMSO	dimethyl sulphoxide
Dppe	1,2-Bis(diphenylphosphino)ethane
EBHTI	ethylenebis(tetrahydroindenyl)
Et	ethyl
exc.	excess
h	hour
$\Delta H^{\ddagger}$	activation enthalpy
Hal	halogen
Hmpa	hexamethylphosphoric acid triamide, $O=P(NMe_2)_3$
HOMO	highest occupied molecular orbital
Hoz	2-(2'-hydroxyphenyl)-2-oxazoline
hν	light
Hz	Hertz, cycles per second
IHI	Interligand Hypervalent Interaction
J	coupling constant (NMR)
IR	infrared
k	reaction rate constant
KIE	Kinetic isotope effect
L_n	ligand
Ln	lanthanide
LUMO	lowest unoccupied molecular orbital
M	central metal atom in a complex
m	*meta-*
m	multiplet (NMR)
Me	methyl
Mes	mesityl
MO	molecular orbital
ND	neutron diffraction
NMR	nuclear magnetic resonance
NOE	nuclear Overhauser effect

o	*ortho-*
OA	oxidative addition
OTf	triflate
p	*para-*
p	pentet (NMR)
pfb	pentafluorobutyrate
Ph	phenyl
PhMe	toluene
^{i}Pr	isopropyl
^{n}Pr = Pr	propyl
Py	pyridine
q	quartet (NMR)
quant.	quantitative
RE	reductive elimination
RT	room temperature
s	singlet (NMR)
sat	satellite (NMR)
sept	septet (NMR)
$\Delta S^{\ddagger}$	activation entropy
Solv	solvent
t	triplet (NMR)
TBAF	tetrabutylammonium fluoride
tert-, *t*	tertiary
THF	tetrahydrofuran
TFPB	tetrakis(pentafluorophenyl)borate
TM	transition metal
TMS	trimethylsilyl
Tol	tolyl
tss	thiosemcarbazonato silacylaldehyde
VT	variable temperature
vt	virtual triplet (NMR)

UV	ultraviolet
δ	chemical shift
Δ	heat

List of Figures

Figure 1. Coordination of dihydrogen to transition metal complexes and the 2c-3e bond concept for H_3^+, CH_5^+, and polyboranes 6

Figure 2. Nonclassical Si-H interactions in the coordination sphere of transition metals . 7

Figure 3. DCD type model for the 3c-2e Si-H-M bonding. 8

Figure 4. Classification of Si-H···M agostic complexes. 10

Figure 5. Zirconium (**II-15** – **II-17**) and lanthanide (**II-18**) β-agostic silylamido complexes. 15

Figure 6. Effect of the nature of the substituent X in **II-17** on the NSi-H···Zr interaction. 17

Figure 7. Agostic coordination modes for the bis(dimethylsilyl)amide ligand in **II-18**.. 18

Figure 8. DFT model for the formation of complex **II-29** and $(Ar'N\text{-}SiHCl)_2$. 22

Figure 9. MO diagram for the insertion of terminal (**a**) and internal (**b**) alkynes into M-H bond of the catalyst. 39

Figure 10. *N*-based chiral ligands effectively applied in the Rh(I)-catalyzed hydrosilation. 47

Figure 11. Rh(I) carbene complex **II-83** active in the hydrosilation of aryl/alkyl and dialkyl ketones. 49

Figure 12. Salalen ligand and Abu-Omar's Mo(VI) salalen oxo complex **II-103**..... 55

Figure 13. Rhenium complexes containing Re=X multiple bonds (X = O, NAr, N) active hydrosilation of carbonyl compounds. 57

Figure 14. Base-stabilized iridium silylene complexes **II-127** – **II-129**..... 64

Figure 15. Zirconium catalyst for the reduction of CO_2 with hydrosilanes. 93

Figure 16. Mo(IV) imido complexes active in hydrosilation catalysis. 97

Figure 17. Suggested intermediates for reactions of **III-22** and **III-23** with $HSiCl_3$..... 109

Figure 18. ORTEP plot of the molecular structure of (ArN)$MoCl_2(PMe_3)_3$ (**III-47**) (hydrogen atoms are omitted for clarity). Anisotropic displacement parameters are plotted at 50 % probability. 110

Figure 19. Canonical forms for the bonding in d^2 agostic silylamide complexes..... 113

Figure 20. ORTEP plot of the molecular structure of (ArN)$Mo(SiH_2Ph)(\eta^3$-NAr-SiHPh-H)(PMe_3) (**III-1**) (hydrogen atoms except Si*H* are omitted for clarity). Anisotropic displacement parameters are plotted at 50 % probability. 117

Figure 21. ORTEP plot of the molecular structure of complex **III-77** (hydrogen atoms, except SiH and MoH, are omitted for clarity). Anisotropic displacement parameters are plotted at 50 % probability. 126

Figure 22. Molybdenum silyl complexes **III-81** – **III-84**..... 128

Figure 23. ^{1}H-NMR spectrum of **III-1** (mixture of two diastereomers) at –50 °C. 133

Figure 24. ^{29}Si INEPT+ NMR spectra of **III-1** at –49 (**A**), –19 (**B**), 0 (**C**), 21 (**D**), 39 (**E**), 55 (**F**), and 68 °C (**G**). 134

Figure 25. The affect of the temperature on the $^1J_{Si\text{-}H}$ values for agostic Si center in **III-1**. 135

Figure 26. ^{1}H-^{1}H EXSY NMR spectrum (22 °C) of the mixture of **III-1** and $PhSiH_3$.. 136

Figure 27. ORTEP plot of the molecular structure of complex **III-3** (one of two independent molecules is shown; hydrogen atoms are omitted for clarity). Anisotropic displacement parameters are plotted at 50 % probability. 146

Figure 28. Possible products formed in the reaction of **III-1** with 1-hexene..... 148

Figure 29. ^{31}P{^{1}H}-NMR spectra of the reaction mixture of **III-1** and ^{t}PrCN (the signals at 10.5, -3.8, and -4.4 ppm correspond to **III-1**, **III-106**, and **III-110**, respectively). 154

Figure 30. ^{1}H-^{13}C HMBC NMR spectrum of **III-110** taken directly from the reaction mixture (proton signals at 5.4, 3.9, and 1.8 ppm correspond to SiH, CH and CH_3, respectively). 155

Figure 31. Dependence of the rate constant of the reaction of **III-3** with $PhSiH_3$ at 50 °C on concentration of $PhSiH_3$..... 157

Figure 32. Dependence of the rate constant of the reaction of **III-3** with 10 $PhSiH_3$ (pseudo-first-order regime) at 50 °C on concentration of PMe_3..... 159

Figure 33. ORTEP plot of the molecular structure of **III-125** (C-bound H atoms are omitted for clarity). Anisotropic displacement parameters are plotted at 50 % probability..... 174

Figure 34. EPR spectra (black line) of the frozen solution (top) and fluid solution (bottom) of **III-125** in toluene and their simulation (red line)..... 176

Figure 35. ORTEP plot of the molecular structure of **III-8** (C-bound H atoms are omitted for clarity). Anisotropic displacement parameters are plotted at 50 % probability. 178

Figure 36. ORTEP plot of the molecular structure of **III-7** (H atoms, except Si-H and Mo-H, are omitted for clarity). Anisotropic displacement parameters are plotted at 50 % probability..... 182

Figure 37. ORTEP plot of the molecular structure of **III-6** (H atoms, except Mo-H, are omitted for clarity). Anisotropic displacement parameters are plotted at 50 % probability..... 185

Figure 38. Two addition sites for hydrosilation of 1-octyne..... 187

Figure 39. Dependence of the rate constant of the reaction of **III-6** with PhC(O)H at -5 °C on the concentration of the latter..... 194

Figure 40. ORTEP plot of the molecular structure of **III-138** (hydrogen atoms are omitted for clarity). Anisotropic displacement parameters are plotted at 50 % probability..... 196

Figure 41. Dependence of the rate constant of the reaction of **III-135** with $PhSiH_3$ at 22 °C on the concentration of $PhSiH_3$ (**A**) and PMe_3 (**B**)..... 197

Figure 42. Dependence of the rate constant of the reaction of **III-6** with EtOh at 22 °C on the concentration of EtOH (**A**) and PMe_3 (**B**)..... 198

Figure 43. ORTEP plot of the molecular structure of **III-142** (one of two independent molecules; hydrogen atoms except methylenamide C*H* are omitted for clarity). Anisotropic displacement parameters are plotted at 50 % probability. 200

Figure 44. Dependence of the rate constant of the silyl/silane exchange between **III-7** and $PhSiH_3$ at 30 °C on the concentration of PMe_3 added. 205

Figure 45. ORTEP plot of the molecular structure of **III-145** (H atoms, except CO*H*, are omitted for clarity). Anisotropic displacement parameters are plotted at 50 % probability. 210

Figure 46. Dependence of the rate constant of the reaction of **III-7** with acetone at 22 °C on the concentration of the latter. 213

Figure 47. Dependence of the rate constant of the reaction of **III-7** with acetone (20 equiv.) at 22 °C on the concentration of PMe_3. 213

Figure 48. ^1H-^{13}C HMBC NMR of **III-1** (signals at ~8.43 and at ~7.55 ppm in ^1H-projection correspond to *o*-H of the agostic SiH_2Ph and Mo-bound SiH_2Ph substituents, respectively) 334

Figure 49. Eyring plot for exchange between **III-1** and $PhSiH_3$ (standard error: 0.06). 334

Figure 50. Kinetic profile of the hydrosilation of PhC(O)H with $PhSiH_3$ mediated by **III-1** (1.3 mol. %). 335

Figure 51. Deactivation of the catalyst **III-1** (TOF/time coordinates) in the hydrosilation of PhC(O)H with $PhSiH_3$ (1.3 mol. % load of **III-1**)..... 335

Figure 52. ^1H-^{13}C HMBC NMR spectrum (- 30 °C, toluene-d_8) of **III-107** (protons in ^{t}Bu group (at 1.39 ppm) are coupled to nitrile carbon at 204.4 ppm; no coupling between the Si*H* proton (at 5.66 ppm) and C≡N is observed). 336

Figure 53. –Ln[C]/time dependence for reactions of **III-6** with benzaldehyde at -5 °C. 336

Figure 54. ^1H-^1H EXSY NMR spectrum (RT) of a mixture of **III-6** and PMe_3 showing exchange with *trans*-PMe_3 ligand. 337

Figure 55. 1D ^{1}HEXSY NMR spectrum of a mixture of **III-136** and PhC(O)H (irradiation of the C(O)*H* proton in **III-136** at 5.763 ppm shows exchange with free PhC(O)H (9.63 ppm) and another isomer of **III-136** (5.42 ppm); t_m = 0.3 s). 337

Figure 56. 1D ^{1}H EXSY NMR experiment of **III-136** (irradiation of the PMe_3 protons at 1.572 ppm shows exchange with another PMe_3 ligand (1.29 ppm); t_m = 1.0 s). 338

Figure 57. –Ln[C]/time plot for rearrangement of **III-136** into **III-135** at 22 °C (standard error: 0.068). 338

Figure 58. Eyring plot for the reaction of **III-136** with PhC(O)H (10 eq.)..... 339

Figure 59. –Ln[C]/time dependence for reactions of **III-135** with $PhSiH_3$ at 22 °C in the presence of 20 equiv. of PMe_3. 339

Figure 60. –Ln[C]/time dependence for reactions of **III-135** with $PhSiH_3$ at 22 °C in the presence of excess PMe_3. 340

Figure 61. –Ln[C]/time dependence for reactions of **III-6** with EtOH at 22 °C. 340

Figure 62. –Ln[C]/time dependence for reactions of **III-6** with EtOH at 22 °C in the presence of excess PMe_3. 341

Figure 63. Eyring plot for exchange between SiH_2Ph substituent in **III-7** and free $PhSiH_3$ (standard error 0.06)..... 341

Figure 64. Eyring plot for exchange between SiH_2Ph substituent in **III-7** and free $PhSiH_3$ in the presence of 7 equiv. of PMe_3 (standard error 0.08). 342

Figure 65. Eyring plot for intramolecular phosphine exchange in **III-7** (standard error 0.17). 342

Figure 66. Eyring plot for intermolecular phosphine exchange between **III-7** and free PMe_3 (standard error 0.18)..... 343

Figure 67. Eyring plot for intermolecular phosphine exchange between **III-7** and free PMe_3 in the presence of 10 equiv. of $PhSiH_3$ (standard error 0.13). 343

Figure 68. –Ln[C]/time dependence for reactions of **III-7** with acetone at 22 °C (50 % conversion)..... 344

Figure 69. –Ln[C]/time dependence for reactions of **III-7** with acetone at 22 °C (50 % conversion) in the presence of PMe_3. 344

Figure 70. Eyring plot for the reaction of **III-7** with 20 equiv, of acetone (50 % conversion; standard error 0.18). 345

List of Schemes

Scheme 1. Catalytic reduction of C-X (X = C, N, O, S) multiple bonds. 1

Scheme 2. Generally accepted Chalk-Harrod mechanism of TM catalyzed hydrosilation reactions. 2

Scheme 3. Reactions of (Ar'N)Mo(PMe_3)$_3$ (**I-2**) with Me_2SiCl and $MeSiHCl_2$..... 3

Scheme 4. Isolobal analogy between half-sandwich and imido complexes..... 4

Scheme 5. Preparation of agostic silylamides **II-21**, **II-22** and silyl derivatives **II-23**.... 19

Scheme 6. Suggested mechanism for the reaction of **II-20** with $HSiClR'_2$..... 20

Scheme 7. Reaction of **II-24** with $HSiMe_nCl_{3-n}$ (n = 0 – 2). 20

Scheme 8. Reactivity of (Ar'N)Mo(PMe_3)$_3$ (**II-26**) towards chlorohydrosilanes..... 21

Scheme 9. Reactions **II-31** (A) and **II-32** (B) with hydrosilanes..... 22

Scheme 10. Diversity of catalytic hydrosilation of unsaturated organic molecules..... 24

Scheme 11. Chalk-Harrod mechanism for TM mediated hydrosilation of alkenes. 25

Scheme 12. Experimental evidence in favour (**A**, **B**) and against (**C**) Chalk-Harrod mechanism. 26

Scheme 13. Modified Chalk-Harrod mechanism for TM mediated hydrosilation..... 27

Scheme 14. Insertion of ethylene into the Fe-Si bond of Cp*Fe($SiMe_3$)$(CO)_2$ (**II-35**). .. 28

Scheme 15. Classification of silane redistribution side-reactions in the hydrosilation catalysis..... 29

Scheme 16. OA – RE sequences for the catalytic redistribution of silanes..... 30

Scheme 17. Seitz-Wrighton mechanism for the hydrosilation and dehydrogenative silation of alkenes. 30

Scheme 18. Reaction pathways of CpRh(η^2-CH_2=CH_2)(SiR_3)(H) (**II-40**). 31

Scheme 19. Duckett-Perutz "two-silicon cycle" mechanism for hydrosilation of alkenes. 32

Scheme 20. Mechanism of catalytic hydrosilation of ethylene mediated by $Cp_2Ta(\mu\text{-}CH_2)_2Ir(CO)_2$ (**II-50**). 34

Scheme 21. Activation of silanes in hydrosilation by zwitterionic Rh and Ir complexes. 34

Scheme 22. Glaser-Tilley mechanism for hydrosilation of alkenes with primary silanes. 35

Scheme 23. Silylene extrusion from Ph_2SiH_2 or $PhSiH_3$ by **II-57**. 36

Scheme 24. Regio- and stereoselectivity of TM catalyzed hydrosilation of terminal and internal alkynes. 37

Scheme 25. Combined scheme for Chalk-Harrod (**A**) and Crabtree-Ojima (**B**) mechanisms for the TM catalyzed hydrosilation of alkynes. 38

Scheme 26. Formation of $[Rh(cod)(PPh_3)_2][Cl]$ (**II-62**) and $[Rh(cod)(NCR)_2][Cl]$ (**II-64**). 42

Scheme 27. Intramolecular hydrosilation of alkynyl silyl ethers catalyzed by neutral (**a**) and cationic (**b**) ruthenium complexes. 42

Scheme 28. Mechanism of Ru-mediated intramolecular hydrosilation of alkynyl silyl ethers. 43

Scheme 29. Formation of α-vinylsilanes by regioselective hydrosilation of alkynes. 44

Scheme 30. Catalytic hydrosilation of carbonyls and imines. 45

Scheme 31. Ojima's mechanism of ketone hydrosilation mediated by Wilkinson's catalyst. 46

Scheme 32. Chan's mechanism of catalytic hydrosilation of α,β-unsaturated carbonyl compounds mediated by $(Ph_3P)_4RhH$ (**II-81**). 48

Scheme 33. Hydrosilation of 3,5-dimethylcyclohex-2-enone with $HSiMe_2Ph$ mediated by $(Ph_3P)_4RhH$ (**II-81**). 49

Scheme 34. Suggested mechanism of hydrosilation of ketones with secondary silanes mediated by **II-83**. 50

Scheme 35. Buchwald's mechanism for the asymmetric hydrosilation of ketones mediated by (*R*,*R*)-(EBHTI)TiF_2 (**II-84**)/$PhSiH_3$/R'OH system. 51

Scheme 36. Floriani's mechanism for ketone hydrosilation in the presence of $ZnEt_2$/diamine (**II-85**). 52

Scheme 37. Toste's mechanism for the hydrosilation of carbonyl compounds mediated by $(Ph_3P)_2Re(O)_2I$ (**II-86**). 53

Scheme 38. Romao's mechanism for the hydrosilation of carbonyl compounds mediated by MoO_2Cl_2 (**II-96**) 55

Scheme 39. Abu-Omar's mechanism for the hydrosilation of carbonyl compounds mediated by [Re(O)$(hoz)_2$(MeCN)][TFPB] (**II-104**) 56

Scheme 40. Original (**A**) and revised (**B**) mechanism of carbonyl hydrosilation mediated by **II-107 – II-109** 58

Scheme 41. Berke's mechanism for ketone hydrosilation mediated by $Re(NCMe)_3Br_2(NO)$ (**II-113**). 59

Scheme 42. Mindiola's mechanism for ketone hydrosilation mediated by $[(PN^{iPr3})Ni(\mu^2\text{-}Br)]_2$ (**II-119**). 60

Scheme 43. Mechanism of the reaction of [(PNP)(H)Ir=SiRR'][$B(C_6F_5)_4$] (**II-123**) with ketones. 61

Scheme 44. Tilley's mechanism of ketone hydrosilation mediated by [(PNP)(H)Ir=SiRR'][$B(C_6F_5)_4$] (**II-123**). 63

Scheme 45. Buchwald's mechanism of asymmetric hydrosilation of imines mediated by (EBHTI)TiF_2 (**II-84**)/$PhSiH_3$/R'OH system. 65

Scheme 46. Alternative mechanism of hydrosilation of imines in the presence of primary amines mediated by **II-84**/$PhSiH_3$/R'OH system. 66

Scheme 47. Suggested mechanism for the catalytic hydrosilation of imines mediated by $Yb(\eta^2\text{-}Ph_2C{=}NAr)(hmpa)_n$ (**II-136**). 67

Scheme 48. Mechanism for imine hydrosilation catalyzed by $\{Ru(CO)_2(SiTol_2H)\}_2(\mu$-dppm)$(\mu$-$\eta^2$:$\eta^2$-$H_2SiTol_2)$ (**II-139**). 67

Scheme 49. Applications of silylated imines R'CH=N(SiR_3) in organic synthesis..... 69

Scheme 50. Murai's mechanism of nitrile hydrosilation mediated by $Co_2(CO)_8$ (**II-144**). 69

Scheme 51. Addition of nitriles to a bissilyl platinum diphosphine complex $Pt(SiHPh_2)_2(PMe_3)_2$ (**II-148**). 70

Scheme 52. Mechanism of nickel-catalyzed addition of 1,2-bis(dimethylsilyl)carborane to organic nitriles. 71

Scheme 53. Potential mechanism of stoichiometric nitrile hydrosilation promoted by $\{Ru(CO)_2(SiTol_2H)\}_2(\mu$-dppm$)(\mu$-$\eta^2$:$\eta^2$-$H_2SiTol_2)$ (**II-139**)..... 71

Scheme 54. Potential mechanism of stoichiometric nitrile hydrosilation promoted by Cp*(CO)(H)Ru=Si(H)[$C(SiMe_3)_3$] (**II-124**). 72

Scheme 55. Tobita's mechanism for the addition of RCN (R = Me, Ph) to Cp*(CO)(H)Ru=Si(H)[$C(SiMe_3)_3$] (**II-124**). 73

Scheme 56. Tobita's mechanism for the addition of RCN (R = Me, ^{t}Bu) to Cp'$(CO)_2$(H)W=Si(H)[$C(SiMe_3)_3$] (**II-125**)..... 74

Scheme 57. Catalytic alcoholysis and aminolysis of hydrosilanes. 75

Scheme 58. Mechanism of silane alcoholysis mediated by $Co_2(CO)_8$ (**II-144**)..... 76

Scheme 59. Mechanisms of silane alcoholysis mediated by $[IrH_2(THF)_2(PPh_3)_2][SbF_6]$ (**II-168**) (**A**) and $Rh_2(pfb)_4$ (**II-172**) (**B**). 77

Scheme 60. Generation of cationic η^2-silane complexes $[Cp(CO)(PR_3)Fe(\eta^2$-$HSiEt_3)]^+$ (**II-175**, R = Pe, Et). 78

Scheme 61. Brookhart's mechanism of catalytic silane alcoholysis mediated by $[Cp(CO)(PR_3)Fe(\eta^2$-$HSiEt_3)]^+$ (**II-175**, R = Pe, Et)..... 79

Scheme 62. Mechanism of silane alcoholysis mediated by $CpZr(acac)_2Cl$ (**II-180**) / ^{n}BuLi. 80

Scheme 63. Mechanism of silane alcoholysis promoted by AuCl(Xantphos) (**II-184**). .. 80

Scheme 64. Activation of amines in catalytic silane aminolysis in the presence of Yb(η^2-Ph_2C=NAr)$(hmpa)_n$ (**II-136**) (**A**) and $[(Et_3N)_3U][BPh_4]$ (**II-188**) (**B**)..... 81

Scheme 65. Abu-Omar's mechanism for silane hydrolysis and alcoholysis catalyzed by $[Re(O)(hoz)_2(Solv)][B(C_6F_5)_4]$ (**II-104**). 83

Scheme 66. Reactivity of $[(PNP)(H)Ir{=}SiPh_2][B(C_6F_5)_4]$ (**II-123**) towards alcohols and the mechanism of the reaction with ROH. 84

Scheme 67. Tilley's mechanism of silane alcoholysis catalyzed by $[(PNP)(H)Ir{=}SiPh_2][B(C_6F_5)_4]$ (**II-123**)..... 85

Scheme 68. Stoichiometric reactivity of Cp_2ZrR_2 (R = Et, ^{n}Bu) (**196**) with H_2SiPh_2..... 86

Scheme 69. Mechanism for alkene hydrosilation with the use of $Cp_2M(^nBu)_2$ (M = Zr (**II-194**), Ti (**II-200**), Hf (**II-201**)). 87

Scheme 70. Coupling reaction between $Cp_2Zr(\eta^2$-$C_2H_4)$ (**II-202**) with SiH_4. 87

Scheme 71. Mechanisms for the 1,4-hydrosilation of dienes (**A**) and dehydrogenative double silation of dienes (**B**) promoted by Cp_2TiF_2 (**II-203**). 88

Scheme 72. Hydrosilation of alkynes with the use of Cp_2TiCl_2 (**II-204**) / ^{n}BiLi..... 89

Scheme 73. Mechanism of **II-205**-catalyzed hydrosilation of ketones. 90

Scheme 74. Titanocene catalyzed hydrosilation of esters. 90

Scheme 75. Cp_2TiMe_2 (**II-211**) catalyzed hydrosilation of pyridine. 92

Scheme 76. MoO_2Cl_2 (**II-96**) catalyzed hydrosilation of amides..... 93

Scheme 77. MoO_2Cl_2 (**II-96**) catalyzed hydrosilation of sulphoxides..... 93

Scheme 78. Cp_2TiCl_2 (**II-204**) / ^{n}BuLi catalyzed silation of diols. 94

Scheme 79. Intarmolecular alcoholysis and aminolysis reactions catalyzed by Cp_2TiMe_2 (**II-211**) and (EBTHI)$TiMe_2$ (**II-220**). 95

Scheme 80. Proposed synthesis of imido silylamide and hydride complexes. 96

Scheme 81. Preparation of $(RN)_2NoCl_2(DME)$ (**III-11 – III-15**). 98

Scheme 82. Preparation of Mo(IV) and W(IV) bis(imido) phosphine compounds. 99

Scheme 83. Preparation of bis(imido) ethylene adducts **III-30** and **III-31**. 101

Scheme 84. Reactivity of $(RN)_2Mo(PMe_3)_n$ with $HSiClR'_2$ and $HSiMeCl_2$. 103

Scheme 85. Degenerate exchange in complex **III-38** (two enantiomers, "**A**" and "**B**") and proposed mechanism for this process. 105

Scheme 86. Reactivity of $(RN)_2M(PMe_3)_{n-1}L$ (M = Mo, W; L = PMe_3, η^2-C_2H_4) with $HSiCl_3$. 107

Scheme 87. Reaction of $(ArN)_2Mo(\eta^2\text{-}C_2H_4)(PMe_3)_2$ (**III-31**) with $HSiCl_3$ and BPh_3.. 108

Scheme 88. Proposed mechanism for the reaction of **III-23** with $HSiCl_3$. 112

Scheme 89. Reaction of $(ArN)_2Mo(PMe_3)_3$ (**III-22**) with $PhSiH_3$ 114

Scheme 90. Reaction of $(ArN)_2Mo(\eta^2\text{-}CH_2{=}CH_2)(PMe_3)_2$ (**III-31**) with $PhSiH_3$ and BPh_3. 118

Scheme 91. Reaction of $(ArN)_2Mo(PMe_3)_3$ (**III-22**) with $PhSiH_3$ and H_2 purging. 118

Scheme 92. Reaction of **III-23** with $PhSiH_3$ and BPh_3. 120

Scheme 93. Reactivity of $(Ar'N)_2Mo(PMe_3)_3$ (**III-4**) towards $PhSiH_3$. 121

Scheme 94. NMR scale reaction of $(Ar'N)_2Mo(PMe_2Ph)_3$ (**III-26**) with $PhSiH_3$. 123

Scheme 95. Reactions of $(^tBuN)_2Mo(PMe_3)L$ (L = PMe_3 (**III-27**), η^2-C_2H_4 (**III-30**) with $PhSiH_3$. 125

Scheme 96. NMR scale reaction of $(^tBuN)_2Mo(PMe_3)L$ (L = PMe_3 (**III-27**), η^2-C_2H_4 (**III-30**)) with $PhMeSiH_2$. 129

Scheme 97. Reactions of $(RN)_2Mo(PMe_3)_n$ (**III-22** and **III-27**) with $(EtO)_3SiH$. 131

Scheme 98. Possible pathways for the reactivity of agostic silylamides 132

Scheme 99. Suggested dynamic process in complex **III-1**. 135

Scheme 100. Silane/silyl exchange in **III-1** *via* the silanimine intermediate **III-2**. 138

Scheme 101. Silane/silyl exchange in **III-1** *via* the dissociation of Si-H···Mo bond. 138

Scheme 102. Reactions of complex **III-1** with ethylene and styrene..... 145

Scheme 103. Possible mechanism for the formation of ethyl (vinylsilyl)amide **III-3**... 149

Scheme 104. Reactions of **III-1** with olefins in the presence of BPh_3..... 149

Scheme 105. Reactions of **III-1** with ketones forming compounds **III-96** and **III-97**.. 150

Scheme 106. Reaction of **III-97** with acetophenone..... 151

Scheme 107. Reaction of **III-1** with benzaldehyde and formation of complex **III-100**. 152

Scheme 108. Reaction of **III-31** with BPh_3 and benzaldehyde..... 152

Scheme 109. Reactivity of **III-1** towards organic nitriles..... 153

Scheme 110. Thermal stability of **III-3** and its reactions with hydrosilanes and H_2. 156

Scheme 111. Mechanism of the reaction of **III-3** with $PhSiH_3$ in the presence of PMe_3. 158

Scheme 112. Formation and reactivity of complex **III-113**..... 160

Scheme 113. Suggested mechanism for the reaction of **III-114** with excess $PhSiH_3$.... 162

Scheme 114. Suggested mechanism for the hydrosilation of alkenes mediated by **III-3**. 167

Scheme 115. Preparation of **III-93** and **III-115** and their reactions with $PhSiH_3$. 168

Scheme 116. Reactions of complex **III-112** with acetone and benzonitrile. 169

Scheme 117. Possible mechanism for the reaction of **III-112** with benzaldehyde..... 170

Scheme 118. Preparation of complex **III-118** and its reaction with $PhSiH_3$..... 171

Scheme 119. Reaction of **III-3** with phenylacetylene..... 171

Scheme 120. Preparation of $(ArN)_2Mo(\eta^2\text{-}BH_4)_2(PMe_3)$ (**III-125**). 173

Scheme 121. Preparation of Mo(IV) bis(borohydride) complexes **III-128** and **III-8**. .. 177

Scheme 122. Reactions of borohydrides **III-128** and **III-8** with silanes..... 180

Scheme 123. Preparation of $(ArN)Mo(H)(Cl)(PMe_3)_3$ (**III-6**)..... 183

Scheme 124. Preparation of the dihydride complex **III-131**..... 184

Scheme 125. Preparation of silylhydrides **III-7**, **III-133**, and **III-134**. 186

Scheme 126. Mechanism for the hydrosilation of PhC(O)H with $PhSiH_3$ mediated by complex **III-6**. 193

Scheme 127. Preparation of (ArN)Mo(Cl)(OCy)$(PMe_3)_3$ (**III-138**). 195

Scheme 128. Mechanism for the ethanolysis of $PhSiH_3$ mediated by **III-6**. 199

Scheme 129. Reactions of (ArN)Mo(H)(Cl)$(PMe_3)_3$ (**III-6**) with nitriles. 200

Scheme 130. Reactions of **III-142** with benzaldehyde and L-Selectride. 202

Scheme 131. Reaction of (ArN)Mo(H)(Cl)$(PMe_3)_3$ (**III-6**) with styrene. 203

Scheme 132. Silyl/silane exchange for complex **III-7**. 205

Scheme 133. Suggested mechanism for the silyl/silane exchange for complex **III-7**. .. 206

Scheme 134. Dissociative and non-dissociative mechanisms for the exchange processes between **III-7**, $PhSiH_3$, and PMe_3 (Gibbs free energies are expressed in $kcal \cdot mol^{-1}$). 208

Scheme 135. Reactivity of complex **III-7** towards benzaldehyde. 209

Scheme 136. DFT calculated mechanism for the reaction of model complex **III-7'** with MeC(O)H and $MeSiH_3$ (Gibbs free energies are expressed in $kcal \cdot mol^{-1}$). 211

Scheme 137. Preparation of complex **III-147** and its reactivity. 212

Scheme 138. Reactions **III-147** with carbonyls and PhCN. 215

Scheme 139. Low temperature NMR scale reaction of complex **III-147** with $PhSiH_3$. 215

Scheme 140. DFT calculated mechanism for the reaction of model complex **III-7'** with acetone and $MeSiH_3$ (Gibbs free energies are expressed in $kcal \cdot mol^{-1}$). 216

Scheme 141. Suggested mechanism for the catalytic hydrosilation of acetone with $PhSiH_3$ in the presence of **III-7**. 217

Scheme 142. Reaction of (ArN)Mo(H)$(SiH_2Ph)(PMe_3)_3$ (**III-7**) with benzonitrile. 218

Scheme 143. Proposed catalytic cycles for hydrogentation of olefins (**A**) and hydroboration of nitriles (**B**) mediated by **IV-12**. 221

List of Tables

Table 1. Selected IR and NMR data for **II-16**, **II-17** and $Me_2HSi\text{-}NH^tBu$ 16

Table 2. Hydrosilation of 1-hexyne mediated by neutral Rh and Rh-Co complexes..... 41

Table 3. Selected NMR and IR data for β-agostic silylamido molybdenum complexes 106

Table 4. Selected bond distances (Å) and angles (°) for complex **III-47**..... 111

Table 5. Selected bond distances (Å) and angles (°) for complex **III-1**..... 117

Table 6. Selected bond distances (Å) and angles (°) for complex **III-77**..... 127

Table 7. Catalytic hydrosilation of ketones and aldehydes mediated by **III-1**. 140

Table 8. Reactions alkenes and alkynes with hydrosilanes in the presence of **III-1**. 142

Table 9. Hydrosilation of nitriles and pyridines as well as alcoholysis and aminolysis of silanes mediated by **III-1**. 143

Table 10. Selected bond distances (Å) and angles (°) for complex **III-3**..... 147

Table 11. Hydrosilation of alkenes and polymerization of phenylacetylene mediated by **III-3**..... 163

Table 12. Hydrogenation (~ 1.5 atm.) of alkenes and alkynes mediated by **III-3**. 163

Table 13. Hydrosilation of carbonyls and nitriles, alcoholysis and aminolysis of $PhSiH_3$ mediated by **III-3**. 164

Table 14. Selected bond distances (Å) and angles (°) for complex **III-125**..... 175

Table 15. Selected bond distances (Å) and angles (°) for complex **III-8**..... 179

Table 16. Selected bond distances (Å) and angles (°) for complex **III-7**..... 182

Table 17. Selected bond distances (Å) and angles (°) for complex **III-6**..... 185

Table 18. Catalytic hydrosilation of aldehydes and ketones mediated by **III-6**. 188

Table 19. Catalytic hydrosilation of alkenes and alkynes and alcoholysis and hydrolysis of $PhSiH_3$ mediated by **III-6**..... 190

Table 20. (**III-7**)-catalyzed hydrosilation of nitriles and alcoholysis of $PhSiH_3$ (5 mol %). 191

Table 21. Catalytic hydrosilation of aldehydes and ketones mediated by **III-7** (5.0 mol %). 192

Table 22. Selected bond distances (Å) and angles (°) for complex **III-138**..... 196

Table 23. Selected bond distances (Å) and angles (°) for complex **III-142**..... 201

Table 24. Selected bond distances (Å) and angles (°) for complex **III-145**..... 210

Table 25. Crystal structure determination parameters for **III-47**..... 346

Table 26. Crystal structure determination parameters for **III-1**..... 347

Table 27. Crystal structure determination parameters for **III-7**..... 348

Table 28. Crystal structure determination parameters for **III-77**..... 349

Table 29. Crystal structure determination parameters for **III-3**..... 350

Table 30. Crystal structure determination parameters for **III-125**..... 351

Table 31. Crystal structure determination parameters for **III-8**..... 352

Table 32. Crystal structure determination parameters for **III-6**..... 353

Table 33. Crystal structure determination parameters for **III-138**..... 354

Table 34. Crystal structure determination parameters for **III-142**..... 355

Table 35. Crystal structure determination parameters for **III-145**..... 356

I. Introduction

The development of synthetic methodologies that allow the selective and efficient reduction of multiple carbon-carbon or carbon-heteroatom (heteroatom = N, O, S) bonds is a fundamental problem of organic and organometallic chemistry.[1] Whereas simple, selective and high yielding organic transformations of this type are scarce,[2] the ability of transition metal compounds to induce stoichiometric and catalytic reactions of this kind has been recognized and extensively used for many years.[1, 3] The homogeneous transition metal mediated reduction of unsaturated organic molecules can be divided into four major categories: hydrogenation,[1, 3, 4] hydroboration,[3, 5] hydroamination[6] and hydrosilation[7] reactions (Scheme 1). All these methods are commonly found in the literature; however, the availability, cost and stability of reagents as well as simplicity of experimental procedures have drawn the special attention of chemists to the hydrosilation methodology. Moreover, catalytic addition of hydrosilanes to carbon-heteroatom multiple bonds provides simultaneous protection of the heteroatom in the reduction product, making it amenable for further transformations, thus resulting in additional advantage of this approach comparatively to other reduction methods.[7]

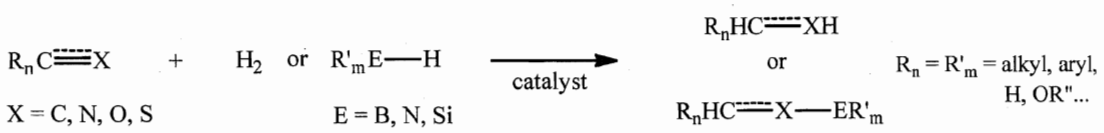

Scheme 1. Catalytic reduction of C-X (X = C, N, O, S) multiple bonds.

The majority of known hydrosilation catalysts are based on late transition metal systems, such as those involving rhodium, ruthenium, platinum, palladium, etc.[7] Despite the high catalytic activity of such complexes, the cost and toxicity of the late transition metal compounds hamper the output of the hydrosilation process making it less profitable and less environmentally benign. On the other hand, early transition metal complexes are, in general, relatively cheap and exhibit much reduced toxicity, attracting the attention of chemists to the application of such systems in catalysis.[7b]

Stoichiometric reductions of multiple bonds by early transition metal hydrides are well established,[8] but little is known about their catalytic variants including hydrosilation

reactions.[9] Until very recently, it has been generally believed that addition of hydrosilanes to unsaturated organic molecules mediated by both early and late metals proceeds *via* a Chalk-Harrod type sequence,[10] starting with Si-H activation and silyl migration, followed by either a σ-bond metathesis (for early TM)[9e] or reductive C-H elimination (for late TM).[10] However, very little mechanistic data is available, and in no case were all the key steps observed on a single metal center.[10b-d] A few other catalytic cycles have been proposed in the last decades, however, the experimental evidence for these mechanisms is scarce and sometimes questionable.[a]

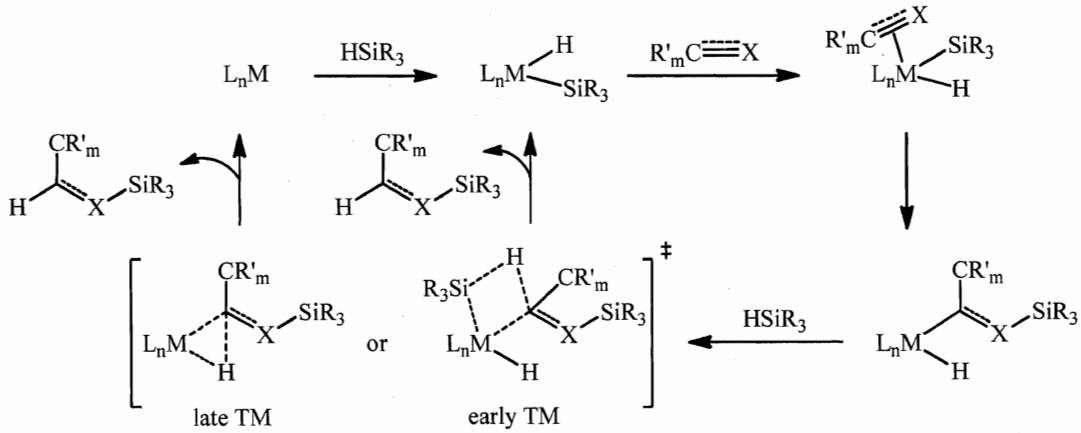

Scheme 2. Generally accepted Chalk-Harrod mechanism of TM catalyzed hydrosilation reactions.[10]

The development of hydrosilation catalysis and the constant search for efficient and air stable catalysts has led to the recent discovery of the catalytic activity of transition metal oxo complexes in hydrosilation reactions.[a] Recently, Toste *et al.* provided compelling evidence that hydrosilation by a Re(V) dioxo complex includes the Si-H addition to the Re=O bond in the silane activation step.[11] Related catalysis by oxo complexes of molybdenum seems to follow a similar mechanism.[12] However, kinetic studies by Abu-Omar *et al.* suggest that this pathway may not be generally applicable even for other Re(V) oxo complexes.[13]

The interest of Nikonov's group in the activation of hydrosilanes by transition metal complexes resulted recently in the discovery of a novel coupling reaction between the imido moiety of early transition metal imido compounds $CpM(NR)L'_n$ (**I-1**, M = Ta, Nb;

[a] See the historical section of this thesis and references therein.

L' = phosphine) and the Si-H bond of silanes.[14] In addition, their studies revealed that the treatment of the isolobal molybdenum bis(imido) derivative $(Ar'N)_2Mo(PMe_3)_3$ (**I-2**) with chlorohydrosilanes (Me_2SiHCl and $MeSiHCl_2$) affords metastable imido β-agostic silylamides $(Ar'N)Mo(Cl)(\eta^3\text{-}NAr'\text{-}SiMeR\text{-}H)(PMe_3)_2$ (R = Me (**I-3**) and Cl (**I-4**); Scheme 3), which decompose to mono(imido) dichloride species $(Ar'N)MoCl_2(PMe_3)_3$ (**I-5**) *via* the release of a silanimine dimer.[15] This reactivity strongly resembles addition of the Si-H bond across the Re=O bond in Re(V) dioxo complexes reported by Toste *et al.*[11] Despite the fact that oxo compounds are, in general, less air- and moisture-sensitive than analogous imido complexes,[11-13] the utilization of the latter for the activation of hydrosilanes has some advantages:[14-16] (i) imido NR^{2-} groups form strong bonds to the metal, being good supporting ligands (4 or 6 electron donors) and stabilizing the electron deficiency at the metal center; (ii) the steric and electronic properties of the system can be easily adjusted by varying the R substituents in the NR^{2-} ligands.

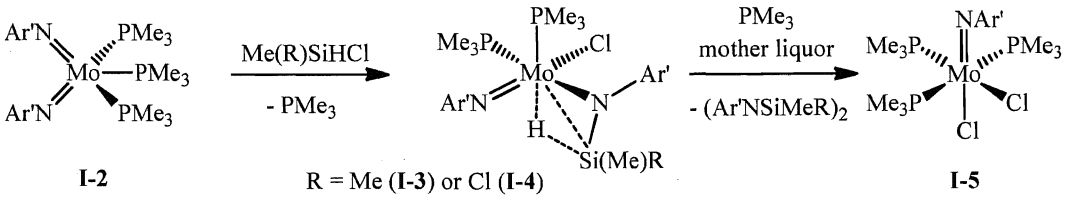

Scheme 3. Reactions of $(Ar'N)Mo(PMe_3)_3$ (**I-2**) with Me_2SiCl and $MeSiHCl_2$.[15]

As a continuation of Nikonov's research in the field of transition metal imido complexes, a significant part of the present study is devoted to the investigation of the imido/silane coupling between imido moiety of molybdenum(IV) and tungsten(IV) bis(imido) compounds $(RN)_2M(PR'_3)_n$ (R = Ar' (**I-2**), Ar (**I-6**), ^{t}Bu (**I-7**), etc., n = 2, 3) and chloro-substituted hydrosilanes and the mechanistic aspects of this process. The results of the extension of the imido/silane coupling methodology to reactions of Mo(IV) and W(IV) bis(imides) with chlorine-free hydrosilanes, in particular $PhSiH_3$, $PhMeSiH_2$ and $(EtO)_3SiH$, will be also presented here.

Although agostic silylamido complexes $L_nM(\eta^3\text{-}NR\text{-}SiR'_2\text{-}H)$ (**I-8**) have been known since 1992, their reactivity has not been studied, so they mainly remained a laboratory curiosity.[17] On the other hand, it is often assumed that these species could present a model for key intermediates in the activation of hydrosilanes by transition metal

complexes.[17] In this respect, the major objectives of the second part of the present research are the preparation and study of the reactivity of the novel Mo(IV) imido agostic silylamide, (ArN)Mo(SiH_2Ph)(η^3-NAr-SiHPh-H)(PMe_3) (**I-9**), available by the coupling between the imido moiety of $(ArN)_2Mo(PMe_3)_3$ (**I-6**) and $PhSiH_3$. For the first time, we present the catalytic and stoichiometric reactions of a compound of this type and provide evidence for the intermediacy of a silanimine complex, (ArN)Mo(η^2-ArN=SiHPh)(PMe_3) (**I-10**). Mechanistic studies of the hydrosilation reactions mediated by **I-9** will be discussed. The reactions of agostic complex **I-9** with olefins leading to the formation of the products of Si-C coupling, (ArN)Mo(R)(η^3-NAr-SiHPh-CH=CHR')(PMe_3) (**I-11**), will also be presented in this part of the thesis along with the stoichiometric and catalytic reactivity of **I-5** and the mechanism of its reaction with phenylsilane.

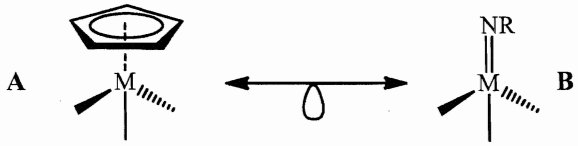

Scheme 4. Isolobal analogy between half-sandwich and imido complexes.

The chemistry of transition metal hydride cyclopentadienyl sandwich and half-sandwich complexes has been intensively studied because of their important role in many transformations as catalysts[18] and key intermediates.[19] At the same time, compounds with N-based ligands isolobal to Cp^- (Scheme 4, **A**) (such as RN^{2-} and RPN^{2-}; Scheme 4, **B**)[14] have also been successfully applied in a variety of transition metal mediated transformations, including catalytic hydrogenation, hydrosilation and olefin polymerization reactions.[20] However, relatively little is known about the structure, stability and reactivity of their hydride derivatives.[21] The preparation and structure of novel mono(imido) Mo(IV) hydride complexes as well as their stoichiometric and catalytic reactivity will be the subject of the research in the last part of this thesis. Detailed mechanistic studies of the hydrosilation of carbonyl compounds and alcoholysis of hydrosilanes will be also presented in Chapter III.

The historical section of the present thesis precedes the results and discussion section and includes an account of the structural and spectroscopic features of silane σ- and agostic Si-H···M complexes as well as the recent advances in the chemistry of β-agostic

NSi-H···M compounds. This is followed by the detailed overview of available mechanistic studies of transition metal catalyzed hydrosilation reactions and recent advances in the field of early transition metal hydrosilation catalysis.

II. Historical

II.1 Agostic Si-H···M interactions in transition metal complexes

The study of nonclassical interactions in the coordination sphere of transition metal complexes started with the Kubas discovery[22] of the coordination of an H_2 molecule to transition metals to form a dihydrogen σ-complex **II-1**.[23, 24] By definition, a nonclassical complex is the compound, in which one or several metal-ligand and/or ligand-ligand bonds are involved in nonclassical interactions. This bonding situation cannot be described by a single Lewis structure (2 center – 2 electron interactions) and, usually, include a significant delocalization of σ-bonds over three or more centers. Thus, complexation of H_2 in **II-1** can be understood as a 3 center–2 electron (3c-2e) interaction (Figure 1). The same concept was earlier applied to describe bonding in trihydrogen cation H_3^+ (**II-2**), methonium ion CH_5^+ (**II-3**), and polyboranes (**II-4**).[17]

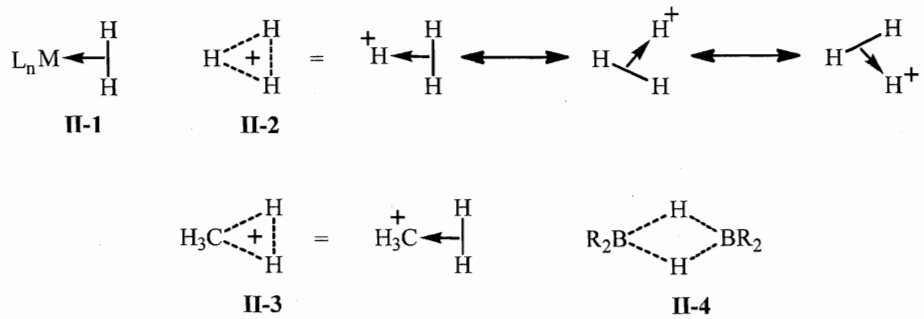

Figure 1. Coordination of dihydrogen to transition metal complexes and the 2c-3e bond concept for H_3^+, CH_5^+, and polyboranes

The discovery of H-H and E-H (E = C, Si, etc.) σ-bond coordination to transition metals[17, 22-25] was quickly realized to be highly relevant to transition metal mediated activation of small molecules and, eventually, to catalysis.[24-26] Originally, the idea of nonclassical Si-H complexes was developed almost 35 years ago.[27] Only later, in the 1980s, the interest in silane σ-complexes **II-5**[28] (Figure 2) resulted in a significant improvement in the understanding of Si-H activation, important in the investigation of various catalytic reactions (such as hydrosilation, dehydrogenative silane coupling, etc.) and for the design of new catalysts. Nowadays, there are four types of nonclassical Si-H

interactions known in organometallic chemistry, which can be classified as silane σ-complexes (**II-5**), Si-H···M agostic compounds (**II-6**), complexes with *I*nterligand *H*ypervalent *I*nteractions (*IHI*) (**II-7**), and polyhydride silyl compounds with multicenter Si-H interactions, such as in **II-8**, (Figure 2; dotted line represents the nonclassical bonding between the silicon atoms and hydride ligands (Figure 2).[17]

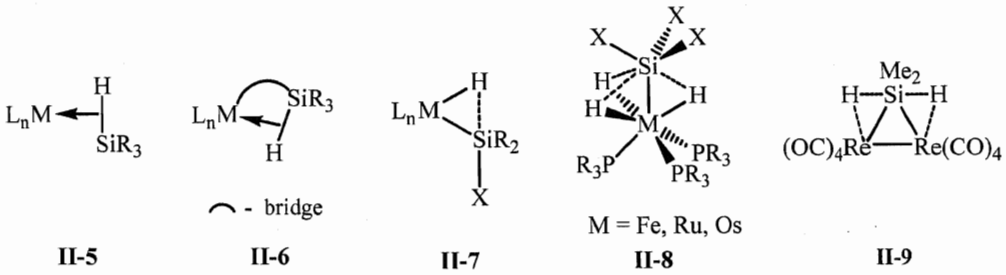

II-5 **II-6** **II-7** **II-8** **II-9**

Figure 2. Nonclassical Si-H interactions in the coordination sphere of transition metals

Since this thesis relates only to agostic NSi-H···M complexes, the following part of the literature review will describe only this kind of interaction as well as closely related bonding in silane σ-complexes. The intent of this chapter is to discuss the nature, general features and ideas of agostic Si-H···M bonding and to review recent experimental and theoretical achievements in the field of agostic NSi-H···M complexes.

II.1.1 Bonding aspects of Si-H···M agostic and silane σ-complexes

The formation of complexes **II-5** and **II-6** can be viewed as a result of incomplete Si-H bond activation by an electrophilic transition metal center[24b, 29] ("arrested" oxidative addition[30]). Initially, the formation of a structure of this type was proposed by Graham *et al.* for the dinuclear rhenium silane complex $Re_2(\mu\text{-}H_2SiMe_2)(CO)_8$ (**II-9**; Figure 2).[27, 28] Although the hydrogen atoms were not seen in the X-ray analysis, the Si-H contact for **II-9** was estimated to be longer than for a normal Si-H bond (1.57 Å *vs.* 1.48 Å, respectively). This and the small value of the coupling constant between the methyl groups and hydrogen atoms at silicon ($^3J_{H\text{-}H}$ = 1.5 Hz compared to 4.2 Hz in Me_2SiH_2) in the ^{1}H-NMR spectrum suggested the presence of nonclassical interactions. Similar arguments were used to assign a nonclassical structure to $W_2(\mu\text{-}H_2SiMe_2)(CO)_8$ (**II-10**),[31] however, reliable structural and spectroscopic evidence for nonclassical Si-H bonding was still absent. In 1982, Corriu *et al.* suggested an effective test for the presence of

nonclassical Si-H interactions based on the observation of significantly reduced (compared to free hydrosilanes) value of $^1J_{Si\text{-}H}$.[32] Thus, the value of $^1J_{Si\text{-}H}$ of 65 Hz in the half-sandwich manganese silane complex Cp'Mn(η^2-H-SiPh$_3$)(CO)$_2$ (**II-11**) is much smaller than for silanes (>180 Hz), but larger than the coupling constant in classical silylhydride complexes (3-10 Hz).[32] In addition, ND analysis for the related compound Cp'Mn(η^2-H-SiFPh$_2$)(CO)$_2$ (**II-12**) reported by Schubert *et al.* indicated the presence of an elongated Si-H contact of 1.802(5) Å (vs. 1.48 Å for Si-H in hydrosilanes).[33] The answer regarding the nature of such unusual spectroscopic and structural characteristics is lying in the description of the 3c-2e bond,[23, 26a] which could be carried out using the well-known Dewar-Chatt-Duncanson (DCD) scheme[17, 34] (Figure 3). The 3c-2e bond is formed

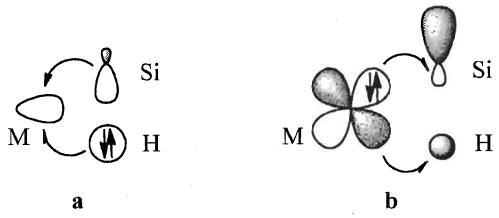

Figure 3. DCD type model for the 3c-2e Si-H-M bonding.[17]

by mixing a vacant orbital of one of the centers with a 2e σ-bond between two others (Figure 3, **a**). In the case of silane agostic and σ-complexes, the 3c-2e bonding corresponds to the complexation of the Si-H bond to a metal or, if another approach is applied, to the protonation of the M-Si bond.[29] However, this bonding description can be correctly applied only if the metal center is in the d^0 configuration. In the case of d^n ($n \geq 1$) complexes, the back-donation from the occupied metal d-orbital on the antibonding σ*(Si-H) orbital (Figure 3, **b**) cannot be ignored. In fact, for the majority of d^n ($n \geq 1$) complexes the strength of back-donation from the metal is the key factor controlling the stability of the σ-bond complexation.[23-24, 34] The overall scheme shown in Figure 3 is close to the DCD model originally designed to describe bonding in olefin complexes.[35]

The presence of substituents at the silicon center also affects the coordination of silanes to the metal *via* steric and electronic factors. According to the DCD model, the introduction of electron-donating groups in silanes makes both σ(Si-H) and σ*(Si-H) orbitals be higher in energy,[36] thus, increasing the donation but decreasing the back-donation components. In contrast, electron-withdrawing substituents bring both the

bonding and antibonding orbitals of the Si-H bond down in energy, decreasing the donation and increasing the back-donation components (Figure 3). This leads to weakening of the Si-H bonding, and, eventually, in the case of a very strong back-donation, results in complete oxidative addition (OA) of the Si-H bond to the metal center forming a silylhydride complex.[17] However, the presence of several very strong π-acidic ligands, usually carbonyls,[37] at the metal fragment could inhibit the complete OA of silanes, stabilizing the σ-Si-H coordination. Since for d^n ($n \geq 1$) systems the back-donation is the most crucial factor affecting the stability of the Si-H bond coordination, anything that reduces this component will lead to the increase of the residual Si-H σ-bonding. These factors are:[17, 23] (i) the presence of a metal from the first transition series (d-orbitals of these metals do not provide efficient overlapping with ligand orbitals); (ii) the presence of strong π-acidic ligands (such as CO or PF_3) and/or electron-withdrawing substituents at the metal (such as halogens) that bring the d-level down in energy; (iii) the presence of a metal in high oxidation state and/or a positively charged metal center, which contracts d-orbitals preventing sufficient orbital overlap.

II.1.2 Structural features of Si-H···M agostic and silane σ-complexes

Since the bonding in Si-H···M agostic compounds is usually described in the same manner as in σ-complexes, both species are identified by the same structural and spectroscopic parameters. The structural difference between σ-complexation and an agostic bond is the presence of a supportive link to the metal in the latter species, which can be either a sequence of atoms, as in the case of β- (one atom), γ- (two atoms), δ- (three atoms) and so on, or just a chemical bond between the metal and silicon (α-agostic interaction; Figure 4).[17] The properties of Si-H···M agostic compounds depend on the length of the chain between metal and silicon centers and, in the case of reasonably long and flexible bridges, do not differ significantly from silane σ-complexes.[17, 29] However, the presence of short and rigid chains may affect the interaction between the metal and the Si-H bond. The α-agostic interaction (Figure 4) is a recently discovered phenomenon and its theoretical aspects are still not completely understood.[17] Analogously to dihydrogen complexation, a more advanced oxidative addition of the Si-H bond to a metal results in shorter M-Si and M-H bonds and a longer Si- H distance. However,

X_n - number of atoms between M and Si

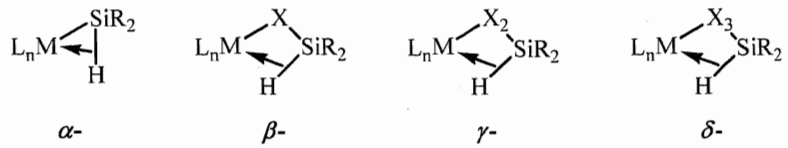

Figure 4. Classification of Si-H···M agostic complexes.

recent theoretical and experimental results indicate that the straightforward assignment of the presence of nonclassical Si-H interactions based on these criteria is not always correct.[17] The main limitation of this approach is the presence of substituents at the silicon center and the difference in electronegativities between the hydrogen and silicon atoms.[17, 29] As mentioned above, the extent of silane OA to a metal and, therefore, the value of the Si-H distance are dictated mostly by the strength of back-donation from the metal to the antibonding σ*(Si-H) orbital.[23, 24b, 34] However, the back-donation component of the DCD model (Figure 3) depends strongly on several factors, which make the application of a simple threshold value of a bond length as a criterion for Si-H interactions problematic. Furthermore, in the case of *β*-agostic Si-H···M compounds (Figure 4) the value of the Si-H distance is often affected by the nature of the atom in the *α*-position and, according to numerous X-ray studies, appears to be somewhat shorter than in silane *σ*-complexes.[17, 38] In 1990, Schubert suggested that the shortest nonbonding Si-H contact can be estimated as 2.0 Å.[38] This structural criterion, widely used in the 1990s to establish the presence of silane *σ*-complexes,[29, 39] is based on the concept of atomic radii and obtained by summing up half of the nonbonding Si-Si distance in 1,3-cyclodisiloxanes (2.3-2.4 Å)[40] with half of the H-H distance, at which the H-H interaction is supposed to be weak (1.85 Å).[38] However, the known range for a single Si-Si bond is 2.33-2.70 Å[41] exceeding the nonbonding Si-Si distance in 1,3-cyclodisiloxanes.[40] Furthermore, some examples of complexes with rather long Si-H distances (2.0-2.2 Å) recently appeared in the literature.[17] In addition, a short distance between atoms may not necessarily mean the presence of a chemical bond and could be due to the presence of some steric factors.[40] These arguments suggest that the structural criterion suggested by Schubert for the presence of silane *σ*-complexation should be used with caution.

The influence of substituents at silicon on the magnitude of Si-H contacts is also questionable. Experimental data for R_3Si-H contacts (where R is an electron-donating or electron-withdrawing group) reported to date are not always in agreement with theoretical predictions made by the DCD scheme (Figure 3; see the discussion above). Thus, the X-ray study of a series of manganese complexes Cp"Mn(η^2-H-SiR_3)(CO)L (**II-13**, L – CO or another two electron ligand, Cp" – Cp, Cp', Cp*) with different R's revealed a rather narrow range of Si-H contacts (1.75(4)-1.802(5) Å, the upper limit was found by ND), showing, contrary to expectations based on the DCD model, no significant effect of substituents at silicon on the Si-H bond magnitude.[17, 32, 33, 38] In addition to X-ray studies, recent computational studies on the system **II-13** also supported this conclusion.[42]

Taking into account the elongation of the M-H bond in dihydrogen complexes,[22, 23, 43] one could expect to observe a similar phenomenon for silane complexation.[33] However, in the case of agostic Si-H···M and silane σ-complexes, the situation is less straightforward and depends on the particular system. Thus, numerous X-ray and computational data[17, 23, 29, 38, 44] as well as the ND study of complex **II-12**[29] show no significant elongation of the M-H bond in the case of silane complexation.[b] For example, the X-ray diffraction studies of a series of complexes **II-13** with different substituents at the metal and silicon atoms showed the M-H distance being in the range 1.47(3)-1.569(4) Å (seven compounds with Δ = 0.11(3) Å).[23, 29, 38] Despite the inaccuracy of hydride positions found by X-ray, this data does not allow us to draw any accurate conclusions regarding the influence of substituents on the M-H distance. However, in some cases more advanced OA of silane leads indeed to the observation of a reduced M-H contact. This, for example, was demonstrated by comparing the Mo-H distances for Mo(η^2-$HSiPh_3$)(CO)$(dppe)_2$ (**II-14**, Mo-H 1.70(5) Å) and Mo(η^2-H_2SiPh_2)(CO)$(dppe)_2$ (**II-15**, Mo-H 2.04(5) Å, $\Delta_{Mo\text{-}H}$ = 0.34(7) Å), the shortening of which correlates with the somewhat stronger silane complexation (Si-H: 1.78(6) Å for **II-14** *vs.* 1.66(6) Å for **II-15** ($\Delta_{Si\text{-}H}$ = 0.12(8) Å); $^1J_{H\text{-}Si}$: 39 Hz for **II-14** *vs.* 50 Hz for **II-15**, see the discussion of spectroscopic features below).[32, 38] For β-agostic Si-H···M complexes, M-H distances are

[b] It is well-known that X-ray diffraction is inaccurate in locating hydrogen atoms in the vicinity of heavy elements. This may provide significant error in the values of M-H distances determined by X-ray.

also close to those observed for classical hydrides.[17] Some particular examples of β-agostic NSi-H···M compounds and their structural characteristics will be discussed below.

Since the M-Si contact may be accurately determined by X-ray crystallography, it was initially suggested as a criterion to indicate the strength of OA of silane to the metal. Despite the fact that the M-Si distance varies significantly depending on the nature of the metal (especially on the size of the metal atom) and substituents at silicon, the value of this contact should undergo critical change upon silane complexation (compared to M-H and Si-H).[17] The nature of this phenomenon could be explained by the difference in the electronegativities of H and Si, which leads to the fact that the bonding σ(Si-H) orbital as well as the negative charge are mostly localized on the hydrogen end of the Si-H bond and the antibonding σ*(Si-H) orbital is more localized on the silicon atom.[36] Addition of silane to the metal fragment starts with initial interaction *via* hydrogen atom making the M-H distance somewhat similar to that one usually observed for hydride complexes.[17, 38] This interaction eventually brings the silicon atom in a closer proximity with the metal.[38] As mentioned above, the introduction of electronegative substituents at the silicon center increases the population of the antibonding σ*(Si-H) orbital (increased back-donation; Figure 3) and decreases direct donation from the bonding σ(Si-H) orbital to the metal (this orbital goes down in energy). Such a compensation of the Si-H bond weakening and the M-H bond strengthening should theoretically result in just minor changes of the Si-H and M-H contacts. On the other hand, the value of the M-Si distance should be considerably dependant on the strength of silane addition.[17, 29] This prediction is, however, complicated by the fact that in classical silyl complexes the M-Si distance is also affected by the substitution at the silicon and by steric factors. Thus, the correct structural assignment for the presence of Si-H interactions requires a proper choice of a reference classical silyl system.

Another structural criterion that is often used to determine the presence of Si-H complexation in β-agostic Si-H···M complexes is the reduced M-X-Si angle (X = CH_2, N, etc.).[14, 15, 45] However, since this parameter is strongly affected by the steric repulsions in the coordination sphere of metal, the appropriate choice of a reference system is required.

II.1.3 Spectroscopic features of Si-H···M agostic and silane σ-complexes

Apart from structural studies, the presence of nonclassical Si-H interactions can be also identified using IR and NMR analysis.[17, 29, 38] The general feature of the majority of compounds with Si-H σ-complexation is a characteristic high-field shift of the Si-H proton signal in ^{1}H-NMR spectra. Depending on the strength of the residual Si-H interaction, the silicon bound proton can be found in the typical Si-H region (if the Si-H interaction is strong, which is the case of d^0 complexes without back-donation) or close to the hydride region (for stretched Si-H bonding in d^n ($n \geq 1$) complexes with significant back-donation). However, the nature of this phenomenon is not fully understood.[17]

Another feature characteristic for Si-H···M agostic and silane σ-complexes is the observation of reduced (relatively to silanes) coupling constant between the silicon and hydrogen atoms. As was mentioned above, in 1982 Corriu *et al.* discovered[32] that coordination of silanes to transition metals leads to the observation of $^1J_{Si\text{-}H}$ values intermediate between those found for hydride silyl species (3-10 Hz)[38] and free silanes (about 200 Hz). Later, in 1990 Schubert suggested an approximate limit for the $^1J_{Si\text{-}H}$ in silane complexes of 10-20 Hz. Values below this threshold were postulated to signify the absence of any significant Si-H bonding.[38] However, similarly to the structural criteria discussed above, the observed $^1J_{Si\text{-}H}$ are highly affected by the nature of substituents at the silicon atom. Thus, several independent studies of a series of complexes **II-13** revealed that introduction of electronegative substituents at silicon leads to more advanced OA of coordinated silanes.[29, 38, 46, 47] For example, the compound $CpMn(HSiCl_3)(CO)_2$ was found to be close to the Mn(III) limit than to Mn(I) complex.[46b,d,c] In contrast, the observed $^1J_{Si\text{-}H}$ of 55 Hz in the related $Cp'Mn(HSiCl_3)(CO)_2$[47b] is close to the range for nonclassical Si-H complexes **II-13** (63-69 Hz)[29, 38] and is much larger than the Schubert's criterion (20 Hz).[38] This confusing influence of substituents at silicon can be explained by Bent's rule, which states that *more electronegative substituents prefer hybrid orbitals having less s character, and more electropositive substituents prefer hybrid orbitals having more s character.*[48, 49] In accordance with Bent's rule, the introduction of more electronegative substituents in hydrosilanes brings more Si 3s character to the bond with the hydride.[50] At the same time, the presence of electron-withdrawing groups at silicon lowers the energies of both σ(Si-

H) bonding and σ*(Si-H) antibonding orbitals decreasing the donation and increasing the back-donation from the metal centre.[17] In this situation, a weak silane donation compensates strong metal back-donation and leads to the formation of a complex with nonclassical Si-H interaction. Since the value of the coupling constant between two elements X and Y mostly depends on the s character of the X-Y bond, the introduction of electron-withdrawing groups at Si in $HSiR_3$ increases the value of $^1J_{Si-H}$ in free silane (370 Hz for $HSiCl_3$ *vs.* < 200 Hz for $HSiR_3$, where R = alkyl, aryl).[17] Similar trends could be also found for silane complexes, indicating that the rather large $^1J_{Si-H}$ of 55 Hz in $Cp'Mn(HSiCl_3)(CO)_2$ is the result of relatively large Si 3s character in the residual Si-H bond, rather than a strong Si-H interaction.

The additional information about the presence and the strength of residual Si-H bonding in agostic and silane complexes is also provided by the sign of the observed J_{Si-H},[17, 46e] which can be viewed as a result of combination of one-bond (Si-H) and two-bonds (Si-M-H) interactions: $^{obs}J_{H-Si} = {}^1J_{H-Si} + {}^2J_{H-Si}$.[17] Since $^1J_{H-Si}$ is known to be negative and in many cases $^2J_{H-Si}$ are found to be positive, the relative signs and magnitudes of these constants will determine the sign and the magnitude of $^{obs}J_{H-Si}$.[51] Thus, the observation of a negative value for $^{obs}J_{H-Si}$ indicates the dominance of $^1J_{H-Si}$ over $^2J_{H-Si}$ and serves as an additional argument for the presence of nonclassical Si-H bonding.

Not quantitative, but qualitative analysis of Si-H···M agostic and silane σ-complexes is provided by IR spectroscopy. Analogously to dihydrogen bonding M-H···H-A,[52] complexation of the Si-H bond to transition metal causes significant shift of the Si-H stretch[53] to longer wavelengths, which can be used for identification of silane agostic and σ-complexes. For the majority of compounds with significant Si-H bond activation, the M-H and Si-H vibrations are strongly coupled and the stretch is often observed in a typical hydride region.[45d,e] However, the origin of this phenomenon has not been clearly established and in some cases the band is found even below the usual M-H region.[17]

In conclusion, both structural (Si-H, M-H, and M-Si distances, as well as M-X-Si angles in β-agostic Si-H compounds) and spectroscopic (J_{Si-H}, and SiH chemical shift in ^{1}H-NMR, as well as ν_{Si-H} in IR) criteria for the presence and strength of the Si-H complexation should be used with caution and a careful choice of a reference system should be made.[17] A justified conclusion for the presence of nonclassical Si-H

interactions can only be made using a combination of several independent structural (X-Ray, ND), spectroscopic (NMR, IR, etc.), and computational methods.

II.1.4 Recent advances in the chemistry of β-agostic NSi-H···M complexes

β-Agostic Si-H···M complexes are probably the most studied class of Si-H agostic transition metal compounds. Such interactions are known for carbon, phosphorus, and nitrogen bridging atoms.[17] Most β-agostic Si-H···M complexes exhibit $^{1}J_{Si\text{-}H} > 100$ Hz, which is intermediate between the values normally observed in silane σ-complexes (range 40-80 Hz)[17, 29, 38] and free silanes (180-200 Hz).[54] The M-Si and M-H distances in the majority of known Si-H β-agostic compounds are close to those found in classical silyl and hydride species,[38] whereas the Si-H bonds appear to be somewhat shorter than in silane σ-complexes. Since this thesis covers only β-agostic Si-H···M bonding in silylamido complexes, only compounds with the nitrogen bridge will be discussed below.

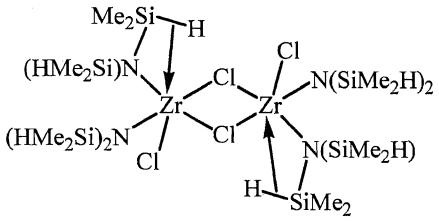

II-15

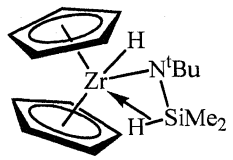

II-16

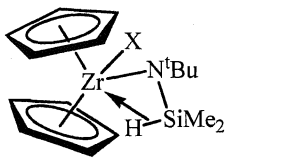

X = Cl, Br, I, F

II-17

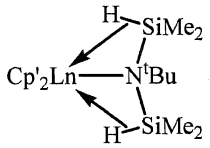

II-18

Figure 5. Zirconium (**II-15** – **II-17**) and lanthanide (**II-18**) β-agostic silylamido complexes.

Historically, the majority of known β-agostic NSi-H···M compounds have been prepared by the substitution of readily displaced leaving groups (such as halogens) with silylated amines $(HR_2Si)(R')NH$ or amides $(HR_2Si)(R')NLi$.[17] For the first time, this type of agostic interaction was observed for the dinuclear zirconium complex **II-15** (Figure 5).[45d] In **II-15** the complexation of the Si-H bond of one of silylamido substituents to

Table 1. Selected IR and NMR data for **II-16**, **II-17** and $Me_2HSi\text{-}NH^tBu$

Compound	IR	^{1}H-NMR	^{29}Si-NMR	
	ν(SiH), cm^{-1}	δ, ppm	δ, ppm	$J_{Si\text{-}H}$, Hz
$Cp_2Zr(H)(\eta^3\text{-}HSiMe_2N^tBu)$	1912	1.21	-73.4	113.2
$Cp_2Zr(I)(\eta^3\text{-}HSiMe_2N^tBu)$	1960	1.69	-62.0	118.7
$Cp_2Zr(Br)(\eta^3\text{-}HSiMe_2N^tBu)$	1975	2.24	-56.1	123.2
$Cp_2Zr(Cl)(\eta^3\text{-}HSiMe_2N^tBu)$	1981	2.58	-52.3	126.5
$Cp_2Zr(F)(\eta^3\text{-}HSiMe_2N^tBu)$	1998	2.84	-42.0	135.4
$Me_2HSi\text{-}NH^tBu$	2107	4.83	-18.3	192.6

zirconium results in significantly reduced Zr-N-Si angle (102.8(2)° *vs.* 129.5(1), 117.2(2), and 126.9(2)° for three others Zr-N-Si angles). This distortion brings the silicon atom closer to the metal so that the Zr-Si distance in **II-15** comes close to a normal Zr-Si bond (2.943(1) Å *vs.* 2.654(1)-2.815(1) Å for silyl substituted zirconium compounds). However, the rather long Zr-H contact of 2.40(3) Å and the normal Si-H distance (1.45(2) Å) suggest only weak coordination of the Si-H bond.[45d] Additional proof for the Si-H coordination in **II-15** is the observation of a characteristic red shift of the Si-H stretch in IR spectrum, which was found at 1948 cm^{-1}, whereas the normal range for the noncoordinated Si-H bond is 2080-2280 cm^{-1}.[17]

Berry *et al.* thoroughly investigated agostic interactions in the system $Cp_2Zr(H)(\eta^3\text{-}N^tBu\text{-}SiMe_2\text{-}H)$ (**II-16**; Figure 5), which was prepared by the treatment of $[CpZrHCl]_n$ with $LiN^tBuSiMe_2H$.[45e] Further exchange of the hydride ligand in **II-16** for halogens allowed for systematic investigation of the effect of halide substituents on the extent of Si-H···Zr bonding (Figure 6). As shown in Table 1, the Si*H* resonances of **II-16** and $Cp_2Zr(X)(\eta^3\text{-}N^tBu\text{-}SiMe_2\text{-}H)$ (**II-17**; X =F, Cl, Br, I) are shifted from the typical Si*H* region (~ 3.5-5.0 ppm) in the ^{1}H-NMR spectra and undergo significant high-field shift indicating a considerable perturbation of the Si-H environment.[17, 29, 38] Furthermore, the presence of Si-H complexation in **II-16** is also evident from the observation of a doublet for the hydride signal at 5.53 ppm ($^2J_{H\text{-}H}$ = 3.1 Hz) due to coupling to the agostic Si*H* proton. A similar finding was made for the fluoride signal in the ^{19}F-NMR spectrum of $Cp_2Zr(F)(\eta^3\text{-}N^tBu\text{-}SiMe_2\text{-}H)$ (**II-17$_F$**), which gives rise to a doublet at 15.72 ppm with $^2J_{F\text{-}H}$ = 8.1 Hz (the same coupling constant was found for the Si*H* signal in the ^{1}H-NMR

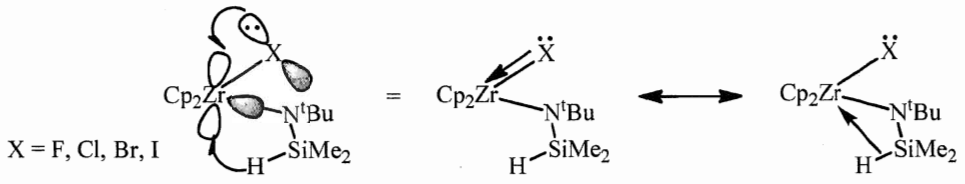

II-17

Figure 6. Effect of the nature of the substituent X in **II-17** on the NSi-H···Zr interaction.[45e]

spectrum of **II-17$_F$**). Since the coordination of the Si-H bond to the metal results in significant weakening of the bond,[17, 29, 38] the values of the $^1J_{Si-H}$ for **II-16** and **II-17** were found to be notably smaller than for Me_2HSi-NH^{t}Bu (113.2–135.4 Hz *vs.* 192.6 Hz, respectively). The IR data for **II-16** and **II-17**[45e] are also in a good agreement with the presence of nonclassical Si-H···Zr interactions[17] in these species (the red shift of Si-H stretches characteristic for Si-H complexation was observed for all cases; see Table 1). Comparison of the NMR and IR parameters for the series of **II-16** and **II-17** suggested that the strength of the agostic interaction between the Si-H σ-bond and the Zr center of $Cp_2Zr(X)(\eta^3$-N^{t}Bu-$SiMe_2$-H) is decreasing in order X = H > I > Br > Cl > F.[45e] In their manuscript Berry *et al.* also presented X-ray diffraction analyses for complex **II-16** and for its choloro-substituted analog $Cp_2Zr(Cl)(\eta^3$-N^{t}Bu-$SiMe_2$-H) (**II-17$_{Cl}$**). Both structures revealed relatively short Zr-Si contacts (2.857(2) Å and 2.931(1) Å for **II-16** and **II-17$_{Cl}$**, respectively) and small Zr-N-Si angles (93.9° and 99.1 °, respectively), suggesting the η^2-cordination of the Si-H bond to Zr.[45e] Additionally, the location of the amido group for both **II-16** and **II-17$_{Cl}$** appears to be near the center of the metallocene equatorial wedge, which is consistent with the Cp_2ML_3 coordination environment. For $Cp_2Zr(Cl)(\eta^3$-N^{t}Bu-$SiMe_2$-H) (**II-17$_{Cl}$**), the Si-H bond complexation leads to significant elongation of the Zr-Cl distance (2.523(1) Å), which was explained by the redistribution of the electron density around Zr. Thus, the σ-donation from the agostic Si-H bond leads to a more electron rich zirconium center, which should result in less π-donation from the chloride ligand to the metal making the Zr-Cl bond longer. Similar reasoning could be used to explain the trend for the strength of the NSi-H···Zr bonding in other halosubstituted complexes **II-17**.[45e] Taking into account the presence of a competing electron donation from the halide and the Si-H, it is clear that the strongest NSi-H···Zr interaction would be

observed for the weakest π-donor X (Figure 6). Within the series of halide derivatives **II-17**, the degree of nonclassical Si-H interaction is strongest in the case of iodide and weakest for fluoride,[45e] indicating that the fluoride is the best π-donor to zirconium and iodide is the weakest. The same trend was earlier observed for boron trihalides: the strong π-donation of the fluoride makes BF_3 the weakest Lewis acid for that series.[55]

A similar NSi-H···M agostic interaction was reported by Anwander *et al.* for a series of d^0 lanthanide silylamide complexes $Cp'_2Ln(N(SiMe_2H)_2)$ (**II-18**) (Ln – lanthanide metal, Cp' – substituted cyclopentadienyl, ansa-fluorenyl, and indenyl ligands).[45f-i] Depending on the steric hindrance of the Cp' groups and the metal size, the bis(dimethylsilyl)amide ligands in complexes **II-18** adopt various agostic coordination modes (Figure 7).[45i] In all cases, the presence of a NSi-H···Ln bond was established by a characteristic red shift in the Si-H absorptions (by ~200 – 300 cm^{-1}) in the IR spectra, a high-field shift of the SiH resonances and reduced $^1J_{Si-H}$ coupling constants (133 – 155 Hz *vs.* ~200 Hz for non-

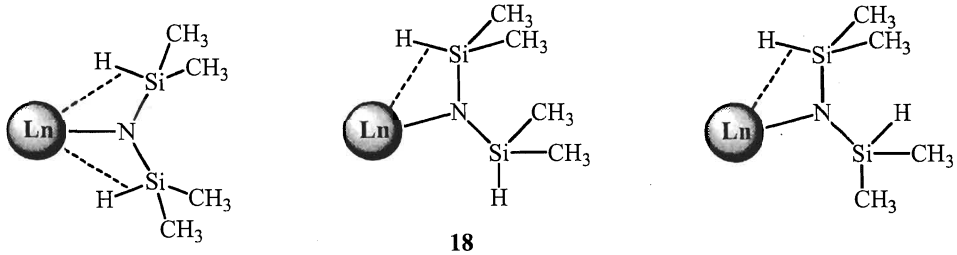

Figure 7. Agostic coordination modes for the bis(dimethylsilyl)amide ligand in **II-18**.

coordinated Si-H bond) in the ^{1}H-NMR spectra, and acute M-N-Si bond angles (down to 98 (1)°) from the X-ray diffraction data. Furthermore, for the bis(agostic) coordination mode (Figure 7, **a**) large values of Si-N-Si bond angles (as large as 160.1(2)°) were observed.[45i] Based on spectroscopic and structural data, Anwander *et al.* concluded that for system **II-18** smaller metals have a stronger interaction with the Si-H bond.[45f-i] Almost at the same time, Schumann *et al.* described similar polyagostic Si-H interactions for the erbium tris(disilyl)amido complex $Er[N(SiMe_3)(SiMe_2H)]_3$ (**II-19**) on the basis of IR and X-ray evidence.[45j]

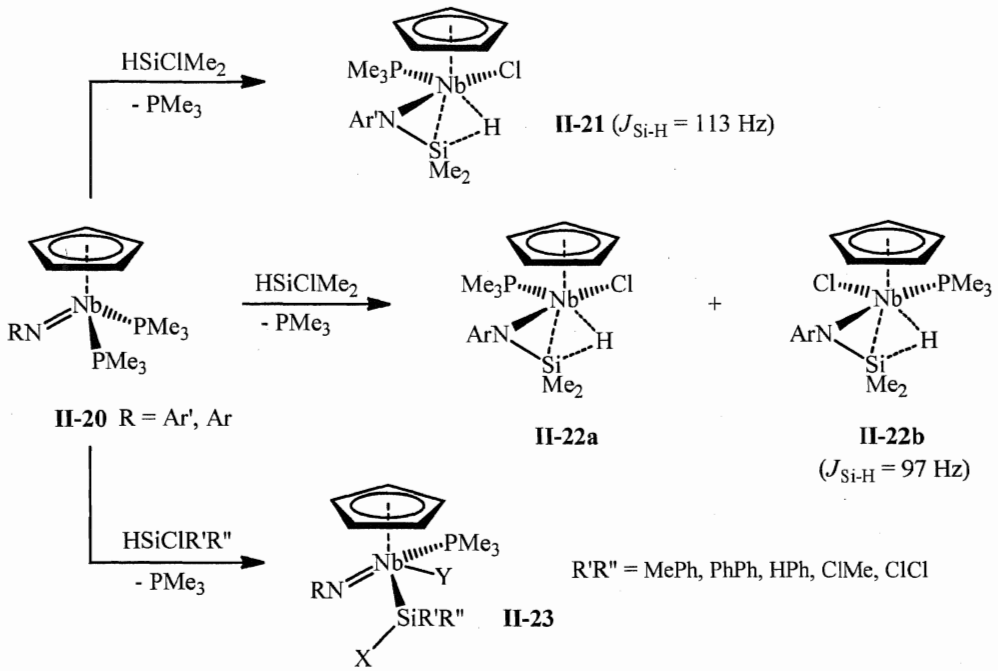

Scheme 5. Preparation of agostic silylamides **II-21**, **II-22** and silyl derivatives **II-23**.[14]

Recently, a novel way for the preparation of silylamido β-agostic transition metal complexes was discovered in our group. This approach is based on the direct coupling reaction between an imido $(RN)^{2-}$ ligand of the complex and chlorohydrosilanes.[14, 15, 17] Thus, half-sandwich niobium agostic silylamides CpNb(Cl)(η^3-NR-SiMe$_2$-H)(PMe$_3$) (R = Ar' (**II-21**) and Ar (**II-22a,b**)) were synthesized by the treatment of the corresponding imido precursors CpNb(NR)(PMe$_3$)$_2$ **II-20** with dimethylchlorosilane (Scheme 5).[14] The formation of a mixture of isomers for complex **II-22** was explained in terms of steric repulsions between the bulky 2,6-diisopropylphenyl group and the phosphine ligand. For Ar' the repulsion is smaller, and PMe$_3$ can be accommodated *trans-* to the Si-H bond, resulting in a weaker Si-H bond activation ($^1J_{Si-H}$ = 113 Hz for **II-21** vs. $^1J_{Si-H}$ = 97 Hz for **II-22b**). On the basis of combined experimental and theoretical studies, Nikonov *et al.* suggested a possible mechanism for this reaction (Scheme 6), which involves direct coupling of silane with the imido moiety. The reaction is highly dependent on the substitution at silicon and imido nitrogen. Changing the sterics and the acidity of the silane leads to migration of the silyl group from the imido nitrogen to the metal affording imido silyl derivatives CpNb(NR)(SiR'R"X)(Y)(PMe$_3$) (**II-23**, R = Ar', Ar; X = Cl, H; Y = Cl, H; R'R" = MePh, PhPh, HPh, ClMe, ClCl; Scheme 1).[14] Analogous reactions of the

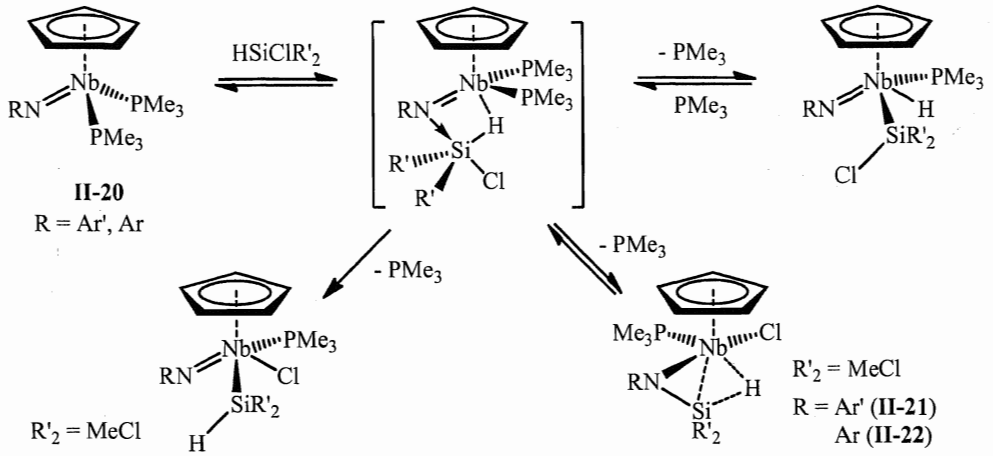

Scheme 6. Suggested mechanism for the reaction of **II-20** with $HSiClR'_2$.

tantalum compound $CpTa(NAr)(PMe_3)_2$ (**II-24**) with chlorosilanes $HSiMe_nCl_{3-n}$ (n = 0 - 2) also do not afford β-agostic species; the silylhydride complexes $CpTa(NAr)(H)(SiX_2Cl)(PMe_3)$ (**II-25**, X = Me, Cl; Scheme 7) are formed instead.[14h]

Agostic complexes **II-21** and **II-22** present the first examples of compounds with stretched β-agostic Si-H···M interactions.[17] Similarly to the systems described above, the presence of the Si-H···Nb bonding was established from spectroscopic features of **II-21** and **II-22**, X-ray diffraction analysis of **II-21** and **II-22a**, and DFT calculations of model complexes. Both **II-21** and **II-22** exhibit characteristic red shift of the Si-H stretches in the IR spectra, high-field shift of Si*H* resonances and reduced $^1J_{Si\text{-}H}$ coupling in the ^{1}H-NMR spectra. The values of these parameters were found to be smaller than normally

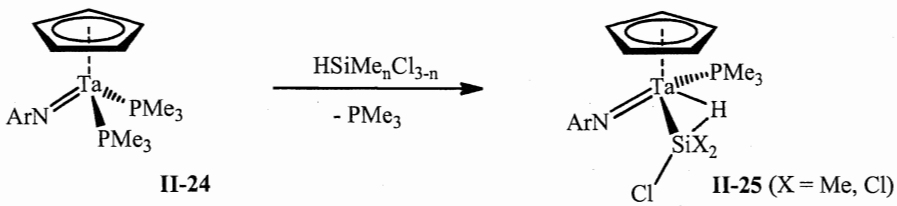

Scheme 7. Reaction of **II-24** with $HSiMe_nCl_{3-n}$ (n = 0 – 2).

detected for d^0 β-agostic silylamides **II-15** – **II-19**,[45d-j] which can be accounted for stronger Si-H bond activation due to partial back-donation from the d^2 niobium center.[48] This leads to a more advanced OA of the Si-H bond to the metal and results in a greater high-field shift of the Si*H* resonances (-3.76 ppm and -3.41 ppm for **II-22b** and **II-21**,

respectively), smaller $^1J_{Si-H}$ constants (113 Hz for **II-21** and 97 Hz for **II-22a**), and longer Si-H bonds (1.52(5) Å for **II-22a** *vs.* 1.45(2) Å for **II-15**).[14, 17]

Imido/silane coupling was later extended to the bis(imido) molybdenum chemistry. In 2004, Nikonov *et al.* reported reactions of the Mo(IV) complex $(Ar'N)_2Mo(PMe_3)_3$ (**II-26**), isolobal to **II-20**, with HSiCl(Me)R (R = Me, Cl) which lead to the formation of the β-agostic imido silylamides $(Ar'N)Mo(Cl)(\eta^3\text{-}NAr'\text{-}Si(Me)R\text{-}H)(PMe_3)_2$ (R = Me (**II-27**), Cl (**II-28**); Scheme 8).[15] The presence of NSi-H···Mo agostic bonding was suggested from the observation of reduced $^1J_{Si-H}$ values (97 Hz for **II-27** and 129 Hz for **II-28**) and was further supported by X-ray structure analyses. The analogous treatment of **II-26** with more acidic $HSiCl_3$ leads to the double Si-Cl bond activation and formation of the dichloride derivative $(Ar'N)MoCl_2(PMe_3)_3$ (**II-29**) and the silanimine dimer $(Ar'N\text{-}SiHCl)_2$ (Scheme 8).[15] The detailed mechanistic studies of this reaction will be discussed in the course of this thesis.

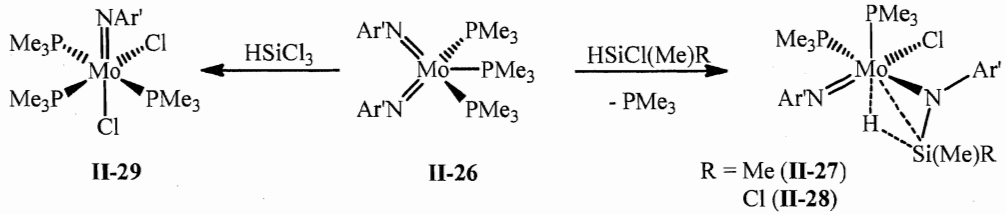

II-29 **II-26** R = Me (**II-27**) Cl (**II-28**)

Scheme 8. Reactivity of $(Ar'N)Mo(PMe_3)_3$ (**II-26**) towards chlorohydrosilanes.

One could expect that substitution at the silicon center with more electronegative groups should result in more advanced OA of the Si-H agostic bond to the metal.[29, 38] However, the observation of a larger $^1J_{Si-H}$ of 129 Hz for complex **II-28** compared to **II-27** (97 Hz) contradicts this common expectation. The X-ray diffraction analysis for both complexes **II-27** and **II-28** revealed no effect of the substitution at silicon on the values of M-H and Si-H distances. However, the Mo-Si bond (2.657(1) Å) in **II-28** appears to be somewhat shorter than in **II-27** (2.668(1) Å), suggesting stronger Si-H bond activation for the chloromethylsilyl group.[15] DFT calculations of a series of model complexes $(MeN)Mo(Cl)(\eta^3\text{-}NMe\text{-}SiMe_nCl_{2-n}\text{-}H)(PMe_3)_2$ (**II-30**, n = 0 – 2) showed that the substitution at the silicon center with Cl leads to weaker OA of the Si-H bond.[15] These unexpected results were rationalized in terms of a revised DCD diagram taking in account the effects of substituents (see above).[17] According to Bent's rule,[48, 49] introduction of

electron-withdrawing Cl groups at a silicon centre provides more Si 3s character in the Si-H bond. This leads to decrease of the donation component in the DCD scheme (Figure 3) and increase in the value of the Si-H coupling constant. On the other hand, substitution with Cl increases Lewis acidity of the Si atom making the Mo→σ*(Si-H) back-donation stronger.[17] Since σ(Si-H) is more localized on the hydrogen atom and σ*(Si-H) has a larger contribution from Si, these changes result in the shortening of the Mo-Si bond and elongation of the Mo-H bond.[15]

Formation of **II-29** and $(Ar'N\text{-}SiHCl)_2$ in the reaction of **II-26** with $HSiCl_3$ can be explained by the strengthening of the Si-H bond upon increased Cl substitution at silicon. Thus, DFT calculations, reported by Nikonov *et al.* for the model system $(MeN)Mo(Cl)(\eta^3\text{-}NMe\text{-}SiHCl\text{-}Cl)(PMe_3)_2$ (**II-31b**) gave an energy of only *ca.* 1 kcal above that of agostic compound **II-31a** (Figure 8).[15] Further *β*-Cl elimination from **II-31b** would lead to the formation of dichloride complex and silanimine dimer.

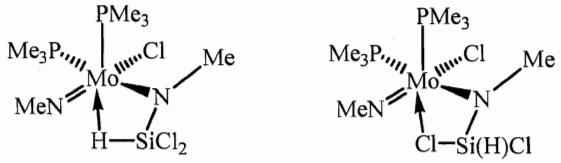

II-31a **II-31b**

Figure 8. DFT model for the formation of complex **II-29** and $(Ar'N\text{-}SiHCl)_2$.[15]

Some examples of the reaction of silanes and an imido moiety of TM complexes have also been reported by groups of Tilley[16] and Fryzuk.[56] The imido/amido compound $Cp^*Ta(X)[L(SiMe_3)]$ (**II-32**, X = Me, Cl) undergoes an exchange with $PhSiH_3$ *via* the

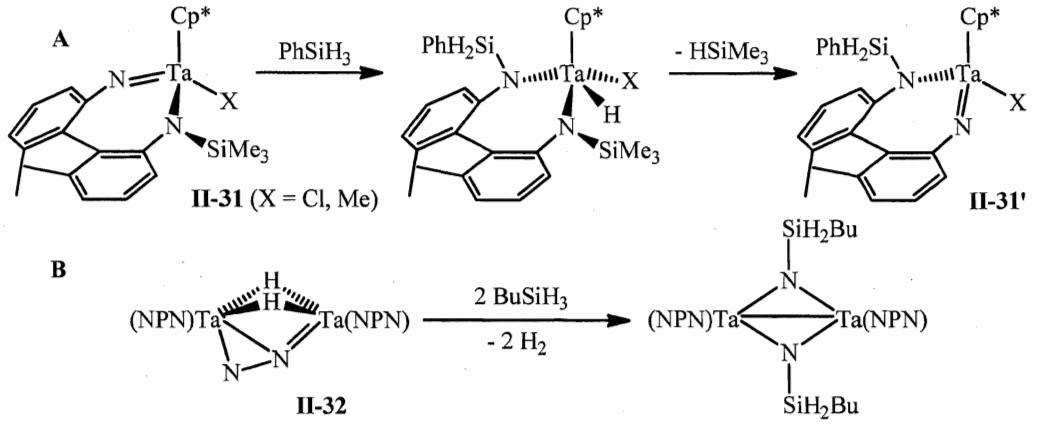

Scheme 9. Reactions **II-31** (A) and **II-32** (B) with hydrosilanes.[16, 56]

imido/silane coupling route (Scheme 9, **A**).[16] In 2003, Fryzuk *et al.* demonstrated the hydrosilation of the dinitrogen tantalum complex ([NPN]Ta)$_2$(μ-H)$_2$(μ-η^1:η^2-N$_2$) (**II-32**, NPN = (PhNSiMe$_2$CH$_2$)$_2$PPh; Scheme 9, **B**), which also proceeds via the addition of BuSiH$_3$ to the Ta=N bond.[56]

II.2 Homogeneous hydrosilation of unsaturated organic molecules

The term *hydrosilation* (or *hydrosilylation*) refers to the addition of silicon hydrides (usually organosilanes R_3SiH) across multiple bonds. Nowadays, the hydrosilation process is known for carbon-carbon, carbon-heteroatom (i.e. carbon-oxygen, carbon-nitrogen, and carbon sulphur), and heteroatom-heteroatom (such as nitrogen-nitrogen and nitrogen-oxygen) bonds (Scheme 10).[7] Taking into account the high energy of the Si-H bond in R_3SiH (for example: 74.6 kcal/mol for R = Me, 96.8 kcal/mol for R = OEt, and 100 kcal/mol for R = F),[29] the activation of silanes usually requires harsh conditions, such as elevated temperatures (> 250°C), UV irradiation, and/or free-radicals generation.[7] The first example of a hydrosilation process, namely the reaction of 1-octene with $HSiCl_3$ in the presence of acetyl peroxide, appeared in the literature in 1947.[57] However, the era of homogeneous catalytic hydrosilation began only decade later, with a discovery by Speier from Dow Corning Co. in 1957 of $H_2[PtCl_6]$ (**II-33**) as an efficient precursor to the Pt-catalyst.[58] As a result, it ultimately replaced all previous systems, considerably extending the synthetic possibilities of catalytic hydrosilation.[7] Since then this field has grown rapidly and to-date, the majority of known laboratory and industrial hydrosilation reactions employ transition metal catalysis. This part of the literature review describes the general mechanistic aspects of the transition metal catalyzed hydrosilation of the main classes of unsaturated organic molecules (alkenes, alkynes, carbonyls, imines, nitriles, and pyridines), alcoholysis and aminolysis of silanes, as well as recent advances in early transition metal hydrosilation catalysis.

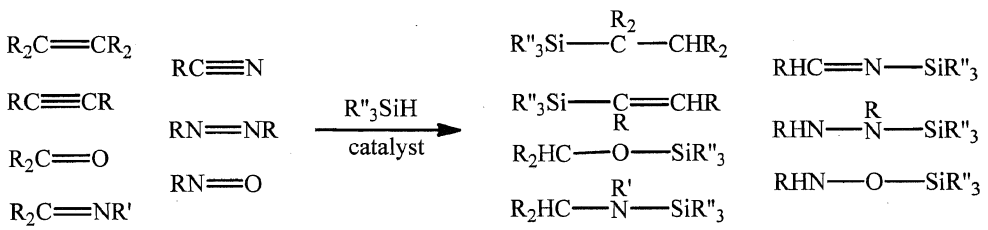

Scheme 10. Diversity of catalytic hydrosilation of unsaturated organic molecules.

II.2.1 Mechanisms of TM catalyzed hydrosilation of alkenes

The catalytic addition of silicon hydrides to alkenes, arylalkenes, and cycloalkenes, as well as their derivatives with functional groups, leads to corresponding alkyl derivatives of silicon and occurs with anti-Markovnikov regioselectivity.[7] However, under some conditions (e. g. in the presence of Pd catalysts) the anti-Markovnikov product is accompanied by an α-adduct, i. e. the one containing an internal silyl group. The mechanism catalytic processes strongly depends on the type of catalyst. While platinum and other late transition metal complexes are believed to catalyze the hydrosilation of carbon-carbon bond via oxidative addition of silicon hydrides to metal, the hydrosilation catalyzed by early transition metal complexes often occurs *via* σ-bond metathesis, which does not include oxidative addition of the Si-H bond.[7]

Speier's discovery that homogeneous hydrosilation of olefins can be practically catalyzed by $H_2[PtCl_6]$ (**II-33**)[58] provoked extensive developments in this field.[7] Nowadays, the catalytic addition of hydrosilanes to alkenes is one of the most useful ways for the preparation of alkyl substituted silanes, which have found wide application in the silicon polymer industry as precursors to silicon rubbers, liquid injection molding products, paper release coatings, and pressure-sensitive adhesives.[59]

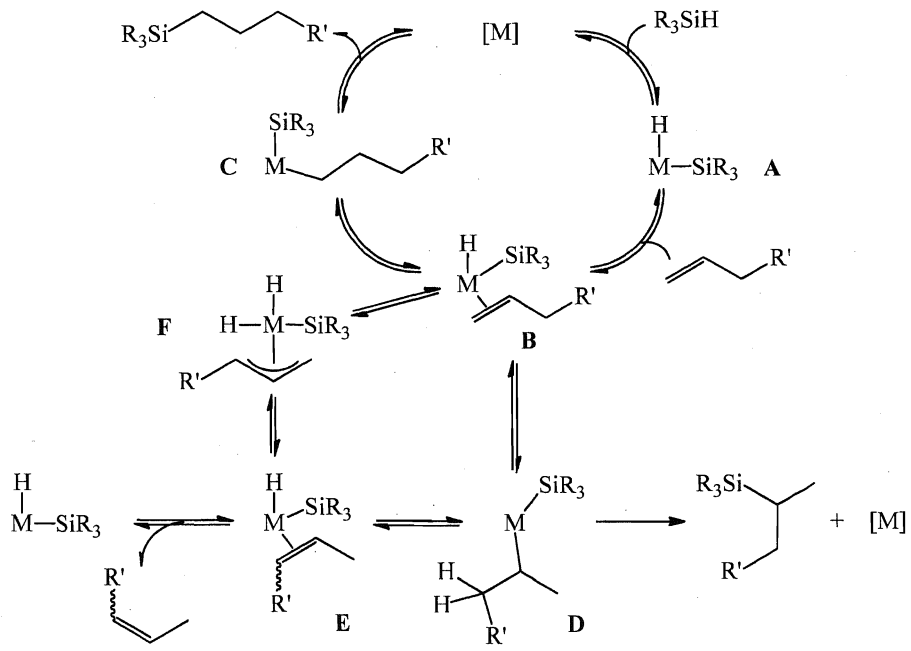

Scheme 11. Chalk-Harrod mechanism for TM mediated hydrosilation of alkenes.[10a]

Despite the large number of publications on catalytic hydrosilation over last 60 years, in no case has a proposed mechanism for this process been completely supported experimentally. The most common mechanism for the hydrosilation of alkenes is depicted in Scheme 11,[19e] the essential features of which were first postulated in 1965 by Chalk and Harrod.[10a] This mechanism, originally derived from the studies of chloroplatinic acid as a precursor (Pt-catalyst), for many years provided a qualitative rationale catalysis by other transition metal complexes.[7] This mechanistic scheme presents the conventional sequence of oxidative addition – reductive elimination steps: the OA of silanes R_3SiH to a metal, coordination of alkene, migratory insertion of olefin into the M-H bond, followed by reduction elimination of Si-C bond from resulting silyl/alkyl derivative regenerates the starting metal complex (Scheme 11). Initially, the Chalk-Harrod mechanism was based only on experimental evidence. Later, a detailed theoretical study of the $Pt(PH_3)_2$-catalyzed hydrosilation of ethylene[60] supported this suggestion. The reversibility of all steps was established by conducting numerous deuterium labelled experiments.[61] For instance, the reaction of $DSiCl_3$ with isobutene mediated by **II-33** resulted in almost statistical scrambling of the deuterium over all carbon atoms in the product and on the silicon atom (Scheme 12, **A**).[61] The possibility of double bond migration was suggested based on the hydrosilation of 4-methylcyclohexene (Scheme 12, **B**) and 1-hexene, in which the formation of silyl substituted derivatives of isomerized substrates was observed.[61] Furthermore, for the reaction of 1-hexene with

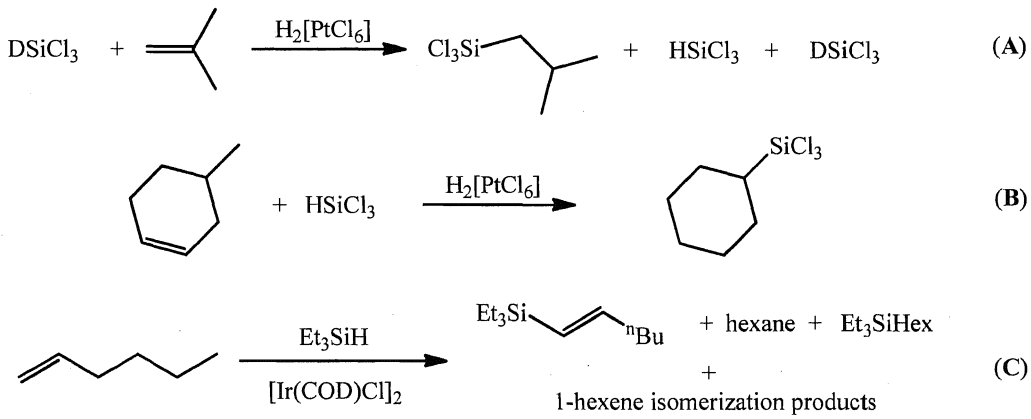

Scheme 12. Experimental evidence in favour (**A**, **B**) and against (**C**) Chalk-Harrod mechanism.

Et_3SiH almost complete conversion of the substrate to internal olefins was found after only 10 % of hydrosilation.[62] The isomerization of alkene substrates, concurrent with hydrosilation, could be explained by π-σ reversible rearrangement (Scheme 11, route from **B** to **E**) and/or by the formation of a π-allyl complex (Scheme 6, **F**).[7]

Careful screening of alkene substrates allowed for further conclusions on the mechanistic aspects of the hydrosilation process, which are the following: (i) addition of silyl group is preferred at terminal olefin positions over internal positions;[61, 62] (ii) addition of the silicon and hydrogen atoms to the double C=C bond is *cis*;[63] (iii) OA of silane to the metal and overall process of hydrosilation proceeds with the retention of configuration at silicon.[64, 65]

For a variety of transition metal catalysts, the experimental evidence supports the steps in the proposed by Chalk and Harrod mechanism (Scheme 11), however, in no case were all these key steps observed on a single metal center.[10b-d, 66] Furthermore, the original Chalk-Harrod scheme does not explain the formation of vinylsilanes and alkanes as well as other side-reactions (such as redistribution of silanes, etc.) often observed in catalytic hydrosilation of alkenes. For instance, the $[Ir(COD)Cl]_2$ (**II-34**) catalyzed reaction of

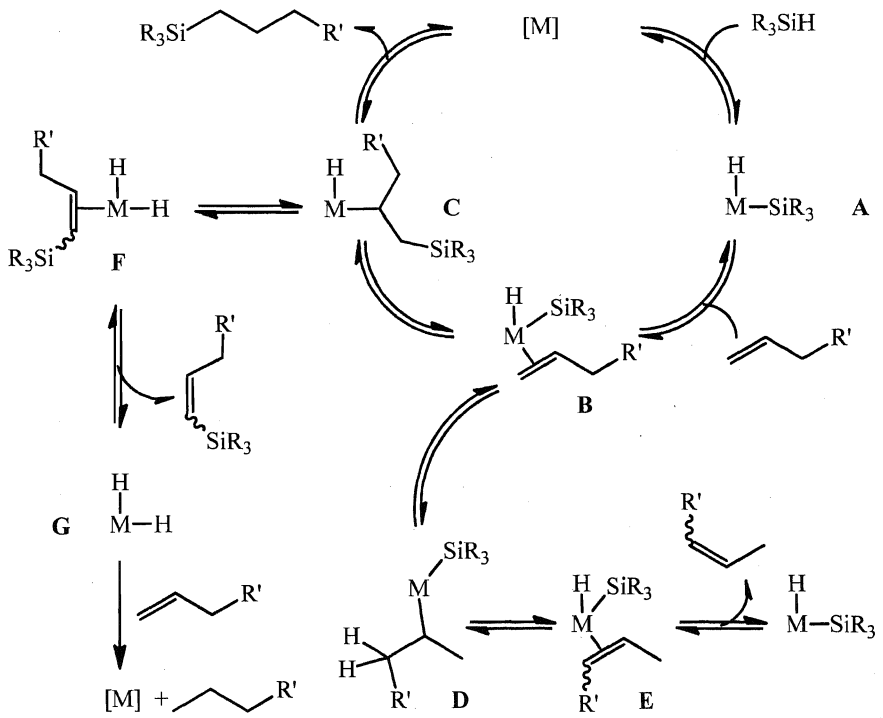

Scheme 13. Modified Chalk-Harrod mechanism for TM mediated hydrosilation.

1-hexene with Et_3SiH generates almost 50 % of vinylsilane in addition to the hydrosilation product and isomerized alkenes (Scheme 12, **C**). This unexpected result was explained by a modified Chalk-Harrod mechanism, which includes olefin insertion into the M-Si bond (silyl migration pathway; Scheme 13, **B** → **C**), followed by well-established in organometallic chemistry C-H bond reductive elimination.[c, 67] The silyl migration route can account for all other features of the original Chalk-Harrod scheme, as well as offers a ready explanation for the appearance of vinylsilanes, which presumably form *via* the β-C-H bond activation in the silylated alkyl substituent (Scheme 13, **C** → **F**). The dihydride species **G**, forming during this transformation, can hydrogenate the olefin substrates, affording corresponding alkanes.[68]

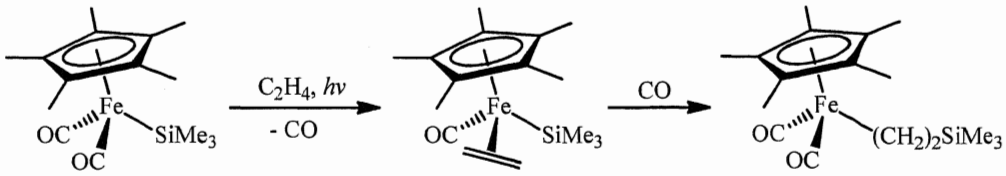

II-35 **II-36** **II-37**

Scheme 14. Insertion of ethylene into the Fe-Si bond of $Cp^*Fe(SiMe_3)(CO)_2$ (**II-35**).

Additional support for the modified Chalk-Harrod mechanism was obtained by direct observation of silyl migration to olefin in the stoichiometric reaction between $Cp^*Fe(SiMe_3)(CO)_2$ (**II-35**) and ethylene outlined in Scheme 14. After pre-coordination of C_2H_4 to form the complex $Cp^*Fe(SiMe_3)(CO)(\eta^2\text{-}CH_2{=}CH_2)$ (**II-36**), migration occurs at 25 °C with the formation of $Cp^*Fe[(CH_2)_2SiMe_3](CO)_2$ (**II-37**). The latter affords 65 % of vinylsilane and 15 % of **II-36** upon irradiation.[69] A few more examples of olefin insertion into the M-Si bond appeared later,[70] however, the demonstration that this key step is possible for a particular stoichiometric reaction does not necessarily imply that it occurs in catalysis, since the probability of steps in a catalytic cycle always depends on their relative rates.

The redistribution reactions at the silicon atom catalyzed by transition metal complexes were reviewed by Curtis and Epstein in 1981,[71] while those observed under the hydrosilation conditions were discussed by Speier in 1979.[72] The main types of silane

[c] The original Chalk-Harrod cycle (Scheme 11) involves reductive elimination of the Si-C bond, which is also known in stoichiometric organometallic chemistry, but less common than C-H reductive elimination. For example, see refs. 19e and 66.

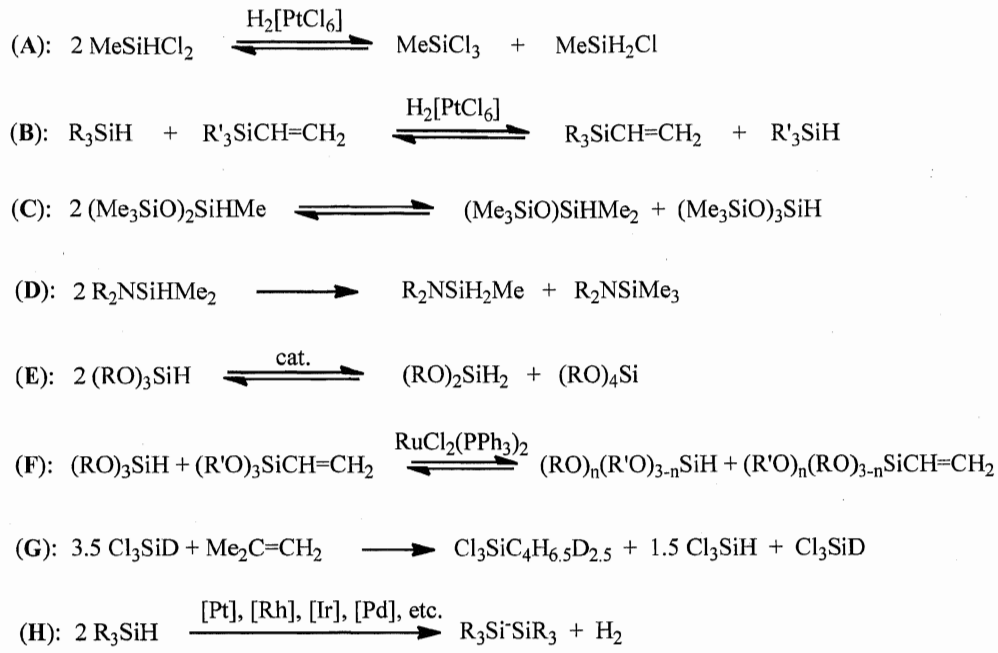

Scheme 15. Classification of silane redistribution side-reactions in the hydrosilation catalysis.

redistribution reactions leading to the formation of by-products in hydrosilation are summarized in Scheme 15. They can be classified as: H/Cl (**A**), vinyl/H (**B**), Me_3SiO/Me (**C**), Me/H (**D**), H/OR (**E**), RO/R'O (**G**), H/D (**H**), and SiR_3/H (**F**) exchange processes. Some of these reactions may be initiated by homolysis or by catalytic activation, or even by conventional acid or base catalysis, but a few occur more readily in the presence of olefins.[7a] Furthermore, the silane redistribution products may also participate in hydrosilation, leading to even larger number of by-products. The majority of transition metal catalyzed silane redistribution reactions occur when at least one Si-H bond is present in the molecule[71, 72] and, depending on the oxidation state of the metal, require a series of silane oxidative addition reduction and elimination sequences (Scheme 16).

The hydrosilation of olefins catalyzed by transition metal complex can be also accompanied by other side-reactions, such as reduction of organic compounds (this is particularly observed in the reduction of allyl acetate and halides to propene)[7a] and metathesis processes (for instance, the evalution of ethylene in the Ru-catalyzed hydrosilation of vinyltrialkoxysilanes points to a competitive metathesis process).[73]

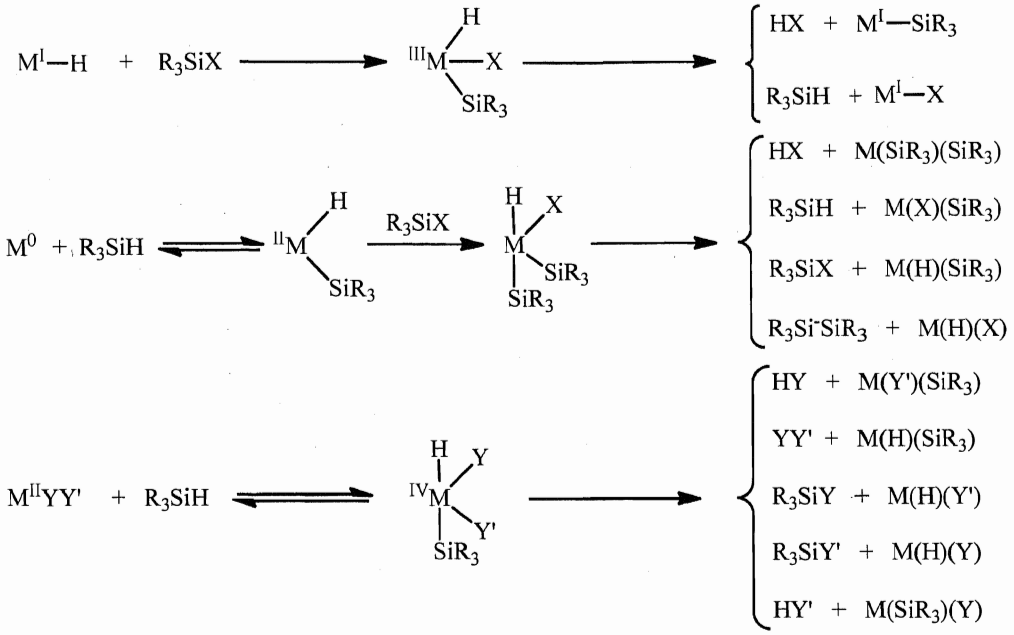

Scheme 16. OA – RE sequences for the catalytic redistribution of silanes.

The discovery of the Chalk-Harrod type mechanisms for the hydrosilation of olefins (Schemes 11 and 13) stimulated research in this field, and several other mechanistic studies of hydrosilation reactions appeared in the literature in the late 1980s – early 1990s.[7, 19d, 74] Thus, in 1988, Seitz and Wrighton reported the study of photochemically initiated hydrosilation of alkenes mediated by the cobalt silyl complex $Co(CO)_4(SiMe_3)$ (**II-38**).[74] The cycle proposed in this work (Scheme 17) incorporated silyl migration to the olefin and alkylsilane reductive elimination steps, but did not involve the formation of

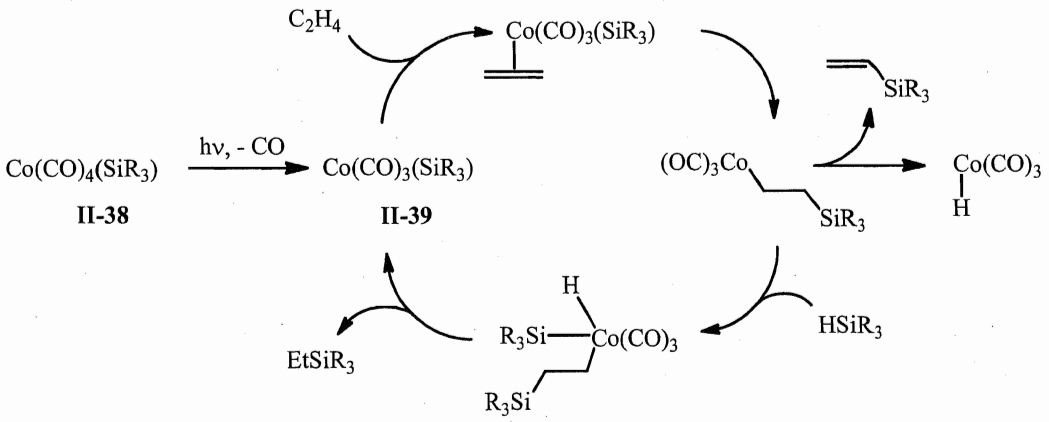

Scheme 17. Seitz-Wrighton mechanism for the hydrosilation and dehydrogenative silation of alkenes.

a metal alkene silylhydride intermediate. The suggested catalytic scheme includes a photochemical initiation step *via* the dissociation of CO, followed by coordination of ethylene. The intramolecular insertion of a C_2H_4 molecule into the Co-Si bond and oxidative addition of silane results in the formation of the silyl(alkyl) silylhydride species **II-39**, which undergoes reductive elimination of $EtSiMe_3$ recovering the catalyst.[74]

In 1985, Perutz *et al.* reported for the first time the isolation and characterization of the rhodium ethylene silylhydride derivative $CpRh(\eta^2\text{-}CH_2{=}CH_2)(SiR_3)(H)$ (**II-40**; R = Me, Et) prepared by photolysis of $CpRh(\eta^2\text{-}CH_2{=}CH_2)_2$ (**II-41**) in the presence of R_3SiH.[75] This molecule contains all the essential ligands for the key intermediate in the Chalk-Harrod catalytic scheme. Moreover, Perutz *et al.* showed that the formation of complex **II-40** at ambient temperature is accompanied by hydrosilation and silation products, however, the low temperature experiment proceeds without hydrosilation.[75b] Almost at the same time, a few other examples of ethylene silylhydride compounds appeared in the literature, but no detailed mechanistic investigations of their stoichiometric and catalytic reactivity were reported.[76] To shed more light on the mechanism of the hydrosilation process, Perutz *et al.* investigated the reactivity of complex **II-40** towards ethylene and

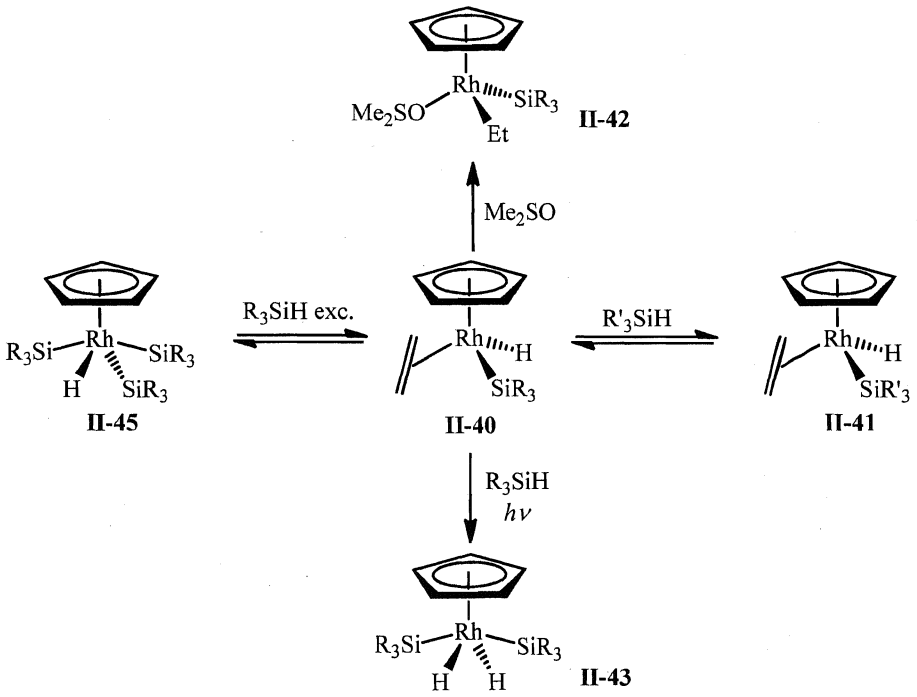

Scheme 18. Reaction pathways of $CpRh(\eta^2\text{-}CH_2{=}CH_2)(SiR_3)(H)$ (**II-40**).

various trialkylsilanes under stoichiometric and catalytic conditions.[19d, 77] The study of stoichiometric reactivity of **II-40** revealed three reaction pathways illustrated in Scheme 18: (i) trialkylsilane may be eliminated leading to silane exchange in the presence of another trialkylsilane, R'_3SiH; (ii) the hydride may reversibly migrate onto ethylene (this process leads to a slow exchange between the hydride and ethylene in **II-40** and upon addition of Me_2SO affords the ethyl derivative $CpRh(Et)(SiR_3)(OSMe_2)$ (**II-42**)); (ii) ethylene may be expelled by the treatment of **II-40** with R_3SiH giving the Rh(V) complex $CpRh(SiR_3)_2(H)_2$ (**II-43**) (the substitution of ethylene in **II-40** was also observed in the reaction with Me_2SO, which gives complex **II-42** in a mixture with $CpRh(SiR_3)(H)(OSMe_2)$ (**II-44**)). The hydride migration postulated for the formation of **II-42** also takes place upon treatment of **II-40** with excess R_3SiH, which was found to proceed *via* R_3SiEt elimination and formation of the tris(silyl) derivative $CpRh(SiR_3)_3(H)$ (**II-45**; Scheme 18). These observations together with various isotopic labelling experiments with C_2D_4 and R_3SiD, as well as kinetic studies of hydrosilation and cross-silane reactions allowed Duckett and Perutz to conclude that addition of hydrosilanes to alkenes by complex **II-40** does not proceed *via* the Chalk-Harrod mechanism or its variants involving silyl migration (Schemes 11 and 13). Instead, Duckett and Perutz

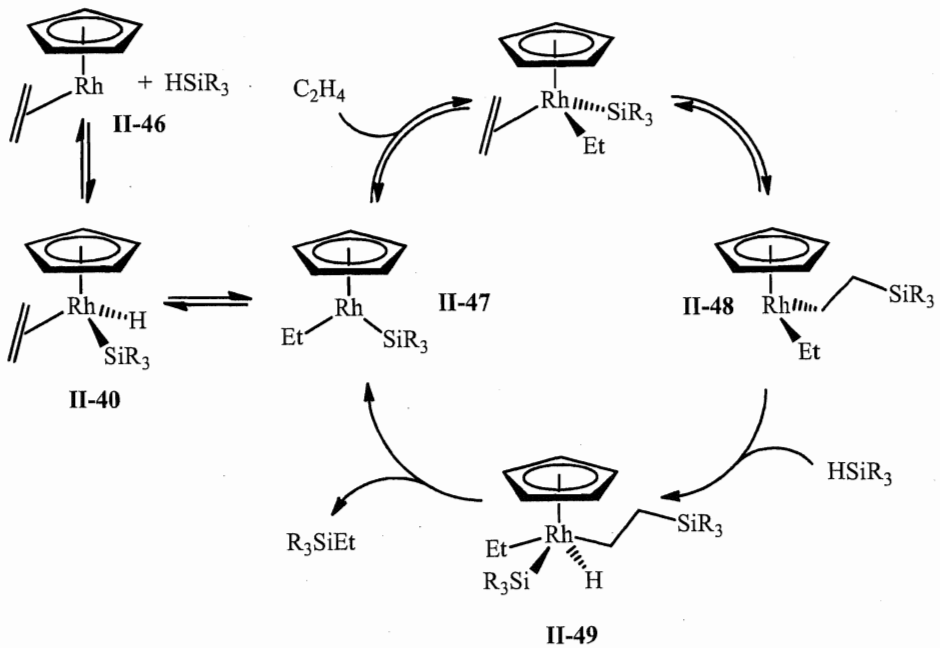

Scheme 19. Duckett-Perutz "two-silicon cycle" mechanism for hydrosilation of alkenes.

suggested an alternative mechanism based on a "two-silicon cycle" (Scheme 19), characterized by the following criteria: (i) the ethylene silylhydride complex **II-40** is not involved directly in the catalytic cycle, (ii) $CpRh(\eta^2\text{-}CH_2{=}CH_2)$ (**II-46**) is not participating in hydrosilation, and (iii) the integrity of the original ethylene ligand is retained (established by catalytic hydrosilation of C_2D_4 with R_3SiH, where no deuterium incorporation into the ethylene ligand of **II-40** was observed).[19d] Duckett and Perutz proposed that the catalytic cycle is initiated *via* a 1,3- hydrogen shift forming the electron-deficient complex $CpRh(Et)(SiR_3)$ (**II-47**) (see Scheme 19), which, coordinates another molecule of ethylene, followed by silyl migration to the olefin to give $CpRh(Et)[(CH_2)_2SiR_3]$ (**II-48**). Further oxidative addition of R_3SiH generates the Rh(V) species $CpRh(SiR_3)(Et)[(CH_2)_2SiR_3]$ (**II-49**), which upon release of R_3SiEt regenerates the catalyst **II-47** (Scheme 19).[19d, 75, 77] The formation of the Rh(V) complex **II-49** is consistent with previous Perutz's and Duckett's demonstrations that compounds of the type $CpRh(SiR_3)_2(H)_2$ (**II-43**) and $CpRh(SiR_3)_3(H)$ (**II-45**) are accessible at room temperature (Scheme 18).[77] The well-known instability of alkyl hydride compounds relative to the corresponding silyl hydrides analogues is only in agreement with a fast catalytic cycle. It should be also noted that the addition of silane to the intermediate **II-48** must occur stereoselectively, since no formation of ethane was detected in the reaction, and therefore, the hydride and ethyl substituents in **II-49** cannot be *cis-* to each other.

Many other mechanistic studies of the catalytic hydrosilation of alkenes have appeared in the literature recently,[7b, 76d, 78, 79, 80, 81] however, most of them present variations in the original or modified Chalk-Harrod schemes. In all commonly accepted proposals, the bond formation occurs *via* the coordination of both silane and olefin to the transition metal, followed by either reductive elimination[78, 81a] or σ-bond metathesis,[81b,c] forming the hydrosilation product. Nevertheless, some of these systems, such as complexes with metal-ligand cooperative reactivity,[82, 83] require our particular attention.

In 1993, Bergman *et al.* reported the preparation and catalytic reactivity of the dimetallic complex $Cp_2Ta(\mu\text{-}CH_2)_2Ir(CO)_2$ (**II-50**). Based on stoichiometric reactivity and various kinetic and thermodynamic studies of this compound, they proposed a hydrosilation mechanism in which the bridging methylene groups of **II-50** exhibit non-innocent behaviour (Scheme 20).[82] According to Bergman's suggestion, oxidative

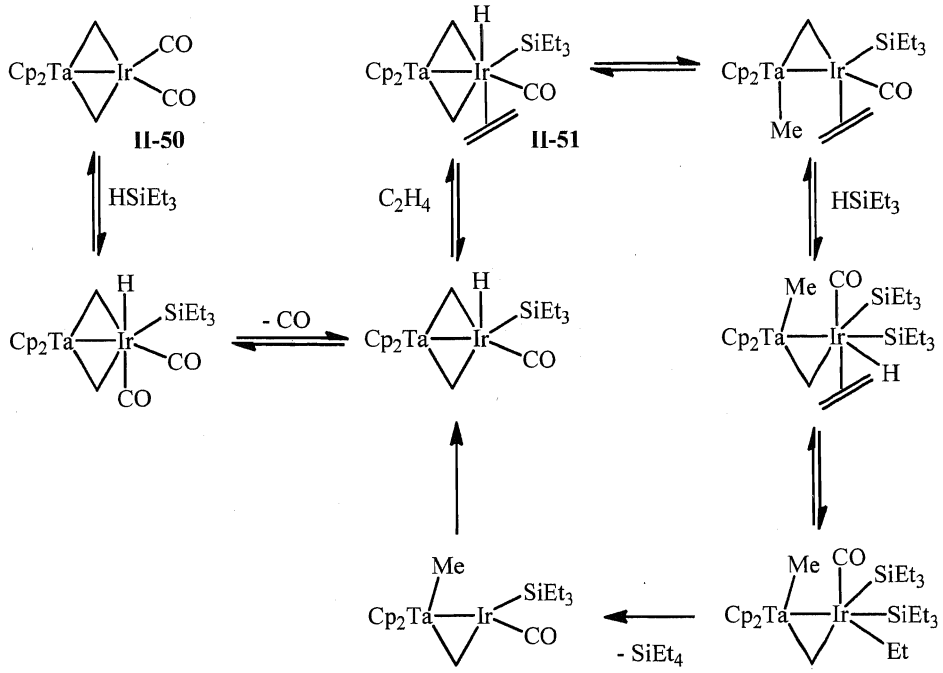

Scheme 20. Mechanism of catalytic hydrosilation of ethylene mediated by $Cp_2Ta(\mu\text{-}CH_2)_2Ir(CO)_2$ (**II-50**).

addition of silane to **II-50** followed by coordination of the alkene forms the species **II-51**, having the hydride ligand and the ethylene *trans*- to each other. Reductive elimination of the C-H bond of one of the methylene bridges generates the electron deficiency on the Ir centre necessary for activation of the second silane molecule. Further alkene insertion into the Ir-H bond, reductive elimination of the hydrosilated product and oxidative addition of the tantalum bound methyl group closes the cycle (Scheme 20).[82]

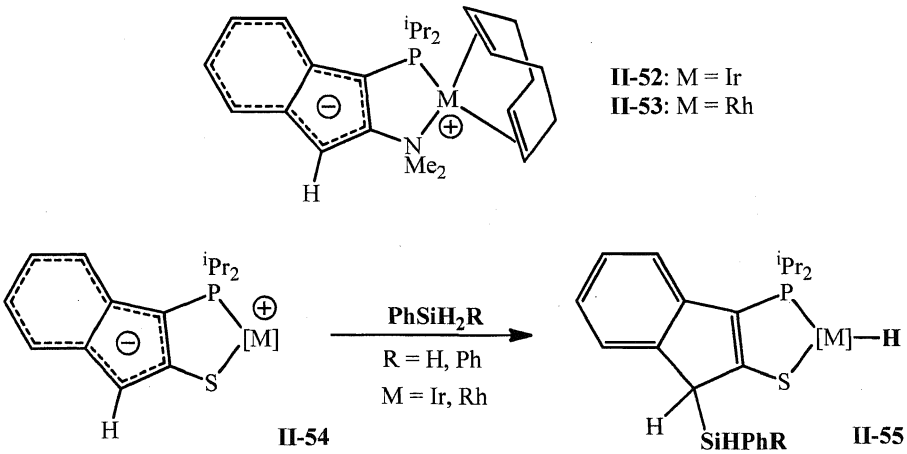

Scheme 21. Activation of silanes in hydrosilation by zwitterionic Rh and Ir complexes.

More recently, Stradiotto *et al.* showed that activation of silanes in the hydrosilation of alkenes could be achieved by a metal-ligand cooperative reactivity of iridium (**II-52**) and rhodium zwitterionic complexes (**II-53**) (Scheme 21).[83] Stoichiometric reactivity of analogous rhodium and iridium complexes **II-54** with hydrosilanes was reported later and supported the non-innocent behaviour of zwitterionic ligands.[83c]

An alternative mechanism for the hydrosilation of alkenes with primary silanes mediated by $[\{Cp^*(P^iPr_3)H_2Ru{=}SiHPh\}Et_2O][B(C_6F_5)_4]$ (**II-56**) was proposed by Glaser and Tilley in 2003.[84] The suggested scheme includes activation of two (sp^2)Si-H bonds of the silane substrate, direct addition of (sp^2)Si-H to the alkene and finally the 1,2-H-migration and reductive elimination step (Scheme 22). The crucial point of this mechanism is the direct insertion of the alkene into the Si-H bond of a ruthenium-silylene complex, which proceeds without preliminary coordination of the alkene to the ruthenium centre.[84] DFT calculations performed for model systems by Beddie and Hall[85] as well as by Bohme *et al.*[86] provided theoretical evidence for the importance of Glaser-Tiller catalytic scheme. They found that the rate determining transition state for the proposed cycle is more than 8 kcal/mol lower in energy than the highest energy transition state in the original and modified Chalk-Harrod mechanisms. Furthermore, the DFT study also revealed that the catalytically active complex has a nonclassical η^3-bonded silane ligand (the Ru-Si bond is bridged by two hydrogen atoms as highlighted in Scheme 20).[86] Unfortunately, the application of the Glaser-Tilley scheme is restricted to the use of only primary silanes, i.e. $RSiH_3$, required for the formation of hydrogen substituted silylene

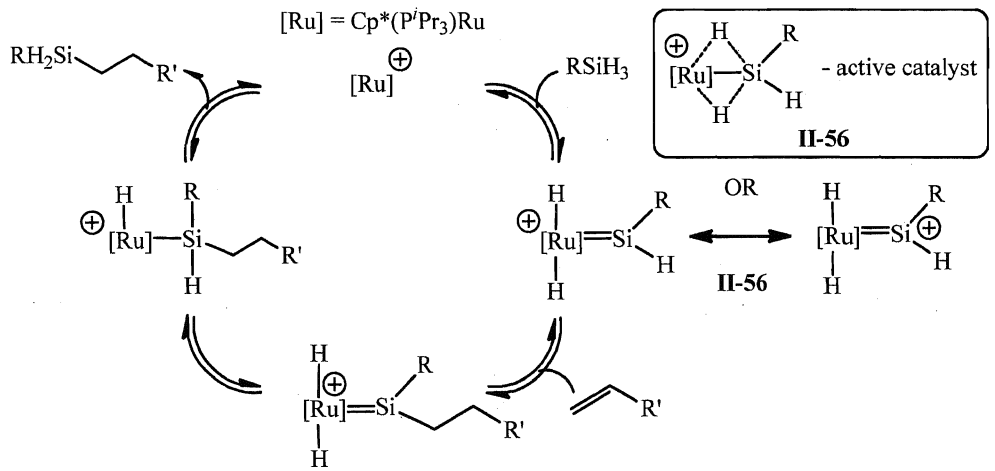

Scheme 22. Glaser-Tilley mechanism for hydrosilation of alkenes with primary silanes.

ligands in **II-56**.

The evidence for the key-step in the Glaser-Tilley catalytic scheme has been shown by Stradiotto *et al.*, who conducted stoichiometric reactions of the ruthenium cationic complex Cp*Ru(κ^2-P,N)$^+$ (**II-57**) with Ph_2SiH_2 and $PhSiH_3$ leading to a silylene extrusion and formation of ruthenium silylene complexes **II-59** (Scheme 23).[87] However, base-stabilization of the Ru=Si species with an amino substituent of the indene ligand provided negligible catalytic turnover in the hydrosilation of alkenes. Poor catalytic activity as well as the lack of stoichiometric reactivity of **II-59** towards 1-hexene and styrene provided further empirical evidence for the required intermediacy of a base-free Ru=Si species in the Glaser-Tilley mechanism.

Mechanistic studies discussed above demonstrate that there is no common mechanism for the alkene hydrosilation reaction catalyzed by transition metal complexes. Each particular catalytic system possesses characteristic nuances, which depend on the nature

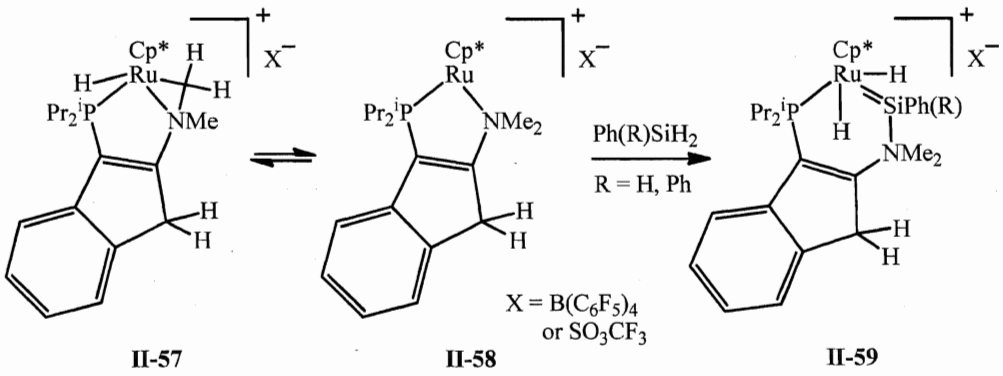

II-57 **II-58** **II-59**

Scheme 23. Silylene extrusion from Ph_2SiH_2 or $PhSiH_3$ by **II-57**.

of the transition metal, the acidity of silanes employed, and the steric and electronic properties of ligands. In the chemistry of late transition metals, for instance, Pt complexes tolerate a wide range of hydrosilanes, such as $HSiCl_nMe_{3-n}$ (n = 1 – 3), $HSi(OR)_3$, or H_nSiR_{4-n} (n = 1 – 3; R = alkyl or Ph), while Pd complexes are applicable mostly to $HSiCl_nR_{3-n}$ (n = 2, 3) and Rh catalysts preferably to tertiary silanes $HSiR_3$.[53, 54] A comprehensive discussion of recent advances in early transition metal hydrosilation systems and their mechanistic aspects is given below.

II.2.2 Mechanisms of TM catalyzed hydrosilation of alkynes

Transition metal catalyzed hydrosilation of alkynes is an efficient and mild method for the preparation of vinylsilanes. The design and the development of highly efficient and selective catalytic systems for the synthesis of alkenylsilanes have been the subject of extensive study due to the wide application of vinylsilanes as versatile building blocks in organic synthesis and material science.[7, 88-91] The unsaturated hydrosilation products RHC=C(R')(SiR"$_3$) provide ample opportunities for further transformations *via* oxidation (Tamao-Fleming protocol),[88] electrophilic substitution, nucleophilic addition,[89] cross-coupling (Hiyama coupling),[90] etc. Furthermore, the ease of handling, low cost and toxicity, as well as compatibility with a range of organic transformations have greatly stimulated their synthetic applications. For example, the recent demonstration of palladium catalyzed cross-coupling of vinylsilanols with vinyl and aryl halides provided an alternative to the use of highly toxic organostannanes.[91] However, transition metal catalyzed preparation of vinylsilanes usually requires high levels of regio- and stereocontrol.[7b] This part of the literature review describes general mechanistic aspects of transition metal catalyzed hydrosilation of alkynes as well as stereo- and regioselectivity of this process.

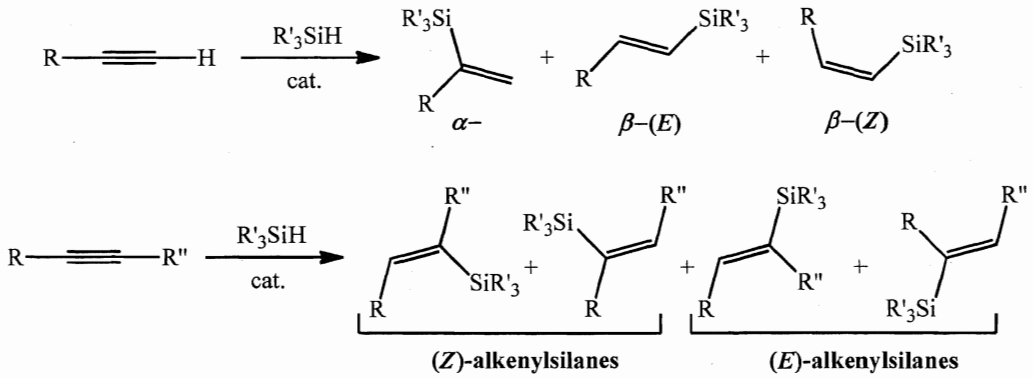

Scheme 24. Regio- and stereoselectivity of TM catalyzed hydrosilation of terminal and internal alkynes.

Hydrosilation of a terminal alkyne can result in three isomeric vinylsilanes: the α-silyl product, and two β-stereoisomers, *E* and *Z* (Scheme 24). On the other hand, the hydrosilation of internal alkynes offers a greater synthetic challenge because of the possibility of a broader product distribution. Thus, catalytic addition of hydrosilanes to

alkynes can potentially give four isomeric disubstituted alkenylsilanes (Scheme 24). The selectivity of hydrosilation depends upon several factors, such as the nature of the catalyst, the substitution of the alkyne and/or hydrosilane, and the reaction conditions (solvent, temperature, and catalyst loading). The reaction mechanism, and therefore, the distribution of products, depends not only on the metal used but also on the electronic and steric properties of ligands.[7b]

Analogously to hydrosilation of alkenes (see above), there are two generally accepted mechanisms describing the catalytic addition of hydrosilanes to alkynes: the original (**A**) and the modified[d] (**B**) Chalk-Harrod mechanisms (Scheme 25).[7] The original Chalk-Harrod scheme is based on Si-H oxidative addition, migratory insertion of alkyne into M-H bond, and reductive C-Si elimination. It has been successfully applied to explain hydrosilation of terminal alkynes in the presence of platinum complexes, which usually proceeds *via* exclusive *cis*-addition to form α- and β-(*E*)-alkenylsilanes, with the latter ones being predominant (anti-Markovnikov addition). The regioselectivity of the hydro-

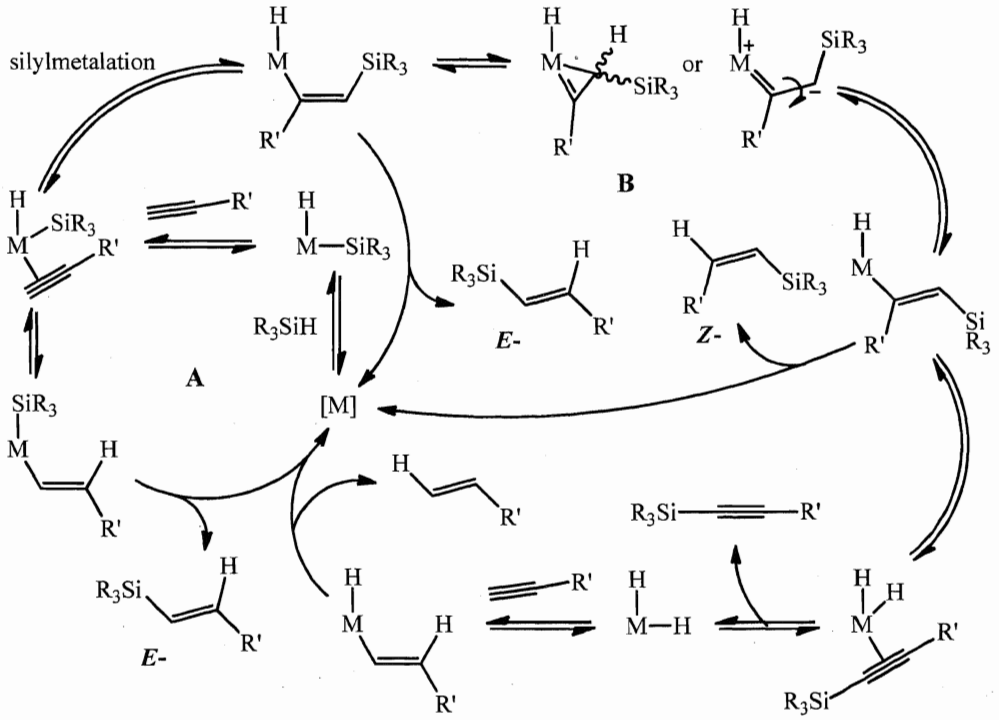

Scheme 25. Combined scheme for Chalk-Harrod (**A**) and Crabtree-Ojima (**B**) mechanisms for the TM catalyzed hydrosilation of alkynes.[7, 92]

[d] This mechanism of catalytic hydrosilation of alkynes is often called Crabtree-Ojima scheme.

silation process could be explained using Figure 9, which illustrates an interaction between the frontier orbital of the catalyst and alkyne orbitals.[7a] The π-HOMO orbital of the alkyne interacts with an unoccupied d^2-p^2-hybrid orbital of the catalyst and the π*-LUMO of the alkyne interacts with the bonding σ-MO ($d^2p_\sigma{}^2$-s_σ) of the complex (only two of four frontier orbitals are shown in Figure 9 for simplicity). Thus, in the case of terminal alkynes (Figure 9, **a**) the largest p coefficient of the π*-LUMO is localized on C_R atom, and therefore, nucleophilic attack by a hydride can take place on the C_H. For disubstituted alkynes (Figure 9, **b**), the differences in relative values of the sp coefficients for π-HOMO and π*-LUMO are smaller, and in the extreme case of symmetrical substrates RC≡CR, the migration of the hydride to both carbon atoms is equally probable. However, in the real catalytic system steric effects of the substituents on the alkyne should be also taken into account.[7a]

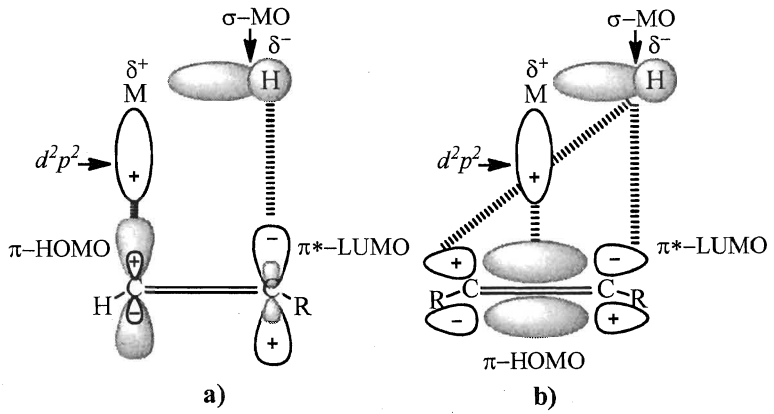

Figure 9. MO diagram for the insertion of terminal (**a**) and internal (**b**) alkynes into the M-H bond of the catalyst.[7a]

While the *β*-(*E*)-alkenylsilanes are obtained with high selectivity using Pt and Pd-based complexes, the selective formation of the stereoisomeric *β*-(*Z*)-vinylsilanes is generally achieved using Rh, Ir, and Ru catalysts. In the latter cases, the hydrosilation of terminal alkynes proceeds predominantly *via* a *trans*(*anti*-)-fashion leading to the formation of thermodynamically unfavourable *Z*-alkenylsilanes as the major products. Furthermore, similarly to the hydrosilation of olefins, the catalytic addition of hydrosilanes to alkynes often results in the products of dehydrogenative silation, $R'C{\equiv}CSiR_3$, and in products of reduction, $R'HC{=}CH_2$. These observations do not cleanly

fit the original Chalk-Harrod mechanism (Scheme 25, route **A**). In order to explain the predominant appearance of the unusual *trans*-addition products as well as the formation of alkenes and silylated alkynes, in the beginning of the 1990s Crabtree and Ojima proposed a modified Chalk-Harrod scheme, which is based on the silylmetalation of an alkyne, followed by *E*/*Z* isomerization (Scheme 25, route **B**).[92] According to this proposal, the exclusive insertion of the alkyne into the M-Si bond leads to the formation of a (*Z*)-silylvinyl complex, which, due to steric repulsion of the silyl group from the substituted metal atom, isomerizes to the thermodynamically favourable (*E*)-silylvinyl derivative. In principle, this isomerization could go *via* either a zwitterionic carbene species (as suggested by Ojima *et al.* for a Rh-catalyzed reaction)[92b] or *via* a metallacyclopropene intermediate (postulated by Crabtree *et al.* for an Ir catalyst).[92a] Further reductive elimination of the C-H bond leads to the formation of (*Z*)-alkenylsilanes as the kinetic products. At the same time, the formation of dehydrogenative silation products $R'C{\equiv}CSiR_3$ could be described in terms of β-hydrogen activation of the (*E*)-silylvinyl substituent affording a dihydride derivative, which, in principle, is capable of alkyne hydrogenation *via* the sequence of insertion of alkyne into the M-H bond and reductive elimination reactions (Scheme 25).

The Crabtree-Ojima mechanistic proposal perfectly explains the product distribution in hydrosilation of alkynes mediated by Rh, Ir, and Ru (and in some cases Pt and Pd) complexes. Thus, electron-rich hydrosilanes (such as trialkyl-substituted silanes) and relatively unhindered terminal alkynes usually give (*Z*)-alkenylsilanes as the major products, while catalytic hydrosilation using hydrosilanes with electron-withdrawing groups (such as alkoxy or halogens) generally provides access to (*E*)-products.[7] Furthermore, the desired *Z*/*E* selectivity of the hydrosilation process could be also achieved by tuning the sterics of the alkyne substrates and utilized silanes. Thus, hydrosilation of alkynes bearing bulky cycloalkyl or tertiary alkyl groups usually affords (*E*)-alkenylsilanes with decent selectivity.[7b] The electronics and sterics of the transition metal catalysts also have a great impact on the stereoselectivity of hydrosilation. For example, catalysis by cationic rhodium complexes exhibits high (*E*)-selectivity, whereas the neutral rhodium catalysts usually give (*Z*)-isomers.[93] Probably, the first examples of successful stereocontrol in the catalytic hydrosilation of alkynes were reported by the

groups of Takeuchi[93] and Ojima.[92b, 94] Some of their results are presented in Table 2 illustrating the role of silane substituents in the hydrosilation of 1-hexyne mediated by neutral Rh and Rh-Co complexes. This table clearly indicates that introduction of electron-rich groups at silicon leads to the predominant formation of *β*-(*Z*)-vinylsilanes. Furthermore, the stereoselectivity of the homogeneous alkyne hydrosilation is also highly sensitive to the properties of utilized solvent. Thus, using a series of Rh-based catalysts in the hydrosilation of 1-hexyne, Takeuchi *et al.* demonstrated the effect of solvent on the stereoselectivity of catalysis and the yield of alkenylsilanes.[93b] For example, addition of Et_3SiH to 1-hexyne mediated by $[Rh(cod)Cl]_2$ (**II-60**) in ethanol or DMF resulted in selective formation of the *Z*-product in 94 and 97 %, respectively. At the same time, $RhCl(PPh_3)_3$ (**II-61**) catalyzed reaction using ethanol or dimethylfomamide shows poor

Table 2. Hydrosilation of 1-hexyne mediated by neutral Rh and Rh-Co complexes

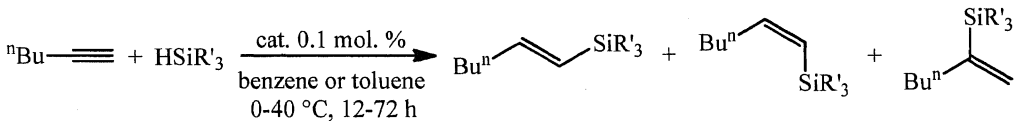

Catalyst	Silane R'_3SiH	Yield (GS) (%)	β-(*E*)/β-(*Z*)/α
$RhCl(PPh_3)_3$	Et_3SiH	100	3/94/3
$RhCo_3(CO)_{12}$	Et_3SiH	100	2/96/2
$Rh_2Co_2(CO)_{12}$	Et_3SiH	100	2.5/95/2.5
$Rh_4(CO)_{12}$	Et_3SiH	100	5/90/5
$Rh_4(CO)_{12}$	$PhMe_2SiH$	100	27/60/13
$Rh_4(CO)_{12}$	$(MeO)_3SiH$	98	95/0/5
$Rh_4(CO)_{12}$	Me_2ClSiH	76	80/0/20
$Rh_4(CO)_{12}$	$MeCl_2SiH$	70	65/0/35

stereoselectivity and leads to the formation of alkenylsilanes with 55/44 and 70/29 *β-Z/β-E* ratio, respectively (in both cases ~1 % of *α*-product was observed). Changing the solvent to nitrile (CH_3CN or PrCN) results in complete reversal of the stereoselectivity of the process, and formation of 95 % of the *E*-isomer. Hydrosilation of 1-hexyne catalyzed by **II-60** in acetonitrile is non-selective (*β-Z/β-E/α* = 36/33/31) and the products are isolated in poor yields. On the other hand, the **II-60**/PPh_3–catalyzed reaction gives a result comparable to that of the **II-61**–catalyzed process.[93b] Takeuchi suggested that

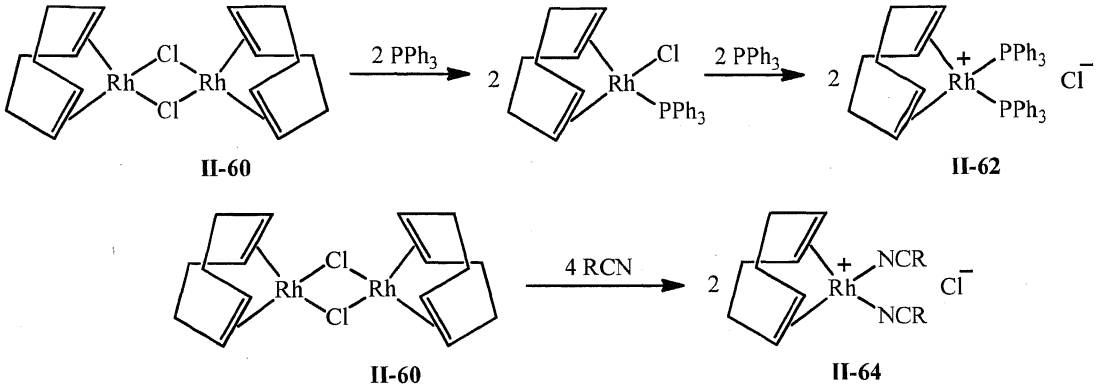

Scheme 26. Formation of $[Rh(cod)(PPh_3)_2][Cl]$ (**II-62**) and $[Rh(cod)(NCR)_2][Cl]$ (**II-64**).[95 - 97]

hydrosilation goes *via* the insertion of alkyne into the Rh-Si bond, followed by isomerization of the silylvinylene intermediate into a zwitterionic carbene species (Scheme 25, route **B**). Formation of this species leads to significant solvent control on the hydrosilation process. Thus, polar solvents, such as EtOH and DMF, should provide additional stability for the zwitterionic intermediate, increasing the *Z*-selectivity of the reaction.[93b] At the same time, *E*-stereoselective hydrosilation by the **II-60**/PPh_3 system was accounted for by the *in situ* formation of the cationic Rh(I) species $[Rh(cod)(PPh_3)_2][Cl]$ (**II-62**) that could be generated in polar solvents as described in Scheme 26.[95, 96] A reference catalytic reaction in the presence of $[Rh(cod)_2][BF_4]$ (**II-63**) / PPh_3 proved this suggestion by showing extremely high *E*-stereoseletivity.[93b] However, in their work Takeuchi *et al.* did not take into account the well-known basic nature of nitriles, which can form Rh(I) cationic complexes $[Rh(cod)(NCR)_2][Cl]$ (**II-64**) even in

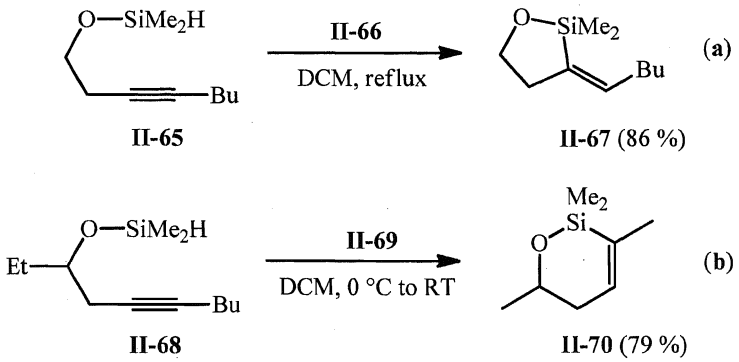

Scheme 27. Intramolecular hydrosilation of alkynyl silyl ethers catalyzed by neutral (**a**) and cationic (**b**) ruthenium complexes.[98, 99]

the absence of phosphine additives (Scheme 26).[97] Unfortunately, no catalytic reactions in CH_3CN or PrCN under phosphine-free conditions were reported.[93b]

The intramolecular hydrosilation of alkynes is also generally assumed to proceed *via* Chalk-Harrod or Crabtree-Ojima catalytic schemes. For example, Denmark *et al.* in 2002 reported a highly regio- and stereoselective anti-intramolecular hydrosilation of alkynyl silyl ethers **II-65** catalyzed by the ruthenium arene complex $[(C_6H_6)RuCl_2]_2$ (**II-66**) (Scheme 27, **a**).[98] The reaction goes in a 5-*exo*-dig manner to give the exocyclic *Z*-vinylsilane product **II-67**, which was *in situ* subjected to Pd-catalyzed cross coupling generating homoallylic trisusbstituted alkenes.

Trost *et al.* demonstrated that hydrosilation of the similar substrates using $[Cp^*Ru(NCMe)_3][PF_6]$ (**II-69**) leads to the formation of the 6-*endo*-dig products (Scheme 27, **b**).[99] Although, the 5-*exo*-dig cyclization could be explained by the *cis*-hydrosilation/isomerization mechanism proposed by Crabtree and Ojima (Scheme 25, route **B**), the formation of the *endo*-dig products most likely does not go *via* a similar rearrangement due to the strained structure of the intermediate **II-74** (Scheme 28). Instead, Trost *et al.* suggested that formation of the *endo*-products could be a result of direct *trans*-addition of the Ru-Si bond across the orthogonal π-systems of the alkyne.[99] However, the real mechanism could be more complicated and may include formation of polynuclear aggregates, as was showed by Oro and co-workers.[100]

As was mentioned above, transition metal catalyzed hydrosilation of alkynes leads mostly to the formation of *β*-alkenylsilanes, although, selective production of *α*-products

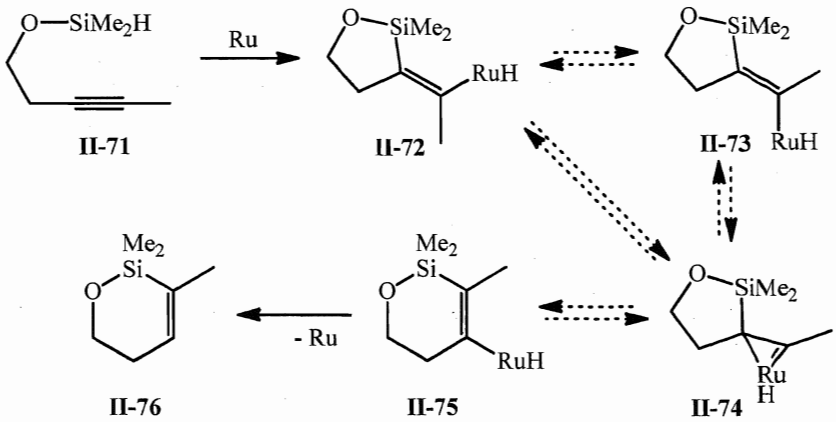

Scheme 28. Mechanism of Ru-mediated intramolecular hydrosilation of alkynyl silyl ethers.

was showed for a few catalytic systems. Thus, Chang *et al.* demonstrated the use of $[RuCl_2(p\text{-cymene})]_2$ (**II-77**) in highly regioselective addition of silanes to alkyne substrates having a hydroxyl group at the β-position to the triple bond (Scheme 29, **a**).[101a] Unfortunately, the nature of such OH-directed regioselective transformation was not explored, and no reasonable explanation was suggested. However, rather low isolated yields of the hydrosilation products, observation of a competitive O-silation processes and the fact that analogous reaction with O-protected substrate selectively provided regioisomeric β-vinylsilane suggest the non-innocent role of the hydroxyl proton.[101a]

In 2001, Trost *et al.* also reported non-directed regioselective hydrosilation of alkynes mediated by $[Cp^*Ru(NCMe)_3][PF_6]$ (**II-78**) (Scheme 29, **b**).[101b] The 9:1 – 20:1 of α:β selectivity was discovered but, again, relatively little mechanistic data were discussed.[102]

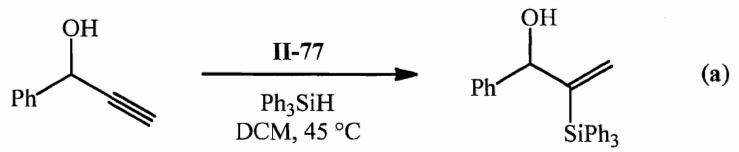

98:2 selectivity for α-isomer, 60 % yield

20:1 selectivity for α-isomer, 87 % yield

Scheme 29. Formation of α-vinylsilanes by regioselective hydrosilation of alkynes.

III.2.3 Mechanisms of TM catalyzed hydrosilation of C=X (X = O, N) bonds

The catalytic reduction of C=O and C=N bonds can be realized with the use of a number of reducing agents, with dihydrogen being the most frequently applied.[1-6] However, hydrogenation reactions as well as the reactions involving stoichiometric reducing reagents are often limited by the selectivity, cost, and difficulty of experimental procedures.[1-4] The development of the hydrosilation methodology as an alternative method for reduction of carbonyls and imines started in the early 1970s with the discovery by Ojima *et al.* of the high activity of Wilkinson's catalyst $RhCl(PPh_3)_3$ (**II-79**) for the catalytic addition of hydrosilanes to ketones.[103] Nowadays, the homogeneous catalytic hydrosilation of C=O and C=N bonds presents one of the most important, mild

and convenient methods for the preparation of secondary alcohols and amines.[7] Furthermore, the asymmetric version of this process provides optically active alcohols and amines, which could be further transformed into more complicated pharmaceutically relevant chiral molecules.

The hydrosilation of ketones and aldehydes (imines) produces in a single step the silyl ethers (silylamines), which can be easily transformed into alcohols (amines) *via* hydrolysis (Scheme 30). It should be also noted that among C=O or C=N containing substrates, the α,β-unsaturated derivatives form a unique class. In this case, the regioselectivity (1,2- or 1,4-addition) of the reaction crucially depends on the type of the catalyst and silane. In the literature, the 1,4- hydrosilation/hydrolysis sequence is often referred to as the conjugate reduction.[7]

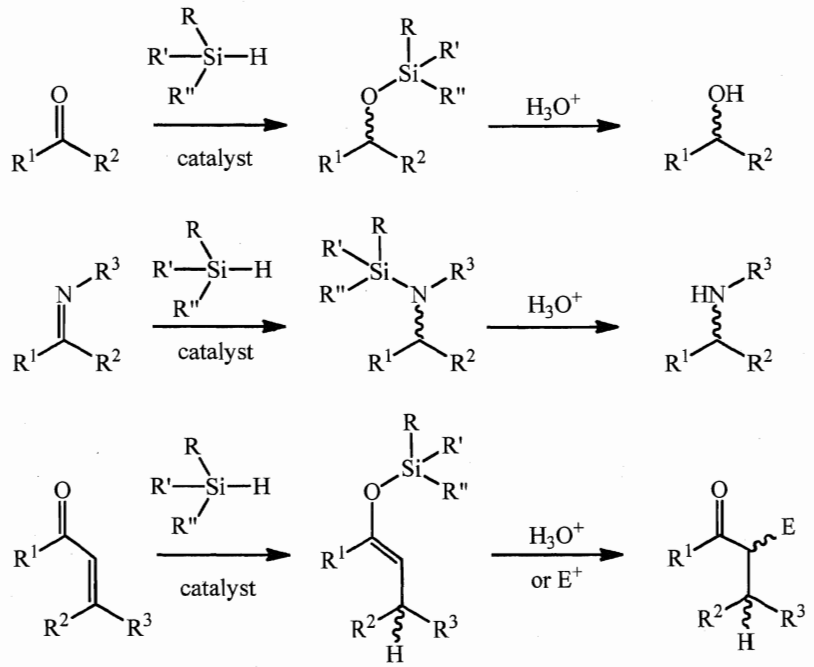

Scheme 30. Catalytic hydrosilation of carbonyls and imines.

This part of the literature review describes general mechanistic aspects of transition metal catalyzed hydrosilation of carbonyl compounds and nitriles. The regioselectivity of such reductions is also discussed.

II.2.3.1 Hydrosilation of carbonyl compounds

The first examples of hydrosilation of carbonyls mediated by metal chlorides (such as $NiCl_2$, $ZnCl_2$, and $H_2[PtCl_6]$) appeared in the literature in the late 1950s.[104] However, the first highly effective catalytic addition of silanes to carbonyls was demonstrated by Ojima *et al.* only in 1972 using Wilkinson's catalyst.[103] Based on the isolation of the Rh(III) silyl intermediate $Rh(H)(SiEt_3)(Cl)(PPh_3)_2$ (**II-80**), Ojima proposed the mechanism shown in Scheme 31.[10b, 103, 105] Since then, it has been generally believed that in most cases catalytic addition of hydrosilanes to carbonyls proceeds according to the Ojima's scheme, which is similar to the modified Chalk-Harrod catalytic cycle for the hydrosilation of alkenes (see Scheme 13).[10a] Ojima's mechanism includes the following steps: (i) the oxidative addition of silane to the transition metal centre; (ii) migratory insertion of the organic substrate into the M-Si bond giving a α-(silylalkoxy)alkyl hydride derivative; and (iii) reductive elimination of the C-H bond (Scheme 31).[10b, 103, 105] Analogously to saturated substrates, the mechanism presented in Scheme 31 in most cases could be also applied to the catalytic hydrosilation of α,β-unsaturated carbonyl compounds.[10b,c,d, 103, 105]

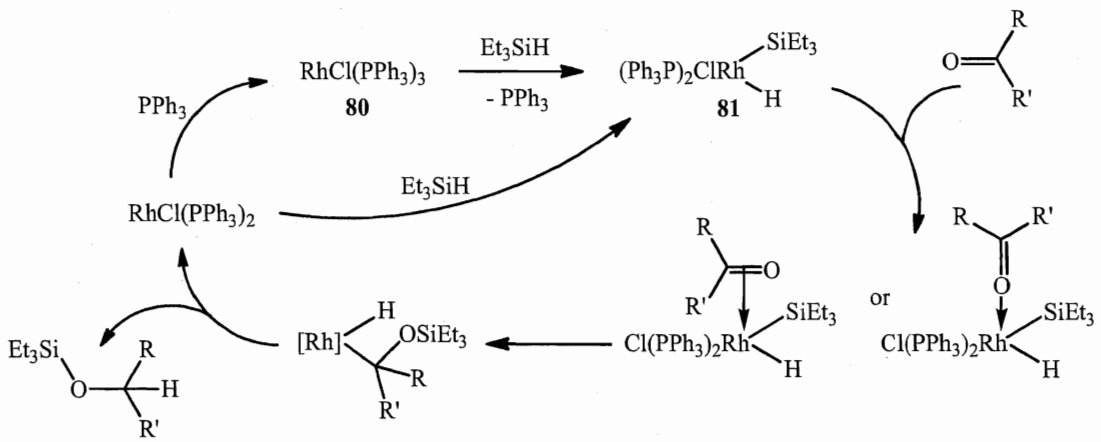

Scheme 31. Ojima's mechanism of ketone hydrosilation mediated by Wilkinson's catalyst.

The discovery of Ojima *et al.* started a "new wave" in the development of efficient catalytic systems for carbonyl hydrosilation. In 1972, Kagan *et al.* reported the first example of asymmetric hydrosilation of ketones mediated by a Rh(I)-DIOP (DIOP - 2,3-*O,O'*-isopropylidene-2,3-dihydroxy-1,4-bis(diphenylphosphino)butane) catalyst.[106] Since

then, a variety of late transition metal catalytic systems have been designed for the asymmetric version of this reaction using a diversity of chiral ligands (usually *N*- and *P*-based ligands) and molecular hydrosilanes, which reduce a large range of carbonyl compounds in high yields with moderate to high enantioselectivities.[107] Some of the *N*-based chiral ligands that are effectively applied nowadays in asymmetric Rh(I)-catalyzed

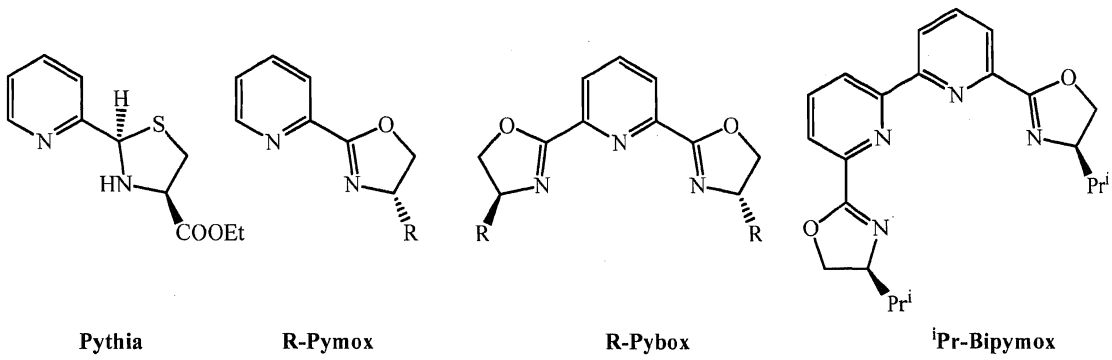

Figure 10. *N*-based chiral ligands effectively applied in Rh(I)-catalyzed hydrosilation.

hydrosilation are presented in Figure 10.[107, 108] Most of these catalytic processes are assumed to proceed *via* the general Ojima's scheme, which also explains the formation silyl enol ethers and alcohols as products of dehydrogenative silation and reduction of carbonyls, respectively.[109]

In 1995, Chan and co-workers reported the application of the Rh(I) hydride complex $(Ph_3P)_4RhH$ (**II-81**) for the catalytic hydrosilation of α,β-unsaturated carbonyl compounds. It was found that, depending on the substitution of the silane, the reactions proceed *via* either regioselective 1,2- (for di- and trihydridosilanes) or 1,4-addition (for monohydrosilanes).[110] Deuterium labelling studies performed for the addition of polyhydrosilanes and monohydrosilanes to acetophenone revealed $k_H/k_D = 2$ and $k_H/k_D = 1$, respectively. Based on these observations, Chan *et al.* proposed an alternative mechanism, which includes carbonyl coordination to the silicon atom of the silyl ligand, followed by a hydride shift (Scheme 32). It was also suggested that the absence of any significant isotope effect in the reaction with monohydrosilanes indicates that neither the formation of a silylhydrido rhodium complex (**A**) or elimination of **C** to **D** can be the rate-determining step. On the other hand, the observation of a significant primary kinetic isotope effect in the reaction with dihydrosilanes is consistent with the possibility that the

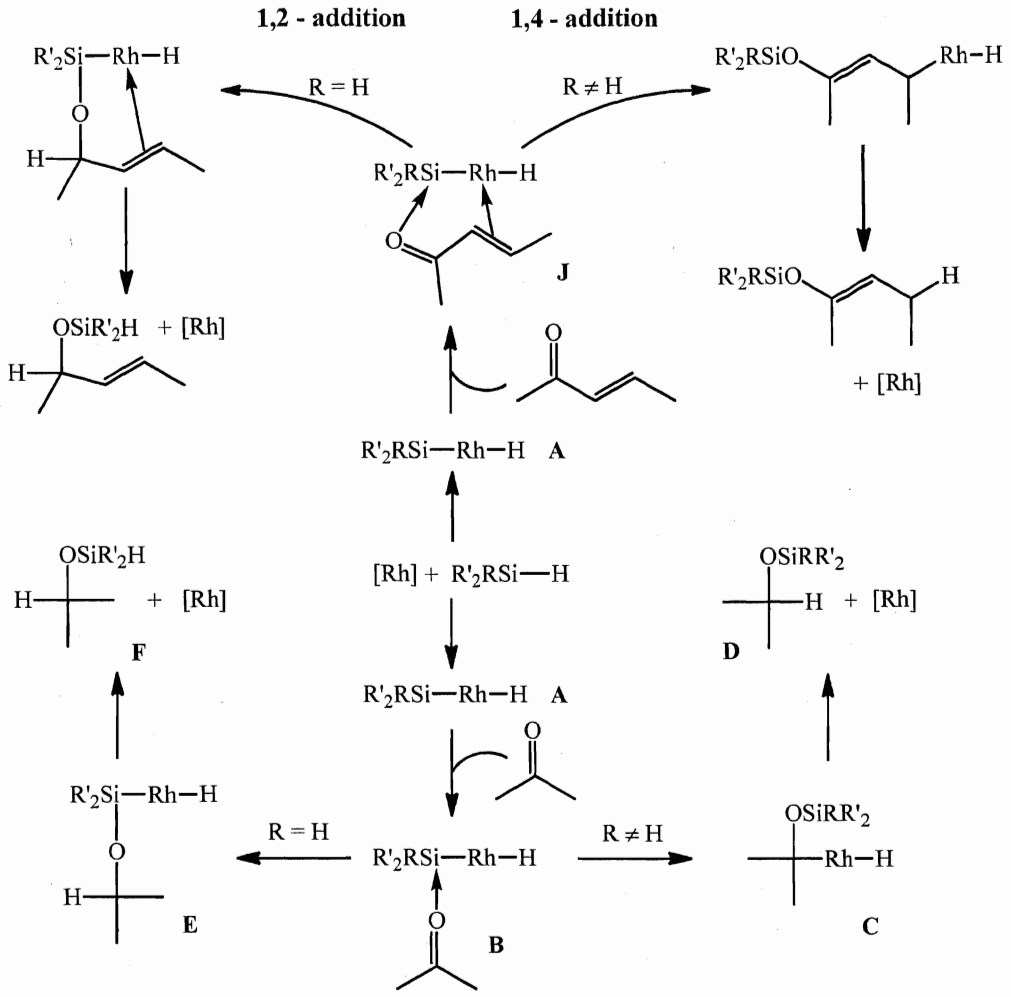

Scheme 32. Chan's mechanism of catalytic hydrosilation of α,β-unsaturated carbonyl compounds mediated by $(Ph_3P)_4RhH$ (**II-81**).

rate-determining step is the formation of intermediate **E** from the complex **B**.[110] For the addition of silanes to α,β-unsaturated carbonyls the formation of adduct **J** was suggested to be the rate-limiting for both di- and trisubstituted silanes (k_H/k_D = 1) (Scheme 32). Coordination of the ketone as the rate-determining step was also proposed earlier by Kolb and Hetflejs[111] for the catalytic hydrosilation of *tert*-butyl phenyl ketone mediated by $[Rh(1,5\text{-cod})\{(-)\text{-DIOP}\}]^+ClO_4^-$ (**II-82**) (DIOP–2,3-*O*,*O*'-isopropylidene-2,3-dihydroxy-1,4-bis(diphenylphosphino)butane).

The presence of C=C bond coordination to the rhodium centre in **J** can also account for the stereoselectivity (*cis*:*trans* = 92:8) observed by Chan *et al.* for the catalytic

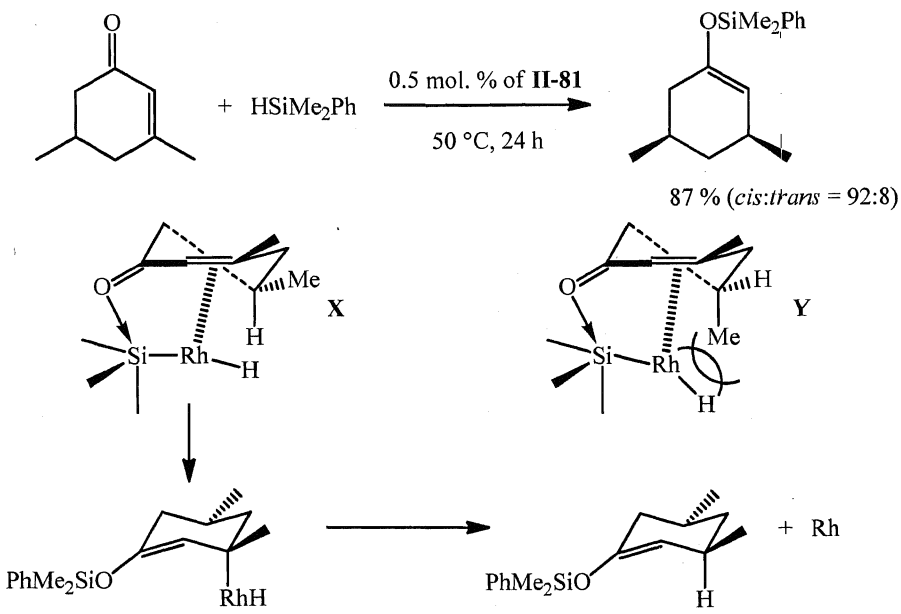

Scheme 33. Hydrosilation of 3,5-dimethylcyclohex-2-enone with $HSiMe_2Ph$ mediated by $(Ph_3P)_4RhH$ (**II-81**).

1,2-reduction of 3,5-dimethylcyclohex-2-enone (Scheme 33).[110] In this particular case, the intermediate **X** would be favoured over the intermediate **Y**, which possesses more steric repulsions between the axial methyl group and the rhodium moiety. Further substrate insertion and reductive elimination would then give *cis*- product selectively.

Results contradicting Chan's catalytic scheme were obtained recently by Gade, Hofmann and co-workers.[112] Their initial work on the catalytic activity of the carbene Rh(I) complex (**II-83**, Figure 11) for the hydrosilation of both alkyl/aryl and dialkyl ketones[113] was followed by the computational study of full catalytic cycles for the latter

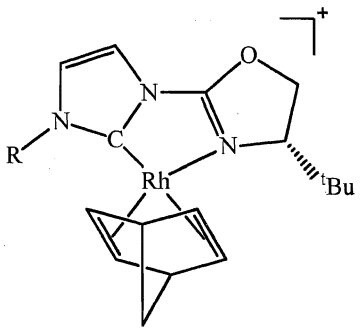

II-83
R = Mes, $(1\text{-naphthyl})_2CH$

Figure 11. Rh(I) carbene complex **II-83** active in hydrosilation of aryl/alkyl and dialkyl ketones.

system.[112] Interestingly, the deuterium labelling experiment for the **II-83**–mediated hydrosilation of acetophenone revealed no kinetic isotope effect (*KIE*) for tertiary silanes (in particular, $PhMe_2SiH$ and $PhMe_2SiD$ were used), whereas reaction with disubstituted silanes (Ph_2SiH_2 and Ph_2SiD_2) was found to be characterized by an inverse *KIE* of 0.8.[112a] These observations are incompatible with the previously postulated Chan's mechanism (Scheme 32).[110] The DFT calculations performed by Gade and Hofmann resulted in suggestion of a new mechanistic pathway, which involves a silylene intermediate and applicable only in the case of secondary silanes (Scheme 34).[112]

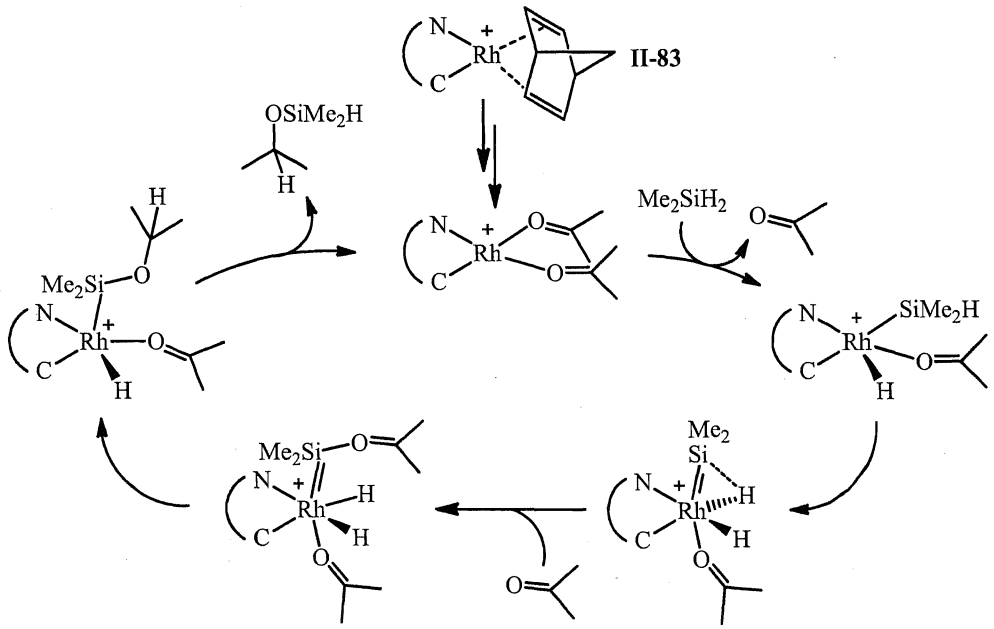

Scheme 34. Suggested mechanism of hydrosilation of ketones with secondary silanes mediated by **II-83**.[112]

Probably the major breakthrough in the catalytic hydrosilation of alkenes was achieved in the late 1980's – beginning of 1990's with the development of titanocene catalysts that proved highly efficient for the enantioselective reduction of both imines and carbonyls.[7, 9, 107, 108] In the 1990's, Buchwald *et al.* proposed a novel mechanism for asymmetric ketone hydrosilation mediated by (*R*,*R*)-(EBHTI)TiF_2 (**II-84**), where EBHTI is ethylenebis(tetrahydroindenyl).[9e] The originality of Buchwald's scheme is in the final step leading to the catalyst recovery, which presents a Ti-O/H-Si σ-bond metathesis (Scheme 35). The hydrosilation of ketones by **II-84**/$PhSiH_3$ system slowly proceeds

without any additives; however, addition of few equivalents of alcohol (such as MeOH, ^{i}PrOH, and ^{n}BuOH) significantly increases the rate of the process. The smaller size of the OR' group, relatively to O(CH(R^1)R^2), enhances the rate of the σ-bond metathesis in the rate determining step. Unfortunately, the lack of experimental evidence for the proposed mechanism makes the scheme totally speculative.[9e] Furthermore, the presence of fluoride ions in the catalytic system could also lead to the hydrosilation of ketones.[114]

Reduction of ketones by **II-84**/PhSiH$_3$/R'OH does not present a clear case for carbonyl hydrosilation, i.e. the addition of hydrosilanes across C=O bond. Instead, the cycle proposed by Buchwald *et al.* can be better classified as an intramolecular hydrogen

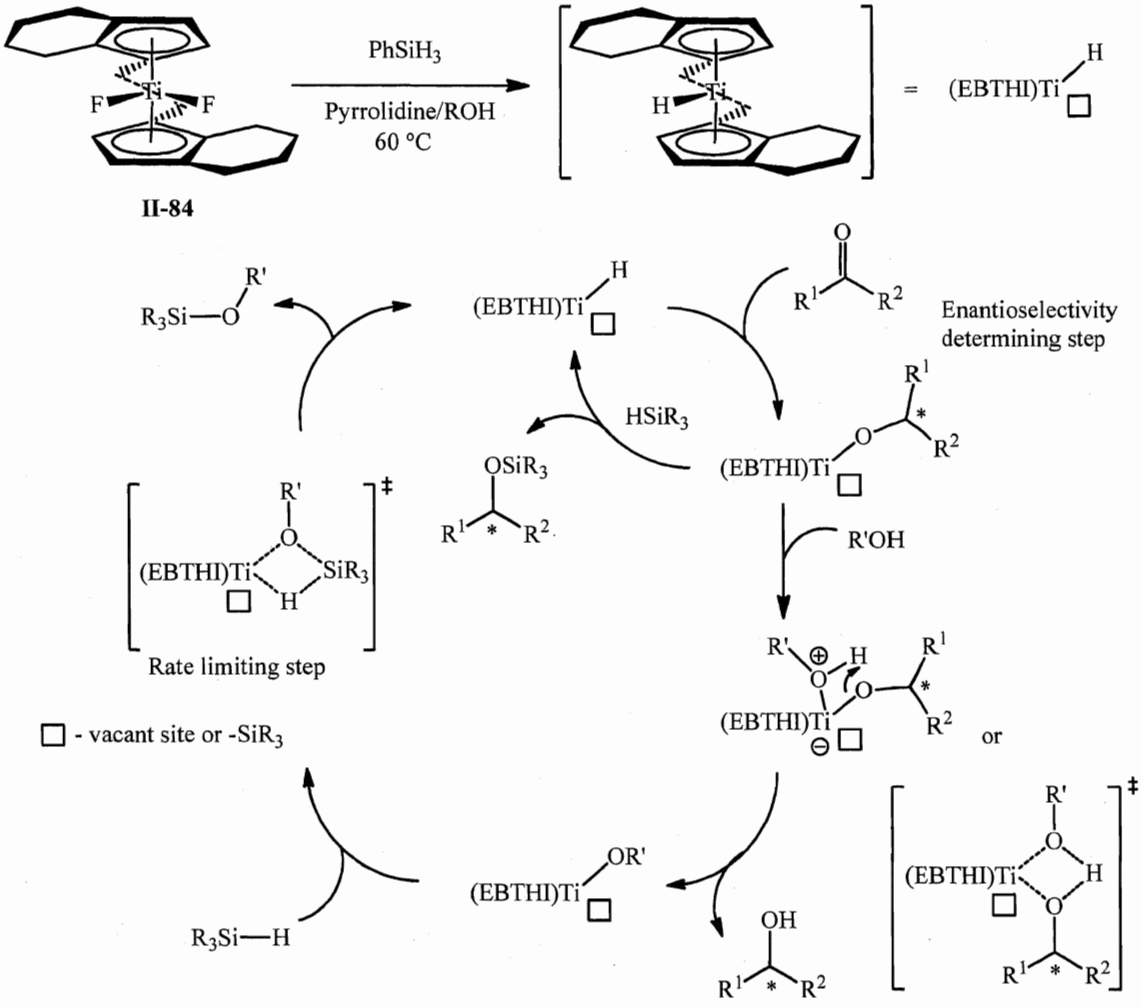

Scheme 35. Buchwald's mechanism for the asymmetric hydrosilation of ketones mediated by (*R*,*R*)-(EBHTI)TiF$_2$ (**II-84**)/PhSiH$_3$/R'OH system.

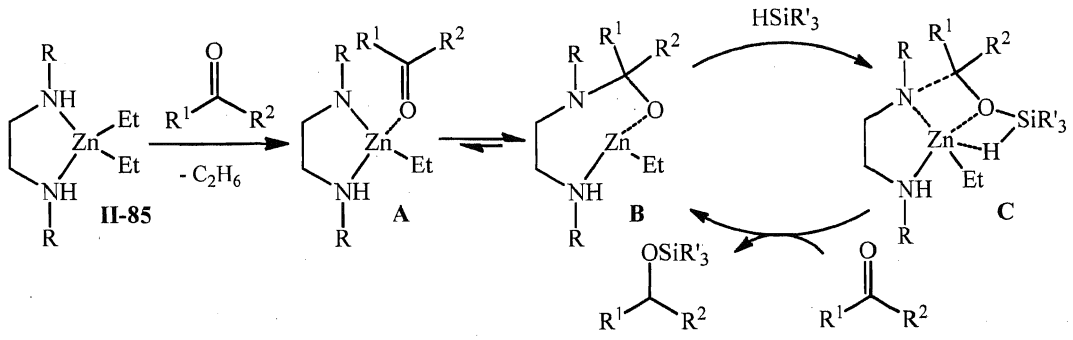

Scheme 36. Floriani's mechanism for ketone hydrosilation in the presence of $ZnEt_2$/diamine (**II-85**).

transfer reaction; the silane, however, is needed for the catalyst recovery.

Another novel mechanism for the catalytic hydrosilation of carbonyl compounds was presented by Floriani *et al.* for the combination of $ZnEt_2$ with chiral diamines (**II-85**).[115] Isolation of a seven-membered dimeric zinc complex (**B**), in which the ketone inserts into a Zn-N bond suggests that the diamine is not an ancillary but plays an active role in the hydrosilation process. A plausible mechanism proposed by Floriani and co-workers is depicted in Scheme 36 and involves the coordination of a ketone substrate to zinc (**A**), followed by insertion into the Zn-N bond (**B**) and σ-bond metathesis with the silane (**C**).[115]

Immense progress in the hydrosilation of carbonyls was made in the last decade, when traditional catalytic systems were expanded with novel organometallic compounds. Thus, in 2003, Toste *et al.* applied high oxidation transition metal complexes, usually employed in oxidation and oxygen atom transfer reactions, in hydrosilation.[11a, 116] This allows them to avoid many of the limitations typically associated with traditional hydrosilation catalysts, which often suffer from air and moisture sensitivity, functional group incompatibility, and the requirement to use reactive polyhydric silanes.[7, 107]

Studying the hydrosilation of carbonyl compounds mediated by $(Ph_3P)_2Re(O)_2I$ (**II-86**) Toste *et al.* proposed an unprecedented mechanism shown in Scheme 37 (**A**),[11a, 116] which was later confirmed by a computational study carried out by Lin, Wu, and co-workers.[11b] In contrast to traditional hydrosilation catalysts, which are known to generate a hydride species *via* Si-H oxidative addition to transition metal; the activation of silanes by high oxidation complexes and the formation of hydride derivatives proceed *via* an

alternative [2+2]-type addition of the Si-H bond to a metal-ligand π-bond (usually M=S, M=O, and M=N) (Scheme 37, **B**, path I).[14, 15, 117] The choice of a dioxo Re(V) catalyst was made in the hope that the reactivity of the metal-oxygen double bond would be enhanced by the presence of the second oxo ligand (the spectator oxo effect).[116] Thus,

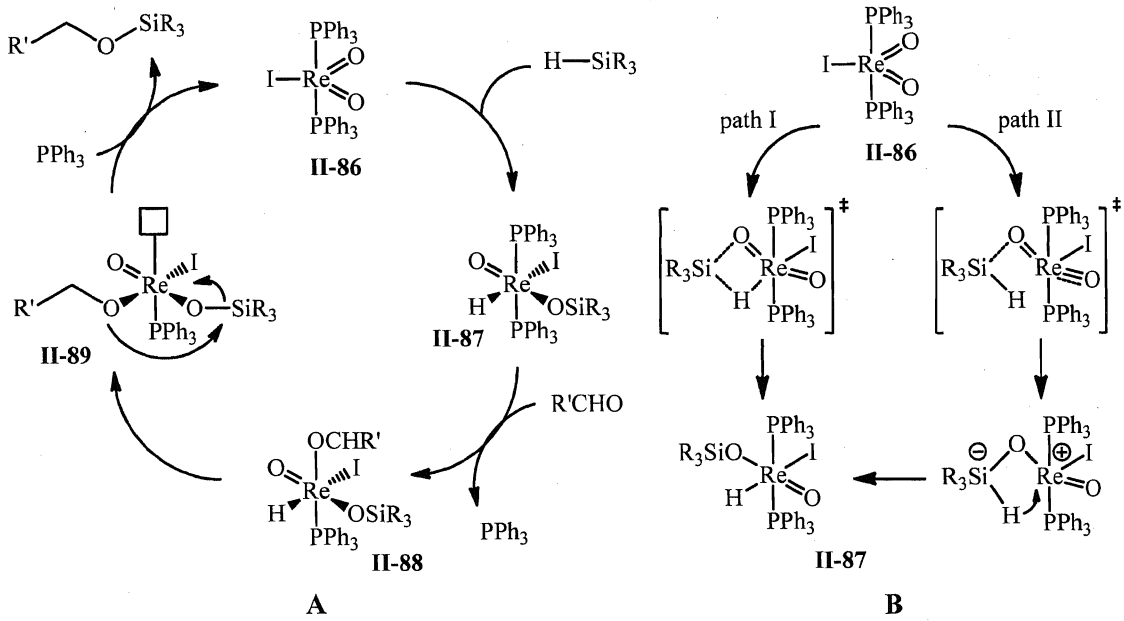

Scheme 37. Toste's mechanism for the hydrosilation of carbonyl compounds mediated by $(Ph_3P)_2Re(O)_2I$ (**II-86**).[11a, 116]

treatment of **II-86** with hydrosilanes $HSiR_3$ leads to the conversion of a strongly oxidizing oxo-complex to an isolable silyloxy-substituted metal hydride derivative $(Ph_3P)_2Re(O)(OSiR_3)(H)I$ (**II-87**), which could potentially be employed as a reductant. In contrast to the [2+2]-addition of R_3Si-H across Re=O, the formation of complex **II-87** could be achieved through a Lewis base – Lewis acid interaction forming Si^-/Re^+ zwitterions, followed by the hydride transfer (Scheme 37, **B**, path II).[11a] The kinetic experiments performed by Toste *et al.* proved that the formation of **II-87** undergoes without PPh_3 dissociation, which is incompatible with the computational reports published by Wu.[11b] Based on kinetic studies and the observation of all intermediates in stoichiometric and, in some cases, catalytic reactions, Toste *et al.* stated that complexation of the aldehyde or ketone is preceded by dissociation of one phosphine ligand from **II-86** and affords the siloxyrhenium hydride **II-88**. Subsequent insertion of

the carbonyl substrate into the Re-H bond yields the siloxyrhenium alkoxide derivative **II-89**, which regenerates the dioxo complex **II-86** by reassociation of PPh_3 and liberation of the silyl ether product *via* a formal retro-[2+2] reaction between the alkoxy and siloxy ligands (Scheme 37, **A**).[11a, 116] Depending on the nature of the utilized silane, the rate limiting step of the Toste's hydrosilation cycle could be either formation of the siloxy intermediate **II-87** (determined for Ph_2MeSiH) or insertion of coordinated carbonyl in **II-88** into the Re-H bond to give **II-89** (determined for Me_2PhSiH).[11a] Numerous DFT studies performed for Re dioxo catalytic systems are, in general, in good agreement with the proposed scheme and also conclude that the presence of the second oxo ligand promotes the [2+2] silane addition (kinetically and thermodynamically) in comparison to the neutral mono(oxo) complex $Re(O)Cl_3(PMe_3)_2$ (**II-90**).[11b, 118]

The advantage of the Toste's catalytic system is that metal-oxo compounds are usually resistant to further oxidation, which makes them attractive air-, moisture-, and reagent-tolerant catalysts.[119] Furthermore, hydrosilation of carbonyls mediated by $(Ph_3P)_2Re(O)_2I$ (**II-86**) was found to be highly chemoselective, tolerating functional groups such as cyano and esters, for example.[11a, 116] Similar catalytic activity in the hydrosilation of carbonyl compounds was also found for other polyoxo rhenium complexes, such as Re_2O_7 (**II-91**), $ReMeO_3$ (**II-92**), $CpReO_3$ (**II-93**), $ReO_2Cl(DMSO)_2$ (**II-94**), and $ReO_2Me(PhC{\equiv}CPh)$ (**II-95**).[12a]

The discovery of catalytic hydrosilation of carbonyls mediated by transition metal oxo complexes led to a whole new field of hydrosilation research. Thus, shortly after Toste's original report regarding the application of **II-86**, analogous reactivity in hydrosilation was shown for related molybdenum(VI) dioxo compounds, MoO_2Cl_2 (**II-96**), $MoO_2(acac)_2$ (**II-97**), $CpMoO_2Cl$ (**II-98**), $MoO_2(Mes)_2$ (**II-99**), and for polymeric organotin-oxomolybdates $(R_3Sn)_2MoO_4$ (R = ^{n}Bu, ^{t}Bu, Me) (**II-100**).[12b,c] Similar to complex **II-86**, the catalytic cycle mediated by **II-96** starts with the addition of the Si-H bond of hydrosilanes across the Mo=O bond. Spectroscopic and computational studies performed for complex **II-96** initially suggested that a radical mechanism could be involved in the hydrosilation reaction, where the Mo-H homolytic bond cleavage is taking place in the presence of an aldehyde or ketone (Scheme 38).[12b,c] However, complete DFT studies reported by Romao, Calhorda and co-workers for the proposed

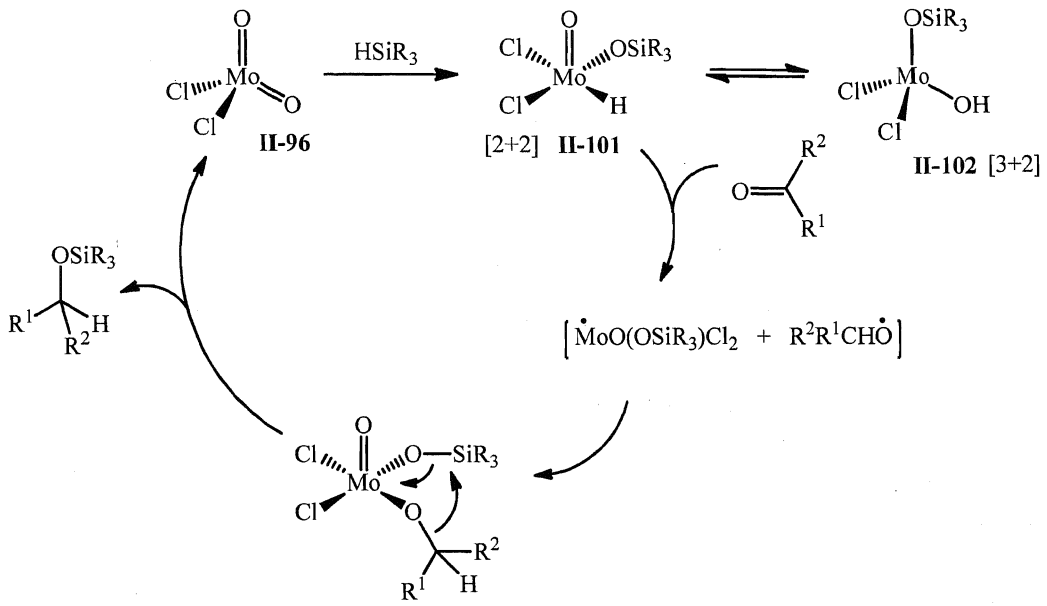

Scheme 38. Romao's mechanism for the hydrosilation of carbonyl compounds mediated by MoO_2Cl_2 (**II-96**).

mechanism could not distinguish between the different possible pathways for the initial silane activation: the [2+2]-reaction versus the [3+2]-addition known for C-H activation[118] (Scheme 38). The role of the carbonyl compound in the suggested scheme also remains unclear.[12c] In 2007, Strassner *et al.* presented an independent computational study on the hydrosilation mediated by **II-96**, which led to the conclusion that [3+2]-activation of silanes and the formation of the hydroxyl derivative **II-102** are strongly unfavourable.[118] A similar conclusion about the involvement of a radical mechanism has been recently made by Abu-Omar *et al.* during their investigation of the hydrosilation of carbonyls in the presence of $Mo(O)_2$(salalen-3,5-R_2) (**II-103**, R = H, ^{t}Bu; Figure 12).[120]

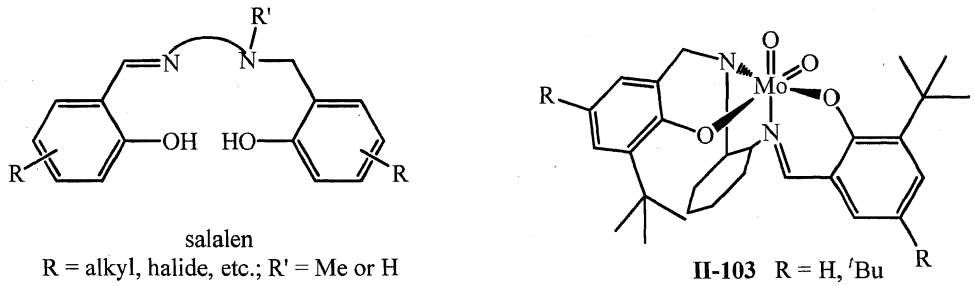

Figure 12. Salalen ligand and Abu-Omar's Mo(VI) salalen oxo complex **II-103**.

Almost at the same time, Abu-Omar *et al.* reported the utilization of a modified oxo rhenium catalyst [Re(O)(hoz)$_2$(MeCN)][TFPB] (**III-104**, hoz = 2-(2'-hydroxyphenyl)-2-oxazoline(-); TFPB = tetrakis(pentafluorophenyl)borate) for the hydrosilation of carbonyl compounds.[13a] The important features of the **III-104**-catalyzed hydrosilation include the following: (i) the high efficiency of the catalysis under ambient temperature and atmosphere with low catalyst loading (0.1 mol. %); (ii) the transformation may be performed without a solvent, wherein the catalyst precipitates at the end of the reaction (this minimizes the organic waste generated and facilitates catalyst separation). Abu-Omar proposed that activation of silanes mediated by **II-104** does not include the [2+2] addition of Si-H across the Re=O bond, which was stated for the dioxo rhenium[11a, 12a, 116] and molybdenum compounds.[12b,c] Instead, based on preliminary kinetic and ^{18}O-labeling experiments, the authors initially suggested that the catalytic cycle starts with the OA of R_3SiH to the cationic Re centre affording the silane σ-complex **II-105**. Addition of the carbonyl leads to a metathesis-like reaction (**II-106**, Scheme 39) and does not include the formation of a rhenium hydride species, which are not sufficiently hydridic in order to reduce organic carbonyl group.[13a] An analogous metathesis-like transformation has been

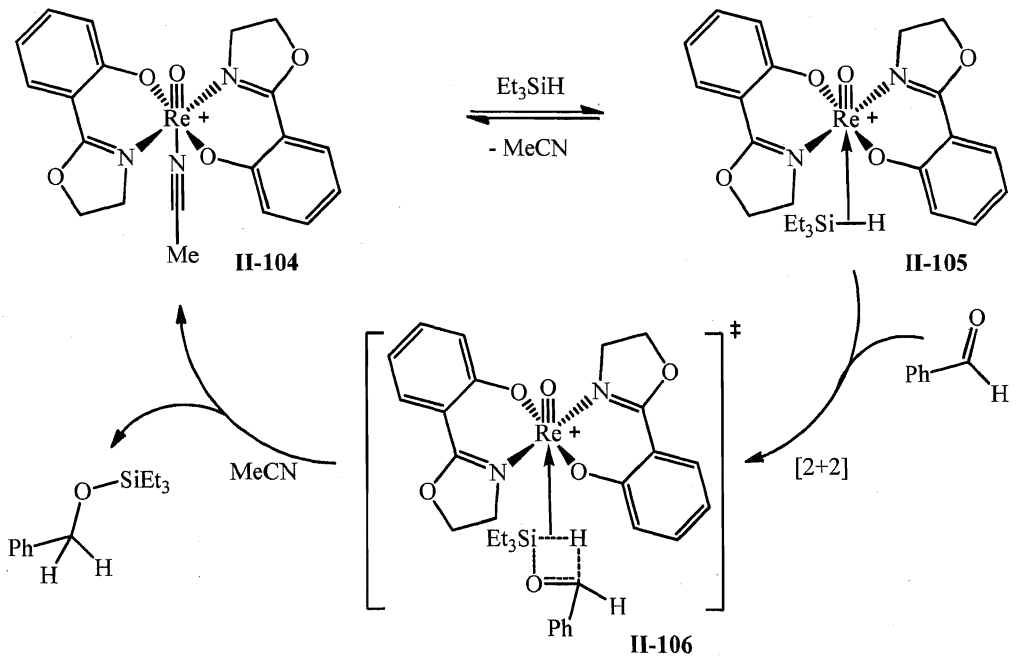

Scheme 39. Abu-Omar's mechanism for the hydrosilation of carbonyl compounds mediated by [Re(O)(hoz)$_2$(MeCN)][TFPB] (**II-104**).[13a]

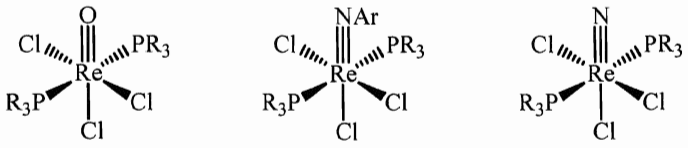

R = Ph, Cy — **II-107**

Ar = Mes, Ph; R = Ph, Cy — **II-108**

R = Ph, Cy — **II-109**

Figure 13. Rhenium complexes containing Re=X multiple bonds (X = O, NAr, N) active hydrosilation of carbonyl compounds.

documented in recent years by Bullock *et al.* for ionic hydrogenation reactions[121] and was suggested for other monooxo rhenium catalysts.[13b,d]

The stoichiometric reactivity studies as well as various kinetic experiments conducted by Abu-Omar *et al.* for a series of catalytically active rhenium complexes **II-107** – **II-109** containing Re=X multiple bonds (where X = O, NAr, N) (Figure 13) led to reconsideration of the initially proposed hydrosilation mechanism.[13c,e] The investigation of stoichiometric reactivity of the $Re(O)Cl_3(PPh_3)_2$ (**II-107**) system independently established three transformations: (i) formation of the rhenium hydride $Re(O)Cl_2(H)(PPh_3)_2$ (**II-110**) *via* chloride abstraction with silane, (ii) insertion of aldehydes into the Re-H bond to form the rhenium alkoxide $Re(O)Cl_2(OCH_2Ph)(PPh_3)_2$ (**II-111**), and (iii) silyl ether formation from the reaction of **II-111** with silane to regenerate the rhenium hydride **II-110**.[13c] All of these reactions could be hypothetically combined in a catalytic cycle for the hydrosilation of aldehydes illustrated in Scheme 40 (**A**). However, kinetic studies for each particular step in this cycle did not fit in with the overall picture. For example, a strong dependence of the rate of catalysis on the PPh_3 added (inhibition of the reaction) was found. All this led Abu-Omar *et al.* to the conclusion that complexes **II-110** and **II-111** are not the major players in the catalytic pathway, although they are capable of hydrosilation catalysis. The analogous observations were also made for the imido and nitride compounds **II-108** and **II-109**, respectively (Figure 13).[13c] In total, Abu-Omar *et al.* considered four pathways by which silane can be activated by $Re(X)Cl_n(PR_3)_2$: (1) activation by the Re=X bond *via* a [2+2] cycloaddition across the Re=X bond; (2) silane-ligand (chloride or alkoxide) metathesis; (3) oxidative addition of silane to Re(V); or (4) a heterolytic cleavage *via* a σ-bonded η^2-

silane adduct. Although, neither intermediate was observed, the first three possibilities were ruled out based on the result of kinetic experiments. Moreover, by analogy to dihydrogen activation, OA *via* homolytic cleavage of the Si-H bond is unlikely for electrophilic metals like Re(V).[13c] All this brought Abu-Omar and co-workers to a conclusion that the catalytic hydrosilation of carbonyl compounds mediated by complexes **II-107 – II-109** most likely proceeds *via* initial coordination of the silane followed by heterolytic cleavage of the Si-H bond (Scheme 40, **B**). Although, in some cases the Re-H hydride species (**II-112**) was observed during catalysis its reactivity was not sufficient in order to participate in the catalytic cycle.[13c,e]

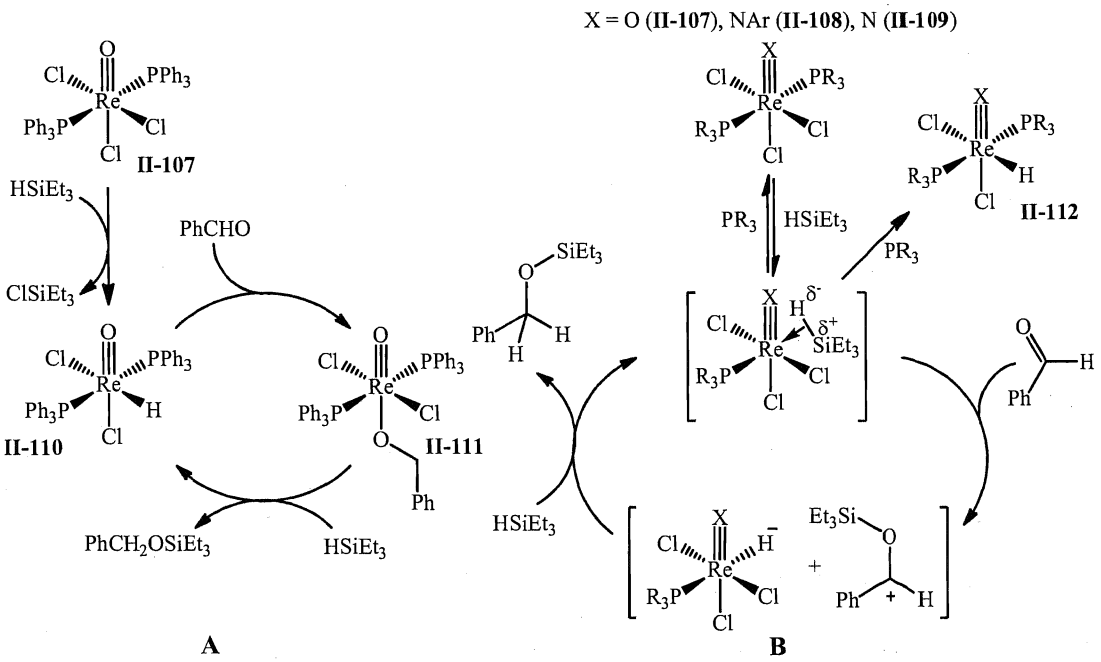

Scheme 40. Original (**A**) and revised (**B**) mechanism of carbonyl hydrosilation mediated by **II-107 – II-109**.

Despite the recent interest in the application of high oxidation transition metal complexes (such as oxo rhenium and molybdenum compounds) in hydrosilation,[11a,b, 12, 13, 116, 119-120] a few novel low-valent systems have appeared in the literature in the past two years. In 2009, Berke *et al.* presented a convenient and efficient method for the hydrosilation of ketones and aldehydes with the use of $Re(NCMe)_3Br_2(NO)$ (**II-113**) and $Re(THF)(NCMe)_2Br_2(NO)$ (**II-114**).[122] When the hydrosilation of aromatic aldehydes

was conducted, both complexes **II-113** and **II-114** showed a tolerance for a variety of electron-withdrawing and electron-donating substituents in the aryl rings. Berke *et al.* also found that this reaction is quite sensitive to the solvent applied and the fastest hydrosilation and the highest yields were observed for dichloromethane, 1,4-dioxane, and

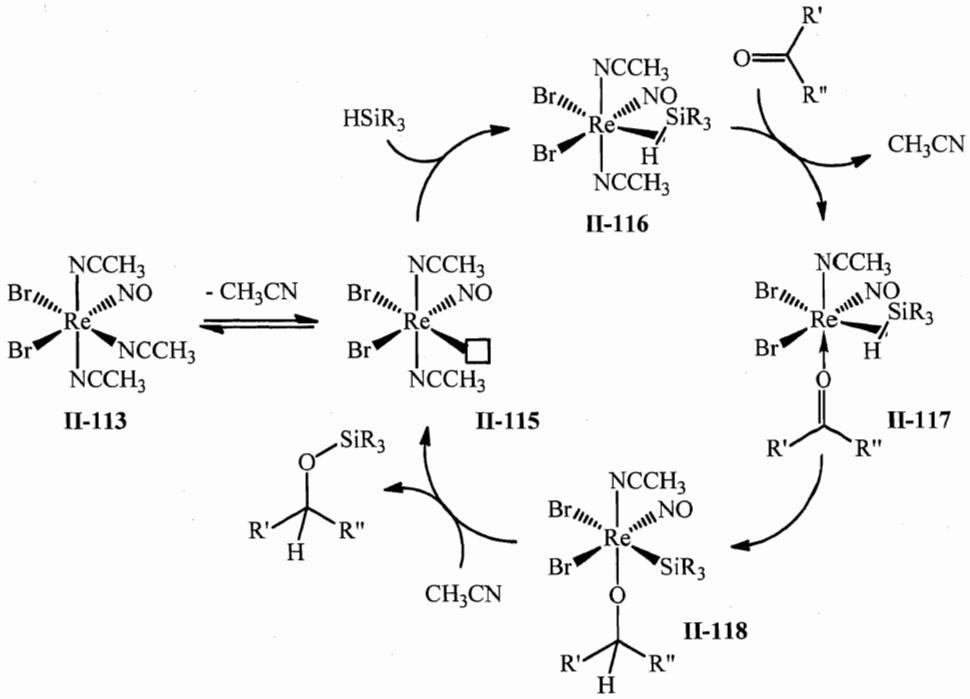

Scheme 41. Berke's mechanism for ketone hydrosilation mediated by $Re(NCMe)_3Br_2(NO)$ (**II-113**).

chlorobenzene. Utilization of coordinating solvents, such as CH_3CN and THF, afforded only modest yields of silyl ethers, suggesting the presence of a ligand dissociation step in the catalytic cycle. The proposed mechanism for the catalytic ketone hydrosilation mediated by **II-113** is shown in Scheme 41 and includes the following steps: (i) CH_3CN dissociation (observed by ^{1}H-NMR), (ii) addition of silane leads to the formation of the η^2-$HSiR_3$ intermediate **II-116** (alternatively, oxidative addition of silane affording silyl hydride species was suggested but no experimental evidence for this was obtained by NMR), (iii) coordination of the ketone and direct inter-ligand transfer of a hydride from the silane ligand (or hydride shift from the metal in the case of silane oxidative addition) gives the silyl organyloxy complex **II-118**, which reductively eliminates the silyl ether regenerating the catalyst **II-115**.[122] The formation of the silane σ-complex **II-116** was

suggested based on the ^{1}H NOE NMR experiment when saturation of the dissociated acetonitrile methyl group gave rise to a very broad (> 100 Hz) NOE signal, which was assigned to the Re attached Si-H group. In addition, a long range $^{13}C,^{1}H$-correlation NMR experiment did not reveal the simultaneous presence of a classical rhenium-bound hydride and coordinated acetonitrile in the ligand sphere. Despite the reported NMR studies, the proposed mechanism still remains speculative and requires more detailed investigation.[122]

The migratory insertion of carbonyl into the M-H bond was postulated recently by Mindiola and co-workers for the catalytic pathway promoted by $[(PN^{iPr3})Ni(\mu^2\text{-}Br)]_2$ (**II-119**, PN^{iPr3} = *N*-(2-(diisopropylphosphino)-4-methylphenyl)-2,4,6-triisopropylanilide) and $[(PN^{Me3})Ni(\mu^2\text{-}Cl)]_2$ (**II-120**, PN^{Me3} = *N*-(2-(diisopropylphosphino)-4-methylphenyl)-2,4,6-trimethylanilide).[123] No physicochemical studies were performed on the system, however, on the basis of stoichiometric reactivity of complexes **II-119** and **II-120** as well as careful NMR analysis of the catalytic and stoichiometric reaction mixtures Mindiola *et al.* suggested a mechanism depicted in Scheme 42. Activation of the catalyst requires the addition of KO^{t}Bu, followed by the treatment with Et_3SiH, which generate the nikel hydride species **II-121** *in situ*. Unfortunately, all attempts to isolate and characterize complex **II-121** were unsuccessful. However, upon stoichiometric treatment of **II-119** with KO^{t}Bu/Et_3SiH, Mindiola *et al.* did observe the formation of such hydrides in solution on the basis of combined ^{1}H- and ^{31}P-NMR studies.[123] No further reaction with

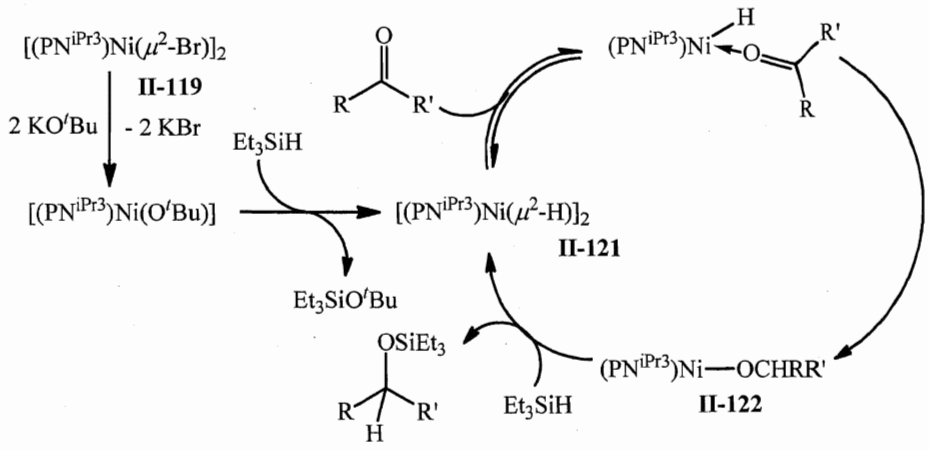

Scheme 42. Mindiola's mechanism for ketone hydrosilation mediated by $[(PN^{iPr3})Ni(\mu^2\text{-}Br)]_2$ (**II-119**).

Et_3SiH was detected. Introduction of the ketone to the mixture leads to initial coordination of the carbonyl, followed by a 1,3-hydride shift to afford the alkoxy intermediate **II-122**, which upon further treatment with the silane undergoes alkoxide/hydride exchange (σ-bond metathesis) releasing the silyl ether and regenerating the catalyst.[123] A process, similar to the last step, has been previously observed in the copper-based hydrosilation catalysis.[124]

The most recent example of the mechanistic studies of carbonyl hydrosilation was demonstrated by Tilley *et al.* for cationic PNP-supported iridium silylnene complexes $[(PNP)(H)Ir{=}SiRR'][B(C_6F_5)_4]$ (R = R' = Ph; R = H, R' = Mes) (**II-123**).[125] Analogously to the activation of alkenes by transition metal hydride silylene compounds,[84-86, 126, 127a] insertion of carbonyls into the Si-H bond of the silylene fragment was demonstrated for for $Cp^*(CO)(H)Ru{=}SiH(C(SiMe_3)_3)$ (**II-124**) and $Cp(CO)_2(H)W{=}SiH(C(SiMe_3)_3)$ (**II-**

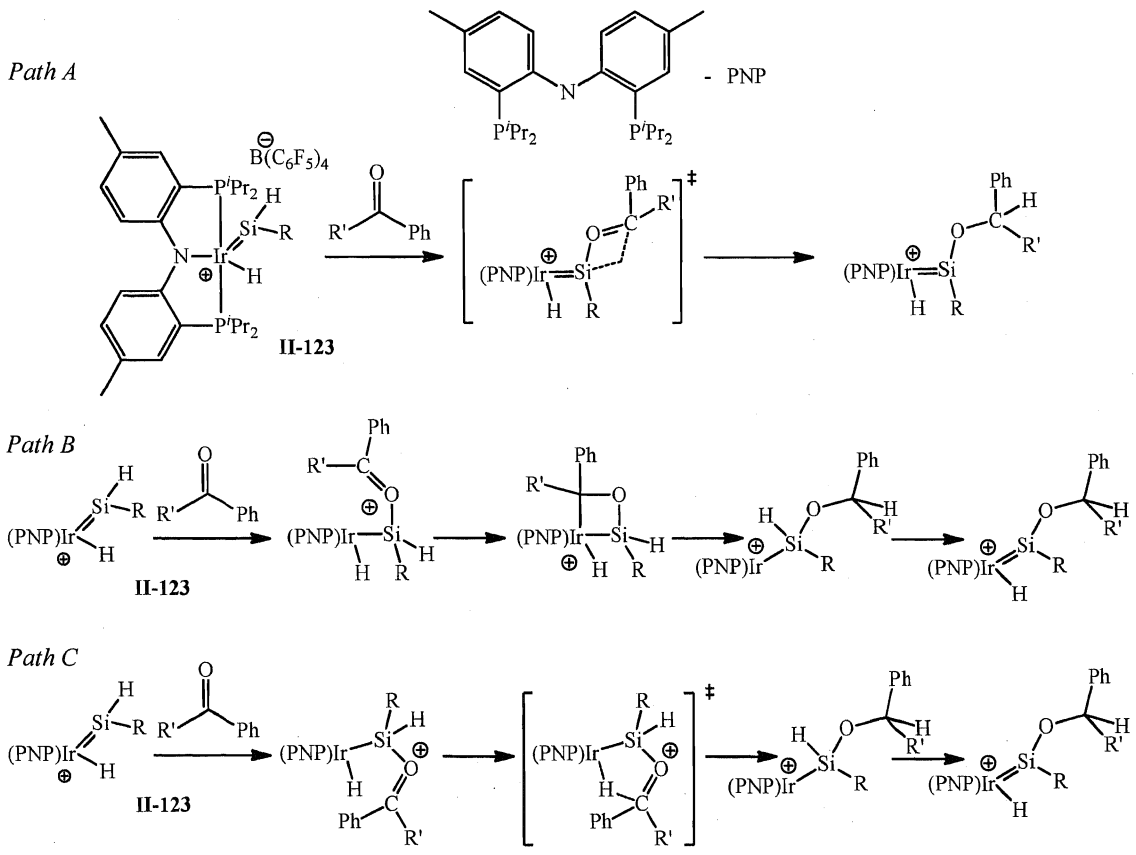

Scheme 43. Mechanism of the reaction of $[(PNP)(H)Ir{=}SiRR'][B(C_6F_5)_4]$ (**II-123**) with ketones.

125) by Tobita *et al.*[127b,c] and for $[Cp^*(PMe_3)(H)Ir{=}SiR_2][B(C_6F_5)_4]$ (R = Ph, Mes) (**II-126**) by the group of Tilley.[128] The last complex was also found to be active in catalytic hydrosilation of ketones, however, no detailed mechanistic studies for this process were reported at that time. Based on the available experimental evidence and literature data for the reactivity of silylene compounds towards organic substrates, Tilley *et al.* postulated three pathways for the reactivity of **II-123** towards ketones (Scheme 43).[125] One of them (*A*) involves direct addition of the carbonyl group to the Si-H bond. A similar process was suggested for the reactions of alkenes with $[\{Cp^*(P^iPr_3)(H)_2Ru{=}SiH(Ph)\}(Et_2O)][B(C_6F_5)_4]$ (**II-56**) (see Glaser-Tilley hydrosilation mechanism, Scheme 22).[84-86] A second path includes a [2+2]-cycloaddition to afford an intermediate metallocycle, which could reorganize *via* reductive elimination of the C-H bond, followed by α-hydrogen migration (Scheme 43, *path B*). Such a cycloaddition process has been previously described for reactions with isocyanates.[129] A third route (*C*) implies the formation of a base-stabilized silylene complex, which activates the carbonyl substrate to the reaction with the hydride ligand, followed by α-hydrogen migration. Recently, Tobita *et al.* proposed mechanisms *B* and *C* for the reaction of **II-124** with ketones and aldehydes.[127c] However, further theoretical investigations of the reaction of the related compound **II-125** with acetone supported a reaction sequence similar to that presented in path *C*. This path involves the initial formation of a base-stabilized silylene complex, followed by a nucleophilic attack of the transition metal hydride.[130]

The overall cycle suggested by Tilley *et al.* for the catalytic hydrosilation of ketones with complex **II-123** is presented in Scheme 44 and includes two possible routes.[125] Similar to the Ojima's traditional scheme,[10b, 105] the first step of *route A*, α-migration from iridium silylene complex **II-123**, generates a transient silyl complex (**A**). Subsequent coordination of the ketone to the vacant site on the iridium (**B**), followed by insertion into the Ir-Si bond, generates an iridium alkyl derivative (**C**). The release of the product could then proceed *via* activation of the silane substrate by the Si-H oxidative addition, followed by reductive elimination of the product to complete the catalytic cycle.

A second possible mechanism (Scheme 44, *route B*) proceeds *via* a silylene complex and, analogously to the pathway postulated for the stoichiometric reactivity of **II-123** with carbonyl compounds (Scheme 43, *path A*), involves coordination of the ketone

substrate to the silicon center to form a base-stabilized silylene ligand (**E**). Similar complexes were reported by Tilley *et al.* for the stoichiometric reaction of **II-123** with 4-dimethylaminopyridine (DMAP), DMF and benzophenone leading to the formation of the adducts [(PNP)(H)Ir=SiPh$_2$(DMAP)][B(C$_6$F$_5$)$_4$] (**II-127**), [(PNP)(H)Ir=SiH(Mes)(DMF)][B(C$_6$F$_5$)$_4$] (**II-128**), and [(PNP)(H)Ir=SiPh$_2$(O=CPh$_2$)][B(C$_6$F$_5$)$_4$] (**II-129**), respectively (Figure 14).[125] Such coordination of a ketone to the Lewis basic silylene substituent increases the electrophili-

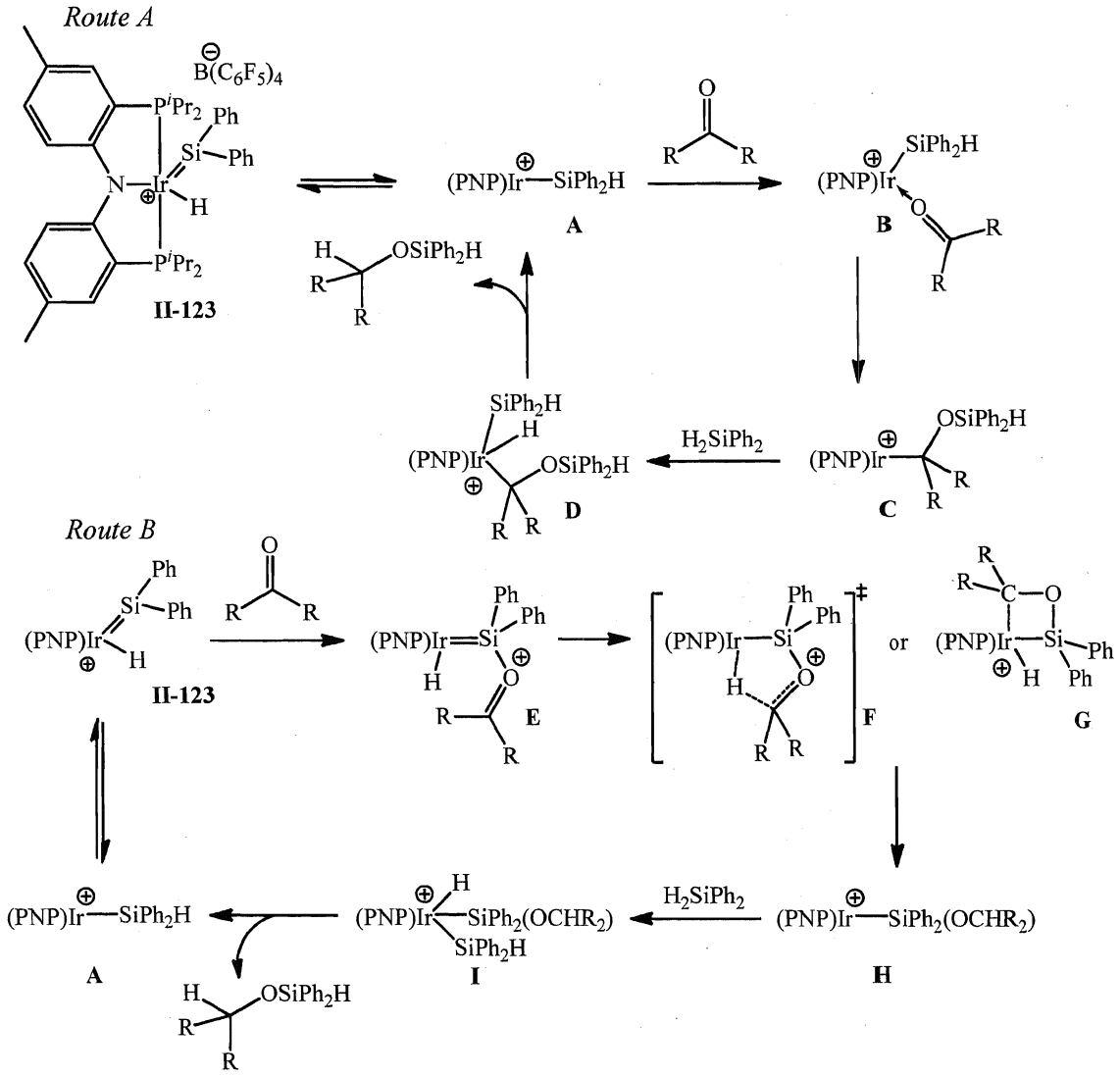

Scheme 44. Tilley's mechanism of ketone hydrosilation mediated by [(PNP)(H)Ir=SiRR'][B(C$_6$F$_5$)$_4$] (**II-123**).

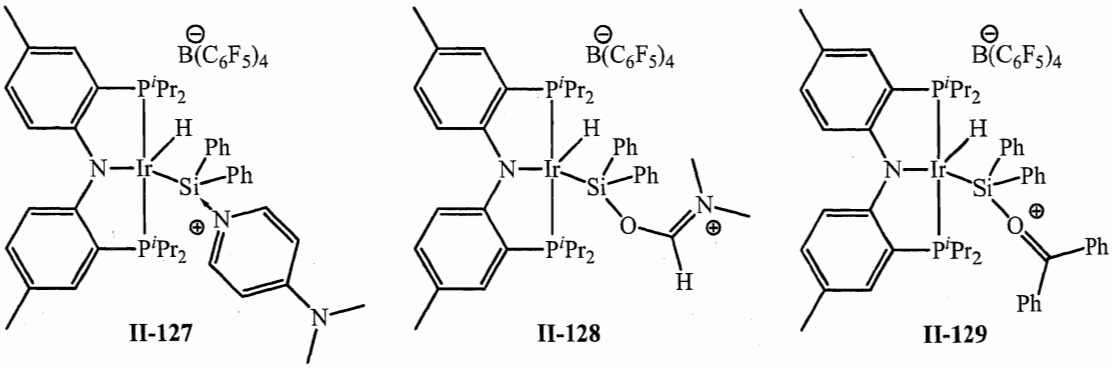

Figure 14. Base-stabilized iridium silylene complexes **II-127 – II-129**.

city of the carbonyl carbon, therefore activating it for further transformations. Taking this into account, one could suggest the shift of the iridium bound hydride to the carbonyl group *via* a five-membered transition state (**F**) to give a silyl intermediate (**H**). Alternatively, **H** could be produced by a [2+2]-cycloaddition of the ketone (**G**), followed by C-H reductive elimination. Further oxidative addition of Ph_2SiH_2 (**G** → **I**) and reductive elimination of the product generates a transient silyl complex (**A**), which after α-migration of the hydride could regenerate the silylene catalyst and complete the catalytic cycle.[125] Unfortunately, deuterium labelling stoichiometric experiments, performed by Tilley *et al.* in order to differentiate between the two pathways, did not provide insight into the mechanism and suggest the presence of more than one catalytic schemes. NMR studies of the catalytic reaction using 10 mol. % of **II-123**, Ph_2SiH_2 and benzophenone revealed the presence of a base-stabilized complex **II-129** as the major species in the mixture, which suggests that the reaction predominantly goes *via* the *route B*. On the other hand, *route A* could not be completely excluded as the observed intermediate **E** could be in equilibrium with the silyl derivative **B** (Scheme 44).[125]

II.2.3.2 Hydrosilation of imines

The mechanistic aspects concerning the hydrosilation of imines are generally considered to be analogous to those reported for carbonyls.[7, 107, 108] Nevertheless, a few different mechanisms have been suggested in the literature on the basis of available theoretical and experimental data. Thus, Buchwald *et al.* in 1996 demonstrated the application of the (EBHTI)TiF_2 (**II-84**)/$PhSiH_3$/R'OH system for the asymmetric catalytic

addition of hydrosilanes to imines.[131a] They suggested that once the active catalyst, (EBHTI)TiH (**II-130**), has been generated, the reaction proceeds by a catalytic cycle similar to that for the titanocene-catalyzed hydrosilation of ketones.[9e] Insertion of the imine into the Ti-H bond of **II-130** would give the corresponding amido-titanium complex **II-131**. Subsequent σ-bond metathesis of **II-131** with $PhSiH_3$ *via* a four-centered

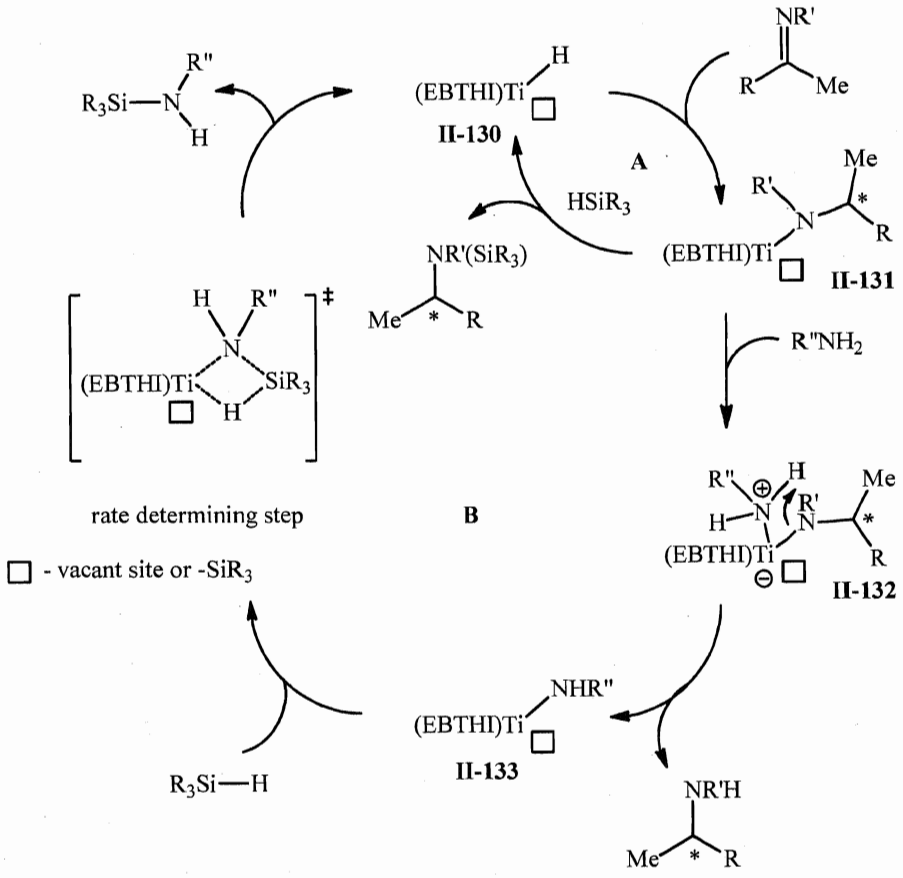

Scheme 45. Buchwald's mechanism of asymmetric hydrosilation of imines mediated by (EBHTI)TiF_2 (**II-84**)/$PhSiH_3$/R'OH system.

transition state would afford the silylated amine and regenerate the titanium hydride compound **II-130** (Scheme 45, **A**). An analogous scheme has been also proposed for titanocene-catalyzed hydrogenation of imines on the basis of kinetic and thermodynamic studies.[131] A few years later, Buchwald and co-workers found that the introduction of the primary amine additives to the reaction mixture significantly enhances the catalysis.[131b] The catalytic cycle initially proposed for this process is analogous to that suggested for

the addition of silanes to ketones (see Scheme 35)[9e] and is based on the intramolecular hydrogen transfer from the primary amine into an amido substituent in **II-132** leading to the formation of amide **II-133**. Further σ-bond metathesis of **II-133** with silane affords silylated amine and recovers the catalyst (Scheme 45, **B**). Alternatively, the effect of added amine could be explained by the route depicted in Scheme 46, which presents the case of intramolecular amine exchange. Unfortunately, the viability of these pathways has not been approved experimentally.[131b]

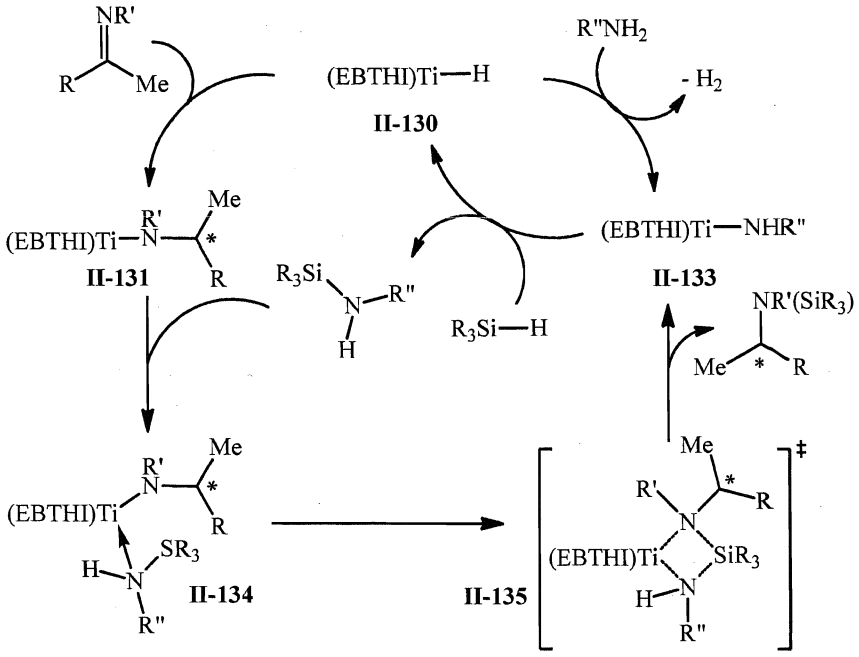

Scheme 46. Alternative mechanism of hydrosilation of imines in the presence of primary amines mediated by **II-84**/$PhSiH_3$/R'OH system.

A mechanism for the catalytic hydrosilation of imines, identical to Buchwald's original cycle (Scheme 45, **A**), was also proposed by the group of Takaki[132] for Yb(η^2-Ph_2C=NAr)$(hmpa)_n$ (**II-136**, Ar = Ph, *p*-C_6H_4F; hmpa = hexamethylphosphoric acid triamide, $O=P(NMe_2)_3$; Scheme 47). Based on the stoichiometric reactivity of **II-136** they suggested a catalytic cycle, which involves formation of the hydride species **II-137**,[e] followed by insertion of the imine into the Yb-H bond to form the bisamide derivative **II-**

[e] Takaki *et al.* do not specify the origin of the reaction of **II-36** with $PhSiH_3$, which leads to the formation of hydride species **II-137**. See ref. 132.

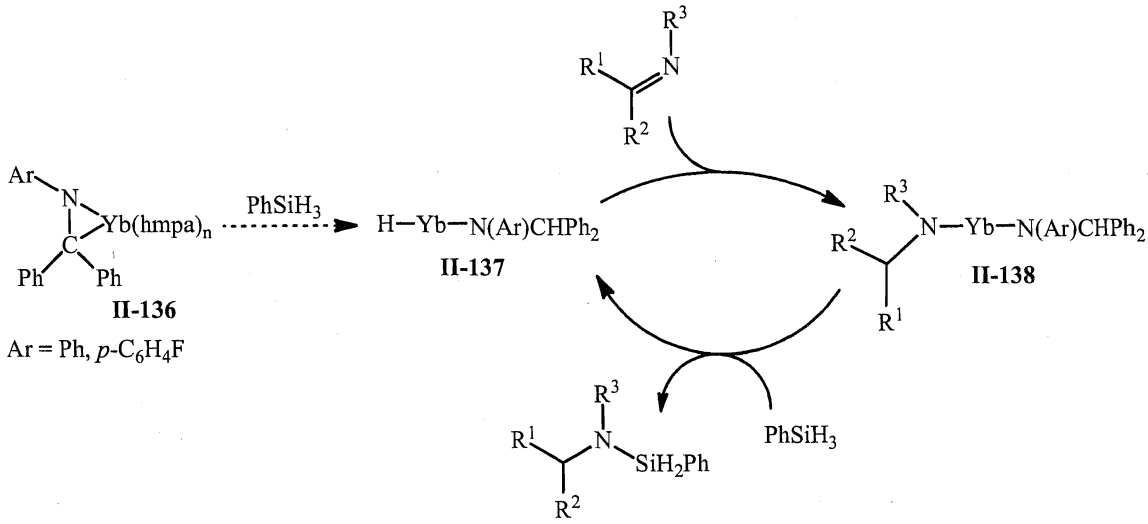

Scheme 47. Suggested mechanism for the catalytic hydrosilation of imines mediated by Yb(η^2-Ph_2C=NAr)$(hmpa)_n$ (**II-136**).

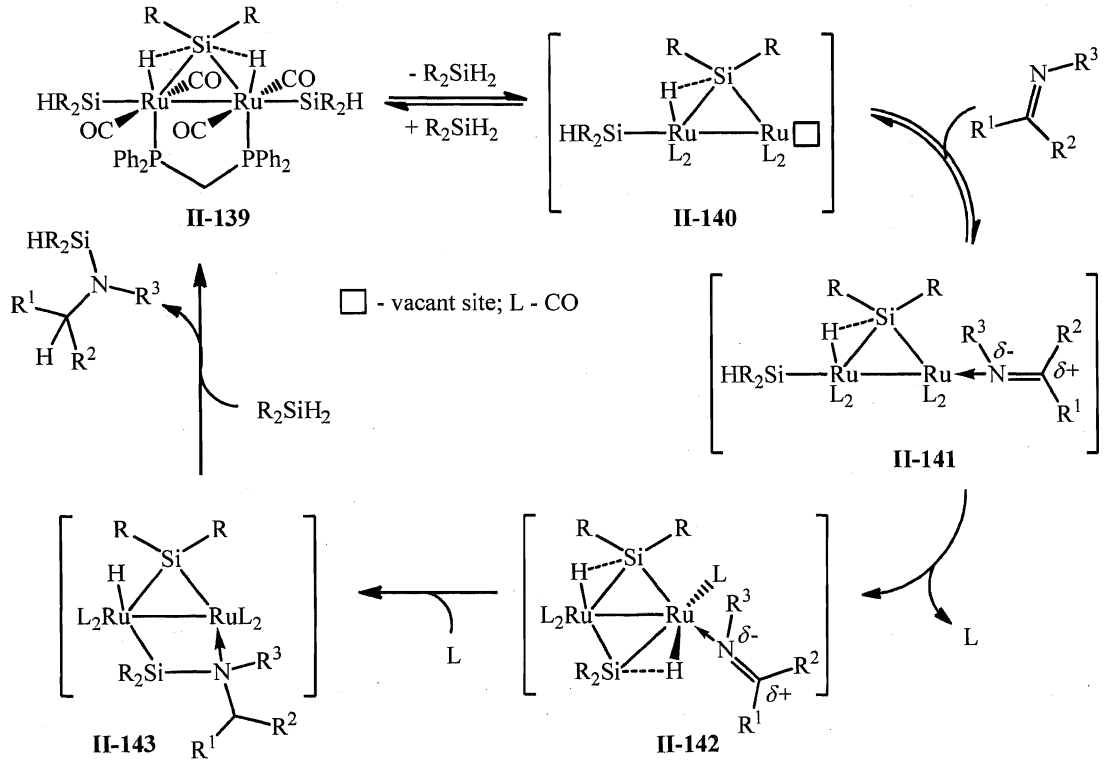

Scheme 48. Mechanism for imine hydrosilation catalyzed by $\{Ru(CO)_2(SiTol_2H)\}_2$(μ-dppm)(μ-η^2:η^2-H_2SiTol_2) (**II-139**).

138. Subsequent σ-bond metathesis of **II-138** with $PhSiH_3$ furnishes the cycle recovering the catalyst **II-137**.[132]

A novel scheme for catalytic hydrosilation of imines was postulated by Kira *et al.* for the μ-silane diruthenium complex $\{Ru(CO)_2(SiTol_2H)\}_2(\mu\text{-dppm})(\mu\text{-}\eta^2\text{:}\eta^2\text{-}H_2SiTol_2)$ (**II-139**).[133] The proposed cycle is based on the labile nature of the $\mu\text{-}\eta^2\text{:}\eta^2\text{-}H_2SiTol_2$ ligand in **II-139**, which could account for the formation of the unsaturated intermediate **II-140** (Scheme 48). Further coordination of the imine substrate to **II-140** and dissociation of the carbonyl ligand, followed by Si-H activation of the silyl substituent and insertion of the imine, affords the μ-aminosilyl complex **II-143**. Treatment of the latter with R_2SiH_2 gives the hydrosilation product and recovers the catalyst.[133] It should be noted that, although a number of nonclassical complexes bearing M···H-Si interactions were reported (see chapt. II.1), compound **II-139** presents the rare example of the catalysts of this type.[134] The catalytic cycle involving the cooperative functions of the two Ru metals was originally suggested for the hydrosilation of imines and, moreover, μ-iminosilyl intermediates similar to **II-143** (Scheme 48) were isolated and fully characterized.[133]

II.2.4 Mechanisms of TM catalyzed hydrosilation of nitriles

The transition metal mediated hydrosilation of nitriles is an extremely rare case of a catalytic process.[7] Depending on the system, addition of hydrosilanes to the C≡N bond provides a cheap and efficient method for the production of silylated imines and bis(silyl) amines. These products find wide applications in a variety of organic transformations, including the preparation of biologically active and pharmaceutically relevant molecules (Scheme 49).[135] The first example of transition metal catalyzed hydrosilation of organic nitriles was reported in 1970 by Chalk for $Co_2(CO)_8$ (**II-144**). Thus, expanding the scope of alkene substrates for Rh- and Co-catalyzed hydrosilation reactions, Chalk found that treatment of methacrylonitrile with chlorodimethylsilane in the presence of complex **II-144**, surprisingly, yields the product of 1,4-silane addition, $Me_2HC\text{-}CH{=}CH\text{-}N(SiMe_2Cl)_2$.[136] However, only in 1985, Murai *et al.* expanded the scope of Co-catalyzed hydrosilation of nitriles and suggested a plausible mechanism for this process (Scheme 50).[137] On the basis of the stoichiometric reactivity of complex **II-144** towards silanes, Murai and co-workers postulated that the active catalyst for hydrosilation may be the

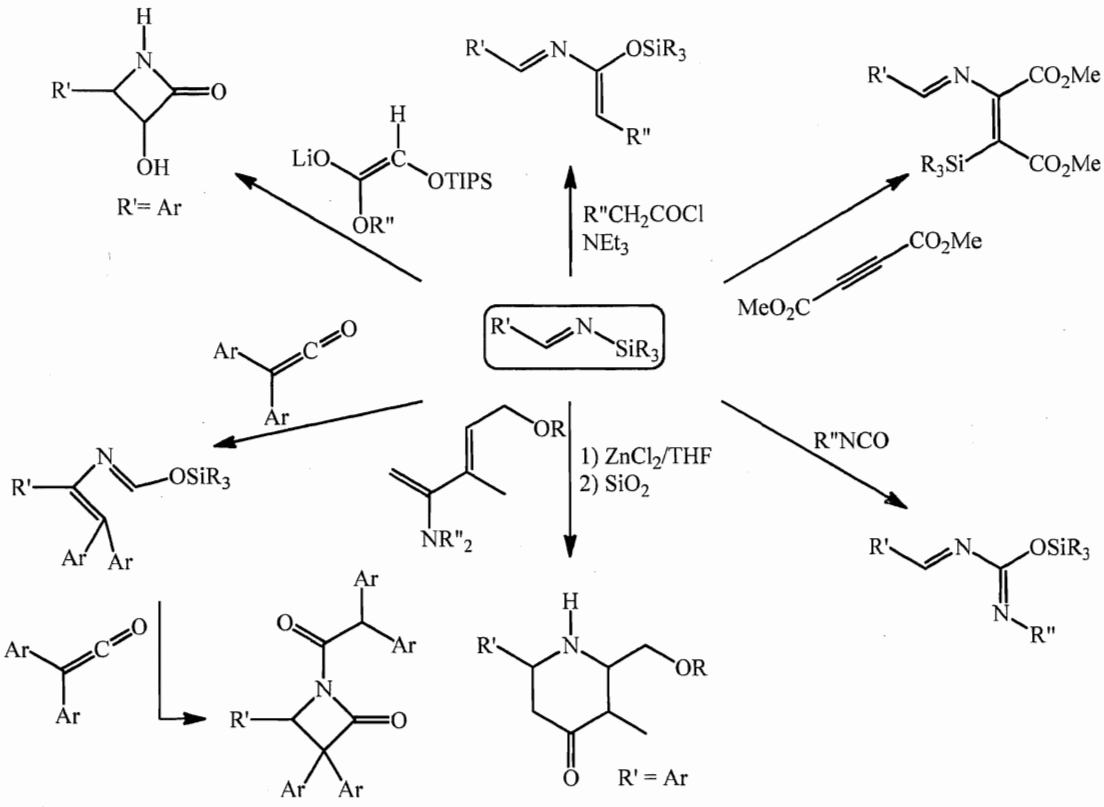

Scheme 49. Applications of silylated imines R'CH=N(SiR_3) in organic synthesis.[135]

(trialkylsilyl)cobalt carbonyl complex $R_3SiCo(CO)_4$ (**II-145**), which is easily generated from a hydrosilane and **II-144**.[137b] Further nucleophilic attack of the nitrile lone pair on **II-145** could lead to the heterolytic splitting of the Si-Co bond and generation of the *N*-silylnitrilium intermediate **II-146** and the anionic cobalt species $Co(CO)_4^-$. Subsequent hydrogen transfer to **II-146** from $HSiR_3$ or $HSiR_3Nu$ (a pentacoordinate silicon, where

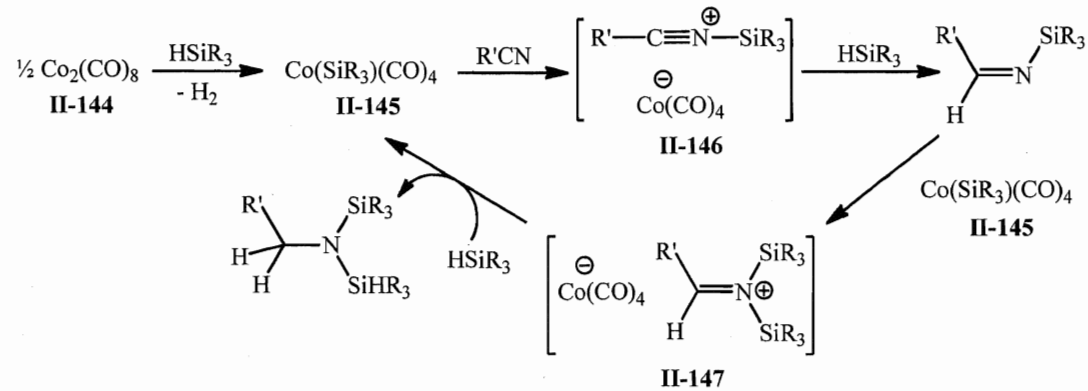

Scheme 50. Murai's mechanism of nitrile hydrosilation mediated by $Co_2(CO)_8$ (**II-144**).

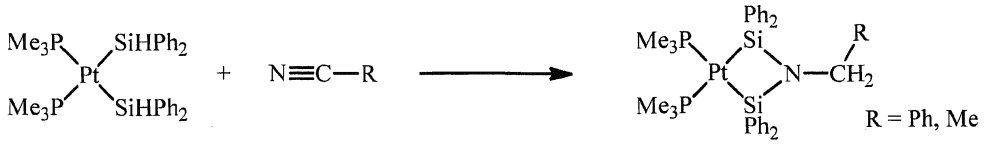

II-148 **II-149**

Scheme 51. Addition of nitriles to a bissilyl platinum diphosphine complex $Pt(SiHPh_2)_2(PMe_3)_2$ (**II-148**).

Nu may be $Co(CO)_4^-$) would result in the formation of a silylimine. A similar process may be repeated for R'HC=N(SiR_3) to give the bis(silylated) amine as the final product (Scheme 50).[137] The feasibility of the proposed catalytic scheme was further supported by stoichiometric experiments, which indicated the transformation of *N*-alkylnitrilium ion **II-146** to the imine upon treatment with $HSiEt_3$.[138] Furthermore, the observation of fast (compared with PhCN) hydrosilation of PhHC=N(SiR_3) led Murai *et al.* to the conclusion that the formation of the *N*-alkylnitrilium **II-146** and *N,N*-disilyliminium **II-147** ions is the rate-determining step in the postulated catalytic cycle.[137b]

A few other rhodium, ruthenium, iridium, and platinum catalytic systems active in the hydrosilation of organic nitriles appeared in the literature in early 1980's – late 1990's, however no mechanistic studies were reported.[139] The main stoichiometric hydrosilation reactions of nitriles were carried out in the beginning of 2000's. Thus, in 2001, Osakada and co-workers established that the stoichiometric double addition of the Si-H bonds of $Pt(SiHPh_2)_2(PMe_3)_2$ (**II-148**) to nitriles afforded 3-aza-2,4-disilaplatinacyclobutanes (**II-149**) (Scheme 51).[140] At the same time, Ko *et al.* showed the addition of 1,2-bis(dimethylsilyl)carborane to organic nitriles catalyzed by a nickel complex containing *o*-carboranylene unit, $(Et_3P)_2Ni[o\text{-}(SiMe_2)_2C_2B_{10}H_{10}]$ (**II-150**).[141] The postulated mechanism for Ko's transformation (Scheme 52) starts with the insertion of the cyano group into one Ni-Si bond leading to the formation of a seven-membered intermediate **II-151**. Such a coupling of the M-Si bond and unsaturated organic molecules was previously demonstrated by Berry *et al.*,[142] and Tilley *et al.*[143] Subsequent migration of the other silicon atom to nitrogen affords the carbene derivative **II-152**, which after 1,3-hydrogen shift from the alkyl substituent to the Ni center generates the σ-vinyl complex **II-153**. The *N,N*-bis(silyl)enamine **II-154** is then formed *via* a reductive elimination step with the

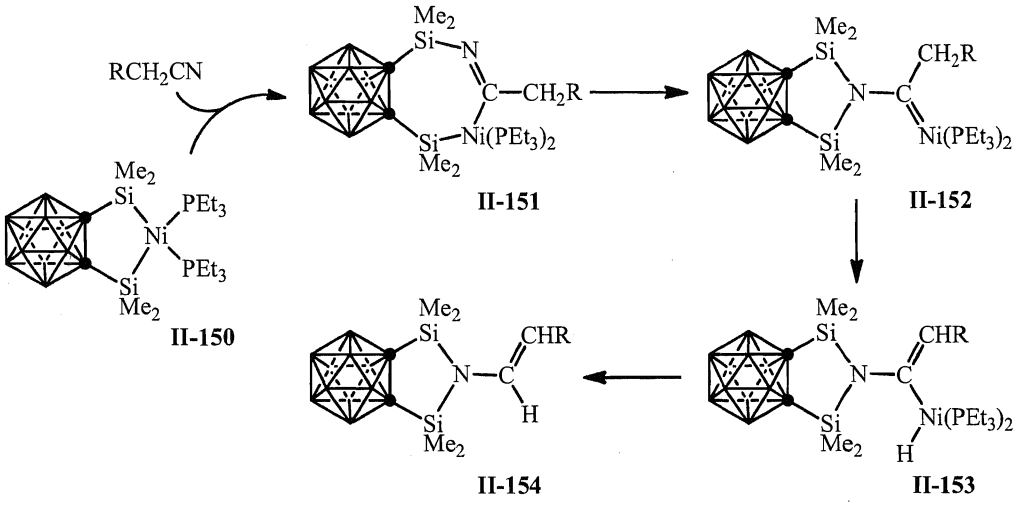

Scheme 52. Mechanism of nickel-catalyzed addition of 1,2-bis(dimethylsilyl)carborane to organic nitriles.

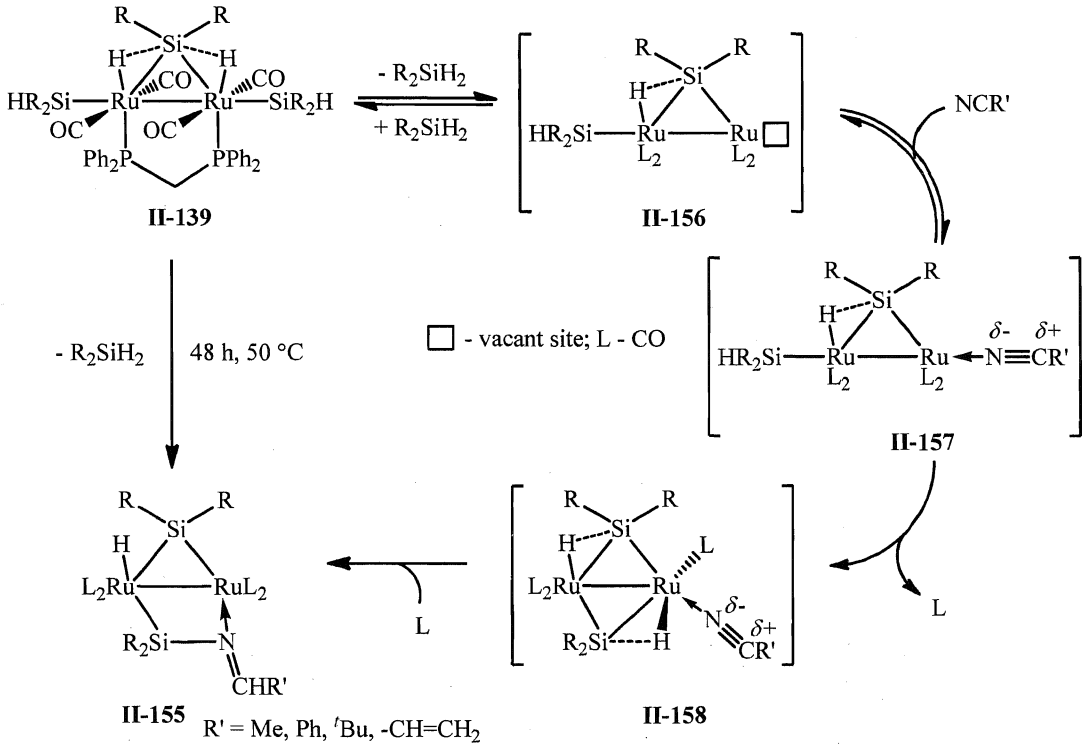

Scheme 53. Potential mechanism of stoichiometric nitrile hydrosilation promoted by $\{Ru(CO)_2(SiTol_2H)\}_2(\mu\text{-dppm})(\mu\text{-}\eta^2\text{:}\eta^2\text{-}H_2SiTol_2)$ (**II-139**).[133]

extrusion of $Ni(PEt_3)_2$. The suggested scheme is in a good agreement with catalytic experimental data presented by Ko and co-workers, however, no detailed mechanistic studies were performed.[141]

In 2003, Kira *et al.* succeeded in an unusual stoichiometric hydrosilation of organic nitriles using the μ-silane diruthenium complex $\{Ru(CO)_2(SiTol_2H)\}_2(\mu\text{-dppm})(\mu\text{-}\eta^2\text{:}\eta^2\text{-}(H_2SiTol_2)$ (**II-139**).[133] Isolation of μ-iminosilyl intermediates $Ru_2(CO)_4(\mu\text{-dppm})(\mu\text{-}SiTol_2)(\mu\text{-R'CH=NSiTol}_2)$ (**II-155**) contributed to the development of a cycle (Scheme 53) similar to that described above for the hydrosilation of imines (see Scheme 48). However, the addition of nitrile to **II-139** proceeded only stoichiometrically and the formation of the final product, a silylated imine, was not observed in the reaction. Unfortunately, Kira and co-workers did not present any reasoning for the incomplete formation of silylated imine.[133]

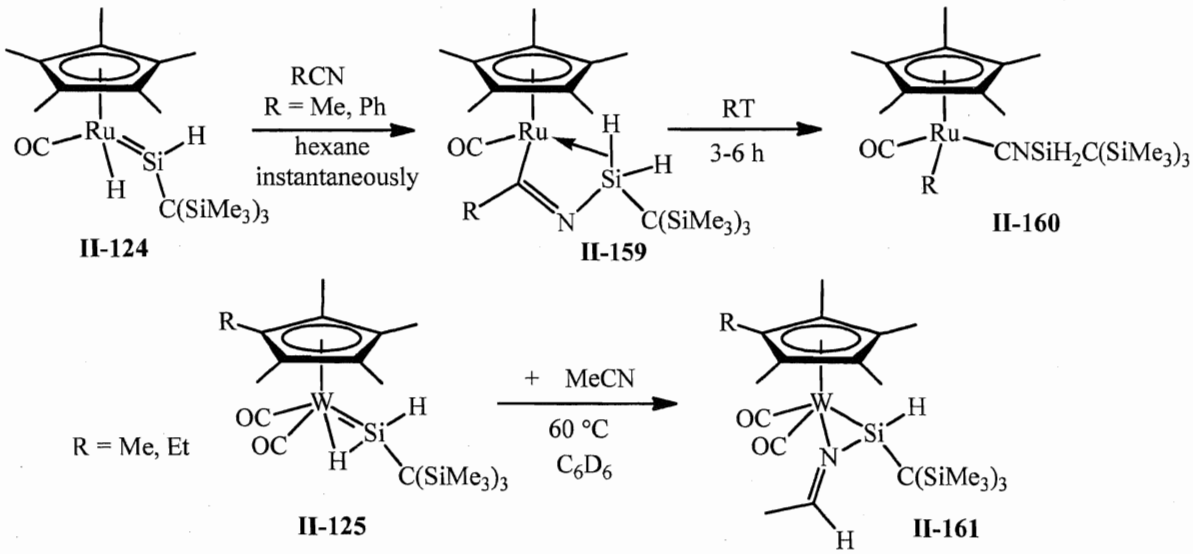

Scheme 54. Potential mechanism of stoichiometric nitrile hydrosilation promoted by $Cp^*(CO)(H)Ru=Si(H)[C(SiMe_3)_3]$ (**II-124**).

Stoichiometric addition of organic nitriles to silylene complexes, $Cp^*(CO)(H)Ru=Si(H)[C(SiMe_3)_3]$ (**II-124**) and $Cp'(CO)_2(H)W=Si(H)[C(SiMe_3)_3]$ (Cp' = Cp*, η^5-C_5Me_4Et) (**II-125**) were also reported recently by Tobita *et al.* (Scheme 54).[127b,c, 144] Thus, treatment of **II-124** with acetonitrile or benzonitrile initially leads to the formation of a product of nitrile insertion into the Ru-Si bond, the iminoacyl complex

$Cp^*(CO)Ru\{C(R)=NSiH_2C(SiMe_3)_3\}$ (**II-159**, R = Me, Ph), which was detected by NMR spectroscopy for R = Ph and isolated for R = Me. Further rearrangement of **II-159** *via* C-R bond cleavage affords the final product, $Cp^*(CO)(R)Ru\{CNSiH_2[C(SiMe_3)_3]\}$ (**II-160**). This second step is closely related to the C-C bond activation of nitriles by rhodium and iron silyl complexes, giving slilylisocyanide derivatives, reported earlier by Brookhart *et al.* and Nakazawa *et al.*[145] Based on the available literature data, Tobita and co-workers proposed two possible mechanisms for the nitrile addition to **II-124**, which are depicted in the Scheme 55.[127a] One mechanism is likely to proceed through 1,2-H migration to give a 16-electron silyl complex **A**, coordination of nitrile molecule to Ru to

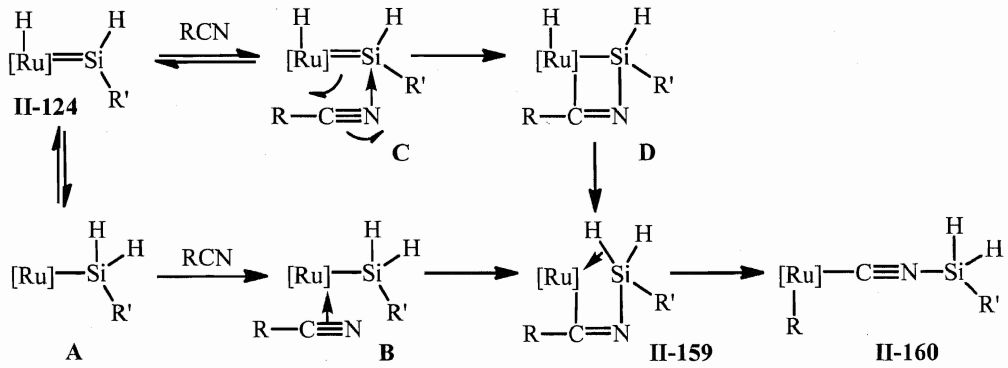

Scheme 55. Tobita's mechanism for the addition of RCN (R = Me, Ph) to $Cp^*(CO)(H)Ru=Si(H)[C(SiMe_3)_3]$ (**II-124**).

give **B**, silyl ligand migration to nitrogen, and η^2-coordination of an Si-H bond. This route is similar to the Brookhart-Nakazawa mechanism that produces metal—C≡N three-membered-ring iminoacyl compounds.[145] In contrast, the other pathway suggested by Tobita starts from the coordination of the nitrile molecule to the silylene silicon to generate **C**. Then, a [2+2]-cycloaddition reaction affords the four-membered metallacycle **D**, followed by hydride migration to silicon to form **II-59**. Further decomplexation of the η^2-Si-H bond and intramolecular C-C bond oxidative addition yields the final product **II-160**. Despite the fact that both proposed schemes seem feasible, mechanistic stoichiometric studies indicated the initial formation of a base-stabilized silylene intermediate **C**, wich could be further converted to the silyl complex **B** or form the metallacycle derivative **D**. All attempts to establish experimentally which mechanism is operative were unsuccessful.[127a]

The treatment of the silylene tungsten complex $Cp'(CO)_2(H)W{=}Si(H)[C(SiMe_3)_3]$ (**II-125**) with MeCN surprisingly leads to the formation of the {κ^2(*N,Si*)-ethylideneamino}silyl complex $Cp'(CO)_2W[\kappa^2(N,Si)\text{-}Si(H)(N{=}CHMe)\{C(SiMe_3)_3\}]$ (**II-161**) (Scheme 54), which could be accounted for by cooperative reactivity of the hydrido and silylene ligands in **II-125**.[144] Analogous stoichiometric reaction of **II-125** with ^{t}BuCN revealed the formation of $Cp'(CO)_2(H)W{=}Si\text{-}(N{=}CH^tBu)\{C(SiMe_3)_3\}$ (**II-162**) as a by-product. Based on these observations and the reactivity of related silylene complexes towards carbonyl compounds (see above),[125, 127-130] Tobita *et al.* postulated the mechanism illustrated in Scheme 56. Similarly to the ruthenium complex **II-124**, it was suggested that the reaction of **II-125** with nitriles starts with the formation of a base-stabilized silylene derivative.[130, 144]

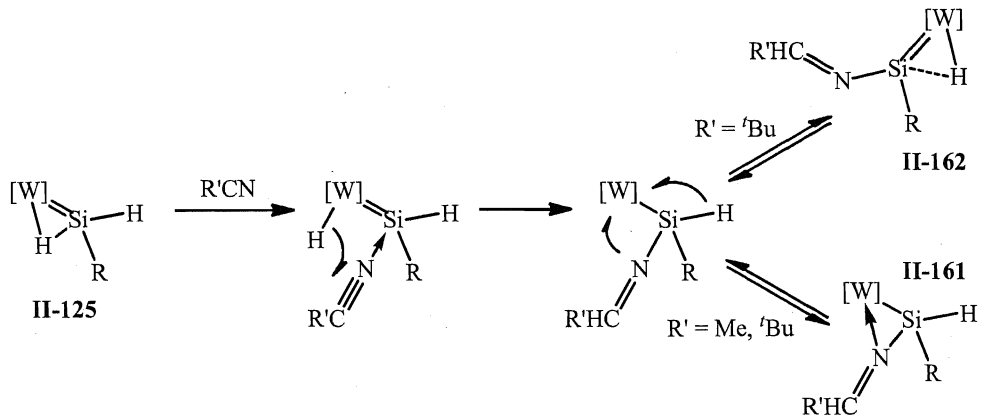

Scheme 56. Tobita's mechanism for addition of RCN (R = Me, ^{t}Bu) to $Cp'(CO)_2(H)W{=}Si(H)[C(SiMe_3)_3]$ (**II-125**).

Lastly, selective monosubstitution of CH_3CN with hydrosilanes to form silylated imines $MeHC{=}N(SiR_3)$ was accidentally observed by Pitter *et al.* during the catalytic hydrosilation of CO_2 mediated by ruthenium acetonitrile complexes $RuX_3(NCMe)_3$ (**II-163**) and $RuX_2(NCMe)_4$ (**II-164**) (X = Br, Cl).[146] The authors were unable to isolate the product $MeHC{=}N(SiR_3)$, which is known to be particularly unstable due to the imine-enamine tautomerism.[147] However, their preliminary results on the hydrosilation of ^{t}BuCN with Me_2PhSiH in the presence of catalytic amounts of *mer*-$[RuCl_3(MeCN)_3]$ indicated that ^{t}Bu-CH=N($SiMe_2Ph$) could be formed with approximately 70 % yield.[146]

No studies on the mechanistic aspects of this process have been reported, neither has a catalytic cycle been proposed to date.[146]

II.2.5 Mechanisms of TM catalyzed silane alcoholysis and aminolysis

The silane alcoholysis and aminolysis reactions constitute an extremely mild and efficient method of protecting hydroxyl and amino functions by trialkyl or aryl-silyl groups (Scheme 57).[148] Apart from the importance of the silyl ethers as protecting groups in organic chemistry, they also play a valuable role in inorganic, material, and polymer chemistry as precursors to sol-gels and other condensed siloxane products.[149] At the same time, transition metal catalysed aminolysis of silanes provides an elegant and alternative route to silazanes, which are attractive precursors for important silicon nitride materials.[150] The classical way of making silazanes is based on the aminolysis or ammonolysis of chlorosilanes, with the disadvantages being the formation of large amounts of ammonium halide by-products.[151]

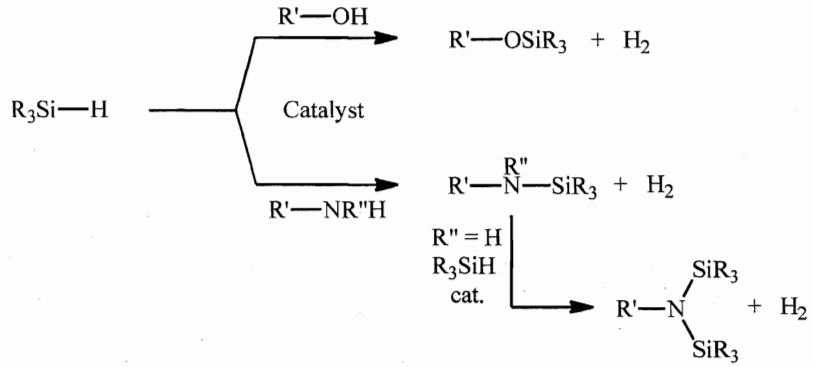

Scheme 57. Catalytic alcoholysis and aminolysis of hydrosilanes.

The high enthalpic driving force for the formation of oxygen-silicon and nitrogen-silicon bonds, together with the entropically favourable generation of dihydrogen, generally results in clean and quantitative conversions of these reactions. However, the alcoholysis and aminolysis of hydrosilanes require a catalyst because alcohols and amines are not generally sufficiently nucleophilic to attack hydrosilanes. Strongly nucleophilic or electrophilic catalytic systems can be used to promote these transformations,[149c] and a large variety of transition metal complexes have been reported to be active in the catalytic alcoholysis and/or aminolysis of R_3SiH substrates.[125, 152-163, 165] Since both processes are

strongly related, this chapter will mostly describe transition metal mediated dehydrogenative additions of hydrosilanes to alcohols, although few examples of mechanistic studies of catalytic aminolysis will be also discussed.

Despite the diversity of catalytic systems for silane alcoholysis, most of the known mechanisms of this process imply silane activation by an electrophilic metal center, making it amenable to an attack by an external nucleophile.[152-159] For the first time, homogeneous stoichiometric silation of alcohols and amines mediated by silylcobalt carbonyls $Co(SiR_3)(CO)_4$ (**II-145'**) appeared in the literature in 1969.[65b, 152a] The intensive studies of the transition metal catalyzed homogeneous alcoholysis of hydrosilanes started in 1970's with the use of cobalt complexes $Co_2(CO)_8$ (**II-144**)[153] and $CoH_2(PPh_3)_3[Si(OEt)_3]$ (**II-165**),[154] as well as Wilkinson's catalyst, $RhCl(PPh_3)_3$ (**II-79**).[155] Thus, in 1970, Chalk demonstrated for the first time the **II-144**-catalyzed coupling of hydrosilanes with alkyl and aryl alcohols and proposed the mechanism outlined in Scheme 58.[153] A year later, a similar transformation was shown by Haszeldine *et al.* for **II-165**.[154] Later, Parish *et al.* proposed an analogous scheme for the iridium chloride complexes $[IrCl(C_8H_{14})_2]_2$ (**II-166**) and $IrCl(CO)_2(H_2NC_6H_4Me\text{-}p)$ (**II-167**), which catalyze silane alcoholysis *via* the oxidative addition of hydrosilanes, followed by exchange between a silyl intermediate and an alcohol to form a dihydride species.[156] The latter upon oxidative addition of another molecule of silane recovers the hydride silyl catalyst with the release of a molecule of H_2.

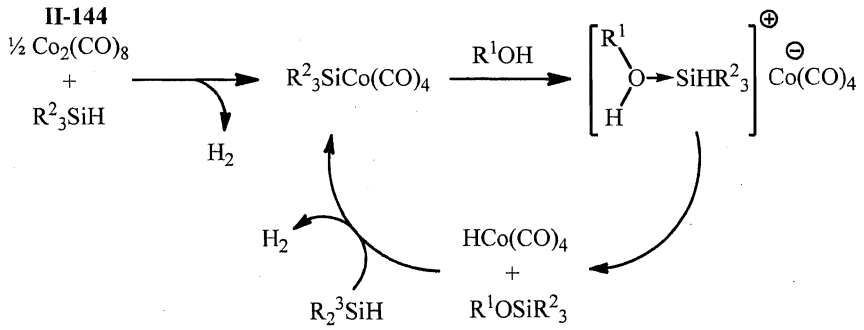

Scheme 58. Mechanism for silane alcoholysis mediated by $Co_2(CO)_8$ (**II-144**).[153]

Nucleophilic attack on hydrosilanes activated by transition metals (activation of a hydrosilane implies ethier the formation of a η^2-silane or a silylhydride complex) was also suggested for silane alcoholysis and hydrolysis reactions catalyzed by rhodium,

iridium, ruthenium, rhenium, nickel, manganese, and iron compounds in the 1980's – 1990's.[157] However, only few of the proposed catalytic cycles were supported experimentally. For example, in 1989, based on kinetic experiments and the stoichiometric reactivity of cationic iridium complexes Crabtree *et al.* postulated the mechanism of silane alcoholysis mediated by $[IrH_2(THF)_2(PPh_3)_2][SbF_6]$ (**II-168**) (Scheme 59, **A**).[157b] According to this suggestion, the displacement of the coordinated THF molecule in **II-168** by MeOH followed by addition of the Et_3SiH would generate η^2-silane intermediate **II-169**, which upon intramolecular nucleophilic attack of coordinated MeOH releases silyl ether to form the η^2-dihydrogen species **II-170**. The coordinated H_2 molecule in **II-170** could be further substituted with methanol finishing the catalytic cycle.[157b] The analogous scheme was also suggested by Crabtree *et al.* for the $[Ni(tss)]_2$ (**II-171**, tss – thiosemicarbazonato silacylaldehyde) catalyzed addition of silanes to alcohols on the basis of kinetic studies.[157d]

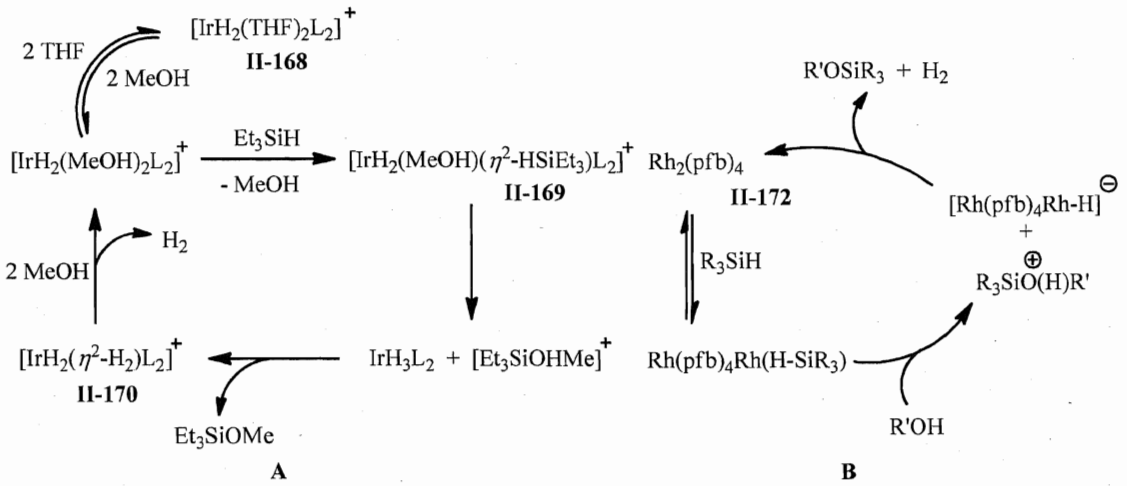

Scheme 59. Mechanisms of silane alcoholysis mediated by $[IrH_2(THF)_2(PPh_3)_2][SbF_6]$ (**II-168**) (**A**) and $Rh_2(pfb)_4$ (**II-172**) (**B**).

In 1990, a similar activation of hydrosilanes was proposed by Doyle and co-workers for the catalytic silane alcoholysis mediated by $Rh_2(pfb)_4$ (**II-172**, pfb – perfluorobutyrate).[157c] The cycle presented in Scheme 59 (**B**) resulted from the spectroscopic (NMR spectroscopy) observation of intermediates and their generation in stoichiometric manner. The catalytic scheme closely related to Doyle's was also

developed in the early 1990's for $Re_2(CO)_{10}$ (**II-173**)[157e] and $[Mn(CO)_4Br]_2$ (**II-174**).[157f] Probably, one of the most interesting and most studied systems for the catalytic alcoholysis of silanes was reported in 1998 by Brookhart *et al.* for the cationic η^2-silane iron complexes $[Cp(CO)(PR_3)Fe(\eta^2\text{-}HSiEt_3)]^+$ (**II-175**, R = Pe, Et).[157h] These catalysts can be generated either by treatment of cationic carbene derivatives $[Cp(Co)(PR_3)Fe{=}CHR'][BF_4]$ (**II-176**) with Et_3SiH[157g] or *via* the protonation of neutral compounds $Cp(CO)(PR_3)Fe(X)$ (**II-177**, X = $SiEt_3$ or Me) with $H(OEt_2)_2BAr'$ (Ar' = 3,5-$(CF_3)_2C_6H_3$) in the presence of Et_3SiH (Scheme 60).[157g,h] In the course of studies on the stoichiometric reactivity of **II-175** it was found that its hydrolysis forms rapidly Et_3SiOH and the η^2-dihydrogen species $[Cp(CO)(PR_3)Fe(\eta^2\text{-}H_2)]^+$ (**II-178**); the latter can displace a molecule of H_2 with silane to generate the complex **II-175**.[157g] The hydrolysis of silanes was also studied under catalytic conditions, and Brookhart and co-workers demonstrated

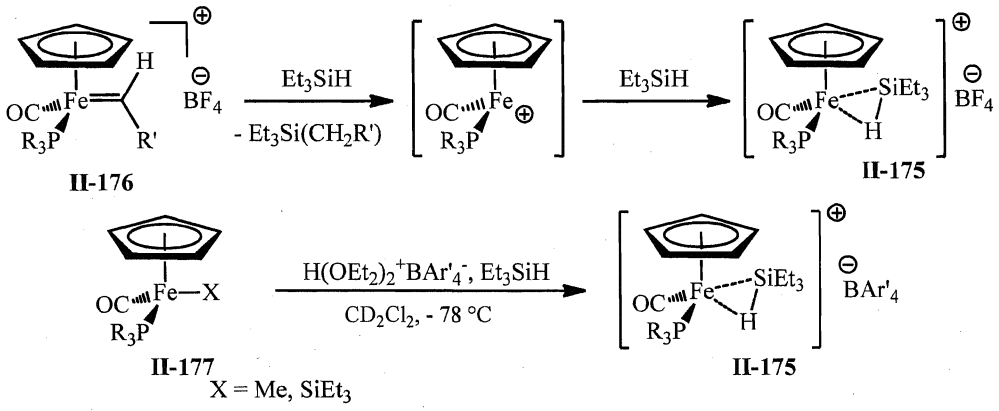

Scheme 60. Generation of cationic η^2-silane complexes $[Cp(CO)(PR_3)Fe(\eta^2\text{-}HSiEt_3)]^+$ (**II-175**, R = Pe, Et).[157g,h]

the utilization of **II-175** in catalytic silane alcoholysis. The proposed mechanism for this process is depicted in Scheme 61 and is based on the isolation and stoichiometric reactivity of the η^2-silane complexes **II-175** and the determination and full characterisation of η^2-H_2 derivatives **II-178**. All steps of the proposed cycle were modelled under stoichiometric conditions and the reactions were monitored by VT (*v*ariable *t*emperature) NMR, which allowed the observation and spectroscopic characterization of key intermediates.[157h] Later, Bühl *et al.* presented DFT data supporting the proposed scheme.[158] Furthermore, analogous NMR studies of the silation

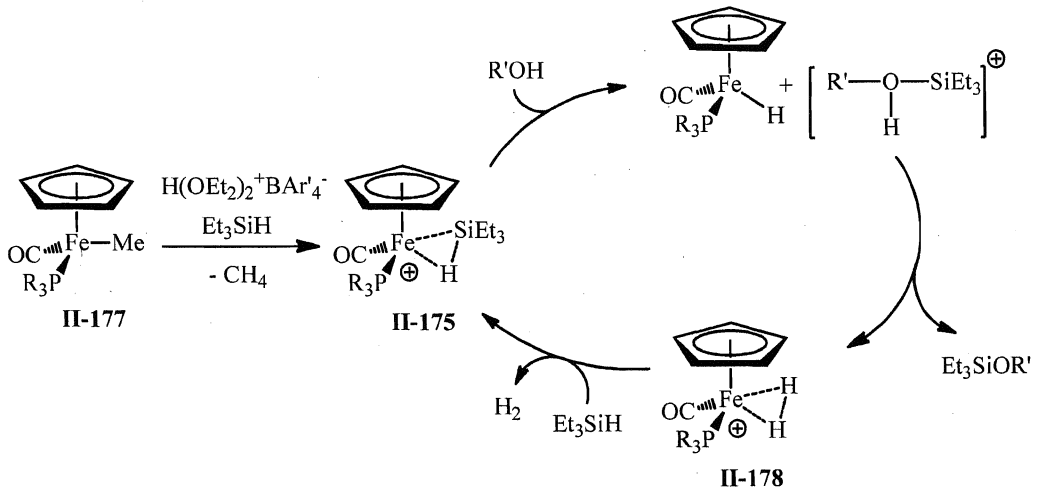

Scheme 61. Brookhart's mechanism of catalytic silane alcoholysis mediated by $[Cp(CO)(PR_3)Fe(\eta^2\text{-}HSiEt_3)]^+$ (**II-175**, R = Pe, Et).[157h, 158]

of alcohols in the presence of related [*mer*-$Mn(CO)_3\{P(OCH_2)_3CMe\}_2(DCM)][BAr_F]$ (**II-179**) were performed by Kubas *et al.* in 2000, who suggested a catalytic scheme identical to that by Brookhart *et al.*[159]

A significant development in understanding the mechanistic aspects of transition metal catalyzed dehydrogenative addition of hydrosilanes to alcohols occurred over the last decade.[125, 160-162] Thus, in 2001, Lee *et al.* applied a mixture of $CpZr(acac)_2Cl$ (**II-180**) and ^{n}BuLi in alcoholysis of phenylsilane.[160] In contrast to earlier suggested schemes,[153-159] the mechanism proposed for this catalyst involves the initial activation of alcohol instead of convenient activation of silanes (Scheme 62). Unfortunately, no mechanistic studies for the suggested cycle were performed, leaving it totally speculative. The pathways postulated by Lee and co-workers pathway includes the following steps: (i) treatment of **II-180** with ^{n}BuLi in the presence of $PhSiH_3$ to give the hydride derivative $CpZr(acac)_2H$ (**II-181**); (ii) coordination of the alcohol to the Zr centre followed by the evolution of H_2 to form the alkoxy intermediate $CpZr(acac)_2(OR)$ (**II-182**); and (iii) coordination of the silane and intramolecular nucleophilic attack of the alkoxy group on the η^2-H-SiH_2Ph ligand leading to the formation of $ROSiH_2Ph$, furnishing the cycle. In principle, such a sequence could be repeated affording a mixture of mono-, bis- and even tris(silylated) products $ROSiH_2Ph$, $(RO)_2SiHPh$, and $(RO)_3SiPh$, respectively (Scheme 62).[160]

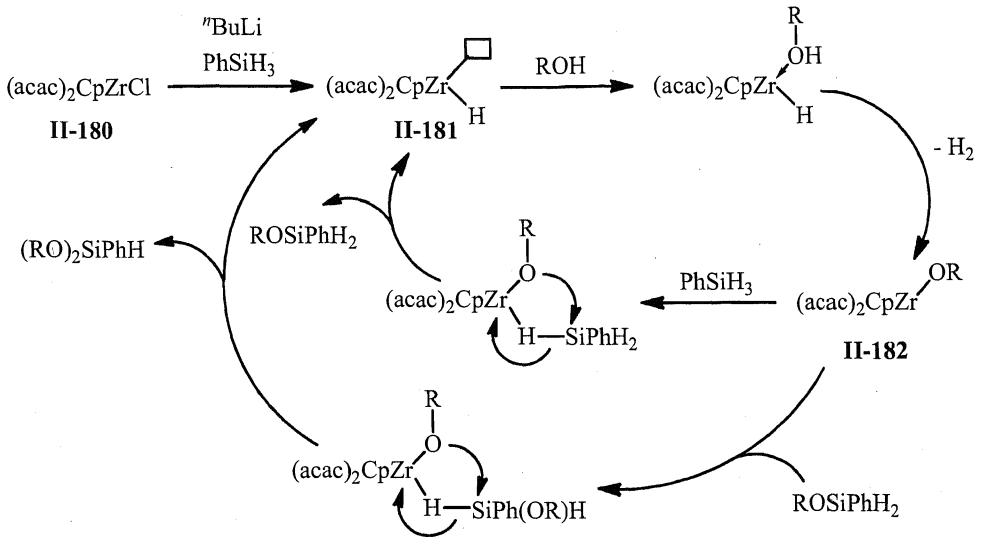

Scheme 62. Mechanism for silane alcoholysis mediated by $CpZr(acac)_2Cl$ (**II-180**) / $^{n}BuLi$.[160]

The activation of an alcohol by AuH(Xantphos) (**II-183**), which can be generated from the chloride derivative AuCl(Xantphos) (**II-184**) in the presence of R_3SiH, was also postulated in 2005 by Sawamura *et al.* for the highly chemoselective catalytic silane alcoholysis.[161] The proposed catalytic cycle is depicted in Scheme 63 and includes the

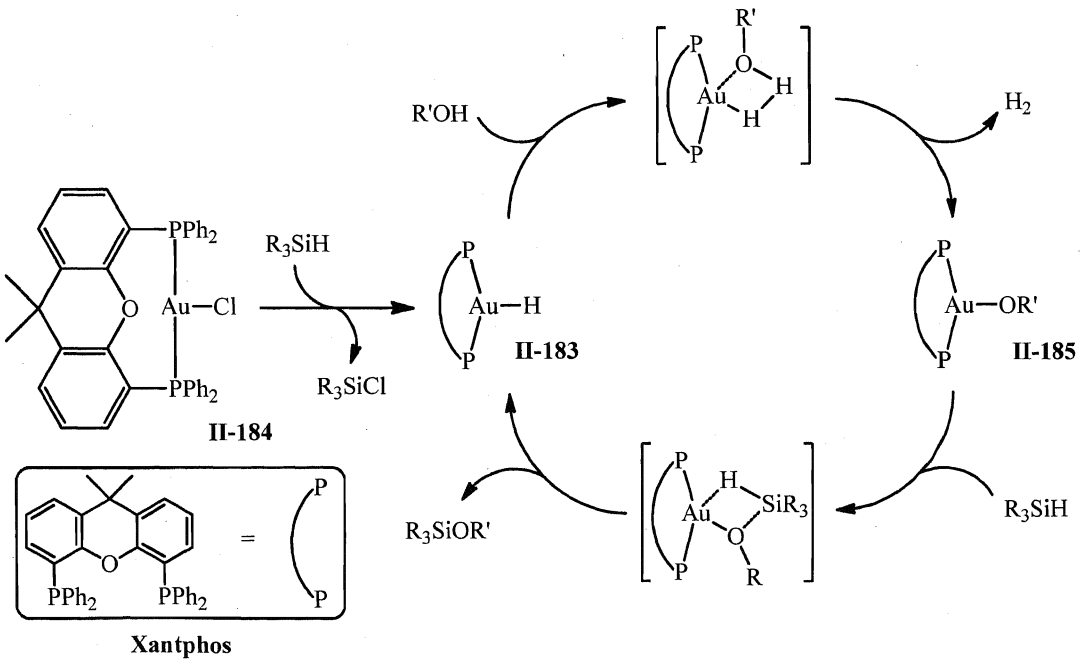

Scheme 63. Mechanism of silane alcoholysis promoted by AuCl(Xantphos) (**II-184**).[161]

initial formation of the alkoxy derivative **II-185**, followed by metathesis with silane. Furthermore, the authors stated that: (1) the monomeric structure is essential for each metathesis reaction in the cycle; and+ (2) the large P-Au-P bite angles induced by the Xanphos ligand help to activate the Au-X (X = Cl, H, OR') bonds. The OH silation by **II-184** was found to be tolerant to a variety of functionalities, such as –C=C–, –C≡C–, –Hal, –COOR, –COR, –CHO, –OCONHR, and –C=CCOR. Again, no experimental evidence for the suggested transformation was reported.[161]

Similar to the alcoholysis of silanes, the catalytic dehydrogenative coupling of hydrosilanes with amines can proceed in two ways: the traditional cycle starting with the activation of silanes[162] and another one, which includes the initial addition of amines to transition metal center.[132a, 163] For instance, in 1999, Takaki *et al.* succeeded in the catalytic aminolysis of hydrosilanes with the use of the ytterbium imine complex Yb(η^2-Ph_2C=NAr)$(hmpa)_n$ (**II-136**, Ar = Ph, *p*-C_6H_4F; hmpa = hexamethylphosphoric acid triamide, $O=P(NMe_2)_3$).[132a] In contrast to the earlier described catalytic hydrosilation of imines in the presence of **II-136** (see Scheme 47, **A**), dehydrogenative coupling of amines

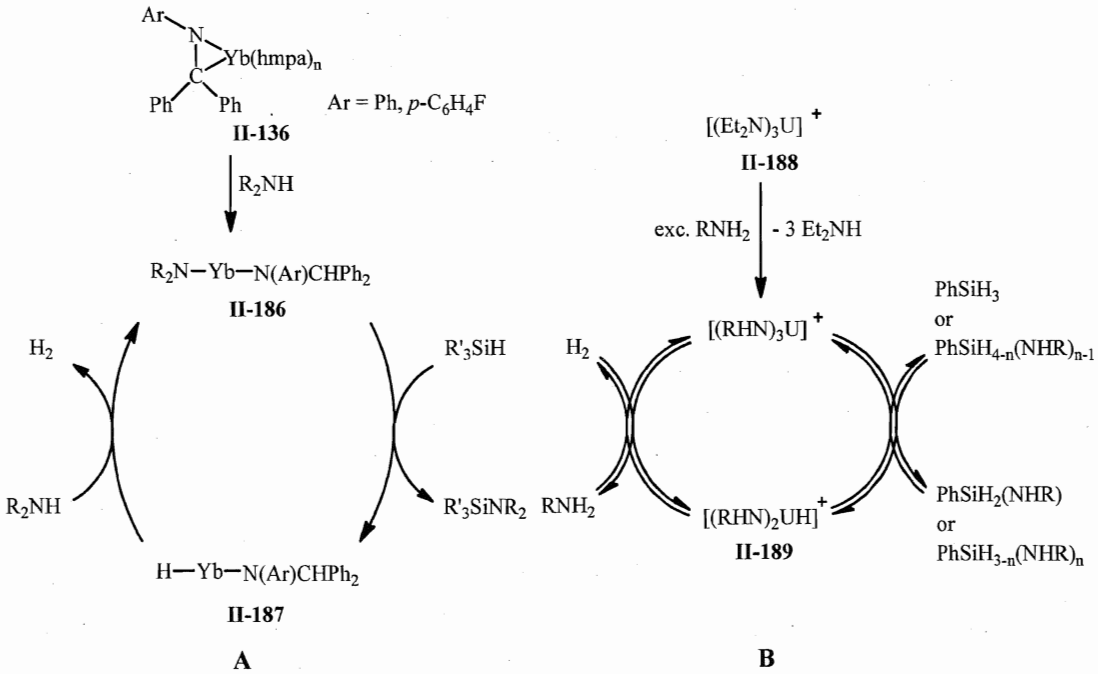

Scheme 64. Activation of amines in catalytic silane aminolysis in the presence of Yb(η^2-Ph_2C=NAr)$(hmpa)_n$ (**II-136**) (**A**) and $[(Et_2N)_3U][BPh_4]$ (**II-188**) (**B**).

with hydrosilanes starts with the initial amine R_2NH addition followed by a σ-bond metathesis between the amide intermediate $Yb(NR_2)(N(Ar)CHPh_2)$ (**II-186**) and R'_3SiH to give the hydride derivative $Yb(H)(N(Ar)CHPh_2)$ (**II-187**) and the silylated amine (Scheme 64, **A**). Subsequent addition of R_2NH to **II-187** furnishes the catalytic cycle regenerating the amide **II-186**. Later, activation of amines as the first step in catalytic silane aminolysis was also proposed by Eisen and co-workers for $[(Et_2N)_3U][BPh_4]$ (**II-188**) (Scheme 64, **B**).[163] The reasoning for the suggested scheme resulted from the stoichiometric reactivity of complex **II-188** towards primary amines. Thus, treatment of **II-188** with $^nPrNH_2$ after 5 min. at ambient temperature showed exchange of the Et_2N and ^nPrNH substituents in the coordination sphere of uranium. Furthermore, the observation of $[(Et_2N)_2UH][BPh_4]$ (**II-189**) upon the stoichiometric treatment of **II-188** with $PhSiH_3$ also supported the proposed catalytic scheme indicating that complex **II-189** could be an active intermediate. Similar exchange reactions of transition metal amides with group 14 hydridoorganic compounds to give hydride species were previously reported.[164]

Very recently, the success in the development of a new non-trivial catalytic system for the hydrosilation of carbonyl compounds and imines has been transferred to the alcoholysis of silanes and novel mechanisms were proposed for this process.[125, 165] Thus, in 2009, Abu-Omar *et al.* applied $[Re(O)(hoz)_2(Solv)][B(C_6F_5)_4]$ (**II-104**, hoz = 2-(2'-hydroxyphenyl)-2-oxazoline, Solv = H_2O or CH_3CN) for the catalytic hydrolysis and alcoholysis of organic silanes.[165] The advantage of the oxo rhenium catalytic system is that the reactions could be carried out under open-flask conditions with reasonably low catalyst loads ($\leq$ 1 mol. %). Initially, two possible catalytic cycles were suggested for the **II-104**-mediated formation of silyl ethers (Scheme 65). The first one involves activation of the catalyst in the form of alkoxy or hydroxyl derivatives **II-190**, which could further react with R_3SiH to give the oxo rhenium hydride intermediate **II-191**. The latter could react with a proton to evolve H_2 and regenerate the active cationic species (Scheme 65, **A**). An alternative pathway would start with the rate-determining oxidative addition of the organosilane to the metal to give a transient Re(VII) complex **II-192** (Scheme 65, **B**). Subsequent nucleophilic attack of water or alcohol would lead to the production of a silanol or silyl ether, respectively. The cycle is completed by H_2 formation from the reaction of the rhenium oxo hydride and H^+.[165] Both schemes are consistent with the

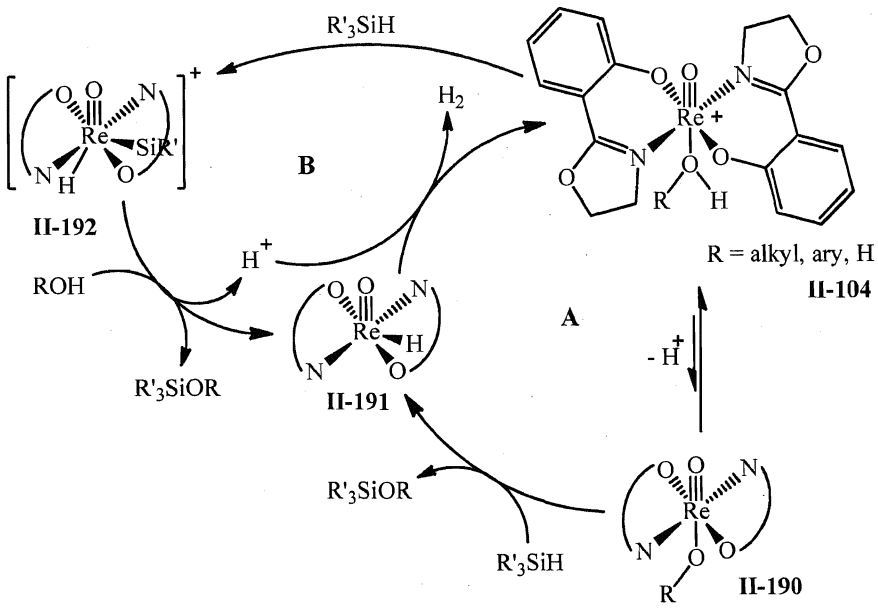

Scheme 65. Abu-Omar's mechanism for silane hydrolysis and alcoholysis catalyzed by $[Re(O)(hoz)_2(Solv)][B(C_6F_5)_4]$ (**II-104**).

kinetic studies, which indicated negative values of $\Delta S^{\ddagger}$, modest values of $\Delta H^{\ddagger}$ and primary isotope effects of 1.3 and 1.4 for Et_3Si-H/D reactions with H_2 and MeOH, respectively. However, the ^{18}O-labeling and kinetic studies performed by Abu-Omar *et al.* suggested that path **A** plays a predominant role in the catalytic hydrolysis and alcoholysis of hydrosilanes.[165]

In 2010, Tilley *et al.* reported that the catalytic alcoholysis and aminolysis of hydrosilanes could be carried out with the use of the iridium silylene complex $[(PNP)(H)Ir{=}SiPh_2][B(C_6F_5)_4]$ (**II-123**).[125] It was shown that stoichiometric reactions of **II-123** with alcohols lead to the formation of (alkoxy)silyl derivatives **II-193** (Scheme 66). Analogous reactions were also found for amines. Similarly to the activation of carbonyl compounds discussed above (see Schemes 43 and 44), three different pathways were suggested for the reactivity of **II-123** towards alcohols and amines (Scheme 66). One mechanism involves the addition of the O-H bond of alcohol across the Ir=Si double bond of the complex, followed by migration of the iridium bound hydride to the amido group of the PNP ligand (*path A*). Alternatively, the O-H activation can occur *via path B*, in which the alcohol coordinates to the silicon centre to form a base-stabilized silylene complex (such base-stabilized derivatives were reported to form upon treatment of **II-123**

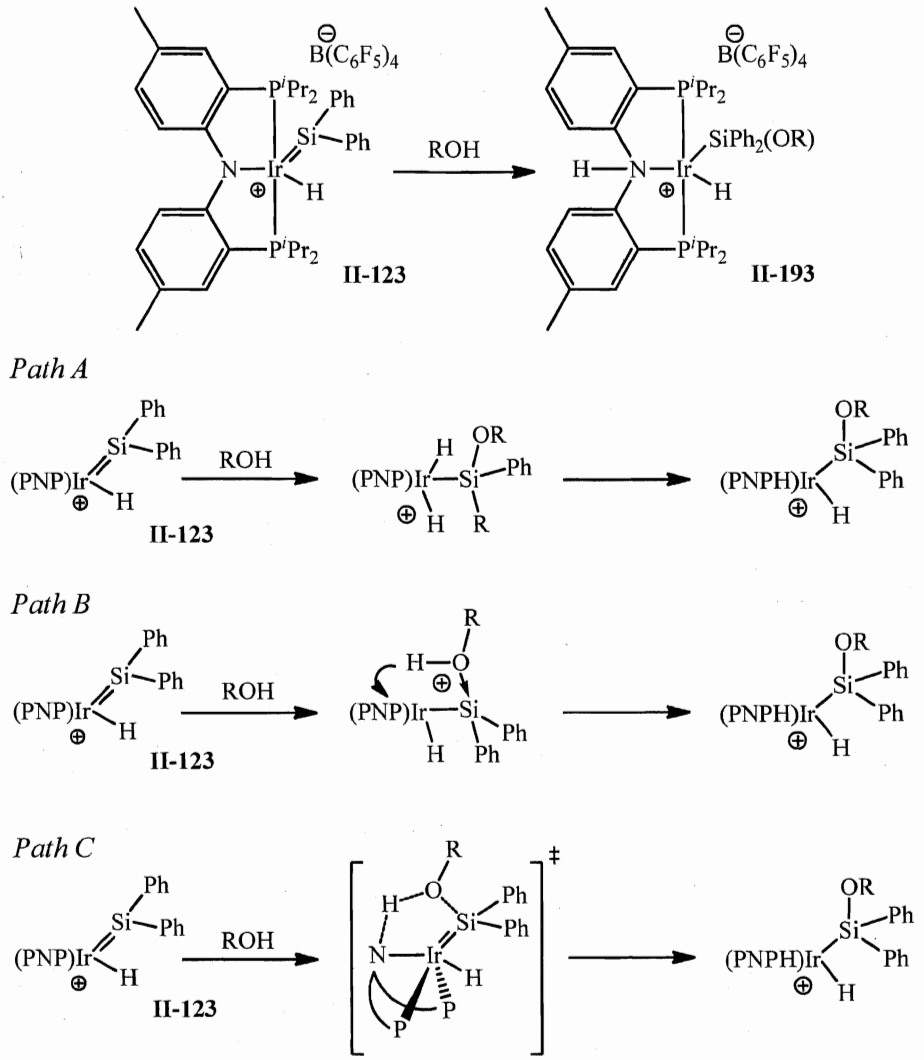

Scheme 66. Reactivity of [(PNP)(H)Ir=$SiPh_2$][$B(C_6F_5)_4$] (**II-123**) towards alcohols and the mechanism of the reaction with ROH.[125]

with DMAP, DMF, and benzophenone), followed by deprotonation by the amido nitrogen. Lastly, the third pathway involves a process initiated by intermolecular proton transfer from the alcohol to the amido group with the concurrent formation of the Si-O bond (Scheme 66, *path C*).[125] Deuterium labelling experiments with ROD performed by Tilley *et al.* revealed an almost statistical redistribution of D between hydride and amine positions. This fact suggested the realization of *path A* (Scheme 66), in which H-migration to the amide of the PNP ligand could occur from either of the iridium hydrides. However, the possibility of intramolecular hydride scrambling was also mentioned.[125]

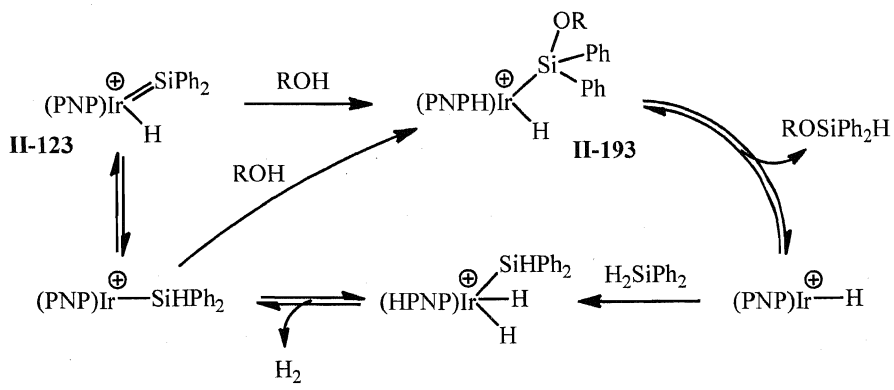

Scheme 67. Tilley's mechanism of silane alcoholysis catalyzed by $[(PNP)(H)Ir{=}SiPh_2][B(C_6F_5)_4]$ (**II-123**).[125]

Taking into account the reactivity of silynene complex **II-123** towards alcohols, Tilley *et al.* proposed a mechanism for the catalytic alcoholysis of organic silanes depicted in Scheme 67. NMR studies of the coupling of diphenylsilane with 3,5-di-*tert*-butylphenol under catalytic conditions (1-5 mol. % of **II-123**) revealed the presence of an alcohol insertion product $[(PNPH)IrH(SiPh_2OAr^{tBu})][B(C_6F_5)_4]$ (**II-193**), which supports the postulated scheme. Aminolysis of hydrosilanes in the presence of **II-123** is believed to proceed in a similar manner.[125]

II.2.6 Early TM catalyzed hydrosilation reactions

Historically, the catalytic hydrosilation of unsaturated organic compounds and related dehydrogenative silation of alcohols and amines started with the application of late transition metal complexes, such as compounds of Pt, Pd, Rh, Ru, Ir, Ni, Co, Fe, etc.[7] However, the toxicity and high cost of these catalytic systems prompted the search and development of early transition metal catalysts.[7b] The advantage of early TM is that they are much cheaper and show reduced toxicity. This part of the literature review describes recent advances in this field, classified by the types of hydrosilation reactions and organic substrates.

II.2.6.1 Hydrosilation of alkenes

The first example of early TM catalyzed hydrosilation of alkenes appeared in the literature in 1991. Thus, Negishi and Takahashi *et al.* reported the catalytic activity of zirconocene Cp_2ZrR_2 (R = Et, ^{n}Bu) (**II-194**), which can be generated *in situ* by the

reaction of Cp_2ZrCl_2 (**II-195**) with RMgBr or RLi.[166] Interestingly, the system Cp_2ZrCl_2 (**II-195**) / ^{n}BuLi (ca. 3 equiv.) promotes the hydrosilation of styrene according to the Markovnikov rule, while a ½ ratio of **II-195** and ^{n}BuLi leads to the reverse regioselectivity.[167] The stoichiometric treatment of **II-194** with hydrosilanes revealed the formation of unsaturated silyl hydride species $[Cp_2Zr(H)(SiHPh_2)]$ (**II-196**) as possible intermediates in the actual catalytic cycle (Scheme 68). Such zirconocene silyl hydrides can be stabilized by the addition of phosphines. They were shown to react with alkenes giving hydrosilation products. However, no stoichiometric hydrosilation of 1-octene was observed for $[Cp_2Zr(SiHPh_2)(\mu\text{-}H)]_2$ (**II-197**). Based on these observations, Negishi and Takahashi proposed that under the catalytic conditions, the monomer **II-196** is generated

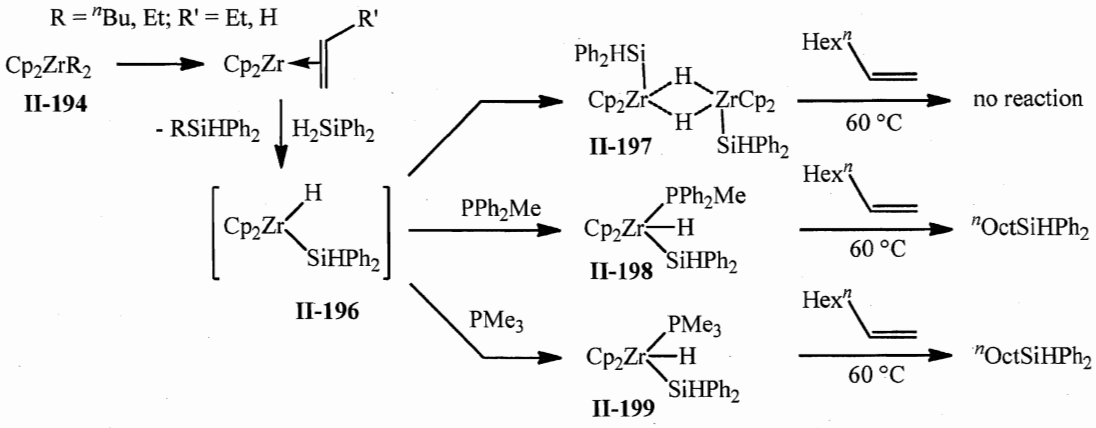

Scheme 68. Stoichiometric reactivity of Cp_2ZrR_2 (R = Et, ^{n}Bu) (**196**) with H_2SiPh_2.

in situ and reacts with alkenes to give hydrosilated products before dimerization to produce **II-197**. The cycle may involve either hydrozirconation or silylzirconation of the olefin, followed by RE to form the C-H or the C-Si bond, respectively.[166] Shortly thereafter, stoichiometric reactivity studies of complex **II-194** and the related complex Cp_2MR_2 (M = Ti (**II-200**), Hf (**II-201**)) reported by groups of Waymouth *et al.* and Corey *et al.* suggested that the catalytic reactions may go *via* a σ-bond metathesis (Scheme 69).[168] This conclusion was further substantiated by the fact that the OA – RE sequence is rare for early transition metal d^0 systems. On the other hand, σ-bond metathesis reactions have been well documented in the literature and were shown to proceed through concerted, four-centre transition states.[168a] Furthermore, all literature reports relevant to zirconocene catalyzed hydrosilation suggest that catalysis by the Cp_2Zr moiety involves a

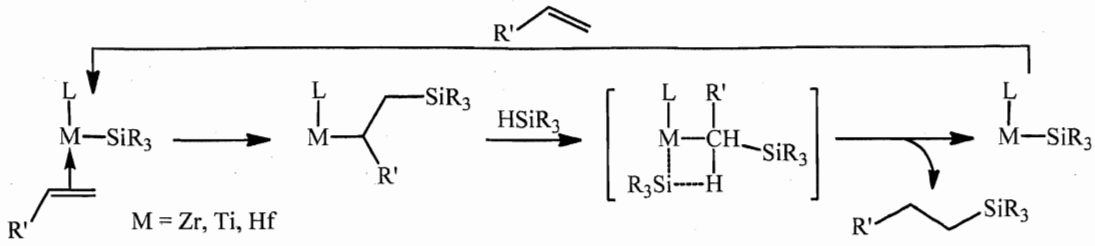

Scheme 69. Mechanism for alkene hydrosilation with the use of $Cp_2M(^nBu)_2$ (M = Zr (**II-194**), Ti (**II-200**), Hf (**II-201**)).

coupling reaction between Cp_2Zr(alkene) and silane, rather than either alkene insertion into the Zr-H or Zr-SiR_3 bonds.[166, 168] A similar coupling was reported by Takahashi and collaborators for the treatment of $Cp_2Zr(\eta^2\text{-}C_2H_4)$ (**II-202**) with chlorosilanes and their Ge and Sn analogues, $ClEPh_3$ (E = Si, Ge, Sn) (Scheme 70).[169] Comprehensive theoretical studies of Cp_2Zr-catalyzed hydrosilation of ethylene by monosilane confirmed the coupling mechanism. Such coupling reaction between **II-202** and SiH_4 proceeds through a reactant-like transition state to give a silane σ-complex with significant bonding overlap between the Si-H σ^*-orbital and d_π-π^* back-donation orbital. From this adduct either hydride migration or silyl migration to ethylene to give a silyl alkyl or hydride alkyl derivative, respectively, can occur with comparably small barriers. Neither species can eliminate the silane product. However, ethylene coordination facilitates significantly the H-C and Si-C reductive elimination.[170] A similar conclusion was made for the Ti-mediated hydrosilation on the basis of calculations on model systems TiH_2 and $TiCl_2$.[171]

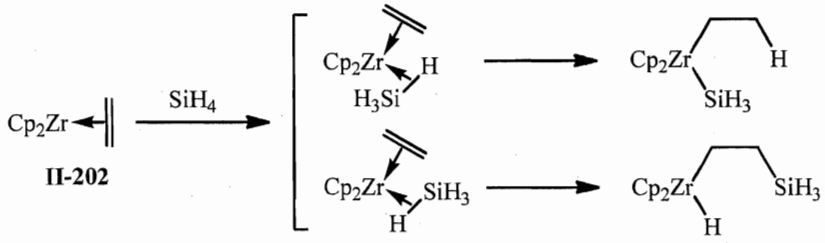

Scheme 70. Coupling reaction between $Cp_2Zr(\eta^2\text{-}C_2H_4)$ (**II-202**) with SiH_4.[169]

A novel route to the *anti*-1,4-hydrosilation of dienes using the air-stable titanium pre-catalyst Cp_2TiF_2 (**II-203**) has been published recently by Moïse *et al.*[172] The reaction proceeds with an unprecedented regio- and diastereoselectivity to give *E*-allylsilanes in good to excellent yields. Similarly to Buchwald's system reported for the catalytic hydro-

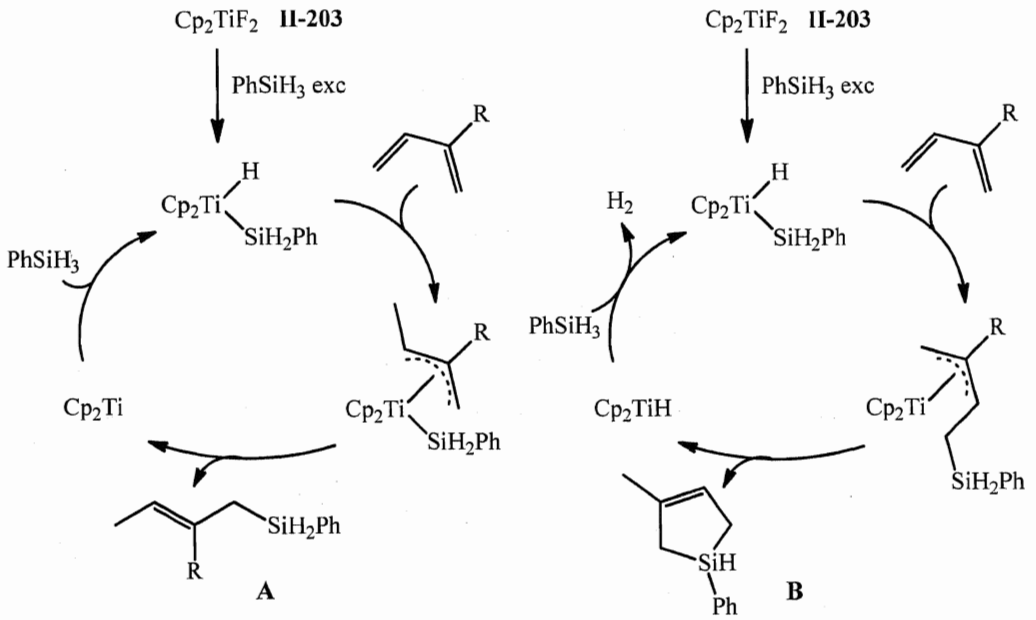

Scheme 71. Mechanisms for the 1,4-hydrosilation of dienes (**A**) and dehydrogenative double silation of dienes (**B**) promoted by Cp_2TiF_2 (**II-203**).[172]

silation of carbonyl compounds and imines,[9e] the activation of the catalyst requires an excess $PhSiH_3$ to form the Ti-H species *in situ*. Upon variation of the activation conditions, Moïse *et al.* found that in addition to the selective 1,4-addition of silanes, complex **II-203** can also promote the dehydrogenative double silation of dienes (Scheme 71).[172]

II.2.6.2 Hydrosilation of alkynes

In contrast to late transition metal catalysis, Pt, Pd, Rh, etc., examples of early TM catalyzed hydrosilation of alkynes are extremely rare.[7] A few examples of lanthanide and actinide complexes that mediate catalytic addition of hydrosilanes to alkynes have appeared since 1995, however, the application of these systems is limited mostly to hydrosilation by Lewis acidic primary silanes $RSiH_3$.[173] Furthermore, Lewis-acid catalyzed *trans*-hydrosilation of alkynes using Group IV tetrachlorides, MCl_4 (M = Ti, Zr, and Hf) is also well established in the literature.[174] However, despite the known catalytic activity of group IV metallocene complexes in hydrosilation of alkenes, the utilization of these compounds in catalytic addition of hydrosilanes to alkynes is limited. Thus, the only example was reported in 2003 by Takahashi *et al.* who succeeded in the

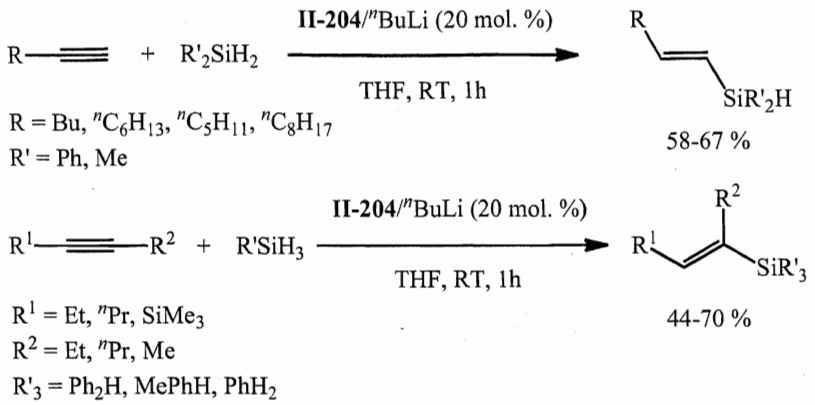

Scheme 72. Hydrosilation of alkynes with the use of Cp_2TiCl_2 (**II-204**) / ^{n}BiLi.[175]

highly regioselective *syn*-hydrosilation of terminal and internal alkynes promoted by the Cp_2TiCl_2 (**II-204**) / ^{n}BuLi system (Scheme 72).[175] *E*-alkenylsilanes were efficiently obtained under mild conditions in good yields, however a very high catalyst loading (20 mol. %) is required for this process. By analogy with the catalytic scheme proposed for the Group IV metallocene catalyzed hydrosilation of alkenes (see Schemes 69 and 70),[166-171] Takahashi *et al.* suggested a mechanism, which involves the simultaneous coordination of the alkyne substrate and silane to the Ti centre, followed by an intramolecular coupling.[175] Unfortunately, no experimental evidence confirming this postulated mechanism was presented.

II.2.6.3 Hydrosilation of carbon-heteroatom multiple bonds

The first early transition metal catalyzed hydrosilation of carbonyl compounds was reported in 1988 by Nagai *et. al.* who demonstrated the use of the air stable titanocene complex Cp_2TiPh_2 (**II-205**) for the catalytic addition of phenyl-, diphenyl-, and methylphenylsilane to ketones.[176] Thus, dialkylketones were transformed into the corresponding silyl ethers with the yields of up to 91 %. However, the reported reaction conditions were rather extreme: 90 – 120 °C, 5 – 20 h. The mechanism proposed for **II-205** (Scheme 73) involves formation of titanium hydride species. No experimental evidence was presented by Nagai and co-workers and the the catalytic cycle was proposed based on the addition of carbonyls to titanium hydrides demonstrated earlier by Sato *et al.*[177]

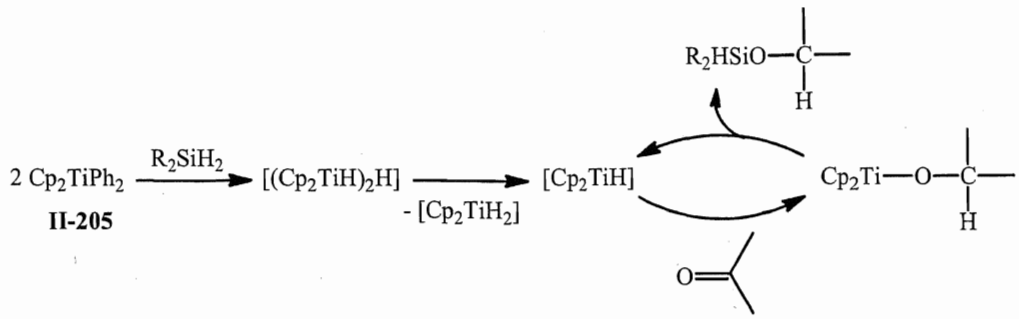

Scheme 73. Mechanism of **II-205**-catalyzed hydrosilation of ketones.

The discovery of Nagai *et al.* inspired numerous studies in the field of Group IV catalyzed hydrosilation reactions of carbonyls and imines.[7b] In 1991, Buchwald *et al.* reported the application of the $CpTiCl_2$ (**II-206**) / ^{n}BuLi system for the hydrosilation of esters with $HSi(OEt)_3$ (Scheme 74, **A**).[178] The reaction was found to proceed under mild conditions (room temperature, 0.5-2 h) with reasonably low pre-catalyst loadings (5 mol. %) affording selective reduction of the ester group to the corresponding alcohols with moderate to high isolated yields. Furthermore, it was also shown that **II-206**/^{n}BuLi promoted addition of $HSi(OEt)_3$ to the carbonyl group of esters is highly chemoselective, tolerating potentially reactive functionalities such as hydroxy, amino, and cyclopropyl groups, as well as isolated and conjugated C=C double bonds. However, esters containing terminal carbon-carbon double bonds or epoxy groups required the use of the more hindered titanium derivative, (EBHTI)$TiCl_2$ (**II-207**) (EBHTI – ethylene-1,2-bis(η^5-4,5,6,7-tetrahydro-1-indenyl)).[178]

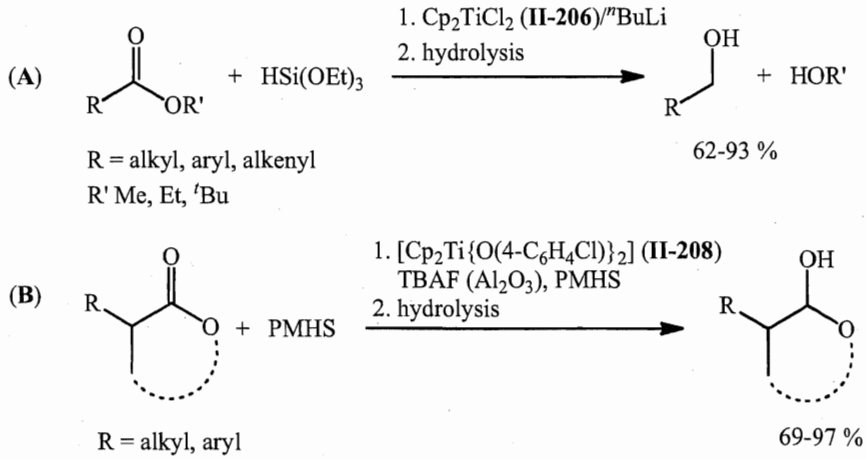

Scheme 74. Titanocene catalyzed hydrosilation of esters.[178]

The reaction protocol for the titanocene catalyzed hydrosilation of carbonyl compounds was further improved and the use of PMHS as a stoichiometric reductant and EtMgBr instead of ^{n}BuLi for the generation of active catalyst was shown.[179] More recent reports on the titanocene mediated hydrosilation of carbonyls and imines are mostly focused on variations of substituents at the Cp rings and titanium center in order to improve the regioselectivity, to introduce enantioselectivity, and expand the scope of substrates.[9, 107d, 108, 180] For example, the efficient hydrosilation of five- and six-membered ring lactones with PMHS as a hydride source was reported by Buchwald *et al.* in 1995 (Scheme 74, **B**).[180a] After hydrolytic work up, the corresponding lactols were obtained with moderate to high isolated yields (69-97 %) under mild conditions. The procedure involves the *in situ* generation of an active catalyst (assumed to be titanocene(III) hydride) by the treatment of $Cp_2Ti(OC_6H_4Cl\text{-}4)_2$ (**II-208**) with TBAF and PMHS. Catalytic asymmetric hydrosilation of carbonyls and imines promoted by (*R,R*)-(EBHTI)TiF_2 (**II-84**) was studied by Buchwald *et. al.* in the middle of 1990's and was described previously (see Schemes 35 and 46).[9e, 180b] Cp_2ZrMe_2 (**II-209**) was also found active in hydrosilation of ketones with $PhSiH_3$.[9f] Depending on the steric properties of the utilized ketone substrates, the reaction leads to the formation of a mixture of mono-, di- or trialkoxysilanes.

Another example of titanium-catalyzed hydrosilation of carbonyls is the $Ti(O^{i}Pr)_4$ (**II-210**) promoted of $HSi(OEt)_3$ to esters.[181] This reaction can be carried out in air, without solvent, and displays a high level of functional group compatibility. An improved protocol, employing Ti(IV) isopropoxides or Zr(IV) ethoxides and less expensive PMHS, was reported later.[182]

The unprecedented homogeneous catalytic hydrosilation of pyridines with $PhSiH_3$ and $PhMeSiH_2$ mediated by Cp_2TiMe_2 (**II-211**) and Cp*CpTiMe_2 (**II-212**) was reported by Harrod *et al.* (Scheme 75).[19g, 183] The corresponding products were obtained with moderate to high yields and the selectivity as well as the level of reduction were shown to be sensitive to the ring substitution. The initial step of the reaction was proposed to be the addition of a Ti-Si species to the carbon-nitrogen bond of the pyridine to form an *N*-silyldihydropyridine.

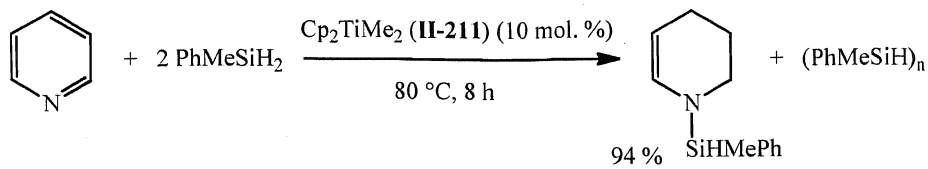

Scheme 75. Cp_2TiMe_2 (**II-211**) catalyzed hydrosilation of pyridine.[19g]

During last two decades, the hydrosilation of carbonyl compounds was shown to proceed in the presence of molybdenum and tungsten carbonyl complexes.[130, 144, 184] For example, the anionic μ-hydride carbonyls $[HM_2(CO)_{10}]^-$ (M = Mo (**II-213**), W (**II-214**)) were found to catalyze the hydrosilation of simple ketones and aldehydes with Et_3SiH to give silyl ethers in high yields.[184a] Cabonyl molybdenum and tungsten oxadiene derivatives $M(CO)_2(oxadiene)_2$ (M = Mo (**II-215**), W (**II-216**); oxadiene = pulegone, pinocarvone, and (*E*)-5methyl-3-hexen-2-one) exhibit catalytic activity for the $PhSiH_3$ addition to unsaturated ketones and aldehydes.[184b] Solvent free hydrosilation reactions of ketones with Et_3SiH was achieved with cationic $[CpW(CO)_2IMes][B(C_6F_5)_4]$ (**II-217**). Importantly, the catalyst precipitates at the end of the reaction because of the decreased polarity of the media and can be recycled.[184d] The photocemically initiated addition of Ph_2SiH_2 to RMeC(O) (R = Me, ^{i}Pr, Pr, Ph) was discovered for $W(CO)_6$ (**II-218**).[184e] Lastly, in 2006, Tobita *et al.* reported the stoichiometric hydrosilation of acetone and nitriles (see Scheme 56) with the novel silylene tungsten complex $Cp^*(CO)_2(H)W{=}SiH\{C(SiMe_3)_3\}$ (**II-125**).[144] The mechanism of this reaction has been investigated with the help of DFT calculations.[130]

The discovery of Toste *et al.* in 2003 of the catalytic activity of the high valent rhenium complex $(Ph_3P)_2Re(O)_2I$ (**II-86**) in the hydrosilation of carbonyl compounds[116] has inspired a quest for similar early transition metal systems.[12b,c, 118, 185] Thus, Romao *et al.* reported the MoO_2Cl_2 (**II-96**) catalyzed addition of Me_2PhSiH to aldehydes and ketones to afford the corresponding dimethylphenylsilyl ethers in moderate to high yields (see Scheme 38).[185a] A few other oxo molybdenum catalytic systems, such as $CpMoO_2Cl$ (**II-98**), $MoO_2(Mes)_2$ (**II-99**), $(R_3Sn)_2MoO_4$ (R = ^{n}Bu, ^{t}Bu, Me) (**II-100**), MoO_2(salalen-3,5-R_2) (**II-103**, R = H, ^{t}Bu; Figure 12) appeared in the literature shortly thereafter and the scope of organic substrates was expanded to include secondary and tertiary amides (Scheme 76).[12b,c, 120, 185b,c]

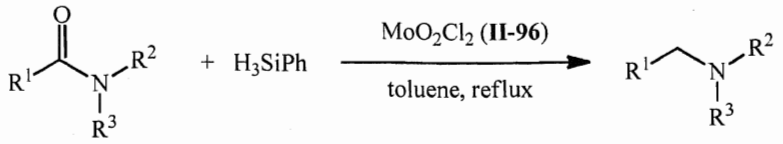

R^1 = Me, aryl; R^2 = H; R^3 = aryl, benzyl
R^1 = Me; NR^2R^3 = N-heterocycle

Scheme 76. MoO_2Cl_2 (**II-96**) catalyzed hydrosilation of amides.[185]

Apart from the catalytic addition of hydrosilanes to carbonyls, there are examples of early transition metal catalyzed hydrosilation of CO_2[186] and sulphoxides.[187] Thus, the homogeneous reduction of carbon dioxide with silanes was found for the zirconium complex **II-219** (Figure 16) combined with $B(C_6F_5)_3$.[186] Depending on the utilized silane and the ratio **II-219**/$B(C_6F_5)_3$, the hydrosilation products, bis(silyl)acetals, such as $(Et_3SiO)_2CH_2$ and $(Ph_3SiO)_2CH_2$, could be obtained in 82 and 64 % yield, respectively.

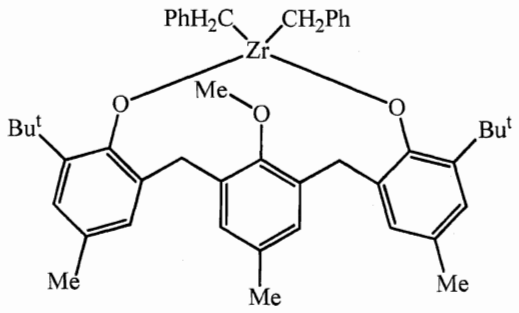

II-219

Figure 15. The zirconium catalyst for the reduction of CO_2 with hydrosilanes.[186]

The catalytic sulphoxide reduction with hydrosilanes to give corresponding sulphides (Scheme 77) was discovered for MoO_2Cl_2 (**II-96**).[187] Such a transformation in the presence of **II-96** has been shown to be highly selective for the S=O bond, tolerating, for example, C=C bonds or ester groups. An additional advantage of this system includes the use of PMHS in an open-flask protocol, which can be carried out in methanol or even in

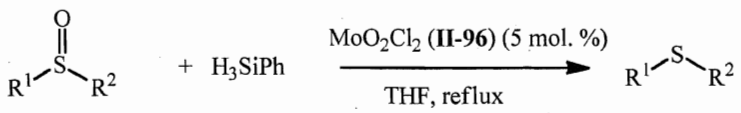

R^1 = aryl, alkyl
R^2 = aryl, alkyl, $HC{=}CH_2$, CH_2COOMe

Scheme 77. MoO_2Cl_2 (**II-96**) catalyzed hydrosilation of sulphoxides.[187]

water, making the transformation environmentally friendly.

II.2.6.4 Hydrolysis, alcoholysis and aminolysis of silanes

The homogeneous catalytic alcoholysis and aminolysis of hydrosilanes by late transition metal complexes is very well established and has been known for several decades. Although a few examples of early transition metal systems,[160, 188, 189] as well as lanthanide and actinide compounds[132a, 163] are also active in these transformations.

The first early transition metal (in particular, Cp_2TiCl_2 (**II-204**) / ^{n}BuLi and Cp_2TiPh_2 (**II-205**)) mediated alcoholysis of silanes appeared in the literature in the beginning of 1990's.[188] For example, Corey *et al.* in 1992 demonstrated the use of the **II-204**/^{n}BuLi system, well known for the hydrosilation of alkenes, alkynes and carbonyls, and in catalytic dehydrogenative coupling of hydrosilanes with aliphatic and aromatic alcohols.[188b] Depending on the steric properties of the utilized R_3SiH, the reaction was shown to proceed either at room temperature or in refluxed THF with a reasonably low pre-catalyst loading (3.3 mol. %) to afford mono-, di- or trialkoxysilanes in moderate to good yields. A similar catalytic activity of **II-204**/^{n}BuLi was also found in the silation of polyfunctional alcohols (Scheme 78).[188b]

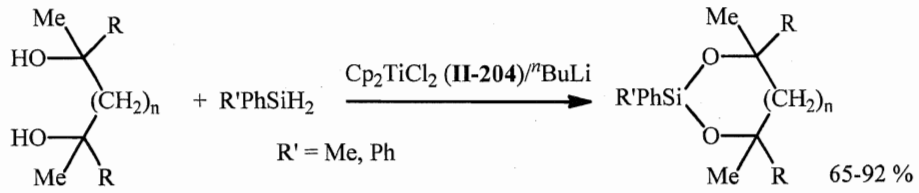

Scheme 78. Cp_2TiCl_2 (**II-204**) / ^{n}BuLi catalyzed silation of diols.[188b]

In 1995, Harrod and co-workers expanded the application of titanocene catalysts by conducting reactions of hydrosilanes with allylic alcohols in the presence of Cp_2TiMe_2 (**II-211**) and (EBTHI)$TiMe_2$ (**II-220**, EBTHI = ethylene-1,2-bis(η^5-4,5,6,7-tetrahydro-1-indenyl); Scheme 79).[189] It was reported that the addition of primary and tertiary silanes ($PhSiH_3$, Me_2PhSiH, $MePh_2SiH$) to allyl alcohols leads to selective OH silation, however, the use of Ph_2SiH_2 and $MePhSiH_2$ is not chemoselective and after the Si-O bond formation further intamolecular hydrosilation of C=C bond was also observed.

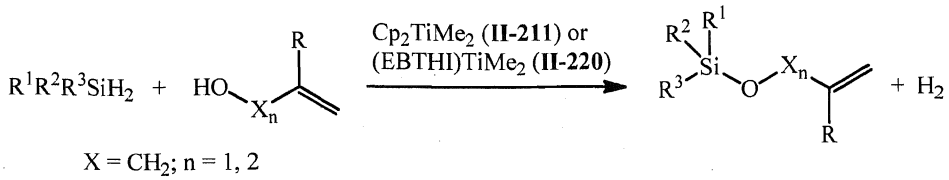

Scheme 79. Intramolecular alcoholysis and aminolysis reactions catalyzed by Cp_2TiMe_2 (**II-211**) and (EBTHI)$TiMe_2$ (**II-220**).[189]

Recently, the silation of aliphatic and allyl alcohols with $PhSiH_3$ catalyzed by a mixture of $CpZr(acac)_2Cl$ (**II-180**) and ^nBuLi was reported by Lee *et al.*[160] The reaction was shown to proceed under mild conditions (1 mol. % of **II-180**, room temperature) to give a mixture of mono-, di- and trialkoxy substituted products in moderate yields. The suggested mechanism is discussed earlier (see Scheme 62) and includes the formation of a zirconium hydride species followed by activation of the alcohol substrate to form an alkoxy derivative. Such interactions of early transition metal hydrides with acidic alcohols are well documented in literature.[190]

III. Results and Discussion

III.1 Introduction

As has been already mentioned in the introduction to the thesis (Chapter I), the present research is devoted to the synthesis and reactivity study of novel molybdenum and tungsten imido agostic silylamido and hydride complexes, including the catalytic activity of these species in hydrosilation reactions. The preparation of the target compounds, proposed in Scheme 80, is based on the imido/silane coupling approach between bis(imido) complexes and hydrosilanes, previously discovered in our group for isolobal mono(imido) tantalum derivatives.[14] The first part of this chapter will present a brief discussion of the synthetic methodologies used for the preparation of the bis(imido) molybdenum and tungsten precursors. The results of the reactivity studies of Mo(IV) and W(IV) bis(imido) phosphine compounds towards chloro-substituted hydrosilanes and mechanistic aspects of their reactions with $HSiCl_3$ are discussed in the second section of this chapter.

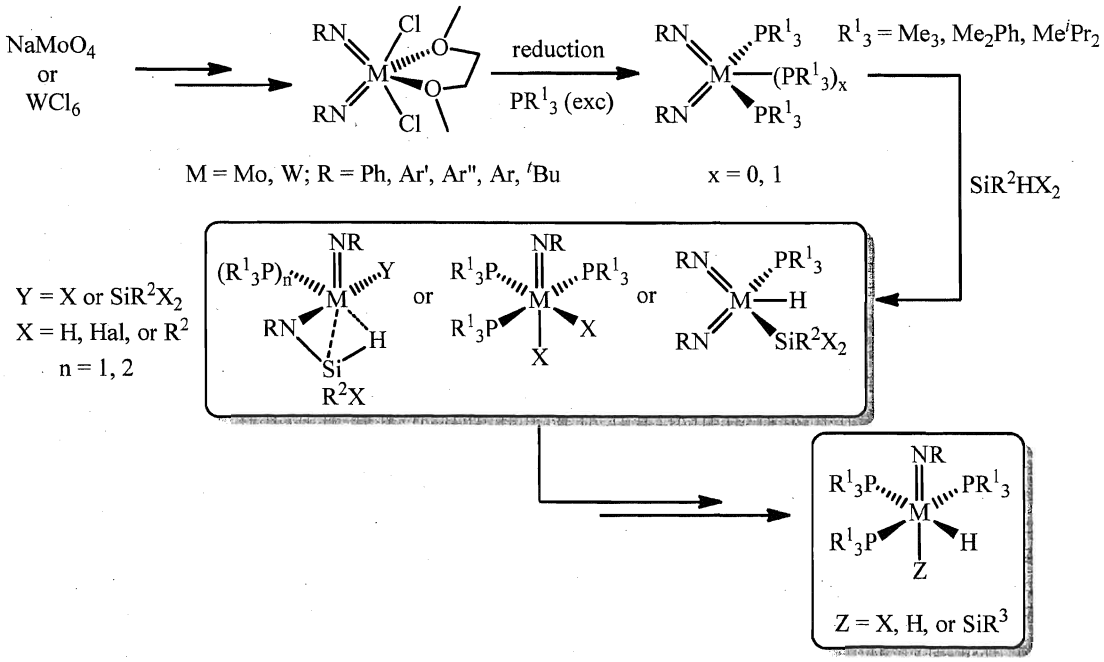

Scheme 80. Proposed synthesis of imido silylamide and hydride complexes.

A significant part of this chapter deals with the reactivity of Mo(IV) and W(IV) bis(imides) with chlorine-free hydrosilanes, such as $PhSiH_3$, $PhMeSiH_2$. Using this approach we present the preparation of a novel Mo(IV) imido silyamido agostic derivative (ArN)Mo(SiH_2Ph)(η^3-NAr-SiHPh-H)(PMe_3) (**III-1**; Figure 16) and show its unprecedented stoichiometric and catalytic reactivity, involving the intermediacy of the silanimine complex, (ArN)Mo(η^2-ArN=SiHPh)(PMe_3) (**III-2**; Figure 16). The mechanistic aspects of both catalytic and stoichiometric reactions are also discussed. Furthermore, the discovery of stoichiometric Si-C coupling reactions of **III-1** with olefins have led to the isolation of the (vinylsilyl)amide derivative (ArN)Mo(Et)(η^3-NAr-SiHPh-CH=CH_2)(PMe_3) (**III-3**; Figure 16), whose reactivity is also presented.

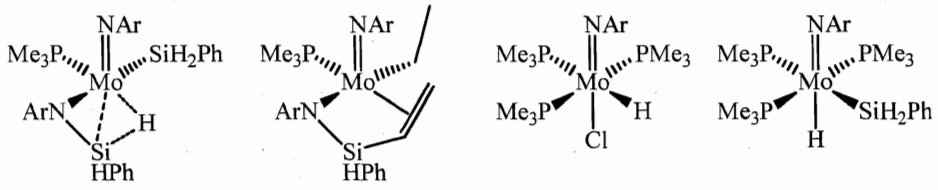

Figure 16. Mo(IV) imido complexes active in hydrosilation catalysis.

Recently, Nikonov *et al.* demonstrated that the treatment of (Ar'N)$_2$Mo(PMe_3)$_3$ (**III-4**) with $HSiCl_3$ affords the Mo(IV) dichloride compound (Ar'N)$MoCl_2$(PMe_3)$_3$ (**III-5**), accompanied by release of the silanimine dimer (Ar'N-SiHCl)$_2$.[15] In the present study, this approach is extended to other Mo(IV) bis(imido) derivatives, affording a series of Mo mono(imido) dichlorides. The well-known rich reactivity of transition metal hydride complexes[18, 19] as well as the general interest in the Nikonov group in the chemistry of the early transition metal hydrides inspired the development of an efficient approach to novel Mo(IV) imido hydride compounds (ArN)Mo(H)(Cl)(PMe_3)$_3$ (**III-6**) and (ArN)Mo(H)(SiH_2Ph)(PMe_3)$_3$ (**III-7**) (Figure 16). The preparation, structural features, stoichiometric and catalytic reactions of these species, as well as detailed mechanistic studies of hydrosilation catalysis are presented in the last part of this chapter. Furthermore, in the course of this study, we also performed an isolation and reactivity study of the imido complex (ArN)Mo(η^2-BH_4)$_2$(PMe_3)$_2$ (**III-8**), which is a rare example of bis(borohydride) derivative.[191]

III.2 Preparation of bis(imido) complexes of molybdenum and tungsten

Despite the variety of common methods for the introduction of an imido moiety in transition metal complexes,[192] the choice of an appropriate procedure for any particular TM system is dictated by the availability of the starting materials, cost of the reagents, and the simplicity of the experimental manipulations. Certain types of imido complexes can be prepared in high yields most simply by adding a primary or silylated amine to a metal oxo complex to produce water or siloxane as a by-plroduct.[192] Similarly, the preparation of bis(imido) Mo(VI) complexes in the present work is based on the procedure developed by Schrock *et al.*,[193] which starts from the commercially available, air-stable and inexpensive molybdates, $(NH_4)_2Mo_2O_7$ (**III-9**) or $NaMoO_4$ (**III-10**). Thus, the treatment of the molybdenum precursor **III-10** with two equivalents of amine RNH_2 (R = Ar, Ar', Ar", Ph, ^{t}Bu) in dimethoxyethane in the presence of excess NEt_3 and Me_3SiCl affords the bis(imido) molybdenum dichloride species, $(RN)_2MoCl_2(DME)$ (R = Ar (**III-11**), Ar' (**III-12**), Ar" (**III-13**), Ph (**III-14**), ^{t}Bu (**III-15**); Scheme 81). Excess triethylamine and Me_3SiCl is required in order to effectively remove the released HCl and water, respectively. Alternatively, for the addition of alkyl substituted amines, like ^{t}BuNH$_2$, excess amine substrate could be used instead of NEt_3. The reaction does not require the use of extremely dry conditions and reproducibly affords bis(imido) molybdenum complexes in high to quantitative yields close to those reported by Schrock *et al.*[193] The analogous tungsten bis(imido) dichloride $(ArN)_2WCl_2(DME)$ (**III-16**) had been prepared previously in our group following literature procedure[194] and was generously donated by Dr. Nikonov.

The reduction of the dichloride precursors $(RN)_2MCl_2(DME)$ had been reported earlier to give several types of compounds. Sodium amalgam reduction of **III-16** in the presence

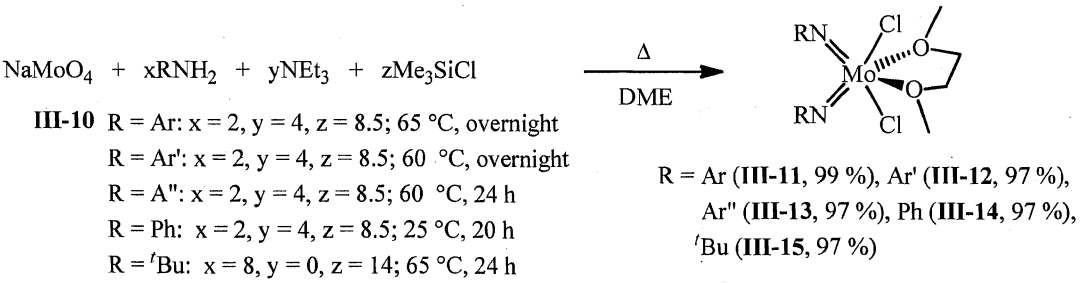

Scheme 81. Preparation of $(RN)_2NoCl_2(DME)$ (**III-11 – III-15**).

of PMe_2Ph or $PMePh_2$ affords the bis(phosphine) compound $(ArN)_2W(PR_3)_2$ (R_3 = Me_2Ph (**III-17**) or $MePh_2$ (**III-18**)).[195] Gibson has reported the X-ray structure of the related molybdenum compound $(ArN)_2Mo(PMe_3)_2$ (**III-19**) synthesized by the reduction of **III-11** with magnesium.[196] On the other hand, Sundermeyer *et al.* provided evidence that for the less bulky imido group (R = Mes) the tris(phosphine) compound $(MesN)_2Mo(PMe_3)_3$ (**III-20**) exists in equilibrium with its bis(phosphine) form and free PMe_3.[197] In contrast, the magnesium reduction of $(^tBuN)_2MoCl_2(DME)$ (**III-15**) was reported to furnish the imido-bridged dimer $[(^tBuN)(Me_3P)Mo(\mu\text{-}N^tBu)]_2$ (**III-21**).[198] In this work, we found that magnesium reduction of $(RN)_2MCl_2(DME)$ (R = Ar (**III-11**, **III-16**) or Ar' (**III-12**)) in the presence of excess PMe_3 always gives tris(phosphine) compounds $(RN)_2M(PMe_3)_3$ (M = Mo (**III-4**, **III-22**), W (**III-23**)) existing in solution in equilibrium with the corresponding bis(phosphine) derivatives and free PMe_3 (Scheme 82). Introduction of a bulky phosphine substituent (PMe_2Ph or PMe^iPr_2) leads to the formation of diphosphine complexes $(ArN)_2Mo(PMe_2Ph)_2$ (**III-24**) and $(Ar'N)_2Mo(PMe^iPr_2)_2$ (**III-25**). However, for the relatively small imido group Ar'N reduction in the presence of PMe_2Ph affords the tris(phosphine) derivative, $(Ar'N)_2Mo(PMe_2Ph)_3$ (**III-26**).

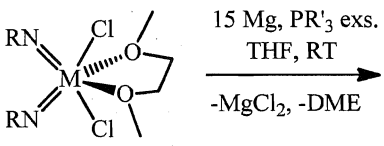

M = Mo (**III-11** - **III-15**)
W (**III-16**)

Mo:
III-4 (88 %): R = Ar', $R'_3 = Me_3$, n = 1
III-22 (97 %): R = Ar, $R'_3 = Me_3$, n = 1
III-24 (50 %): R = Ar, $R'_3 = Me_2Ph$, n = 0
III-25 (23 %): R = Ar', $R'_3 = Me^iPr_2$, n = 0
III-26 (42 %): R = Ar', $R'_3 = Me_2Ph$, n = 1
III-27 (55 %): R = ^{t}Bu, $R'_3 = Me_3$, n = 0
W:
III-23 (70 %): R = Ar, $R'_3 = Me_3$, n = 1

Scheme 82. Preparation of Mo(IV) and W(IV) bis(imido) phosphine compounds.

In the case where R = ^{t}Bu, the magnesium reduction of $(^tBuN)_2MoCl_2(DME)$ (**III-15**) in the presence of 5 to 7 equivalents of PMe_3 affords a mixture of a new bis(phosphine) compound $(^tBuN)_2Mo(PMe_3)_2$ (**III-27**; Scheme 82) and the previously reported dimer $[(^tBuN)(PMe_3)Mo(\mu\text{-}N^tBu)]_2$ (**III-21**).[198] The yield of **III-27** increases when more phosphine is used. Addition of excess PMe_3 to **III-21** does not convert it into the monomeric **III-27**, even upon heating to 70 °C for several days. However, we found that

very prolonged heating (3 weeks) of a mixture of **III-27** and **III-21** at 75 °C results in selective decomposition of the latter into insoluble product(s) of unknown composition, leaving monomer **III-27** as the single component of the solution. Interestingly, there is no formation of free phosphine during this decomposition, suggesting that the product is a higher oligomer of $\{(^t\text{BuN})_2(\text{PMe}_3)\text{Mo}\}$ having the same composition. Furthermore, in the presence of excess PMe_3, degradation of **III-21** slows significantly, suggesting that phosphine elimination is the rate determining step.

The reduction of molybdenum dichloride compounds $(\text{RN})_2\text{MoCl}_2(\text{DME})$ containing relatively non-bulky aromatic imido groups (R = Ar" (**III-13**) and Ph (**III-14**)) is not reproducible and leads mostly to decomposition of target phosphine complexes $(\text{RN})_2\text{Mo}(\text{PMe}_3)_3$ (R = Ar" (**III-28**) and Ph (**III-29**)) to a mixture of unidentified products.

Despite the experimental simplicity of the reaction of Mo(VI) and W(VI) diclorides with magnesium, the isolation of corresponding Mo(IV) and W(IV) phosphine derivatives is complicated due to the formation of the soluble $\text{MgCl}_2(\text{THF})_x$ by-product, which could be separated from the desired molybdenum and tungsten complexes only by the extraction of the latter with hexanes. However, the poor solubility of $(\text{RN})_2\text{M}(\text{PR'}_3)_n$ in hexanes makes the work-up procedure expensive and time consuming. Moreover, the preparation of $(\text{RN})_2\text{M}(\text{PR'}_3)_n$ requires the presence of excess phosphine PR'_3 in order to prevent a dimerization by-process.[f] This significantly increases the cost of the reaction and generates large amount of toxic waste.

Due to these factors, in the present work the preparation of Mo(IV) bis(imido) complexes was also performed using an alternative approach suggested by Gibson *et al.*, which involves the treatment of the dichloride precursors $(\text{RN})_2\text{MoCl}_2(\text{DME})$ with Grignard reagents.[199] Thus, the reaction of $(^t\text{BuN})_2\text{MoCl}_2(\text{DME})$ (**III-15**) with two equivalents of EtMgCl in the presence of an equivalent of PMe_3 affords the Mo(IV) ethylene adduct $(^t\text{BuN})_2\text{Mo}(\eta^2\text{-CH}_2\text{=CH}_2)(\text{PMe}_3)$ (**III-30**) in 50 % yield (Scheme 83). $(\text{ArN})_2\text{Mo}(\eta^2\text{-CH}_2\text{=CH}_2)(\text{PMe}_3)_2$ (**III-31**) was obtained analogously in 70 % yield from **III-11** using two equivalents of PMe_3. Both compounds **III-30** and **III-31** undergo ethy-

[f] In the absence of phosphine, the reduction of $(\text{RN})_2\text{MoCl}_2(\text{DME})$ with magnesium seems to form complexes with bridged imido ligands.[192] For example, see the above discussion of the reaction of $(^t\text{BuN})_2\text{MoCl}_2(\text{DME})$ (**III-15**) with Mg.

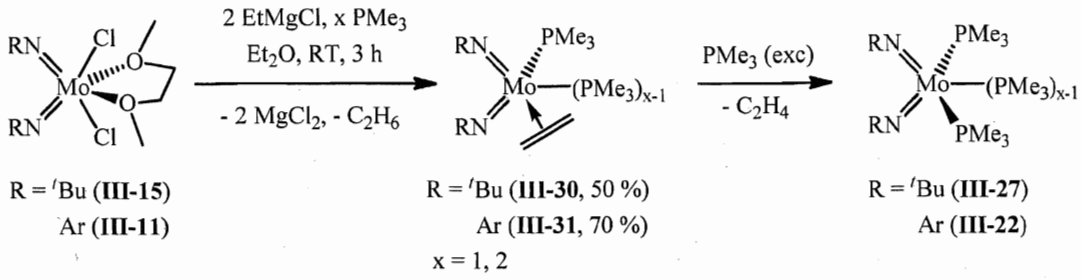

Scheme 83. Preparation of bis(imido) ethylene adducts **III-30** and **III-31**.

lene/phosphine exchange[196, 199] and in the presence of excess PMe_3 can be quantitatively converted to phosphine derivatives ($^tBuN)_2Mo(PMe_3)_2$ (**III-27**) and $(ArN)_2Mo(PMe_3)_3$ (**III-22**) derivatives, respectively.

Bis(imido) complexes $(RN)_2Mo(PR'_3)_n$ (M = Mo, W, n = 2, 3), except compound **III-25**, are highly fluxional at room temperature, and ^{31}P-NMR spectra show broad resonances for the PR'_3 (R'_3 = Me_3 and Me_2Ph) substituents: two broad signals for the tris(phosphine) derivatives and one signal for the bis(phosphine) compounds. Such a fluxionality of $(RN)_2M(PR'_3)_n$ could be a result of intra- and intermolecular phosphine exchange, which proceeds *via* PR'_3 dissociation. In fact, the dissociative mechanism of exchange is further supported by the previously reported substitution of the PMe_3 ligand in **III-22** with olefin and alkyne substrates.[196] Furthermore, addition of an equivalent of BPh_3 to a solution of **III-22** in C_6D_6 leads to the abstraction of one phosphine ligand forming quantitatively $Ph_3B{\cdot}PMe_3$ and $(ArN)_2Mo(PMe_3)_2$ (**III-19**). Analogous abstraction of PMe_3 with BPh_3 is also possible for ethylene complex **III-31** affording the mono(phosphine) derivative $(ArN)_2Mo(\eta^2\text{-}CH_2{=}CH_2)(PMe_3)$ (**III-32**).

III.3 Reactivity of $(RN)_2M(PR'_3)_n$ with chlorohydrosilanes

III.3.1 Reactions of $(RN)_2Mo(PR'_3)_n$ with mono- and dichlorosilanes

The reactivity of early transition metal imido complexes towards chloro-substituted hydrosilanes has been studied in our research group since 2001.[14, 15] Within the last decade it has been shown that, depending on the electronic and steric properties of the ligand sphere as well as the nature of transition metal, the treatment of $L_nM(=NR)$ with $HSiR'_2Cl$ leads to the formation of either silyl products, $L_n(RN=)M(H)(SiR'_2Cl)$ and

$L_n(RN=)M(Cl)(SiR'_2H)$, or β-agostic silylamides, $L_nM(\eta^3\text{-}NR\text{-}SiR'_2\text{-}H)(Cl)$.[14, 17] This research started with the study of the reactivity of half-sandwich imido complexes of tantalum, $Cp(RN)Ta(PMe_3)_2$ (**III-33**, R = Ar, Ar'), and niobium, $Cp(RN)Nb(PMe_3)_2$ (**III-34**, R = Ar) towards $HSiR'_2Cl$. For niobium, the reactions proceed *via* a novel imido/silane coupling route followed by the Si-Cl bond activation and formation of metastable silylamido agostic derivatives (see Schemes 5 and 6, chapt. II.1.4).[14] In all cases, the initial formation of imido silylhydride species $Cp(RN)M(H)(SiR_2Cl)(PMe_3)$ (**III-35**) was detected. For $R_2=Me_2$, this species rearranges into the agostic complex $CpNb(Cl)(\eta^3\text{-}NR\text{-}SiMe_2\text{-}H)(PMe_3)$ (**III-36**; see Scheme 5, chapt. II.1.4) For more Lewis acidic silanes, the initial silyl hydride species rearranges into silyl chloride species *via* hydride/chloride exchange, forming a mixture of imido silyl derivatives $CpNb(NR)(SiR'_2X)(Y)(PMe_3)$ (R = Ar', Ar; X = Cl, H; Y = Cl, H; R'_2 = MePh, Ph_2, HPh, ClMe, Cl_2) (**III-37**).[14] In contrast, tantalum agostic silylamides were not observed, presumably, due to the fast SiR'_2H migration process (see Scheme 7, chapt. II.1.4).[14h]

Recently, we have became interested in the development of analogous imido/silane coupling reactions for bis(imido) molybdenum and tungsten systems. Preliminary research by Nikonov *et al.*[15] has showed that the reactions of $(Ar'N)Mo(PMe_3)_3$ (**III-4**) with the chlorosilanes $HSiMe_2Cl$ and $HSiMeCl_2$ afford exclusively the β-agostic Si-H···Mo d^2 complexes $(Ar'N)Mo(\eta^3\text{-}NAr'\text{-}Si(Me)R\text{-}H)(Cl)(PMe_3)_2$ (R = Me (**III-38**), Cl (**III-39**); see Scheme 8, chapt. II.1.4). At the same time, the treatment of **III-4** with $HSiCl_3$ results in the formation of dichloride $(Ar'N)MoCl_2(PMe_3)_3$ (**III-5**) and the release of the silanimine dimer $(Ar'N\text{-}SiHCl)_2$ (Scheme 8, chapt. II.1.4).[15] DFT calculations of a series of model complexes $(MeN)Mo(Cl)(\eta^3\text{-}NMe\text{-}SiMe_nCl_{2-n}\text{-}H)(PMe_3)_2$ (**III-40**, n = 0 – 2) suggested that the formation of **III-5** could be a result of the strengthening of the residual Si-H bond in agostic species upon increased Cl substitution at silicon. This could lead to the rearrangement of the molecule to form a Cl-bridged intermediate $(MeN)Mo(Cl)(\eta^3\text{-}NMe\text{-}SiMe_nHCl_{1-n}\text{-}Cl)(PMe_3)_2$ (**III-41**, n = 0 – 1), which upon the β-Cl elimination in the presence of phosphine can form dichloride the **III-5** and $(Ar'N\text{-}SiHCl)_2$.[15] In the course of the present work the scope of molybdenum bis(imido) complexes in silane/imido coupling reaction was expanded to Ar and ^{t}Bu compounds and screened for variety of chloro-substituted hydrosilanes.

Similarly to complex **III-4**, compounds $(ArN)_2Mo(PMe_3)_3$ (**III-22**) and $(^tBuN)_2Mo(PMe_3)_2$ (**III-27**) react with mono- and dichlorosilanes to give exclusively the β-Si-H agostic derivatives $(RN)Mo(Cl)(\eta^3\text{-}RN\text{–}SiR'_2\text{-}H)(PMe_3)_2$ (R'_2 = Me_2 (**III-42a,c**), MePh (**III-43a-c**), MeCl (**III-44a,c**), PhH (**III-45a,b**), and Ph_2 (**III-46b,c**); Scheme 84). Formation of the compound **III-42c**, with the intermediacy of $(^tBuN)Mo(Cl)(\eta^3\text{-}^tBuN\text{-}SiMe_2\text{-}H)(\eta^2\text{-}CH_2{=}CH_2)(PMe_3)$ (**III-47**), was also observed upon treatment of the ethylene adduct $(^tBuN)_2Mo(\eta^2\text{-}CH_2{=}CH_2)(PMe_3)$ (**III-30**) with Me_2SiHCl. The original Nikonov's synthesis of $(Ar'N)_2Mo(Cl)(\eta^3\text{-}NAr'\text{–}SiR'_2\text{-}H)(PMe_3)_2$ (R'_2 = Me_2 (**III-38**) and MeCl (**III-39**)) was also repeated in the course of the present work in order to obtain more detailed spectroscopic characteristics. In contrast to the chemistry of the half-sandwich imido complexes of niobium and tantalum,[14] the formation of the isomeric silylhydride compounds $(RN)_2Mo(SiR'_2Cl)(H)(PMe_3)$ was not observed even when the reactions were monitored by low temperature NMR spectroscopy. It should be noted that the agostic compounds **III-38**, **III-39**, **III-42** – **III-46** are metastable in solution and leaving the reaction mixture at room temperature leads to a slow decomposition to the thermodynamically stable products $(RN)MoCl_2(PMe_3)_3$ (R = Ar (**III-47**) and ^{t}Bu (**III-48**); Scheme 84), analogous to that reported for the Ar'-substituted imido complex.[15] The main silicon co-product of this reaction is the silanimine dimer $(RN\text{-}SiR'_2)_2$, whose formation manifests productive coupling of the imido ligand with the silane. The same behaviour has been previously observed for additions of chloro-substituted silanes to the isolobal Group 5 compounds $Cp(RN)M(PMe_3)_2$ (M = Ta (**III-33**), Nb (**III-34**); R = Ar or

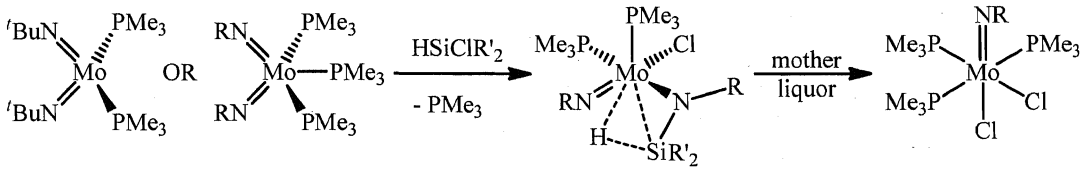

III-27 R = Ar (**III-22**), Ar' (**III-4**)

R = Ar: R'_2 = Me_2 (**III-42a**), MePh (**III-43a**), MeCl (**III-44a**), PhH (**III-45a**)

R = Ar': R'_2 = Me_2 (**III-38**), MePh (**III-43b**), MeCl (**III-39**), PhH (**III-45b**), Ph_2 (**III-46b**)

R = ^{t}Bu: R'_2 = Me_2 (**III-42c**), MePh (**III-43c**), MeCl (**III-44c**), Ph_2 (**III-46c**)

R = Ar' (**III-5**), Ar (**III-47**), ^{t}Bu (**III-48**)

Scheme 84. Reactivity of $(RN)_2Mo(PMe_3)_n$ with $HSiClR'_2$ and $HSiMeCl_2$.

Ar'), for which the initial agostic or silylhydride products were found to be intermediates on the way to dichlorides $Cp(RN)MCl_2(PMe_3)$ (**III-49**) and $CpMCl_2(PMe_3)_3$ (**III-50**).[14]

The rate of silane addition to complexes **III-4**, **III-22**, and **III-27** appears to be controlled by steric factors. Thus, the relatively unhindered compounds **III-4** and **III-27** react over a period of several hours. Compound **III-22**, bearing the relatively bulky Ar group at the imido nitrogen, reacts with $HSiMe_2Cl$ overnight, whereas its reaction with the more hindered HSiMePhCl takes several days and is accompanied by significant decomposition to **III-47**. The reactivity study of **III-22**, conducted previously by Nikonov *et al.*, revealed no reaction of the bis(imido) complex with $HSiPh_2Cl$ even after several days. In contrast to trimethylphosphine complexes, the reaction of reasonably bulky $(Ar'N)_2Mo(PMe^iPr)_2$ (**III-25**) with $PhSiH_2Cl$ is not clean and after 5 min. at room temperature shows formation of a difficult-to-characterize mixture of unknown decomposition products.

Agostic compounds **III-38**, **III-39**, and **III-42 – III-46** were characterized by IR and multinuclear NMR spectroscopy. The X-ray structure determinations for compounds **III-38** and **III-39** were previously reported by Nikonov *et al.*[15, 17] Apart from X-ray parameters, which were already obtained and discussed prior to this work, the presence of the agostic Si-H···Mo bond has been established spectroscopically. For example, the ^{1}H-NMR spectrum of compound **III-44c** exhibits the characteristic agostic Si–H···M hydride as a phosphorus-coupled up-field shifted signal at 1.45 ppm (dd, $^2J_{H\text{-}P}$ = 3.6 Hz and 0.9 Hz), two nonequivalent ^{t}Bu signals at 1.54 ppm (imido) and 1.15 ppm (amido), and the SiMe signal at 1.18 ppm. The agostic hydride gives rise to a band at 2128 cm^{-1} in the IR spectrum. Compounds **III-38**, **III-39**, **III-43b,c**, **III-44a**, and **III-46c** are fluxional in solution and their room temperature ^{1}H-NMR spectra show only featureless signals in the aliphatic and aromatic regions. However, lowering the temperature down to -40 – -70 °C affords the observation of distinct resonances of pure silylamides, similar to those described for **III-44c**. Selected NMR data for the β-agostic silylamido molybdenum complexes are summarized in Table 3.

The nature of the fluxionality of agostic complexes **III-38** and **III-39** was suggested by Nikonov *et al.* on the basis of VT NMR studies, which revealed the pairwise methyl group degenerate exchange processes $Me^2 \leftrightarrow Me^1$, $Me^7 \leftrightarrow Me^6$, $Me^8 \leftrightarrow Me^9$, and $Me^3 \leftrightarrow$

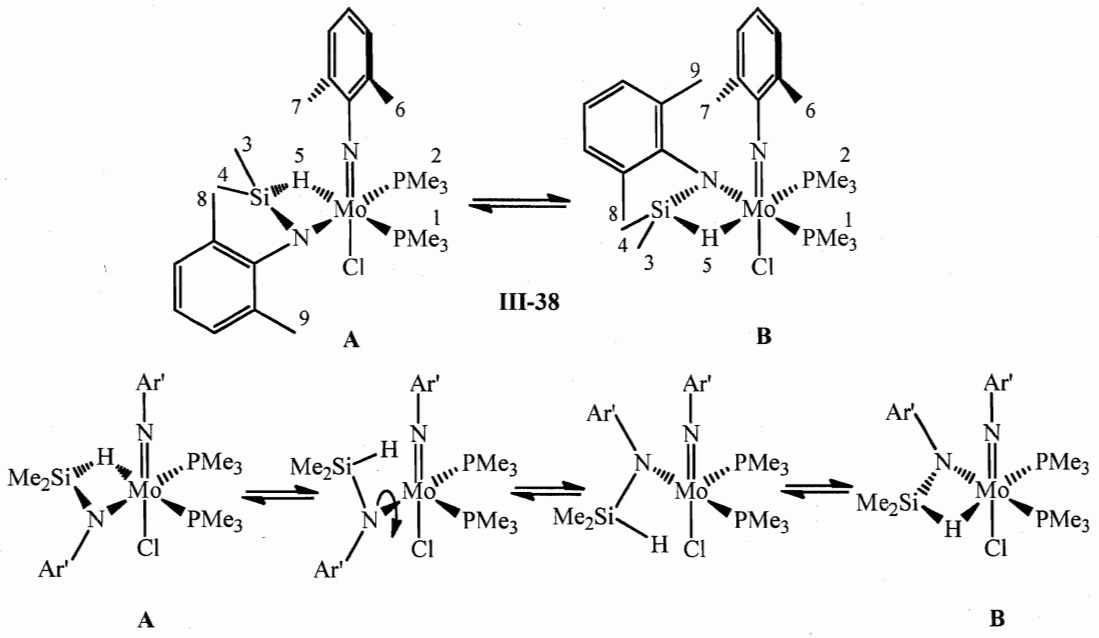

Scheme 85. Degenerate exchange in complex **III-38** (two enantiomers, "**A**" and "**B**") and proposed mechanism for this process.

Me[4] (Scheme 85). Careful line shape analysis of Me signals in ^{1}H-NMR spectra provided activation parameters for the exchange in **III-38**, consistent with the proposed mechanism presented in Scheme 85.[g] For the silylamide **III-39**, the situation is more complicated due to the presence of two chiral centers in the molecule (molybdenum and silicon) and thus the possibility of diastereomerism (the second diastereomer of **III-39** was observed by Nikonov *et al.* in the ^{1}H- and ^{31}P-NMR spectra acquired at - 40 °C).

The formulation of compounds **III-38**, **III-39**, **III-42a,c**, **III-43b,c**, and **III-44a,c** as agostic species is further supported by the measurements of silicon-hydride coupling constants from the ^{29}Si- and ^{29}Si INEPT+ NMR spectra (Table 3). These values are about half of those in the parent silanes but significantly larger than for non-interacting silyl and hydride groups (3-10 Hz).[38] Notably, the $^{1}J_{Si-H}$ of 98 and 97 Hz in **III-3** and **III-42a**, respectively, are the same as silicon-proton coupling constant observed previously for the structurally characterized isolobal compound CpNb(Cl)(η^3-ArN–SiMe$_2$H)(PMe$_3$) (**III-36$_{Me2}$**).[14a] As can be seen from Table 3, chlorine substitution at silicon leads to increased

[g] The mechanism depicted in Scheme 85 was proposed based on the observation of somewhat negative values of the $\Delta S^{\ddagger}$ = -10 – -15 cal mol^{-1} K^{-1}, ruling out phosphine dissociation as a possible step in exchange.

Table 3. Selected NMR and IR data for β-agostic silylamido molybdenum complexes.

Compound	δ ^{1}H: Si-*H*, ppm (J_{H-P}, Hz)	δ ^{29}Si, ppm[a]	$^1J_{Si-H}$, Hz[a]	υ_{Si-H}, cm^{-1}
III-38	1.68[f] (dd; 3.5, 23.5)	-63.8[f]	98[f]	1910
III-39	2.02[g] (dd, 4, 20)	70.1 70.5[f]	129 135.6[f]	1920
III-42a	0.88 (t; 7.5)	-64.9	97	1943
III-42c	1.4[b,c]	-76.0	93	1992
III-43b	2.14[c,d] (t; 22.0)	-69.3[d]	98[d]	1906
III-43c	1.83[b,c,e]	-79.9	94	2121
III-44a	1.23[b,c,f]	-68.7[f]	130[f]	2167
III-44c	1.45 (dd; 3.6, 0.9)	-74.2	123	2128

[a] At room temperature unless otherwise stated. [b] The signal is obscured by other resonances. [c] Found from ^{1}H-^{29}Si HSQC. [d] at – 40 °C. [e] at – 20 °C. [f] at – 50 °C. [g] at – 70 °C.

Si-H coupling constants (for instance, 123 Hz in **III-44c** and 130 Hz in **III-44a** *vs.* 93 Hz for **III-42c** and 97 Hz for **III-42a**); however, this increase in $^1J_{Si-H}$ values does not correspond to a stronger residual Si-H bonding but is instead a result of rehybridization at the silicon center in accordance with Bent's rule[48, 49] and the revised DCD model (see chapt. II.1.3).[15, 17] Surprisingly, no correlation was found between the values of $^1J_{Si-H}$ and the Si-H band in the IR spectrum. Thus, an insignificant increase in the $^1J_{Si-H}$ for complex **III-42c**, comparable with **III-38**, is accompanied by a significant low-frequency shift of the Si-H band from 1992 to 1910 cm^{-1}. In contrast, in the chloride-substituted silylamido compounds the increase of $^1J_{Si-H}$ from **III-44c** to **III-44a** (from 123 Hz to 130 Hz, respectively) corresponds to the expected shift of the hydride stretch to higher frequencies (from 2128 cm^{-1} to 2167 cm^{-1}, respectively), closer to the typical silane region. This difference emphasizes again the fact that the observed agostic "hydride" band in the IR spectra stems from the coupled M-H and Si-H stretches whose dependence on the substitution at silicon can be difficult to rationalize.[17]

III.3.1 Reactions of $(RN)_2M(PR'_3)_{n-1}L$ with $HSiCl_3$

As was already mentioned, the treatment of $(Ar'N)_2Mo(PMe_3)_3$ (**III-4**) with trichlorosilane has been reported to give a novel Mo(IV) mono(imido) complex $(Ar'N)MoCl_2(PMe_3)_3$ (**III-5**) accompanied by the release of the silanimine dimer $(Ar'N\text{-}SiHCl)_2$.[15] In the course of the present work, a similar reactivity towards $HSiCl_3$ has been shown for the Ar and ^{t}Bu molybdenum derivatives **III-22** and **III-27**, respectively, as well as for the tungsten analog $(ArN)_2W(PMe_3)_3$ (**III-23**) (Scheme 86). The reactions proceed at room temperature and are reasonably fast (minutes – overnight) affording selectively the mono(imido) compounds $(RN)MoCl_2(PMe_3)_3$ (R = Ar (**III-47**) and ^{t}Bu (**III-48**)) and $(ArN)WCl_2(PMe_3)_3$ (**III-51**) in moderate to high yields (42 % - 82 %, depending on the time of the experiment).[200] Interestingly, the treatment of the bis(imido) complex **III-22** with Me_2SiCl_2 does not lead to the formation of the corresponding mono(imido) derivative **III-47**. No reaction was observed after one week at room temperature even in the presence of an equivalent of BPh_3. Such lack of reactivity of **III-22** with dichlorodimethylsilane compared to $HSiCl_3$ and other chlorohydrosilanes $HSiCl_nR_{3-n}$ (n = 1 – 3) could be a result of the steric control. In this regard, the presence of chloride and R substituents at silicon (both are more sterically demanding than hydride) could prevent the coordination of the silane to the imido nitrogen, which was shown to be necessary for further Si-Cl bond activation.[14, 15, 17]

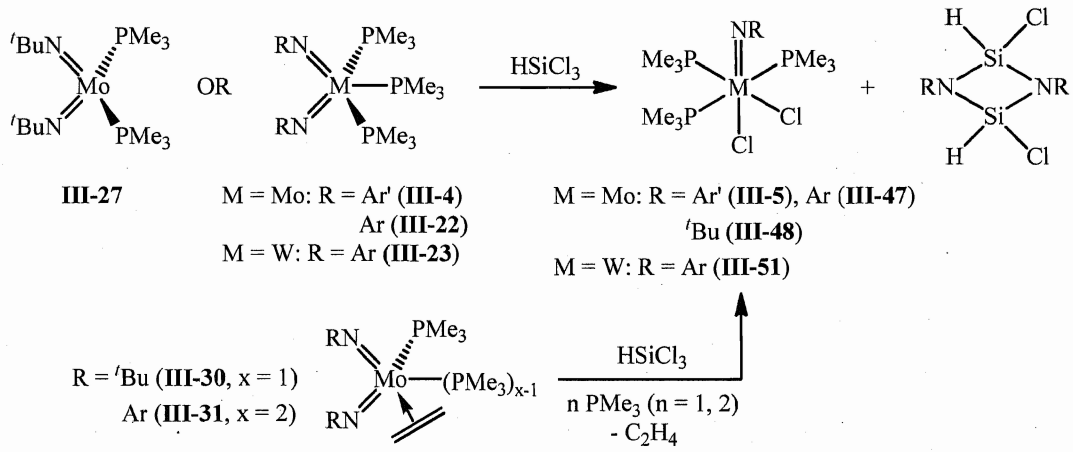

Scheme 86. Reactivity of $(RN)_2M(PMe_3)_{n-1}L$ (M = Mo, W; L = PMe_3, η^2-C_2H_4) with $HSiCl_3$.

Alternatively, molybdenum dichlorides **III-47** and **III-48** could be obtained by the reaction of the corresponding bis(imido) ethylene adducts $(ArN)_2Mo(\eta^2\text{-}CH_2{=}CH_2)(PMe_3)_2$ (**III-31**) and $(^tBuN)_2Mo(\eta^2\text{-}CH_2{=}CH_2)(PMe_3)$ (**III-30**) with $HSiCl_3$ in the presence of one or two equivalents of PMe_3, respectively (Scheme 86). The reactions were initially performed on the NMR scale showing quantitative formation of dichloride complexes. However, preparative scale transformation using **III-31** proved to be much less selective affording a difficult-to-separate mixture of compound **III-47** and an unknown by-product. On the other hand, treatment of **III-31** with $HSiCl_3$ in the presence of one equivalent of BPh_3 leads to a completely different reactivity and NMR monitoring of the reaction showed, after 5 min. at room temperature, the formation of $(ArN)Mo(Cl)(SiHCl_2)(\eta^2\text{-}CH_2{=}CH_2)(PMe_3)$ (**III-52**; Scheme 87) and the release of the $Ph_3B{\cdot}PMe_3$ adduct. The structure of **III-52** was suggested on the basis of NMR analysis, which shows the presence of one imido ArN^{2-} ligand, a classical Si*H* proton (P-coupled doublet at 6.7 ppm ($^3J_{H\text{-}P}$ = 2.4 Hz) in the ^{1}H-NMR spectrum), and a coordinated ethylene ligand (ethylene protons give rise to signals at 2.89, 2.46, and 2.22 ppm in the ^{1}H-NMR spectrum)).

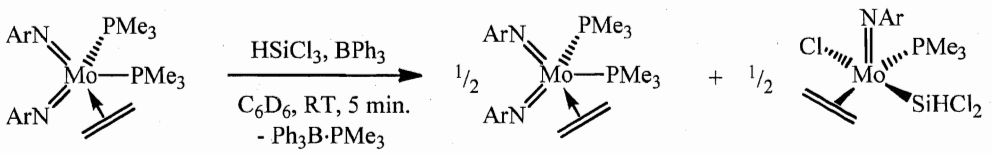

III-31 **III-31** **III-52**

Scheme 87. Reaction of $(ArN)_2Mo(\eta^2\text{-}C_2H_4)(PMe_3)_2$ (**III-31**) with $HSiCl_3$ and BPh_3.

DFT calculations reported earlier by Nikonov *et al.*[15] for the model system $(MeN)Mo(Cl)(\eta^3\text{-}NMe\text{-}SiMe_nCl_{2\text{-}n}\text{-}H)(PMe_3)_2$ (**III-53**, n = 0 – 2) suggested that the formation of mono(imido) molybdenum complexes $(RN)MoCl_2(PMe_3)_3$ could be a result of rearrangement of the initially formed agostic intermediate $(RN)Mo(\eta^3\text{-}NR\text{-}SiCl_2\text{-}H)(Cl)(PMe_3)_3$ into a Cl-bridged species $(RN)Mo(\eta^3\text{-}NR\text{-}Si(Cl)H\text{-}Cl)(Cl)(PMe_3)_3$. Such a rearrangement takes place due to the strengthening of the Si-H bonding upon Cl substitution at silicon due to increased Si 3s contribution in accordance with Bent's rule.[48, 49] To shed more light on the mechanism of the reaction of $(ArN)_2Mo(PMe_3)_3$ (**III-22**) with $HSiCl_3$ we performed low temperature VT NMR studies in an attempt to trap a

key-intermediate of this process. At –30 °C, the formation of an initial bis(phosphine) complex having two broad ^{31}P NMR singlets of equal intensity at 20.0 and –2.6 ppm was observed. In the ^{1}H-NMR spectra, this compound shows a down-field Si*H* signal at 7.10 ppm coupled in the ^{1}H-^{29}Si HSQC with the ^{29}Si NMR signal at –31.8 ppm with $^{1}J_{H\text{-}Si}$ = 337.5 Hz (found from ^{29}Si INEPT+ NMR spectroscopy). The large value of $^{1}J_{H\text{-}Si}$ and the fact that neither the Si-bound proton nor the ^{29}Si-NMR signal are coupled to the phosphorus atom suggest the absence of the Si-H bond coordination to metal. These features are consistent with the initial formation of a silylamido complex (ArN)Mo(Cl)(η^2-NAr-SiHCl-Cl)(PMe_3)$_2$ (**III-54a**; Figure 17), which presumably has an additional coordination of one of the Si-bound chlorides to molybdenum, allowing for the formation of a 18e species. Unfortunately, we have no evidence for the formation of the Si-Cl-Mo bridge, but this inference seems to be a reasonable alternative to the otherwise 16-electron imido/amido derivative, (ArN)Mo(Cl)(NAr{$SiCl_2H$})(PMe_3)$_2$ (**III-54b**). Moreover, according to DFT calculation reported by Nikonov *et al.*, optimization of the HSi–Cl···Mo bonded structure gives an energy only *ca.* 1 kcal above the agostic ClSi–H···Mo structure.[15]

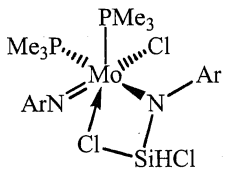

III-54a

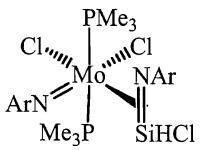

III-55

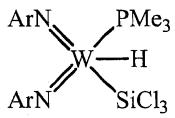

III-56

Figure 17. Suggested intermediates for reactions of **III-22** and **III-23** with $HSiCl_3$.

Warming the reaction mixture to –15 °C – 0 °C leads to a slow rearrangement of the initial product into another bis(phosphine) compound exhibiting a large $^{2}J_{P\text{-}P}$ coupling constant of 223.5 Hz, suggesting the trans- arrangement of phosphine ligands. In the ^{1}H-NMR spectrum, this derivative shows a downfield Si*H* signal at 6.01 ppm coupled to one of the phosphines with the $^{3}J_{H\text{-}P}$ of 9.0 Hz and also coupled in the ^{1}H-^{29}Si HSQC NMR spectrum to the ^{29}Si NMR signal at –42.4 ppm (appears in the ^{29}Si INEPT+ NMR spectrum as a doublet of doublets with $^{1}J_{Si\text{-}H}$ = 327.0 Hz and $^{2}J_{Si\text{-}P}$ = 22.1 Hz). The large value of $^{1}J_{Si\text{-}H}$ is consistent with the Si-H bond being uncoordinated to the metal, whereas the large $^{2}J_{Si\text{-}P}$ and small $^{3}J_{SiH\text{-}P}$ constants show that the silicon atom is directly bound to

molybdenum. All together these NMR features suggest the formation of the silanimine complex (ArN)$MoCl_2(\eta^2$-ArN=SiHCl)$(PMe_3)_2$ (**III-55**, Figure 17), which could be a direct precursor to the dichloride complex (ArN)$MoCl_2(PMe_3)_3$ (**III-47**). Consistent with the description, addition of an equivalent of PMe_3 to this mixture results in immediate formation of **III-47**.

Compound **III-47** was characterized by X-ray diffraction (see chapt. VI, Table 25 for crystal structure determination parameters). The complex adopts an octahedral geometry, with one of the chloride substituents lying trans- to the imido group (Figure 18). The second chloride occupies an equatorial position (*cis*- to ArN^{2-}) and is co-planar with all three PMe_3 ligands. The imido moiety in **III-47** is almost linear (Mo1-N1-C1 angle is 172.7(3)°; Table 4), which indicates that the ArN^{2-} ligand acts as a 6 electron donor to the metal stabilizing the 18e valence shell. Analogous structural parameters were reported earlier for (^{t}BuN)$MoCl_2(PMe_3)_3$ (**III-48**) by Green *et al.*[200]

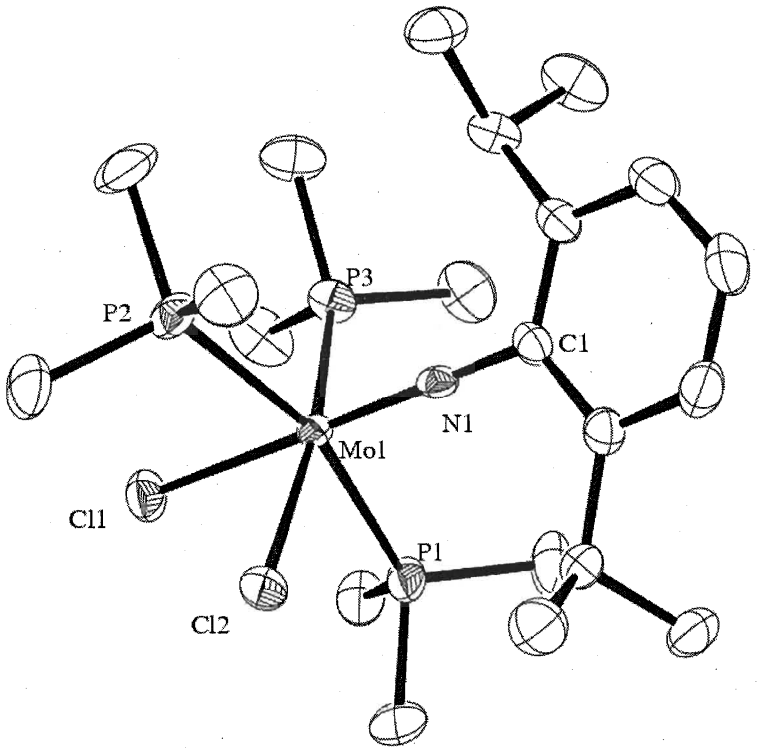

Figure 18. ORTEP plot for the molecular structure of (ArN)$MoCl_2(PMe_3)_3$ (**III-47**) (hydrogen atoms are omitted for clarity). Anisotropic displacement parameters are plotted at 50 % probability.

Table 4. Selected bond distances (Å) and angles (°) for complex **III-47**.

distances, Å		Angles, °	
Mo1-N1	1.753(4)	Mo1-N1-C1	172.7(3)
Mo1-Cl1	2.5079(14)	N1-Mo1-Cl1	179.28(13)
Mo1-Cl2	2.5206(13)	Cl1-Mo1-Cl2	85.31(5)
Mo1-P1	2.5080(15)	N1-Mo1-Cl2	94.95(13)
Mo1-P2	2.5158(14)	P1-Mo1-P2	163.84(5)
Mo1-P3	2.4987(15)	P1-Mo1-P3	90.45(5)
N1-C1	1.405(6)	P2-Mo1-P3	99.51(5)

In contrast to the Mo chemistry, a low temperature (-20 °C) NMR scale reaction of $(ArN)_2W(PMe_3)_3$ (**III-23**) with $HSiCl_3$ in the presence of an equivalent of BPh_3 revealed the formation of a bis(imido) intermediate. In the ^{1}H-NMR, this compound shows a W-bound hydride signal at 11.04 ppm coupled to the phosphine ($^2J_{H\text{-}P}$ = 58.8 Hz) and tungsten ($^1J_{H\text{-}W}$ = 31.8 Hz). A weak coupling of the hydride to the ^{29}Si signal at 73.8 ppm is also observed in the ^{1}H-^{29}Si HSQC NMR. These spectroscopic features are consistent with the formation of a silylhydride derivative $(ArN)_2W(H)(SiCl_3)(PMe_3)$ (**III-56**; Figure 17). A similar complex, $(ArN)_2W(H)(SiMeCl_2)(PMe_3)$ (**III-57**), was obtained earlier by Nikonov *et al.* by the reaction of **III-23** with $MeSiHCl_2$.[h] Furthermore, the formation of bis(imido) silylhydride tungsten species *vs.* imido silylamides, described above for molybdenum, is in agreement with the well-known fact of greater stability of W(VI) compounds compared to Mo(VI) species. Gradually warming the reaction mixture up to room temperature leads to decomposition of **III-56** to a mixture of $(ArN)WCl_2(PMe_3)_3$ (**III-51**) and several uncharacterized hydride products. Despite the lack of observation of the agostic compound $(ArN)W(\eta^3\text{-}NAr\text{-}SiCl_2\text{-}H)(Cl)(PMe_3)$ (**III-58**) and the Cl-bridged species $(ArN)W(\eta^3\text{-}NAr\text{-}SiClH\text{-}Cl)(Cl)(PMe_3)$ (**III-59**), their formation seems to be a reasonable step in the path to complex **III-51**. This is further supported by the recent success in the isolation of $(RN)W(\eta^3\text{-}NR\text{-}SiR'_2\text{-}H)(Cl)(PMe_3)$ prepared by the reaction between $(RN)_2W(PMe_3)_3$ and $HSiR'_2Cl$ (R = Ar, Ar'; R'_2 = MeCl, Me_2).[h] Moreover,

[h] This research has been combined with the present study of the reactivity of bis(imido) molybdenum complexes and was published in *Inorg. Chem.* **2009**, *48*, 9605.

Nikonov *et al.* demonstrated that treatment of **III-57** with PMe_3 affords the Si-Cl-W bridged complex (ArN)W(η^2-NAr-SiMeH-Cl)(Cl)(PMe_3) (**III-60**), which slowly rearranges in solution to (or is in equilibrium with) the β-Si-H agostic compound (ArN)W(η^3-NAr-SiMeCl-H)(Cl)(PMe_3) (**III-61**).

Combining all the observations, the overall suggested mechanism for the reaction of **III-23** with $HSiCl_3$ could be described as shown in Scheme 88 and includes the following steps: (i) formation of the silylhydride intermediate **III-56** as a kinetic product, (ii) rearrangement of the latter into the Cl-bridged species (ArN)W(η^2-NAr-SiHCl-Cl)(Cl)(PMe_3) (**III-62**), which upon (iii) β-chloride elimination releases a silanimine dimer and gives the dichloride complex **III-51**. This scheme is reminiscent of the earlier reported reactions of the isolobal half-sandwich niobium imides CpNb(NR)(PMe_3)$_2$ (**III-34**) with silanes, where the initially formed silylhydrides CpNb(NR)(H)(SiR'$_2$Cl)(PMe_3) rearrange into the agostic products CpNb(Cl)(η^3-NR-SiR'$_2$-H)(PMe_3) (for R'$_2$ = Me_2, MePh) or silyl chloride compound CpNb(NR)(Cl)(SiR'$_2$H)(PMe_3) (for R'$_2$ = MeCl). Both of these reactions are catalyzed by PMe_3.[14e]

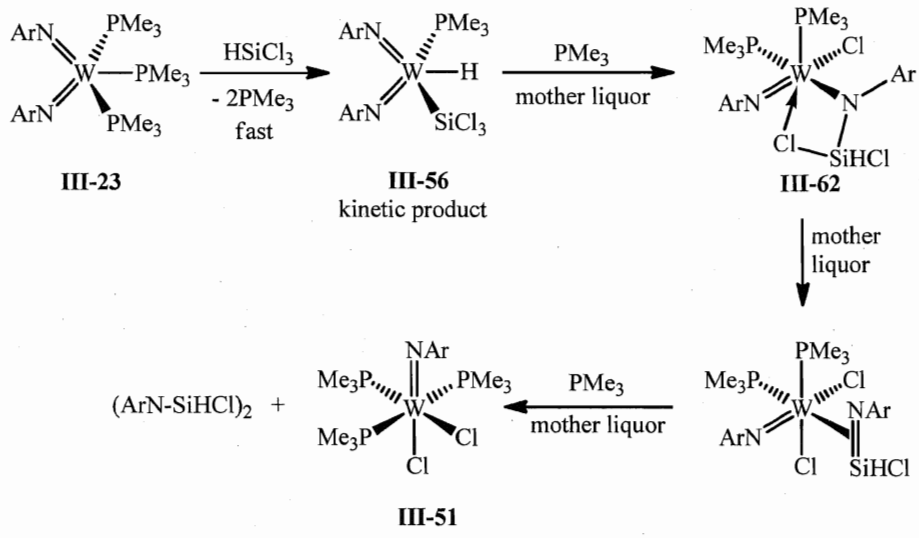

Scheme 88. Proposed mechanism for the reaction of **III-23** with $HSiCl_3$.

III.4 Reactivity of $(RN)_2M(PR'_3)_{n-1}L$ towards hydrosilanes

After the discovery of the imido/silane coupling reactions between chloro-substituted hydrosilanes and Mo and W bis(imido) phosphine complexes, we have become interested in the study of reactivity of these imido compounds towards chlorine-free hydrosilanes. We anticipated that these reactions would lead to the formation of stable chlorine-free

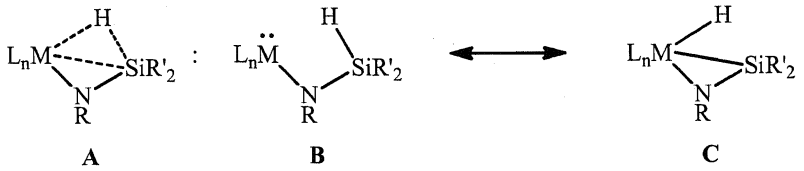

Figure 19. Canonical forms for the bonding in d^2 agostic silylamide complexes.

agostic silylamide derivatives, which were expected to have a greater extent of Si-H bond activation due to the absence of additional lone-pair donation from the halogen substituent. The possibility of such coupling between the imido moiety and chlorine-free hydrosilanes was demonstrated recently by groups of Tilley[16] and Fryzuk[56] for tantalum complexes (see Scheme 9, chapt. II.1.4). The bonding situation in such d^2 β-agostic silylamides $L_nM(\eta^3\text{-NR-SiR'}_2\text{-H})$ (**A**; Figure 19) can be represented by two canonical forms, **B** and **C**, one of which has a silanimine character (**C**). This fact suggests that compounds of the type **A** could serve as synthons for silanimine complexes, which, although very scarce,[142, 201] are known to exhibit a wealth of reactivity.[142] In this regard, we proposed that variation of substituents at silicon and imido nitrogen could result in a compound with a trapped silanimine ligand. Taking into account the fact that our synthetic approach starts with the coordination of silane to the imido nitrogen,[14, 15, 17] the choice of hydrosilane substrates suitable for the test reactions was made for the reasonably Lewis acidic silanes $PhSiH_3$, $PhMeSiH_2$, and $(EtO)_3SiH$.

III.4.1 Reactions of $(RN)_2M(PR'_3)_{n-1}L$ with $PhSiH_3$

III.4.1.1 Reactions of Ar and Ar' complexes

Initially, the reactions of bis(imido) phosphine complexes $(RN)_2M(PR'_3)_n$ with phenylsilane were studied on the NMR scale. Thus, treatment of $(ArN)_2Mo(PMe_3)_3$ (**III-22**) with an equivalent of $PhSiH_3$ in C_6D_6 at room temperature leads instantaneously to

the release of two equivalents of phosphine and formation of a 1:1 mixture of the starting complex and a novel highly fluxional compound, showing broad resonance for the PMe_3 ligand in the ^{31}P-NMR spectrum. Leaving the reaction mixture at room temperature for few hours results in decomposition of the initial product to give a difficult-to-separate mixture of imido polyhydride derivatives. Formation of the same mixture is also observed when excess $PhSiH_3$ is used. Careful analysis of NMR data allowed us to assign the signals of the decomposition products to $(ArN)MoH_4(PMe_3)_3$ (**III-63**) and [η^3-SiH(Ph)-N(Ar)-SiHPh-H]$MoH_3(PMe_3)_3$ (**III-64**) (3:5 ratio according to $^{31}P\{^1H\}$-NMR; Scheme 89). All attempts to separate **III-63** and **III-64** *via* recrystallization were not successful; however, addition of excess $PhSiH_3$ to the mixture leads to a very slow conversion (few weeks) of the tetrahydride **III-63** to a disilyl trihydride **III-64**, increasing their ratio to 3:7. The ^1H-NMR spectrum of complex **III-63** shows an up-field shifted signal for all four equivalent hydride substituents at –5.27 ppm (quartet, $^2J_{H\text{-}P}$ = 29.4 Hz) coupled to the ^{31}P NMR signal for three equivalent PMe_3 ligands at 4.8 ppm. The ^{31}P-NMR coupled to proton and selectively decoupled from Me groups at phosphorus gives rise to a pentet with the same H-P coupling constant, confirming the presence of four hydride substituents in **III-63**. The silicon substituted by-product **III-64** is highly fluxional at room temperature, but cooling the sample down to –45 °C allows for the observation of three non-equivalent hydride resonances of equal intensity at -8.82 (d, $^2J_{H\text{-}P}$ = 19.2 Hz), -6.58 (t, $^2J_{H\text{-}P}$ = 36.0 Hz), and -5.61 ppm (d, $^2J_{H\text{-}P}$ = 53.4 Hz) in the ^1H-NMR. The Si-bound protons of the silyl ligand [η^3-SiH(Ph)-N(Ar)-SiHPh-H] give rise to broad singlets

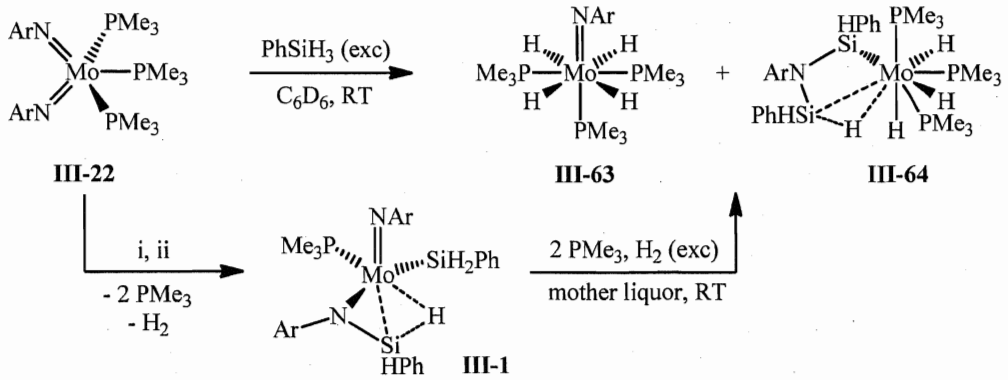

i - low temperature NMR scale reaction with 1 equiv. of $PhSiH_3$ (50 % yield according to NMR)
ii - preparative scale reaction with 2 equiv. of $PhSiH_3$ and N_2 purging (77 % yield)

Scheme 89. Reaction of $(ArN)_2Mo(PMe_3)_3$ (**III-22**) with $PhSiH_3$

at 5.22 and 5.63 ppm, coupled in the ^{1}H-^{29}Si HSQC NMR to the ^{29}Si signals at -14.2 and 51.3 ppm, respectively. Also, the presence of two SiHPh groups is confirmed by the observation of two doublets for ortho protons of two non-equivalent Si*Ph* groups at 8.90 and 8.47 ppm in the ^{1}H-NMR spectrum. At room temperature, the PMe_3 signals in the ^{31}P-NMR spectrum merge into one broad singlet at -7.7 ppm, however, at -45 °C the ^{31}P-NMR spectrum shows three non-equivalent resonances at -8.8 (t, $^{2}J_{P\text{-}P}$ = 40.0 Hz), -6.6 (dd, $^{2}J_{P\text{-}P}$ = 21.9 and 40 Hz), and 3.7 ppm (dd, $^{2}J_{P\text{-}P}$ = 21.9, 40.0 Hz). Unfortunately, the agostic Si-H···Mo hydride was not found by NMR spectra, however, the formulation of **III-64** as a Mo(IV) agostic species seems to be more reasonable than the formation of a Mo(V) bis(silyl) derivative [η^2-SiH(Ph)-N(Ar)-SiHPh]$MoH_3(PMe_3)_3$, which should be paramagnetic.

The reaction of **III-22** with an equivalent of $PhSiH_3$ at low temperature was followed by NMR spectroscopy. At -30 °C, 50 % conversion of the starting complex and formation of a novel agostic silylamide derivative (ArN)Mo(SiH_2Ph)(η^3-NAr-SiHPh-H)(PMe_3) (**III-1**) was observed (Scheme 89). In the presence of PMe_3 and H_2 complex **III-1** is not stable at room temperature and decomposes to a mixture of **III-63** and **III-64**. Nonetheless, the preparative scale reaction of **III-22** with two equivalents of $PhSiH_3$ under N_2 purging (in order to remove effectively the released H_2 and PMe_3) allowed us to isolate **III-1** in 77 % yield. Instead of running this reaction under N_2 purging, an alternative method to remove PMe_3 and H_2 would be to add two equivalents of BPh_3, forming the adduct $Ph_3B{\cdot}PMe_3$. However, in this case the reaction is not clean and the isolation is complicated due to the similar solubility of the product and $Ph_3B{\cdot}PMe_3$. Silylamide **III-1** was fully characterized by multinuclear NMR, IR and X-Ray diffraction (structure determination parameters are listed in Table 26, chapt. VI), which confirmed the β-agostic NSi-H···Mo structure. **III-1** is fluxional at room temperature, but at –50 °C the ^{1}H-NMR spectrum shows the presence of two silicon centers: the silyl group with two diastereotopic Si*H* signals at 5.97 and 5.68 ppm, coupled to a ^{29}Si-NMR signal at 1.2 ppm (t, $^{1}J_{Si\text{-}H}$ = 153.5 Hz; found by ^{29}Si NEPT+ NMR spectroscopy), and silylamido ArN-SiH_2Ph ligand, in which one SiH_a proton gives rise to an up-field resonance at 4.35 ppm (bm), coupled with a small $^{2}J_{H\text{-}H}$ of 5.4 Hz to another Si*H* proton at 6.03 ppm (bd). Both Si-bound proton signals of the silylamide substituent are coupled in the ^{1}H-^{29}Si HSQC NMR spectrum to one silicon

signal at -72.9 ppm (dd, $^1J_{Si\text{-}Ha}$ = 113.0 Hz, $^1J_{Si\text{-}H}$ = 245.3 Hz; found by ^{29}Si INEPT+ NMR spectroscopy). These spectroscopic features, in particular the up-field SiH_a shift in the ^{1}H NMR, the up-field shifted ^{29}Si NMR signal, and the small value of $^1J_{Si\text{-}Ha}$, suggest coordination of the Si-H bond to molybdenum.[17] Additionally, the presence an agostic bonding is supported by IR spectroscopy, in which the agostic Si-H_a bond gives rise to a red-shifted band at 1694 cm^{-1}, whereas three other classical Si-H stretches are found at 2014, 2041, and 2165 cm^{-1} (see the discussion in chapt. II.1.3). At -30 °C, the coupled-to-proton ^{31}P-NMR spectrum of **III-1** with selective decoupling from the Me groups shows a doublet for PMe_3 at 10.6 ppm due to the coupling to the agostic SiH_a ($^2J_{H\text{-}P}$ = 9.3 Hz). The observation of a slightly increased, compared to CpNb(Cl)(η^3-NAr-SiMe$_2$-H)(PMe_3) (**III-37**) and (Ar'N)Mo(η^3-NAr'-SiMe$_2$-H)(Cl)(PMe_3)$_2$ (**III-39**), value of the $^1J_{Si\text{-}Ha}$ coupling constant for **III-1** (96.0[14a] and 97.0 Hz[15] *vs.* 113.0 Hz, respectively) may indicate a smaller extent of Si-H activation, owing to a greater electron deficiency of the 16e Mo(IV) center in **III-1**.[i]

The molecular structure of complex **III-1** can be described as a distorted molybdenum-centered trigonal bipyramid having the PMe_3 group and the agostic hydride ligand in the apical positions (Figure 20). The Mo1-Si1 distance involving the agostic silyl group (2.634(1) Å; Table 5) is significantly longer than the Mo1-Si2 bond for the terminal silyl group (2.495(1) Å), but is comparable with the M-Si bonds for agostic silylamido ligands in the related chloro-substituted complexes **III-37** (2.646(1) Å)[14a] and **III-39** (2.668(1) Å).[15] The agostic hydride ligand is found at a long Mo1-H1b distance of 1.92(5) Å, whereas the Si1-H1b bond of 1.49(5) Å is normal (compare to the Si2-H2a distance of 1.44(6) Å and the Si2-H2b distance of 1.54(6) Å; Table 5), indicating weak Si-H bond activation.[17] As expected, the Mo1-N1 bond (2.062(4) Å) is significantly larger than the Mo1-N2 distance (1.754(4) Å). The Mo1-N2-C2 linkage is approximately linear (169.5(3)°; Table 5) suggesting that the ArN^{2-} ligand may, in principle, act as a 6 electron donor to the metal stabilizing the 16 electron valence shell.[192]

[i] The energy barrier for activation of the Si-H bond depends on the extent of back-donation.[17] Assuming a triple-bond character for $Ar'N^{2-}$, **III-37** and **III-39** are 18e complexes, whereas **III-1** is a 16e compound.

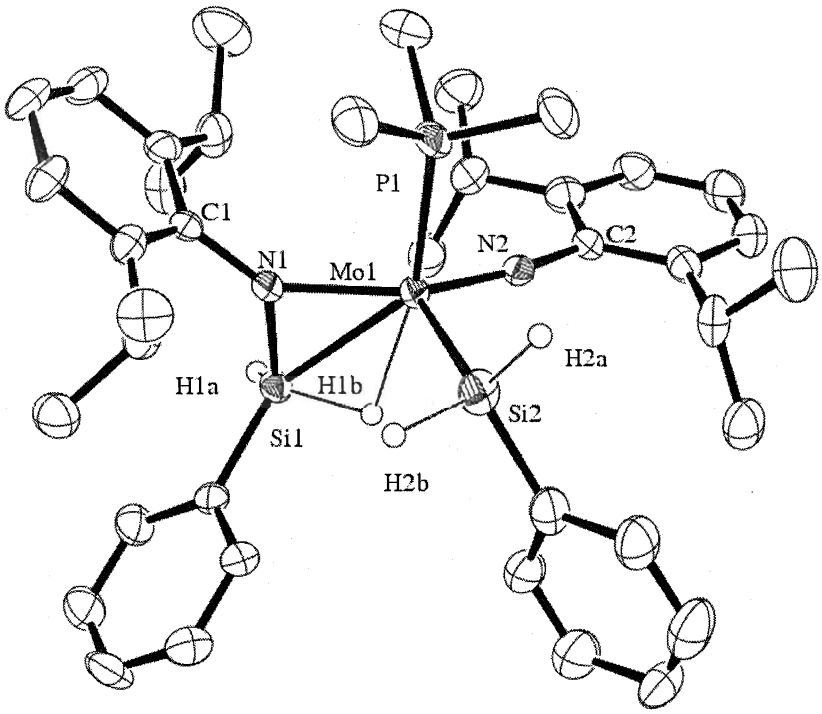

Figure 20. ORTEP plot of the molecular structure of (ArN)Mo(SiH_2Ph)(η^3-NAr-SiHPh-H)(PMe_3) (**III-1**) (hydrogen atoms except Si*H* are omitted for clarity). Anisotropic displacement parameters are plotted at 50 % probability.

Table 5. Selected bond distances (Å) and angles (°) for complex **III-1**.

distances, Å		Angles, °	
Mo1-Si1	2.634(1)	Mo1-N1-Si1	88.50(16)
Mo1-Si2	2.495(1)	Mo1-Si1-N1	51.49(12)
Mo1-N1	2.062(4)	Mo1-N1-C1	140.0(3)
Si1-N1	1.694(4)	Mo1-N2-C2	169.5(3)
Mo1-N2	1.754(4)	P1-Mo1-Si2	89.61(5)
Mo1-H1b	1.92(5)	P1-Mo1-Si1	136.55(4)
Si1-H1a	1.43(4)	N1-Mo1-N2	144.13(15)
Si1-H1b	1.49(5)	P1-Mo1-H1b	162.3(17)
Si2-H2a	1.44(6)	Si1-Mo1-N2	121.87(12)
Si2-H2b	1.54(6)	N1-Mo1-Si1	40.01(10)

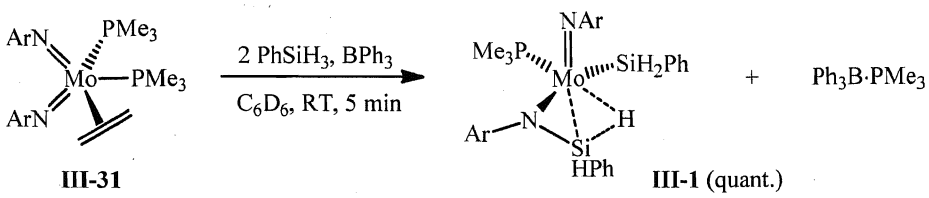

III-31 **III-1** (quant.)

Scheme 90. Reaction of $(ArN)_2Mo(\eta^2\text{-}CH_2{=}CH_2)(PMe_3)_2$ (**III-31**) with $PhSiH_3$ and BPh_3.

Formation of the agostic complex **III-1** was also observed by NMR spectroscopy upon treatment of $(ArN)_2Mo(\eta^2\text{-}CH_2{=}CH_2)(PMe_3)_2$ (**III-31**) with 2 equiv. of $PhSiH_3$ (Scheme 90). Similarly to the compound **III-22**, the room temperature reaction of **III-31** in C_6D_6 affords a difficult-to-separate mixture of **III-1**, **III-63**, and **III-64**. The formation of a small amount of the product of ethylene hydrosilation, $PhEtSiH_2$,[202] was also observed. The selectivity of the reaction of **III-31** with $PhSiH_3$ can be significantly increased by the addition of an equivalent of BPh_3, which leads to quantitative production of **III-1** in a mixture with the $Ph_3B{\cdot}PMe_3$ adduct. The isolation from the latter can be easily achieved by the extraction of the molybdenum product with hexanes.

The compound $(ArN)Mo(H)_4(PMe_3)_3$ (**III-63**) is of interest due to the well-known rich reactivity of transition metal hydride complexes.[18, 19] Its preparation was attempted but, unfortunately, no improvement in the selectivity was observed upon the treatment of complex **III-22** with $PhSiH_3$ in atmosphere of hydrogen (~ 1.5 atm.) in an NMR tube. At the same time, the preparative scale reaction of **III-22** with $PhSiH_3$ under H_2 purging surprisingly leads to the release of $ArNH_2$ to give the novel complex $(ArN)Mo(H)(SiH_2Ph)(PMe_3)_3$ (**III-7**), which was isolated in 26 % yield by recrystallization from hexane solution at –30 °C (Scheme 91). To the best of our knowledge, complex **III-7** presents the first example of a Mo(IV) imido hydride species. On the other hand, no reaction was observed upon treatment of the agostic silylamide **III-**

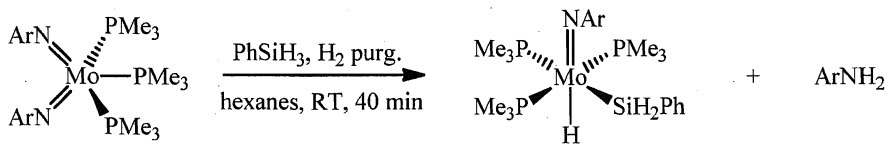

III-22 **III-7** (26 %)

Scheme 91. Reaction of $(ArN)_2Mo(PMe_3)_3$ (**III-22**) with $PhSiH_3$ and H_2 purging.

1 with dihydrogen.

Compound **III-7** was fully characterized by multinuclear NMR and IR spectroscopy, and X-Ray diffraction (crystal structure parameters are listed in Table 27, chapt. VI). The ^{1}H NMR spectrum of **III-7** shows an up-field hydride signal at -3.92 ppm (dt, $^2J_{P\text{-}H}$ = 18.6 Hz, $^2J_{P\text{-}H}$ = 65.4 Hz) coupled to two equivalent PMe_3 ligands (*cis*- to the silyl) and one *trans*- to the silyl PMe_3 substituent. Equivalent protons of the SiH_2Ph group give rise to a triplet at 5.75 ppm ($^3J_{H\text{-}P}$ = 7.8 Hz, $^1J_{H\text{-}Si}$ = 147.0 Hz), coupled in the ^{1}H-^{29}Si HSQC spectrum to the ^{29}Si-NMR signal at 0.2 ppm ($^2J_{Si\text{-}P}$ = 9.6 and 21.7 Hz, $^1J_{Si\text{-}H}$ = 154.4 Hz; found by ^{29}Si INEPT+ NMR spectroscopy). The large value of $^1J_{Si\text{-}H}$ in **III-7** suggests that the Si-H bonds of the SiH_2Ph ligand are not coordinated to molybdenum. The classical silylhydride structure of **III-7** is also confirmed by the observation of normal Mo-H and Si-H IR stretches at 1699 cm^{-1} and 1998 cm^{-1}, respectively. The discussion of structural parameters of complex **III-7** is presented below (see Figure 36, chapt. III.7.1).

Changing the substitution on the phosphine ligands does not affect significantly the reactivity of bis(imido) Mo(IV) complexes with $PhSiH_3$. Thus, the treatment of sterically hindered $(ArN)_2Mo(PMe_2Ph)_2$ (**III-24**) with phenylsilane leads to the formation of the agostic silylamide $(ArN)Mo(SiH_2Ph)(\eta^3$-NAr-SiHPh-H$)(PMe_2Ph)$ (**III-65**), analogous to **III-1**. Complex **III-65** was characterized by NMR, which revealed the presence of the classical SiH_2Ph group (broad signal at 5.89 ppm for Si*H* protons in the ^{1}H-NMR spectrum) and the agostic silylamide ligand (the terminal Si*H* proton gives rise to a broad signal at 5.87 ppm and the agostic Si*H* proton is found at 3.85 ppm). Unfortunately, the product was found to be unstable and decomposes in solution *via* phosphine dissociation within two hours, hampering its full characterization and isolation. Analogous reaction of $(Ar'N)_2Mo(PMe_2{}^iPr_2)_2$ (**III-25**) with $PhSiH_3$ also affords the agostic species $(Ar'N)Mo(SiH_2Ph)(\eta^3$-NAr'-SiHPh-H$)(PMe^iPr_2)$ (**III-66**; see experimental section for details). Similarly to the complex **III-65**, all attempts to isolate compound **III-66** were unsuccessful due to its instability (full decomposition to a mixture of unidentified products was observed by NMR spectroscopy after two hours at room temperature).

In contrast, the reaction of the tungsten analogue $(ArN)_2W(PMe_3)_3$ (**III-23**) with one equivalent of $PhSiH_3$ in the presence of two equivalents of BPh_3 results in the formation of the bis(imido) silyl hydride derivative $(ArN)_2W(H)(SiH_2Ph)(PMe_3)$ (**III-68**; Scheme

92). This result is similar to the observation of complexes **III-56** and **III-57** in the reaction of **III-23** with $HSiCl_3$ and $MeSiHCl_2$, respectively (see the discussion above; Scheme 88). Complex **III-68** is not stable in solution at room temperature and slowly (within few hours) decomposes to a mixture of unidentified products. Possibly, the decomposition process occurs *via* the migration of the SiH_2Ph substituent from tungsten to the imido ligand, forming fluxional agostic and Cl-bridged silylamide species. An analogous rearrangement has been previously documented for $SiCl_3$ and $SiCl_2Me$ derivatives (see above; Scheme 88).

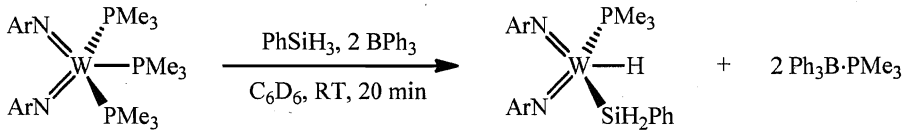

III-23 **III-68** (quant. by NMR)

Scheme 92. Reaction of **III-23** with $PhSiH_3$ and BPh_3.

Similarly to complex **III-22**, treatment of $(Ar'N)_2Mo(PMe_3)_3$ (**III-4**) with $PhSiH_3$ after 10 min. at room temperature affords the silyl silylamido derivative $(Ar'N)Mo(SiH_2Ph)(NAr'\{SiH_2Ph\})(PMe_3)_2$ (**III-69**; Scheme 93). When a stoichiometric reaction between **III-4** and $PhSiH_3$ was conducted at low temperature, no intermediates such as $(Ar'N)Mo(H)(NAr'\{SiH_2Ph\})(PMe_3)_n$ were detected and only the formation of complex **III-69** was observed after 15 min. at -5 °C (50 % conversion of the starting material). Compound **III-69** is highly fluxional. Its room temperature ^{1}H-NMR spectrum shows broad featureless resonances in the aliphatic and aromatic regions. Nevertheless, the ^{1}H-NMR spectrum of **III-69** acquired at -71 °C reveals two pairs of diastereotopic Si*H* signals for the Mo-bound silyl group and for the silylamide ligand at 5.71, 5.80, 5.96, and 6.02 ppm. These signals are coupled in the ^{1}H-^{29}Si HSQC NMR spectrum to two ^{29}Si-NMR resonances at 1.3 ppm and -32.1 ppm, corresponding to Mo-bound silyl and silylamide, respectively. In contrast to its agostic analogue **III-1**, no coupling of the silylamide Si-bound protons to phosphorus nuclei can be seen in the ^{1}H- and ^{1}H-^{31}P HSQC NMR spectra, suggesting the absence of any Si-H bond coordination to molybdenum. In the ^{31}P-NMR spectrum, two non-equivalent PMe_3 ligands of **III-69** give rise to two doublets at -9.3 and -13.6 ppm, coupled to each other. The large value of the

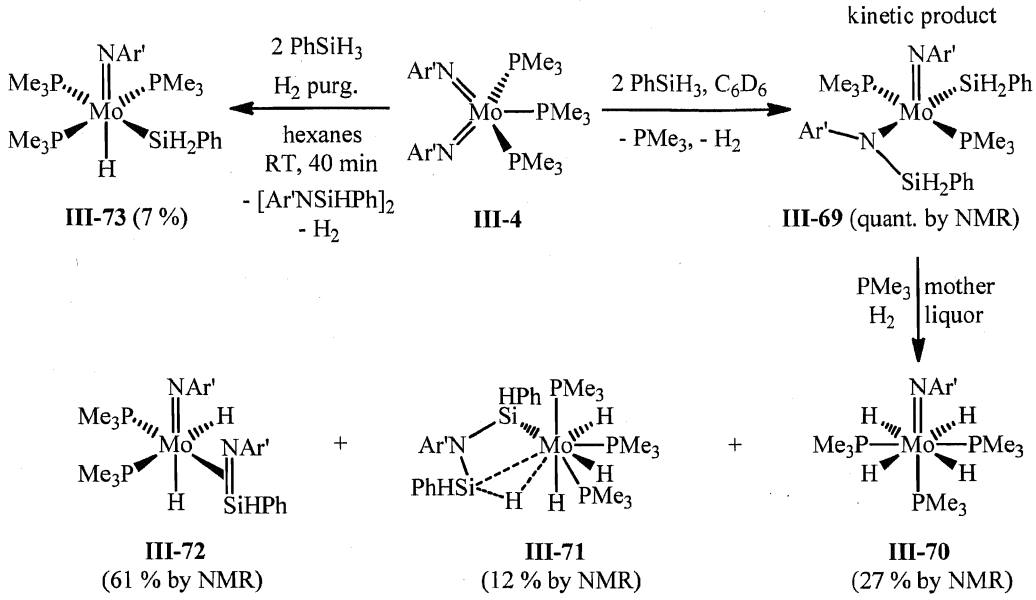

Scheme 93. Reactivity of $(Ar'N)_2Mo(PMe_3)_3$ (**III-4**) towards $PhSiH_3$.

$^2J_{P\text{-}P}$ coupling constant of 199.2 Hz suggests the *trans*- arrangement of phosphines. Similarly to the agostic compound **III-1**, complex **III-69** is not stable in solution in the presence of PMe_3 and H_2 and decomposes overnight at room temperature into a difficult-to-separate mixture of $(Ar'N)MoH_4(PMe_3)_3$ (**III-70**) and [η^3-PhHSi-N(Ar')-SiHPh-H]$MoH_3(PMe_3)_3$ (**III-71**), spectroscopic features of which are analogous to those for compounds **III-63** and **III-64**, respectively.

The decomposition of **III-69** is also accompanied by the formation of a large amount (61 %) of a complex with trapped silanimine ligand, $(Ar'N)Mo(\eta^2$-Ar'N=SiHPh)$(H)_2(PMe_3)_2$ (**III-72**; Scheme 93). Formation of such a product was not observed in the case of the decomposition of compound **III-1**. The structure of **III-72** was proposed on the basis of NMR analysis. Thus, the room temperature ^{1}H-NMR spectrum shows up-field resonances for two non-equivalent Mo-bound hydrides at -4.76 (ddd, $^2J_{H\text{-}P}$ = 45.3, 55.3 Hz, $^2J_{H\text{-}H}$ = 8.5 Hz) and -2.46 ppm (ddd, $^2J_{H\text{-}P}$ = 15.3, 31.6 Hz, $^2J_{H\text{-}H}$ = 8.5 Hz). The Si-bound proton of the silanimine ligand gives rise to a down-field signal at 6.36 ppm (dd, $^3J_{H\text{-}P}$ = 2.3, 15.0 Hz), coupled in the ^{1}H-^{31}P HSQC spectrum to two non-equivalent mutually coupled ^{31}P-NMR signals at 4.2 and 8.4 ppm, and in the ^{1}H-^{29}Si HSQC NMR spectrum with the ^{29}Si-NMR signal at –12.1 ppm (d, $^1J_{H\text{-}Si}$ = 218.8 Hz, found by ^{29}Si-NMR spectroscopy). The small value of the $^2J_{P\text{-}P}$ (15.8 Hz) indicates the

cis- arrangement of the PMe_3 ligands. The formulation of **III-72** as a silanimine complex and, in particular, the direct bonding between the molybdenum and silicon atoms is supported by the observation of a reasonably large $^2J_{SiH-P}$ constant (15.0 Hz), whereas the large value of $^1J_{H-Si}$ (218.8 Hz) is consistent with the Si-H bond being uncoordinated to the metal.

Addition of excess $PhSiH_3$ to a mixture of **III-70**, **III-71** and **III-72** (27, 12, and 61 %, respectively) leads after one hour at 100 °C to the disappearance of **III-72** and the increase of the **III-70** and **III-71** content. Furthermore, this transformation is accompanied by the release of a silanimine dimer $(Ar'N\text{-}SiHPh)_2$, suggesting the intermediacy of silanimine complex **III-72** in the formation of polyhydride products. All attempts to isolate compound **III-72** by the addition of one equivalent of BPh_3 to a mixture of **III-4** and $PhSiH_3$ were unsuccessful. These conditions increase the content of **III-72** (up to 75 %) in the mixture with **III-70** and **III-71**, however, similar solubility of latter two compounds hampers the isolation of this silanimine derivative in an analytically pure form.

The preparative scale reaction of $(Ar'N)_2Mo(PMe_3)_3$ (**III-4**) with two equivalents of $PhSiH_3$ under nitrogen purging through the solution does not allow for the isolation of the kinetic product, $(Ar'N)Mo(SiH_2Ph)(NAr'\{SiH_2Ph\})(PMe_3)_2$ (**III-69**). Instead, similar to the NMR scale reaction, the formation of a difficult-to-separate mixture of compounds **III-70**, **III-71**, and **III-72** was observed. An analogous result was also achieved upon the low temperature (-5 – 0 °C) treatment of **III-4** with $PhSiH_3$. On the other hand, H_2 purging changes the reaction pathway, leading to the formation of the mono(imido) silylhydride derivative $(Ar'N)Mo(H)(SiH_2Ph)(PMe_3)_3$ (**III-73**; Scheme 93), which was isolated in analytically pure form in 7 % yield.

Complex **III-73** was characterized by IR and multinuclear NMR spectroscopy. The ^{1}H-NMR spectrum of **III-73** exhibits the Mo-bound hydride as a P-coupled up-field signal at -3.56 ppm (dt, $^2J_{H-P}$ = 18.5 and 65.4 Hz). Two equivalent Si*H* protons of the SiH_2Ph group give rise to a triplet at 5.83 ($^3J_{H-P}$ = 7.8 Hz) coupled in the ^{1}H-^{29}Si HSQC spectrum with the ^{29}Si-NMR signal at 1.7 ppm (t, $^1J_{Si-H}$ = 157.4 Hz; found from ^{29}Si INEPT+ NMR spectroscopy). The down-field chemical shift for the Si*H* signal in ^{1}H-NMR and the large value of the $^1J_{Si-H}$ coupling constant suggest the classical structure of

III-73.[17] As is typical for triphosphine imido compounds,[15] the ^{31}P-NMR spectrum of complex **III-73** exhibits two mutually coupled signals: a doublet for two equivalent ligands at –1.5 ppm ($^2J_{P\text{-}P}$ = 23.1 Hz) and a triplet for the unique *trans*-PMe_3 at 10.5 ppm. The absence of nonclassical interactions in the silylhydride **III-73** is supported by the observation of normal Mo-H and Si-H stretches[17] at 1647 and 2152 cm^{-1} in the IR spectrum, respectively.

Substitution of PMe_3 with PMe_2Ph in $(Ar'N)_2Mo(PR'_3)_3$ does not change the reactivity towards phenylsilane. The treatment of $(Ar'N)_2Mo(PMe_2Ph)_3$ (**III-26**) with excess $PhSiH_3$ selectively affords $(Ar'N)Mo(SiH_2Ph)(NAr'\{SiH_2Ph\})(PMe_2Ph)_2$ (**III-74**; Scheme 94), analogous to complex **III-69**. Leaving the reaction mixture overnight at room temperature results in partial decomposition of the compound **III-74** to a novel mono(imido) silylhydride derivative $(Ar'N)Mo(H)(SiH_2Ph)(PMe_2Ph)_3$ (**III-75**, Scheme 94). All attempts to isolate the silylamide **III-74** gave a difficult-to-separate mixture of the starting **III-26** and complexes **III-74** and **III-75**.

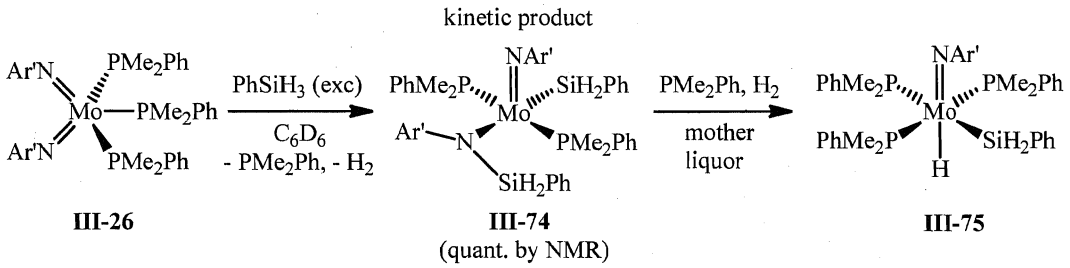

Scheme 94. NMR scale reaction of $(Ar'N)_2Mo(PMe_2Ph)_3$ (**III-26**) with $PhSiH_3$.

III.4.1.2 Reactions of $(^tBuN)_2Mo(PMe_3)L$

The reaction of $(^tBuN)_2Mo(PMe_3)_2$ (**III-27**) with an equivalent of $PhSiH_3$ was initially studied by low temperature NMR spectroscopy. At -30 °C, NMR spectra showed 50 % conversion of **III-27** and selective formation of a novel complex (^{t}BuN)Mo(H)(η^3-PhHSi-N(^{t}Bu)-SiHPh-H)(PMe_3)$_2$ (**III-76**; as a mixture of two isomers in 1:2 ratio; Scheme 95). Complex **III-76** presents the first example of a double silane addition to the metal-imido bond. No intermediates of silane monoaddition were seen in NMR. At –30 °C, the ^{1}H-NMR spectrum of the major isomer of the compound **III-76** exhibits signal of a Mo-bound hydride at -4.40 ppm (dd, $^2J_{H\text{-}P}$ = 15.8 Hz and 48.4 Hz) and the Si*H* resonance for

the classical NSiH(Ph)Mo fragment at 6.91 ppm, coupled in the ^{1}H-^{29}Si HSQC spectrum to the ^{29}Si-NMR signal at 5.2 ppm (d, $^{1}J_{Si-H}$ = 172.3 Hz; found by ^{29}Si INEPT+ NMR spectroscopy). In the major isomer of **III-76**, the terminal and agostic protons of the $NSiH_2Ph$ moiety give rise to a broad singlet at 6.82 ppm, coupled in the ^{1}H-^{29}Si HSQC spectrum to a ^{29}Si-NMR signal at -16.2 ppm (dd, $^{1}J_{Si-H}$ = 34.9 and 195.6 Hz; found by ^{29}Si INEPT+ NMR spectroscopy). The significantly reduced value of the $^{1}J_{Si-Ha}$ coupling constant is in agreement with the proposed structure and indicates coordination of one of the Si-H bonds of $NSiH_2Ph$ to the molybdenum center.[17] The *cis*- arrangement of the non-equivalent phosphine substituents in the major isomer of compound **III-76** is evident from the ^{31}P-NMR spectrum, which at –25 °C shows two doublets, at -7.0 and -0.8 ppm ($^{2}J_{P-P}$ = 43.7 Hz), coupled to each other. Addition of another equivalent of phenylsilane to **III-76** and warming the sample up to 0 °C leads to selective formation of the metastable[j] Mo(VI) complex (^{t}BuN)Mo(H)(SiH_2Ph){$(SiHPh)_2(\mu$-N^{t}Bu)}$(PMe_3)_2$ (**III-77**; Scheme 95), which is presumably produced *via* further oxidative addition of the agostic Si-H bond in **III-76** to molybdenum affording a Mo(VI) dihydride species, which after dihydrogen elimination adds $PhSiH_3$. The formation of complex **III-77** presents a rare example of triple silane addition to a TM centre.[203]

The formation of **III-77** is also observed by NMR spectroscopy upon treatment of the bis(imido) precursor **III-27** with three equivalents of $PhSiH_3$ at room temperature (Scheme 95), however the reaction is complicated by a decomposition by-process, leading to a novel silanimine compound (η^2-^{t}BuN=SiHPh)$MoH_4(PMe_3)_3$ (**III-78**; mixture of two isomers). The structure of **III-78** was suggested on the basis of NMR data. Thus, the ^{1}H-NMR spectrum shows the presence of four equivalent Mo-bound hydrides at -5.82 ppm, coupled with a large coupling constant ($^{2}J_{H-P}$ = 27.2 Hz) to the ^{31}P-NMR signal at -12.4 ppm of equivalent PMe_3 groups. The Si*H* proton of the silanimine η^2-^{t}BuN=SiHPh ligand gives rise to a down-field shifted singlet at 8.31 ppm, which is also coupled to the phosphorus signal in the ^{1}H-^{31}P HSQC spectrum when a small J_{H-P} of 15 Hz is applied. Selective decoupling of the ^{31}P-NMR signal from the methyl groups of PMe_3 leads to the observation of a pentet, additionally confirming the presence of four hydrides on Mo. The

[j] (^{t}BuN)Mo(H)(SiH_2Ph){$(SiHPh)_2(\mu$-N^{t}Bu)}$(PMe_3)_2$ (**III-77**) is not stable at room temperature in solution and in the absence of $PhSiH_3$ fully decomposes within a few hours to a mixture of unidentified products.

$^{29}Si\{^{1}H\}$-NMR spectrum of complex **III-78** contains only one signal for the silanimine ligand, which appears at 6.2 ppm as a quartet due to coupling to three PMe_3 ligands ($^{2}J_{Si\text{-}P}$ = 13.1 Hz). The large value of $^{2}J_{Si\text{-}P}$ and the coupling of the Si-bound proton to the ^{31}P-NMR signal in the ^{1}H-^{31}P HSQC NMR spectrum are in agreement with the proposed structure, suggesting the presence of a direct bonding between silicon and molybdenum.

Selective generation of compound **III-77** can be achieved by the reaction of the bis(imido) complex **III-27** with excess $PhSiH_3$ at room temperature (Scheme 95). Alternatively, **III-77** can be isolated in 82 % yield using a low temperature (-30 — -5 °C; see experimental details) preparative scale reaction of **III-27** with three equivalents of phenylsilane (Scheme 95). Analogously to the reaction of complex **III-27**, treatment of bis(imido) ethylene adduct (^{t}BuN)$_2$Mo(η^2-CH_2=CH_2)(PMe_3) (**III-30**) with three equivalents of phenylsilane and an equivalent of PMe_3 results after 10 min. at room temperature in the release of ethylene and the quantitative formation of **III-77**.

Complex (^{t}BuN)Mo(H)(SiH_2Ph){($SiHPh$)$_2$(μ-N^{t}Bu)}(PMe_3)$_2$ (**III-77**) was characterized by IR and multinuclear NMR spectroscopy, and single crystal X-Ray diffraction. The molecular structure of **III-77** is depicted in Figure 21 (crystal data and

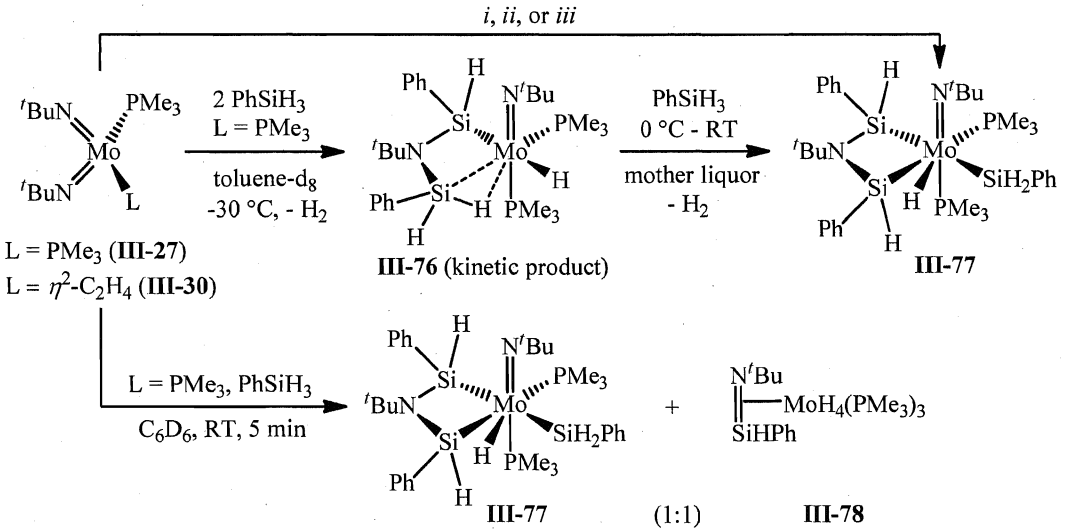

i - L = PMe_3: $PhSiH_3$ (exc), C_6D_6, RT, 5 min, quantitative yield; *ii* - L = PMe_3: 3 $PhSiH_3$, hexanes, -30 – -5/0 °C, 82 % yield; *iii* - L = η^2-C_2H_4: 3 $PhSiH_3$, PMe_3, C_6D_6, RT, 10 min, quantitative yield.

Scheme 95. Reactions of (^{t}BuN)$_2$Mo(PMe_3)L (L = PMe_3 (**III-27**), η^2-C_2H_4 (**III-30**) with $PhSiH_3$.

structure refinement parameters are listed in Table 28, chapt. VI). The ^{1}H-NMR spectrum of **III-77**, acquired at –28 °C, shows four non-equivalent Si*H* signals of equal intensity at 5.13 ppm (bd, $^{2}J_{H\text{-}P}$ = 19.6 Hz) and 5.60 ppm (dd, $^{3}J_{H\text{-}P}$ = 14.9 Hz, $^{2}J_{H\text{-}H}$ = 7.5 Hz) for the SiH_2Ph group and at 6.03 ppm (dd, $^{3}J_{H\text{-}P}$ = 9.6, 3.7 Hz) and 6.67 ppm (ddd, $^{2}J_{H\text{-}H}$ = 5.9 Hz, $^{3}J_{H\text{-}P}$ = 11.6, 17.2 Hz) for the {(SiHPh)$_2$(μ-N^{t}Bu)} ligand. The Mo-bound hydride gives rise to a P-coupled signal at 1.54 ppm (d, $^{2}J_{H\text{-}P}$ = 21.0 Hz). The formulation of the complex **III-77** as a classical silyl species is supported by the observation of large values of $^{1}J_{Si\text{-}H}$ coupling constants (154.5, 186.0, and 166.9 Hz) for all three silicon signals (found in the ^{29}Si INEPT+ NMR spectrum at -14.3, -5.0, and 1.4 ppm, respectively) and absence of any reduced coupling to the Mo-bound hydride. Furthermore, the ^{29}Si RF INEPT NMR experiment at –18 °C shows the presence of the only one Si-bound proton on each silicon center of the {(SiHPh)$_2$(μ-N^{t}Bu)} ligand. The observation of relatively large values of $^{3}J_{Si\text{-}P}$ coupling constants (25.0 and 20.3 Hz) for the {(SiHPh)$_2$(μ-N^{t}Bu)}

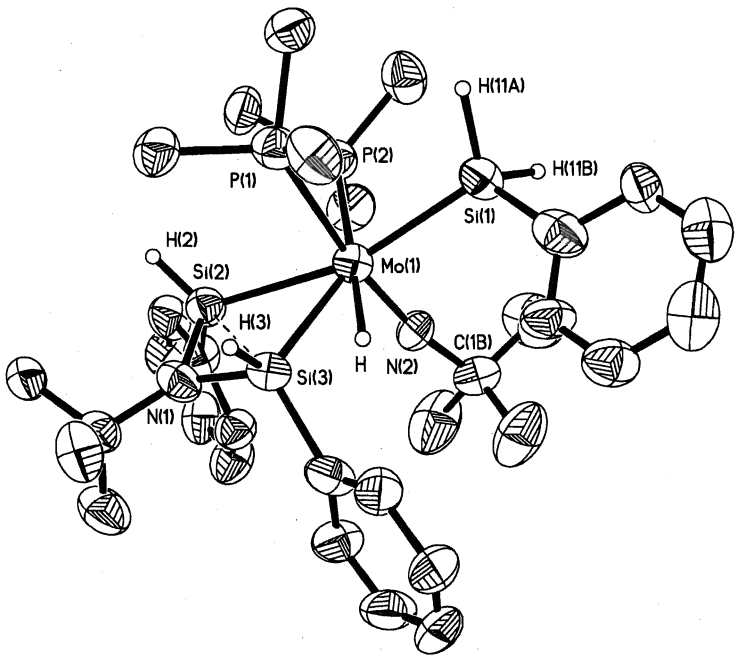

Figure 21. ORTEP plot of the molecular structure of complex **III-77** (hydrogen atoms, except SiH and MoH, are omitted for clarity). Anisotropic displacement parameters are plotted at 50 % probability.

Table 6. Selected bond distances (Å) and angles (°) for complex **III-77**.

distances, Å		angles, °	
Mo1···N1	3.365	Mo1-N2-C1b	170.5(7)
Mo1-N2	1.726(7)	N2-Mo1-P1	167.8(3)
Mo1-Si1	2.568(3)	Si1-Mo1-Si2	164.08(10)
Mo1-Si2	2.614(3)	Si3-Mo1-P2	142.81(10)
Mo1-Si3	2.560(3)	P1-Mo1-P2	87.44(10)
Si2-Si3	2.621(5)	Mo1-Si2-N1	99.0(3)
Si2-N1	1.749(9)	Mo1-Si3-N1	101.9(3)
Si3-N1	1.719(9)	Si2-N1-Si3	98.2(4)
Mo1-H	1.55(9)	Si2-Mo1-Si3	60.86(10)
Mo1-P1	2.686(3)	P1-Mo-H	79(3)
Mo1-P2	2.532(4)	P2-Mo-H	162(3)
N2-C1b	1.467(13)		

fragment found by ^{29}Si INEPT+ NMR spectroscopy indicates the presence of direct bonding between silicon atoms and molybdenum. The Si-H bonds of **III-77** give rise to bands at 1825, 1890, 2037, and 2142 cm^{-1} in the IR spectrum, further supporting the classical structure of the complex.

The molecular structure of complex **III-77** adopts an octahedral geometry with one of the PMe_3 groups being *trans*- to imido ligand (Figure 21). Another phosphine group is lying *cis*- to the imido substituent and is co-planar with the SiH_2Ph and {$(SiHPh)_2(\mu$-N^{t}Bu)} fragments. The Mo1-N2-C1b linkage is almost linear (170.5(7) °; Table 6) suggesting that the imido ligand, in principle, can act as a 6 electron donor to the d^0 molybdenum center, stabilizing the 18-electron valence shell. The Mo-HSi distances in **III-77** are too large (3.387, 3.498, 3.462, and 3.354 Å; Table 6) to allow for presence of Si-H bond coordination to molybdenum.[17] In contrast to the spectroscopic features of **III-77** showing the absence of nonclassical (2c-3e) bonding between the Mo-bound hydride and the Si3 atom of the {$(SiHPh)_2(\mu$-N^{t}Bu)} ligand, the rather short Si3-HMo distance (1.553 Å) may indicate the opposite.[17] At the same time, the Mo1-H bond length is normal (1.704 Å). Taking into account the spectroscopic parameters of **III-77** and the well-known inaccuracy of finding hydride positions by X-ray, these data do not allow us

to draw any accurate conclusion regarding the presence or absence of Si-H···Mo agostic bonding in the compound **III-77**. DFT calculations would provide more insight into the structure.

Some other structural data for complex **III-77** have also been found to be unusual. Thus, a short Si2-Si3 contact of 2.621(5) Å, close to the upper end of single Si-Si bonds (2.33 – 2.70 Å),[17, 204] is observed for the {$(SiHPh)_2(\mu$-N^{t}Bu)} ligand. Similar Si-Si bonding was described previously for the tungsten complex, $Cp_2W\{(SiMe_2)_2(\mu$-O)} (**III-79**; Si-Si 2.594(3) Å),[205] and the isolobal niobium derivative, $Cp_2Nb(H)\{(SiMe_2)_2(\mu$-N^{t}Bu)} (**III-80**; 2.654(2) Å).[206] Interestingly, whereas the Mo1-Si1 bond (2.568(3) Å) for the silyl SiH_2Ph ligand in **III-77** is normal,[207] the Mo1-Si2 distance in {$(SiHPh)_2(\mu$-N^{t}Bu)} is significantly elongated (2.614(3) Å). At the same time both the Mo1-Si2 and Mo1-Si3 (2.560(3) Å) distances are longer than those for the related molybdenum compounds $Cp_2Mo\{(SiMe_2)_2(\mu$-S)} (**III-81**; 2.558(2) and 2.550(2) Å),[208] $Cp(CO)_2Mo\{(SiMe_2)_2(\mu$-OMe)} (**III-82**; 2.4804(9) and 2.4795(9) Å), and $Cp(CO)_2Mo\{(SiMe_2)_2(\mu$-NEt$_2$)} (**III-83**; 2.4996(9) and 2.5008(9) Å)[209], reported earlier (Figure 22). Such elongation of the Mo1-Si2 bond relatively the Mo1-Si3 bond (Δ = 0.054 Å) could be accounted for by the exceptional property of the silyl group as a *trans*-influencing ligand (the Si1-Mo1-Si2 angle is 164.08(10) °).[210] A similar *trans*-influence was previously observed by Minato *et al.* for $[P_4Si^1]MoH_2(Si^2H_2Ph)$ (**III-84**; Figure 22), where the Mo-Si^2 bond was found to be 2.620(2) Å (compare with the Mo-Si^1 distance of 2.559(2) Å).[207b]

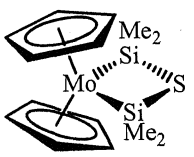

III-81

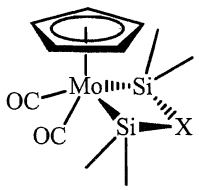

X = OMe (**III-82**), NEt_2 (**III-83**)

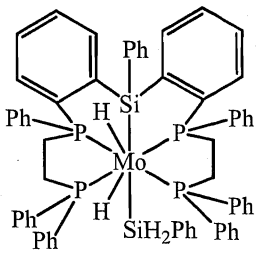

III-84

Figure 22. Molybdenum silyl complexes **III-81** – **III-84**.

III.4.2 Reactions of $(RN)_2M(PR'_3)_{n-1}L$ with $PhMeSiH_2$ and $(EtO)_3SiH$

In order to investigate the impact of the electronic (Lewis acidity) and steric properties of hydrosilanes on their reactivity with bis(imido) molybdenum(IV) and tungsten(IV) complexes we performed NMR studies of the reactions of $(RN)_2M(PR'_3)_{n-1}L$ (where L = PR'_3 or η^2-C_2H_4) with $PhMeSiH_2$ and $(EtO)_3SiH$. Preliminary mechanistic studies of the reactions of $L_nM(NR)(PR'_3)_m$ with chlorohydrosilanes performed by Nikonov *et al.*[14, 15, 17] showed that the imido/silane coupling process is initiated by the direct attack of the silane to the imido nitrogen, generating a Lewis acid-base adduct $L_nM\{=N(R)\rightarrow SiR'_2H\}$ (see the discussion above). The formation of such adduct is required for further Si-H (or Si-Cl) bond activation by the metal center, affording either Si-H agostic or Cl-bridged species.[14, 15] The latter in most of the cases decompose either *via* migration of the silyl group to metal (like for tungsten complexes) or *via* dissociation of a silanimine ligand (observed for molybdenum compounds).[15] Intuitively, increasing the steric hindrance as well as decreasing the acidity of utilized silanes should hamper the formation of the initial Lewis adduct and, therefore, decrease the reactivity with $(RN)_2M(PR'_3)_{n-1}L$. Indeed, treatment of $(RN)Mo(PMe_3)_3$ (R = Ar' (**III-4**), Ar (**III-22**)) with $PhMeSiH_2$ at room temperature results in no reaction. Heating the mixture at 50 – 100 °C leads only to phosphine dissociation and formation of a mixture of unidentified decomposition products. In contrast, no reaction was also observed between $PhMeSiH_2$ and bulkier $(ArN)_2Mo(PMe_2Ph)_2$ (**III-24**). Further addition of an equivalent of BPh_3 to the reaction mixture leads to a decomposition process and formation of a difficult-to-characterize mixture of unknown compounds.

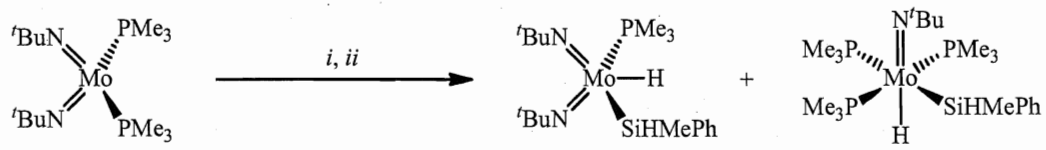

III-27 **III-85** **III-86**

i: $PhMeSiH_2$, C_6D_6, RT, 5 min, 55 % of **III-85** by ^{31}P-NMR.
ii: $PhMeSiH_2$, 2 PMe_3, C_6D_6, RT, overnight, 42 % of **III-85** and 8 % of **III-86** by ^{31}P-NMR.

Scheme 96. NMR scale reaction of $(^tBuN)_2Mo(PMe_3)_2$ (**III-27**) with $PhMeSiH_2$.

Changing the electronic properties of the imido substituent from aryl to alkyl, e.g. ArN^{2-} to $^tBuN^{2-}$, results in a completely different reactivity for bis(imido) phosphine complexes. Thus, a stoichiometric NMR scale reaction of $(^tBuN)_2Mo(PMe_3)_2$ (**III-27**) with $PhMeSiH_2$ at room temperature leads only after 5 min. to a 55 % conversion (according to the $^{31}P\{^1H\}$-NMR spectrum) of the starting material and formation of novel a Mo(VI) bis(imido) silylhydride complex, $(^tBuN)_2Mo(H)(SiHMePh)(PMe_3)$ (**III-85**; Scheme 96). The instability of the product prohibited its isolation; however, available NMR data allow us to assign the structure of **III-85** with certainty. Thus, the ^1H-NMR spectrum of **III-85** exhibits coupled-to-phosphorus down-field hydride and Si*H* signals at 3.71 ppm (d, $^2J_{H\text{-}P}$ = 57.6 Hz) and 6.23 ppm (bq + sat, $^3J_{H\text{-}H}$ = 3.8 Hz, $^1J_{H\text{-}Si}$ = 173.5 Hz), respectively. The large value of $^1J_{H\text{-}Si}$ for the SiHMePh group and large $^2J_{H\text{-}P}$ for the hydride ligand are in agreement with the formulation of **III-85** as a classical silylhydride species.

Presumably, decomposition of **III-85** starts with phosphine dissociation followed by migration of the silyl substituent from the imido nitrogen to molybdenum, forming a mono(imido) silylamide species, similar to those observed previously by Nikonov for tungsten analogues (see above). All attempts to synthesize complex **III-85** by a preparative scale reaction of **III-27** with $PhMeSiH_2$ under N_2 purging were unsuccessful. A difficult-to-separate mixture of $(^tBuN)Mo(H)(SiHMePh)(PMe_3)_3$ (**III-86**) and unknown products was observed. Similar to the Ar and Ar' silylhydrides **III-7** and **III-73**, the ^1H-NMR spectrum of **III-86** shows an up-field hydride signal at -3.93 (dt, $^2J_{H\text{-}P}$ = 63.9, 20.7 Hz), coupled to PMe_3, and a down-field Si*H* resonance at 5.59 ppm (broad signal), coupled in ^1H-^{31}P HSQC to ^{31}P-NMR signals. The COSY NMR spectrum of **III-86** also shows coupling between the Si*H* proton signal and a resonance for the Si-bound methyl group, found in the ^1H-NMR spectrum at 0.47 ppm (broad signal). The unique phosphine ligand of **III-86** lying *trans*- to SiHMePh gives rise to a doublet of doublets at 14.9 ppm ($^2J_{P\text{-}P}$ = 23.1 Hz and 24.7 Hz) in the ^{31}P-NMR spectrum. Due to the presence of a chiral silicon center in the SiHMePh substituent, two *trans*-PMe_3 groups appear in the ^{31}P-NMR as two overlapping doublet of doublets of doublets at 2.5 ppm ($^2J_{P\text{-}P}$ = 23.1 Hz and 24.7 Hz).

Addition of two equivalents of PMe_3 to a mixture of **III-27** and $PhMeSiH_2$ significantly slows down the reaction and only 42 % of **III-85** was observed after overnight at room temperature. This suggests that the process starts with reversible dissociation of PMe_3, followed by the oxidative addition of the silane. Furthermore, the presence of PMe_3 complicates the outcome of the reaction of **III-27** with $PhMeSiH_2$ forming 8 % of the mono(imido) silylhydride by-product, (^{t}BuN)Mo(H)(SiHMePh)(PMe_3)$_3$ (**III-86**; Scheme 96). Formation of an analogous mixture of **III-85** and **III-86** is also observed upon the treatment of the bis(imido) ethylene adduct (^{t}BuN)$_2$Mo(η^2-CH_2=CH_2)(PMe_3) (**III-30**) with methylphenylsilane. Similar reaction in the presence of two equivalents of PMe_3 leads to decomposition to a difficult-to-characterize mixture of unidentified products. Only trace formation of the complex **III-86** was observed.

The room temperature NMR scale reaction of (^{t}BuN)Mo(PMe_3)$_2$ (**III-27**) with more acidic $(EtO)_3SiH$ leads mostly to decomposition. Only traces of a novel tris(phosphine) product were observed in the $^{31}P\{^1H\}$-NMR spectrum: a triplet for one PMe_3 at 14.8 ppm ($^2J_{P\text{-}P}$ = 24.3 Hz) and a doublet for two equivalent phosphines at 3.4 ppm ($^2J_{P\text{-}P}$ = 24.3 Hz). The structure of this complex is not clear at this point, however the appearance of new signals for the OEt group in the ^{1}H-NMR spectrum as well as the absence of Si-bound or Mo-bound protons suggest the formation of (^{t}BuN)Mo(OEt)$_2$(PMe_3)$_3$ (**III-87**; Scheme 97).

This conclusion is also based on the analogy with the reaction of **III-27** with $HSiCl_3$ affording (^{t}BuN)$MoCl_2$(PMe_3)$_3$ (**III-48**; see above). Unfortunately, full characterization of **III-87** by NMR is prevented due to the overlap of its signals with the resonances of the

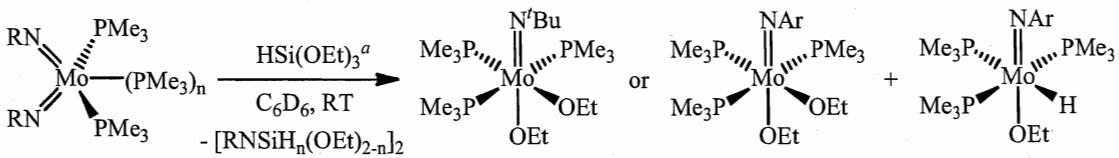

III-22: R = Ar, n = 1 **III-87** **III-88** **III-89**
III-27: R = ^{t}Bu, n = 0

[a] for complex **III-27** an equivalent of PMe_3 was added

Scheme 97. Reactions of $(RN)_2Mo(PMe_3)_n$ (**III-22** and **III-27**) with $(EtO)_3SiH$.

decomposition products. A similar result was also obtained in the reaction of $(ArN)_2Mo(PMe_3)_3$ (**III-22**) with an equivalent of triethoxysilane (Scheme 97), which, presumably, gives the related compound $(ArN)Mo(OEt)_2(PMe)_3$ (**III-88**) in a mixture with another triphosphine complex (~ 1:1 according to the $^{31}P\{^1H\}$-NMR spectrum). The structure of the second product was tentatively assigned to $(ArN)Mo(H)(OEt)(PMe_3)_3$ (**III-89**), which could be formed *via* the Si-H bond activation in the initial Lewis acid-base adduct $(ArN)Mo\{N(Ar)\rightarrow SiH(OEt)_3\}(PMe_3)_n$, followed by addition of the Si-O bond to molybdenum and release of the silanimine dimer $[ArN\text{-}Si(OEt)]_2$. Unfortunately, the Mo*H* resonance of **III-88** is not evident from the ^1H-NMR spectrum, however, the hydride structure was suggested by analogy with $(ArN)Mo(H)(Cl)(PMe_3)_3$ (**III-6**) discussed below.

III.5 Reactivity of $(ArN)Mo(SiH_2Ph)(\eta^3\text{-}NAr\text{-}SiHPh\text{-}H)(PMe_3)$ (III-1)

As was already mentioned, β-agostic silylamido complexes of general formula $L_nM(\eta^3\text{-}NR\text{-}SiR'_2\text{-}H)$ have been known since 1992,[14,15, 45d-i] however, their reactivity has been virtually unstudied, so they largely remain a laboratory curiosity.[17] Hypothetically, one could imagine that the reactivity pathways of agostic silylamides could be associated with either decrease in electron deficiency (dissociation of the Si-H···M bond; Scheme 98, path **A**) or increase in the oxidation state (full OA of the Si-H bond; Scheme 98, path **B**) of the metal center. The complete oxidative addition of the agostic Si-H bond would form

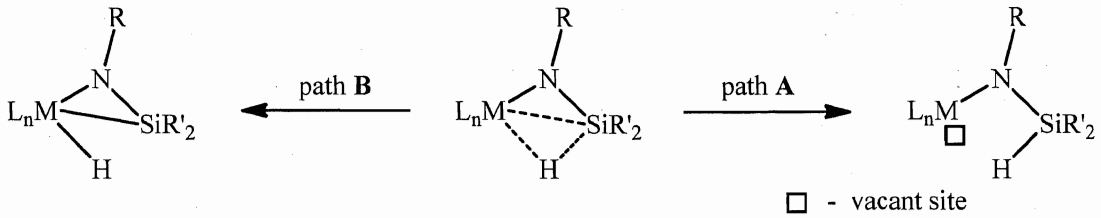

Scheme 98. Possible pathways for the reactivity of agostic silylamides.

in situ a silanimine hydride complex $L_nM(H)(\eta^2\text{-}RN{=}SiR'_2)$, which could also exhibit two reactivity sites: the M-H bond and the silanimine fragment. In contrast to the well-known reactivity of transition metal hydrides, examples of silanimine transition metal derivatives are extremely rare.[142, 201] However, they are known to exhibit facile coupling with unsaturated molecules.[142] In particular, insertion of unsaturated organic nolecules, CO,

and CO_2 into the Zr-Si bond of a zirconocene silanimine $Cp_2Zr(\eta^2$-^{t}BuN=SiMe$_2$)(PMe$_3$) (**III-90**) were illustrated by Berry *et al.* in 1990's.[142] In this part of the results and discussion chapter, we present the first example of a study of stoichiometric and catalytic reactivity of the molybdenum agostic silylamide (ArN)Mo(SiH$_2$Ph)(η^3-NAr-SiHPh-H)(PMe$_3$) (**III-1**) and provide evidence for the intermediacy of the 16-electron silanimine complex, (ArN)Mo(η^2-ArN=SiHPh)(PMe$_3$) (**III-2**). The nature of fluxionality of **III-1** has been also studied and is discussed below.

III.5.1 VT NMR study of complex III-1

As mentioned above, complex (ArN)Mo(SiH$_2$Ph)(η^3-NAr-SiHPh-H)(PMe$_3$) (**III-1**) is fluxional at room temperature in solution, which could be accounted for by several reasons. First of all, the dynamic process could be a result of exchange between two enantiomeric forms of **III-1** (a similar process was previously studied by Nikonov *et al.* for compound **III-38** and is discussed in chapt. III.3.1). Such an exchange, however, is degenerate and indistinguishable by NMR spectroscopy. Secondary, the presence of a chiral silicon center in the [η^3-NAr-SiHPh-H] ligand suggests the existence of two diastereomers of complex **III-1**.

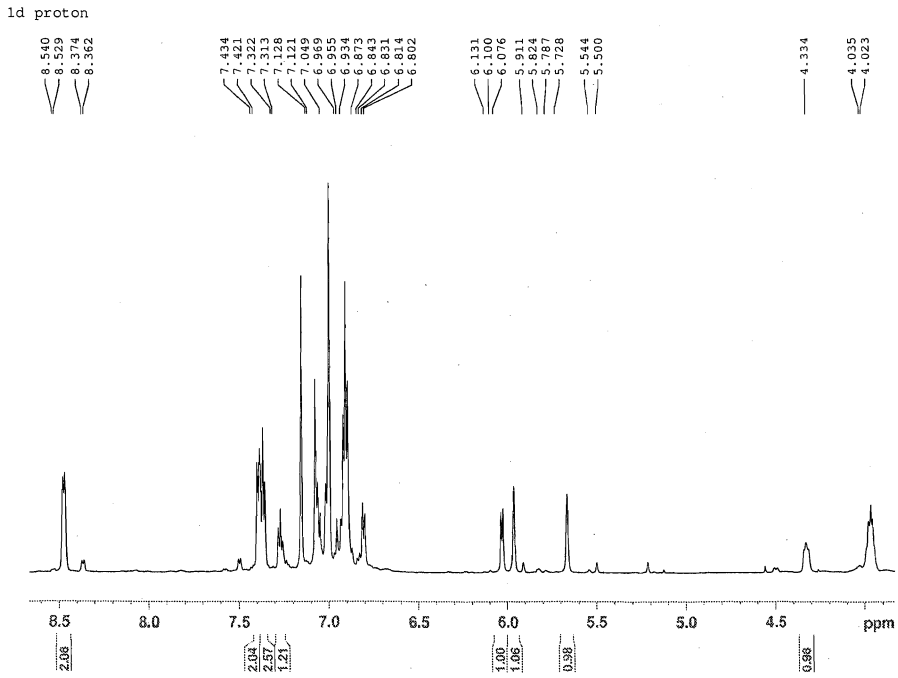

Figure 23. ^{1}H-NMR spectrum of **III-1** (mixture of two diastereomers) at –50 °C.

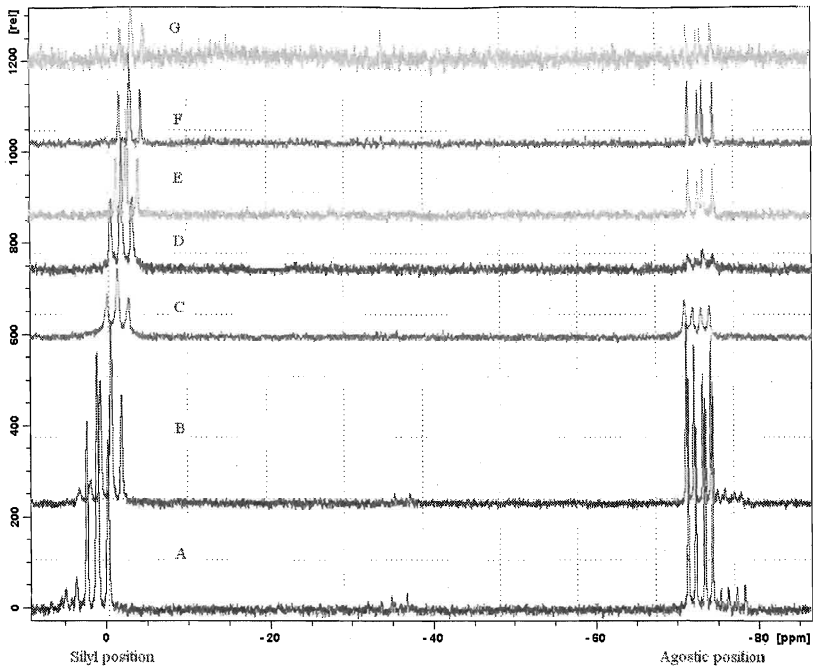

Figure 24. ^{29}Si INEPT+ NMR spectra of **III-1** at –49 (**A**), –19 (**B**), 0 (**C**), 21 (**D**), 39 (**E**), 55 (**F**), and 68 °C (**G**).

To gain an understanding of the dynamic process involved, VT NMR studies were performed. The ^{1}H-NMR spectrum at –50 °C reveals the presence of the second isomer, **III-1'** (Figure 23; small signals at 8.37 (d), 7.43(d), 5.91(s), 5.50 (s), 5.22 (s), and 4.03 (bs) correspond to the *o*-H of Si*Ph* and four non-equivalent Si*H* protons of the minor isomer, respectively). Unfortunately, the low abundance of the minor isomer (~ 5 %) hampered quantitative analysis. The second isomer of the silylamide **III-1** is also observed in the ^{29}Si INEPT+ NMR spectrum, which at –49 °C exhibits two nearly overlapping pairs of signals for the classical silyl and agostic silicon centers (Figure 24). In order to understand the nature of isomerism in the compound **III-1**, variable temperature (-49 – 68 °C) ^{29}Si-NMR studies were performed. Thus, the increase in the temperature of the ^{29}Si-NMR experiment leads to merging of the ^{29}Si resonances of **III-1** and **III-1'** (Figure 24). Furthermore, the increase in the temperature brings the $^{1}J^{ag}_{Si\text{-}H}$ and $^{1}J^{term}_{Si\text{-}H}$ coupling constants for the [η^3-NAr- SiHPh-H] ligand closer to each other in values (Figure 25), whereas the $^{1}J_{Si\text{-}H}$ for the SiH_2Ph ligand virtually remains the same. These observations suggest the presence of two diastereomeric forms of the agostic silylamide **III-1**. Additionally, the ^{1}H-^{1}H EXSY NMR experiments, performed at –44 and

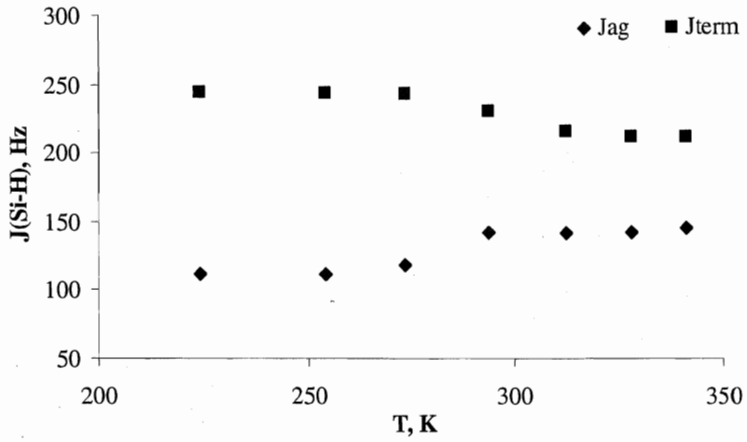

Figure 25. The affect of the temperature on the $^{1}J_{Si\text{-}H}$ values for agostic Si center in **III-1**.

and –6 °C for a solution of **III-1** in toluene-d_8, revealed an exchange between two non-equivalent Si-bound protons of the [η^3-NAr-SiHPh-H] fragment, indicating the feasibility of agostic Si-H bond dissociation. Thus, the dynamics process in complex **III-1** could be represented by Scheme 99 and includes dissociation of the agostic Si-H^a bond, followed by rotation around the N-Si bond. Further coordination of another Si-H^b bond to the molybdenum center furnishes the second diastereomer **III-1'**.

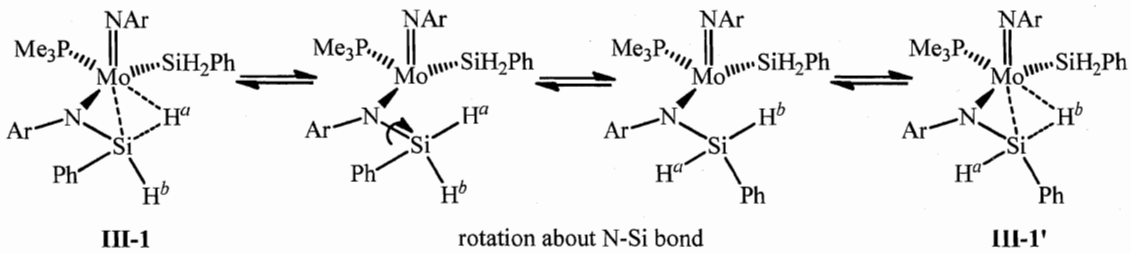

Scheme 99. Suggested dynamic process in complex **III-1**.

III.5.2 Reactions of complex III-1 with hydrosilanes

Addition of excess $PhSiH_3$ (10 equivalents) to a solution of complex **III-1** in C_6D_6 results in a slow silane coupling and redistribution process, indicating the possibility of the Si-H bond activation.[211] The reaction proceeds at room temperature and after overnight gives a 70 % conversion of $PhSiH_3$ to a mixture of Ph_2SiH_2 (34 %), SiH_4 (34 %), and $PhH_2Si\text{-}SiH_2Ph$ (2 %). Full conversion of phenylsilane was observed upon

heating the mixture overnight at 50 °C affording Ph_2SiH_2, SiH_4 and $PhH_2Si\text{-}SiH_2Ph$ in 47, 47, and 6 % yield (determined by ^{1}H-NMR spectroscopy), respectively. To gain an understanding of the catalytic silane activation mediated by the silylamide **III-1**, NMR studies of its reactions with hydrosilanes were performed.

Thus, variable temperature (-4 – 22 °C) ^{1}H-^{1}H EXSY NMR experiments of a stoichiometric mixture of the agostic complex **III-1** and $PhSiH_3$ showed an exchange process between the silane and the classical SiH_2Ph ligand, but not within the SiH_2Ph group of the agostic silylamide fragment (Figure 26). On the other hand, an NMR experiment with a labelled silane $PhSiD_3$ revealed, after 5 min. at room temperature, a nearly statistical redistribution of deuterium on all the silicon centers in (ArN)Mo(SiD_2Ph)(η^3-NAr-SiDPh-D)(PMe_3) (**III-1d$_4$**), suggesting a fast exchange between the Si-bound protons of both silyl groups and the free silane (Scheme 100). Hypothetically, such substitution of SiH by deuterium could proceed without exchange of silicon centers between free silane and silyl groups of **III-1**. This suggestion was

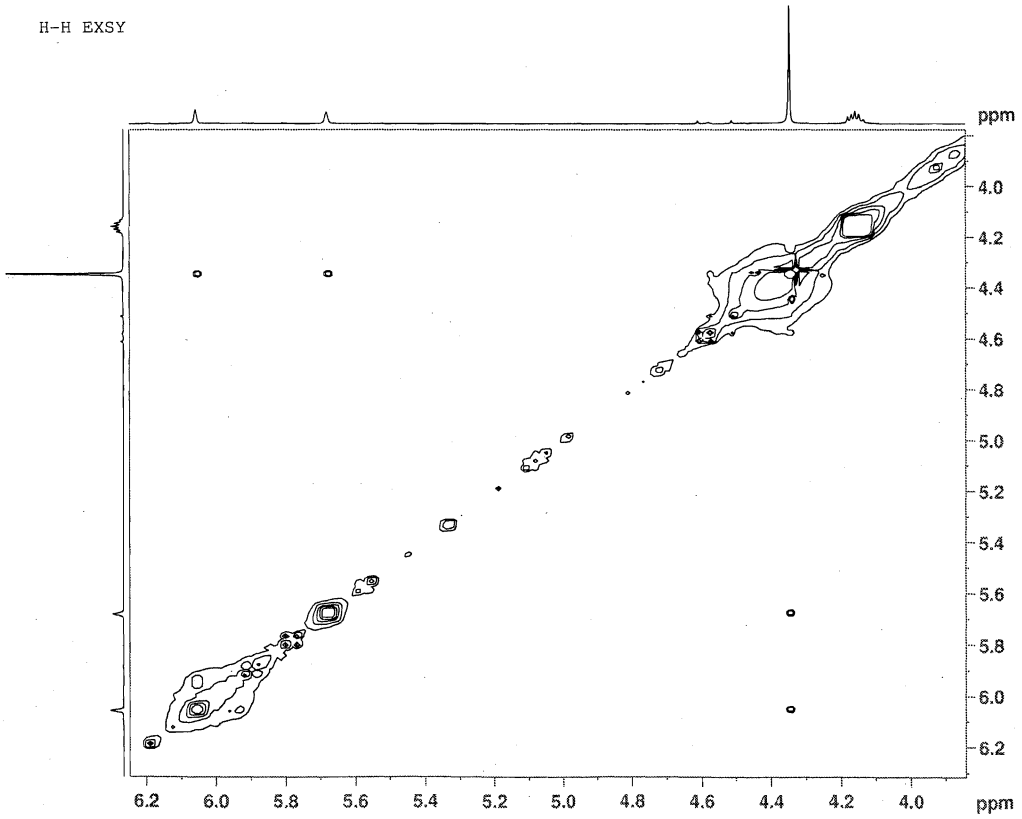

Figure 26. ^{1}H-^{1}H EXSY NMR spectrum (22 °C) of the mixture of **III-1** and $PhSiH_3$.

examined using another labeling experiment with (*m*-Tol)SiH_3. Thus, the treatment of **III-1** with (*m*-Tol)SiH_3 leads, after 10 min at room temperature, to the replacement of the classical SiH_2Ph ligand with the tolylsilyl group forming **III-1$_{tol}$** (43 % conversion; Scheme 100), in which the SiH_2Ph group of the agostic ligand remains unreacted (as indicated by the ^1H-^{13}C HMBC-GP NMR spectroscopy[k]; Figure 48, chapt. VI). Furthermore, analogous treatment of the silylamide **III-1** with excess $PhMeSiH_2$ also leads to a partial displacement of the classical SiH_2Ph ligand with SiHMePh. These observations suggest a mechanism of silane/silyl exchange depicted in Scheme 100, which includes the intermediate formation of a 16-electron silanimine complex (ArN)Mo(η^3-NAr-SiHPh)(PMe_3) (**III-2**).

Alternatively, the selective exchange of the classical SiH_2Ph ligand with an external silane (for example, (*m*-Tol)SiH_3) could proceed *via* the dissociation of the agostic Si-H···Mo bond, generating a species with the vacancy at the molybdenum center, e.g. (ArN)Mo(SiH_2Ph){NAr(SiH_2Ph)}(PMe_3) (**III-91**; Scheme 101). Such dissociation of the Si-H···Mo bond is, for instance, responsible for the fluxionality of complex **III-1** (see above). In this case, the formation of compound **III-1$_{tol}$** could proceed *via* the coordination of (*m*-Tol)SiH_3 to the unsaturated molybdenum center in **III-91**, followed by $PhSiH_3$ dissociation.

The activation parameters, calculated using variable temperature 1D ^1H EXSY NMR experiments[212] for a mixture of **III-1** and phenylsilane, showed a large negative entropy of activation, $\Delta S^{\ddagger}$ = -36.7 ± 2.2 cal·mol^{-1}·K^{-1} ($\Delta H^{\ddagger}$ = 7.7 ± 0.7 kcal·mol^{-1}, $\Delta G^{\ddagger}_{295.1}$ = 18.5 ± 1.3 kcal·mol^{-1}), which indicates an associative mechanism of the process (see Figure 49, chapt. VI). Such a transformation most likely occurs *via* dissociation of the NSi-H···Mo bond and addition of an external silane as depicted in Scheme 101. However, there still remains a possibility of the silanimine pathway (Scheme 100), which was initially suggested on the basis of labelling experiments with $PhSiD_3$ and (*m*-Tol)SiH_3 (see above). Furthermore, the arguments in favour of intermediacy of the silanimine (ArN)Mo(η^2-ArN=SiHPh)(PMe_3) (**III-2**) were obtained from the study of the stoichiometric reactivity of complex **III-1** with unsaturated organic molecules. In these reactions, the release of one equivalent of $PhSiH_3$, presumably preceding the coupling of

[k] HMBC-GP: *H*eteronuclear *M*ultiple *B*ond *C*orrelation with *G*radient *P*ulse

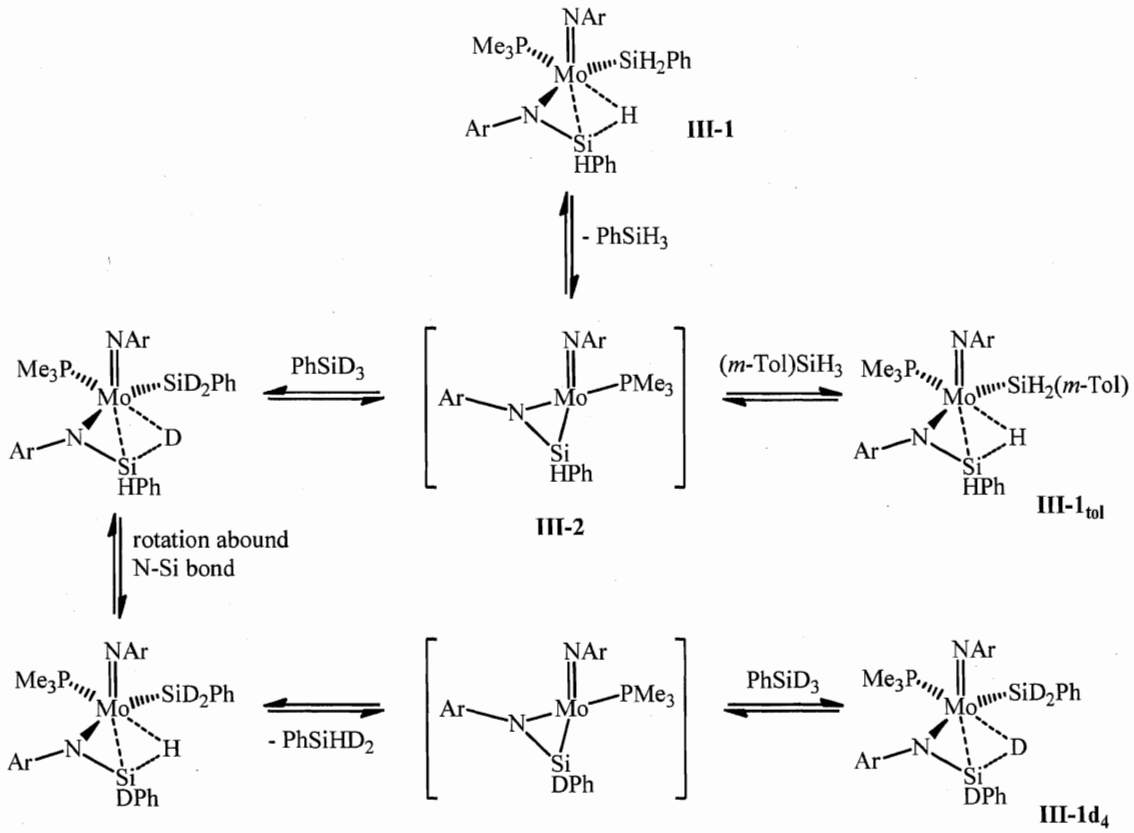

Scheme 100. Silane/silyl exchange in **III-1** *via* the silanimine intermediate **III-2**.

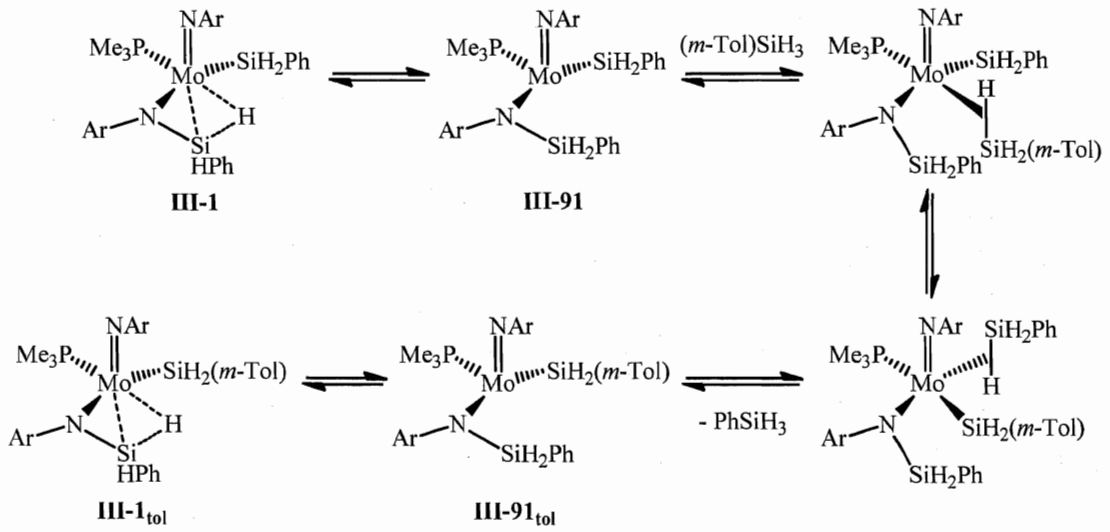

Scheme 101. Silane/silyl exchange in **III-1** *via* the dissociation of Si-H···Mo bond.

organic substrates with **III-2**, was observed by NMR spectroscopy (see the discussion below, chapt. III.5.4). Most likely, the exchange between the external silane and classical SiH_2Ph ligand in **III-1** involves both the silanimine and silylamide pathways.

III.5.3 Catalytic reactivity of complex III-1

The discovery of the catalytic dehydrogenative coupling and redistribution of $PhSiH_3$ mediated by **III-1**, as well as the intermediacy of either the silanimine **III-2** or classical silylamide **III-91** derivatives (both are electron deficient complexes) have inspired an investigation of the catalytic activity of the agostic compound **III-1** in the hydrosilation of unsaturated organic molecules.

Indeed, compound **III-1** was found to catalyze a surprising variety of hydrosilation processes (Tables 7-9).[l, 213] Thus, the 1:1 reaction of benzaldehyde with $PhSiH_3$ in the presence of 0.5 mol. % of complex **III-1** gives a 100 % conversion of the substrate after 16 hours, affording a mixture of mono- ($PhH_2Si(OBn)$) and bis(substituted), ($PhHSi(OBn)_2$) silyl ethers in 43 % and 57 %, respectively (Table 7, entry 1).[160, 214, 215b] Changing the ratio of PhC(O)H and $PhSiH_3$ to 2:1 and increasing the load of the catalyst to 1.3 mol. % leads to increased reaction time and gives a 100 % conversion of the benzaldehyde after one week at room temperature. At the same time, almost exclusive formation of $PhHSi(OBn)_2$ (95 % according to ^{1}H-NMR spectroscopy) is observed in the latter case (Table 7, entry 2). Monitoring the reaction by ^{1}H-NMR spectroscopy (Figures 50 and 51, chapt. VI) has revealed fast deactivation of the catalyst **III-1**.

The catalytic hydrosilation of benzaldehyde was proved to be highly sensitive to the acidity and steric hindrance of the applied silane. Thus, treatment of PhC(O)H with $PhMeSiH_2$ in the presence of 1.6 mol. % of **III-1** gives, after 6 days at room temperature, only 28 % conversion of benzaldehyde to form exclusively $PhMeHSi(OBn)$[215] exclusively (Table 7, entry 3). At the same time, the reaction of benzaldehyde with more acidic $(EtO)_3SiH$[216] and 1.0 % of **III-1** results in even lower conversion of PhC(O)H (10 % after 4 days at room temperature). However, this result could be accounted for by the occurance of a competing redistribution[7a, 72] in the hydrosilated product $(EtO)_3Si(OBn)$,[216a] affording a mixture of silyl ethers, one of which was assigned to

[l] For reviews in transition metal mediated homogeneous hydrosilation of unsaturated organic molecules see, for example, refs. 7, 19c, 80, 107, and 108.

Table 7. Catalytic hydrosilation of ketones and aldehydes mediated by **III-1**.

Entry	Organic substrate[a]	Silane	cat., mol. %	T, °C / time	Products[b]	Substrate. Conv.[c]	Yield[c]	TON
1	PhC(O)H	$PhSiH_3$	0.5	RT / 16 h	$PhSiH_2(OBn)$	100 %	43 %	192
					$PhSiH(OBn)_2$		57 %	
2[d]			1.3	RT / 7 days	$PhSiH_2(OBn)$	100 %	5 %	82
					$PhSiH(OBn)_2$		95 %	
3		$PhMeSiH_2$	1.6	RT / 6 days	PhMeHSi(OBn)	28 %	28 %	16
4		$(EtO)_3SiH$	1.0	RT / 4 days	$(EtO)_3Si(OBn)$	10 %	8 %	10
					$(EtO)Si(OBn)_3$		< 2 %	
5				50 °C / 12 days	$(EtO)_3Si(OBn)$	100 %	10 %	98
					$(EtO)_2Si(OBn)_2$		32 %	
					$(EtO)Si(OBn)_3$		47 %	
					$Si(OBn)_4$		11 %	
6	PhC(O)Me	$PhSiH_3$	1.0	RT / 20 days	$PhH_2Si[OCH(Me)Ph]$	100 %	44 %	107
					$PhHSi[OCH(Me)Ph]_2$		29 %	
					$PhSi[OCH(Me)Ph]_3$		21 %	
					$PhCH_2CH_3$		6 %	
7	$Me_2C(O)$	$PhSiH_3$	1.0	RT / 5 days	$PhH_2Si(O^iPr)$	79 %	34 %	77
					$PhHSi(O^iPr)_2$		42 %	

[a] The ratio of organic substrate and silane is 1:1. [b] Reactions with $PhSiH_3$ give Ph_2SiH_2 and SiH_4 as by-products produced by the catalytic redistribution of substituents at the silicon centre.[211] Increase of the temperature increases the amount of Ph_2SiH_2 and SiH_4 formed. [c] Detected by ^{1}H-NMR spectroscopy using tetramethylsilane as an internal standard. [d] The reaction was done with 2:1 ratio of PhC(O)H and $PhSiH_3$, respectively.

$(EtO)Si(OBn)_3$ (Table 7, entry 4). At 50 °C, the reaction of PhC(O)H with $(EtO)_3SiH$ goes to completion after 12 days, giving only 10 % of $(EtO)_3Si(OBn)$. The other 90 % of the silicon containing products were found to be $(EtO)_2Si(OBn)_2$ (32 %), $(EtO)Si(OBn)_3$ (47 %), and $Si(OBn)_4$ (11 %), produced by the catalytic redistribution of benzoxy(triethoxy)silane (Table 7, entry 5).

In contrast to the reaction of benzaldehyde with phenylsilane, the catalytic hydrosilation of ketones (acetophenone and acetone) by $PhSiH_3$ at room temperature is very sluggish (Table 7, entries 6 and 7). An increase of the reaction time and/or temperature leads to competing silane redistribution[211] and to partial carbonyl reduction to alkanes.[217]

Interestingly, complex **III-1** turned out to be inactive in the hydrosilation of alkenes and alkynes (Table 8). Thus, reactions of $PhSiH_3$ with 1-hexene, cyclohexene, and styrene result only in partial reduction to the corresponding alkanes.[68] For instance, stoichiometric treatment of 1-hexene with $PhSiH_3$ in the presence of 5.0 mol. % of **III-1** after three days at room temperature leads to only a 20 % conversion of the substrate, forming hexane in 15 % yield (5 % of the isomerised product, 2-hexene,[218] were also observed by ^{1}H-NMR spectroscopy; Table 8, entry 1). An increase of the reaction time (37 days) and temperature (50 °C) affords 100 % conversion of 1-hexene and production of 71 % of hexane in a mixture with 2-hexene (26 %) and hydrosilation products[219] (less than 3 %) (Table 8, entry 2). The treatment of the less sterically unhindered olefine, ethylene, by $PhSiH_3$ gives, however, hydrosilation products (a mixture of $PhEtSiH_2$, $PhEt_2SiH$, and $PhEt_3Si$)[202] in 49 % yield after 15 hours at 50 °C (Table 8, entry 11). Similarly to other alkenes, the formation of 31 % of ethane was also detected by ^{1}H-NMR analysis.

Neither hydrosilation nor reduction processes were observed upon room temperature reaction of phenylacetylene with $PhSiH_3$ in the presence of 2.7 mol. % of complex **III-1**. Instead, catalytic polymerization[220] takes place leading, after 17 hours, to 100 % conversion of phenylacetylene and formation of polyphenylacetylene (turnover number (TON) = 34, turnover frequency (TOF) = 2; Table 8, entry 7). Surprisingly, the absence of silane significantly decreases the turnover number of the reaction and leads to only 25 % conversion of alkyne after 24 hours at room temperature. In the last case, the increase

Table 8. Reactions alkenes and alkynes with hydrosilanes in the presence of **III-1**.

Entry	Organic substrate[a]	Silane	cat., mol. %	T, °C / time	Products[b]	Substrate conv.[c]	Yield[c]	TON
1	1-hexene	$PhSiH_3$	5.0	RT / 3 days	2-hexene	20 %	5 %	4
					Hexane		15 %	
2				50 °C / 37	2-hexene	100 %	26 %	20
				days	hexane		71 %	
					hydrosilation products		< 3 %	
3	Cyclohexene	$PhSiH_3$	5.0	RT / 2 days	Cyclohexane	< 5 %	< 5 %	—
4				50 °C / 39	Cyclohexane	28 %	28 %	6
				days				
5	Styrene	$PhSiH_3$	3.0	RT / 24 h	no reaction	—	—	—
6				50 °C / 23 h	$PhCH_2CH_3$	6 %	6 %	1.3
7	Phenylacetylene	$PhSiH_3$	2.7	RT / 17 h	Polyphenylacetylene	100 %	100 %	34
8		—	3.0	RT / 24 h	Polyphenylacetylene	25 %	25 %	8
9				50 °C / 24 h	Polyphenylacetylene	45 %	45 %	15
10	Ethylene	$PhSiH_3$	3.3	RT / 0.5 h	no reaction	—	—	—
11				50 °C / 15 h	$PhEtSiH_2$	80 %	19 %	24
					$PhEt_2SiH$ + $PhEt_3Si$		30 %	
					Ethane		31 %	

[a] The ratio of organic substrate and silane is 1:1 [b] Formation of Ph_2SiH_2 and SiH_4 as by-products due to the catalytic redistribution of $PhSiH_3$[211] was observed. Increase of the temperature increases the amount of Ph_2SiH_2 and SiH_4 formed. [c] Detected by ^{1}H-NMR spectroscopy using tetramethylsilane as an internal standard.

Table 9. Hydrosilation of nitriles and pyridines as well as alcoholysis and aminolysis of silanes mediated by **III-1**.

Entry	Organic substrate[a]	Silane	cat., mol. %	T, °C / time	Products[b]	Substrate conv.[c]	Yield[c]	TON
1	CH_3CN	$PhSiH_3$	5.0	RT / 14 h	no reaction	—	—	—
2				50 °C / 51 h	$Et(SiH_2Ph)_2$	< 3 %	< 3 %	—
3	PhCN	$PhSiH_3$	5.0	RT / 24 h	no reaction	—	—	—
4				50 °C / 6 days	$PhHC{=}N(SiH_2Ph)$	20 %	20 %	4
5	Pyridine	$PhSiH_3$	0.6	RT / 5 days	*N*-(phenylsilyl)-4-hydropyridine	< 5 %	all together < 5 %	—
					N-(phenylsily)-2-hydropyridine			
6	EtOH	$PhSiH_3$	5.0	RT / 5 min	$PhH_2Si(OEt)$	100 %	33 %	20
					$PhHSi(OEt)_2$		67 %	
7[d]				RT /25 min	$PhH_2Si(OEt)$	100 %	11 %	41
					$PhHSi(OEt)_2$		89 %	
8	$^{i}PrOH$	$PhSiH_3$	5.0	RT / 5 min	$PhH_2Si(O^{i}Pr)$	100 %	18 %	20
					$PhHSi(O^{i}Pr)_2$		82 %	
9	$PhNH_2$	$PhSiH_3$	5.0	RT / 20 min	$PhHN(SiH_2Ph)$	100 %	100 %	20

[a] The ratio of organic substrate and silane is 1:1. [b] Reactions with $PhSiH_3$ give Ph_2SiH_2 and SiH_4 as by-products produced by the catalytic redistribution of substituents at the silicon centre.[211] Increase of the reaction temperature increases the amount of Ph_2SiH_2 and SiH_4 formed. [c] Detected by ^{1}H-NMR spectroscopy using tetramethylsilane as an internal standard. [d] The reaction was performed with 2:1 ratio of EtOH and $PhSiH_3$, respectively.

of the temperature of the process up to 50 °C does not affect significantly the yield of the polymer product (Table 8, entries 8 and 9). These observations suggest that $PhSiH_3$ plays an important role in either activation or, more likely, in the recovery of the actual catalyst in the polymerization reaction.

Catalytic alcoholysis of $PhSiH_3$ by an equivalent of ethanol or isopropanol mediated by complex **III-1** is a fast process and gives a 100 % conversion in only 5 min. at room temperature (TON = 20, TOF = 241; Table 9, entries 6 and 8).[m] The stoichiometric reaction of $PhSiH_3$ with either EtOH or ^{i}PrOH in the presence of 5.0 mol. % of **III-1** affords a mixture of mono- and disubstituted products $PhH_2Si(OR)$ (R = Et (33 %), ^{i}Pr (18 %)) and $PhHSi(OR)_2$ (R = Et (67 %), ^{i}Pr (82 %)),[160, 221] respectively. Addition of two equivalents of ethanol to phenylsilane results in a longer reaction time (25 min.), but almost selectively forms diethoxyphenylsilane (89 %; TON = 41, TOF = 98; Table 9, entry 7). Analogous high activity of complex **III-1** was also found for the aminolysis[m] of $PhSiH_3$ by aniline under catalytic conditions (5.0 mol. % cat. loading, TON = 20, TOF = 60; Table 9, entry 9).

Finally, the agostic silylamide complex **III-1** was found to mediate the addition of phenylsilane to nitriles. Unfortunately, only traces (< 3 %) of the hydrosilation product, $EtN(SiH_2Ph)$, were observed in the reaction of $PhSiH_3$ with CH_3CN even after heating the reaction mixture at 50 °C for 51 h (Table 9, entry 2). On the other hand, the stoichiometric treatment of PhCN with $PhSiH_3$ in the presence of 5.0 mol. % of **III-1** gives exclusively the silylated imine $PhCH{=}N(SiH_2Ph)$ with 20 % conversion of nitrile after 6 days at 50 °C (TON = 4, Table 9, entry 4). To the best of our knowledge, such a selective monoaddition is very rare[146] in the catalytic hydrosilation of nitriles.[133, 136, 137b, 138a, 141, 222]

III.5.4 Stoichiometric reactivity of complex III-1

To shed more light on the catalytic processes, stoichiometric reactions of the agostic silylamido complex **III-1** with unsaturated organic molecules were attempted. First of all, it should be noted that all transformations of the compound **III-1** with organic substrates

[m] For transition metal mediated alcoholysis and aminolysis of hydrosilanes, see chapts. II.2.5 and II.2.6.4 and references therein.

performed in stoichiometric ratio lead to the release of a molecule of $PhSiH_3$, suggesting further oxidative addition of the agostic NSi-H···Mo bond as an initial step of these reactions. This chapter describes the reactivity of **III-1** towards alkenes, alkynes, carbonyls, and organic nitriles. The stoichiometric reaction between **III-1** and $PhSiH_3$ in the presence of BPh_3 is also discussed.

III.5.4.1 Reactions of complex III-1 with alkenes

Treatment of complex **III-1** with olefins leads to the products of Si_{ag}-C coupling, containing only one classical Si-H group. Thus, a reaction of **III-1** with ethylene cleanly gives the ethyl vinylsilyl derivative (ArN)Mo(Et)(η^3-NAr-SiHPh-CH=CH_2)(PMe_3) (**III-3**; Scheme 102), which was characterized by spectroscopic methods (IR and multinuclear NMR) and by X-ray diffraction (Figure 27). Compound **III-3** can be also obtained in 52 % yield by the reaction of the bis(imido) complex $(ArN)_2Mo(\eta^2\text{-}CH_2{=}CH_2)(PMe_3)_2$ (**III-31**) with two equivalents of $PhSiH_3$ and excess ethylene (Scheme 102). The ^{1}H-NMR spectrum of **III-3** exhibits a down-field singlet for the Si*H* proton at 6.48 ppm, coupled in the ^{1}H-^{29}Si HSQC spectrum to a ^{29}Si-NMR signal at –28.2 ppm. The observation of a doublet for the silicon signal in the ^{29}Si INEPT+ NMR spectrum and the large value of $^1J_{Si\text{-}H}$ = 207.8 Hz suggest the presence of only classical Si*H* proton. Furthermore, the absence of an additional NSi-H···Mo bonding in **III-3** is supported by the absence of the coupling of the Si*H* signal to the ^{31}P-NMR signal in the ^{1}H-^{31}P HSQC NMR spectrum

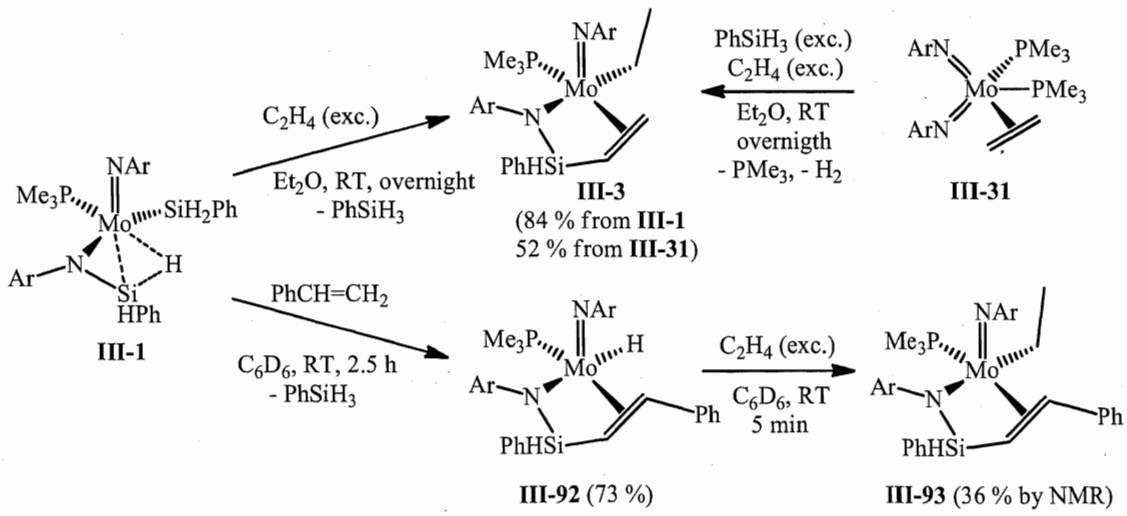

Scheme 102. Reactions of complex **III-1** with ethylene and styrene.

and observation of a characteristic Si-H stretch at 2105 cm^{-1} in the IR spectrum. The coordination of the vinyl moiety of the (vinylsilyl)amide ligand to the molybdenum results in the appearence of three CH signals of equal intensity at 2.95 (dd, $^3J_{H-H}$ = 13.0, 15.6 Hz), 4.09 (m, obscured by a signal from the ^{i}Pr group of NAr), and 4.30 ppm (dd, $^3J_{H-H}$ = 3.9, 13.0 Hz) in the ^{1}H-NMR spectrum. The up-field shift of these C*H* resonances in the ^{1}H-NMR spectrum, their coupling in the ^{1}H-^{31}P HSQC NMR spectrum to a phosphorus nucleus, as well as the significant up-field shift of vinyl carbons in the ^{13}C-NMR (49.9 and 75. 4 ppm, coupled to phosphorus with $^2J_{C-P}$ = 4.7 and 13.2 Hz, respectively) also imply the formation of an η^2-olefin adduct.

Similarly to the agostic silylamide **III-1**, the molecular structure of complex **III-3** (Figure 27) can be described as a distorted molybdenum-centered trigonal bipyramid, having the PMe_3 group and the coordinated vinyl ligand in the apical positions (selected bond distances and angles are listed in Table 10; the crystal structure parameters are

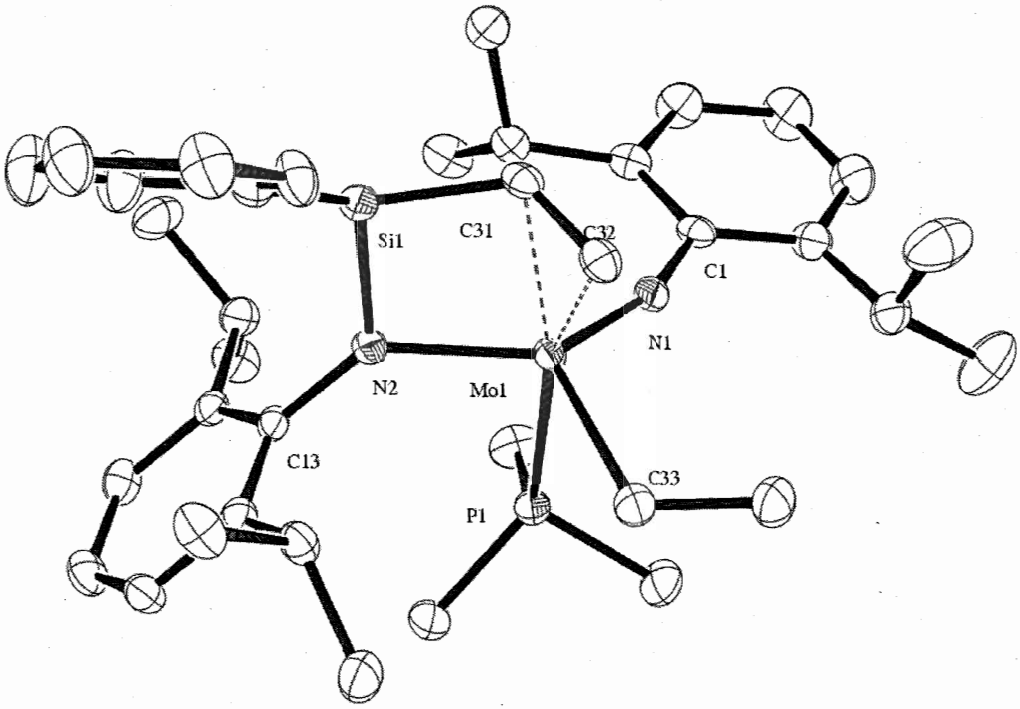

Figure 27. ORTEP plot of the molecular structure of complex **III-3** (one of two independent molecules is shown; hydrogen atoms are omitted for clarity). Anisotropic displacement parameters are plotted at 50 % probability.

Table 10. Selected bond distances (Å) and angles (°) for complex **III-3**.

distances, Å		angles, °	
Mo1-N1	1.769(2)	Mo1-N1-C1	161.3(2)
Mo1-N2	2.068(2)	Mo1-N2-Si1	99.02(10)
Mo1-C31	2.283(3)	N2-Si1-C31	95.92(11)
Mo1-C32	2.238(3)	N1-Mo1-N2	139.72(10)
Mo1-C33	2.216(3)	N1-Mo1-C33	108.77(11)
Mo1-Si1	2.9036(8)	N2-Mo1-C33	111.01(10)
Mo1-P1	2.5757(8)	N1-Mo1-P1	84.79(8)
Si1-N2	1.740(2)	N2-Mo1-P1	94.23(6)
Si1-C31	1.841(3)	C33-Mo1-P1	82.52(8)

presented in Table 29, chapt. VI). The Mo1-N1-C1 bond angle in the imido ArN^{2-} moiety of **III-3** is 161.3(2) ° (Table 10), which indicates that the imido ligand can act as a 6-electron donor to molybdenum, stabilizing the 18-electron species. Coordination of the vinyl ligand leads to the observation of decreased Mo-C_{vinyl} distances of 2.238(3) and 2.283(3) Å (compared to the Mo1-C33 bond of 2.216(3) Å for the Mo-bound ethyl ligand; Table 10). The quite large Mo-Si separation of 2.9038(8) Å testifies against the presence of any nonclassical Si-H···Mo bonding in **III-3** (compare to the Mo-Si_{ag} distance of 2.634(1) Å in the agostic complex **III-1**; Table 5).

The NMR scale reaction of agostic silylamide **III-1** with an equivalent of styrene gives the hydrido vinylsilane complex (ArN)Mo(H)(η^3-NAr-SiHPh-CH=CHPh)(PMe_3) (**III-92**; Scheme 102). The presence of a hydride ligand in the compound **III-92** is evident from the IR spectrum, which exhibits stretches at 1812 and 2098 cm^{-1} assigned to the Mo-H and Si-H vibrations, respectively. The ^{1}H-NMR spectrum of **III-92** shows a down-field Si*H* signal at 6.15 ppm (d, $^4J_{H\text{-}P}$ = 6.6 Hz), coupled in the ^{1}H-^{29}Si HSQC NMR spectrum to a ^{29}Si-NMR resonance at -8.2 ppm, and a down-field Mo-H signal at 3.05 ppm (d) with the large $^2J_{H\text{-}P}$ of 43.2 Hz (the same coupling constant was observed for the ^{31}P-NMR signal upon selective decoupling from the methyl substituents). Despite the coupling of the Si*H* proton signal to phosphorus ($J_{H\text{-}P}$ = 6.6 Hz), the large value of $^1J_{S\text{-}H}$ = 197.9 Hz (found by ^{29}Si INEPT+ NMR spectroscopy) suggests that the Si-H bond is not coordinated to the molybdenum. Similarly to **III-3**, the η^2-coordination of the vinyl

ligand –CH=CHPh in **III-92** is established from its ^{1}H-NMR spectrum, in which the alkene protons give rise to doublets at 3.30 and 6.22 ppm ($^{3}J_{H\text{-}H}$ = 15.0 Hz), coupled in the ^{1}H-^{31}P HSQC spectrum to the phosphorus signal at -19.2 ppm. An analogous up-field shift of the resonances of the vinyl carbons is observed in the ^{13}C NMR spectrum, where corresponding signals can be found at 37.5 ppm (d, $^{2}J_{C\text{-}P}$ = 6.8 Hz) and 83.4 ppm (d, $^{2}J_{C\text{-}P}$ = 3.4 Hz). The bonding between the silicon atom and vinyl carbon in **III-92** was established by the ^{1}H-^{13}C HMBC NMR experiment, which revealed coupling between the Si*H* proton and the vinyl carbon. Analogously, the ^{1}H-^{13}C HMBC spectrum showed the positioning of the phenyl substituent of the vinyl group at the carbon atom *β*- to Si, which could be accounted for by the presence of steric repulsions with the Ph substituent at silicon.

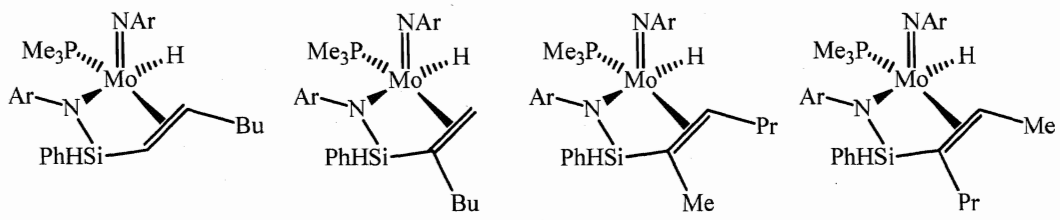

Figure 28. Possible products formed in the reaction of **III-1** with 1-hexene.

The reaction of **III-1** with 1-hexene seems to go *via* the same Si$_{ag}$-C coupling route, however, the formation of a mixture of isomers for the vinylsilyl derivative as well as the concurrent reaction with 2-hexene, formed by an isomerisation side-process, hampered the isolation and characterization of the product (Figure 28).

Interestingly, a similar alkene insertion into the Zr-Si bond has been observed previously by Berry *et al.* for the silanimine complex Cp$_2$Zr(η^2-^{t}BuN=SiMe$_2$)(PMe$_3$) (**III-90**).[142a,b] Taking this into account and keeping in mind that the reaction of **III-1** with olefins leads to the release of an equivalent of PhSiH$_3$, the insertion of alkenes into the NSi-H···Mo agostic fragment of silylamide **III-1** could proceed *via* the formation of a silanimine intermediate (ArN)Mo(η^2-ArN=SiHPh)(PMe$_3$) (**III-2**). Further coupling of the electron deficient complex **III-2** with olefins[142a,b] and C-H bond activation at the *β*- to Mo carbon of the CH$_2$CHR substituent afforded a hydrido (vinylsilyl)amido derivative, which in the case of the relatively small ethylene reacts further to give the complex **III-3** (Scheme 103). A similar insertion of C$_2$H$_4$ into the Mo-H bond is observed upon a room

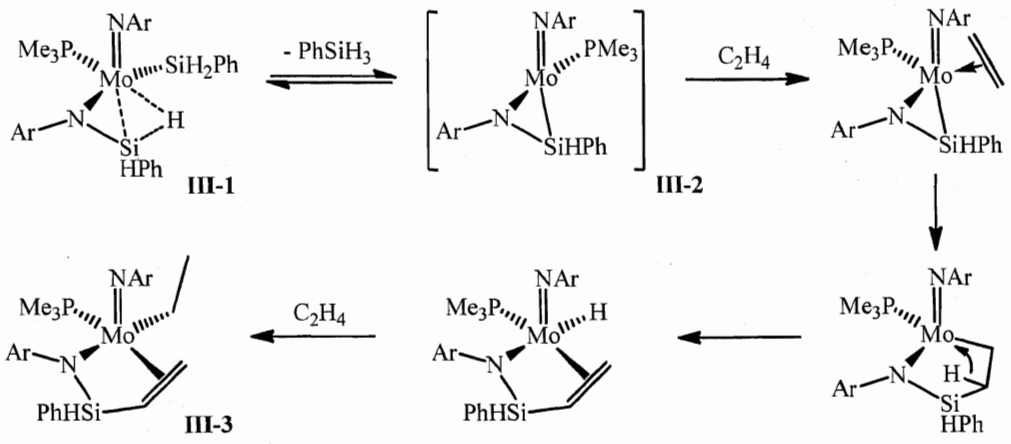

Scheme 103. Possible mechanism for the formation of ethyl (vinylsilyl)amide **III-3**.

temperature NMR scale reaction of compound **III-92** with ethylene, which gives the ethyl derivative (ArN)Mo(Et)(η^3-NAr-SiHPh-CH=CHPh)(PMe_3) (**III-93**; Scheme 102).

The formation of the Si_{ag}-C coupling products in the reactions of **III-1** with olefins (styrene and ethylene) can be suppressed by the addition of an equivalent of BPh_3. In this case, the process goes *via* abstraction of the PMe_3 ligand to release the Lewis adduct $Ph_3B{\cdot}PMe_3$ and give η^2-alkene silylamido agostic complexes, (ArN)Mo(η^3-NAr-SiHPh-H)(η^2-CH_2=CHR) (R = Ph (**III-94**), H (**III-95**); Scheme 104). Unfortunately, all attempts to isolate compounds **III-94** and **III-95** were unsuccessful due to their high instability. Nevertheless, the structures of these products were supported by NMR and IR analysis, which indicate the presence of classical and agostic silyl groups as well as the η^2-coordinated alkene ligand (see experimental details). The position of the η^2-olefin ligand *trans*- to the Si-H···Mo unit is suggested by analogy with the structure of the phosphine precursor (ArN)Mo(η^3-NAr-SiHPh-H)(PMe_3) (**III-1**) and, logically, explains the absence of insertion of the coordinated alkene into the Mo-Si_{ag} bond. Furthermore, addition of an

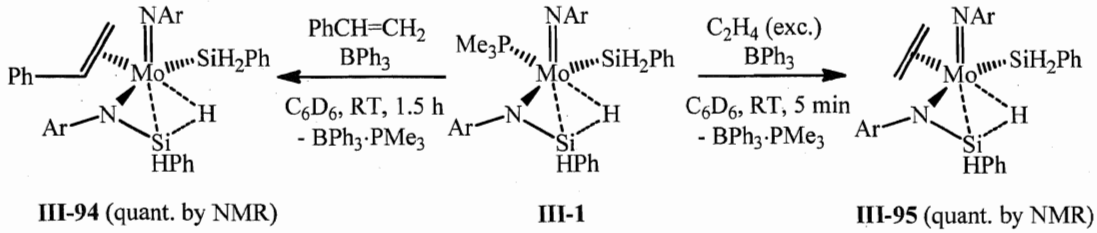

Scheme 104. Reactions of **III-1** with olefins in the presence of BPh_3.

equivalent of phosphine to adducts **III-94** and **III-95** selectively recovers the starting compound **III-1** with the release of a molecule of olefin. Further reaction of the agostic complex **III-1** with an alkene affords (ArN)Mo(R)(η^3-NAr-SiHPh-CH=CHR')(PMe_3) (**III-3**: R = Et, R' = H; **III-92**: R = H, R' = Ph).

III.5.4.2 Reactions with ketones and aldehydes

The reactions of agostic silylamide **III-1** with ketones (acetone and acetophenone), surprisingly, do not afford products of insertion into the Mo-Si_{ag} bond. Instead, the formation of bis(imido) carbonyl adducts $(ArN)_2Mo(\eta^2\text{-}O{=}CMe_2)(PMe_3)$ (**III-96**)[223] and $(ArN)_2Mo(\eta^1\text{-}O{=}CMePh)(PMe_3)$ (**III-97**)[224] was observed by NMR (Scheme 105). The reactions are accompanied by the evolution of one equivalent of $PhSiH_3$ and give a difficult-to-characterize mixture of silicon-containing compounds. All attempts to trace the fate of the extruded silylene fragment :SiHPh were unsuccessful. The coordination mode for acetone (η^2) and acetophenone (η^1) is suggested from the available NMR and IR data (see experimental details). The treatment of **III-96** and **III-97** with an excess of $PhSiH_3$ results in initial elimination of the ketone and selective regeneration of the agostic silylamido complex **III-1** (Scheme 105). Hydrosilation of ketones by the agostic compound **III-1** to give corresponding silyl ethers was also observed.

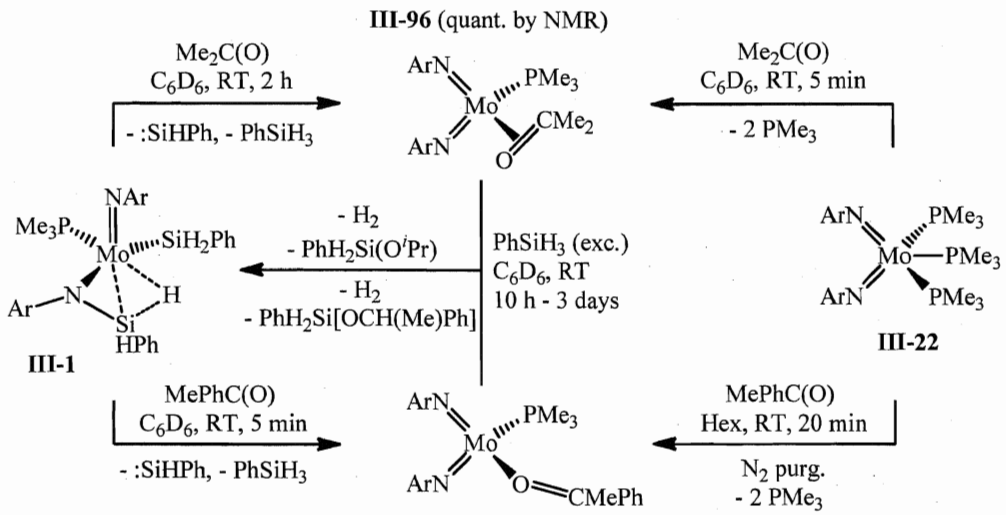

Scheme 105. Reactions of **III-1** with ketones forming compounds **III-96** and **III-97**.

Carbonyl adducts **III-96** and **III-97** can also be easily prepared by the reaction of $(ArN)_2Mo(PMe_3)_3$ (**III-22**) with the corresponding ketone (Scheme 105). In this way, compound **III-97** was isolated in 41 % yield, whereas all attempts to obtain its acetone analogue **III-96** were unsuccessful due to its instability and decomposition into the starting complex **III-22**. This observation suggests the reversibility of carbonyl addition to **III-22**. Interestingly, the treatment of **III-22** with excess acetophenone and increasing both the reaction time (up to 4 days) and temperature (up to 50 °C) lead to coupling of the initial product **III-97** with MePhC(O) affording the pinacole derivative $(ArN)_2Mo\{O\text{-}C(Me)Ph\text{-}C(Me)Ph\text{-}O\}\text{-}(PMe_3)$ (**III-98**; 82 % by $^{31}P\{^1H\}$-NMR; Scheme 106).

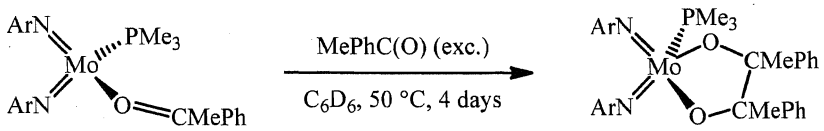

III-97 **III-98** (82 % by NMR)

Scheme 106. Reaction of **III-97** with acetophenone.

In contrast to ketones, the reaction of **III-1** with benzaldehyde gives a highly fluxional product, which in its ^{1}H-NMR spectrum exhibits a doublet at 13.28 ppm coupled to the phosphorus nucleus with $J_{H\text{-}P}$ = 7.2 Hz and assigned to the O=C*H* proton. This fact and the observation of a down-field Si*H* signal at 6.83 ppm (1 H) coupled to phosphorus in the ^{1}H-^{31}P HSQC spectrum suggest the formation of a silanimine complex bearing the coordinated benzaldehyde $(ArN)Mo(\eta^2\text{-}ArN{=}SiHPh)(O{=}CHPh)(PMe_3)$ (**III-99**; Scheme 107).[223, 224] As for ketones, the reaction of $(ArN)_2Mo(PMe_3)_3$ (**III-22**) with benzaldehyde gives an η^2-carbonyl compound[223] $(ArN)_2Mo)(\eta^2\text{-}O{=}CHPh)(PMe_3)$ (**III-100**), characterized by an up-field O=C*H* signal at 5.69 ppm in its ^{1}H-NMR spectrum. A slow (2.5 weeks) formation of complex **III-100** was also observed upon stoichiometric treatment of the acetophenone derivative **III-97** with benzaldehyde at room temperature (Scheme 107). At the same time, the reaction of $(ArN)_2Mo(\eta^2\text{-}CH_2{=}CH_2)(PMe_3)$ (**III-101**; generated *in situ* from $(ArN)_2Mo(\eta^2\text{-}CH_2{=}CH_2)(PMe_3)_2$ (**III-31**) and BPh_3) with PhHC(O), surprisingly, does not stop at the formation of **III-100** and goes further affording the coupling[225, n] product$(ArN)_2Mo(\eta^2\text{-}O{=}C(Ph)OBn)(PMe_3)$ (**III-103**; Scheme

[n] The coupling of aldehydes to form esters is often called the Tishchenko reaction.[225]

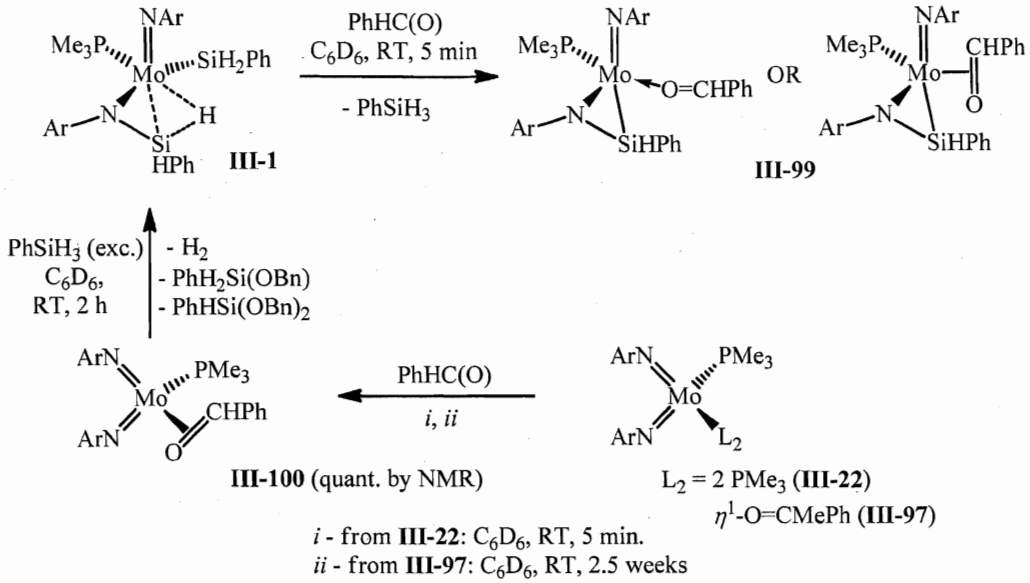

Scheme 107. Reaction of **III-1** with benzaldehyde and formation of complex **III-100**.

108) in a mixture with **III-101** and $(ArN)_2Mo(\eta^2\text{-}CH_2{=}CH_2)(\eta^1\text{-}O{=}CHPh)(PMe_3)$ (**III-104**). All attempts to obtain complex **III-103** independently *via* the treatment of bis(imido) phosphine compounds **III-22** or **III-31** with benzyl benzoate were unsuccessful.

Analogously to the reactions of **III-96** and **III-97**, treatment of complex **III-100** with an excess of $PhSiH_3$ also leads to the formation of agostic silylamide **III-1** (Scheme 107). The released benzaldehyde is transformed to $PhH_2Si(OBn)$, and $PhHSi(OBn)_2$.[160, 214, 215b] However, the formation of **III-99** in the reaction of the complex **III-1** with benzaldehyde suggests that in the **III-1**-mediated hydrosilation of carbonyl compounds the active catalyst is probably formed from complex **III-1** after silane elimination, but before the silylene extrusion from $(ArN)Mo(\eta^2\text{-}ArN{=}SiHPh)(PMe_3)$ (**III-2**). In order to confirm this

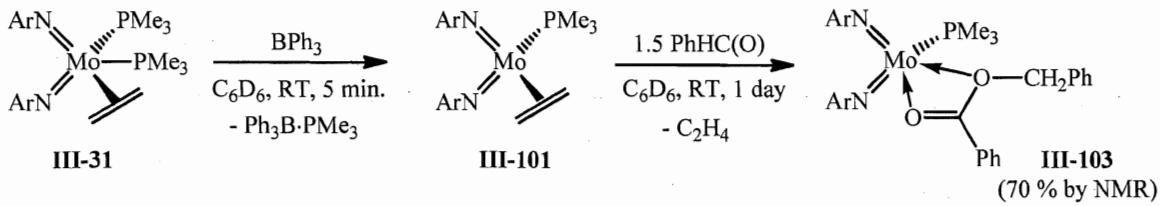

Scheme 108. Reaction of **III-31** with BPh_3 and benzaldehyde.

assumption, complex **III-97** was subjected to the catalytic hydrosilation of acetophenone with $PhSiH_3$, which revealed a much slower process than in the case of **III-1**, showing only 35 % conversion of MePhC(O) after 20 days at room temperature (TON = 38 *vs.* TON = 107 with 100 % conversion of MePhC(O) for **III-1** when the same conditions are applied; Table 7, entry 6). This fact indicates that, as proposed, the formation of bis(imido) carbonyl adducts is not involved in the actual catalytic cycle of carbonyl hydrosilation mediated by silylamide **III-1**.

III.5.4.3 Reactions with organic nitriles

As in the reaction with acetone, room temperature treatment of **III-1** with nitriles (CH_3CN, PhCN, ^{i}PrCN, and ^{t}BuCN) gives initially the η^2-adducts (ArN)Mo(η^2-ArN=SiHPh)(η^2-N≡CR)(PMe_3) (R = Me (**III-104**), Ph (**III-105**), ^{i}Pr (**III-106**), and ^{t}Bu (**III-107**); Scheme 109), evidenced by the diagnostic ^{13}C-NMR signals at 187-204 ppm for the carbon nucleus of the nitrile group.[226] The rate of the reaction depends on the steric demands of the R group and varies from 10 min for R = Me to a couple of hours for R = ^{t}Bu. The initial adducts **III-104** – **III-107** are unstable in solution and undergo a slow rearrangement through the insertion of the C≡N moiety into the Mo-Si bond of the silanimine fragment to give (ArN)Mo(η^2-NAr-SiHPh-C(R)=N)(PMe_3) (R = Me (**III-108**), Ph (**III-109**), ^{i}Pr (**III-110**), and ^{t}Bu (**III-111**); Scheme 109 and Figure 29). The rate of the rearrangement is also highly dependent on the bulkiness of the nitrile substituent (as expected, the slowest reaction was observed for the R = ^{t}Bu complex **III-107**). Rearrangement of the methyl derivative **III-104** is complicated, owing to the additional activation of the C-H bond of the CH_3CN ligand.[227] Surprisingly, NMR studies of the final products suggest the formation of a [PhHSi-C(R)=N] fragment, rather than *N*-addi-

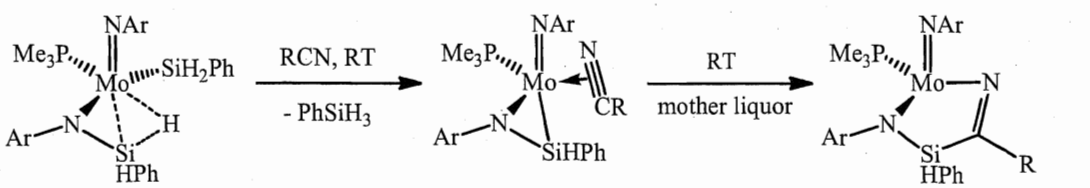

III-1

R = Me (**III-104**), Ph (**III-105**)
^{i}Pr (**III-106**), ^{t}Bu (**III-107**)

R = Me (**III-108**), Ph (**III-109**)
^{i}Pr (**III-110**), ^{t}Bu (**III-111**)

Scheme 109. Reactivity of **III-1** towards organic nitriles.

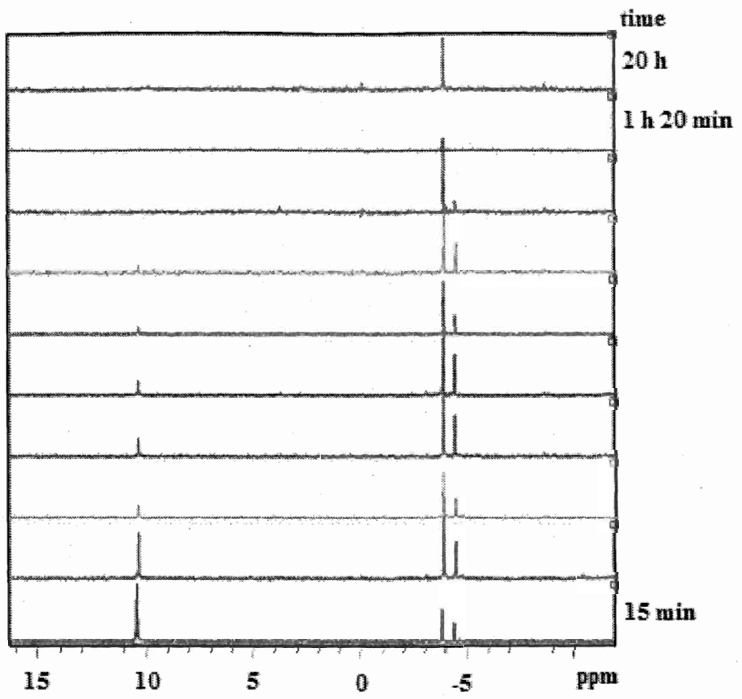

Figure 29. $^{31}P\{^{1}H\}$-NMR spectra of the reaction mixture of **III-1** and $^{i}PrCN$ (the signals at 10.5, -3.8, and -4.4 ppm correspond to **III-1**, **III-106**, and **III-110**, respectively).

tion to silicon.[133, 222c] In particular, a long-range ^{1}H-^{13}C HMBC NMR study of **III-110** shows the coupling of Si*H*, C*H*, and CH_3 protons to the imine carbon nucleus, thus, indicating the presence of direct bonding between the silicon atom and the imine carbon atom (Figure 30, see also Figure 52, chapt. VI). Such a selective *N*-addition of the RC≡N ligand to molybdenum is probably accounted for by the highly electron deficient nature of compounds **III-108** – **III-111**, in which the direct bonding between the molybdenum and imine nitrogen centres allows for additional lone-pair donation from the latter to the former, stabilizing the 16-electron valence shell. Despite the electron deficiency at the Mo center in complexes **III-108** – **III-111**, down-field shifts of the Si*H* signals (5.31 - 6.56 ppm) in the ^{1}H-NMR spectrum, large values of $^{1}J_{Si\text{-}H}$ coupling constants (218.3 - 225.4 Hz) in the ^{29}Si INEPT+ NMR specrum, as well as the observation of normal Si-H stretches at 2103-2118 cm^{-1} in the IR spectra suggest the absence of Si-H bond coordination to molybdenum.[17]

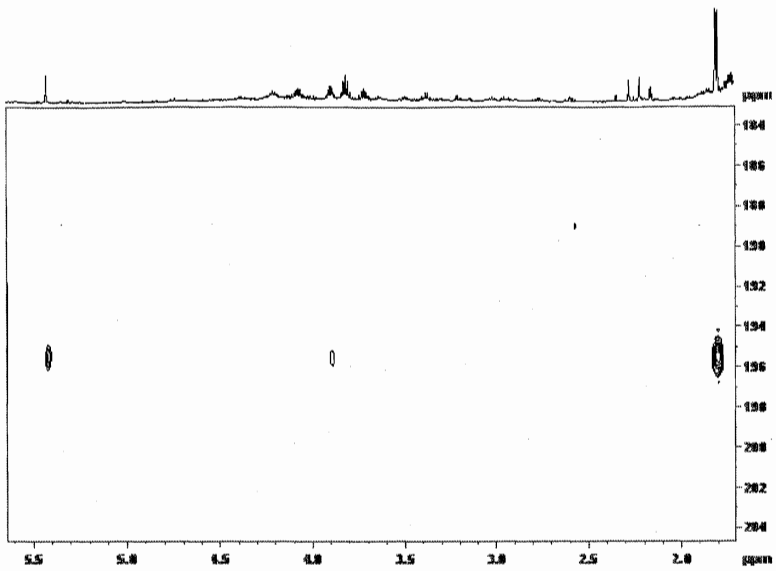

Figure 30. ^{1}H-^{13}C HMBC NMR spectrum of **III-110** taken directly from the reaction mixture (proton signals at 5.4, 3.9, and 1.8 ppm correspond to SiH, CH and CH_3, respectively).

Treatment of (ArN)Mo(η^2-NAr-SiHPh-C(^{i}Pr)=N)(PMe_3) (**III-110**) with excess $PhSiH_3$ at room temperature leads to a slow (4 days) conversion into the agostic complex (ArN)Mo(η^3-NAr-SiHPh-H)(PMe_3) (**III-1**; 65 %), accompanied by the formation of a difficult-to-characterize mixture of silicon containing products.

III.6 Reactivity of (ArN)Mo(Et)(η^3-NAr-SiHPh-CH=CH_2)(PMe_3) (III-3)

Similar to the agostic silylamido complex (ArN)Mo(SiH_2Ph)(η^3-NAr-SiHPh-H)(PMe_3) (**III-1**), the reactivity of the (vinylsilyl)amido derivative (ArN)Mo(Et)(η^3-NAr-SiHPh-CH=CH_2)(PMe_3) (**III-3**) could be induced by the presence of the labile η^3-NAr-SiHPh-CH=CH_2 ligand. We initially suggested that dissociation of either the coordinated vinyl group or PMe_3 ligand would provide a vacant site at the molybdenum center in **III-3**, making it amenable to activation of hydrosilanes and/or small organic molecules. In order to verify this assumption, the study of the reactivity of complex **III-3** towards $PhSiH_3$ and dihydrogen was performed. The discussion of the catalytic activity of **III-3** in hydrosilation and hydrogenation reactions as well as its stoichiometric reactions with unsaturated organic molecules is also presented in this chapter.

III.6.1 Reactions of III-3 with hydrosilanes and H_2

Compound **III-3** is stable at room temperature, however, heating a solution of **III-3** in C_6D_6 at 50 °C overnight results in the slow evolution of ethylene and the production of the hydride derivative (ArN)Mo(H)(η^3-NAr-SiHPh-CH=CH_2)(PMe_3) (**III-112**; 40% yield according to ^{31}P-NMR spectroscopy; Scheme 110). Complex **III-112** is similar to **III-92**, which was obtained from **III-1** by the treatment with styrene (see Scheme 102). The thermolysis of **III-3** presumably proceeds *via* a β-proton shift from the ethyl substituent to molybdenum. Formation of the hydride **III-112** is also observed upon treatment of **III-3** with a 20-fold excess of $PhSiH_3$ at room temperature, which after two days gives only 17 % conversion of the starting material accompanied by the evolution of $PhEtSiH_2$.[202] Full conversion of **III-3** and selective production of **III-112** can be achieved upon treatment with $PhSiH_3$, H_2, or $PhMeSiH_2$ at 50 °C overnight, accompanied by the release of $PhEtSiH_2$, ethane or PhMeEtSiH, respectively (Scheme 110). Surprisingly, the addition of one equivalent of PMe_3 to a mixture of **III-3** and silane significantly increases the rate of the reaction, affording higher yields of **III-112**. This fact suggests that the transformation of complex **III-3** into **III-112** does not necessarily involve phosphine dissociation in the first step. Alternatively, hydride derivative **III-112** could be obtained in 66 % yield by a preparative scale reaction between the ethyl precursor **III-3** and $PhSiH_3$ in the presence of stoichiometric amounts of PMe_3 (Scheme 110).

Complex **III-112** was fully characterized by multinuclear NMR and IR analysis. The spectroscopic features of **III-112** are similar to those observed for its ethyl analogue **III-3**, except the presence of a Mo-bound hydride ligand, which gives rise to an up-field P-coupled signal at 2.69 ppm (d, $^2J_{H\text{-}P}$ = 41.7 Hz) in the ^{1}H-NMR spectrum. In accordance

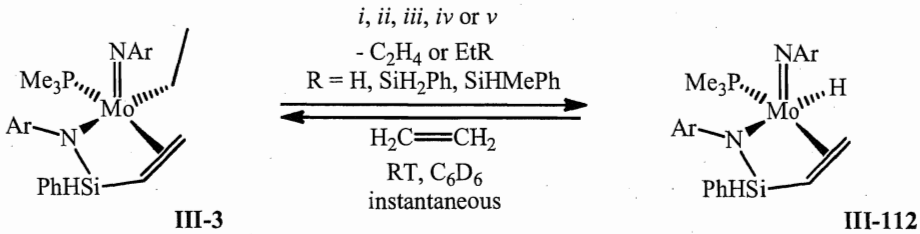

i - C_6D_6, 50 °C, overnight, 40 % yield by NMR; *ii* - 20 $PhSiH_3$, C_6D_6, RT, 2 days, 17 % yield by NMR
iii - 1.2 $PhSiH_3$, PMe_3, toluene, 50 °C, overnight, 66 % yield; *iv* - $PhMeSiH_2$, PMe_3, C_6D_6, 50 °C, overnight, 50 % yield; *v* - H_2 (~ 1.5 atm.), C_6D_6, 50 °C, 36 h, 67 % yield by NMR

Scheme 110. Thermal stability of **III-3** and its reactions with hydrosilanes and H_2.

with the proposed classical structure of **III-112**, the IR spectrum shows two characteristic stretches at 2098 cm^{-1} and 1796 cm^{-1}, which have been assigned to the Si-H and Mo-H vibrations, respectively.

The mechanism of the reaction of **III-3** with hydrosilanes was scrutinized by conducting D-labelling and kinetic NMR experiments. Thus, treatment of **III-3** with $PhSiD_3$ at 50 °C affords exclusively (ArN)Mo(D)(η^3-NAr-SiHPh-CH=CH_2)(PMe_3) (**III-112$_D$**) and $PhEtSiD_2$, indicating that the hydride in **III-112** is transferred from the silane, and is not formed *via* the β-C-H activation of the ethyl ligand in **III-3**. The fact that addition of PMe_3 to a mixture of **III-3** and $PhSiH_3$ increases the reaction rate suggests that the process does not necessarily start with phosphine dissociation. Instead, the reactivity of **III-3** could be related to the dissociation of the coordinated vinyl fragment. To provide more insight into the mechanism of the formation of hydride **III-112**, kinetic studies of the reaction of complex **III-3** with $PhSiH_3$ at 50 °C were performed. At large silane concentrations, the reaction obeys pseudo-first-order kinetics (k_{eff}(50 °C) = (2.8 ± 0.1) × 10^{-4} s^{-1}; Figure 31), consistent with a rate-limiting either PMe_3 or η^3-NArSiHPhCH=CH_2 dissociation, followed by the fast addition of $PhSiH_3$. At the same time, the dependence of the reaction rate in the pseudo-first-order regime (10-fold excess

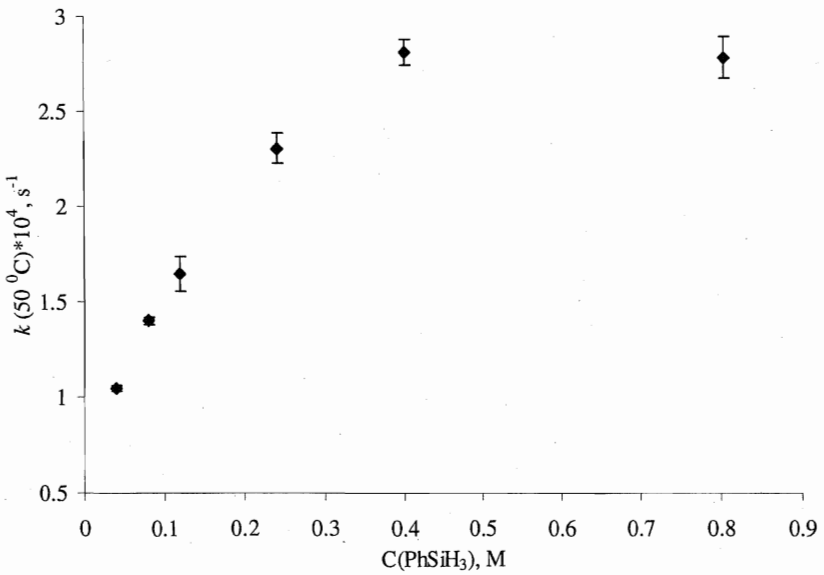

Figure 31. Dependence of the rate constant of the reaction of **III-3** with $PhSiH_3$ at 50 °C on concentration of $PhSiH_3$.

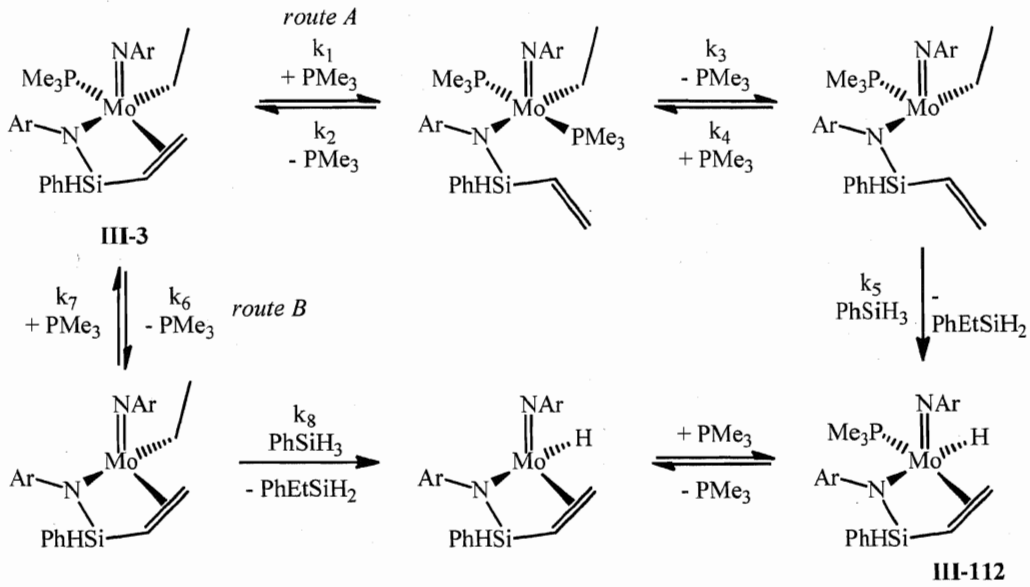

Scheme 111. Mechanism of the reaction of **III-3** with $PhSiH_3$ in the presence of PMe_3.

$PhSiH_3$) on the concentration of phosphine proved to be more complicated (Figure 32), suggesting the occurrence of several pathways for the process. A possible mechanism consistent with this dependence of k_{eff} on PMe_3 concentration is shown in Scheme 111. This mechanism starts with the competing rate-determining steps. *Route A* starts with PMe_3-assisted vinyl dissociation. The competing *route B* involves dissociation of PMe_3. In both cases, the hydride complex **III-112** is furnished by a σ-bond metathesis between $PhSiH_3$ and the ethyl group, which is well-established in the literature for hydrosilation reactions mediated by early transition metal complexes (see chapt. II.2.6 and references therein). The alternative OA of silane cannot be excluded but is lesslikelyas it would require a Mo(VI) intermediate. Taking into account two competing pathways, the consumption of the compound **III-3** is described as (for $k_{1\text{-}8}$, see Scheme 111):

$$-\frac{d[\mathbf{III\text{-}3}]}{dt} = \frac{k_1k_3k_5k_7[PhSiH_3][PMe_3]^2 + (k_1k_3k_5k_8[PhSiH_3] + k_2k_4k_6k_8)[PhSiH_3][PMe_3] + (k_2k_5k_6k_8 + k_3k_5k_6k_8)[PhSiH_3]^2}{k_2k_4k_7[PMe_3]^2 + (k_2k_5k_7 + k_3k_5k_7 + k_2k_4k_8)[PhSiH_3][PMe_3] + (k_2k_5k_8 + k_3k_5k_8)[PhSiH_3]^2}[\mathbf{III\text{-}3}]$$

$k_1k_3k_5k_7[PhSiH_3] = \mathbf{A}$

$(k_1k_3k_5k_8[PhSiH_3] + k_2k_4k_6k_8)[PhSiH_3] = \mathbf{B}$

$(k_2k_5k_6k_8 + k_3k_5k_6k_8)[PhSiH_3]^2 = \mathbf{C}$

$k_2k_4k_7 = \mathbf{D}$

$(k_2k_5k_7 + k_3k_5k_7 + k_2k_4k_8)[PhSiH_3] = \mathbf{E}$

$(k_2k_5k_8 + k_3k_5k_8)[PhSiH_3]^2 = \mathbf{H}$

$$-\frac{d[\mathbf{III\text{-}3}]}{dt} = \frac{\mathbf{A}[PMe_3]^2 + \mathbf{B}[PMe_3] + \mathbf{C}}{\mathbf{D}[PMe_3]^2 + \mathbf{E}[PMe_3] + \mathbf{H}}[\mathbf{III\text{-}3}]$$

$$k_{eff} = \frac{\mathbf{A}[PMe_3]^2 + \mathbf{B}[PMe_3] + \mathbf{C}}{\mathbf{D}[PMe_3]^2 + \mathbf{E}[PMe_3] + \mathbf{H}}$$

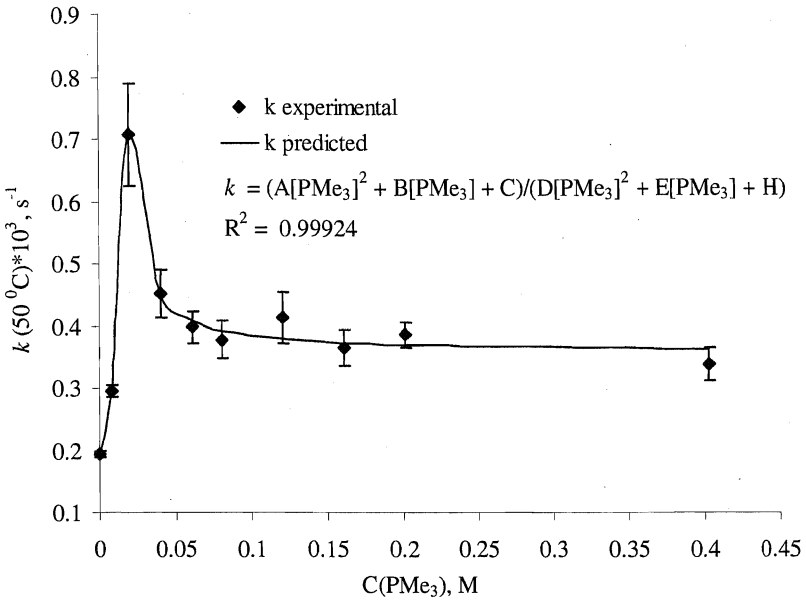

Figure 32. Dependence of the rate constant of the reaction of **III-3** with 10 $PhSiH_3$ (pseudo-first-order regime) at 50 °C on concentration of PMe_3.

At large $PhSiH_3$ concentrations (pseudo-first-order regime) the function $k_{eff}([PMe_3])$ perfectly fits the experimental data for the dependence of the effective reaction rate constant on the concentration of the external PMe_3 (Figure 32).

Abstraction of PMe_3 from **III-3** with BPh_3 in the presence of $PhSiH_3$ results in the formation of an agostic silylamide (ArN)(SiH_2Ph)(η^3-NAr-Si(Et)Ph-H)(η^2-CH_2=CH_2) (**III-113**; Scheme 112). An NMR experiment with the labelled silane $PhSiD_3$ affords (ArN)(SiD_2Ph)(η^3-NAr-Si(Et_D)Ph-H)(η^2-CH_2=CH_2) (**III-113$_D$**), showing incorporation of deuterium in the ethyl, but not in the agostic Si*H* position. This suggests that the SiEtPhH fragment in **III-113** stems from the hydrogenation of the (vinyl)silyl fragment in **III-3** rather than from coupling of $PhSiD_3$ with the ethyl ligand and the subsequent reaction of $PhEtSiH_2$ with the imido ligand. The isolation of **III-113** is hampered by its decomposition under vacuum, which presumably occurs *via* dissociation of coordinated ethylene. Nevertheless, the structure of compound **III-113** was suggested on the basis of VT NMR and IR analysis. At -53 °C, the ^{1}H-NMR spectrum of **III-113** reveals the presence of three non-equivalent Si*H* signals at 6.07, 5.75 an 4.99 ppm for two diastereotopic protons of SiH_2Ph ligand and the agostic Si*H* proton of the η^3-NArSi(Et)-

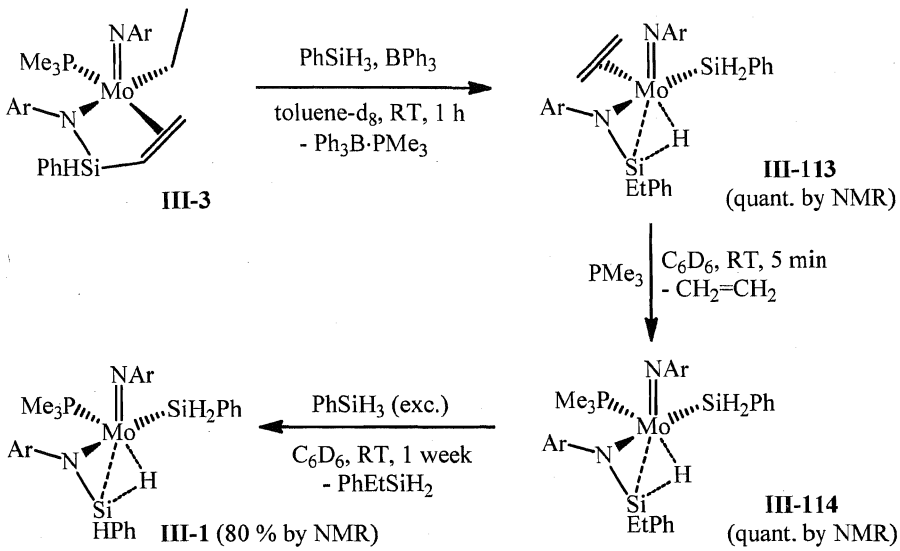

Scheme 112. Formation and reactivity of complex **III-113**.

Ph-H fragment, respectively. The coordination of ethylene to molybdenum results in four non-equivalent protons giving rise to broad up-field shifted signals at 3.42, 3.24, 3.13, and 1.84 ppm, coupled in the ^{1}H-^{13}C HSQC spectrum to the up-field ^{13}C NMR signals at 44.0 and 51.2 ppm. The presence of the NSi-H···Mo agostic bonding in **III-113** is supported by the ^{29}Si INEPT+ NMR spectrum, showing two silicon resonances at 0.9 ppm (dd, $^{1}J_{Si-H}$ = 173.0, 163.4 Hz) and -64.4 ppm (d, $^{1}J_{Si-H}$ = 107.3 Hz) for the classical SiH_2Ph ligand and agostic Si(Et)PhH group, respectively. Such coordination of the Si-H bond to the Mo also affects the IR spectrum of **III-113**,[17] which shows a normal Si-H stretch (2077 cm^{-1}) for classical SiH_2Ph ligand and a red-shifted Si-H_{ag} band (1772 cm^{-1}) for the η^2-NAr-Si(Et)Ph-H. The $^{1}J_{Si-H}$ coupling constant for the agostic Si-H_{ag} bond in **III-113** is slightly reduced in comparison with the value observed for **III-1** (107.3 Hz *vs.* 113.0 Hz, respectively), which may indicate a greater extent of the Si-H activation.[17] This result is surprising taking into account that ethylene is better π-acceptor than PMe_3 and hence less back-donation on the σ*(Si-H) antibonding orbital in **III-113** is expected. In contrast to (ArN)Mo(SiH_2Ph)(η^3-NArSiHPh-H)(PMe_3) (**III-1**), a stronger NSi-H···Mo bond in **III-113** results in a much slower exchange with $PhSiH_3$. Thus, no exchange of complex **III-113** with $PhSiH_3$ was observed in ^{1}H-^{1}H EXSY NMR experiment at room temperature. This fact, in addition to the activation parameters of such exchange for **III-1** (see above), could be accounted for by the associative mechanism of exchange, which

starts with dissociation of the Si-H agostic bond, followed by addition of silane (see the discussion above; Scheme 101).

Addition of an equivalent of PMe_3 to the compound **III-113** results in the almost instantaneous release of a molecule of ethylene and the formation of (ArN)(SiH_2Ph)(η^3-NAr-Si(Et)Ph-H)(PMe_3) (**III-114**) as a mixture of two diastereomers (2:1, according to $^{31}P\{^1H\}$-NMR spectroscopy), due to the chirality at the agostic silicon center (Scheme 112). The spectral (NMR and IR spectroscopy) features of compound **III-114** are similar to those observed for **III-1** and **III-113** and indicate[17] the presence of an agostic NSi-H···Mo interaction (see experimental details). Like in **III-113**, the $^1J_{Si\text{-}Hag}$ for both diastereomers of **III-114** (105.4 and 107.1 Hz) are slightly reduced in comparison with **III-1** ($^1J_{Si\text{-}Hag}$ = 113.0 Hz). This can be accounted for by the substitution of the terminal Si-bound proton at the agostic silicon center for the group, which in accordance with Bent's rule (assuming that Et is more electron-donating than H) brings less *s* character of silicon in the Si-H···Mo bond, thus decreasing the $^1J_{Si\text{-}H}$ values.[17, 48-50] On the other hand, the electron-donating properties of the ethyl group and hydride are very close, and the application of Bent's rule in this particular case is questionable.

Analogously to the ethylene adduct **III-113**, the ^1H-^1H EXSY NMR experiment did not reveal any exchange between **III-114** and excess $PhSiH_3$. Again, this observation supports an associative mechanism for the exchange with silane: smaller $^1J_{Si\text{-}Hag}$ results in more difficult dissociation of the NSi-H···Mo bond, necessary for the silane addition to Mo. Leaving a mixture of these compounds for one week at room temperature leads to slow conversion of the complex **III-114** into the silyamide compound **III-1**, accompanied by a release of $PhEtSiH_2$ (Scheme 113). A similar observation has been also made for the reaction of the hydride derivative **III-112** with an excess of $PhSiH_3$, which affords **III-1** and $PhEtSiH_2$. For both processes, the evolution of ethylphenylsilane suggests a pathway involving the cleavage of the N-Si bond of the silylamide ligand η^3-NAr-Si(R)Ph-H. Additionally, this suggestion was supported by a labelling experiment. When compound **III-114** was reacted with (*m*-Tol)SiH_3, the first process observed was the exchange between (*m*-Tol)SiH_3 and the SiH_2Ph group followed by the slow release of $PhEtSiH_2$ and the formation of complex **III-1$_{tol}$**, in which the tolyl group is scrambled over two possible silicon positions (established by ^1H-^{13}C HMBC NMR spectroscopy).

Furthermore, treatment of **III-114** with $PhSiD_3$ selectively gives PhEtSiHD and **III-1d$_4$**. These observations allowed us to draw a plausible mechanism for the reaction of **III-114** with phenylsilane (Scheme 113), based on coordination of the external silane *via* the coordination to the imido nitrogen of **III-114** to give a silylamido ligand and elimination of $PhEtSiH_2$ from the other silylamide. A similar pathway has been previously suggested by Tilley *et al.* for the silane exchange in a silylamido complex of tantalum (see Scheme 9, **A**).[16] Taking into account the stoichiometric coupling of agostic compound **III-1** with alkenes and nitriles (see the discussion above), such a cooperative Mo/NAr^{2-} reactivity of imido silylamido complexes towards hydrosilanes could be involved in the catalytic cycle of hydrosilation reactions mediated by complex **III-1**.

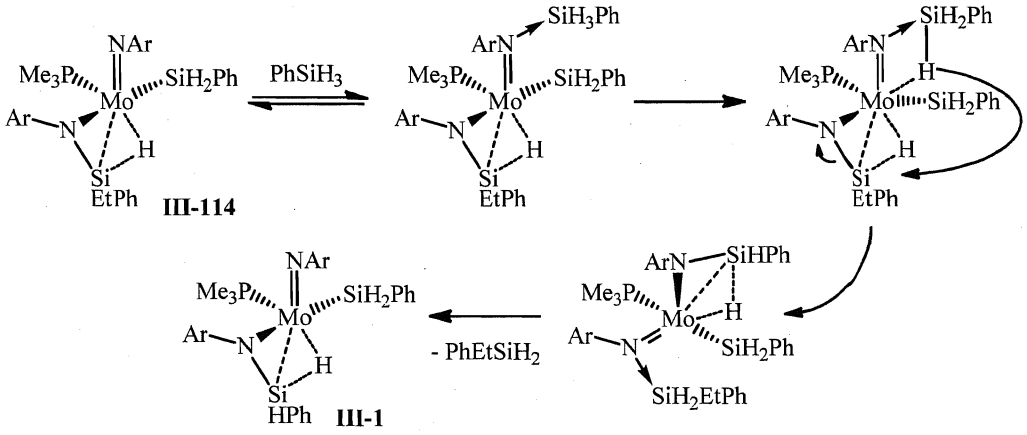

Scheme 113. Suggested mechanism for the reaction of **III-114** with excess $PhSiH_3$.

III.6.2 Catalytic reactivity of complex III-3

The observation of the formation of $PhEtSiH_2$ and ethane in the reactions of (vinylsilyl)amide complex (ArN)Mo(Et)(η^3-NAr-SiHPh-CH=CH$_2$)(PMe_3) (**III-3**) with $PhSiH_3$ and H_2, respectively, inspired the study of the catalytic activity of compound **III-3** in the hydrosilation of unsaturated organic molecules and hydrogenation of alkenes (Tables 11-13). Thus, the treatment of ethylene with $PhSiH_3$ in the presence of 5.0 mol. % of complex **III-3** gives, after 22.3 hours at 50 °C, 45 % conversion of C_2H_4 and formation of $PhEtSiH_2$ in 39 % yield (according to ^{1}H-NMR; Table 11, entry 1).[202] Polymerization of ethylene under catalytic hydrosilation conditions was also observed as a side-process (~ 6 % conversion of C_2H_4). Similar to the catalysis mediated by the

Table 11. Hydrosilation of alkenes and polymerization of phenylacetylene mediated by **III-3**.

Entry	Organic substrate[a]	Silane	cat., mol. %	T, °C / time	Products[b]	Substrate conv.[c]	Yield[c]	TON
1	ethylene	$PhSiH_3$	5.0	50 °C / 22.3 h	$PhEtSiH_2$	45 %[d]	39 %	9
2	1-hexene	$PhSiH_3$	5.0	50 °C / 14.8 h	hexane	48 %	31 %	9.6
					2-hexene		13 %	
					$PhH_2Si(Hex)$		4 %	
3	styrene	$PhSiH_3$	5.0	50 °C / 14.8 h	$PhCH_2CH_3$	19 %	14 %	3.8
					$PhH_2Si(CH_2)_2Ph$		5 %	
4	Phenylacetylene	$PhSiH_3$	5.0	50 °C / 19 h	Polyphenylacetylene	28 %	28 %	5.6

[a] The ratio of organic substrate and silane is 1:1. [b] Reactions with $PhSiH_3$ give Ph_2SiH_2 and SiH_4 as by-products produced by catalytic redistribution of substituents at the silicon centre.[211] Increase of the reaction temperature increases the amount of Ph_2SiH_2 and SiH_4 formed. [c] Detected by ^{1}H-NMR spectroscopy using tetramethylsilane as an internal standard. [d] Catalytic hydrosilation of ethylene with $PhSiH_3$ gives also formation of small amount of polyethylene.

Table 12. Hydrogenation (~ 1.5 atm.) of alkenes and alkynes mediated by **III-3**.

Entry	Organic substrate	cat., mol. %	T, °C / time	Products[a]	Substrate conv.[a]	Yield[a]	TON
1	styrene	5.0	50 °C / 7 h	$PhCH_2CH_3$	100 %	100 %	20
2	cyclohexene	5.0	50 °C / 16 h	Cyclohexane	94 %	94 %	18.8
3	1-hexene	5.0	50 °C / 1.8 h	Hexane	66 %	44 %	13.2
				2-hexene		22 %	

[c] Detected by ^{1}H-NMR spectroscopy using tetramethylsilane as an internal standard.

Table 13. Hydrosilation of carbonyls and nitriles, alcoholysis and aminolysis of $PhSiH_3$ mediated by **III-3**.

Entry	Organic substrate	Silane	Cat., mol. %	T, °C / time	Products[a]	Substrate conv.[b]	Yield[b]	TON
1	PhC(O)H	$PhSiH_3$	5.0	RT / 20 min	$PhSiH_2(OBn)$	100 %	28 %	20
					$PhSiH(OBn)_2$		72 %	
2	$Me_2C(O)$	$PhSiH_3$	5.0	RT / 2.3 h	$PhSiH_2(O^iPr)$	95 %	71 %	19
					$PhSiH(O^iPr)_2$		24 %	
3	PhMeC(O)	$PhSiH_3$	5.0	RT / 25.7 h	$PhH_2Si[OCH(Me)Ph]$	47 %	32 %	9.4
					$PhHSi[OCH(Me)Ph]_2$		9 %	
					$PhSi[OCH(Me)Ph]_3$		6 %	
4	EtOH	$PhSiH_3$	5.0	RT / 5 min	$PhH_2Si(OEt)$	100 %	21 %	20
					$PhHSi(OEt)_2$		67 %	
					$PhSi(OEt)_3$		12 %	
5	^iPrOH	$PhSiH_3$	5.0	RT / 5 min	$PhSiH_2(O^iPr)$	100 %	82 %	20
					$PhSiH(O^iPr)_2$		18 %	
6	$PhNH_2$	$PhSiH_3$	5.0	RT / 19.9 h	$PhH_2Si(NHPh)$	86 %	50 %	17.2
					$PhHSi(NHPh)_2$		36 %	
7	CH_3CN	$PhSiH_3$	5.0	50 °C / 25.5 h	$EtN(SiH_2Ph)_2$	31 %	30 %	6.2
					$PH_2Si(N=CHMe)$		1 %	
8	PhCN	$PhSiH_3$	5.0	RT / 23.8 h	$PhH_2Si(N=CHPh)$	5 %	5 %	1
9				50 °C / 25.5 h	$PhH_2Si(N=CHPh)$	8 %	8 %	1.6

[a] Reactions with $PhSiH_3$ give Ph_2SiH_2 and SiH_4 as by-products produced by the catalytic redistribution of substituents at the silicon centre.[211] Increase of the reaction temperature increases the amount of Ph_2SiH_2 and SiH_4 formed. [b] Detected by ^1H-NMR spectroscopy using tetramethylsilane as an internal standard.

agostic complex (ArN)Mo(Et)(η^3-NAr-SiHPh-H)(PMe_3) (**III-1**), the hydrosilation with $PhSiH_3$ catalyzed by **III-3** is also accompanied by the concurrent redistribution of the silane affording Ph_2SiH_2 and SiH_4.[211] Analogous reactions of $PhSiH_3$ with 1-hexene and styrene at 50 °C result in only partial reduction of olefin substrates to the corresponding alkanes[68] with the trace formation of hydrosilated products (Table 11, entries, 2 and 3).[78f, 168b, 209, 228] At the same time, compound **III-3** was found to catalyze the isomerisation of 1-hexene into 2-hexene[218] and polymerization of phenylacetylene[220] (Table 1, entry 4).

The catalytic hydrogenation of alkenes mediated by complex **III-3** presents more promising results, being a rare example of an early transition metal complex for the hydrogenation of olefins.[121] For instance, heating a solution of styrene and 5.0 mol. % of **III-3** at 50 °C in a hydrogen atmosphere (~ 1.5 atm.) for 7 hours leads to full conversion of $PhCH{=}CH_2$ and quantitative formation of ethylbenzene (TON = 20; Table 12, entry 1) High activity of **III-3** was also found in the hydrogenation of cyclohexene, which after 16 hours at 50 °C affords 94 % of cyclohexane (Table 12, entry 2). A more sluggish reaction was found in the case of 1-hexene (66 % conversion after 1.8 h at 50 °C), however, this result may be accounted for by the concurrent isomerisation of 1-hexene to 2-hexene (22 %; Table 12, entry, 3).[218]

Surprisingly, compound **III-3** was also found to catalyze a variety of carbonyl hydrosilation reactions.[7, 80, 107, 108, 201] Thus, stoichiometric treatment of benzaldehyde with $PhSiH_3$ in the presence of 5.0 mol. % of complex **III-3** results in full conversion of PhCH(O) to form a mixture of $PhH_2Si(OBn)$ (28 %) and $PhHSi(OBn)_2$ (72 %) after only20 min. at room temperature (TON = 20, TOF = 60; Table 13, entry 1).[160, 214, 215b] The activity of **III-3** in the catalytic hydrosilation of ketones (acetone and acetophenone) is slightly lower, being highly sensitive to the steric properties of the utilized substrate. For example, a 95 % conversion was found in the reaction of acetone with $PhSiH_3$ at room temperature in the presence of 5.0 mol. % of **III-3** (2.3 hours, TON = 19, TOF = 8.3; Table 13, entry 2),[13a, 184e, 229] whereas similar catalytic conditions result in only 47 % conversion of acetophenone to a mixture of $PhH_2Si[OCH(Me)Ph]$ (32 %), $PhHSi[OCH(Me)Ph]_2$ (9 %), and $PhSi[OCH(Me)Ph]_3$ (6 %) after 25.7 hours (Table 13, entry 3).[215] In contrast to the agostic complex **III-1**, no reduction of ketones to alkanes was observed.[217]

Catalytic alcoholysis of $PhSiH_3$ by an equivalent of ethanol or isopropanol mediated by the compound **III-3** is a fast process and gives 100 % conversion of alcohol in only 5 min. at room temperature (TON = 20, TOF = 241; Table 13, entries 4 and 5). Both EtOH and ^{i}PrOH lead to the formation of mixtures of mono-, bis- and, in the case of ethanol, tris(substituted) products: $PhH_2Si(OR)$, $PhHSi(OR)_2$, and $PhSi(OR)_3$ (R = Et (21, 67, and 12 %, respectively; R = ^{i}Pr (82, 18, and 0 %, respectively)).[160, 221] In contrast, complex **III-3** turned out to be less active than (ArN)Mo(SiH_2Ph)(η^3-NAr-SiHPh-H)(PMe_3) (**III-1**) in the aminolysis of $PhSiH_3$ with aniline. After 19.9 hours at room temperature with the 5.0 mol. % loading of the catalyst 86 % conversion and production of a mixture of $PhH_2Si(NHPh)$ (50 %) and $PhHSi(NHPh)_2$ (36 %) was observed (TON = 17.2, TOF = 0.9; Table 13, entry 6).[162, 163]

Lastly, (ArN)Mo(Et)(η^3-NAr-SiHPh-CH=CH_2)(PMe_3) (**III-3**) catalyzes the addition of phenylsilane to organic nitriles, albeit the activity is low. At 50 °C, the reaction of acetonitrile with $PhSiH_3$ with 5.0 mol. % loading of **III-3** yields mostly the bis(silylated) amine $EtN(SiH_2Ph)_2$ (30 %)[162, 163] with only trace formation of a mono(substituted) product, CH_3CH=$N(SiH_2Ph)$ (assigned by the ^{1}H and ^{13}C NMR signals; Table 13, entry, 7). On the other hand, substitution of CH_3CN with PhCN leads to a decreased reactivity towards $PhSiH_3$ affording only 5 % of PhCH=$N(SiH_2Ph)$ after 23.8 hours at room temperature (Table 13, entry 8; compare to the reaction catalyzed by **III-1**). Heating the mixture at 50 °C does not significantly increase the yield of the hydrosilation product (8 %; Table 13, entry 9), but accelerates the concurrent redistribution of $PhSiH_3$ to give Ph_2SiH_2 and SiH_4 by-products.[211] Despite the low conversion of benzonitrile, such selective formation of PhCH=$N(SiH_2Ph)$ presents a rare example of transition metal mediated monoaddition of hydrosilanes to nitriles.[133, 136, 137b, 138a, 141, 146, 222]

III.6.3 Reactions of III-3 and III-112 with unsaturated organic molecules

To gain an understanding of the mechanism of the catalytic hydrosilation processes, (ArN)Mo(Et)(η^3-NAr-SiHPh-CH=CH_2)(PMe_3) (**III-3**) and its hydride analogue (ArN)Mo(H)(η^3-NAr-SiHPh-CH=CH_2)(PMe_3) (**III-112**) were tested in stoichiometric reactions with unsaturated organic compounds. The formation of hydride complex **III-112** from **III-3** and $PhSiH_3$ and the reverse reaction of ethylene with **III-112** to give **III-3**

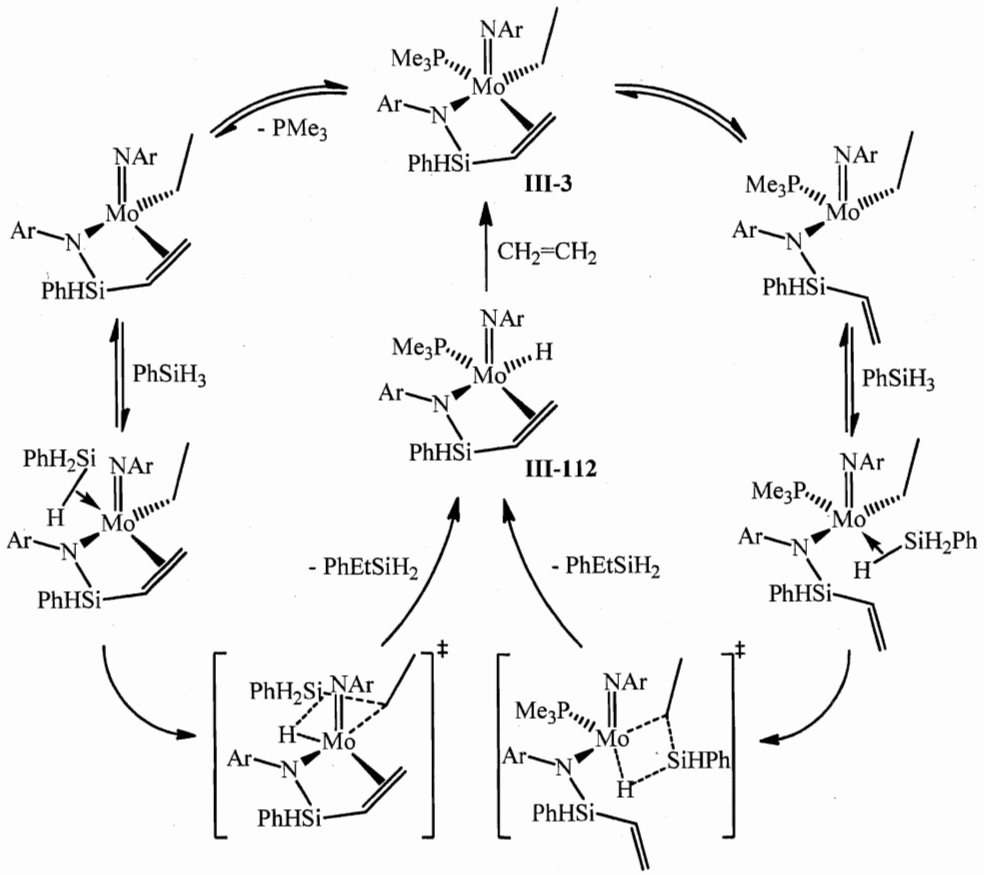

Scheme 114. Suggested mechanism for the hydrosilation of alkenes mediated by **III-3**.

suggest the involvement of **III-112** in the catalytic cycle of alkene hydrosilation. As was already mentioned, **III-112** is most likely formed *via* a σ-bond metathesis (see chapt. II.1.4 and references therein) between the alkyl ligand and hydrosilane as depicted in Scheme 114.[o] In order to verify this hypothesis, we carried out reactions presented in Scheme 115. Thus, the treatment of compound **III-112** with one equivalent of styrene at room temperature gives the product of olefin insertion into the Mo-H bond, (ArN)Mo(CH_2CH_2Ph)(η^3-NAr-SiHPh-CH=CH_2)(PMe_3) (**III-115**). NMR features of **III-115** are close to those of the ethyl derivative **III-3**. The presence of the CH_2CH_2Ph ligand is evident from the ^{1}H-NMR spectrum, in which the –CH_2-CH_2– fragment gives rise to four mutually coupled (proved by ^{1}H-^{1}H COSY NMR spectroscopy) signals of equal intensity at 3.66 (ddd, $^2J_{H\text{-}H}$ = 4.5 Hz, $^3J_{H\text{-}H}$ = 13.2, 18.0 Hz), 3.24 (ddd, $^2J_{H\text{-}H}$ = 3.6 Hz,

[o] The possibility of OA-RE reaction sequence can not be completely excluded in the reaction of **III-3** with $PhSiH_3$, but this route is less likely as it would require formation of a Mo(VI) intermediate.

$^3J_{H\text{-}H}$ = 13.2, 18.0 Hz), 2.72 (m, obscured by CH resonance of NAr), and 1.69 ppm (m). The substitution of molybdenum with CH_2CH_2Ph in **III-115** is also supported by the observation of reasonably large values of $J_{C\text{-}P}$ coupling constants for the carbon resonances of the $-CH_2\text{-}CH_2-$ fragment found at 41.0 (d, $^2J_{C\text{-}P}$ = 6.8 Hz) and 41.7 ppm (d, $^3J_{C\text{-}P}$ = 5.3 Hz) in the ^{13}C-NMR spectrum.

At 50 °C, the reaction of (ArN)Mo(CH_2CH_2Ph)(η^3-NAr-SiHPh-CH=CH_2)(PMe_3) (**III-115**) with $PhSiH_3$ in the presence of an equivalent of PMe_3 leads to selective formation of the starting hydride complex (ArN)Mo(H)(η^3-NAr-SiHPh-CH=CH_2)(PMe_3) (**III-112**) and evolution of a molecule of $Ph(CH_2)_2SiH_2Ph$ (Scheme 115). Similar observations were made for the reaction of $PhSiH_3$ with (ArN)Mo(Et)(η^3-NAr-SiH-CH=CHPh)(PMe_3) (**III-93**; Scheme 115) leading to selective formation of $PhEtSiH_2$.[202]

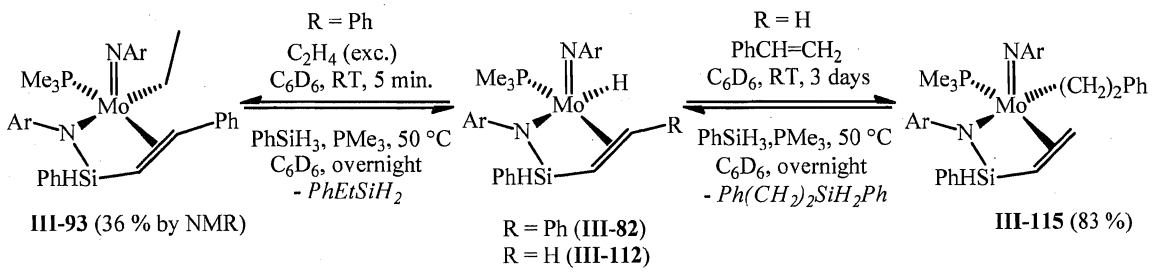

Scheme 115. Preparation of **III-93** and **III-115** and their reactions with $PhSiH_3$.

The Mo-H insertion pathway has been also observed upon the treatment of **III-112** with both acetone and benzonitrile[230] affording the isopropoxy (ArN)Mo(O^{i}Pr)(η^3-NAr-SiH-CH=CH_2)(PMe_3) (**III-116**) and methylenamide (ArN)Mo(N=CHPh)(η^3-NAr-SiH-CH=CH_2)(PMe_3) (**III-117**) derivatives, respectively (Scheme 116). The instability of complex **III-116** hampered its isolation. However the formation of the Mo-O^{i}Pr moiety is evident from the NMR spectra (see experimental details). At the same time, compound **III-117** was isolated in 78 % yield and fully characterized by IR and multinuclear NMR spectroscopy. The ^{1}H-NMR spectrum of **III-114** shows a down-field signal for the imine proton as at 8.59 ppm, coupled in the ^{1}H-^{13}C HSQC NMR spectrum to the characteristic imine ^{13}C-NMR signal at 153.7 ppm[230] and in the ^{1}H-^{31}P HSQC NMR spectrum to the ^{31}P-NMR signal at -16.4 ppm. The Si*H* proton gives rise to a singlet at 6.23 ppm in the ^{1}H-NMR spectrum, coupled in the ^{1}H-^{29}Si HSQC NMR spectrum to a silicon resonance

at -30.2 ppm (d, $^1J_{Si-H}$ = 206.2 Hz; found by ^{29}Si INEPT+ NMR spectroscopy). The large value of the $^1J_{Si-H}$ coupling constant indicates the absence of any nonclassical Si-H···Mo interactions in the compound **III-114**.[17] Additionally, the classical structure of **III-114** is supported by the observation of a normal Si-H stretch at 2104 cm^{-1} in the IR spectrum,[17] which also exhibits the C=N band at 1591 cm^{-1}.[230c, 231]

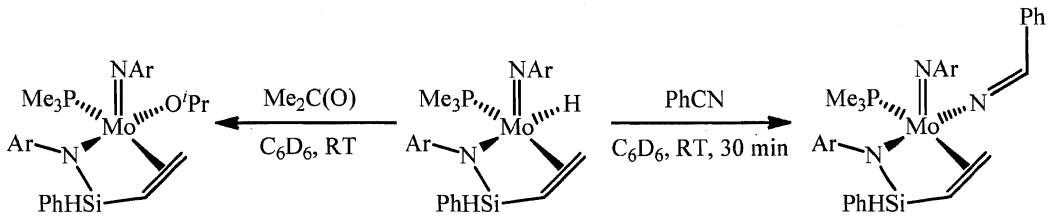

III-116 **III-108** **III-117** (78 %)

Scheme 116. Reactions of complex **III-112** with acetone and benzonitrile.

Compound **III-117** does not react with $PhSiH_3$ at room temperature (no reaction was seen after two hours even with a 10-fold excess of phenylsilane), however heating the reaction mixture at 50 °C overnight leads mainly to decomposition, giving only traces of (ArN)Mo(H)(η^3-NAr-SiH-CH=CH$_2$)(PMe$_3$) (**III-112**) and $PhH_2Si(N{=}CHPh)$. Initially, we suggested that the transformation of **III-117** into **III-112** could proceed *via* coordination of silane to the nitrogen atom of the methylenamide, followed by the Si-H bond activation. The observed lack of reactivity of **III-117** with $PhSiH_3$ could be accounted for by the additional donation of the methylenamide nitrogen lone pair to molybdenum, which is induced by the electron deficiency of the Mo center[p] and leads to the decreased basicity of the N=CHPh ligand. This also explains the low conversion of organic nitriles (acetonitrile and benzonitrile) in their reactions with $PhSiH_3$ mediated by (ArN)Mo(H)(η^3-NAr-SiH-CH=CH$_2$)(PMe$_3$) (**III-3**) (Table 13, entries 7 – 9).

In contrast to the reaction with acetone, the treatment of the hydride complex (ArN)Mo(H)(η^3-NAr-SiHPh-CH=CH$_2$)(PMe$_3$) (**III-112**) with an equivalent of benzaldehyde gives, unexpectedly, the bis(imido) benzaldehyde adduct (ArN)$_2$Mo(η^2-O=CHPh)(PMe$_3$) (**III-100**), accompanied by the formation of $PhH_2Si(CH{=}CH_2)$. The reaction was found to be unclean and poorly reproducible, often leading to full decompo-

[p] Even if the imido ligand is a 6-electron donor in the limit of π-saturation, the complex is formally 16e. This allows for additional π-interaction with the amido ligand.[230, 231]

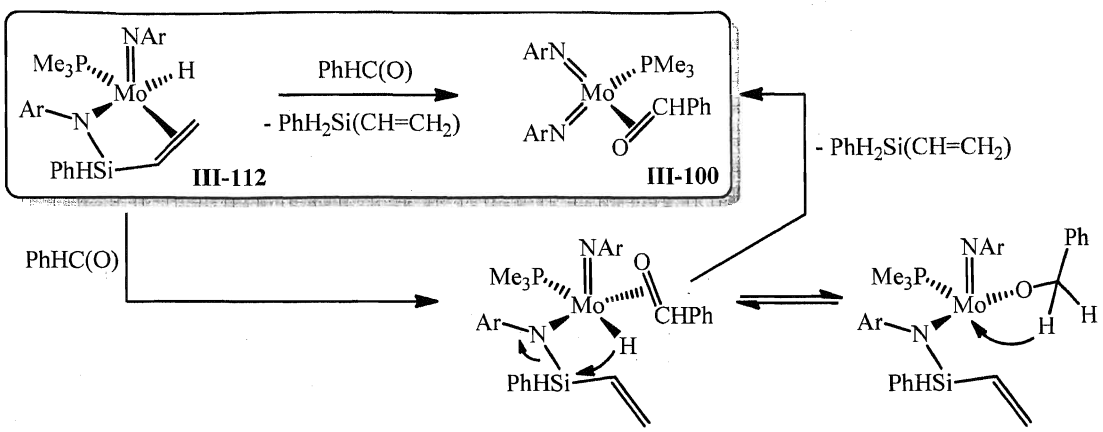

Scheme 117. Possible mechanism for the reaction of **III-112** with benzaldehyde.

sition. The mechanism of this reaction is not fully understood at the moment. Nonetheless, one could suggest that such an unusual N-Si bond cleavage in **III-112** is induced by the aldehyde assisted dissociation of the coordinated vinyl fragment (an analogous process was proposed for the reaction of **III-3** with $PhSiH_3$ in the presence of PMe_3; see above), followed by 1,3-hydride shift (Scheme 117).

No reaction was observed upon the room temperature treatment of the ethyl substituted compound (ArN)Mo(Et)(η^3-NAr-SiHPh-CH=CH_2)(PMe_3) (**III-3**) with acetone. On the other hand, addition of benzaldehyde surprisingly leads to the insertion into the Si-H bond and formation of (ArN)Mo(Et)(η^3-NAr-Si(OBn)Ph-CH=CH_2)(PMe) (**III-118**; Scheme 118). An NMR experiment with the labelled molybdenum complex (ArN)Mo(Et)(η^3-NAr-SiDPh-CH=CH_2)(PMe) (**III-3$_D$**) revealed selective formation of (ArN)Mo(Et)(η^3-NAr-Si(OCH(D)Ph)Ph-CH=CH_2)(PMe) (**III-118$_D$**; mixture of diastereomers due to the chirality at the Si center), indicating that the reaction does not go *via* either Si-H or ethyl C-H bond activation. Alternatively, dissociation of either the vinyl substituent or the PMe_3 ligand of **III-3**, coordination of benzaldehyde to Mo and further migration of the PhHC(O) ligand to silicon could happen. To the best of our knowledge such insertion of carbonyls into the Si-H bond is extremely rare and known only for silylene complexes L_nM(=SiHR), reported by the groups of Tobita[127b,c] and Tilley.[125, 128]

Similarly to (ArN)Mo(Et)(η^3-NAr-SiHPh-CH=CH_2)(PMe_3) (**III-3**), heating a mixture of **III-118** with an equivalent of $PhSiH_3$ at 50 °C affords the hydride derivative (ArN)Mo-

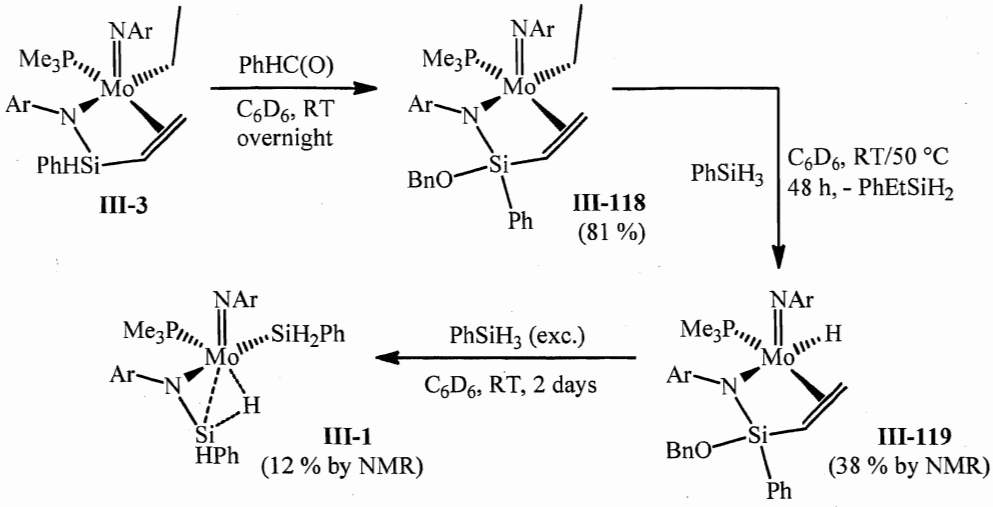

Scheme 118. Preparation of complex **III-118** and its reaction with $PhSiH_3$.

(H)(η^3-NAr-Si(OBn)Ph-CH=CH_2)(PMe) (**III-119**), which upon prolonged (two days) room temperature treatment with phenylsilane forms the agostic complex (ArN)Mo(SiH_2Ph)(η^3-NAr-SiHPh-H)(PMe_3) (**III-1**) (Scheme 118).

Complex **III-3** was found to be unreactive with 1-hexene upon treatment at room temperature, however, leaving the reaction mixture overnight at 50 °C leads to the isomerisation of 1-hexene into 2-hexene with a trace formation of the hydride derivative (ArN)Mo(H)(η^3-NAr-SiHPh-CH=CH_2)(PMe_3) (**III-112**). Such isomerisation of hexene most likely proceeds *via* the thermolysis of **III-3** to give **III-112**, followed by insertion of 1-hexene into the Mo-H bond. Further β-C-H activation[218] in the hexyl intermediate (ArN)Mo(Hex)(η^3-NAr-SiHPh-CH=CH_2)(PMe) (**III-120**), release of 2-hexene and reinsertion of ethylene present in the reaction mixture furnish the compound **III-3**.

The reaction of **III-3** with phenylacetylene is not clean and is poorly reproducible, however, the formation of alkenyl derivatives (a mixture of isomers of (ArN)Mo(CH=CH_2Ph)(η^3-NAr-SiHPh-CH=CH_2)(PMe) (**III-121**); Scheme 119) was

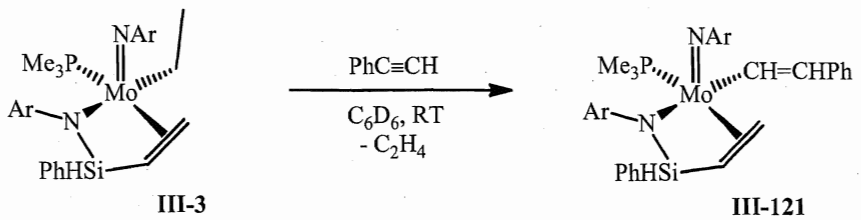

Scheme 119. Reaction of **III-3** with phenylacetylene.

suggested on the basis of ^{1}H-NMR spectroscopy.

All attempts to elucidate the mechanism of aminolysis and alcoholysis of $PhSiH_3$ mediated by (ArN)Mo(Et)(η^3-NAr-SiHPh-CH=CH_2)(PMe_3) (**III-3**) by stoichiometric reactions of the latter with amines and ethanol were unsuccessful. Thus, the treatment of **III-3** with either $ArNH_2$ or $PhNH_2$ at 50 °C leads only to formation of the hydride derivative (ArN)Mo(H)(η^3-NAr-SiHPh-CH=CH_2)(PMe_3) (**III-112**) and an equivalent of ethylene. At the same time, addition of EtOH to a solution of **III-3** gives free $ArNH_2$ and an unknown diphosphine compound. The $^{31}P\{^1H\}$-NMR spectrum of the latter shows two doublets at 1.8 and -1.7 ppm with the large value of $^2J_{P\text{-}P}$ = 170.1 Hz, which indicates the *trans*- arrangement of PMe_3 ligands. However, the structure of this product is not clear at the moment and the reaction of complex (ArN)Mo(Et)(η^3-NAr-SiHPh-CH=CH_2)(PMe_3) (**III-3**) with ethanol requires more detailed study.

III.7 Preparation and reactivity of molybdenum imido hydride complexes

Research in the field of imido hydrides originally stemmed from our interest in hydride derivatives in metallocene-like ligand platforms.[14a,h, 232] Transition metal compounds bearing N-based ligands (such as R_3PN^-, RN^{2-}, and cyclic triamines) have been recently successfully applied for the systematic design of post-metallocene ligand environments, primarily for application in catalytic olefin polymerization,[20] however, the chemistry of their hydride derivatives is underdeveloped.[21, 233] This chapter describes the preparation of bis- and mono(imido) borohydride as well as mono(imido) hydride complexes of molybdenum and study of their reactivity in stoichiometric and catalytic reactions. The results of detailed investigations of the mechanism of hydrosilation catalysis are also discussed here.

III.7.1 Mono- and bis(imido) molybdenum borohydrides

The majority of transition metal hydride complexes usually conform to the effective electron number rule, i.e., exhibit either an 18 or 16 (for the d^8 species) valence electron count.[234] Although compounds with an odd valence shell have become quite common, odd-electron hydrides (e.g., the 17 and 19 valence electron species) are relatively rare.[235] Steric protection can stabilize electron-deficient centers, as is the case in Poli's 15

valence electron compound (η-$C_5H_2{}^tBu_3$)Mo(H)(PMe_3)$_2$ (**III-122**),[236] but "electron rich" 19e and 20e configurations usually occur only if there are strong π-accepting ligands, such as CO, NO, and PF_3, which can delocalize the "excess" electron density from the metal.[234]

Based on the isolobal analogy with metallocene trihydride compounds $[Cp_2M(H)_3]^x$ (M = Nb or Ta, x = 0; M = Zr, x = 1-) we targeted the preparation of molybdenum bis(imido) species $(RN)_2Mo(H)_2(PMe_3)$ (**III-123**), related to the complex (PhN)W{$(NSiMe_3)_2C_6H_4$}$(H)_2(PMe_3)$ (**III-124**), reported by Boncella *et al.*[233] In the course of this work, we encountered an unusual paramagnetic borohydride compound $(ArN)_2Mo(\eta^2$-$BH_4)(PMe_3)_2$ (**III-125**), which lacks strongly π-stabilizing ligands such as CO or an alkene.

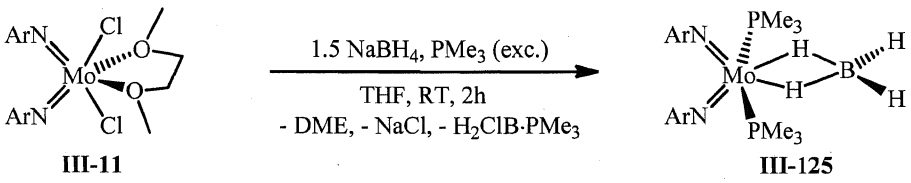

Scheme 120. Preparation of $(ArN)_2Mo(\eta^2$-$BH_4)_2(PMe_3)$ (**III-125**).

As shown in Scheme 120, compound **III-125** was prepared by the addition of a solution of the Mo(VI) bis(imido) complex $(ArN)_2MoCl_2$(DME) (**III-11**) in THF to a mixture of PMe_3 (ca. 6 equiv.) and $NaBH_4$ (1.5 equiv.). While a large number of Mo(IV) and Mo(VI) bis(imido) compounds are known,[192] complex **III-125** is a very rare example of a monomeric Mo(V) bis(imido) derivative, and only one other has been structurally authenticated.[237] Bis(imido) Mo(V) compounds are usually dimeric and have a Mo-Mo bond.[192] Additionally, although transition metal borohydride compounds have been extensively studied,[235b-d] few structurally characterized molybdenum (or Group 6 in general) derivatives are known,[238] these all being diamagnetic with formally Mo(0)[238a,c,d] or Mo(II) centers.[238b] In contrast to **III-125**, most borohydride complexes generally conform to the 18 valence electron rule, in particular those with one BH_4 ligand.[239] Paramagnetic borohydride compounds are rather uncommon.[235b-d] Finally, it should be noted that imido transition metal borohydrides themselves are unusual[192, 240] and only one example has been structurally authenticated, namely Ti(NAr){ArNC(Me)CHC(Me)CH^{t}Bu}(η^3-BH_4) (**III-126**).[241]

The ^{1}H-NMR spectrum of $(ArN)_2Mo(\eta^2\text{-}BH_4)(PMe_3)_2$ (**III-125**) features broad resonances consistent with a paramagnetic compound. At the same time, the presence of the η^2-BH_4 ligand is evident from the IR spectrum, which exhibits υ(B-H) bands at 2389, 2358, and 2102 cm^{-1}.[235b] Collaboration between the Nikonov group and the groups of Mountford and Green at the University of Oxford resulted in the characterization of complex **III-125** by X-Ray analysis (see Table 30, chapt. VI), EPR spectroscopy, and a DFT study.

In the solid state, molecules of **III-125** contain six-coordinate Mo(V) centers with *cis*-arylimido ligands and *trans*-PMe_3 ligands (Figure 33). The atoms of the $Mo(\mu\text{-}H)_2B$ unit are effectively coplanar with the MoN_2 moiety. The terminal H atoms (H3, H4) of the borohydride lie above and below this plane with dihedral angles P1-Mo1···B1-H4 and P2-Mo1···B1-H3 of 3 and 1°, respectively. The bidentate coordination mode of the BH_4 ligand is consistent with the IR spectrum. The Mo-N-C_{ipso} linkages (168.5(2) and 172.5(2)°; Table 14) are approximately linear, suggesting that each ArN^{2-} ligand may, in principle, act as a 6 electron donor to the metal.

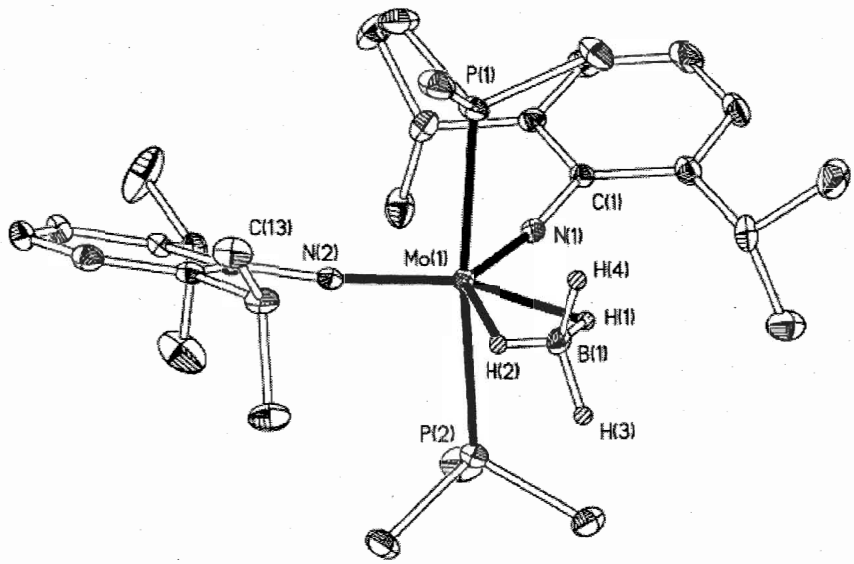

Figure 33. ORTEP plot of the molecular structure of **III-125** (C-bound H atoms are omitted for clarity). Anisotropic displacement parameters are plotted with 50 % probability.

Table 14. Selected bond distances (Å) and angles (°) for complex **III-125**.

distances, Å		angles, °	
Mo1-N1	1.822(2)	N1-Mo1-N2	127.59(10)
Mo1-N2	1.808(2)	P1-Mo1-P2	173.42(3)
Mo1-H1	2.01(1)	N1-Mo1-B1	116.87(11)
Mo1-H2	2.00(1)	N2-Mo1-B1	115.03(11)
Mo1···B1	2.461(3)	Mo1-N1-C1	168.5(2)
B1-H1	1.05(4)	Mo1-N2-C13	172.5(2)
B1-H2	0.83(4)	H1-Mo1-H2	42.0(15)
B1-H3	1.04(3)	H1-B1-H2	99.0(17)
B1-H4	1.17(3)	P1-Mo1-B1	86.88(9)
		P2-Mo1-B1	88.21(9)

As mentioned above, only one bis(imido) molybdenum(V) compound has been structurally authenticated recently, namely the "ate" complex $(ArN)_2Mo\{\mu,\kappa_{C,N}^2\text{-}2\text{-}C_6H_4CH_2\text{-}NMe_2\}_2Li$ (**III-127**), which has an approximately tetrahedral Mo(V) center.[237] The Mo-NAr distances in **III-127** (average 1.771 Å) are somewhat shorter than those in **III-125** (average 1.815 Å), probably reflecting the higher coordination number of the latter. The ArN-Mo-NAr angle of 121.8 ° (average for two crystallographically independent molecules) is also somewhat less than that in **III-125** (127.59(10)°). Two structurally characterized bis(arylimido) Mo(IV) complexes have been reported previously: $(ArN)_2Mo(PMe_3)_2$ (**III-19**; average Mo-NAr 1.805 Å, average ArN-Mo-NAr 137°)[196] and $(ArN)_2Mo(\eta^2\text{-}C_2H_4)(PMe_3)_2$ (**III-31**; average Mo-NAr 1.828 Å, ArN-Mo-NAr 143.1(2)°).[198] A more comprehensive comparison can be made with a series of Mo(VI) five coordinate bis(arylimido) compounds $(ArN)_2Mo(L)_3$ (17 examples: average Mo-NAr 1.75 ± 0.02 Å, average ArN-Mo-NAr 109 ± 7°) and six-coordinate bis(arylimido) compounds $(RN)_2MoCl_2L_2$ (R = 2,6-disubstituted phenyl, 14 examples: average Mo-NAr 1.75 ± 0.03 Å, average ArN-Mo-NAr 104 ± 3°) in general.[242] The Mo-NAr distances in **III-125** are significantly longer than those in either the five- or six-coordinate Mo(VI) compounds, consistent with the higher formal oxidation state of the latter set but rather similar to those of the two Mo(IV) examples. The ArN-Mo-NAr angle

of 127.59(10)° (Table 14) in **III-125** lies between the values for the Mo(IV) and Mo(VI) systems, and this is in accord with theoretical expectations.[243]

Interestingly, the Mo1···B1 distance in $(ArN)_2Mo(\eta^2\text{-}BH_4)(PMe_3)_2$ (**III-125**) (2.461(3) Å; Table 14) lies at the long end of the limited number of previously characterized molybdenum borohydride compounds, even though its formal oxidation state is significantly higher than in the previous examples: $[Mo^0(CO)_4(\eta^2\text{-}BH_4)]^-$ (Mo···B = 2.41(2) Å);[238a] *trans*-$Mo^{II}(PMe_3)_4(H)(\eta^2\text{-}BH_4)$ (Mo···B = 2.468(12) Å);[238b] $Mo^0(\eta^7,\eta^1\text{-}C_7H_6\text{-}2\text{-}C_6H_4P^iPr_2)(\eta^2\text{-}BH_4)$ (Mo···B = 2.358 Å);[238c] $Mo^0(\eta\text{-}C_7H_7)(PCy_3)(\eta^2\text{-}BH_4)$ (Mo···B = 2.379 Å).[238d]

The EPR spectra[q] of $(ArN)_2Mo(\eta^2\text{-}BH_4)(PMe_3)_2$ (**III-125**) as frozen and fluid toluene solutions are shown in Figure 34 along with their simulations and are consistent with the structure. Thus, the spectra are characteristic of an $S = 1/2$ species, being in agreement with the formulation of **III-125** as a Mo(V) d^1 compound. The fluid solution spectrum shows a central 1:2:1 triplet hyperfine multiplet, centered at $g_{iso} = 1.969$. This is either due to the interaction of the unpaired electron (*upe*) with two equivalent ^{31}P nuclei (I = 1/2, 100 %) or with the two ^1H substituents (I = 1/2, 100 %) of the BH_4^- ligand. Further

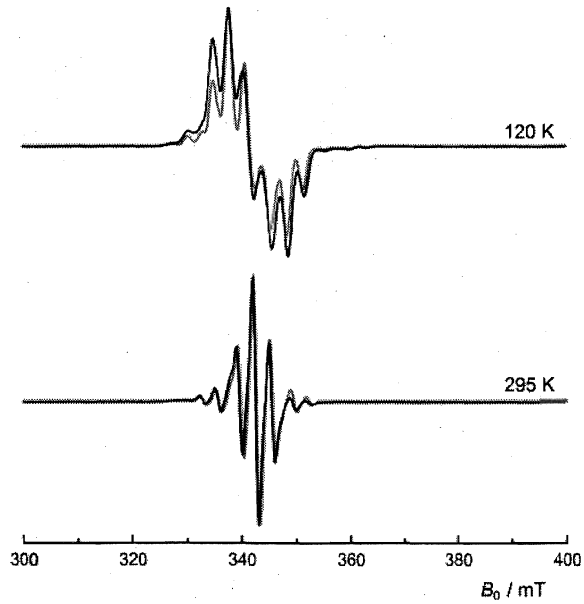

Figure 34. EPR spectra (black line) of the frozen solution (top) and fluid solution (bottom) of **III-125** in toluene and their simulation (red line).

[q] EPR study was performed by Dr. McInnes (the University of Manchester, UK).

transitions are observed in the "wings" of the spectrum, and these are satellites due to hyperfine coupling of the *upe* with ^{95,97}Mo (nuclear spin I = 5/2, sum to 25 % natural abundance). The frozen solution spectrum shows an overlapping rhombic pattern of g-values (rhombic symmetry), each of which is split into a 1:2:1 triplet by the interaction of the *upe* with two equivalent ^{31}P or ^{1}H atoms. Again, additional features due to the Mo satellites are observed in the "wings" of the spectrum. The simulation of EPR parameters for **III-125** (red line, Figure 34) gives the spectra similar to the experimental ones.

In contrast to the bis(imido) dichloride $(ArN)_2MoCl_2(DME)$ (**III-11**), the mono(imido) complex $(ArN)MoCl_2(PMe_3)_3$ (**III-22**) does not show any reaction with excess $NaBH_4$. Surprisingly, no reactivity was observed even upon treatment of **III-22** with $MeLi/H_2$, $Na(Hg)/H_2$, and KC_8/H_2. On the other hand, addition of a solution of $LiBH_4$ (2 equiv.) in THF at room temperature to the mono(imido) dichloride complexes $(RN)MoCl_2(PMe_3)_3$ (R = Ar' (**III-5**), Ar (**III-22**)) in toluene affords diamagnetic mono(imido) bis(borohydride) derivatives $(RN)Mo(\eta^2\text{-}BH_4)_2(PMe_3)_2$ (R = Ar' (**III-128**) or Ar (**III-8**); Scheme 121).

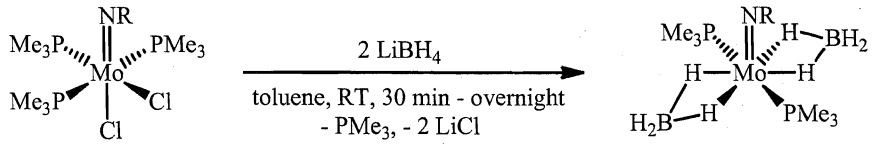

R = Ar' (**III-5**), Ar (**III-22**)

R = Ar' (**III-128**, 67 %), Ar (**III-8**, 51 %)

Scheme 121. Preparation of Mo(IV) bis(borohydride) complexes **III-128** and **III-8**.

Depending on the substituent in the imido ligand, the reaction takes either 30 min. or overnight. The higher solubility of the Ar derivative **III-8** in non-polar solvents allows its isolation by extraction with hexanes (51 % yield in analytically pure form), whereas the complex **III-128** was isolated *via* extraction with toluene and crystallization from an Et_2O solution (67 % yield). Both **III-128** and **III-8** were characterized by multinuclear NMR, IR, and, in the case of **III-8**, X-ray diffraction analysis.

Typical for borohydride compounds, the ^{1}H-NMR spectra of both **III-128** and **III-8** feature broad resonances for the BH_4 substituents at -0.03 and -0.02 ppm, respectively. Lowering the temperature of the NMR experiment down to -44 ÷ -79 °C led to the observation of two types of signals for bridging and terminal hydrides in the BH_4 ligand

(-5.38 ppm (bs, 2 H, B-H_{bridge}) and -1.10 ppm (bs, 2 H, B-H_{term}) for **III-128**; -5.43 ppm (bs, 2 H, B-H_{bridge}) and -1.16 ppm (bs, 2 H, B-H_{term}) for **III-8**). The ^{31}P-NMR spectra of both Ar'- and Ar-substituted borohydrides do not depend on the temperature and show a singlet for two equivalent *trans*-PMe_3 groups at 1.9 and 1.1 ppm, respectively. The η^2-coordination mode of the BH_4 ligand is evident from the IR spectra, which exhibit multiple B-H stretches at 2111, 2189, 2269, 2371, and 2395 cm^{-1} for the complex **III-128** and 1950, 1969, 2013, 2102, 2266, 2378, and 2405 cm^{-1} for **III-8**.[235b]

The molecular structure of (ArN)Mo(η^2-BH_4)$_2$(PMe_3)$_2$ (**III-8**; Figure 35) was determined by X-ray diffraction at 123 K (see Table 31, chapt. VI). All non-hydrogen atoms were readily located and refined anisotropically. The H atoms of the BH_4 ligands were located from a Fourier difference synthesis and could be positionally refined subject to soft similarity restrains on the B-H distances and with the common isotropic displacement parameter for the H atoms. Complex **III-8** has an octahedral structure with

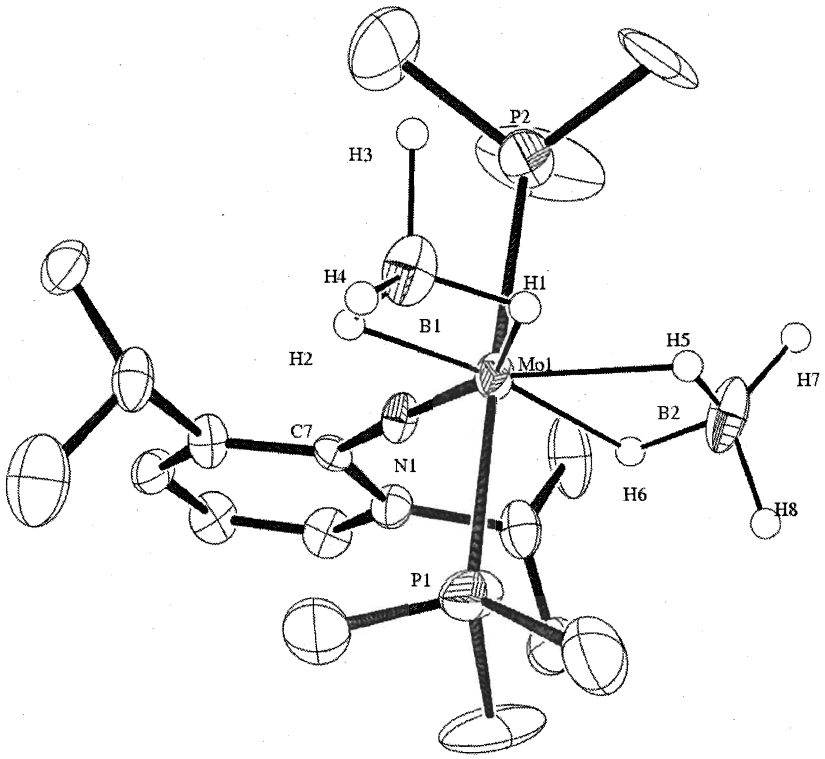

Figure 35. ORTEP plot of the molecular structure of **III-8** (C-bound H atoms are omitted for clarity). Anisotropic displacement parameters are plotted at 50 % probability.

Table 15. Selected bond distances (Å) and angles (°) for complex **III-8**.

distances, Å				angles, °	
Mo1-N1	1.7423(17)	B2-H5	1.17(2)	Mo1-N1-C7	177.0(4)
Mo1-H1	2.07(2)	B2-H6	1.23(3)	N1-Mo1-B1	123.68(9)
Mo1-H2	1.91(3)	B2-H7	1.17(4)	N1-Mo1-B2	116.96(9)
Mo1-H5	2.06(2)	B2-H8	1.19(6)	P1-Mo1-P2	172.14(3)
Mo1-H6	1.88(3)	Mo1···B1	2.484(3)	H1-Mo1-H2	57.9(10)
B1-H1	1.18(3)	Mo1···B2	2.479(3)	H1-B1-H2	103.5(17)
B1-H2	1.27(2)	Mo1-P1	2.481(4)	H5-Mo1-H6	56.4(12)
B1-H3	1.33(5)	Mo1-P2	2.492(4)	H5-B2-H6	102.0(2)
B1-H4	1.03(4)			H2-Mo1-H6	169.0(3)

two bridging hydrides (H1 and H5) of two different Mo(μ-H)$_2$B units lying *trans-* to the imido group ArN^{2-}. The other two bridging hydrides (H2, H6) of two Mo(μ-H)$_2$B are coplanar with the t*rans*-PMe_3 ligands and ArN^{2-} substituent, whereas the terminal H atoms (H3, H4, H7, and H8) of the two borohydrides are positioned above and below the B1-N1-B2 plane, similar to the structure of (ArN)$_2$Mo(η^2-BH_4)(PMe_3)$_2$ (**III-125**; Figure 33). The Mo1···B1 and Mo1···B2 distances in **III-8** (2.484(3) and 2.479(3) Å, respectively; Table 15) lie at the long end of previously characterized molybdenum borohydride compounds (2.358-2.468(12) Å).[238a-d] The Mo1-N1-C7 linkage is approximately linear (177.0(4)°) suggesting that the ArN^{2-} ligand may act as a 6 electron donor to the metal.

Surprisingly, both complexes **III-128** and **III-8** were found to be extremely inert towards Lewis bases. Thus, the treatment of the borohydride derivatives with NEt_3 or PMe_3 does not show any significant reaction even upon heating up to 50 °C. Remarkably, no reaction was also observed in the case of alcohols (ethanol and ethylene glycol) and water! Heating the compound (ArN)Mo(η^2-BH_4)$_2$(PMe_3)$_2$ (**III-8**) up to 100 °C in the presence of excess water gives only slow decomposition of the complex *via* partial hydrolysis of the Mo=NAr moiety and formation of $ArNH_2$.

On the other hand, addition of sufficiently Lewis acidic silanes (chlorohydrosilanes or $PhSiH_3$) to a mixture of **III-128** or **III-8** and excess PMe_3 leads to an extremely slow

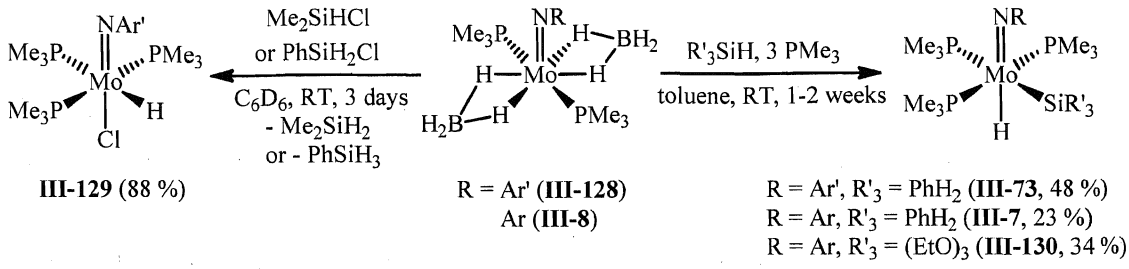

Scheme 122. Reactions of borohydrides **III-128** and **III-8** with silanes.

abstraction of BH_3 and formation of the $H_3B{\cdot}PMe_3$ adduct. For example, an NMR scale reaction of (Ar'N)Mo(η^2-BH_4)$_2$(PMe_3)$_2$ (**III-128**) with mono(chloro) substituted silanes (such as Me_2SiHCl or $PhSiH_2Cl$) in the presence of three equivalents of PMe_3 after three days at ambient temperature gives quantitatively R_2SiH_2 (R = Me_2 or PhH) and a novel hydrido chloride derivative, (Ar'N)Mo(H)(Cl)(PMe_3)$_3$ (**III-129**; Scheme 122). Substitution of chlorohydrosilanes with less Lewis acidic hydrosilanes significantly slows down the abstraction of BH_3. Thus, reactions of both **III-128** and **III-8** with $PhSiH_3$ in the presence of excess PMe_3 (3 equiv.) are much slower and lead, after few weeks at room temperature, to the formation of the silyl hydride complexes, (Ar'N)Mo(H)(SiH_2Ph)(PMe_3)$_3$ (**III-73**, 48 %) and (ArN)Mo(H)(SiH_2Ph)(PMe_3)$_3$ (**III-7**, 23 %), respectively (Scheme 122). The treatment of (ArN)Mo(η^2-BH_4)$_2$(PMe_3)$_2$ (**III-128**) with $HSi(OEt)_3$ under similar conditions affords the (triethoxy)silyl derivative (ArN)Mo(H)($Si(OEt)_3$)(PMe_3)$_3$ (**III-130**, 34 %; Scheme 122), which was found to be metastable and slowly (~ 1 week at room temperature) decomposes in solution to a difficult-to-characterize mixture of products, the main component of which was suggested to be (ArN)Mo(OEt)$_2$(PMe_3)$_3$ (**III-88**; see the discussion in chapt. III.4.2).

All the products of the reactions of bis(borohydride) compounds with silanes were characterized by multinuclear NMR and IR spectroscopy, and, in the case of the complex **III-7**, by X-ray diffraction analysis (see Table 27, chapt. VI). The hydride ligand in (Ar'N)Mo(H)(Cl)(PMe_3)$_3$ (**III-129**) gives rise to a P-coupled down-field signal at 5.38 ppm (dt, $^2J_{H\text{-}P}$ = 51.3 and 29.4 Hz) in the ^{1}H-NMR spectrum. The large difference in the values of $^2J_{H\text{-}P}$ coupling constants ($\Delta \approx 22$ Hz) for the Mo-H signal suggests the *cis*-positioning of the hydride to the ArN^{2-} ligand. This leads to a strong coupling to the unique *trans*-PMe_3 ($^2J_{H\text{-}P}$ = 51.3 Hz) and a significantly weaker coupling to two

equivalent *cis*-PMe_3 groups ($^2J_{H-P}$ = 29.4 Hz). The hydride ligand in **III-129** is also seen from the IR spectrum, which shows a characteristic Mo-H stretch at 1713 cm^{-1}.[17] Similar to dichloride tris(triphosphine) complexes **III-5**, **III-47**, and **III-48**, two *trans*- PMe_3 ligands in **III-129** are equivalent and show up in the ^{31}P-NMR as a doublet at -1.6 ppm ($^2J_{P-P}$ = 14.6 Hz) due to the coupling to the unique PMe_3 *trans*- to hydride PMe_3. The latter phosphine gives rise to a triplet at -17.1 ppm ($^2J_{P-P}$ = 14.6 Hz).

Analogously, the ligation of molybdenum with a hydride in compounds **III-7**, **III-73**, and **III-130** is confirmed by ^{1}H-NMR spectroscopy, revealing up-field P-coupled signals at -3.56 (dt, $^2J_{H-P}$ = 18.5, 65.4 Hz), -3.92 (dt, $^2J_{P-H}$ = 18.6, 65.4 Hz), and -4.73 ppm (dt, $^2J_{P-H}$ = 18.6, 62.1 Hz), respectively. Additionally, the hydride substituents of **III-7** and **III-73**, give rise to characteristic red-shifted Mo-H stretches at 1699 and 1647 cm^{-1} in the IR spectra, respectively. The observation of down-field resonances of the silicon bound protons (5.75 (t, $^3J_{H-P}$ = 7.8 Hz) and 5.83 ppm (t, $^3J_{H-P}$ = 7.8 Hz), respectively) in the ^{1}H-NMR spectra, as well as the large values of the $^1J_{Si-H}$ coupling constants (157.4 and 147.0 Hz, respectively) and normal Si-H stretches in the IR spectra (2152 and 1998 cm^{-1}, respectively) suggest the classical structures of silylhydrides **III-73** and **III-7**.

The molecular structure of (ArN)Mo(H)(SiH_2Ph)(PMe_3)$_3$ (**III-7**), determined at 120 K, revealed that the Mo adopts an octahedral geometry, with the hydride lying *trans*- and the silyl group lying *cis*- to the imido substituent (Figure 36). All three phosphines are coplanar with the silyl ligand and, thus, are *cis*- to the Mo-bound hydride substituent. Such an unusual arrangement of ligands in the compound **III-7** is not consistent with the *trans*-influence of strongly donating ArN^{2-} ligand[244] and is probably due to the presence of steric repulsions between the bulky SiH_2Ph group and phosphine ligands. Complex **III-7** has a classical silyl hydride structure with Mo1-H1 distance of 1.9202 Å, Si1-H2 and Si1-H3 bonds of 1.44(3) and 1.46(3) Å, respectively, and the Si1-Mo1-H1 angle of 61.9° (Table 16). All three PMe_3 groups show approximately equal Mo-P distances, contradicting the expected *trans*- influence of the silyl SiH_2Ph ligand.[210] Slight elongation of the *cis*- to silyl Mo1-P3 bond (2.4861(5) Å *vs.* 2.4671(5) and 2.4699(5) Å for Mo1-P1 and Mo1-P2, respectively) is not significant and could be a result of steric repulsions of phosphine with SiH_2Ph substituent. The Mo1-N1-C1 linkage (174.08(13)°; Table 16) is

almost linear, suggesting that ArN^{2-} acts as a 6 electron donor to the d^2 molybdenum center stabilizing the 18 electron valence shell.

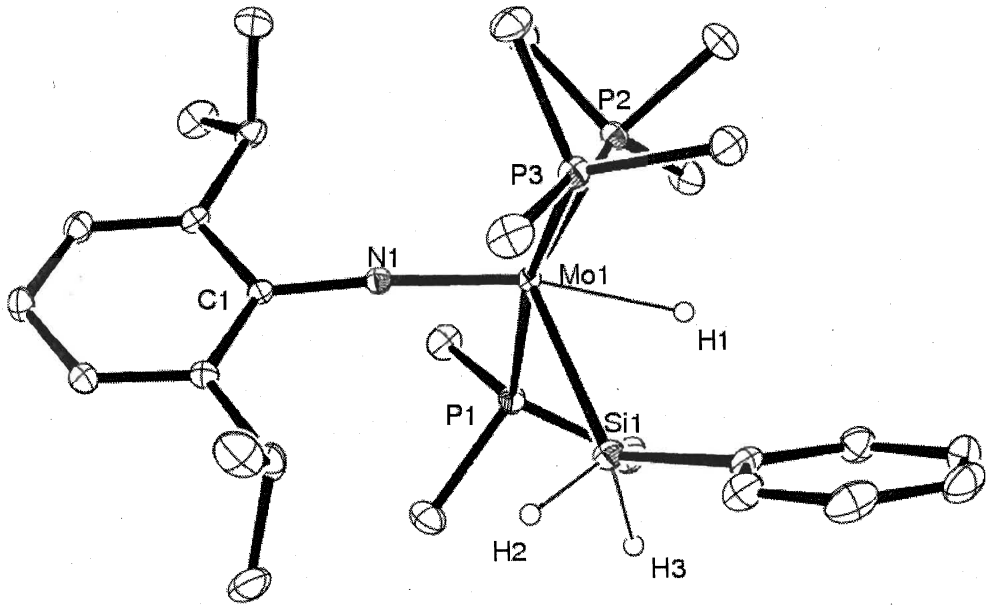

Figure 36. ORTEP plot of the molecular structure of **III-7** (H atoms, except Si-H and Mo-H, are omitted for clarity). Anisotropic displacement parameters are plotted at 50 % probability.

Table 16. Selected bond distances (Å) and angles (°) for complex **III-7**.

distances, Å		angles, °	
Mo1-N1	1.8084(16)	Mo1-N1-C1	174.08(13)
Mo1-H1	1.9202	N1-Mo1-H1	167.4
Mo1-Si1	2.5010(6)	Mo1-Si1-H2	113.3(11)
Si1-H2	1.44(3)	Mo1-Si1-H3	100.9(16)
Si1-H3	1.46(3)	Si1-Mo1-H1	61.9
Si1···H1	2.328	Si1-Mo1-P2	131.78(2)
Mo1-P1	2.4671(5)	P1-Mo1-P3	169.848(18)
Mo1-P2	2.4699(5)	N1-Mo1-Si1	108.24(5)
Mo1-P3	2.4861(5)	Si1-Mo1-P3	87.35(2)

III.7.2 Preparation and reactivity of imido hydride molybdenum complexes

As was already mentioned, the room temperature reaction of (RN)Mo(η^2-BH_4)$_2$(PMe_3)$_3$ (R = Ar' (**III-128**) and Ar (**III-8**)) with $HSiR'_3$ to form the novel complexes (Ar'N)Mo(H)(Cl)(PMe_3)$_3$ (**III-129**) and (RN)Mo(H)(SiR'_3)(PMe_3) (R = Ar', R'_3 = H_2Ph (**III-73**); R = Ar, R'_3 = H_2Ph (**III-7**) and $(OEt)_3$ (**III-130**); Scheme 122) is slow (1-2 weeks), giving irreproducible yields of the hydride products. Increase of the temperature of the reaction does not accelerate the process, leading only to a concurrent silane redistribution.[7a, 72, 211] In order to develop a reliable procedure for the preparation of imido hydride species, we suggested a different approach based on the selective substitution of one chloride in (RN)$MoCl_2$(PMe_3)$_3$ with a hydride, followed by the substitution of the remaining Mo-Cl with silyl ligand. The present chapter describes our results in the development of an efficient methodology for the preparation of Mo(IV) imido hydrides and the study of their stoichiometric and catalytic reactivity. Mechanistic aspects of catalytic hydrosilation reactions mediated by hydride complexes are also discussed.

III.7.2.1 Preparation of molybdenum imido hydride complexes

In accordance with the proposed approach, the treatment of (ArN)$MoCl_2$(PMe_3)$_3$ (**III-47**) with one equivalent of L-Selectride allows for the selective production of a monosubstituted product (ArN)Mo(H)(Cl)(PMe_3)$_3$ (**III-6**; Scheme 123), characterized by multinuclear NMR and IR spectroscopy, and X-ray diffraction analysis (see Table 32, chapt. VI). In contrast to the previously described method starting with bis(borohydride) precursors, this reaction takes only two hours at room temperature and gives **III-6** in 65 % yield reproducibly.

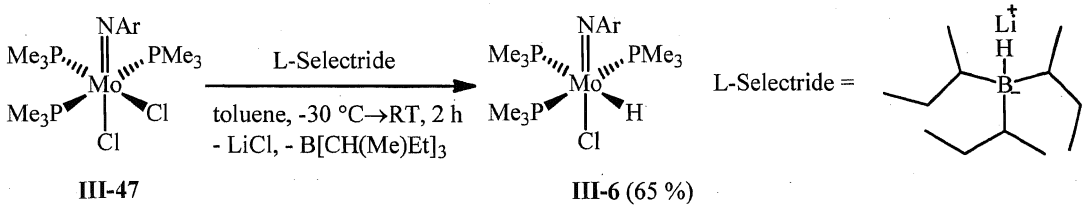

III-47 III-6 (65 %)

Scheme 123. Preparation of (ArN)Mo(H)(Cl)(PMe_3)$_3$ (**III-6**).

The spectroscopic features of **III-6** are similar to those observed for the related Ar' derivative **III-132** discussed above. The ^{1}H-NMR spectrum of **III-6** shows a down-field hydride signal at 5.31 (dt, $^{2}J_{H\text{-}P}$ = 28.5, 51.9 Hz), coupled to two equivalent *cis*-phosphines and the unique *trans*-PMe_3. The presence of the hydride ligand is also evident from the observation of an IR stretch at 1714 cm^{-1} corresponding to the Mo-H stretch. The complex has an octahedral structure (Figure 37), with the chloride lying *trans*- to the imido group (the same geometry was suggested for the Ar' analogue **III-129** based on the NMR data, see above). In contrast to the structures of **III-47** and **III-7**, the PMe_3 *trans*- to hydride in **III-6** forms a longer Mo-P bonds than the *cis*-phosphines (2.572(1) Å for Mo1-P11 *vs.* 2.485(1) and 2.469(1) Å for Mo1-P12 and Mo1-P13, respectively; Table 17). The 18 electron valence shell of complex **III-6** is stabilized by additional donation of the imido nitrogen lone pair to molybdenum resulting in an almost linear Mo1-N1-C1 linkage (170.9(3) °; Table 17).

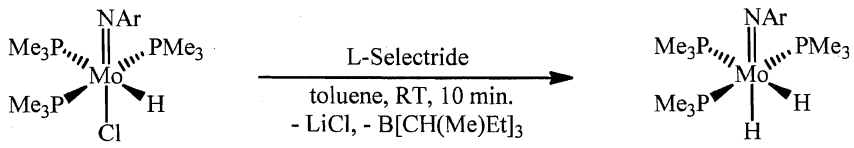

III-6 **III-131** (77 %)

Scheme 124. Preparation of the dihydride complex **III-131**.

Addition of one equivalent of L-Selectride to a solution of (ArN)Mo(H)(Cl)$(PMe_3)_3$ (**III-6**) in toluene selectively affords the dihydride derivative (ArN)Mo$(H)_2(PMe_3)_3$ (**III-131**; Scheme 124). The product is highly fluxional in solution and its room temperature NMR spectra exhibit only broad featureless resonances. However, the $^{31}P\{^{1}H\}$-NMR spectrum of **III-131** registered at -26 °C shows two mutually coupled for two sets of nonequivalent PMe_3 groups, at 14.8 ppm (d) and 13.1 ppm (t) with $^{2}J_{P\text{-}P}$ = 19.4 Hz. At -29 °C, the ^{1}H-NMR spectrum of **III-131** reveals two nonequivalent Mo-bound hydrides, which give rise to resonances at -5.31 ppm (dtd, $^{2}J_{H\text{-}P}$ = 60.6 Hz, $^{2}J_{H\text{-}P}$ = 46.2 Hz, $^{2}J_{H\text{-}H}$ = 7.2 Hz) and 2.08 ppm (multiplet, overlapping with a residual toluene-d_8 signal, $^{2}J_{H\text{-}P}$ = 43.2 Hz, $^{2}J_{H\text{-}H}$ = 7.2 Hz, found by $^{1}H\text{-}^{1}H$ COSY and $^{1}H\text{-}^{31}P$ HSQC NMR experiments). The hydride structure of **III-131** is also seen from the IR spectrum, in which the Mo-H band was detected at 1620 cm^{-1}. Based on these spectroscopic features and the analogy

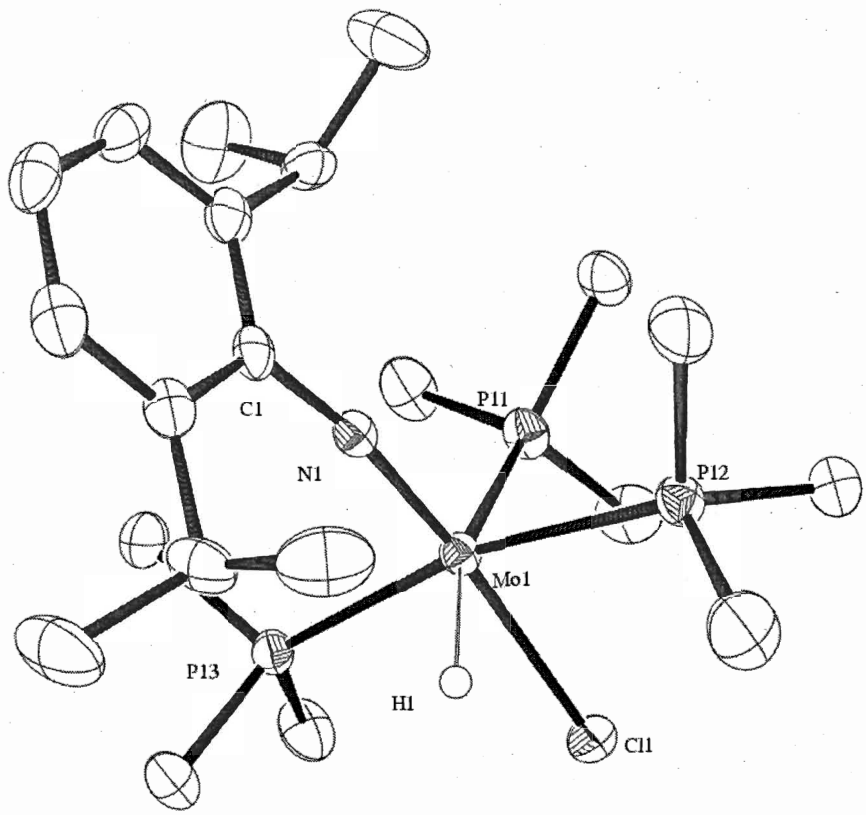

Figure 37. ORTEP plot of the molecular structure of **III-6** (H atoms, except Mo-H, are omitted for clarity). Anisotropic displacement parameters are plotted at 50 % probability.

with (ArN)Mo(H)(Cl)(PMe_3)$_3$ (**III-6**), we suggest an octahedral structure of **III-131** with one of the hydride ligands occupying the apical position. The second Mo-bound hydride lies in the equatorial position being co-planar with PMe_3 substituents.

Despite its unsaturated nature, (ArN)Mo(H)$_2$(PMe_3)$_3$ (**III-131**) does not react with H_2 (see the formation of (ArN)MoH_4(PMe_3)$_3$ (**III-63**) in the room temperature NMR scale reaction of (ArN)$_2$Mo(PMe_3)$_3$ (**III-22**) with excess $PhSiH_3$; Scheme 89), neither with chlorine-free hydrosilanes. At the same time, **III-131** is metastable in solution at room temperature and shows a slow (few days) decomposition to a mixture of unidentified products.

The reaction of (ArN)Mo(H)(Cl)(PMe_3)$_3$ (**III-6**) with an equivalent of $LiBH_4$ or RLi (R = Me or ^{n}Bu) in the presence of $PhSiH_3$ and excess PMe_3 leads to a product of selective chloride substitution, (ArN)Mo(H)(SiH_2Ph)(PMe_3)$_3$ (**III-7**; Scheme 125; the structural and spectroscopic features were already discussed, see above). NMR studies

Table 17. Selected bond distances (Å) and angles (°) for complex **III-6**.

distances, Å		angles, °	
Mo1-N1	1.755(3)	Mo1-N1-C1	170.9(3)
Mo1-H1	1.76(4)	N1-Mo1-Cl1	172.04(10)
Mo1-Cl1	2.5367(11)	N1-Mo1-H1	96.2(13)
Mo1-P11	2.5723(10)	H1-Mo1-P11	160.1(13)
Mo1-P12	2.4854(12)	P12-Mo1-P13	166.78(4)
Mo1-P14	2.4690(12)	H1-Mo1-Cl1	76.4(13)

performed for the reaction between **III-6**, $LiBH_4$, and $PhSiH_3$ suggested the intermediacy of the mono(borohydride) Mo(IV) derivative $(ArN)Mo(H)(\eta^2\text{-}BH_4)(PMe_3)_2$ (**III-132**). The treatment of **III-6** with RLi in the presence of less Lewis acidic and more sterically demanding $PhMeSiH_2$ and $PhMe_2SiH$ results in a more sluggish reaction leading to poor isolated yields of $(ArN)Mo(H)(SiR'_3)(PMe_3)_3$ (R'_3 = PhMeH (**III-133**) and $PhMe_2$ (**III-134**); Scheme 125). The spectroscopic features of compounds **III-133** and **III-134**, in particular the spectroscopic data for the hydride and silyl ligands, reveal the classical structure for these complexes, analogous to the SiH_2Ph derivative **III-7** (see experimental details).

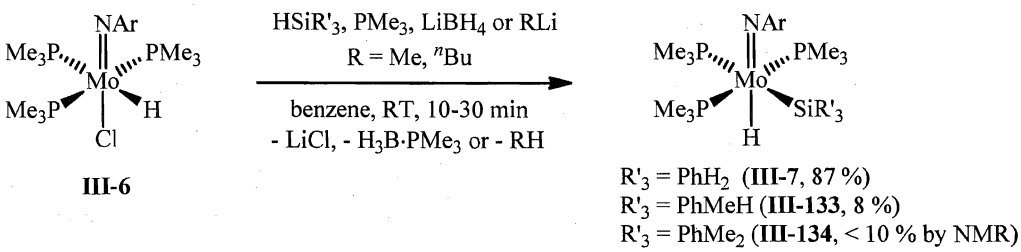

Scheme 125. Preparation of silylhydrides **III-7**, **III-133**, and **III-134**.

III.7.2.2 Catalytic activity of complexes III-6 and III-7

Both hydride compounds $(ArN)Mo(H)(Cl)(PMe_3)_3$ (**III-6**) and $(ArN)Mo(H)(SiH_2Ph)(PMe_3)_3$ (**III-7**) have been found to catalyze a diversity of silane reactions (Tables 18-21),[7] thus presenting only the second and third examples, respectively, of an early TM imido catalyst for hydrosilation (catalytic reactions mediated by the agostic imido silylamide **III-1** are described above). Thus, the room temperature

stoichiometric treatment of benzaldehyde with $PhSiH_3$ in the presence of 5.0 mol. % of **III-6** gives a 100 % conversion of substrate after one day, affording a mixture of $PhH_2Si(OBn)$ and $PhHSi(OBn)_2$ in 37 % and 63 %, respectively (Table 18, entry 1).[160, 214, 215b] An increase of the temperature up to 50 °C leads to a faster reaction and full conversion of PhC(O)H was observed after only 3 hours (Table 18, entry 2). Similar to the hydrosilation mediated by the agostic silylamide **III-1**, addition of $PhSiH_3$ to unsaturated organic molecules in the presence of catalytic amounts of **III-6** is complicated due to the concurrent silane redistribution and coupling, forming Ph_2SiH_2, SiH_4, and $PhH_2Si\text{-}SiH_2Ph$.[7a, 72, 211] The use of $PhMeSiH_2$,[215] $HSi(OEt)_3$,[216] or PMHS[245] instead of $PhSiH_3$ gives more sluggish reactions, with the conversion of benzaldehyde being in the range 50-95 % (Table 18, entries 3-5).

In contrast, $(ArN)Mo(H)(Cl)(PMe_3)_3$ (**III-6**) showed lower activity in the hydrosilation of acetophenone, completing the conversion of the substrate upon treatment with $PhSiH_3$ at 5.0 mol. % load of the catalyst only after 11 days at room temperature (Table 18, entry 6).[215] On the other hand, hydrosilation of PhMeC(O) with PMHS[9d, 115, 246] requires heating (50 °C) and gives 100 % conversion of acetophenone after 48 hours (Table 18, entry 7). Much faster reactions with silanes were shown for the cyclohexanone, which affords a 100 % conversion with $PhSiH_3$ and PMHS after 35 min. and 24 hours, respectively (Table 18, entries 8-10).[9d, 115, 246, 247] Low activity of **III-6** was also found in the hydrosilation of 1-octyne (Table 19, entry 1) leading to only 35 % conversion of the alkyne to form a mixture of $PhH_2Si[\alpha\text{-}(CH{=}CH)Hex]$, $PhH_2Si[\beta\text{-}(CH{=}CH)Hex]$, $PhHSi[\alpha\beta\text{-}(CH{=}CH)Hex]_2$, and $PhHSi[\beta^2\text{-}(CH{=}CH)Hex]_2$ (Figure 38).[248]

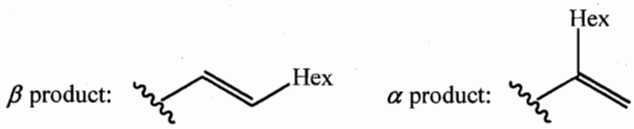

Figure 38. Two addition sites for hydrosilation of 1-octyne.

Surprisingly, $(ArN)Mo(H)(Cl)(PMe_3)_3$ (**III-6**) turned out to be inactive in the hydrosilation of alkenes. Despite the fact that the addition of $PhSiH_3$ to 1-hexene in the presence of 5.0 mol. % of **III-6** gives 86 % conversion of the alkene, the reaction results only in the reduction to hexane[68] and partial formation of 2-hexene[218] (Table 19, entry 2).

Table 18. Catalytic hydrosilation of aldehydes and ketones mediated by **III-6**.

Entry	Org. substrate[a]	Silane	Cat., mol. %	T, °C / time	Products[b]	Substrate conv.[c]	Yield[c]	TON
1	PhC(O)H	$PhSiH_3$	5.0	RT / 24 h	$PhSiH_2(OBn)$	100 %	37 %	20
					$PhSiH(OBn)_2$		63 %	
2			3.0	50 °C / 3 h	$PhSiH_2(OBn)$	100 %	32 %	34
					$PhSiH(OBn)_2$		68 %	
3		$PhMeSiH_2$	5.0	RT / 24 h	PhMeHSi(OBn)	68 %	68 %	14
4		$(EtO)_3SiH$	5.0	RT / 12 days	$(EtO)_3Si(OBn)$	95 %	13 %	19
				and 50 °C /	$(EtO)_2Si(OBn)_2$		40 %	
				24h	$(EtO)Si(OBn)_3$		42 %	
5		PMHS	6.0	50 °C / 48 h	$(BnO)_x$(PMS)	50 %	50 %	8
6	PhMeC(O)	$PhSiH_3$	5.0	RT / 11 days	$PhH_2Si[OCH(Me)Ph]$	100 %	54 %	20
					$PhHSi[OCH(Me)Ph]_2$		23 %	
					$PhSi[OCH(Me)Ph]_3$		12 %	
					$PhCH_2CH_3$		11 %	
7		PMHS	6.0	50 °C / 48 h	$[Ph(Me)CHO]_x$(PMS)	100 %	100 %	17
8	Cyclohexanone	$PhSiH_3$	5.0	RT / 35 min	$PhH_2Si(OCy)$	100 %	79 %	20
					$PhHSi(OCy)_2$		21 %	
9				RT / 3 h	$PhH_2Si(OCy)$	100 %	60 %	20
					$PhHSi(OCy)_2$		40 %	
10		PMHS	6.0	50 °C / 24 h	(cyclohexyl-O)$_x$(PMS)	100 %	100 %	17

[a] 1:1 ratio of substrate and silane. [b] Reactions with $PhSiH_3$ give Ph_2SiH_2 and SiH_4 by-products.[211] [c] Detected by ^{1}H-NMR using tetramethylsilane as a standard.

Ethanolysis of $PhSiH_3$ in the presence of 5.0 mol. % of **III-6** is a fast process (Table 19, entry 3), but is slower than for the agostic compound **III-1** (see above). After one hour at room temperature, the reaction is complete, affording a mixture of silyl ethers $PhH_2(OEt)$ (26 %) and $PhHSi(OEt)_2$ (74 %).[160, 221] Interestingly, a similar reaction of phenylsilane with excess water (ca. 5 equiv.) is more sluggish and leads to the formation of polysiloxane with a 100 % conversion of $PhSiH_3$ after 3 hours at room temperature (Table 19, entry 4).[165]

Lastly, hydrido chloride complex **III-6** was found to mediate the addition of phenylsilane to nitriles, including a rare example of selective catalytic hydrosilation of nitriles to imines.[133, 136, 137b, 138a, 141, 146, 222] Similar to the silylamide **III-1**, the room temperature reaction of PhCN with one equivalent of $PhSiH_3$ and 5.0 mol. % of $(ArN)Mo(H)(Cl)(PMe_3)_3$ (**III-6**) leads to only stoichiometric (5 %) formation of $PhH_2Si(N{=}CHPh)$ (Table 19, entry 6). An increase of the reaction time (up to 13 days) and temperature (up to 50 °C) gives 100 % conversion of benzonitrile producing of a mixture of $PhH_2Si(N{=}CHPh)$ and $PhHSi(N{=}CHPh)_2$ in 76 % and 24 %, respectively (TON = 20, Table 19, entry 7). No product of double addition of silane to PhCN was observed by ^{1}H-NMR.[137b, 139b] In contrast, substitution of benzonitrile with acetonitrile in the reaction with $PhSiH_3$ does not give monoaddition reaction and, after 6 days at 50 °C, 45 % of CH_3CN is converted to the bis(silated) amine $EtN(SiH_2Ph)_2$ (Table 19, entry 5).[137b, 139b, 162, 163]

In comparison with the hydrido chloride complex **III-6**, $(ArN)Mo(H)(SiH_2Ph)(PMe_3)_3$ (**III-7**) shows a much improved catalytic activity in hydrosilation (Tables 20 and 21). Thus, the reactions of benzaldehyde with $PhSiH_3$, $(m\text{-Tol})SiH_3$, $PhMeSiH_2$, and $(EtO)_3SiH$ all give a 100 % conversion of PhHC(O) in 15 min – 18 hours at room temperature (Table 21, entries 1-4).[160, 214, 215b, 216] Similar trends with high yields of silation products have been also found for the (**III-7**)-catalyzed addition of $PhSiH_3$ to ketones[9d, 115, 215, 246, 247] (acetophenone and acetone) and ethanol (Table 21, entries 5, 6 and Table 21, entry 4, respectively). Interestingly, substitution of phenylsilane in the reaction with acetone with the more Lewis acidic PMHS leads to a significantly decreased activity of **III-7**, affording after 3.9 hours at room temperature only 58 % of the hydrosilated product (Table 21, entry 7).

Table 19. Catalytic hydrosilation of alkenes and alkynes and alcoholysis and hydrolysis of $PhSiH_3$ mediated by **III-6**.

Entry	Org. substrate[a]	Silane	cat., mol. %	T, °C / time	Products[b]	Substrate conv.[c]	Yield[c]	TON
1	1-octyne	PhSiH3	5.0	RT / 15 days	$PhH_2Si(CH=CH)Hex(\alpha)$	35 %	4 %	7
					$PhH_2Si(CH=CH)Hex(\beta)$		7 %	
					$PhHSi[(CH=CH)Hex]_2(\alpha\beta)$		12 %	
					$PhHSi[(CH=CH)Hex]_2(\beta^2)$		12%	
2	1-hexene	$PhSiH_3$	5.0	RT / 72 h and	$PhH_2Si(Hex)$	89 %	3 %	18
				60 °C / 24 h	2-hexene		6 %	
					Hexane		80 %	
3	EtOH	$PhSiH_3$	5.0	RT / 1 h	$PhH_2Si(OEt)$	100 %	26 %	20
					$PhHSi(OEt)_2$		74 %	
4	H_2O (exc.)	$PhSiH_3$	5.0	RT / 3 h	polysiloxane and H_2	100 % conv. of $PhSiH_3$	—	20
5	CH_3CN	$PhSiH_3$	5.0	50 °C / 6 days	$EtN(SiH_2Ph)_2$	45 %	45 %	9
6	PhCN	$PhSiH_3$	5.0	RT / 18 h	$PhH_2Si(N=CHPh)$	5 %	5 %	1
7				50 °C / 13 days	$PhH_2Si(N=CHPh)$	100 %	76 %	20
					$PhHSi(N=CHPh)_2$		24 %	

[a] 1:1 ratio of organic sustrate and silane. [b] Reactions with $PhSiH_3$ give Ph_2SiH_2 and SiH_4 as by-products produced by catalytic redistribution of substituents at the silicon centre.[211] Increasing the temperature of the reaction increases the amount of Ph_2SiH_2 and SiH_4 formed. [c] Detected by ^{1}H-NMR spectroscopy using tetramethylsilane as an internal standard.

On the other hand, the activity of (ArN)Mo(H)(SiH_2Ph)(PMe_3)$_3$ (**III-7**) in the hydrosilation of organic nitriles (acetonitrile and benzonitrile) turned out to be somewhat similar to that one showed by (ArN)Mo(H)(Cl)(PMe_3)$_3$ (**III-6**). In particular, only stoichiometric formation of EtN(SiH_2Ph)$_2$ (6 %)[137b, 139b, 162, 163] in the reaction of CH_3CN with $PhSiH_3$ in the presence of 5.0 mol. % of **III-7** was detected after 20 min at room temperature (Table 20, entry 1). No further conversion of acetonitrile was observed during the next 24 hours. At the same time, hydrosilation of benzonitrile selectively gives the monoaddition product PhH_2Si(N=CHPh) in 32 % yield (TON = 6; Table 20, entry 3). Despite the long reaction time and poor yield of PhH_2Si(N=CHPh), complex **III-7** presents the rare example of a catalyst for the selective mono(hydrosilation) of aromatic nitriles.[133, 136, 137b, 138a, 141, 146, 222]

Table 20. (**III-7**)-catalyzed hydrosilation of nitriles and alcoholysis of $PhSiH_3$ (5 mol %).

Entry	Substrate[a]	Silane	Time / T, °C	Products[b]	Conv.[c]	Yield[c]	TON
1	CH_3CN	$PhSiH_3$	20 min / RT	EtN(SiH_2Ph)$_2$	6 %	6 %	1
2	PhCN	$PhSiH_3$	19.7 h / RT	PhH_2Si(N=CHPh)	20 %	20 %	4
3			41.9 h / RT	PhH_2Si(N=CHPh)	32 %	32 %	6
4	EtOH	$PhSiH_3$	20 min / RT	PhH_2Si(OEt)	100 %	67 %	20
				$PhHSi(OEt)_2$		33 %	

[a] 1:1 ratio of organic substrate and silane. [b] Reactions with $PhSiH_3$ give Ph_2SiH_2 and SiH_4 as by-products produced by catalytic redistribution of substituents at the silicon centre.[211] [c] Detected by ^{1}H-NMR spectroscopy using tetramethylsilane as an internal standard.

III.7.2.3 Stoichiometric reactivity of III-6 and the mechanism of hydrosilation of benzaldehyde and alcoholysis of $PhSiH_3$

The mechanism of hydrosilation of benzaldehyde mediated by (ArN)Mo(H)(Cl)(PMe_3)$_3$ (**III-6**) was scrutinized by studying the individual steps under stoichiometric conditions. Complex **III-6** does not react with silane, which is in contrast to the $HSiR_3$ addition to the Re=O bond documented by Toste *et al.*[11a] and the H/Cl exchange observed by Aby-Omar.[13c] However, it undergoes a slow H/D exchange (78 % after 3 days) when reacted with $PhSiD_3$.

On the other hand, compound **III-6** easily reacts with PhC(O)H affording the benzoxy derivative (ArN)Mo(Cl)(OCH_2Ph)(PMe_3)$_3$ (**III-135**), as the major product (slow de-

Table 21. Catalytic hydrosilation of aldehydes and ketones mediated by **III-7** (5.0 mol %).

Entry	Organic substrate[a]	Silane	T, °C / time	Products[b]	Substrate conv.[c]	Yield[c]	TON
1	PhC(O)H	$PhSiH_3$	RT / 15 min	$PhSiH_2(OBn)$	100 %	47 %	20
				$PhSiH(OBn)_2$		53 %	
2		$PhMeSiH_2$	RT / 18 h	PhMeHSi(OBn)	100 %	100 %	20
3		$(EtO)_3SiH$	RT / 18 h	$(EtO)_3Si(OBn)$	100 %	41 %	20
				$(EtO)_2Si(OBn)_2$		29 %	
				$(EtO)Si(OBn)_3$		30 %	
4		(*m*-Tol)SiH_3	RT / 15 min	(*m*-Tol)$SiH_2(OBn)$	100 %	36 %	20
				(*m*-Tol)$SiH(OBn)_2$		64 %	
5	PhMeC(O)	$PhSiH_3$	RT / 48 h and	$PhH_2Si[OCH(Me)Ph]$	94 %	45 %	19
			50 °C / 24 h	$PhHSi[OCH(Me)Ph]_2$		33 %	
				$PhCH_2CH_3$		16 %	
6	$Me_2C(O)$	$PhSiH_3$	RT / 3.4 h	$PhH_2Si(O^iPr)$	90 %	73 %	18
				$PhHSi(O^iPr)_2$		17 %	
7		PMHS	RT / 3.9 h	$(^iPrO)_x$(PMS)	58 %	58 %	12
8			RT / 21 h	$(^iPrO)_x$(PMS)	82 %	82 %	16

[a] 1:1 ratio of organic substrate and silane. [b] Reactions with $PhSiH_3$ give Ph_2SiH_2 and SiH_4 as by-products produced by catalytic redistribution of substituents at the silicon centre.[211] Increasing the temperature of the reaction increases the amount of Ph_2SiH_2 and SiH_4 formed. [c] Detected by ^{1}H-NMR spectroscopy using tetramethylsilane as an internal standard.

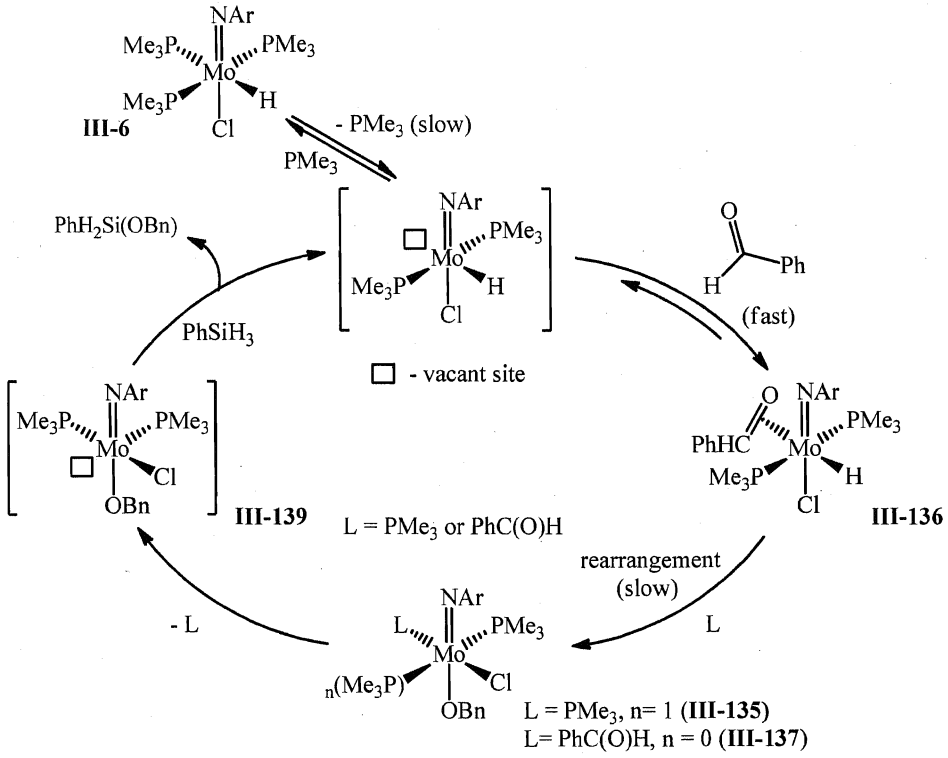

Scheme 126. Mechanism for the hydrosilation of PhC(O)H with $PhSiH_3$ mediated by complex **III-6**.

composition of **III-135** in solution to form $(ArN)MoCl_2(PMe_3)_3$ (**III-22**) was observed by NMR spectroscopy). An intermediate *trans*-(ArN)Mo(H)(Cl)(η^2-PhC(O)H)$(PMe_3)_2$ (**III-136**; Scheme 126), with the aldehyde ligand *trans*- to the hydride, was observed by ^{1}H-NMR spectroscopy. At -5 °C, complex **III-136** is the sole reaction product. The η^2-coordination of benzaldehyde in **III-136** results in an up-field shift of the OC*H* proton (5.77 ppm) and a significant reduction of its C=O IR stretch (1595 cm^{-1}).[195, 223] The nonequivalent *trans*- phosphine groups give rise to a pair of coupled doublets ($^2J_{P\text{-}P}$ = 109.3 Hz) at 1.43 and -5.59 ppm in the ^{31}P-NMR spectrum. At large aldehyde concentration, the reaction obeys the pseudo first order kinetics (k_1(-5 °C) = (7.6 ± 0.19)·10^{-4} s^{-1}; Figure 39; see also Figure 53, chapt. VI), consistent with a rate-limiting elimination of *trans*- to hydride PMe_3 ligand, followed by the fast addition of aldehyde. Such exclusive dissociation of the unique *trans*-PMe_3 is suggested by the comparison of the Mo-P distances in **III-6** (see Table 17) and further supported by the observation of an exchange with an external phosphine in the room temperature ^{1}H-^{1}H EXSY NMR experi-

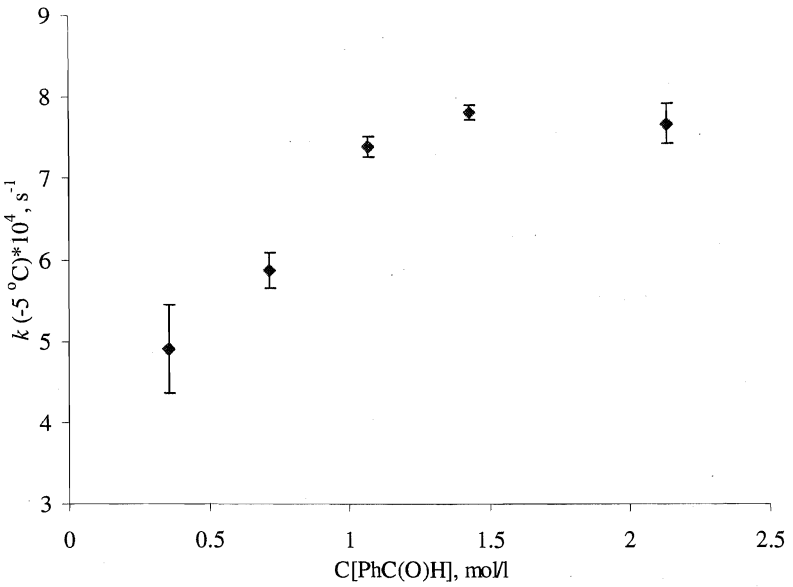

Figure 39. Dependence of the rate constant of the reaction of **III-6** with PhC(O)H at -5 °C on the concentration of the latter.

ment (see Figure 54, chapt. VI). Elimination of PMe_3 from (ArN)Mo(H)(Cl)$(PMe_3)_3$ (**III-6**) in the reaction with benzaldehyde is reversible, as addition of excess phosphine to *trans*-(ArN)Mo(H)(Cl)(η^2-PhC(O)H)$(PMe_3)_2$ (**III-136**) cleanly regenerates complex **III-6** and free PhC(O)H. At the same time, complex **II-136** undergoes a slow intramolecular exchange of the PMe_3 ligands and a fast intermolecular exchange with benzaldehyde (see chapt. VI, Figures 55 and 56).

In the absence of PMe_3, the benzaldehyde adduct **III-136** decomposes within two hours to an intractable mixture of products. But with an equivalent of PMe_3 added, it slowly (five hours) rearranges at room temperature into (ArN)Mo(Cl)$(OCH_2Ph)(PMe_3)_3$ (**III-135**). The reaction is first order on **III-136** (see Figure 57, chapt. VI) and proceeds, most likely, *via* phosphine elimination and readdition to give an isomer where the hydride ligand is *cis*- to the aldehyde. Fast hydride migration to the *cis*-coordinated aldehyde furnishes the benzoxy ligand. Analogous hydride migration has been observed previously for a hydride complex of Re.[13c] The lower k(22 °C) = (2.1 ± 0.03)·10^{-4} s^{-1} of this rearrangement process in comparison with the aldehyde addition step agrees qualitatively well with the difference in *trans*-influence of phosphine and hydride ligands.

Insertion of the coordinated PhC(O)H into the Mo-H bond is also observed upon treatment of **III-136** with excess benzaldehyde affording a mixture of (ArN)Mo(Cl)(OCH_2Ph)(η^2-PhC(O)H)(PMe_3) (**III-137**) and (ArN)Mo(Cl)(OCH_2Ph)(PMe_3)$_3$ (**III-135**).[r] At large benzaldehyde concentrations (ca. 5-15 equiv.), the reaction obeys first order kinetics in **III-136** with k_{eff}(22 °C) = (3.1 ± 0.12)·10^{-4} s^{-1}. The reaction constant does not depend on the concentration of benzaldehyde used, suggesting the rate-limiting PMe_3 dissociation, followed by coordination of PhC(O)H. Such dissociative mechanism for the reaction of *trans*-(ArN)Mo(H)(Cl)(η^2-PhC(O)H)(PMe_3)$_2$ (**III-136**) with benzaldehyde is also consistent with the kinetic VT NMR studies of this process, which reveal large positive value of the activation entropy $\Delta S^{\neq}$ = 29.8 ± 9.2 cal·K^{-1}·mol^{-1} ($\Delta H^{\neq}$ = 30.8 ± 2.7 kcal·mol^{-1}, $\Delta G^{\neq}_{295.1}$ = 22.0 ± 5.4 kcal·mol^{-1}; chapt. VI, Figure 58).

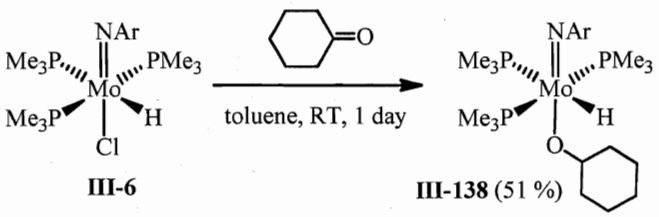

Scheme 127. Preparation of (ArN)Mo(Cl)(OCy)(PMe_3)$_3$ (**III-138**).

Similar to benzaldehyde, the reaction of (ArN)Mo(H)(Cl)(PMe_3)$_3$ (**III-6**) with one equivalent of cyclohexanone gives the cyclohexoxy derivative (ArN)Mo(Cl)(OCy)(PMe_3)$_3$ (**III-138**; Scheme 127).[s] No formation of an η^2-cyclohexanone compound, analogous to the *trans*-(ArN)Mo(H)(Cl)(η^2-PhC(O)H)(PMe_3)$_2$ (**III-136**), was observed upon monitoring the reaction by NMR, suggesting that the rearrangement of such an η^2-adduct into **III-138** is much faster than the transformation of **III-136** into (ArN)Mo(Cl)(OCH_2Ph)(PMe_3)$_3$ (**III-135**). Complex **III-138** was isolated in 51 % yield and characterized by NMR spectroscopy and X-Ray diffraction analysis (see Table 33, chapt. VI). (ArN)Mo(Cl)(OCy)(PMe_3)$_3$ (**III-138**) has an octahedral geometry (Figure 40) and similar to those for compounds **III-6**, **III-7**, and **III-47**. The cyclohexoxy

[r] Generation of (ArN)Mo(Cl)(OCH_2Ph)(η^2-PhC(O)H)(PMe_3) (**III-137**), its characterization and kinetic NMR studies were done by Oleg Shirobokov (PhD student in Nikonov's group).
[s] Preparation and characterization of (ArN)Mo(Cl)(OCy)(PMe_3)$_3$ (**III-138**) was done by Oleg Shirobokov.

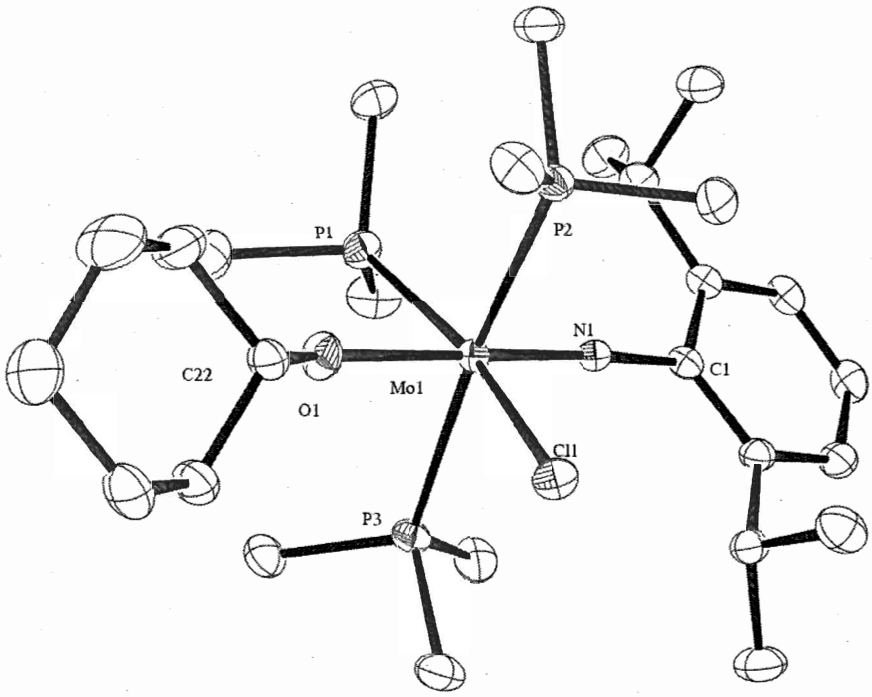

Figure 40. ORTEP plot of the molecular structure of **III-138** (hydrogen atoms are omitted for clarity). Anisotropic displacement parameters are plotted at 50 % probability.

Table 22. Selected bond distances (Å) and angles (°) for complex **III-138**.

distances, Å		angles, °	
Mo1-N1	1.786(3)	Mo1-N1-C1	176.4(2)
Mo1-O1	1.984(2)	N1-Mo1-O1	175.99(11)
Mo1-Cl1	2.5462(8)	P1-Mo1-Cl1	166.80(3)
Mo1-P1	2.4762(9)	P2-Mo1-P3	168.64(3)
Mo1-P2	2.5524(9)	N1-Mo1-Cl1	98.02(8)
Mo1-P3	2.5072(9)	N1-Mo1-P2	90.88(8)

ligand in **III-138** is laying *trans*- to the imido group (O1-Mo1-N1 angle is 175.99(11) °, Table 22), consistent with the *trans*- effect of strongly donating ArN^{2-} ligand[244] and reduced steric repulsions in the molecule.

A fast reaction of (ArN)Mo(Cl)(OCH_2Ph)(PMe_3)$_3$ (**III-135**) with $PhSiH_3$ regenerates the hydride (ArN)Mo(H)(Cl)(PMe_3)$_3$ (**III-6**) and closes the cycle. An NMR experiment with labelled silane $PhSiD_3$ results in exclusive formation of (ArN)Mo(D)(Cl)(PMe_3)$_3$

(**III-6$_D$**). Incorporation of deuterium into the hydride position of **III-6** was also observed upon stoichiometric (100 % load of the catalyst) hydrosilation of benzaldehyde with $PhSiD_3$. Kinetic measurements for the reaction of **III-135** and $PhSiH_3$ in the presence of large excess phosphine revealed a first order dependence on the complex and the silane (the k_{eff} is proportional to the $PhSiH_3$ concentration; Figure 41, **A**; see also Figure 59, chapt. VI). The $1/k_{eff}$ is proportional to phosphine concentration (Figure 41, **B**; see also Figure 60, chapt. VI), which suggests the reaction mechanism depicted in Scheme 126. Taking into account the presence of large excess benzaldehyde (relatively to the catalyst) in the hydrosilation reaction, the catalytic cycle may involve the intermediacy of (ArN)Mo(Cl)(OCH_2Ph)(η^2-PhC(O)H)(PMe_3) (**III-137**) instead of (ArN)Mo(Cl)(OCH_2-

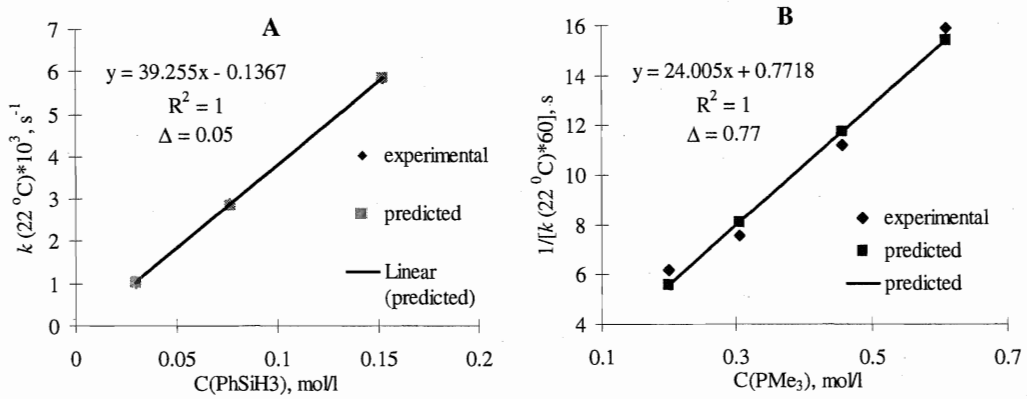

Figure 41. Dependence of the rate constant of the reaction of **III-135** with $PhSiH_3$ at 22 °C on the concentration of $PhSiH_3$ (**A**) and PMe_3 (**B**).

Ph)(PMe_3)$_3$ (**III-135**). In this case, a further reaction of **III-137** with $PhSiH_3$ could proceed *via* either PMe_3 or PhC(O)H dissociation. However, 1D ^{1}H EXSY NMR experiments indicated a reasonably fast exchange between the η^2-PhC(O)H in **III-137** and free benzaldehyde, whereas no phosphine exchange between **III-137** and PMe_3 was observed. Whether silane activation proceeds *via* the Si-H coordination to give a Mo(IV) silane σ-complex or *via* a σ-bond metathesis (or heterolytic silane splitting on the Mo-O bond)[9e] is not clear at this point, however, the pathway involving the oxidative addition of the Si-H bond to the intermediate (ArN)Mo(Cl)(OCH_2Ph)(PMe_3)$_2$ (**III-139**; Scheme 126) to form a Mo(VI) species could be ruled out by the determination of small kinetic isotop effect k_H/k_D = 0.96 ± 0.01 at 10 °C. Thus, the hydrosilation of aldehyde mediated by

(ArN)Mo(H)(Cl)(PMe_3)$_3$ (**III-6**) is different from the previously established schemes in that it (i) does not involve initial activation of the Si-H bond as in Chalk-Harrod mechanism,[10a] (ii) does not proceed *via* the Si-H addition to the M=X bond as in Toste hydrosilylation,[11a] and (iii) does not include an attack of an external carbonyl on coordinated silyl or silane as suggested by Chan *et al.*[110] and Abu-Omar *et al.*[13c]

The study of the reaction between hydrido chloride **III-6** and EtOH revealed a first order kinetics in **III-6** and a saturation behaviour upon the increase of alcohol concentration (the k_{eff} is proportional to the EtOH concentration; Figure 42, **A**; see also Figure 61, chapt. VI). At 20-fold excess of EtOH, the $1/k_{eff}$ is proportional to the phosphine concentration (Figure 42, **B**; see also Figure 62, chapt. VI), which suggests that the reaction starts with a reversible dissociation of PMe_3, followed by the addition of alcohol to molybdenum (Scheme 128). Such an addition probably acidifies the O-H bond enough to allow for proton transfer to the hydride to generate dihydrogen. Elimination of H_2 and phosphine readdition furnishes the product (ArN)Mo(Cl)(OEt)(PMe_3)$_3$ (**III-140**), which like (ArN)Mo(Cl)(OCH_2Ph)(PMe_3)$_3$ (**III-135**)[f]) can react with silanes to give the hydrosilation product R_3SiOEt and **III-6**. In contrast, earlier suggested mechanisms of silane alcoholysis implied silane activation by an electrophilic metal center, making it amenable for an attack by an external nucleophile. Also, the above kinetics (Figure 42) is not consistent with a direct proton transfer from EtOH to **III-6**, which is observed in

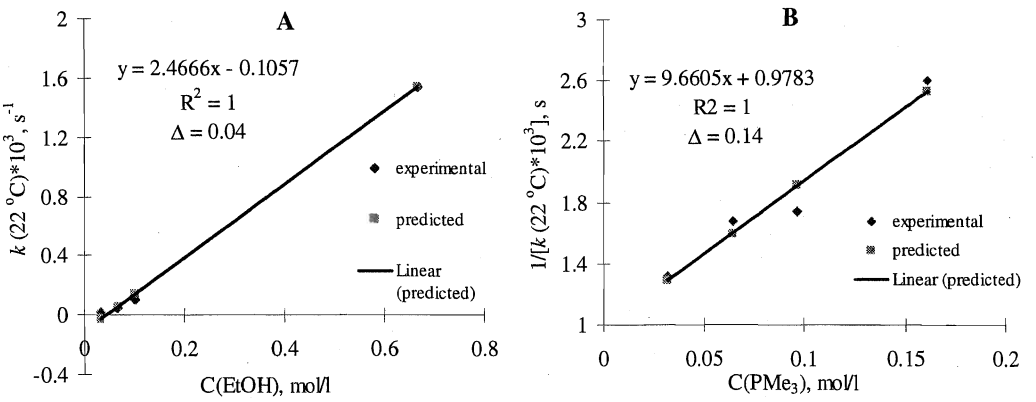

Figure 42. Dependence of the rate constant of the reaction of **III-6** with EtOH at 22 °C on the concentration of EtOH (**A**) and PMe_3 (**B**).

[f] Complex **III-135** can be also obtained by the stoichiometric reaction of (ArN)Mo(H)(Cl)(PMe_3)$_3$ (**III-6**) with $PhCH_2OH$ (see experimental details).

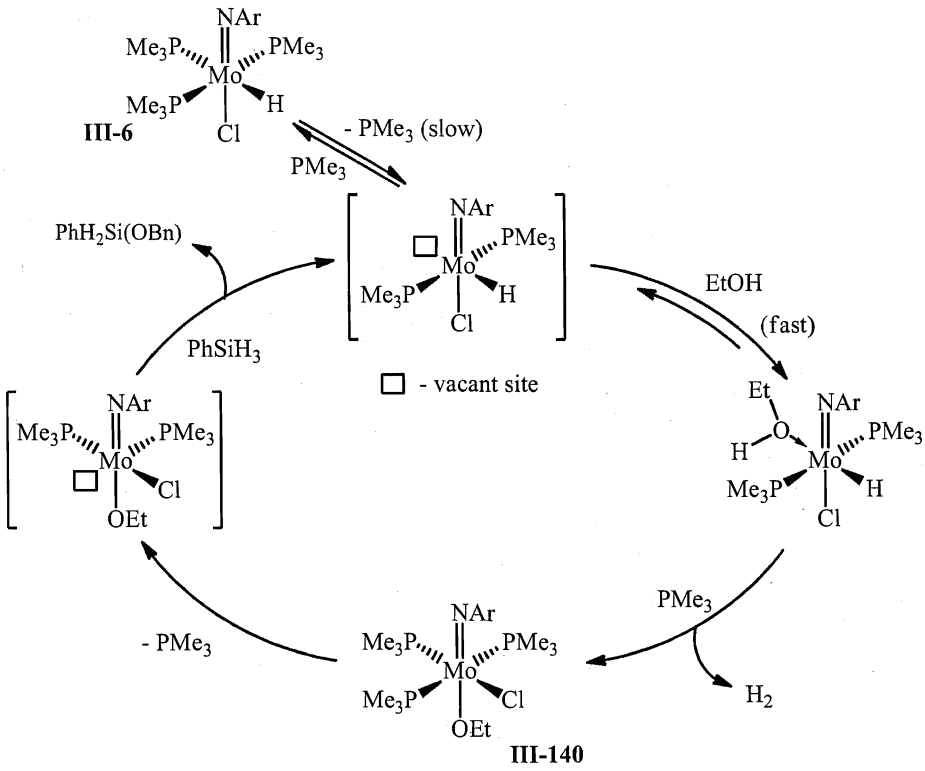

Scheme 128. Mechanism for the ethanolysis of $PhSiH_3$ mediated by **III-6**.

systems with "dihydrogen bonding".[249] The difference likely comes from the lower acidity of EtOH in comparison with perfluoro alcohols, normally used for dihydrogen bonding.

Analogously to the reactions of $(ArN)Mo(H)(Cl)(PMe_3)_3$ (**III-6**) with carbonyls (benzaldehyde and cyclohexanone) and ethanol, the stoichiometric treatment of **III-6** with organic nitriles leads to the formation of the products of nitrile insertion into the Mo-H bond. Thus, the reactions of complex **III-6** with acetonitrile and benzonitrile selectively afford the methylenamide derivatives $(ArN)Mo(Cl)(N{=}CHR)(PMe_3)_2$ (R = Me (**III-141**) and Ph (**III-142**); Scheme 129). Both products were characterized by multinuclear NMR spectroscopy and the structure of **III-142** was also confirmed by X-ray analysis (see Table 34, chapt. VI). The characteristic feature of both products is the methylenamide N=C*H*R proton, which in the ^{1}H-NMR spectrum gives rise to P-coupled up-field signals at 6.15 (m, $^3J_{H\text{-}H}$ = 5.1 Hz) and 7.23 ppm (t, $^4J_{H\text{-}P}$ = 6.0 Hz) for **III-141** and **III-142**, respectively. These proton signals are coupled in the ^{1}H-^{13}C HSQC spectrum to the ^{13}C-NMR resonances at 145.4 (d, $^3J_{C\text{-}P}$ = 11.3 Hz) and 150.2 ppm, respectively.

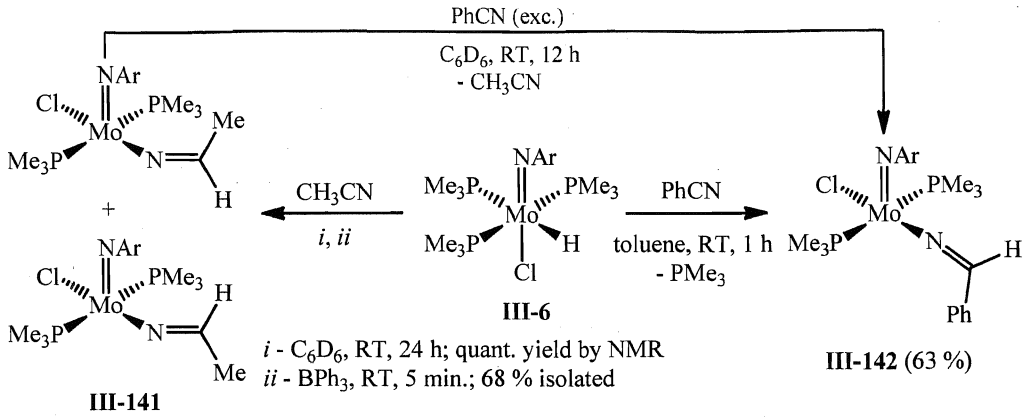

Scheme 129. Reactions of (ArN)Mo(H)(Cl)(PMe_3)$_3$ (**III-6**) with nitriles.

In their IR spectra, complexes **III-141** and **III-142** do not exhibit any characteristic band, which could be assigned to the C=N stretching. Similar observations were also made for the previously reported late transition metal analogues $ReCl_2$(N=HR)LL' (R = Me or Ph, L = py, L' = monophosphine),[231b] *cis*-[ReCl{NC(E)C_6H_4X-4}(dppe)$_2$]Y (E = H, X = OMe, Me, H, F, Cl, Y = BF_4; E = $SiMe_3$, X = Me, Y = CF_3SO_3), and *trans*-[Re-

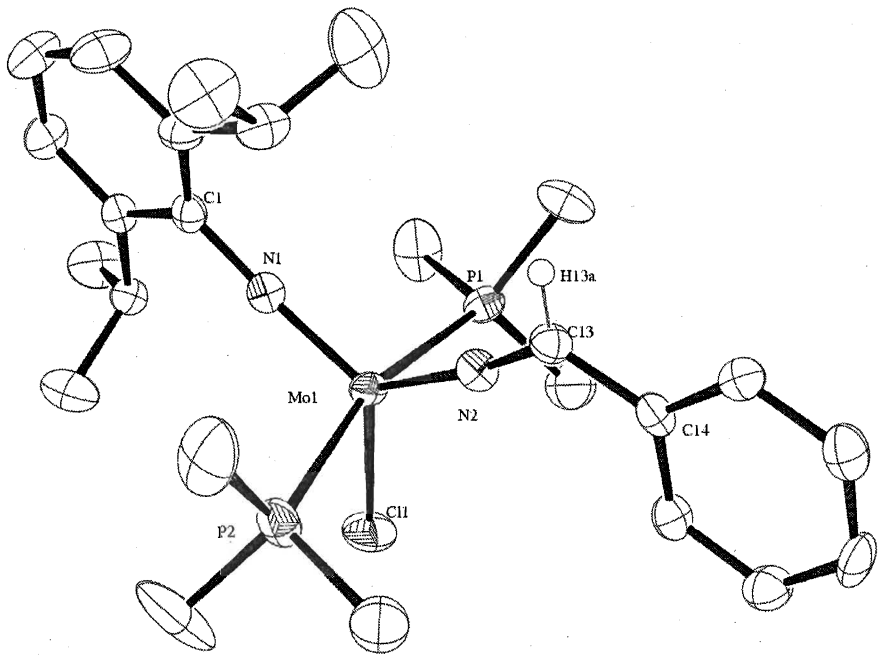

Figure 43. ORTEP plot of the molecular structure of **III-142** (one of two independent molecules; hydrogen atoms except methylenamide C*H* are omitted for clarity). Anisotropic displacement parameters are plotted at 50 % probability.

Table 23. Selected bond distances (Å) and angles (°) for complex **III-142**.

distances, Å		angles, °	
Mo1-N1	1.761(4)	Mo1-N1-C1	175.0(3)
Mo1-N2	1.843(4)	Mo1-N2-C13	172.3(4)
Mo1-Cl1	2.4341(14)	N1-Mo1-N2	116.45(17)
Mo1-P1	2.4929(14)	Cl1-Mo1-N2	122.42(13)
Mo1-P2	2.4846(15)	P1-Mo1-P2	164.60(5)
N2-C13	1.279(6)	P1-Mo1-N2	85.70(5)

$Cl\{NC(H)C_6H_4X\text{-}4\}(dppe)_2][BF_4]$ (X = NEt_2, OMe, H, F, Cl),[250] although there are cases[230c, 231] when the C=N vibrations of methylenamide transition metal compounds were detected as medium to weak bands in the range 1525-1575 cm^{-1}. The strong dependence of the $\nu_{C=N}$ on the nature of co-ligands was demonstrated by Leigh *et al.* for $[Mo(\eta^5\text{-}C_5H_5)L_2\{NC(^tBu)Ph\}]$ (L = CO or PPh_3).[231c]

(ArN)Mo(Cl)(N=CHPh)$(PMe_3)_2$ (**III-142**) adopts a distorted Mo-centred trigonal bipyramidal geometry (Figure 43), with PMe_3 ligands lying in the apical positions. The chloride, imido, and methylenamide substituents are coplanar and occupy equatorial positions with the *trans*- arrangement of the ArN^{2-} and N=CHPh ligands and *trans*-PMe_3 groups. The Mo1-N1-C1 linkage in **III-142** is almost linear (175.0(3) °; Table 23), indicating that the imido group acts as a 6 electron donor to the molybdenum centre.[244b] The electron deficiency at Mo is quenched by additional donation of a lone pair of the methylenamide nitrogen atom, which results in the observation of increased Mo1-N2-C13 angle (172.3 (4) °; Table 23). Such donation increases the Mo1-N2 bond order making it closer to a double bond character (compare the Mo1-N2 and Mo1-N1 distances of 1.843(4) and 1.761(4) Å, respectively (Table 23); also compare with the single Mo1-N1 bond of 2.062(4) Å for the agostic silylamide **III-1** (Table 5)).

Interestingly, (ArN)Mo(Cl)(N=CHPh)$(PMe_3)_2$ (**III-142**) can be also obtained by the treatment of the methyl derivative (ArN)Mo(Cl)(N=CHMe)$(PMe_3)_2$ (**III-141**) with excess benzonitrile (Scheme 129). The reaction takes place overnight at room temperature leading to the release of acetonitrile. Analogous β-C-H activation of methyleneamido ligand with the dissociation of PhCN was also observed in the reaction of **III-142** with benzaldehyde, which affords in the presence of PMe_3 the benzoxy triphosphine complex

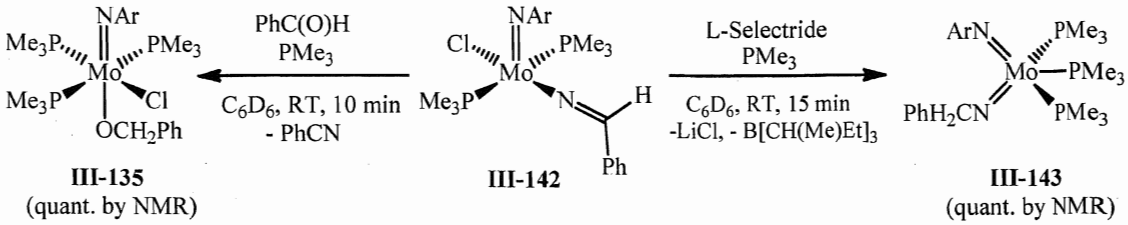

Scheme 130. Reactions of **III-142** with benzaldehyde and L-Selectride.

$(ArN)Mo(Cl)(OCH_2Ph)(PMe_3)_3$ (**III-135**; Scheme 130). In contrast, complex **III-142** does not react with acetonitrile and ketones (acetone or acetophenone) even upon heating the mixture up to 50 °C.

Treatment of compound **III-142** with an equivalent of L-Selectride in the presence of PMe_3 leads to selective formation of an asymmetric bis(imido) complex $(ArN)(PhCH_2N)Mo(PMe_3)_3$ (**III-143**; Scheme 130). The reaction presumably goes *via* the formation of a hydride intermediate, which undergoes intramolecular insertion of the methylenamide fragment into the Mo-H bond, forming the imido substituent. Thus, the reaction sequence including the treatment of $(ArN)Mo(H)(Cl)(PMe_3)_3$ (**III-6**) with organic nitriles, followed by the addition of L-Selectride could be used as a synthetic method for the preparation of a series of asymmetric Mo(IV) bis(imido) phosphine complexes. Such asymmetric bis(imides) have not yet been reported.

To confirm the suggestion of the intermediacy of $(ArN)Mo(Cl)(N{=}CHPh)(PMe_3)_2$ (**III-142**) in the catalytic hydrosilation of benzonitrile mediated by $(ArN)Mo(H)(Cl)(PMe_3)_3$ (**III-6**), we performed a reactivity study of **III-142** towards hydrosilanes. Thus, the reaction of complex **III-142** with $PhSiH_3$ at 50 °C after 2 weeks recovers the starting hydrido chloride **III-6** and shows formation of a mixture of silated imines, $PhH_2Si(N{=}CHPh)$, $PhHSi(N{=}SiHPh)_2$, and $PhCH_2N(SiH_2Ph)$. Similar slow (a few weeks) transformation of **III-142** into **III-6** was also observed upon the treatment with more Lewis acidic silanes, PMHS and $(EtO)_3SiH$. We believe that the reaction starts with the silane attack on the nitrogen atom of the [N=CHPh] ligand. In this respect, the lack of reactivity of $(ArN)Mo(Cl)(N{=}CHPh)(PMe_3)_2$ (**III-142**), as well as the slow catalytic hydrosilation of PhCN, could be accounted for by the significantly reduced basicity of the methylenamide nitrogen, owing to the additional donation of its lone pair to molybdenum.

On the other hand, addition of a reasonably acidic catecholborane to a solution of **III-142** in C_6D_6 leads to formation of the hydrido chloride complex **III-6**, accompanied by the production of a bis(borylated) amine, $PhCH_2N(BCat)_2$. The hydroboration of benzonitrile with CatBH can be done under catalytic conditions using 5.0 mol. % load of $(ArN)Mo(H)(Cl)(PMe_3)_3$ (**III-6**). After overnight at room temperature, the reaction is complete affording selectively $PhCH_2N(BCat)_2$ (TON = 20, TOF = 2). To the best of our knowledge, such catalytic addition of hydroboranes to organic nitriles is unprecedented in the literature.

Addition of styrene to a solution of $(ArN)Mo(H)(Cl)(PMe_3)_3$ (**III-6**) in C_6D_6 does not lead to the insertion of $PhCH{=}CH_2$ into the Mo-H bond. Instead it results in reversible dissociation of PMe_3 and the formation of the adduct $(ArN)Mo(H)(Cl)(PMe_3)_2(\eta^2\text{-}CH_2{=}CHPh)$ (**III-144**; compare with *trans*-$(ArN)Mo(H)(Cl)(\eta^2\text{-}PhC(O)H)(PMe_3)_2$ (**III-136**)) in a mixture with the starting material. Analogous reaction in the presence of an equivalent of BPh_3 quantitatively affords complex **III-144**, accompanied by the release of $Ph_3B{\cdot}PMe_3$ (Scheme 131). In contrast to *trans*-$(ArN)Mo(H)(Cl)(\eta^2\text{-}PhC(O)H)(PMe_3)_2$ (**III-136**), the treatment of compound **III-144** with one equivalent PMe_3 does not afford

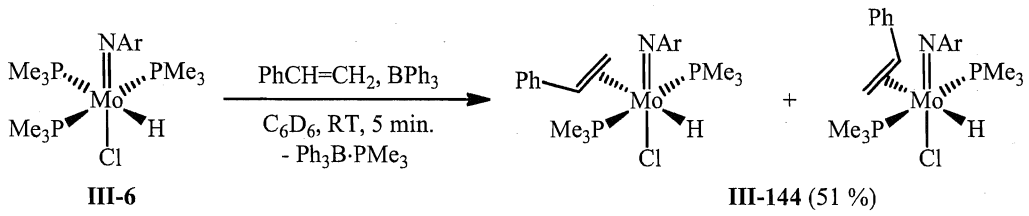

III-6 **III-144** (51 %)

Scheme 131. Reaction of $(ArN)Mo(H)(Cl)(PMe_3)_3$ (**III-6**) with styrene.

an insertion product. The reaction gives only substitution of the $\eta^2\text{-}CH_2{=}CHPh$ ligand to recover the hydrido chloride **III-6**. Compound **III-144** was characterized by IR and multinuclear NMR analysis, which reveals the presence of two isomers, depending on the orientation of the styrene ligand (ratio 7:1, according to $^{31}P\{^1H\}$-NMR analysis). In the ^1H-NMR spectrum, the hydride ligand of the major isomer of **III-144** gives rise to a down-field signal at 6.84 ppm (multiplet), coupled in the $^1H\text{-}^{31}P$ HSQC spectrum at -18 °C to two nonequivalent ^{31}P-NMR resonances at 0.4 (d, $^2J_{P\text{-}P}$ = 111.0 Hz) and 1.0 ppm (d, $^2J_{P\text{-}P}$ = 111.0 Hz). For the minor isomer of **III-144**, the Mo*H* signal shows up as a doublet of doublets at 5.97 ppm ($^2J_{H\text{-}P}$ = 51.3 Hz, $^2J_{H\text{-}P}$ = 31.8 Hz). At -18 °C, the ^{31}P-NMR

spectrum of the minor isomer of **III-144** also contains two coupled to each other signals at -2.2 (d, $^2J_{P\text{-}P}$ = 103.7 Hz) and 0.8 ppm (d, $^2J_{P\text{-}P}$ = 103.7 Hz). The large value of the $^2J_{P\text{-}P}$ coupling constants for both isomers indicate the *trans*- arrangement of PMe_3 ligands consisted with the structure depicted in Scheme 131. IR analysis of **III-144** also supports the presence of the hydride ligand, showing a Mo-H stretch at 1757 cm^{-1}. The η^2-coordination of styrene results in the observation, in the ^{1}H-NMR spectrum, of three nonequivalent up-field shifted C*H* signals at 4.08 ppm, 3.50 ppm, and 2.63 ppm (3.82 ppm, 3.33 ppm, and 3.18 ppm for the minor isomer), coupled in the ^{1}H-^{13}C HSQC spectrum to the ^{13}C-NMR resonances at 60.5 and 49.6 ppm (72.2 and 51.7 ppm for the minor isomer). (ArN)Mo(H)(Cl)$(PMe_3)_2(\eta^2$-CH_2=CHPh) (**III-144**) is thermally unstable in solution and slowly (1 week) decomposes to give $PhCH_2CH_3$ and a difficult-to-characterize mixture of unidentified compounds. The formation of ethylbenzene indicates that the insertion of the coordinated styrene ligand into the Mo-H bond is, indeed, possible but slow.

III.7.2.4 Stoichiometric reactivity of III-7 and the mechanism of carbonyl hydrosilation

To shed more light on the mechanism of carbonyl hydrosilation, we performed stoichiometric reactions. Similarly to (ArN)Mo(H)(Cl)$(PMe_3)_3$ (**III-6**), addition of excess $PhSiH_3$ to (ArN)Mo(H)$(SiH_2Ph)(PMe_3)_3$ (**III-7**) results in a relatively slow silane redistribution and coupling to yield Ph_2SiH_2, SiH_4, and PhH_2Si-SiH_2Ph.[211] The ^{1}H-^{1}H EXSY NMR experiment performed at room temperature did not indicate any exchange between the hydride and silyl in **III-7** and $PhSiH_3$. However, the observation of silyl/silane exchange process becomes possible upon increasing the temperature of the EXSY experiment up to 30 °C and higher. Noteworthy, no hydride/silyl or hydride/silane exchange was observed in the range 30 °C – 50 °C. At the same time, the treatment of compound **III-7** with an equivalent of $PhSiD_3$ after 10 min. at room temperature showed 59 % and 65 % of H/D scrambling in the hydride and silyl positions, respectively (Scheme 132). This fact establishes the possibility of H-Si elimination from **III-7**, albeit at a slower rate than silyl/silane exchange. Addition of (*m*-Tol)SiH_3 to **III-7** leads, after 10 min at room temperature, to a 27 % conversion of (ArN)Mo(H)$(SiH_2Ph)(PMe_3)_3$ (**III**

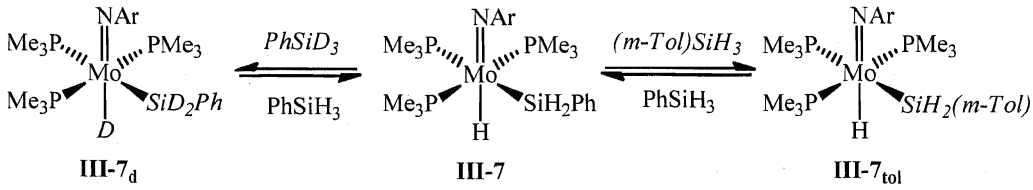

Scheme 132. Silyl/silane exchange for complex **III-7**.

7) into (ArN)Mo(H)[SiH_2(*m*-Tol)](PMe_3)$_3$ (**III-7$_{tol}$**) (Scheme 132). This experiment proves that the silyl group as a whole, not just the Si-bound hydrogens, is involved in exchange with the silane.

The activation parameters of the silyl/silane exchange in **III-7** were calculated (Figure 63, chapt. VI) using 1D ^{1}H EXSY NMR spectroscopy with the initial rate analysis[212, 251] and showed a dissociative mechanism of this process ($\Delta S^{\neq}$ = 34.6 ± 5.6 cal·K^{-1}·mol^{-1}, $\Delta H^{\neq}$ = 31.0 ± 1.7 kcal·mol^{-1}, $\Delta G^{\neq}_{295.1}$ = 20.8 ± 3.4 kcal·mol^{-1}, k(22 °C) = (2.7 ± 0.1)·10^{-3} s^{-1}). The rate of the silyl/silane exchange process depends on the concentration of PMe_3 added. At 35 °C, $1/k_{eff}$ is proportional to the concentration of phosphine and exhibit a saturation behaviour upon the increase of PMe_3 concentration (k_1(35 °C) = (6.7 ± 0.9)·10^{-3} s^{-1}; Figure 44). This observation suggests that the dominating pathway for the silyl/si-

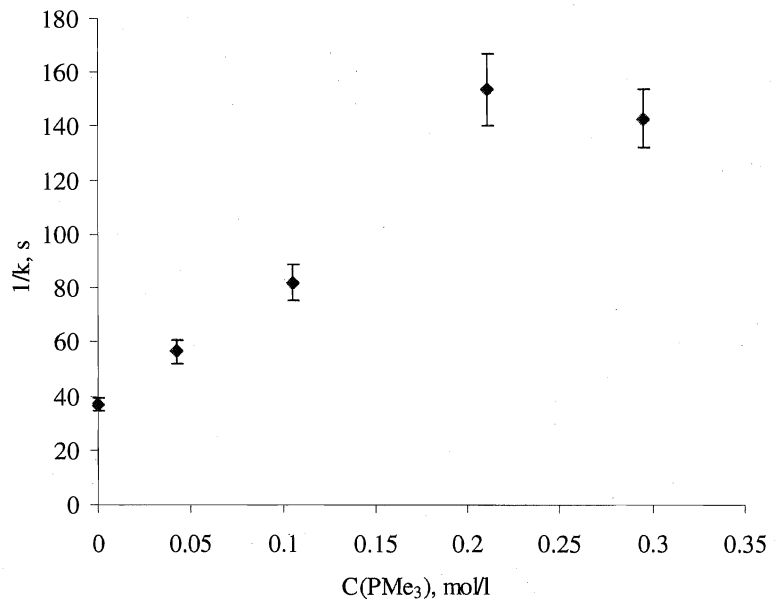

Figure 44. Dependence of the rate constant of the silyl/silane exchange between **III-7** and $PhSiH_3$ at 30 °C on the concentration of PMe_3 added.

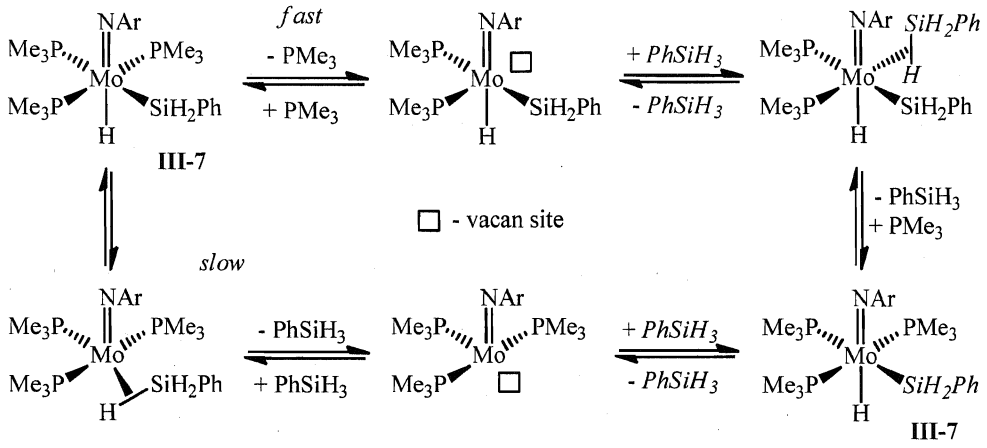

Scheme 133. Suggested mechanism for the silyl/silane exchange for complex **III-7**.

lane exchange involves PMe_3 dissociation. The activation parameters calculated for the silyl/silane exchange between $(ArN)Mo(H)(SiH_2Ph)(PMe_3)_3$ (**III-7**) and $PhSiH_3$ in the presence of excess PMe_3 (ca. 7 equivalents; a pseudo-first order regime) revealed even larger value of the activation entropy ($\Delta S^{\neq}$ = 48.3 ± 7.0 cal·K^{-1}·mol^{-1}, $\Delta H^{\neq}$ = 36.0 ± 2.2 kcal·mol^{-1}, $\Delta G^{\neq}_{295.1}$ = 21.8 ± 4.2 kcal·mol^{-1}), showing slower reaction (k(22 °C) = (6.3 ± 0.1)·10^{-4} s^{-1} *vs.* k(22 °C) = (2.7 ± 0.1)·10^{-3} s^{-1} for the exchange without PMe_3; see Figure 64, chapt. VI). All these observations suggest the mechanism of the exchange between **III-7** and $PhSiH_3$ depicted in Scheme 133, which involves two competing pathways: fast, based on PMe_3 dissociation, and reasonably slow, based on $PhSiH_3$ dissociation.

DFT calculations of the pathways of silyl/silane exchange performed for the model system $(PhN)Mo(H)(SiH_2Me)(PMe_3)_3$ (**III-7'**) and $MeSiH_3$ supported the proposed mechanism (Scheme 133). In accord with our experimental observations, the most plausible intermediates of this reaction are the bis(silyl) dihydride complex $(PhN)Mo(H)_2(SiH_2Me)_2(PMe_3)_2$ (**A**) and the triphosphine imido compound $(PhN)Mo(PMe_3)_3$ (**F**; Scheme 134). Two mechanisms, dissociative and associative, have been considered in calculations but the pathways including the dissociation of either PMe_3 or $MeSiH_3$ have been found to be preferable. Rewardingly, the transition state $\mathbf{TS_E}$ for the route involving dissociation of phosphine is at least 7.5 kcal/mol more stable than the $\mathbf{TS_F}$ for silane dissociation (Scheme 134), which is in accord with our observations by EXSY that the hydride ligand does not contribute to the main exchange pathway.

Surprisingly, the ^{31}P-^{31}P EXSY VT NMR as well as 1D ^{31}P EXSY NMR experiments of a mixture of (ArN)Mo(H)(SiH_2Ph)(PMe_3)$_3$ (**III-7**) and an equivalent of PMe_3 indicate fast intra- and slow intermolecular phosphine exchange ($\Delta S^{\neq}_{intra-}$ = 14.6 ± 5.2 cal·K^{-1}·mol^{-1}, $\Delta H^{\neq}_{intra-}$ = 23.0 ±1.7 kcal·mol^{-1}, $\Delta G^{\neq}_{295.1,\ intra-}$ = 18.7 ± 3.2 kcal·mol^{-1}, k_{intra-}(22 °C) = (9.1 ± 0.1)·10^{-2} s^{-1} (see Figure 65, chapt. VI) *vs.* $\Delta S^{\neq}_{inter-}$ = 30.9 ± 10.6 cal·K^{-1}·mol^{-1}, $\Delta H^{\neq}_{inter-}$ = 30.3 ± 3.4 kcal·mol^{-1}, $\Delta G^{\neq}_{295.1,\ inter-}$ = 21.2 ± 6.5 kcal·mol^{-1}, k_{inter-}(22 °C) = (1.82 ± 0.08)·10^{-3} s^{-1} (see Figure 66, chapt. VI)). Due to the fact that intramolecular exchange occurs easier than the intermolecular one giving the usual strereochemical rigidity of octahedral complexes and the stability of related complex (ArN)Mo(H)(Cl)(PMe_3)$_3$ (**III-6**), we considered the possibility of conversion of **III-7** into a non-rigit species by SiH_2Ph migration to imide, but DFT calculations show that this pathway is energetically too costly. Therefore, we conclude that fast intramolecular PMe_3 exchange in the compound **III-7** proceeds *via* intramolecular "twist" mechanism.[252]

Interestingly, the addition of excess $PhSiH_3$ (ca. 10 equiv.) to a mixture of (ArN)Mo(H)(SiH_2Ph)(PMe_3)$_3$ (**III-7**) and PMe_3 simplifies the intermolecular PMe_3 exchange ($\Delta S^{\neq}_{inter-}$ = 11.7 ± 12.4 cal·K^{-1}·mol^{-1}, $\Delta H^{\neq}_{inter-}$ = 23.9 ± 4.0 kcal·mol^{-1}, $\Delta G^{\neq}_{295.1,\ inter-}$ = 20.5 ± 7.7 kcal·mol^{-1}, k_{inter-}(22 °C) = (4.0 ± 0.04)·10^{-3} s^{-1}; see Figure 67, chapt. VI), indicating that silane can somehow support the PMe_3 dissociation. At the moment, we can not explain this experimental result. Attempted DFT calculations of silane-assisted PMe_3 dissociation have not so far yielded a transition state lower than the $\mathbf{TS_E}$ for direct phosphine dissociation.

Treatment of (ArN)Mo(H)(SiH_2Ph)(PMe_3)$_3$ (**III-7**) with excess PhC(O)H after 5 min. at room temperature initially leads to the elimination of the hydrosilation product, $PhHSi(OBn)_2$,[160, 214, 215b] and exclusive formation of (ArN)Mo(η^2-PhC(O)H)$_2$(PMe_3)$_2$ (**III-145*PMe$_3$**; Scheme 135). The product is highly fluxional even at – 20 °C. However,the $^{31}P\{^1H\}$-NMR spectrum taken at – 60 °C shows two doublets ($^2J_{P\text{-}P}$ = 218.7 Hz) at 8.0 and 6.4 ppm for two nonequivalent *trans*-PMe_3 ligands. Carbonyl protons of two benzaldehyde ligands of **III-145*PMe$_3$** appear in the ^{1}H-NMR spectrum as broad signals at 5.42 (bs) and 5.18 ppm (bd, $J_{H\text{-}P}$ = 9.6 Hz), coupled in the ^1H-^{13}C HSQC spectrum to the carbonyl carbons at 85.2 and 86.1 ppm, respectively. Increasing the temperature of the NMR experiment up to - 40 °C results in PMe_3 dissociation and

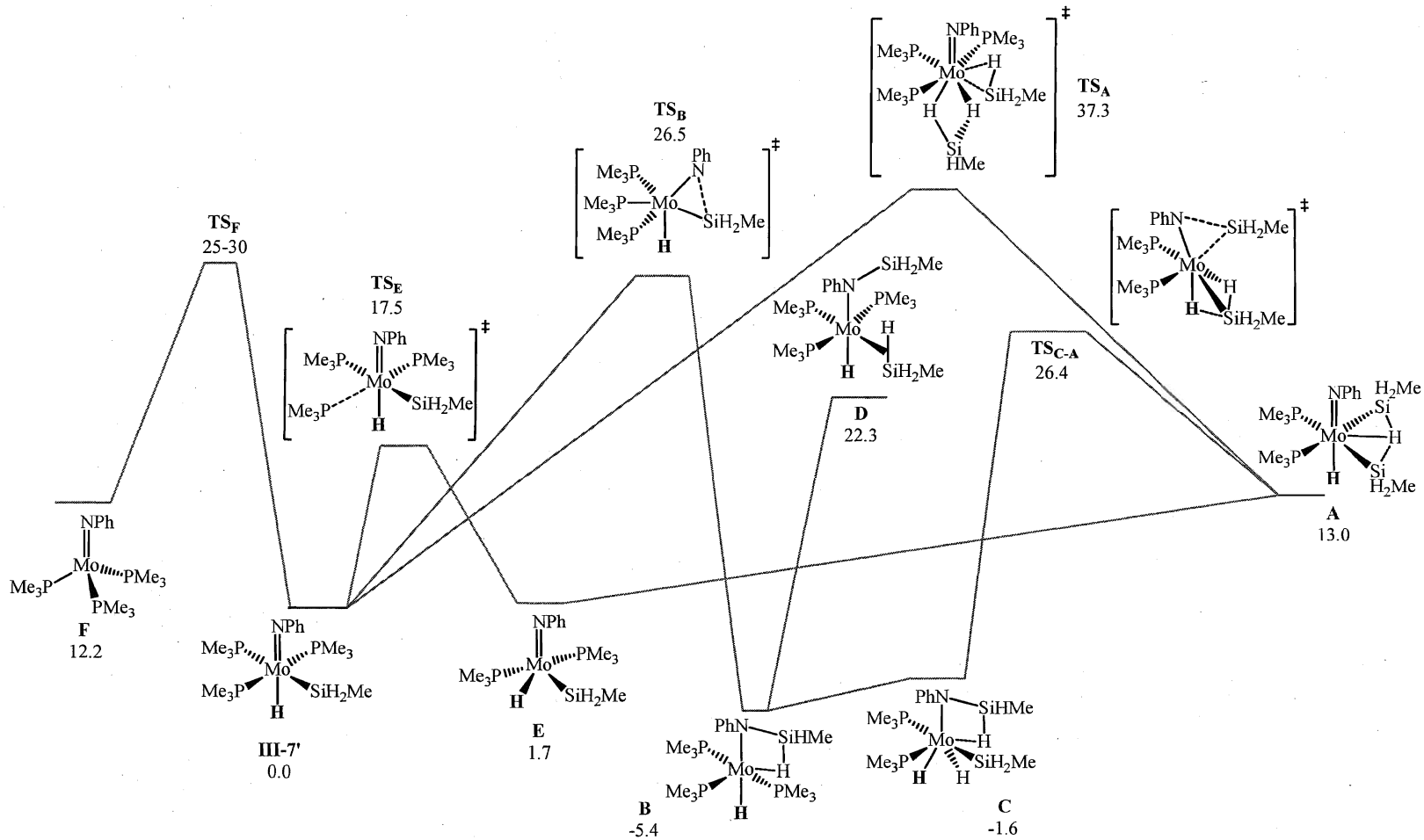

Scheme 134. Dissociative and non-dissociative mechanisms for the exchange processes between **III-7**, $PhSiH_3$, and PMe_3 (Gibbs free energies are expressed in $kcal \cdot mol^{-1}$).

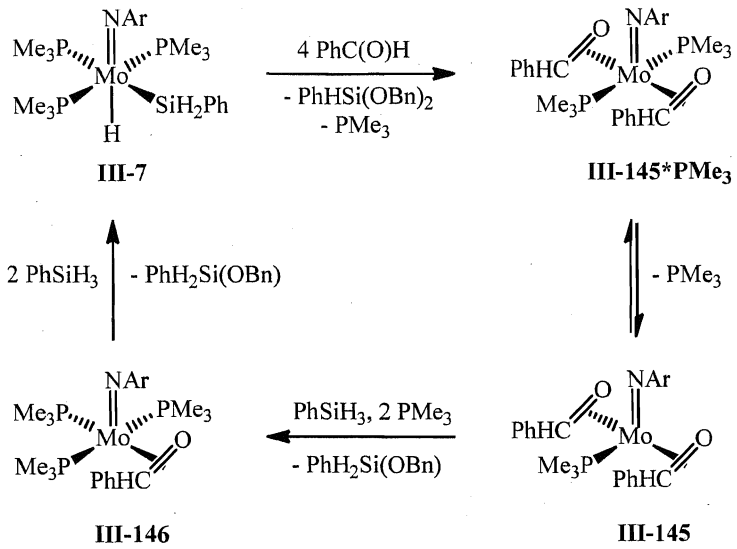

Scheme 135. Reactivity of complex **III-7** towards benzaldehyde.

formation of a mono(phosphine) derivative (ArN)Mo(η^2-PhC(O)H)$_2$(PMe$_3$) (**III-145**) (Scheme 135), which was characterized by IR and multinuclear NMR spectroscopy, and X-Ray diffraction analysis (see Table 35, chapt. VI). The compound is fluxional in the presence of PMe$_3$ and ^{31}P-^{31}P EXSY NMR spectra revealed exchange between **III-145**, **III-145*PMe$_3$** and phosphine even at -30 °C. The ^{1}H-NMR spectrum of **III-145** shows two nonequivalent up-field *H*C=O signals at 5.77 and 3.33 ppm, coupled in the ^{1}H-^{13}C HSQC NMR spectrum to the carbonyl carbons at 74.8 and 84.0 ppm, respectively. The formulation of complex **III-145** as an η^2-adduct is supported by the up-field shift of the carbonyl proton and carbon signals in the ^{1}H- and ^{13}C-NMR spectra, respectively, as well as the red-shift of the C=O stretches in the IR spectrum (1596 cm^{-1}, and 1487 cm^{-1}).[223] The isolation of complex **III-145** is hampered due to its instability in vacuum; however, cooling the reaction mixture down to -30 °C allowed us to crystallize **III-145** in analytically pure form.

(ArN)Mo(η^2-PhC(O)H)$_2$(PMe$_3$) (**III-145**) has a distorted tetrahedral structure (Figure 45) with the imido ligand lying in the apical position and two benzaldehyde ligands in the equatorial positions. The almost linear Mo1-N1-C15 angle of 166.51(18) ° (Table 24) suggests that the imido ligand acts as a 6-electron donor to the metal,[244b] stabilizing the 16 electron valence shell. The slightly different Mo-O (1.9862(18) and 2.0012(18) Å) and Mo-C distances (2.131(3) and 2.126(3) Å) in **III-145** indicate the difference in redistri-

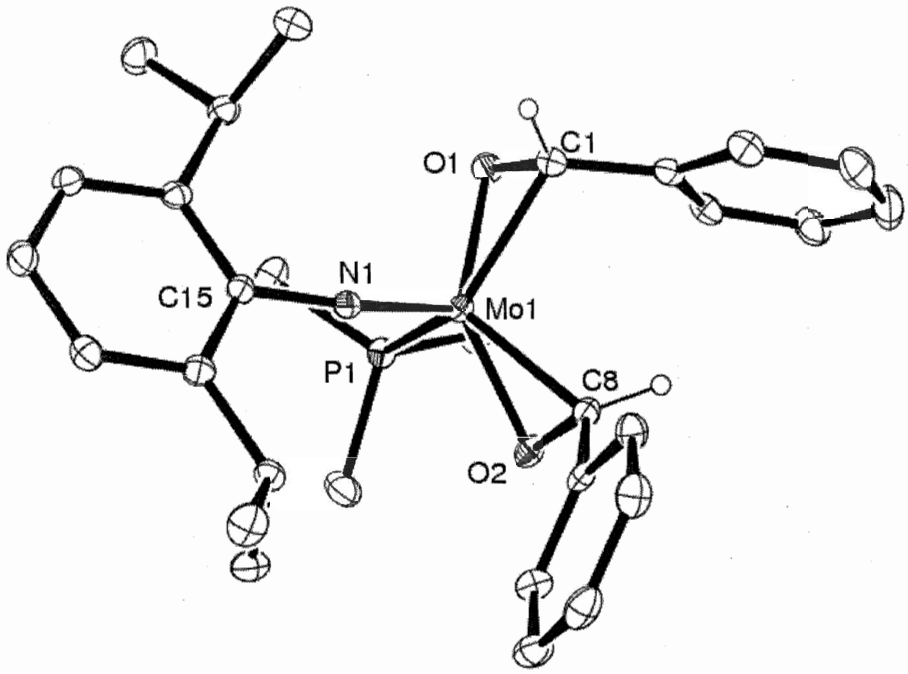

Figure 45. ORTEP plot of the molecular structure of **III-145** (H atoms, except CO*H*, are omitted for clarity). Anisotropic displacement parameters are plotted at 50 % probability.

Table 24. Selected bond distances (Å) and angles (°) for complex **III-145**.

distances, Å		angles, °	
Mo1-N1	1.743(2)	Mo1-N1-C15	166.51(18)
Mo1-O1	1.9862(18)	O1-Mo1-C1	38.71(9)
Mo1-O2	2.0012(18)	O1-Mo1-C8	38.79(8)
Mo1-C1	2.131(3)	O1-C1-Mo1	64.92(13)
Mo1-C8	2.126(3)	O2-C8-Mo1	65.68(13)
Mo1-P1	2.5250(7)	Mo1-O1-C1	76.37(13)
O1-C1	1.371(3)	Mo1-O2-C8	75.53(13)
O2-C8	1.376(3)	N1-Mo1-P1	103.34(7)

bution of electron density between two benzaldehyde ligands (Table 24). The Mo-P bond is significantly elongated (2.5250(7) Å *vs.* 2.4671(5), 2.4699(5), and 2.4861(5) Å for (ArN)Mo(H)(SiH_2Ph)(PMe_3)$_3$ (**III-7**)), most likely, due to the presence of steric repulsions in the complex.

Treatment of (ArN)Mo(η^2-PhC(O)H)$_2$(PMe$_3$) (**III-145**) with an equivalent of PhSiH$_3$ in the presence of two equivalents PMe$_3$ at -15 °C gives hydrosilation of one of benzaldehyde ligands[160, 214, 215b] and formation of (ArN)Mo(η^2-PhC(O)H)(PMe$_3$)$_3$ (**III-146**; Scheme 135). Subsequent addition of excess silane at 0 °C cleanly regenerates (ArN)Mo(H)(SiH$_2$Ph)(PMe$_3$)$_3$ (**III-7**) and releases PhH$_2$Si(OBn). In the absence of PMe$_3$, complex **III-145** slowly reacts with PhSiH$_3$ at 5 °C to give **III-7**, toluene (the result of complete reduction of PhC(O)H), and other unidentified products, which contain either few benzaldehyde or PMe$_3$ ligands. However, the transformations described above are irrelevant to the real catalytic cycle because it runs in the presence of huge excess benzaldehyde and silane.

DFT calculations performed for the model system (PhN)Mo(H)(SiH$_2$Me)(PMe$_3$)$_3$ (**III-7'**) / MeC(O)H / MeSiH$_3$ revealed that the formation of bis(aldehyde) diphosphine complex (PhN)Mo(η^2-MeC(O)H)$_2$(PMe$_3$)$_2$ (**G**; Scheme 136) is profitable by 8.3 kcal/mol.

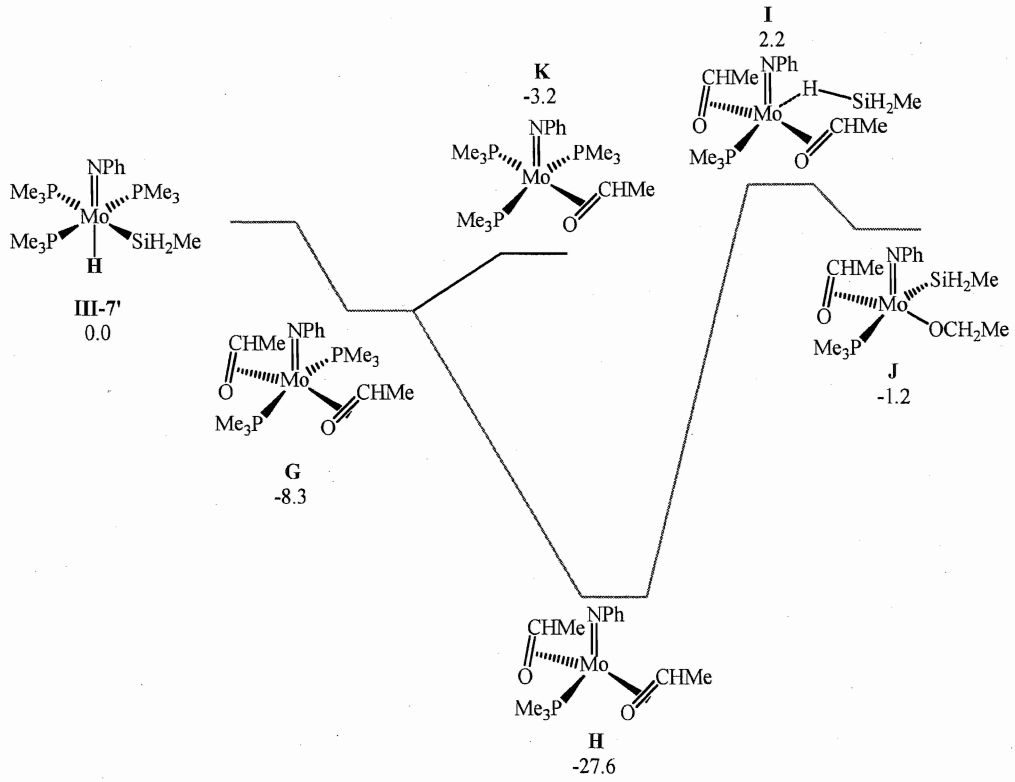

Scheme 136. DFT calculated mechanism for the reaction of model complex **III-7'** with MeC(O)H and MeSiH$_3$ (Gibbs free energies are expressed in kcal·mol^{-1}).

At the same time, the mono(phosphine) derivative (PhN)Mo(η^2-MeC(O)H)$_2$(PMe$_3$) (**H**) is 19.3 kcal/mol more stable than **G**. Addition of silane to compound **I** most likely leads to the formation of a silyl alkoxy derivative (PhN)Mo(SiH$_2$Me)(OCH$_2$Me)(η^2-MeC(O)H)(PMe$_3$) (**J**; ΔG = -1.2 kcal/mol), which could be produced through the η^1-silane intermediate (PhN)M(η^1-H-SiH$_2$Me)(η^2-MeC(O)H)$_2$(PMe$_3$) (**I**; Scheme 136). Although, the triphosphine benzaldehyde adduct (PhN)Mo(η^2-MeC(O)H)(PMe$_3$)$_3$ (**K**) has been found to be 3.2 kcal/mol more stable than the starting (PhN)Mo(H)(SiH$_2$Me)(PMe$_3$)$_3$ (**III-7'**), the intermediacy of the former in the real catalytic cycle is questionable due to the presence of excess aldehyde and silane in the reaction mixture.

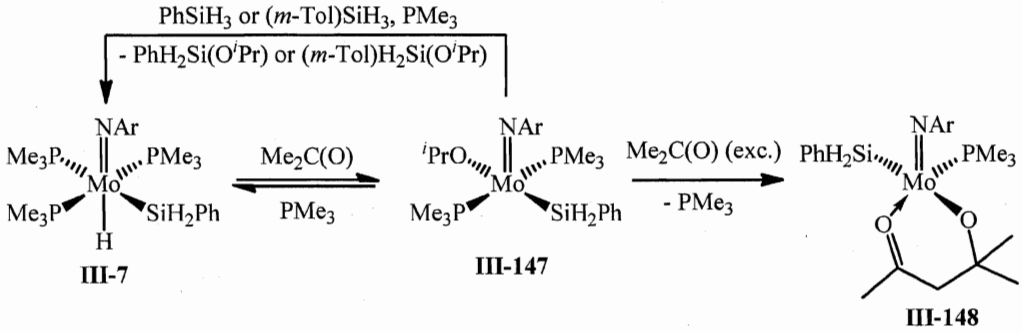

Scheme 137. Preparation of complex **III-147** and its reactivity.

In contrast to benzaldehyde, the reaction of (ArN)Mo(H)(SiH$_2$Ph)(PMe$_3$)$_3$ (**III-7**) with one equivalent of acetone results in the formation of an insertion product (ArN)Mo(SiH$_2$Ph)(O^{i}Pr)(PMe$_3$)$_2$ (**III-147**). Remarkably, the latter exists apparently in equilibrium with the starting material (Scheme 137). Treatment of **III-7** with 5 equivalents of Me$_2$C(O) shifts the equilibrium towards **III-147** showing almost full conversion of the starting material after 30 min. at room temperature. An increase of the reaction time (up to 12 hour) and/or concentration of acetone leads to further reaction affording the acetone coupling product (ArN)Mo(SiH$_2$Ph)(η^2-O-C(Me)$_2$CH$_2$C(O)Me)(PMe$_3$) (**III-148**; Scheme 137). The ^{1}H-NMR spectrum of (ArN)Mo(SiH$_2$Ph)(O^{i}Pr)(PMe$_3$)$_2$ (**III-147**) shows two classical equivalent Si*H* resonances at 5.82 ppm (bs), coupled in the ^{1}H-^{29}Si HSQC NMR spectrum to a ^{29}Si-NMR signal at 4.6 ppm. Two equivalent PMe$_3$ groups appear as a singlet at -5.9 ppm in the ^{31}P{^{1}H}-NMR spectrum suggesting the *trans*- arrangement of phosphine ligands.

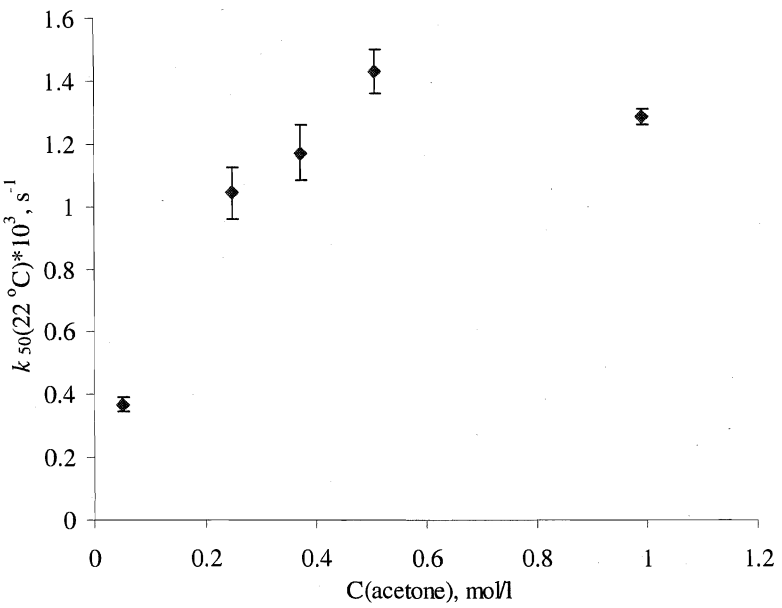

Figure 46. Dependence of the rate constant of the reaction of **III-7** with acetone at 22 °C on the concentration of the latter.

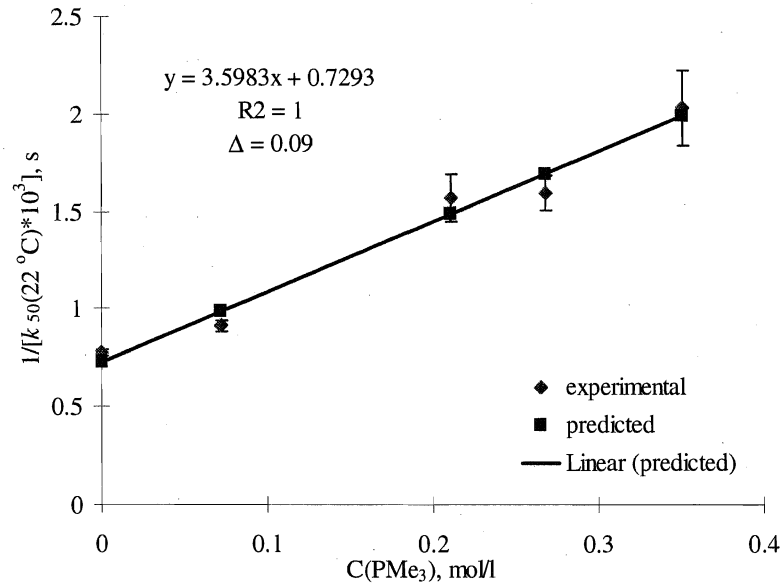

Figure 47. Dependence of the rate constant of the reaction of **III-7** with acetone (20 equiv.) at 22 °C on the concentration of PMe_3.

At large acetone concentrations, the reaction with (ArN)Mo(H)(SiH_2Ph)(PMe_3)$_3$ (**III-7**) obeys the pseudo-first order kinetics (k_1^{50}(22 °C) = (1.29 ± 0.21)·10^{-3} s^{-1}; Figure 46; see also Figure 68, chapt. VI). Furthermore, in the pseudo-first order regime (20-fold excess acetone) $1/k_{eff}$ is proportional to the concentration of added PMe_3 (Figure 47 and also Figure 69 in chapt. VI), which is in accordance with the rate-limiting phosphine dissociation step. Activation parameters for the reaction between **III-7** and excess acetone (ca. 20 equiv.; the pseudo-first order regime) were calculated using kinetic VT NMR experiments and revealed a dissociative mechanism ($\Delta S^{\neq}_{50}$ = 26.1 ± 12.0 cal·K^{-1}·mol^{-1}, $\Delta H^{\neq}_{50}$ = 30.0 ± 3.5 kcal·mol^{-1}, $\Delta G^{\neq}_{50,\ 295.1}$ = 21.3 ± 7.1 kcal·mol^{-1}; see Figure 70, chapt. VI), consistent with the kinetic NMR studies.

Interestingly, addition of excess PMe_3 (15 equiv.) to (ArN)Mo(SiH_2Ph)(O^{i}Pr)(PMe_3)$_2$ (**III-147**) leads to a full conversion of the latter to the starting complex (ArN)Mo(H)(SiH_2Ph)(PMe_3)$_3$ (**III-7**), accompanied by a release of a molecule of acetone. This observation establishes the reversibility of carbonyl insertion into the M-H bond which is unprecedented for early transition metals. The reverse reation most likely occurs *via* the β-CH activation in the O^{i}Pr group by a highly unsaturated Mo center.[u] This suggestion was further confirmed by the treatment of **III-147** with four equivalents of benzaldehyde, which results in the β-hydrogen transfer affording **III-145*PMe$_3$**, PhHSi(OBn)$_2$, and free acetone (Scheme 138). Furthermore, room temperature treatment of **III-147** with cyclohexanone gives the cyclohexoxy derivative (ArN)Mo(SiH_2Ph)(OCy)(PMe_3)$_2$ (**III-149**; could be independently prepared by a reaction of **III-7** with cyclohexanone) in a mixture with the starting material (~ 1:1). The C-H activation in **III-147** is also observed in the reaction with an equivalent of benzonitrile, which after 30 min. at room temperature leads to the formation of the methyleneamide compound (ArN)Mo(SiH_2Ph)(N=CHPh)(η^2-$Me_2C(O)$)(PMe_3)$_2$ (**III-150**, mixture of two isomers; Scheme 138).

[u] Considering ArN^{2-} as a 6 electron donor, the complex (ArN)Mo(SiH_2Ph)(O^{i}Pr)(PMe_3)$_2$ (**III-147**) is a 16 electron compound.

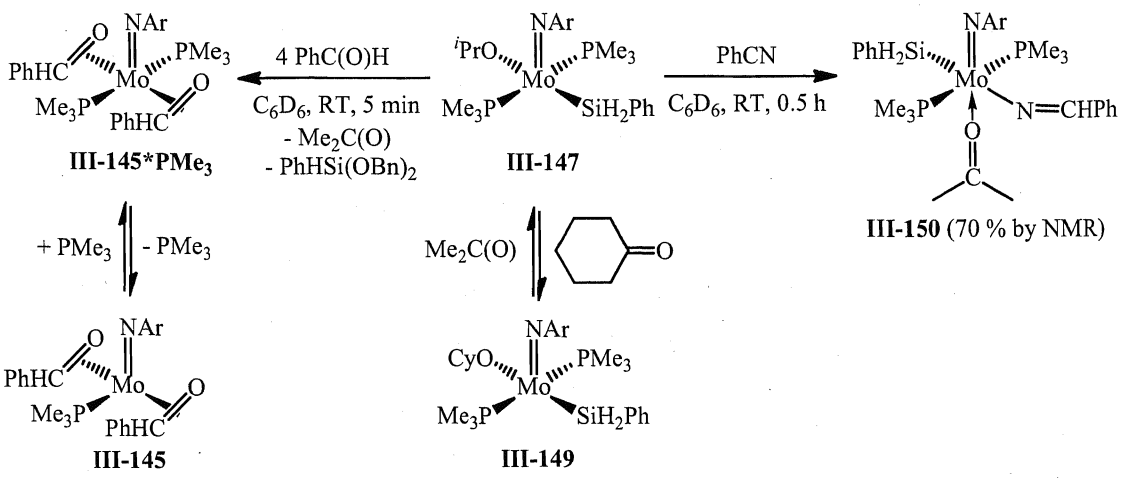

Scheme 138. Reactions **III-147** with carbonyls and PhCN.

In the presence of PMe_3, treatment of (ArN)Mo(SiH_2Ph)(O^iPr)(PMe_3)$_2$ (**III-147**) with one equivalent of $PhSiH_3$ affords the silylhydride complex (ArN)Mo(H)(SiH_2Ph)(PMe_3)$_3$ (**III-7**) and $PhH_2Si(O^iPr)$ (Scheme 137).[160, 221] An experiment with labelling silane (*m*-Tol)SiH_3 leads to the exclusive formation of (*m*-Tol)$H_2Si(O^iPr)$, indicating that the SiH_2Ph ligand of **III-147** is not involved in the hydrosilation process (spectator ligand). The reaction of complex **III-147** with $PhSiH_3$ was monitored by NMR analysis at low temperature. Unfortunately, no intermediate of the addition of silane to the O^iPr ligand was observed in NMR spectra. At -30 °C, a fast abstraction of the isopropoxy group by $PhSiH_3$ leads to the formation of the Mo(VI) bis(silyl) derivative (ArN)Mo(H)$_2$(SiH_2Ph)$_2$(PMe_3)$_2$ (**III-151**; Scheme 139). Interestingly, the intermediacy of a similar Mo(VI) complex (PhN)Mo(H)$_2$(SiH_2Me)(PMe_3)$_2$ (**A**) has been suggested by DFT studies on the exchange between (PhN)Mo(H)(SiH_2Me)(PMe_3)$_3$ (**III-7'**) and $MeSiH_3$ (Scheme 134).

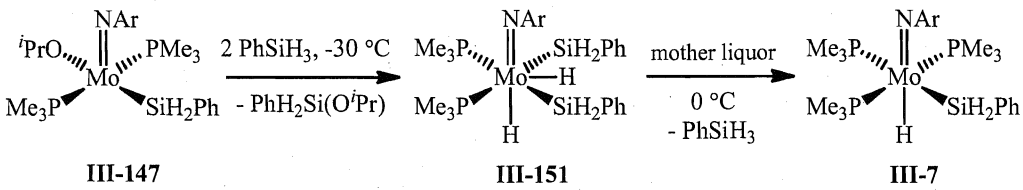

Scheme 139. Low temperature NMR scale reaction of complex **III-147** with $PhSiH_3$.

At -5 °C, the 1D ^{1}H EXSY NMR experiments indicate a fast exchange between $PhSiH_3$ and all Mo- and Si-bound protons of **III-151**, suggesting the intermediate formation of the Mo(IV) silane σ-complex, $(ArN)Mo(H)(SiH_2Ph)(\eta^2\text{-}H\text{-}SiH_2Ph)(PMe_3)_2$ (**III-152**). Warming the reaction mixture up to 0 °C leads to decomposition of the complex $(ArN)Mo(H)_2(SiH_2Ph)_2(PMe_3)_2$ (**III-151**) to a mixture of $(ArN)Mo(H)(SiH_2Ph)(PMe_3)_3$ (**III-7**) and unidentified products.

The mechanism of the catalytic hydrosilation of acetone mediated by **III-7** was elucidated using DFT calculations[v] for the model system $(PhN)Mo(H)(SiH_2Me)(PMe_3)_3$ (**III-7'**) / $Me_2C(O)$ / $MeSiH_3$ (Scheme 140). In accordance with our observations, the

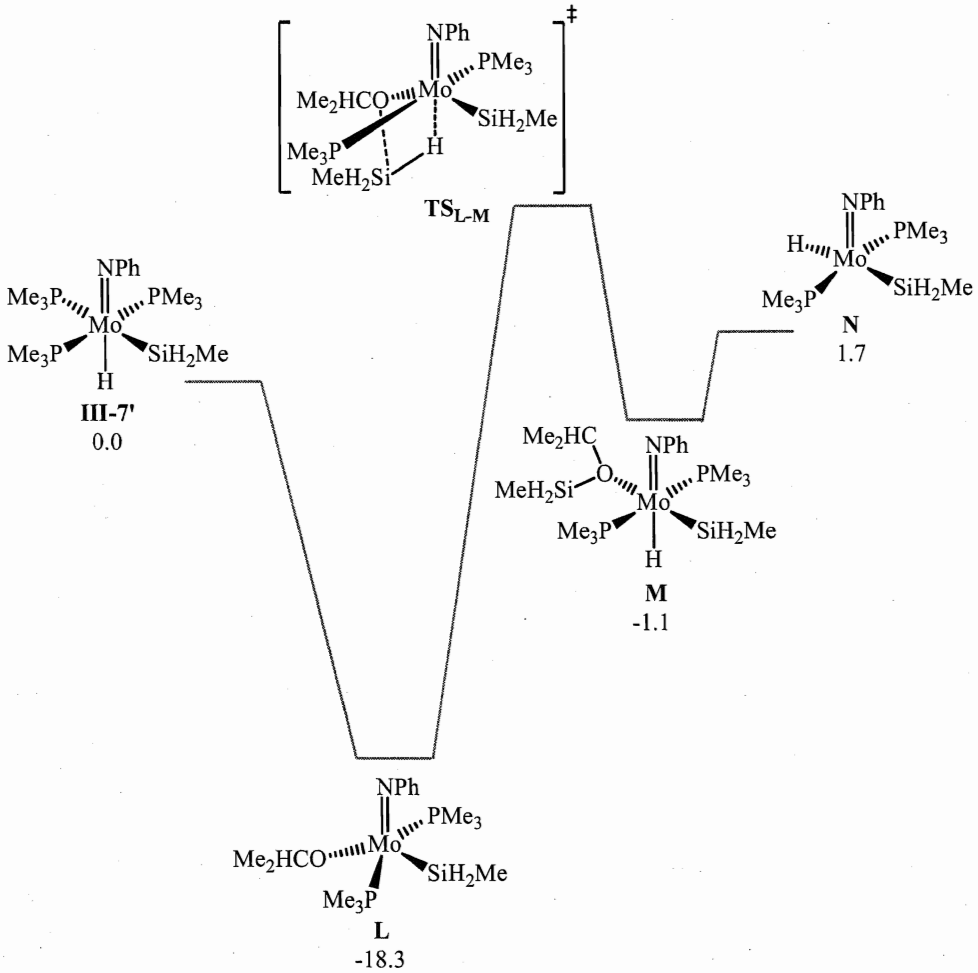

Scheme 140. DFT calculated mechanism for the reaction of model complex **III-7'** with acetone and $MeSiH_3$ (Gibbs free energies are expressed in kcal·mol^{-1}).

[v] The calculations were carried out by Prof. S. K. Ignatov (the University of Nizhnii Novgorod, Russia).

formation of the isopropoxy compound (PhN)Mo(SiH_2Me)(O^iPr)(PMe_3)$_2$ (**L**) stabilizes the system by 18.3 kcal/mol. Further addition of $MeSiH_3$ gives the silylhydride intermediate (PhN)Mo(H)(SiH_2Me)($O(^iPr)SiH_2Me$)(PMe_3)$_2$ (**M**), which, surprisingly, is even more stable than the starting complex **III-7'** by 1.1 kcal/mol (Scheme 140). Unfortunately, the transition state for this transformation has not been found yet. However, the proposed heterolytic Si-H activation pathway ($\mathbf{TS_{L\text{-}M}}$; Scheme 140) seems reasonable. Elimination of the silyl ether $MeH_2Si(O^iPr)$ furnishes the catalytic cycle with (PhN)Mo(H)(SiH_2Me)(PMe_3)$_2$ (**N**), which is destabilized by only 1.7 kcal·mol^{-1} relative to (PhN)Mo(H)(SiH_2Me)(PMe_3)$_3$ (**III-7'**). Thus, combining the experimental and computational observations, the overall catalytic scheme for the hydrosilation of acetone with $PhSiH_3$ in the presence of (ArN)Mo(H)(SiH_2Ph)(PMe_3)$_3$ (**III-7**) is similar to that one for (ArN)Mo(H)(Cl)(PMe_3)$_3$ (**III-6**) and involves the following steps: (i) substitution of PMe_3 with $Me_2C(O)$ and insertion of the latter into the Mo-H bond gives (ArN)Mo(SiH_2Ph)(O^iPr)(PMe_3)$_2$ (**III-147**); (ii) further σ-bond metathesis with $PhSiH_3$ forms the silyl ether adduct (ArN)Mo(H)(SiH_2Ph)($O(^iPr)SiH_2Ph$)(PMe_3)$_2$ (**III-153**),

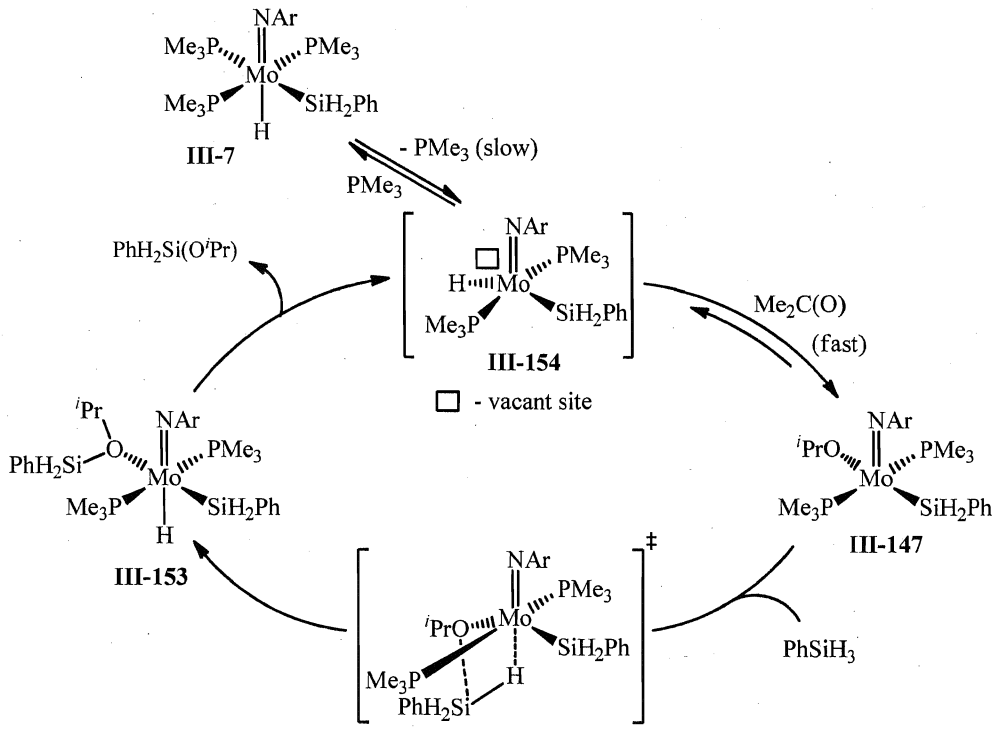

Scheme 141. Suggested mechanism for the catalytic hydrosilation of acetone with $PhSiH_3$ in the presence of **III-7**.

which upon dissociation of the hydrosilation product recovers the actual catalyst (ArN)Mo(H)(SiH_2Ph)(PMe_3)$_2$ (**III-154**; Scheme 141).

III.7.2.5 Reactions of III-7 with EtOH and PhCN

All attempts to elucidate the mechanism of ethanolysis of phenylsilane by the stoichiometric treatment of (ArN)Mo(H)(SiH_2Ph)(PMe_3)$_3$ (**III-7**) with EtOH were unsuccessful. Addition of excess ethanol to a solution of **III-7** in C_6D_6 leads to a fast (5 min at room temperature) decomposition of the complex, forming mainly the tetrahydride Mo(H_4)(PMe_3)$_3$ (**III-155**), which could be responsible for the observed catalysis. Preparation of the compound **III-155** has been previously described in the literature,[253] however, no studies of its catalytic activity were reported.

Analogously to the hydrido chloride derivative (ArN)Mo(H)(Cl)(PMe_3)$_3$ (**III-6**), the reaction of (ArN)Mo(H)(SiH_2Ph)(PMe_3)$_3$ (**III-7**) with two equivalents of benzonitrile affords, after one hour at room temperature, the product of nitrile insertion into the Mo-H bond, (ArN)Mo(SiH_2Ph)(N=CHPh)(NCPh)(PMe_3)$_2$ (**III-156**; Scheme 142). Compound **III-156** is metastable in solution and decomposes overnight *via* PMe_3 dissociation to give exclusively (ArN)Mo(SiH_2Ph)(η^3-N=C(Ph)-N=CHPh)(PMe_3) (**III-157**; Scheme 142), in which the additional coordination of the [N=CHPh] moiety to molybdenum is suggested on the basis of NMR analysis (see experimental details).

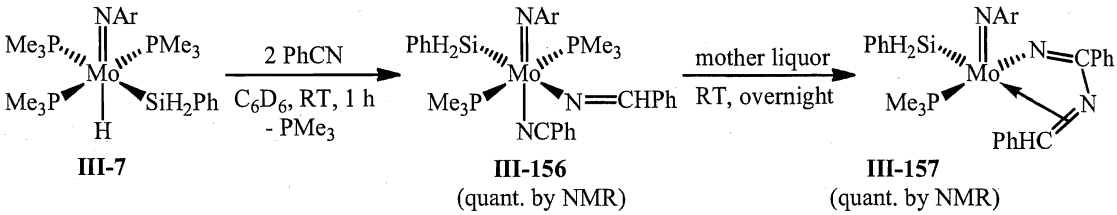

Scheme 142. Reaction of (ArN)Mo(H)(SiH_2Ph)(PMe_3)$_3$ (**III-7**) with benzonitrile.

In conclusion, the proposed mechanism of hydrosilation of unsaturated organic molecules mediated by the silylhydride complex (ArN)Mo(H)(SiH_2Ph)(PMe_3)$_3$ (**III-7**) strongly resembles the scheme suggested for (ArN)Mo(H)(Cl)(PMe_3)$_3$ (**III-6**), which starts with PMe_3 dissociation and insertion of organic substrate into the Mo-H bond. The higher catalytic activity of **III-7**, comparatively to **III-6**, could be explained by the difference in the positioning of the hydride ligand in these complexes (see Figures 36 and

37). Thus, the *cis*-arrangement of all three phosphine ligands and hydride ligand in compound **III-7** results in fast insertion into the Mo-H bond, without the rearrangement process postulated as a rate-determining step in the catalysis mediated by **III-6** (compare Schemes 126 and 141).

IV. Conclusions and Future Work

In the course of the present work we have carried out a detailed investigation of the imido/silane coupling reactions between $(RN)_2M(PR'_3)_n(L)$ (**IV-1**, where R = ^{t}Bu, Ar', Ar; M = Mo, W; R'$_3$ = Me_3, Me_2Ph, Me^iPr_2; L = PMe_3, η^2-C_2H_4) with chloro-substituted and chlorine-free hydrosilanes. For molybdenum, depending on the silane, the reactions lead to the formation of either chloro-substituted or silyl-substituted β-agostic silylamido complexes. In the case of tungsten bis(imides), addition of silanes affords metastable bis(imido) silylhydrides, which were found to decompose *via* the migration of the silyl group from the metal to the nitrogen of the imido ligand. At the same time, treatment of bis(imido) phosphine precursors of Mo and W with $HSiCl_3$ selectively gives the mono(imido) dichloride derivatives $(RN)MCl_2(PMe_3)_3$ (**IV-2**), accompanied by the release of silanimine dimers. Detailed low temperature VT NMR studies suggest the intermediacy of silanimine complexes $(RN)M(\eta^2$-RN=SiHCl$)(PMe_3)_2$ (**IV-3**).

For the fist time, we reported the catalytic and stoichiometric reactions of the novel silyl-substituted agostic silylamide $(ArN)Mo(SiH_2Ph)(\eta^3$-NAr-SiHPh-H$)(PMe_3)$ (**IV-4**) and provided experimental evidence for an unusual mechanism of these processes, which proceed *via* the silanimine intermediate $(ArN)Mo(\eta^2$-ArN=SiHPh$)(PMe_3)$ (**IV-5**). Such coupling of the silanimine moiety of **IV-5** with unsaturated organic molecules suggests the future reactivity study of $(^t$BuN$)Mo(H)(SiH_2Ph)\{(SiHPh)_2(\mu$-N^{t}Bu$)\}(PMe_3)_2$ (**IV-6**), which can be easily obtained by the reaction of $(^t$BuN$)_2Mo(PMe_3)(L)$ (L = PMe_3 (**IV-7**) or η^2-C_2H_4 (**IV-8**)) with excess $PhSiH_3$. By analogy with **IV-4**, we propose the high catalytic activity of complex **IV-6** in hydrosilation reactions.

In the course of investigation of the stoichiometric reactivity of compound **IV-4**, we discovered a novel Si-C coupling reaction with olefins and nitriles, which leads to the formation of $(ArN)Mo(R)(\eta^3$-NAr-SiHPh-CH=CHR'$)(PMe_3)$ (**IV-9**: R = H, R' = Ph; **IV-7**: R = Et, R' = H) and $(ArN)Mo(\eta^2$-NAr-SiHPh-CR=N$)(PMe_3)$ (**IV-10**: R = Ph, ^{i}Pr, ^{t}Bu). Complex **IV-9** was also found to be active in a diversity of hydrosilation reactions, which presumably start with the generation of the hydride derivative $(ArN)Mo(H)(\eta^3$-NAr-SiHPh-CH=$CH_2)(PMe_3)$ (**IV-11**). The mechanism of the formation of **IV-11** has been suggested on the basis of kinetic NMR studies.

Two other major objectives of the present thesis were devoted to the development of efficient synthetic approaches to the novel Mo(IV) mono(imido) hydride derivatives $(ArN)Mo(H)(R)(PMe_3)_3$ (R = Cl (**IV-12**), SiH_2Ph (**IV-13**)), investigation of their structural features and catalytic and stoichiometric reactivity. Compounds **IV-12** and **IV-13** have been found to catalyze a surprising variety of hydrosilation processes, which, according to stoichiometric reactions, kinetic studies of key steps, and model DFT calculations proceed *via* initial substrate activation but not silane addition. These results show promise as a new entry into the family of hydrosilation catalysts based on the early transition metal systems and expand the knowledge about the mechanistic aspects of hydrosilation catalysis, in general.

The study of the stoichiometric reactivity of $(ArN)Mo(H)(Cl)(PMe_3)_3$ (**IV-12**) and $(ArN)Mo(H)(SiH_2Ph)(PMe_3)_3$ (**IV-13**) towards aldehydes, ketones, olefins, and nitriles revealed the formation of products of insertion into the Mo-H bond. Intuitively, such compounds could serve as intermediates not only for hydrosilation but also for hydroge-

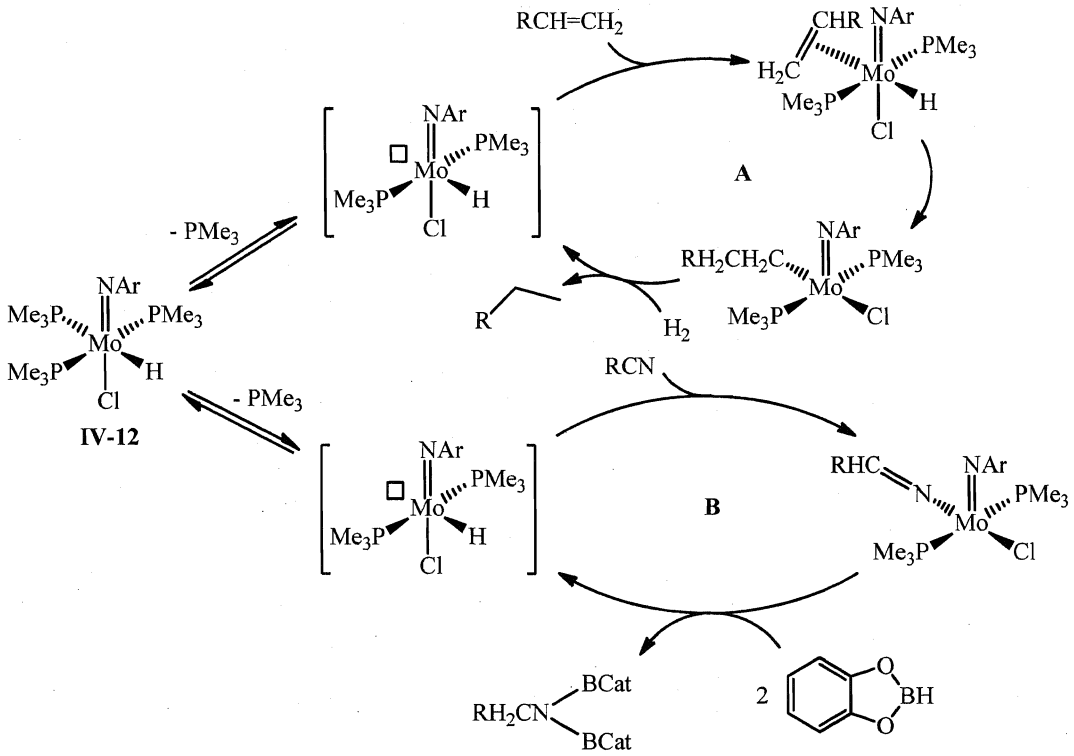

Scheme 143. Proposed catalytic cycles for hydrogentation of olefins (**A**) and hydroboration of nitriles (**B**) mediated by **IV-12**.

nation and hydroboration catalysis. Indeed, our preliminary results indicate that hydrido chloride **IV-12** is active in the unprecedented hydroboration of benzonitrile with catecholborane. More detailed research could result in the design of new hydroboration and hydrogenation catalytic systems based on the early transition metal complexes, which are extremely rare. For instance, plausible catalytic cycles for the hydrogenation of alkenes (**A**) and hydroboration of nitriles (**B**) by **IV-12** are illustrated in Scheme 143.

Lastly, 11 novel molybdenum imido complexes were characterized by single crysral X-ray diffraction. Six compounds, one W(VI) and five Mo(IV) derivatives, were found to be active in the catalytic hydrosilation of unsaturated organic molecules. In all the cases, the hydrosilation catalysis seems to proceed *via* the activation of the organic substrate.

V. Experimental

General methods and instrumentation

All manipulations were carried out using conventional inert atmosphere glove-box and Schlenk techniques. Dry diethyl ether, toluene, hexanes, and acetonitrile were obtained, using Grubbs-type purification columns, other solvents were dried by distillation from appropriate drying agents. C_6D_6, PhMe-d_8 were dried by distillation from K/Na alloy, and $CDCl_3$ was dried by distillation from CaH_2. NMR spectra were obtained with a Bruker DPX-300 and Bruker DPX-600 instruments (^{1}H: 300 and 600 MHz; ^{2}D: 92.1 MHz; ^{13}C: 75.5 and 151 MHz; ^{29}Si: 59.6 and 119.2 MHz; ^{31}P: 121.5 and 243 MHz; ^{11}B: 96.3 and 192.6 MHz). NMR analysis was done at room temperature unless specified. IR spectra were measured on a Perkin-Elmer 1600 FT-IR spectrometer. Elemental analyses were performed in "ANALEST" laboratories (University of Toronto). Correct elemental analyses for $(ArN)_2Mo(\eta^2\text{-}CH_2{=}CH_2)(PMe_3)_2$ and new $(RN)_2Mo(PR')_n$ were not obtained because these compounds are highly sensitive to air and for n = 3 easily loose the phosphine. $PhSiCl_3$, $(EtO)_3SiH$, $SiMe_4$, $SiCl_4$ Me_2SiHCl, MePhSiHCl, $PhMeSiCl_2$, PMe_3, PMe^iPr_2, PPh_3, PMe_2Ph, $BH_3(THF)$, BPh_3, CatBH, EtMgBr, (*m*-Tol)MgCl, $CuCl_2$, CuI, D_2O, $NaBH_4$, and $LiBH_4$ (solution in THF, 1M) were purchased from Aldrich. PEt_3 was generously donated by Cytec Canada Inc. Organic substrates (benzaldehyde, acetophenone, acetone, 1-hexene, cyclohexene, ethylene, styrene, benzonitrile, acetonitrile, ^{i}PrCN, ^{t}BuCN, 1-octyne, phenylacetylene, 3-hexyne, ethanol, and propanol-2) were purchased from Sigma-Aldrich and used without further purification. Amines ($PhNH_2$, $ArNH_2$, Ar'NH_2, Ar"NH_2, ^{t}BuNH$_2$, NEt_3, and 2,6-lutidine) were purchased from Sigma-Aldrich and distilled prior utilization. All catalytic, NMR scale reactions, and kinetic experiments were done under nitrogen atmosphere using NMR tubes equipped with Teflon valves. The structures and yields of all hydrosilated and hydrogenated products were determined by NMR analysis using tetramethylsilane as an internal standard.

Preparation of starting materials and reagents

Preparation of $(ArN)_2MoCl_2(DME)$ (III-11)[193]

$NaMoO_4$ (**III-10**) (5.0 g, 0.024 mol) was suspended in 200 ml of DME. NEt_3 (13.5 ml, 0.097 mol), Me_3SiCl (26.4 ml, 0.206 mol) and $ArNH_2$ (9.16 ml, 0.049 mol) were added sequentially to the suspension at room temperature, each over a period of about 5 min. The reaction mixture was heated at 65 °C overnight. During the heating the colour of the mixture became dark-red. Then the reaction mixture was cooled to room temperature and filtered to remove ammonium salts. The salts were washed with DME until the solvent ran through colorless. The volatile components were removed from the filtrate in vacuum to give a dark-red solid, which was washed three times with 20 ml of cold (-30 °C) hexane. Yield: 14.56 g, 99 %. The NMR spectra and the physical properties of the compound are identical to those previously reported in the literature.[193]

Preparation of $(Ar'N)_2MoCl_2(DME)$ (III-12)[193]

NEt_3 (19 ml, 0.136 mol), Me_3SiCl (37 ml, 0.289 mol), and $Ar'NH_2$ (8.4 ml, 0.068 mol) were added with stirring at room temperature to a suspension of $NaMoO_4$ (**III-10**) (7.0 g, 34 mmol) in 150 ml of DME. After several minutes of stirring, the colour of the reaction mixture turned yellow and then red. The reaction mixture was heated at 60 °C overnight. Then the dark-red solution was filtered and the residue was washed with 300 ml of DME. The solvent was removed in vacuum to give a dark-red solid, which was washed with 50 ml of hexane and dried in vacuum. Yield: 16.29 g, 97 %. The NMR spectra and the physical properties of the compound are identical to those previously reported in the literature.[193]

Preparation of $(Ar''N)_2MoCl_2(DME)$ (III-13)

NEt_3 (10.83 ml, 77.7 mol), Me_3SiCl (21.1 ml, 0.165 mol), and $Ar''NH_2$ (4.85 ml, 38.85 mmol) were added with stirring at room temperature to a suspension of $NaMoO_4$ (**III-10**) (4.0 g, 19.43 mmol) in 150 ml of DME. After 5 min of stirring the solution turned yellow, than brown, then brown-red. The reaction mixture was heated at 60 °C for 24 hours. Then the solution was filtered and the residue was washed with 150 ml of DME. The solvent was removed under reduced pressure to give an orange-yellow powder, which was dried

in vacuum. Yield: 9.37 g, 97 %. ^{1}H-NMR (300 MHz; $CDCl_3$; δ, ppm): 2.19 (s, 12H, Ar"N, *CH*$_3$); 3.90 (bs, 10H, DME); 6.74 (s, 2H, Ar"N, *p-H*); 6.87 (s, 4H, Ar"N, *o-H*). ^{13}C{^{1}H}-NMR (75.5 MHz; $CDCl_3$; δ, ppm): 21.0 (s, Ar"N, *CH*$_3$); 63.7 (bs, O-*CH*$_3$); 71.2 (s, CH_3-O-*CH*$_2$-*CH*$_2$-O-CH_3); 121.6 (s, Ar"N, *o-C*); 129.6 (s, Ar"N, *m-C*); 137.9 (s, Ar"N, *p-C*); 156.4 (s, Ar"N, *i-C*).

Preparation of $(PhN)_2MoCl_2(DME)$ (III-14)[193]

NEt_3 (10.8 ml, 77.7 mol), Me_3SiCl (22.4 ml, 174.9 mmol), and aniline (3.5 ml, 38.9 mmol) were added with stirring at room temperature to a suspension of $NaMoO_4$ (**III-10**) (4.0 g, 19.43 mmol) in 200 ml of DME. The reaction mixture was stirred at room temperature for 20 h. The solution was filtered and DME was removed from the filtrate in vacuum to leave a dark-red solid. Yield: 7.78 g, 91 %. The NMR spectra and the physical properties of the compound are identical to those previously reported in the literature.[193]

Preparation of $(^{t}BuN)_2MoCl_2(DME)$ (III-15)[193]

Me_3SiCl (44 ml, 0.34 mol) was added dropwise to a solution of $^{t}BuNH_2$ (20.4 ml, 0.19 mol) in 130 ml of DME. A white precipitate formed. To this slurry was added $NaMoO_4$ (**III-10**) (5 g, 0.024 mol) all at once as a solid. The reaction mixture was heated at 65 °C for 24 h. Then the solution was filtered and the solvent was removed in vacuum. The residue was extracted with pentane (200 ml). Pentane was removed in vacuum to give a yellow solid, which was dried in vacuum. Yield: 9.38 g, 97 %. The NMR spectra and the physical properties of the compound are identical to those previously reported in the literature.[193]

Preparation of $(ArN)_2Mo(PMe_3)_3$ (III-22)

A solution of $(ArN)_2MoCl_2(DME)$ (**III-11**) (2.95 g, 4.86 mmol) in 50 ml of THF was added at room temperature to a suspension of Mg (1.77g, 72.8 mmol) and PMe_3 (4.0 ml, 38.8 mmol) in 50 ml of THF. After 30 min of stirring the colour of the reaction mixture turned dark-green. The mixture was stirred overnight at room temperature. Then the solvent was removed in vacuum and the residue was extracted with hexane until the filtrate was colourless. All volatiles were pumped off to leave a dark-green solid, which

was dried in vacuum. Yield: 3.16 g, 97 %.[w] ^{1}H-NMR (300 MHz; C_6D_6; δ, ppm): 1.05 (bs, 27H, PMe_3); 1.32 (d, $^3J_{H-H}$ = 6.9 Hz, 24H, 8 *CH*$_3$, *Ar*N); 3.77 (sept, $^3J_{H-H}$ = 6.9 Hz, 4H, 4 *CH*, *Ar*N); 6.91 (t, $^3J_{H-H}$ = 7.5 Hz, 2H, *Ar*N); 7.16 (d, $^3J_{H-H}$ = 7.5 Hz, 4H, *Ar*N). ^{31}P{^{1}H}-NMR (121.5 MHz; C_6D_6; δ, ppm): -12.7 (bs, 2P, 2 *P*Me_3); 23.2 (bs, 1P, *P*Me_3). ^{1}H-NMR (300 MHz, PhMe-d_8, - 40 °C; δ, ppm): 7.18 (d, $^3J_{H-H}$ = 7.5 Hz, 2H, *m*-H, *Ar*N); 7.09 (d, $^3J_{H-H}$ = 7.5 Hz, 2H, *m*-H, *Ar*N); 6.90 (t, $^3J_{H-H}$ = 7.5 Hz, 2H, *p*-H, *Ar*N); 3.81 (sept, $^3J_{H-H}$ = 6.9 Hz, 2H, 2 *CH*, *Ar*N); 3.66 (sept, $^3J_{H-H}$ = 6.9 Hz, 2H, 2 *CH*, *Ar*N); 1.42 (d, $^3J_{H-H}$ = 6.9 Hz, 12H, 4 *CH*$_3$, *Ar*N); 1.29 (d, $^3J_{H-H}$ = 6.9 Hz, 12H, 4 *CH*$_3$, *Ar*N); 1.21 (d, $^2J_{H-P}$ = 7.5 Hz, 9H, P*Me*$_3$), 0.89 (vt, $^2J_{H-P}$ = 2.3 Hz, 18H, 2 P*Me*$_3$). ^{13}C{^{1}H}-NMR (75.4 MHz, PhMe-d_8, - 40 °C; δ, ppm): 128.9; 127.9; 31.7 (*CH*); 31.2 (*CH*); 31.4 (*CH*$_3$, *Ar*N); 29.6 (*CH*$_3$, *Ar*N); 28.8 (P*Me*$_3$); 23.3 (P*Me*$_3$). ^{31}P{^{1}H}-NMR (121.4 MHz, PhMe-d_8, - 20 °C; δ, ppm): -29.9 (s, 1P, *P*Me_3); -5.0 (s, 2P, 2 *P*Me_3).

Preparation of $(ArN)_2Mo(PMe_2Ph)_2$ (III-24)[x]

A solution of $(ArN)_2MoCl_2$(DME) (**III-11**) (500 mg, 0.823 mmol) in 30 ml of THF was added at room temperature to a suspension of Mg (300 mg, 12.35 mmol) and PMe_2Ph (0.35 ml, 2.47 mmol) in 20 ml of THF. The reaction mixture was stirred at room temperature for 5 h. The solvent was removed in vacuum and the residue was extracted with hexane (200 ml). All volatiles were pumped off to give a green solid, which was dried in vacuum. Yield: 297 mg, 50 %. ^{1}H-NMR (300 MHz; C_6D_6; δ, ppm): 1.22 (d, $^3J_{H-H}$ = 6.9 Hz, 24H, 8 *CH*$_3$, *Ar*N); 1.32 (bs, 12H, 4 *CH*$_3$, 2 P*Me*$_2$Ph); 4.13 (sept, $^3J_{H-H}$ = 6.9 Hz, 4H, 4 *CH*, *Ar*N); 6.98-7.19 (m, 12H, *m*-H and *p*-H, 2 Ar*N* and 2 PMe_2*Ph*); 7.46 (m, 4H, *o*-H, 2 PMe_2*Ph*). ^{31}P{^{1}H}-NMR (121.5 MHz; C_6D_6; δ, ppm): 42.2 (bs, 2 *P*Me_2Ph). ^{13}C{^{1}H}-NMR (75.5 MHz; C_6D_6; δ, ppm): 19.0 (bs, 2 P*Me*$_2$Ph); 24.3 (s, 8 *CH*$_3$, 2 *Ar*N); 28.0 (s, 4 *CH*, 2 *Ar*N); 121.1, 122.9, 128.5, 128.8, 130.7, 131.0, 139.7, 155.85 (aromatic carbons of *Ar*N and PMe_2*Ph*).

[w] The product was previously reported as a diphosphine complex $(ArN)_2Mo(PMe_3)_2$ (**III-19**).[196]
[x] The compound was prepared earlier in a different way but no spectroscopic data were reported (see ref. 196).

Preparation of $(Ar'N)_2Mo(PMe_3)_3$ (III-4)[197]

A solution of $(Ar'N)_2MoCl_2(DME)$ (**III-12**) (2.17 g, 4.4 mmol) in 50 ml of THF was added with stirring to a suspension of Mg (1.6 g, 0.066 mol) and PMe_3 (1.8 ml, 0.018 mol) in 50 ml of THF. After 30 min of stirring the colour of the reaction mixture turned dark-green. The reaction mixture stirred overnight. THF was removed in vacuum and the residue was extracted with 200 ml of hexanes. All volatiles were pumped off to give a dark-green solid, which was dried in vacuum. Yield: 2.21 g, 88 %.[209] ^{1}H-NMR (300 MHz; PhMe-d_8; δ, ppm): 0.96 (bs, 27H, 3 P*Me*$_3$); 2.32 (bs, 12H, 8 *CH*$_3$, *Ar'*N); 6.67 (t, $^3J_{H\text{-}H}$ = 7.2 Hz, 2H, *Ar'*N); 7.12 (d, $^3J_{H\text{-}H}$ = 7.2 Hz, 4H, *Ar'*N). ^{31}P{^{1}H}-NMR (121.5 MHz; PhMe-d_8; δ, ppm): -15.0 (bs, 2P, 2 *P*Me$_3$); 25.0 (bs, 1P, *P*Me$_3$). ^{1}H-NMR (300 MHz, PhMe-d_8, - 10 °C; δ, ppm): 7.23 (bs, 2H, *m*-H, *Ar'*N); 7.13 (bs, 2H, *m*-H, *Ar'*N); 6.74 (t, $^3J_{H\text{-}H}$ = 5.7 Hz, 2H, *p*-H, *Ar'*N); 2.43 (bs, 6H, 2 *CH*$_3$, *Ar'*N); 2.29 (bs, 6H, 2 *CH*$_3$, *Ar'*N); 1.27 (d, $^2J_{H\text{-}P}$ = 6.6 Hz, 9H, P*Me*$_3$); 0.80 (bs, 18H, 2 P*Me*$_3$). ^{13}C{^{1}H}-NMR (75.4 MHz, PhMe-d_8, - 10 °C; δ, ppm): 158.7 (*i*-C, *Ar'*N); 125.6; 123.3; 116.4 (all aromatic carbons of *Ar'*N); 25.0 (*CH*$_3$, *Ar'*N); 24.7 (*CH*$_3$, *Ar'*N); 22.0 (P*Me*$_3$); 17.1 (2 P*Me*$_3$). ^{31}P{^{1}H}-NMR (121.4 MHz, PhMe-d_8, - 10 °C; δ, ppm): 31.7 (s, 1P, *P*Me$_3$), - 8.1 (s, 2P, 2 *P*Me$_3$).

Preparation of $(Ar'N)_2Mo(PMe^iPr_2)_2$ (III-25)

A solution of $(Ar'N)_2MoCl_2(DME)$ (**III-12**) (422 mg, 0.852 mmol) in 50 ml of THF was added at room temperature to a suspension of Mg (1.0 g, 41.14 mmol) and PMe^iPr_2 (0.3 ml, 1.91 mmol) in 50 ml of THF. The reaction mixture was stirred at room temperature for 3 h. During this time the colour of the mixture changed from red to green. The solvent was removed in vacuum and the residue was extracted with 300 ml of hexanes. All volatiles were pumped off to give a green solid, which was dried in vacuum. Yield: 117 mg, 23 %. ^{1}H-NMR (300 MHz; C_6D_6; δ, ppm): 7.13 (d, $^3J_{H\text{-}H}$ = 7.8 Hz, 4H, *m*-H, *Ar'*N); 6.93 (t, $^3J_{H\text{-}H}$ = 7.8 Hz, 2H, *p*-H, *Ar'*N); 2.50 (s, 12H, 4 *CH*$_3$, *Ar'*N); 1.72 (m, 4H, 4 *CH*, 2 P^i*Pr*$_2$Me); 1.17 (d, $^2J_{H\text{-}P}$ = 6.9 Hz, 6H, 2 *CH*$_3$, 2 P^{i}Pr$_2$*Me*); 0.97 (m, 24H, 8 *CH*$_3$, P^{i}Pr$_2$Me). ^{31}P{^{1}H}-NMR (121.5 MHz; C_6D_6; δ, ppm): 79.1 (s, 2P, 2 *P*^{i}Pr$_2$Me). ^{13}C{^{1}H}-NMR (150.9 MHz; C_6D_6; δ, ppm): 13.8 (d, $^1J_{C\text{-}P}$ = 15.1 Hz, PMe^{i}Pr$_2$); 18.8 (s, PMe^{i}Pr$_2$); 19.1 (s, PMe^{i}Pr$_2$); 21.2 (s, *CH*$_3$, *Ar'*N); 28.7 (d, $^1J_{C\text{-}P}$ = 24.1 Hz, PMe^{i}Pr$_2$); 120.7 (s, *p*-C, *Ar'*N); 128.1 (s, *m*-C, *Ar'*N); 130.9 (s, *o*-C, *Ar'*N); 159.7 (s, *i*-C, *Ar'*N).

Preparation of $(Ar'N)_2Mo(PMe_2Ph)_3$ (III-26)

A solution of $(Ar'N)_2MoCl_2(DME)$ (**III-12**) (509.4 mg, 0.906 mmol) in 30 ml of THF was added at room temperature to a suspension of Mg (330.3 mg, 13.59 mmol) and PMe_2Ph (0.39 ml, 2.72 mmol) in 20 ml of THF. The reaction mixture was stirred at room temperature for 4 h. The solvent was removed in vacuum and the residue was extracted with hexanes (250 ml). All volatiles were pumped off to give a green solid, which was dried in vacuum. Yield: 288 mg, 42 %. ^{1}H-NMR (300 MHz; C_6D_6; δ, ppm): 7.27 (d, $^3J_{H-H}$ = 7.2 Hz, 4H, *Ar'*N, *m-H*); 7.09 (broad signal, 6H, 3 PMe_2*Ph*, *o*-H); 6.96 (m, 10H, *m*-H and *p*-H of 3 PMe_2*Ph*); 6.85 (t, $^3J_{H-H}$ = 7.2 Hz, 2H, *p*-H, *Ar'*N); 2.25 (s, 12H, 4 *CH*$_3$, *Ar'*N); 1.14 (bs, 18H, 3 P*Me*$_2$Ph). ^{31}P{^{1}H}-NMR (121.5 MHz; C_6D_6; δ, ppm): -7.5 (bs, 2P, 2 *P*Me_2Ph); 34.9 (bs, 1P, *P*Me_2Ph). ^{13}C{^{1}H}-NMR (75.5 MHz; C_6D_6; δ, ppm): 17.6 (bs, P*Me*$_2$Ph); 21.2 (s, *CH*$_3$, *Ar'*N); 117.4 (s, *p*-C, *Ar'*N); 127.9 (s, PMe_2*Ph*); 128.1 (s, *m*-C, *Ar'*N); 130.3 (s, *o*-C, PMe_2*Ph*); 159.2 (s, *o*-C, *Ar'*N).

Preparation of $(^tBuN)_2Mo(PMe_3)_2$ (III-27)

A solution of $(^tBuN)_2MoCl_2(DME)$ (**III-15**) (4.00 g, 10.02 mmol) in THF (100 ml) was added to a mixture of activated Mg (3.67 g, 0.15 mol) and PMe_3 (8.3 ml, 0.08 mol) in 200 ml of THF at room temperature. After 1h of stirring at room temperature the colour of the reaction mixture turned to grey-green. The reaction mixture was left with stirring overnight. The solvent was removed under reduced pressure and the residue was extracted with hexane (350 ml) and dried in vacuum to give a dark-green oily substance. According to NMR analysis, the dark-green substance contains the mixture of $(^tBuN)_2Mo(PMe_3)_2$ (**III-27**) and $[(^tBuN)(PMe_3)Mo(\mu\text{-}N^tBu)]_2$ (**III-21**)[198] in approximate mole ratio 2:1, respectively. The time of the reaction and amounts of PMe_3 utilized in it do not affect the ratio of the products. Furthermore, the separation of the products could not be achieved by recrystallization. However, heating the mixture in toluene at 75 °C for three weeks gives pure monomer **III-27** in solution and dark precipitate. The mixture was filtered, all volatiles were pumped off and the residue was extracted with hexanes (50 ml) to give pure **III-27**, which was isolated as a dark-brown oily substance. Yield: 2.14 g, 55 %.

(^{t}BuN)$_2$Mo(PMe$_3$)$_2$ (**III-27**): ^{1}H-NMR (300 MHz; C_6D_6; δ, ppm): 1.30 (bd, $^2J_{H-P}$ = 7.5 Hz, 18H, 2 P*Me$_3$*); 1.53 (s, 18H, 2 ^{t}*Bu*N). ^{31}P{^{1}H}-NMR (121.5 MHz; C_6D_6; δ, ppm): 31.52 (bs, 2 *P*Me$_3$). ^{1}H-NMR (300 MHz; PhMe-d_8; δ, ppm): 1.32 (bd, $^2J_{H-P}$ = 7.8 Hz, 18H, 2 P*Me$_3$*); 1.48 (s, 18H, 2 ^{t}*Bu*N). ^{31}P{^{1}H}-NMR (121.5 MHz; PhMe-d_8; δ, ppm): 38.5 (bs, 2 *P*Me$_3$). ^{13}C{^{1}H}-NMR (75.5 MHz; PhMe-d_8; δ, ppm): 25.6 (bs, 2 P*Me$_3$*); 35.0 (s, 2 ^{t}*Bu*N). ^{1}H-NMR (300 MHz; PhMe-d_8; - 50 °C; δ, ppm): 1.60 (s, 18H, ^{t}*Bu*N); 1.28 (d, $^2J_{P-H}$ = 7.8 Hz, 18H, 2 P*Me$_3$*). ^{31}P{^{1}H}-NMR (121.5 MHz; PhMe-d_8; - 50 °C; δ, ppm): 39.5 (bs, 2 *P*Me$_3$). ^{13}C{^{1}H}-NMR (75.5 MHz; PhMe-d_8; - 50 °C; δ, ppm): 25.3 (d, $^1J_{C-P}$ = 24.0 Hz, 2 P*Me$_3$*); 34.7 (s, *Me* of 2 ^{t}*Bu*N); 64.5 (s, *C*Me$_3$).

[(^{t}BuN)(PMe$_3$)Mo(μ-N^{t}Bu)]$_2$ (**III-21**):[198] ^{1}H-NMR (300 MHz; C_6D_6; δ, ppm): 1.05 (d, $^2J_{H-P}$ = 7.8 Hz, 18H, 2P*Me$_3$*); 1.28 (s, 18H, 2 ^{t}*Bu*N); 1.99 (s, 18H, 2 ^{t}*Bu*N). ^{31}P{^{1}H}-NMR (121.5 MHz; C_6D_6; δ, ppm): 3.7 (s, 2 *P*Me$_3$).

Preparation of (ArN)$_2$W(PMe$_3$)$_3$ (III-23)[y]

A solution of (ArN)$_2$WCl$_2$(DME) (**III-16**) (0.5 g, 0.72 mmol) in 20 ml of THF was added *via* cannula at room temperature to a mixture of Mg (0.5 g, 20.57 mmol) and PMe$_3$ (0.6 ml, 5.76 mmol) in 20 ml of THF. The reaction mixture was left with stirring overnight at room temperature. All volatiles were pumped off; the residue was dried and extracted with hexanes (4x50 ml). The solvent was removed in vacuum to give a violet powder. Yield: 384 mg, 70 %. ^{1}H-NMR (300 MHz; C_6D_6; δ, ppm): 7.7 (bs, 6H, *m*-H and *p*-H, 2 *Ar*N); 3.7 (bs, 4H, 4 *CH*, 2 *Ar*N); 2.34 (bs, 12H, 4 *CH$_3$*, 2 *Ar*N); 1.30 (bs, 12H, 4 *CH$_3$*, 2 *Ar*N); 1.1 (bs, 27H, 3 P*Me$_3$*). ^{31}P{^{1}H}-NMR (121.4 MHz; C_6D_6; δ, ppm): - 14.1 (bs, 1P, *P*Me$_3$); - 24.0 (bs, 2P, 2 *P*Me$_3$). ^{1}H-NMR (300 MHz, PhMe-d_8, - 20 °C; δ, ppm): 7.00 (d, $^3J_{H-H}$ = 7.5 Hz, 2H, *p*-H, 2 *Ar*N); 6.90 (t, $^3J_{H-H}$ = 7.5 Hz, 4H, *m*-H, 2 *Ar*N); 3.83 (sept, $^3J_{H-H}$ = 6.6 Hz, 2H, 2 *CH*, *Ar*N); 3.51 (sept, $^3J_{H-H}$ = 6.9 Hz, 2H, 2 *CH*, *Ar*N); 1.46 (d, $^2J_{H-P}$ = 8.1 Hz, 9H, P*Me$_3$*); 1.41 (d, $^3J_{H-H}$ = 6.6 Hz, 12H, 4 *CH$_3$*, *Ar*N); 1.25 (d, $^3J_{H-H}$ = 6.9 Hz, 12H, 4 CH$_3$, *Ar*N); 1.08 (vt, $^2J_{H-P}$ = 4.1 Hz, 18H, 2 P*Me$_3$*). ^{13}C{^{1}H}-NMR (75.4 MHz, PhMe-d_8, - 20 °C; δ, ppm): 128.6 (*Ar*N); 127.8 (*Ar*N); 31.6 (*CH*, *Ar*N); 30.8 (*CH*, *Ar*N); 32.7 (P*Me$_3$*); 31.1 (*CH$_3$*, *Ar*N); 31.1 (*CH$_3$*, *Ar*N); 29.2 (P*Me$_3$*). ^{31}P{^{1}H}-NMR (121.4

[y] Similar diphosphine complexes (ArN)$_2$W(PR$_3$)$_2$ (R$_3$ = Me$_2$Ph (**III-17**), MePh$_2$ (**III-18**)) were reported earlier by Gibson *et al.*[195]

MHz, PhMe-d_8, - 20 °C; δ, ppm): - 7.9 (t, $^2J_{P\text{-}P}$ = 18.2 Hz, $^1J_{P\text{-}W}$ = 461 Hz, 1P, PMe_3); - 17.7 (d, $^2J_{P\text{-}P}$ = 18.2 Hz, $^1J_{P\text{-}W}$ = 316 Hz, 2P, 2 PMe_3).

Preparation of (^{t}BuN)$_2$Mo(η^2-CH$_2$=CH$_2$)(PMe$_3$) (III-30)[199]

A solution of EtMgBr in Et_2O (1.26 ml, 3.78 mmol, C = 3.0 M) was added at room temperature to a mixture of (^{t}BuN)$_2$MoCl$_2$(DME) (**III-15**) (754.1 mg, 1.89 mmol) and PMe_3 (0.2 ml, 1.89 mmol) in 50 ml of Et_2O. Immediately after addition the colour of the reaction mixture turned to yellow-green and the formation of yellow precipitate was observed. The mixture was stirred at room temperature for additional 3 h. All volatiles were pumped off and the residue was extracted with hexanes (50 ml). The solvent was removed in vacuum to leave a brown solid, which was recrystallized from concentrated hexane solution at - 30 °C to give yellow crystals. Yield: 323.5 mg, 50 %. The NMR spectra and the physical properties of the compound are identical to those previously reported in the literature.[199]

Preparation of (ArN)$_2$Mo(η^2-CH$_2$=CH$_2$)(PMe$_3$)$_2$ (III-31)

A solution of EtMgBr in Et_2O (2.2 ml, 6.58 mmol, C = 3.0 M) was added at -78 °C to a solution of (ArN)$_2$MoCl$_2$(DME) (**III-11**) (2.0 g, 3.29 mmol) and PMe_3 (0.69 ml, 6.58 mmol) in 100 ml of Et_2O. The reaction mixture was allowed to warm up to room temperature and then was stirred for 3 h. During this time the colour of the mixture changed from red to purple. All volatiles were pumped off; the residue was dried and extracted with hexanes (150 ml). The solvent was removed in vacuum to leave a purple solid. Yield: 1.45 g, 70 %. ^{1}H-NMR (300 MHz; C_6D_6; δ, ppm): 0.97 (bs, 18H, 2 P*Me$_3$*); 1.24 (d, $^3J_{H\text{-}H}$ = 6.9 Hz, 24H, 8 *CH$_3$*, 2 N*Ar*); 1.84 (bs, 4H, η^2-*CH$_2$*=*CH$_2$*); 3.52 (bs, 4H, 4 *CH*, 2 N*Ar*); 6.86 (t, $^3J_{H\text{-}H}$ = 7.5 Hz, 2H, *p*-H, 2 N*Ar*); 7.04 (d, $^3J_{H\text{-}H}$ = 7.5 Hz, 4H, *m*-H, 2 N*Ar*). ^{31}P{^{1}H}-NMR (121.5 MHz; C_6D_6; δ, ppm): -6.9 (bs, 2 PMe_3). ^{13}C{^{1}H}-NMR (75.5 MHz; C_6D_6; δ, ppm): 15.3 (bs, 2 P*Me$_3$*); 24.5 (s, 8 *CH$_3$*, *Ar*N); 27.5 (s, 4 *CH*; *Ar*N); 120.4, 122.7, 138.4, 154.1 (aromatic carbons of 2 *Ar*N).

Reactions of $(RN)_2M(PR'_3)_{n-1}L$ with chlorohydrosilanes

NMR scale reaction of $(ArN)_2Mo(PMe_3)_3$ (III-22) with Me_2SiHCl

NEt_3 (34.4 µl, 0.247 mmol) and Me_2SiHCl (5.5 µl, 0.049 mmol) were added at room temperature to a solution of $(ArN)_2Mo(PMe_3)_3$ (**III-22**) (33.3 mg, 0.049 mmol) in 0.6 ml of C_6D_6 in an NMR tube. No visual changes were observed after addition and the reaction mixture was left at room temperature for 5 min. NMR analysis showed a 50 % conversion of starting material and formation of a difficult-to-separate mixture of starting material and $(ArN)Mo(Cl)(\eta^3\text{-}NAr\text{-}SiMe_2\text{-}H)(PMe_3)_2$ (**III-42a**), whereas NEt_3 remained unreacted. Heating the mixture at 50 °C overnight leads to a decomposition of **III-42a** to $(ArN)MoCl_2(PMe_3)_3$ (**III-47**) (see preparation of **III-47** below).

(ArN)Mo(Cl)(η^3-NAr-SiMe$_2$-H)(PMe$_3$)$_2$ (**III-42a**): ^{1}H-NMR (300 MHz; C_6D_6; δ, ppm): 7.23 (t, $^3J_{H\text{-}H}$ = 4.5 Hz, 1H, *p*-H, *Ar*N); 7.07 (d, $^3J_{H\text{-}H}$ = 4.5 Hz, 2H, *m*-H, *Ar*N); 6.95 (pseudo t, $^3J_{H\text{-}H}$ = 3 Hz, 2H, *m*-H, *Ar*N); 6.84 (dd, $^3J_{H\text{-}H}$ = 3 Hz, $^3J_{H\text{-}H}$ = 6 Hz, 1H, *p*-H, *Ar*N); 4.33 (sept, $^3J_{H\text{-}H}$ = 6.6 Hz, 1H, *CH*, *Ar*N); 3.78 (sept, $^3J_{H\text{-}H}$ = 6.6 Hz, 1H, *CH*, *Ar*N); 3.45 (sept, $^3J_{H\text{-}H}$ = 6.9 Hz, 1H, *CH*, *Ar*N); 3.11 (sept, $^3J_{H\text{-}H}$ = 6.9 Hz, 1H, *CH*, *Ar*N); 1.52 (d, $^3J_{H\text{-}H}$ = 6.6 Hz, 3H, *CH$_3$*, *Ar*N); 1.28 (d, $^2J_{H\text{-}P}$ = 6.0 Hz, 9H, P*Me$_3$*); 1.25 (d, $^3J_{H\text{-}H}$ = 6.9 Hz, 3H, *CH$_3$*, *Ar*N); 1.23 (d, $^3J_{H\text{-}H}$ = 6.6 Hz, 3H, *CH$_3$*, *Ar*N); 1.22 (d, $^3J_{H\text{-}H}$ = 6.6 Hz, 3H, *CH$_3$*, *Ar*N); 1.12 (d, $^2J_{H\text{-}P}$ = 7.5 Hz, 9H, P*Me$_3$*); 1.05 (d, $^3J_{H\text{-}H}$ = 6.6 Hz, 3H, *CH$_3$*, *Ar*N); 1.02 (d, $^3J_{H\text{-}H}$ = 6.9 Hz, 3H, *CH$_3$*, *Ar*N); 1.00 (d, $^3J_{H\text{-}H}$ = 6.9 Hz, 3H, *CH$_3$*, *Ar*N); 0.98 (s, 3H, Si*Me$_2$*); 0.93 (d, $^3J_{H\text{-}H}$ = 6.9 Hz, 3H, *CH$_3$*, *Ar*N); 0.88 (t, $^2J_{H\text{-}P}$ = 7.5 Hz, 1H, Mo*H*Si); 0.65 (s, 3H, Si*Me$_2$*). ^{13}C{^{1}H}-NMR (75.4 MHz; C_6D_6; δ, ppm): 155.0 (s, *i*-C, *Ar*N); 153.2 (s, *i*-C, *Ar*N); 145.9 (s, *o*-C, *Ar*N); 144.6 (s, *o*-C, *Ar*N); 142.2 (s, *o*-C, *Ar*N); 140.0 (s, *o*-C, *Ar*N); 123.7; 123.5; 122.5; 121.9; 29.6 (s, *CH$_3$*, *Ar*N); 27.6 (s, *CH*, *Ar*N); 27.5 (s, *CH*, *Ar*N); 27.3 (s, *CH$_3$*, *Ar*N); 26.5 (s, *CH*, *Ar*N); 24.6 (s, *CH$_3$*, *Ar*N); 24.5 (s, *CH$_3$*, *Ar*N); 24.9 (s, *CH$_3$*, *Ar*N); 23.9 (s, *CH$_3$*, *Ar*N); 23.2 (s, *CH$_3$*, *Ar*N); 22.5 (s, *CH$_3$*, *Ar*N); 21.5 (d, $^1J_{C\text{-}P}$ = 21.3 Hz, P*Me$_3$*); 20.3 (d, $^1J_{C\text{-}P}$ = 21.3 Hz, P*Me$_3$*); 2.8 (s, Si*Me$_2$*); - 0.04 (s, Si*Me$_2$*). ^{31}P{^{1}H}-NMR (121.4 MHz; C_6D_6; δ, ppm): 4.7 (d, $^2J_{P\text{-}P}$ =7.0 Hz, *P*Me$_3$), - 6.8 (d, $^2J_{P\text{-}P}$ = 7.0 Hz, *P*Me$_3$). ^{29}Si-NMR (59.6 MHz; C_6D_6; δ, ppm): - 64.9 (dm, $^1J_{Si\text{-}H}$ = 97.0 Hz, $^2J_{Si\text{-}H}$ = 3.1 Hz, η^3-NAr-*Si*Me$_2$-H). IR (nujol): 1943 cm^{-1} (Si-H).

NMR scale reaction of $(Ar'N)_2Mo(PMe_3)_3$ (III-4) with Me_2SiHCl[15]

Me_2SiHCl (8.6 µl, 0.077 mmol) was added in one portion at room temperature to a solution of $(Ar'N)_2Mo(PMe_3)_3$ (**III-4**) (39.2 mg, 0.077 mmol) in toluene-d_8 in an NMR tube. The colour of the solution turned from green to brown and the reaction mixture was left at room temperature for 10 min. NMR analysis showed the quantitative formation of $(Ar'N)Mo(Cl)(\eta^3\text{-}Ar'N\text{-}SiMe_2\text{-}H)(PMe_3)_2$ (**III-38**). Leaving the reaction mixture at room temperature leads to the decomposition of **III-38** to form $(Ar'N)MoCl_2(PMe_3)_3$ (**III-5**) (see the preparation of **III-5** below).[15]

$(Ar'N)Mo(Cl)(\eta^3\text{-}Ar'N\text{-}SiMe_2\text{-}H)(PMe_3)_2$ (**III-38**): ^{1}H-NMR (500 MHz; toluene-d_8; - 40 °C; δ, ppm): 7.24 (d, $^3J_{H\text{-}H}$ = 7.4 Hz, 1H, *m*-H, *Ar*NSi); 7.10 (d, $^3J_{H\text{-}H}$ = 7.5 Hz, 1H, *m*-H, *Ar*NSi); 7.00 (t, $^3J_{H\text{-}H}$ = 7.4 Hz, 1H, *p*-H, *Ar*NSi); 6.83 (d, $^3J_{H\text{-}H}$ = 7.5 Hz, 1H, *m*-H, *Ar*N); 6.78 (t, $^3J_{H\text{-}H}$ = 7.4 Hz, 1H, *p*-H, *Ar*N); 6.75 (d, $^3J_{H\text{-}H}$ = 7.6 Hz, 1H, *m*-H, *Ar*N); 2.85 (s, 3H, *CH*$_3$, *Ar*NSi); 2.49 (s, 3H, *CH*$_3$, *Ar*NSi); 2.07 (s, 3H, *CH*$_3$, *Ar*NSi); 2.06 (s, 3H, *CH*$_3$, *Ar*N); 1.68 (dqq, $^3J_{H\text{-}H}$ = 2.2 Hz, $^3J_{H\text{-}H}$ = 1.7 Hz, $^2J_{H\text{-}P}$ = 23.3 Hz, 1H, Mo*H*); 1.23 (d, $^2J_{H\text{-}P}$ = 7.1 Hz, 9H, P*Me*$_3$); 0.98 (d, $^2J_{H\text{-}P}$ = 8.5 Hz, 9H, P*Me*$_3$); 0.71 (d, $^3J_{H\text{-}H}$ =1.7 Hz, 3H, Si*Me*); 0.25 (d, $^3J_{H\text{-}H}$ = 2.2 Hz, 3H, Si*Me*). ^{13}C{^{1}H}-NMR (125.7 MHz; toluene-d_8; - 40 °C; δ, ppm): 158.2 (d, $^3J_{C\text{-}P}$ = 2.0 Hz, *i*-C, *Ar*NSi); 154.5 (d, $^3J_{C\text{-}P}$ = 5.6 Hz, *i*-C, *Ar*N); 135.4 (d, $^4J_{C\text{-}P}$ = 2.1 Hz, *o*-C, *Ar*NSi); 133.7 (d, $^4J_{C\text{-}P}$ = 1.6 Hz, *o*-C, *Ar*NSi); 131.3 (d, $^4J_{C\text{-}P}$ = 1.8 Hz, *o*-C, *Ar*N); 128.8 (s, *m*-C, *Ar*N); 128.5 (s, *m*-C, *Ar*NSi); 128.3 (s, *m*-C, *Ar*N); 128.1 (s, *m*-C, *Ar*NSi); 128.0 (s, *o*-C, *Ar*N); 123.3 (s, *p*-C, *Ar*N); 121.0 (s, *p*-C, *Ar*NSi); 21.6 (s, *CH*$_3$, *Ar*NSi); 20.4 (s, *CH*$_3$, *Ar*N); 20.0 (s, *CH*$_3$, *Ar*NSi); 19.9 (s, *CH*$_3$, *Ar*N); 19.5 (d, $^1J_{C\text{-}P}$ = 21.2 Hz, P*Me*$_3$); 18.6 (dd, $^1J_{C\text{-}P}$ = 21.2 Hz, $^3J_{C\text{-}P}$ = 0.8 Hz, P*Me*$_3$). ^{31}P{^{1}H}-NMR (121.4 MHz; toluene-d_8; - 40 °C; δ, ppm): 6.4 (d, $^2J_{P\text{-}P}$ = 9.0 Hz, *P*Me$_3$); - 7.0 (d, $^2J_{P\text{-}P}$ = 9.0 Hz, *P*Me$_3$). ^{29}Si-NMR (119.2 MHz; toluene-d_8; - 50 °C; δ, ppm): - 63.8 (ddd, $^1J_{Si\text{-}H}$ = 98.0 Hz, $^2J_{Si\text{-}H}$ = 7.2 Hz, $^2J_{Si\text{-}P}$ = 21.5 Hz, η^3-Ar'N-*Si*Me$_2$-H). IR (nujol): 1910 cm^{-1} (Si-H, weak).

NMR scale reaction of $(^tBuN)_2Mo(PMe_3)_3$ (III-27) with Me_2SiHCl

Me_2SiHCl (8.6 µl, 0.077 mmol) was added in one portion at room temperature to a solution of $(^tBuN)_2Mo(PMe_3)_2$ (**III-27**) (30.1 mg, 0.077 mmol) in 0.6 ml of C_6D_6 in an NMR tube. The reaction mixture was left at room temperature for an hour, during which

time the colour changed to gray. NMR analysis showed the quantitative formation of (^{t}BuN)Mo(Cl)(η^3-^{t}BuN-SiMe$_2$-H)(PMe$_3$)$_2$ (**III-42c**). Leaving the reaction mixture at room temperature leads to the decomposition of **III-42c** and formation of (^{t}BuN)MoCl$_2$(PMe$_3$)$_3$ (**III-48**) (see the preparation of **III-48** below).

(^{t}BuN)Mo(Cl)(η^3-^{t}BuN-SiMe$_2$-H)(PMe$_3$)$_2$ (**III-42c**): ^{1}H-NMR (300 MHz; C_6D_6; δ, ppm): 1.54 (s, 9H, ^{t}*Bu*N); 1.47 (d, $^2J_{H-P}$ = 7.5 Hz, 9H, P*Me$_3$*); 1.40 (d, $^2J_{H-P}$ = 6.6 Hz, 9H, P*Me$_3$*), ~1.4 (found by ^{1}H-^{29}Si HSQC, Mo*H*); 1.02 (s, 9H, ^{t}*Bu*N); 0.81 (d, $^4J_{H-P}$ = 1.8 Hz, 3H, Si*Me$_2$*); 0.55 (d, $^4J_{H-P}$ = 2.4 Hz, 3H, Si*Me$_2$*). ^{13}C{^{1}H}-NMR (75.4 MHz; C_6D_6; δ, ppm): 68.5 (s, ^{t}*Bu*N); 55.7 (s, ^{t}*Bu*N); 36.0 (s, ^{t}*Bu*N); 31.5 (s, ^{t}*Bu*N); 23.2 (d, $^1J_{C-P}$ = 23.6 Hz, P*Me$_3$*); 22.8 (d, $^1J_{C-P}$ = 21.1 Hz, P*Me$_3$*); 3.4 (s, Si*Me*); 0.9 (s, Si*Me*). ^{31}P{^{1}H}-NMR (121.4 MHz; C_6D_6; δ, ppm): 6.9 (d, $^2J_{P-P}$ = 12.0 Hz, 1P, *P*Me$_3$); 5.0 (d, $^2J_{P-P}$ = 12.0 Hz, 1P, *P*Me$_3$). ^{29}Si-NMR (59.6 MHz; C_6D_6; δ, ppm): -76 (d, $^1J_{Si-H}$ = 93.2 Hz). IR (nujol): 1992 cm^{-1} (weak, Si-H). Elem. Anal.[254] (%): calc. for $C_{16}H_{34}MoN_2P_2SiCl$ (484.63): C 39.63, H 8.94, N 5.78; found: C 38.46, H 8.03, N 5.78.

NMR scale reaction of (^{t}BuN)$_2$Mo(η^2-CH$_2$=CH$_2$)(PMe$_3$) (III-30) with Me$_2$SiHCl

Me$_2$SiHCl (8.2 μl, 0.074 mmol) was added in one portion at room temperature to a solution of (^{t}BuN)$_2$Mo(η^2-CH$_2$=CH$_2$)(PMe$_3$) (**III-30**) (25.3 mg, 0.074 mmol) in 0.6 ml of C_6D_6 in an NMR tube. The reaction mixture was left at room temperature for 5 min. During this time the colour of the solution changed from yellow to brown. NMR analysis showed the formation of an agostic ethylene adduct (^{t}BuN)Mo(Cl)(η^3-^{t}BuN-SiMe$_2$-H)(η^2-CH$_2$=CH$_2$)(PMe$_3$), which slowly releases the molecule of ethylene and rearranges into the bis(phosphine) analog (^{t}BuN)Mo(Cl)(η^3-^{t}BuN-SiMe$_2$-H)(PMe$_3$)$_2$ (**III-42c**), and then decomposes into (^{t}BuN)MoCl$_2$(PMe$_3$)$_3$ (**III-48**).

(^{t}BuN)Mo(Cl)(η^3-^{t}BuN-SiMe$_2$-H)(η^2-CH$_2$=CH$_2$)(PMe$_3$): ^{1}H-NMR (300 MHz; C_6D_6; δ, ppm): 0.63 (d, $^3J_{H-H}$ = 2.4 Hz, 3H, Si*Me$_2$*); 0.82 (d, $^3J_{H-H}$ = 2.4 Hz, 3H, Si*Me$_2$*); 0.83 (s, 9H, ^{t}*Bu*N); 1.41 (d, $^2J_{H-P}$ = 8.4 Hz, 9H, P*Me$_3$*); 1.80 (s, 9H, ^{t}*Bu*N); 2.60 (m, 2H, η^2-*C$_2$H$_4$*); 2.88 (dsept, $^3J_{H-H}$ = 2.4 Hz, $^2J_{H-P}$ = 6.6 Hz, 1H, Si*H*); 3.09 (dddd, $^2J_{H-H}$ = 39.3 Hz, $^3J_{H-H}$ = 10.8 Hz and 12.6 Hz, $^3J_{H-P}$ = 3.9 Hz, 2H, η^2-*C$_2$H$_4$*). ^{31}P{^{1}H}-NMR (121.5 MHz; C_6D_6; δ, ppm): -2.0 (s, *P*Me$_3$). ^{29}Si-NMR (59.6 MHz; C_6D_6; δ, ppm): -75.9 (d, $^1J_{Si-H}$ = 93.6 Hz, η^3-^{t}BuN*Si*HMe$_2$). ^{1}H-^{13}C HSQC NMR (f1: 300 MHz; f2: 75.5 MHz; *J* = 145 Hz; C_6D_6; ^{13}C

projection; δ, ppm): -0.1 (Si*Me*$_2$); 3.3 (Si*Me*$_2$); 19.4 (P*Me*$_3$); 29.0 (^{t}*Bu*N); 36.5 (^{t}*Bu*N); 42.5 (η^2-C_2H_4); 48.9 (η^2-C_2H_4).

NMR scale reaction of (ArN)$_2$Mo(PMe$_3$)$_3$ (III-22) with MePhSiHCl

MePhSiHCl (5.8 µl, 0.039 mmol) was added in one portion at room temperature to a solution of (ArN)$_2$Mo(PMe$_3$)$_3$ (**III-22**) (25.4 mg, 0.039 mmol) in 0.6 ml of C_6D_6 in an NMR tube. Monitoring of the reaction mixture with NMR spectroscopy revealed the slow (several days) formation of (ArN)Mo(Cl)(η^3-ArN-SiMePh-H)(PMe$_3$)$_2$ (**III-43a**), accompanied by a significant decomposition to (ArN)MoCl$_2$(PMe$_3$)$_3$ (**III-47**).

(ArN)Mo(Cl)(η^3-ArN-SiMePh-H)(PMe$_3$)$_2$ (**III-43a**): ^{31}P{^{1}H}-NMR (121.4 MHz; C_6D_6; δ, ppm): 3.4 (bs, 1P, *P*Me$_3$); -6.2 (bs, 1P, *P*Me$_3$).

NMR scale reaction of (Ar'N)$_2$Mo(PMe$_3$)$_3$ (III-4) with MePhSiHCl

MePhSiHCl (7.5 µl, 0.05 mmol) was added in one portion at room temperature to a solution of (Ar'N)$_2$Mo(PMe$_3$)$_3$ (**III-4**) (28.1 mg, 0.05 mmol) in 0.6 ml of toluene-d$_8$ in an NMR tube. The resultant mixture was kept at room temperature for 2 hours, developing brown color. NMR analysis showed the formation of a mixture of (Ar'N)Mo(Cl)(η^3-Ar'N-SiMePh-H)(PMe$_3$)$_2$ (**III-43b**; as a mixture of two isomers) and (Ar'N)MoCl$_2$(PMe$_3$)$_3$ (**III-5**)[15] in a ratio 2:1, respectively.

(Ar'N)Mo(Cl)(η^3-Ar'N-SiMePh-H)(PMe$_3$)$_2$ (**III-43b**): ^{1}H-NMR (300 MHz; toluene-d$_8$; -40 °C; δ, ppm): 8.15 (d, $^3J_{H-H}$ = 7.8 Hz, 4H); 7.52 (d, $^3J_{H-H}$ = 6.9 Hz, 4H); 7.23-6.93 (m); 6.78 (m, 4H); 2.64 (s, 3H, *CH$_3$*, *Ar'*N); 2.69 (s, 3H, *CH$_3$*, *Ar'*N); 2.45 (s, 3H, *CH$_3$*, *Ar'*N); 2.29 (s, 3H, *CH$_3$*, *Ar'*N); 2.24 (s, 3H, *CH$_3$*, *Ar'*N); 2.19 (s, 3H, *CH$_3$*, *Ar'*N); 2.17 (s, 3H, *CH$_3$*, *Ar'*N); 2.14 (t, $^2J_{H-P}$ = 22.0 Hz, 1H, Mo*H*); 2.10 (s, 3H, *CH$_3$*, *Ar'*N); 1.24 (d, $^2J_{H-P}$ = 7.0 Hz, 9H, P*Me$_3$*); 1.23 (d, $^2J_{H-P}$ =7.0 Hz, 9H, P*Me$_3$*); 1.15 (d, $^4J_{H-P}$=1.8Hz, 3H, Si*Me*); 1.00 (d, $^2J_{H-P}$ =8.5 Hz, 9H, P*Me$_3$*); 0.99 (d, $^2J_{H-P}$ = 8.5 Hz, 9H, P*Me$_3$*); 0.58 (d, ^{4}*JH-P* = 1.8 Hz, 3H, Si*Me*). ^{13}C{^{1}H}-NMR (75.4 MHz; toluene-d$_8$; -40 °C; δ, ppm): 157.5, 154.9, 154.4, 136.6, 136.0, 135.5, 135.1, 134.2, 133.3, 132.4, 131.4, 129.9, 127.2, 123.7, 123.6, 121.2, 21.9, 21.5, 20.8, 20.3, 30.0, 19.4 (d, $^1J_{C-P}$ = 21.0 Hz, P*Me$_3$*), 19.3 (d, $^1J_{C-P}$ = 21.6 Hz, P*Me$_3$*), 18.7 (d, $^1J_{C-P}$ = 25.2 Hz, P*Me$_3$*), 18.6 (d, $^1J_{C-P}$ = 25.1 Hz, P*Me$_3$*), 1.0 (s, Si*Me*), -3.4 (s, Si*Me*). ^{31}P{^{1}H}-NMR (121.4 MHz; toluene-d$_8$; 25 °C; δ, ppm): 5.5 (bs, *P*Me$_3$); -7.9 (bs, *P*Me$_3$). ^{29}Si-NMR (59.6 MHz; toluene-d$_8$; 25 °C; δ, ppm): -74.0 (d, $^1J_{Si-H}$ = 100

Hz). $^{29}Si\{^1H\}$-NMR (59.6 MHz; toluene-d_8; -40 °C; δ, ppm): -69.3 (d, $^1J_{Si-H}$ = 98.0 Hz). IR (nujol): 1906 cm^{-1} (weak, Si-H). Elem. Anal. (%): calc. for $C_{24}H_{43}N_2MoP_2SiCl$ (643.116): 54.16, H 7.05, N 4.36; found: C 54.03, H 7.06, N 4.43.

NMR scale reaction of (^{t}BuN)$_2$Mo(PMe$_3$)$_3$ (III-27) with MePhSiHCl

MePhSiHCl (7.5 µl, 0.05 mmol) was added in one portion at room temperature to a solution of (^{t}BuN)$_2$Mo(PMe$_3$)$_2$ (**III-27**) (19.5 mg, 0.05 mmol) in 0.6 ml of C_6D_6 in an NMR tube. The mixture was left to stand at room temperature for an hour to give a dark-brown solution. NMR analysis showed the formation of a mixture of (^{t}BuN)Mo(Cl)(η^3-^{t}BuN-SiPhMe-H)(PMe$_3$)$_2$ (**III-43c**; as a mixture of two isomers; ~ 70 %) and (^{t}BuN)MoCl$_2$(PMe$_3$)$_3$ (**III-48**; ~ 30 %).

(^{t}BuN)Mo(Cl)(η^3-^{t}BuN-SiPhMe-H)(PMe$_3$)$_2$ (**III-43c**): IR (nujol): 2121 cm^{-1} (weak, Si-H). ^{29}Si-NMR (59.6 MHz; 25 °C; C_6D_6; δ, ppm): -79.9 (ddd, $^1J_{Si-H}$ = 94 Hz, $^2J_{Si-H}$ = 3.1 Hz, $^2J_{Si-P}$ = 5.6 Hz). Major isomer of **III-43c**: ^{1}H-NMR(300 MHz; toluene-d_8, -20 °C; δ, ppm): 7.92 (d, $^3J_{H-H}$ = 7.8 Hz, 2H, *o*-H, Si*Ph*); 7.23 (m, 2H, *m*-H, Si*Ph*); 7.14 (m, 1H, *p*-H, Si*Ph*); 1.64 (m, Mo*H*, found from ^{1}H-^{29}Si HSQC); 1.70 (s, 9H, ^{t}*Bu*N); 1.44 (d, $^2J_{H-P}$ = 8.1 Hz, 9H, P*Me$_3$*); 1.37 (d, $^2J_{H-P}$ = 6.9 Hz, 9H, P*Me$_3$*); 0.72 (s, 9H, ^{t}*Bu*N). $^{13}C\{^1H\}$-NMR (75.4 MHz; toluene-d_8, -20 °C; δ, ppm): 140.3 (s, *o*-C, Si*Ph*); 133.4 (s, *p*-C, Si*Ph*); 133.0 (s, *m*-C, Si*Ph*); 55.1 (s, ^{t}*Bu*N); 40.8 (s, ^{t}*Bu*N); 35.5 (s, ^{t}*Bu*N); 27.5 (s, P*Me$_3$*), 27.1 (s, P*Me$_3$*). $^{31}P\{^1H\}$-NMR (121.4 MHz; toluene-d_8, -20 °C; δ, ppm): 12.2 (d, $^2J_{P-P}$ = 12.7 Hz, 1P, *P*Me$_3$); 1.4 (d, $^2J_{P-P}$ = 12.7 Hz, 1P, *P*Me$_3$). Minor isomer of **III-43c**: ^{1}H-NMR(300 MHz; toluene-d_8,-20 °C; δ, ppm): 8.36 (d, $^3J_{H-H}$ = 7.8 Hz, 2H, *o*-H, Si*Ph*); 7.39 (m, 2H, *m*-H, Si*Ph*); 7.21(m, 1H, *p*-H, Si*Ph*); 1.95 (s, 9H, ^{t}*Bu*N); 1.83 (Mo*H*, found from the ^{1}H-^{29}Si HSQC), 1.46 (d, $^2J_{H-P}$ = 6.9 Hz, 9H, P*Me$_3$*); 1.26 (d, $^2J_{H-P}$ = 7.2 Hz, 9H, P*Me$_3$*); 1.05 (s, 9H, ^{t}*Bu*N). $^{13}C\{^1H\}$-NMR (75.4 MHz; toluene-d_8, -20 °C; δ, ppm): 142.8 (s, *o*-C, Si*Ph*); 140.2 (s, *m*-C, Si*Ph*); 134.6 (s, *p*-C, Si*Ph*); 43.0 (s, ^{t}*Bu*N); 27.5 (s, P*Me$_3$*); 27.0 (s, P*Me$_3$*); 36.4 (s, ^{t}*Bu*N). $^{31}P\{^1H\}$-NMR (121.4 MHz; toluene-d_8; -20 °C; δ, ppm): 12.3 (d, $^2J_{P-P}$ = 13.5 Hz, 1P, *P*Me$_3$); -0.3 (d, $^2J_{P-P}$ = 13.5 Hz, 1P, *P*Me$_3$).

NMR scale reaction of (ArN)$_2$Mo(PMe$_3$)$_3$ (III-22) with MeSiHCl$_2$

MeSiHCl$_2$ (6.5 µl, 0.062 mmol) was added at room temperature to a solid (ArN)$_2$Mo(PMe$_3$)$_3$ (**III-22**) (41.7 mg, 0.062 mmol) in 0.6 ml of toluene-d_8 in an NMR

tube. The colour of the solution turned from dark-green to brown and the mixture was left at room temperature for 10 min. NMR analysis showed the quantitative formation of a highly fluxional at room temperature agostic complex (ArN)Mo(Cl)(η^3-NAr-SiMeCl-H)(PMe_3)$_2$ (**III-44a**). The product is unstable at room temperature in solution and decomposes to form (ArN)$MoCl_2(PMe_3)_3$ (**III-47**).

(ArN)Mo(Cl)(η^3-NAr-SiMeCl-H)(PMe_3)$_2$ (**III-44a**): ^{1}H-NMR (300 MHz; toluene-d$_8$; -50 °C; δ, ppm): 4.27 (sept, $^3J_{H-H}$ = 6.6 Hz, 1H, *CH*, *Ar*N); 4.19 (sept, $^3J_{H-H}$ = 6.6 Hz, 1H, *CH*, *Ar*N); 3.74 (sept, $^3J_{H-H}$ = 6.3 Hz, 1H, *CH*, *Ar*N); 2.92 (sept, $^3J_{H-H}$ = 6.3 Hz, 1H, *CH*, *Ar*N); 1.50 (d, $^3J_{H-H}$ = 6.6 Hz, 3H, *CH$_3$*, *Ar*N); 1.47 (d, $^3J_{H-H}$ = 6.6 Hz, 3H, *CH$_3$*, *Ar*N); 1.45 (s, 3H, Si*Me*); 1.39 (d, $^3J_{H-H}$ = 6.3 Hz, 3H, *CH$_3$*. *Ar*N); 1.28 (d, $^3J_{H-H}$ = 6.0 Hz, 3H, *CH$_3$*, *Ar*N); 1.23 (Mo-*H*-Si obscured by a PMe_3 signal but determined from ^{1}H-^{29}Si HSQC at -50 °C); 1.17 (m, Ar signal obscured by PMe_3, 6H, 2 *CH$_3$*, *Ar*N); 1.16 (d, $^2J_{H-P}$ = 7.5 Hz, 9H, P*Me$_3$*); 0.99 (doublet of the Ar signal obscured by PMe_3, 3H, *CH$_3$*, *Ar*N); 0.98 (d, $^2J_{H-P}$ = 8.7 Hz, 9H, P*Me$_3$*); 0.89 (d, $^3J_{H-H}$ = 6.6 Hz, 3H, *CH$_3$*, *Ar*N). ^{13}C{^{1}H}-NMR (75.4 MHz; toluene-d$_8$; -50 °C; δ, ppm): 152.6 (s, *i*-C, N*Ar*); 151.4 (s, *i*-C, N*Ar*); 145.1 (s, *o*-H, N*Ar*); 144.9 (s, *o*-H, N*Ar*); 143.9 (s, *o*-H, N*Ar*); 140.0 (s, *o*-H, N*Ar*); 124.0; 123.9; 123.5; 122.4; 122.3; 29.3 (s, *CH$_3$*, N*Ar*); 28.4 (s, *CH$_3$*, N*Ar*); 27.7 (s, *CH*, N*Ar*); 27.4 (s, *CH*, N*Ar*); 26.6 (s, *CH*, N*Ar*); 26.3 (s, *CH*, N*Ar*); 25.5 (s, *CH$_3$*, N*Ar*); 24.6 (s, *CH$_3$*, N*Ar*); 24.5 (s, *CH$_3$*, N*Ar*); 24.3 (s, *CH$_3$*, N*Ar*); 23.7 (s, *CH$_3$*, N*Ar*); 22.1 (s, *CH$_3$*, N*Ar*); 20.7 (P*Me$_3$*, obscured by toluene); 19.6 (P*Me$_3$*, obscured by toluene); 5.6 (s, Si*Me*). ^{31}P{^{1}H}-NMR (121.4 MHz; toluene-d$_8$; -50 °C; δ, ppm): 10.5 (d, $^2J_{P-P}$ = 8.7 Hz, *P*Me_3); -3.8 (d, $^2J_{P-P}$ = 8.7 Hz, *P*Me_3). ^{31}P{^{1}H}-NMR (121.4 MHz; C_6D_6; 25 °C; δ, ppm): 8.7 (bs, *P*Me_3); - 4.5 (bs, *P*Me_3). ^{29}Si-NMR (119.2 MHz; toluene-d$_8$; -50 °C; δ, ppm): - 68.5 (dd, $^1J_{Si-H}$ = 130.0 Hz, $^2J_{Si-P}$ = 16.2 Hz). IR (nujol): 1919 cm^{-1} (Si-H).

NMR scale reaction of (Ar'N)$_2$Mo(PMe_3)$_3$ (III-4) with $MeSiHCl_2$[15]

$MeSiHCl_2$ (9.4 µl, 0.09 mmol) was added at room temperature to a solution of (Ar'N)$_2$Mo(PMe_3)$_3$ (**III-4**) (45.6 mg, 0.081 mmol) in 0.6 ml of toluene-d$_8$ in an NMR tube. The colour of the solution turned from green to brown and the reaction mixture was left at room temperature for 5 min. NMR analysis showed the quantitative formation of

(Ar'N)Mo(Cl)(η^3-Ar'N-SiMeCl-H)(PMe_3)$_2$ (**III-39**). The product is not stable at room temperature in solution and decomposes forming (Ar'N)$MoCl_2(PMe_3)_3$ (**III-5**).[15]

(Ar'N)Mo(Cl)(η^3-Ar'N-SiMeCl-H)(PMe_3)$_2$ (**III-39**): ^{1}H-NMR (300 MHz; toluene-d_8; - 10 °C; δ, ppm): 7.07 (bd, $^3J_{H-H}$ = 7.6 Hz, 1H, *m*-H, *Ar*N); 6.98 (bd, $^3J_{H-H}$ = 7.5 Hz, 1H, *m*-H, *Ar*N); 6.87 (dd, $^3J_{H-H}$ = 7.5 Hz, 1H, *p*-H, *Ar*N); 6.87 (bs, 3H, *m*-H and *p*-H, *Ar*N); 2.60 (bs, 3H, *CH*$_3$, *Ar*N); 2.39 (bs, 3H, *CH*$_3$, *Ar*N); 2.37 (bs, 6H, 2 *CH*$_3$, *Ar*N); 1.76 (dq, $^2J_{H-P}$ = 18.0 Hz, $^3J_{H-H}$ = 1.5 Hz, 1H, Mo*H*); 1.18 (d, $^2J_{H-P}$ =7.4 Hz, 9H, P*Me*$_3$); 0.99 (d, $^2J_{H-P}$ = 8.5 Hz, 9H, P*Me*$_3$); 0.97 (d, $^3J_{H-H}$ = 1.5 Hz, 3H, Si*Me*). ^{13}C{^{1}H}-NMR (75.4 MHz; toluene-d_8; - 10 °C; δ, ppm): 154.9 (d, $^3J_{C-P}$ = 1.8 Hz, *i*-C, *Ar*N); 154.5 (dd, $^3J_{C-P}$ = 1.8 and 3.5 Hz, *i*-C, *Ar*N); 134.6 (s, *o*-C, *Ar*N); 128.5 (s, *m*-C, *Ar*N); 128.4 (s, *m*-C, *Ar*N); 124.3 (s, *p*-C, *Ar*N); 121.7 (s, *p*-C, *Ar*N); 21.1 (s, *CH*$_3$, *Ar*N); 20.4 (s, *CH*$_3$, *Ar*N); 19.3 (d, $^1J_{C-P}$ = 22.8 Hz, P*Me*$_3$); 18.6 (d, $^1J_{C-P}$ = 25.8 Hz, P*Me*$_3$); 1.8 (s, Si*Me*). ^{31}P{^{1}H}-NMR(121.4 MHz; toluene-d_8; - 60 °C; δ, ppm): 10.2 (bd, $^2J_{P-P}$ = 6.5 Hz, *P*Me$_3$); - 5.0 (bd, $^2J_{P-P}$ = 6.5 Hz, *P*Me$_3$). ^{29}Si-NMR (59.6 MHz; C_6D_6; 25 °C; δ, ppm):- 70.1 (dd, $^1J_{Si-H}$ = 129.0 Hz, $^2J_{Si-P}$ = 7.2 Hz, η^3-Ar'N-*Si*MeCl-H). ^{29}Si-NMR (119.2 MHz; toluene-d_8; - 50 °C; δ, ppm): - 70.5 (dd, $^1J_{Si-H}$ = 135.6 Hz, $^2J_{Si-P}$ = 20.6 Hz, η^3-Ar'N-*Si*MeCl-H). IR (nujol): 1920 cm^{-1} (Si-H, weak). Elem. Anal. (%): calc. for $C_{23}H_{40}N_2MoP_2SiCl_2$ (601.353): C 45.93, H 6.70, N 4.66; found: C 46.23, H 6.93, N 4.74.

NMR scale reaction of (^{t}BuN)$_2$Mo(PMe_3)$_3$ (III-27) with $MeSiHCl_2$

$MeSiHCl_2$ (4.3 µl, 0.041 mmol) was added in one portion at room temperature to a solution of (^{t}BuN)$_2$Mo(PMe_3)$_2$ (**III-27**) (16.0 mg, 0.041 mmol) in 0.6 ml of C_6D_6 in an NMR tube. The mixture was left at room temperature for 10 min., during which time the colour changed to a different tint of brown. NMR analysis showed the quantitative formation of (^{t}BuN)Mo(Cl)(η^3-^{t}BuN-SiMeCl-H)(PMe_3)$_2$ (**III-44c**). The product is not stable at room temperature in solution and decomposes forming (^{t}BuN)$MoCl_2(PMe_3)_3$ (**III-48**).

(^{t}BuN)Mo(Cl)(η^3-^{t}BuN-SiMeCl-H)(PMe_3)$_2$ (**III-44c**): ^{1}H-NMR (300 MHz; C_6D_6; δ, ppm): 1.54 (s, 9H, ^{t}*Bu*N); 1.43 (dd, $^2J_{H-P}$ = 3.6 Hz, 0.9 Hz, 1H, Mo*H*); 1.35 (d, $^2J_{H-P}$ = 8.0 Hz, 9H, P*Me*$_3$); 1.28 (d, $^2J_{H-P}$ = 7.1 Hz, 9H, P*Me*$_3$); 1.19 (s, 3H, Si*Me*Cl); 1.15 (s, 9H, ^{t}*Bu*N). ^{13}C{^{1}H}-NMR (75.4 MHz; C_6D_6; δ, ppm): 69.7 (s, ^{t}*Bu*N); 54.9 (s, ^{t}*Bu*N); 35.2 (s, ^{t}*Bu*N);

31.1 (s, ^{t}*Bu*N); 22.5 (dd, $^{2}J_{C\text{-}P}$ = 2.5 Hz, $^{1}J_{C\text{-}P}$ = 24.8 Hz, P*Me*$_3$); 22.2 (d, $^{2}J_{C\text{-}P}$ = 22.0 Hz, P*Me*$_3$); 3.2 (s, Si*Me*Cl). ^{31}P{$_1$H}-NMR (121.4 MHz; C_6D_6; δ, ppm): 9.8 (d, $^{2}J_{P\text{-}P}$ = 11.8 Hz, 1P, *P*Me$_3$); -3.7 (d, $^{2}J_{P\text{-}P}$ = 11.8 Hz, 1P, *P*Me$_3$). ^{29}Si-NMR (59.6 MHz; C_6D_6; δ, ppm): -74.2 (dd, $^{1}J_{Si\text{-}H}$ = 123 Hz, $^{2}J_{Si\text{-}P}$ = 9 Hz). IR (nujol): 1851 cm^{-1} (weak, Si-H). Elem. Anal.[f] (%): calc. for $C_{15}H_{40}N_2MoCl_2SiP_2$ (505.37): C 35.65, H 7.98, N 5.54; found: C 34.44, H 7.71, N 5.43.

NMR scale reaction of (ArN)$_2$Mo(PMe$_3$)$_3$ (III-22) with PhSiH$_2$Cl

A. NEt$_3$ (35. 5 μl, 0.255 mmol) and PhSiH$_2$Cl (6.8 μl, 0.051 mmol) were added at room temperature to a solution of (ArN)$_2$Mo(PMe$_3$)$_3$ (**III-22**) (34.4 mg, 0.051 mmol) in 0.6 ml of C_6D_6 in an NMR tube. The colour of the solution changed from dark-green to brown almost immediately and the reaction mixture was left at room temperature for 5 min. NMR analysis showed selective formation of (ArN)Mo(Cl)(η^3-NAr-SiHPh-H)(PMe$_3$)$_2$ (**III-45a**). No further reaction of **III-45a** with NEt$_3$ was observed in additional 15 min. All volatiles were pumped off; the residue was dried in vacuum and redissolved in 0.6 ml of fresh C_6D_6. A solution of L-Selectride in THF (51.0 μl, 0.051 mmol, C = 1.0 M) was added at room temperature to a solution of **III-45a**. The reaction mixture was left at room temperature for 5 min. NMR analysis showed formation of a difficult-to-separate mixture of (ArN)$_2$Mo(PMe$_3$)$_3$ (**III-22**), (ArN)Mo(H)(SiH$_2$Ph)(PMe$_3$)$_3$ (**III-7**; see the preparation and characterization below), and (ArN)Mo(SiH$_2$Ph)(η^3-NAr-SiHPh-H)(PMe$_3$) (**III-1**; see the preparation and characterization below).

(ArN)Mo(Cl)(η^3-NAr-SiHPh-H)(PMe$_3$)$_2$ (**III-45a**): ^{1}H-NMR (300 MHz; C_6D_6; δ, ppm): 8.48 (d, $^{3}J_{H\text{-}H}$ = 5.4 Hz, 2H, *o*-H, Si*Ph*); 6.85-7.2 (m, 9H, aromatic protons of *Ar*N and Si*Ph*); 5.4 (bs, 1H, Si*H$_{term}$*); 4.43 (sept, $^{3}J_{H\text{-}H}$ = 6.6 Hz, 1H, *CH*, *Ar*N); 4.08 (bs, 1H, *CH*, *Ar*N); 3.46 (sept, $^{3}J_{H\text{-}H}$ = 6.3 Hz, 1H, *CH*, *Ar*N); 3.18 (sept, $^{3}J_{H\text{-}H}$ = 6.6 Hz, 1H, *CH*, *Ar*N); 2.17 (bs, 1H, Si*H$_{ag}$*); 1.47 (d, $^{3}J_{H\text{-}H}$ = 6.3 Hz, 3H, *CH$_3$*; *Ar*N); 1.30 (d, $^{3}J_{H\text{-}H}$ = 6.6 Hz, 12H, 4 *CH$_3$*; *Ar*N); 1.15 (m, 15H, P*Me*$_3$ and 2 *CH$_3$* of *Ar*N); 0.99 (bm, 9H, P*Me$_3$*); 0.64 (bs, 3H, *CH$_3$*, *Ar*N). ^{31}P{^{1}H}-NMR (121.5 MHz; C_6D_6; δ, ppm): -7.6 (d, $^{2}J_{P\text{-}P}$ = 9.7 Hz, 1P, *P*Me$_3$); 2.6 (d, $^{2}J_{P\text{-}P}$ = 9.7 Hz, 1P, *P*Me$_3$).

B. PhSiH$_2$Cl (4.8 μl, 0.036 mmol) was added at room temperature to a solution of (ArN)$_2$Mo(PMe$_3$)$_3$ (**III-22**) (24.4 mg, 0.036 mmol) in 0.6 ml of benzene in an NMR tube.

The reaction mixture was left at room temperature for 10 min. All volatiles were pumped off; the residue was dried in vacuum and dissolved in C_6D_6. NMR analysis showed the presence of only (ArN)Mo(Cl)(η^3-NAr-SiHPh-H)(PMe_3)$_2$ (**III-45a**). A solution of L-Selectride in THF (36.0 µl, 0.036 mmol, C = 1.0 M) and PMe_3 (3.7 µl, 0.036 mmol) were added simultaneously at room temperature. The colour of the solution changed from brown to dark-green almost immediately. NMR analysis after 5 min at room temperature showed the formation of a difficult-to-separate mixture of (ArN)$_2$Mo(PMe_3)$_3$ (**III-22**), (ArN)Mo(H)(SiH_2Ph)(PMe_3)$_3$ (**III-7**), and (ArN)Mo(SiH_2Ph)(η^3-NAr-SiHPh-H)(PMe_3) (**III-1**).

C. $PhSiH_2Cl$ (4.5 µl, 0.034 mmol) was added at room temperature to a solution of (ArN)$_2$Mo(PMe_3)$_3$ (**III-22**) (22.6 mg, 0.034 mmol) in 0.6 ml of C_6D_6 in an NMR tube. The colour of the solution changed from dark-green to brown almost immediately and the reaction mixture was left at room temperature for 5 min. NMR analysis showed selective formation of (ArN)Mo(Cl)(η^3-NAr-SiHPh-H)(PMe_3)$_2$ (**III-45a**). All volatiles were pumped off; the residue was dried in vacuum and redissolved in 0.6 ml of C_6D_6. NEt_3 (23.3 µl, 0.168 mmol) was added at room temperature to a solution and the mixture was left at 50 °C overnight. NMR analysis revealed the formation of a difficult-to-separate mixture of (ArN)$MoCl_2$(PMe_3)$_3$ (**III-47**), (ArN)Mo(H)(Cl)(PMe_3)$_3$ (**III-6**; see the preparation and characterization below), and (ArN-SiHPh)$_2$.

NMR scale reaction of (Ar'N)$_2$Mo(PMe_3)$_3$ (III-4) with $PhSiH_2Cl$

A. $PhSiH_2Cl$ (7.4 µl, 0.055 mmol) was added at room temperature to a solution of (Ar'N)$_2$Mo(PMe_3)$_3$ (**III-4**) (31.0 mg, 0.055 mmol) in 0.6 ml of C_6D_6 in an NMR tube. The colour of the solution changed from dark-green to brown almost immediately and the reaction mixture was left at room temperature for 5 min. All volatiles were pumped off; the residue was dried in vacuum and redissolved in 0.6 ml of fresh C_6D_6. NMR analysis showed the presence of only (Ar'N)Mo(Cl)(η^3-NAr'-SiHPh-H)(PMe_3)$_2$ (**III-45b**). A solution of L-Selectride in THF (55.0 µl, 0.055 mmol, C = 1.0 M) was added at room temperature to a solution. The reaction mixture was left at room temperature for 5 min. NMR analysis showed the formation of a difficult-to-separate mixture of

$(Ar'N)_2Mo(PMe_3)_3$ (**III-4**) and $(Ar'N)Mo(H)(SiH_2Ph)(PMe_3)_3$ (**III-73**; see the preparation and characterization below).

(Ar'N)Mo(Cl)(η^3-NAr'-SiHPh-H)(PMe_3)$_2$ (**III-45b**): ^{1}H-NMR (300 MHz; C_6D_6; δ, ppm): 8.19 (m, 2H, *o*-H, SiPh); 7.12 (m, 3H, *Ar'*N); 7.04 (d, $^3J_{H-H}$ = 7.2 Hz, 2H, *m*-H, Si*Ph*); 6.87 (t, $^3J_{H-H}$ = 7.5 Hz, 1H, *p*-H, Si*Ph*); 6.78 (bs, 3H, *Ar'*N); 3.79 (bs, 2H, SiH_2Ph); 2.50 (bs, 6H, 2 CH_3, *Ar'*N); 2.26 (s, 6H, 2 CH_3, *Ar'*N); 1.15 (d, $^2J_{H-P}$ = 7.8 Hz, 18H, 2 PMe_3). $^{31}P\{^1H\}$-NMR (121.5 MHz; C_6D_6; δ, ppm): -7.1 (bs, 1P, PMe_3); 2.7 (bs, 1P, PMe_3).

B. $PhSiH_2Cl$ (4.6 µl, 0.034 mmol) was added at room temperature to a solution of $(Ar'N)_2Mo(PMe_3)_3$ (**III-4**) (19.3 mg, 0.034 mmol) in 0.6 ml of C_6D_6 in an NMR tube. The colour of the solution changed from dark-green to brown almost immediately and the reaction mixture was left at room temperature for 5 min. NMR analysis showed selective formation of $(Ar'N)Mo(Cl)(\eta^3$-Ar'N-SiHPh-H$)(PMe_3)_2$ (**III-45b**). All volatiles were pumped off; the residue was dried in vacuum and redissolved in 0.6 ml of C_6D_6. NEt_3 (24.0 µl, 0.172 mmol) was added at room temperature to a solution and the mixture was left at 50 °C overnight. NMR analysis showed the decomposition of **III-48b** and the formation of $(Ar'N)MoCl_2(PMe_3)_3$ (**III-5**) and $(Ar'N\text{-}SiHPh)_2$.[15]

C. $PhSiH_2Cl$ (4.5 µl, 0.034 mmol) was added at room temperature to a solution of $(Ar'N)_2Mo(PMe_3)_3$ (**III-4**) (18.9 mg, 0.034 mmol) in 0.6 ml of C_6D_6 in an NMR tube. The colour of the solution changed from dark-green to brown almost immediately and the reaction mixture was left at room temperature for 5 min. NMR analysis showed selective formation of $(Ar'N)Mo(Cl)(\eta^3$-Ar'N-SiHPh-H$)(PMe_3)_2$ (**III-45b**). All volatiles were pumped off; the residue was dried in vacuum and redissolved in 0.6 ml of C_6D_6. Li[BAF] (20.7 mg, 0.03 mmol) was added at room temperature to a solution and the mixture was left at room temperature for 10 min. NMR analysis showed decomposition of **III-45b** and the formation of a mixture of $(Ar'N)MoCl_2(PMe_3)_3$ (**III-5**)[15] and unidentified products.

NMR scale reaction of $(Ar'N)_2Mo(PMe^iPr_2)_2$ (III-25) with $PhSiH_2Cl$

$PhSiH_2Cl$ (4.8 µl, 0.036 mmol) was added at room temperature to a solution of $(Ar'N)_2Mo(PMe^iPr_2)_2$ (**III-25**) (21.6 mg, 0.036 mmol) in 0.6 ml of C_6D_6 in an NMR tube. The colour of the solution changed from green to brown almost immediately and the reaction mixture was left at room temperature for 5 min. NMR analysis showed the

presence of a difficult-to-characterize mixture of products (at least 4 compounds according to $^{31}P\{^{1}H\}$-NMR) and a large amount of non-coordinated $PMe^{i}Pr_2$.

NMR scale reaction of $(ArN)_2Mo(PMe_3)_3$ (III-22) with Me_2SiCl_2 and BPh_3

A solution of BPh_3 (6.0 mg, 0.025 mmol) and Me_2SiCl_2 (3.0 µl, 0.025 mmol) in 0.6 ml of C_6D_6 was added at room temperature to a solid $(ArN)_2Mo(PMe_3)_3$ (**III-22**) (16.7 mg, 0.025 mmol). The colour of the solution turned to a different tint of green and the mixture was transferred to an NMR tube and left at room temperature overnight. NMR analysis showed the presence of a mixture of $Ph_3B{\cdot}PMe_3$, Me_2SiCl_2, and $(ArN)_2Mo(PMe_3)_2$ (**III-19**).[196] Heating the mixture for 1 h at 50 °C did not promote any further reaction.

NMR scale reaction of $(ArN)_2Mo(PMe_3)_3$ (III-22) with $HSiCl_3$ and BPh_3

A solution of $HSiCl_3$ (4.0 µl, 0.04 mmol) and BPh_3 (9.5 mg, 0.04 mmol) in 0.3 ml of toluene-d_8 was added to an NMR tube containing a frozen solution of $(ArN)_2Mo(PMe_3)_3$ (**III-22**) (26.5 mg, 0.04 mmol) in 0.4 ml of toluene-d_8. The mixture was placed to the NMR spectrometer pre-cooled to - 20 °C and the sample was cooled down to - 70 °C. The mixture was slowly warmed up, and the course of the reaction was monitored by NMR spectroscopy. At - 30 °C, the formation of an initial product with the suggested structure $(ArN)Mo(Cl)(\eta^3\text{-}NAr\text{-}SiHCl\text{-}Cl)(PMe_3)_2$ (**III-54a**) was observed. Warming the mixture up to - 15 °C - 0 °C leads to a slow rearrangement of the initial product into another compound, whose NMR features are consistent with the structure $(ArN)MoCl_2(\eta^2\text{-}ArN{=}SiHCl)(PMe_3)_2$ (**III-55**). Further increase of the temperature to >0 °C leads to fast decomposition to a mixture of $(ArN\text{-}SiHCl)_2$ and $(ArN)MoCl_2(PMe_3)_3$ (**III-47**).

$(ArN)Mo(Cl)(\eta^3\text{-}NAr\text{-}SiHCl\text{-}Cl)(PMe_3)_2$ (**III-54a**): ^{1}H-NMR (600 MHz; -30 °C; toluene-d_8; δ, ppm): 7.44 (bm, 1H,N*Ar*); 7.33 (bm, 1H, N*Ar*); 6.92-7.19 (multiplet overlapping with the residual toluene-d_8 resonances, 4H, N*Ar*); 7.10 (1H, Si*H*, found by ^{1}H-^{29}Si HSQC); 4.85 (bs, 1H, *CH*, N*Ar*); 4.70 (bs, 1H, *CH*, N*Ar*); 3.98 (bs, 1H, *CH*, N*Ar*); 2.79 (bs, 1H, *CH*, N*Ar*); 1.60 (bs, 6H, 2 *CH*$_3$, N*Ar*); 1.49 (bs, 3H, *CH*$_3$, N*Ar*); 1.37 (bs, 6H, 2 *CH*$_3$, N*Ar*); 1.04 (bs, 9H, P*Me*$_3$); 0.94 (bs, 9H, P*Me*$_3$); 0.90 (bs, 3H, *CH*$_3$, N*Ar*); 0.77 (bs, 3H, *CH*$_3$, N*Ar*). $^{31}P\{^{1}H\}$-NMR (243 MHz; -30 °C; toluene-d_8; δ, ppm): 20.0 (bs, *P*Me$_3$); -2.6 (bs, *P*Me$_3$). ^{29}Si INEPT+ NMR (119.2 MHz; -30 °C; toluene-d_8; J = 200 Hz; δ, ppm):

- 31.8 (d, $^1J_{Si-H}$ = 337.5 Hz, Si*H*). ^{1}H-^{13}C HSQC NMR (151 MHz; -30 °C; toluene-d_8; *J* = 145 Hz; δ, ppm): 130.9; 125.1; 124.9; 124.7; 124.1 (all *m*-C and *p*-C of N*Ar*); 28.5; 27.9; 26.5; 25.7 (all *CH*, N*Ar*); 30.5; 27.3; 26.4; 24.7; 23.8; 22.4 (all CH_3, N*Ar*); 20.6 and 18.8 (PMe_3).

(ArN)MoCl$_2$(η^2-ArN=SiHCl)(PMe$_3$)$_2$ (**III-55**): ^{1}H-NMR (600 MHz; -50 °C; toluene-d_8; δ, ppm): 6.81-7.38 (multiplet overlapping with the residual toluene-d_8 resonances, 6H, N*Ar*); 6.01 (bd, $^3J_{H-P}$ = 9.0 Hz, 1H, Si*H*); 4.41 (bs, 1H, *CH*, N*Ar*); 4.11 (bs, 1H, *CH*, N*Ar*); 3.70 (bs, 1H, *CH*, N*Ar*); 3.11 (bs, 1H, *CH*, N*Ar*); 1.60 (bs, 6H, 2 CH_3, N*Ar*); 1.53 (bs, 3H, CH_3, N*Ar*); 1.49 (bs, 3H, CH_3, N*Ar*); 1.39 (bs, 6H, 2 CH_3, N*Ar*); 1.23 (bs, 3H, CH_3, N*Ar*); 1.07 (bs, 3H, CH_3, N*Ar*); 1.19 (bs, 9H, PMe_3), 0.63 (bs, 9H, PMe_3). ^{31}P{^{1}H}-NMR (243 MHz; -50 °C; toluene-d_8; δ, ppm): - 8.6 (d, $^2J_{P-P}$ = 223.5 Hz, *P*Me$_3$), - 17.1 (d, $^2J_{P-P}$ = 223.5 Hz, *P*Me$_3$). ^{29}Si INEPT+ NMR (119.2 MHz; -50 °C; toluene-d_8; *J* = 200 Hz; δ, ppm): - 42.4 (dd, $^1J_{Si-H}$ = 327.0 Hz, $^2J_{Si-P}$ = 22.1 Hz, *Si*H). ^{1}H-^{13}C HSQC NMR (151 MHz; -30 °C; toluene-d_8; *J* = 145 Hz; δ, ppm): 127.8; 124.8; 124.7; 124.3; 123.6 (all *m*-C and *p*-C of N*Ar*); 28.4; 28.2; 27.2; 26.7 (all *CH*, N*Ar*); 30.5; 27.3; 25.9; 25.8; 24.8; 24.7; 24.5; 23.8 (all CH_3, N*Ar*); 16.8 and 15.3 (PMe_3).

NMR scale reaction of (ArN)$_2$W(PMe$_3$)$_3$ (III-23) with HSiCl$_3$ and BPh$_3$

A solution of $HSiCl_3$ (4.2 µl, 0.041 mmol) and BPh_3 (10.0 mg, 0.041 mmol) in 0.4 ml of toluene-d_8 was added at -80 °C to a solution of (ArN)$_2$W(PMe$_3$)$_3$ (**III-23**) (31.5 mg, 0.041 mmol) in 0.4 ml of toluene-d_8 in an NMR tube. The mixture was immediately frozen by liquid nitrogen and placed to a 600 MHz NMR spectrometer pre-cooled to -30 °C, and cooled down to -70 °C. The mixture was slowly warmed up, and the course of thereaction was monitored by NMR spectroscopy. At -20 °C, the selective formation of an initial product with the suggested structure (ArN)$_2$W(H)(SiCl$_3$)(PMe$_3$) (**III-56**) was observed. Warming the mixture up to -10 °C leads to a slow rearrangement of the initial product into other hydride species, which do not contain a coordinated PMe_3 ligand. Addition of excess PMe_3 and warming the mixture up to room temperature results in fast formation of (ArN-SiHCl)$_2$ and (ArN)WCl$_2$(PMe$_3$)$_3$ (**III-51**).

(ArN)$_2$W(H)(SiCl$_3$)(PMe$_3$) (**III-56**): ^{1}H-NMR (600 MHz; -50 °C; toluene-d_8; δ, ppm): 11.04 (d, $^2J_{H-P}$ = 58.8 Hz, 1H, W*H*); 7.00-7.26 (multiplet overlapping with the residual

toluene-d_8 resonances, 6H, N*Ar*); 4.01 (bs, 2H, 2 *CH*, N*Ar*); 3.91 (bs, 1H, *CH*, N*Ar*); 3.56 (bs, 1H, *CH*, N*Ar*); 1.50 (bs, 6H, 2 CH_3, N*Ar*); 1.42 (bs, 3H, CH_3, N*Ar*); 1.31 (m, 12H, 4 CH_3, N*Ar*); 1.19 (bs, 3H, CH_3, N*Ar*), 1.05 (d, $^2J_{H\text{-}P}$ = 7.8 Hz, 9H, PMe_3). $^1H\{^{31}P\}$-NMR (600 MHz; -50 °C; toluene-d_8; δ, ppm; selected resonances): 11.04 (bs, 1H, W*H*); 1.05 (s, 9H, PMe_3). $^{31}P\{^1H\}$-NMR (243 MHz; -50 °C; toluene-d_8; δ, ppm): 3.01 (s+sat, $^1J_{P\text{-}W}$ = 328.0 Hz, *P*Me_3). ^1H-^{29}Si HSQC NMR (119.2 MHz; *J* = 7 Hz; -20 °C; toluene-d_8; δ, ppm): 73.8 (*Si*Cl*3*). ^1H-^{13}C HSQC NMR (151 MHz; *J* = 145 Hz; -30 °C; toluene-d_8; δ, ppm): 127.4; 126.4; 123.9; 123.4; 123.3; 121.9 (all *m*-C and *p*-C of N*Ar*); 27.8; 27.6; 21.7 (all *CH*, N*Ar*); 26.5; 25.9; 25.2; 24.8; 24.0; 23.5; 21.1 (all CH_3, N*Ar*); 18.0 (PMe_3).

(ArN)WCl_2*(*PMe_3*)*$_3$ (**III-51**): ^1H-NMR (300 MHz; C_6D_6; δ, ppm): 7.13(m, 1H, *p*-H, N*Ar*); 6.92 (d, $^3J_{H\text{-}H}$ = 7.2 Hz, 2H, *m*-H, N*Ar*); 4.02 (sept, $^3J_{H\text{-}H}$ = 7.0 Hz, 2H, 2 *CH*, N*Ar*); 4.01 (sept, $^3J_{H\text{-}H}$ = 7.2 Hz, 2H, 2 *CH*, N*Ar*); 1.45 (vt, $^2J_{H\text{-}P}$ = 4.2 Hz, 18H, 2 PMe_3); 1.44 (d, $^2J_{H\text{-}P}$ = 7.1 Hz, 9H, PMe_3); 1.18 (d, $^3J_{H\text{-}H}$ =7.2 Hz, 12H, 4 CH_3, N*Ar*). $^{13}C\{^1H\}$-NMR (125.7 MHz; C_6D_6; δ, ppm): 151.5; 145.1; 125.5 (*p*-C, N*Ar*); 123.7 (*m*-C, N*Ar*); 27.6 (*CH*, NAr); 27.4 (d, $^1J_{C\text{-}P}$ = 27.3 Hz, PMe_3); 25.3 (CH_3, N*Ar*); 18.0 (vt, $^1J_{C\text{-}P}$ = 13.4 Hz, PMe_3). $^{31}P\{^1H\}$-NMR (121.4 MHz; C_6D_6; δ, ppm): - 27.8 (s, 2 *P*Me_3); - 28.8 (s, *P*Me_3).

NMR scale reaction of (^{t}BuN)$_2$Mo(η^2-CH$_2$=CH$_2$)(PMe$_3$) (III-30) with HSiCl$_3$

$HSiCl_3$ (18.2 µl, 0.18 mmol) and PMe_3 (12.4 µl, 0.12 mmol) were added at room temperature to a solution of (^{t}BuN)$_2$Mo(η^2-CH_2=CH_2)(PMe_3) (**III-30**) (20.5 mg, 0.06 mmol) in 0.6 ml of C_6D_6 in an NMR tube. The reaction mixture was left at room temperature for 5 min. During this time the colour of the solution changed from yellow to purple. NMR analysis showed quantitative formation of (^{t}BuN)$MoCl_2(PMe_3)_3$ (**III-48**). A similar low temperature NMR experiment in toluene-d_8 did not provide observation of any intermediates in this reaction.

Reaction of (ArN)$_2$Mo(η^2-CH$_2$=CH$_2$)(PMe$_3$)$_2$ (III-31) with HSiCl$_3$

$HSiCl_3$ (0.45 ml, 4.45 mmol) and PMe_3 (0.23 ml, 2.23 mmol) were added at room temperature to a solution of $(ArN)_2Mo(\eta^2\text{-}CH_2{=}CH_2)(PMe_3)_2$ (**III-31**) (0.93 g, 1.48 mmol) in 50 ml of Et_2O. The reaction mixture was left at room temperature overnight. NMR analysis of the reaction mixture showed formation of a difficult-to-separate mixture of $(ArN)MoCl_2(PMe_3)_3$ (**III-47**; ~70 %) and unidentified products. Ether solution was

concentrated forming a green residue, which was filtered off and washed with 10 ml of hexanes. NMR analysis revealed the presence of the same mixture of **III-47** and unknown conpounds. All attempts to isolate **III-47** in analytically pure form by recrystallization from toluene solution at -30 °C led to the formation of a similar mixture observed before.

NMR scale reaction of $(ArN)_2Mo(\eta^2\text{-}CH_2{=}CH_2)(PMe_3)_2$ (III-31) with $HSiCl_3$ and BPh_3

A solution of $HSiCl_3$ (2.6 µl, 0.026 mmol) and BPh_3 (6.2 mg, 0.026 mmol) in 0.6 ml of C_6D_6 was added at room temperature to a solid $(ArN)_2Mo(\eta^2\text{-}CH_2{=}CH_2)(PMe_3)_2$ (**III-31**) (16.1 mg, 0.026 mmol). The colour of the solution turned to red immediately and the mixture was transferred to an NMR tube and left at room temperature for 5 min. NMR analysis showed the formation of a difficult-to-separate mixture of the starting material and $(ArN)Mo(Cl)(SiHCl_2)(\eta^2\text{-}CH_2{=}CH_2)(PMe_3)_2$ (**III-52**) (~ 1:1 by $^{31}P\{^1H\}$-NMR analysis).

(ArN)Mo(Cl)(SiHCl$_2$)(η^2-CH$_2$=CH$_2$)(PMe$_3$)$_2$ (**III-52**): ^{1}H-NMR (300 MHz; C_6D_6; δ, ppm): 6.84-7.38 (m, 3H, aromatic protons of *Ar*N overlapping with the aromatic signals of $Ph_3B{\cdot}PMe_3$); 6.7 (d, $^3J_{H\text{-}P}$ = 2.4 Hz, 1H, Si*H*Cl$_2$); 4.37 (sept, $^3J_{H\text{-}H}$ = 6.9 Hz, 1H, *CH*, *Ar*N); 4.19 (sept, $^3J_{H\text{-}H}$ = 6.9 Hz, 1H, *CH*, *Ar*N); 2.89 (m, 1H, η^2-C_2H_4); 2.44 (m, 2H, η^2-C_2H_4); 2.22 (m, 1H, η^2-C_2H_4); 1.56 (dd, $^3J_{H\text{-}H}$ = 6.9 Hz, 6H, 2 *CH$_3$*, *Ar*N); 1.51 (d, $^3J_{H\text{-}H}$ = 6.9 Hz, 3H, *CH$_3$*, *Ar*N); 1.16 (d, $^2J_{H\text{-}P}$ = 9.3 Hz, 9H, PMe_3); 1.09 (d, $^3J_{H\text{-}H}$ = 6.9 Hz, 3H, *CH$_3$*, *Ar*N). $^{31}P\{^1H\}$-NMR (121.5 MHz; C_6D_6; δ, ppm): 5.0 (bs, *P*Me$_3$). ^{1}H-^{29}Si HSQC NMR (119.2 MHz; C_6D_6; *J* = 200 Hz; ^{29}Si projection; δ, ppm): -30.8 (Mo*Si*HCl$_2$).

Reactions of $(RN)_2M(PR'_3)_{n-1}L$ with hydrosilanes

NMR scale reaction of $(ArN)_2Mo(PMe_3)_3$ (III-22) with $PhSiH_3$

A: Ambient temperature reaction. $PhSiH_3$ (8.0 µl, 0.063 mmol) was added in one portion at room temperature to a solution of $(ArN)_2Mo(PMe_3)_3$ (**III-22**) (42.5 mg, 0.063 mmol) in 0.6 ml of C_6D_6 in an NMR tube. The reaction mixture was left at room temperature for 6 days. NMR spectra showed the formation of a difficult-to-separate mixture of the products and the starting material: $(ArN)_2Mo(PMe_3)_3$ (**III-22**, 31 %),

(ArN)$MoH_4(PMe_3)_3$ (**III-63**, 21 %), and the tris(phosphine) trihydride agostic complex with suggested structure [η^3-PhHSi-(Ar)N-SiHPh-H]$MoH_3(PMe_3)_3$ (**III-64**, 48 %). $PhSiH_3$ (10.0 μl, 0.081 mmol) was added to the mixture in one portion at room temperature. The reaction mixture was left overnight showing complete conversion of the starting material and formation of a difficult-to-separate mixture of **III-63** and **III-64** (3:5, respectively, according to $^{31}P\{^1H\}$-NMR analysis). The ^1H-NMR spectrum also revealed the presence of Ph_2SiH_2, Ph_3SiH, and SiH_4 formed *via* the catalytic redistribution of $PhSiH_3$.[211] Further addition of excess $PhSiH_3$ (10.0 μl, 0.081 mmol) leads, after overnight at room temperature, to increased amount of Ph_2SiH_2, Ph_3SiH, and SiH_4. Monitoring the mixture with NMR spectroscopy also showed slow (few weeks) conversion of **III-63** into **III-64**, changing the ratio from 3:5 to 3:7, respectively.

(ArN)$MoH_4(PMe_3)_3$ (**III-63**):^1H-NMR (300 MHz; C_6D_6; δ, ppm): -5.27 (q, $^2J_{H-P}$ = 29.4 Hz, 4H, Mo*H*$_4$); 1.24 (bs, 18H, 2 P*Me*$_3$); 1.33 (d, $^3J_{H-H}$ = 6.9 Hz, 12H, 4 *CH*$_3$, *Ar*N); 4.02 (m, 2H, 2 *CH*, *Ar*N); 7.08 (m, 3H, *m-H* and *p-H*, *Ar*N). $^{31}P\{^1H\}$-NMR (121.5 MHz; C_6D_6; δ, ppm): 4.8 (s, 3 *P*Me_3); $^{31}P\{^1H\}$-NMR (243 MHz; C_6D_6; δ, ppm; selectively decoupled from methyl groups): 4.7 (pent, $^2J_{H-P}$ = 29.4 Hz, 3 *P*Me_3).

[η^3-PhHSi-(Ar)N-SiHPh-H]$MoH_3(PMe_3)_3$ (**III-64**): ^1H-NMR (600 MHz; toluene-d_8; -46 °C; δ, ppm): 8.90 (bs, 2H, *o-H*, Si*Ph*); 8.47 (bs, 2H, *o-H*, Si*Ph*); 6.84-7.35 (m, 9H, *m-H* and *p-H* of Si*Ph* and *m-H* and *p-H* of *Ar*N); 5.63 (bs, 1H, Si*H*Ph); 5.22 (bs, 1H, Si*H*Ph); 3.92 (bs, 2H, 2 *CH*, *Ar*N); 1.73 (bs, 12H, 4 *CH*$_3$, *Ar*N); 1.32 (bs, 9H, P*Me*$_3$); 1.08 (bs, 9H, P*Me*$_3$); 0.73 (bs, 9H, P*Me*$_3$); -5.61 (d, $^2J_{H-P}$ = 53.4 Hz, 1H, Mo-*H*); -6.58 (t, $^2J_{H-P}$ = 36.0 Hz, 1H, Mo-*H*); -8.82 (d, $^2J_{H-P}$ = 19.2 Hz, 1H, Mo-*H*). $^{31}P\{^1H\}$-NMR (121.5 MHz; C_6D_6; δ, ppm): -7.7 (s, 3 *P*Me_3). $^{31}P\{^1H\}$-NMR (243 MHz; toluene-d_8; -45 °C; δ, ppm): -8.8 (t, $^2J_{P-P}$ = 40.0 Hz, *P*Me_3); -6.6 (dd, $^2J_{P-P}$ = 21.9 Hz, $^2J_{P-P}$ = 40.0 Hz, *P*Me_3); 3.7 (dd, $^2J_{P-P}$ = 21.9 Hz, $^2J_{P-P}$ = 40.0 Hz, *P*Me_3). $^{29}Si\{^1H\}$-NMR (119.2 MHz; toluene-d_8; δ, ppm): -14.2 (s, *Si*HPh); 51.3 (s, *Si*HPh).

B: Low temperature reaction. $PhSiH_3$ (8.0 μl, 0.063 mmol) was added in one portion to a frozen in liquid nitrogen solution of $(ArN)_2Mo(PMe_3)_3$ (**III-22**) (42.5 mg, 0.063 mmol) in 0.6 ml of toluene-d_8 in an NMR tube. The sample was immediately placed to a precooled to -30 °C NMR machine. The temperature was dropped down to -60 °C and then gradually increased with the monitoring of the reaction by ^1H- and $^{31}P\{^1H\}$-NMR

analysis, showing at -30 °C the release of two equiv. of PMe_3 and selective formation of $(ArN)Mo(SiH_2Ph)(\eta^3\text{-}NAr\text{-}SiHPh\text{-}H)(PMe_3)$ (**III-1**) with a 50 % conversion of starting material. An increase in the temperature leads to a decomposition of **III-1** to a mixture of **III-63** and **III-64**. See the preparation and characterization of compound **III-1** below.

NMR scale reaction of $(ArN)_2Mo(\eta^2\text{-}CH_2{=}CH_2)(PMe_3)_2$ (III-31) with $PhSiH_3$

A. $PhSiH_3$ (14.5 µl, 0.118 mmol) was added in one portion at room temperature to a solution of $(ArN)_2Mo(\eta^2\text{-}CH_2{=}CH_2)(PMe_3)_2$ (**III-31**) (32.4 mg, 0.059 mmol) in 0.6 ml of C_6D_6 in an NMR tube. No visual changes were observed after silane addition. The reaction mixture was left at room temperature overnight. During this time the colour of the solution changed from purple to dark-green. NMR analysis showed formation of a difficult-to-separate mixture of $(ArN)Mo(SiH_2Ph)(\eta^3\text{-}NAr\text{-}SiHPh\text{-}H)(PMe_3)$ (**III-1**), $(ArN)MoH_4(PMe_3)_3$ (**III-63**) and $[\eta^3\text{-}PhHSi\text{-}(Ar)N\text{-}SiHPh\text{-}H]MoH_3(PMe_3)_3$ (**III-64**). The formation of $PhEtSiH_2$ was also observed by NMR spectroscopy.[202]

B. A solution of BPh_3 (13.9 mg, 0.057 mmol) and $PhSiH_3$ (14.2 µl, 0.115 mmol) in 0.6 ml of C_6D_6 was added at room temperature to a solid $(ArN)_2Mo(\eta^2\text{-}CH_2{=}CH_2)(PMe_3)_2$ (**III-31**) (36.0 mg, 0.057 mmol). The colour of the solution turned brown and the reaction mixture was left at room temperature for 5 min. NMR analysis showed quantitative formation of $(ArN)Mo(SiH_2Ph)(\eta^3\text{-}NAr\text{-}SiHPh\text{-}H)(PMe_3)$ (**III-1**) and $Ph_3B{\cdot}PMe_3$.

NMR scale reaction of $(ArN)_2Mo(PMe_2Ph)_2$ (III-24) with $PhSiH_3$

$PhSiH_3$ (4.6 µl, 0.037 mmol) was added in one portion at room temperature to a solution of $(ArN)_2Mo(PMe_2Ph)_2$ (**III-24**) (26.7 mg, 0.037 mmol) in 0.6 ml of C_6D_6 in an NMR tube. The reaction mixture was left for 5 min at room temperature. NMR analysis showed 50 % conversion of starting material and formation of $(ArN)Mo(SiH_2Ph)(\eta^3\text{-}NAr\text{-}SiHPh\text{-}H)(PMe_2Ph)$ (**III-65**) as a mixture of two isomers in a ratio 1:10. One more equivalent of $PhSiH_3$ (4.6 µl, 0.037 mmol) was added to the mixture. NMR analysis after 10 min at room temperature showed complete conversion of **III-24** into agostic complex **III-65**. The product is not stable in solution at room temperature and all attempts to isolate the product gave difficult-to-separate mixtures of **III-24**, **III-65**, and unidentified decomposition products.

(ArN)Mo(SiH$_2$Ph)(η^3-NAr-SiHPh-H)(PMe$_2$Ph) (**III-65**): Major isomer: ^{1}H-NMR (300 MHz; C_6D_6; δ, ppm): 8.29 (d, $^3J_{H-H}$ = 7.2 Hz, 2H, *o*-H, Si*Ph*); 7.38 (m, 2H, *o*-H, Si*Ph*); 6.91-7.30 (m, 17H, *m*-H and *p*-H of Si*Ph*, *m*-H and *p*-H of *Ar*N, *m*-H, *o*-H, and *p*-H of P*Ph*); 5.89 (bs, 1H, Si*H*$_2$Ph); 5.87 (bs, 1H, η^3-NArSi*H*Ph-H); 4.12 (sept, $^3J_{H-H}$ = 6.6 Hz, 2H, 2 *CH*, *Ar*N); 3.85 (bs, 1H, η^3-NArSiHPh-*H*); 3.34(sept, $^3J_{H-H}$ = 6.9 Hz, 1H, *CH*, *Ar*N); 2.77 (sept, $^3J_{H-H}$ = 6.9 Hz, 1H, *CH*, *Ar*N); 1.51 (d, $^2J_{H-P}$ = 8.4 Hz, 3H, *CH*$_3$, P*Me*$_2$Ph); 1.37 (d, $^2J_{H-P}$ = 8.1 Hz, 3H, *CH*$_3$, P*Me*$_2$Ph); 1.23 (d, $^3J_{H-H}$ = 6.6 Hz, 12H, 4 *CH*$_3$, *Ar*N); 1.09 (d, $^3J_{H-H}$ = 6.6 Hz, 6H, 2 *CH*$_3$, *Ar*N); 0.99 (d, $^3J_{H-H}$ = 6.9 Hz, 3H, *CH*$_3$, *Ar*N); 0.30 (bs, 3H, *CH*$_3$, *Ar*N). ^{31}P{^{1}H}-NMR (121.5 MHz; C_6D_6; δ, ppm): 22.0 (s, *P*Me$_2$Ph). Minor isomer: ^{31}P{^{1}H}-NMR (121.5 MHz; C_6D_6; δ, ppm): 22.8 (s, *P*Me$_2$Ph).

NMR scale reaction of (Ar'N)$_2$Mo(PMe^{i}Pr$_2$)$_2$ (III-25) with PhSiH$_3$

PhSiH$_3$ (5.5 μl, 0.043 mmol) was added in one portion at room temperature to a solution of (Ar'N)$_2$Mo(PMe^{i}Pr$_2$)$_2$ (**III-25**) (25.9 mg, 0.043 mmol) in 0.6 ml of C_6D_6 in an NMR tube. Immediately after addition of the silane the colour of the solution changed from green to brown. The reaction mixture was left at room temperature for 15 min. NMR analysis showed 50 % conversion of the starting material and formation of (Ar'N)Mo(SiH$_2$Ph)(η^3-NAr'-SiHPh-H)(PMe^{i}Pr$_2$) (**III-66**). The product is not stable in solution at room temperature and fully decomposes within two hours *via* the dissociation of PMe^{i}Pr$_2$. All attempts to isolate the product gave a mixture of unidentified compounds. *(Ar'N)Mo(SiH$_2$Ph)(η^3-NAr'-SiHPh-H)(PMe^{i}Pr$_2$)* (**III-66**): ^{1}H-NMR (300 MHz; C_6D_6; δ, ppm): 8.18 (d, $^3J_{H-H}$ = 6.6 Hz, 2H, *o*-H, Si*Ph*); 7.37 (d, $^3J_{H-H}$ = 6.9 Hz, 2H, *o*-H, Si*Ph*); 6.55-7.12 (m, 12H, *m*-H and *p*-H of 2 Si*Ph*, *m*-H and *p*-H of 2 *Ar'*N); 6.05 (s, 1H, Si*H*$_2$Ph); 5.66 (s, 1H, Si*H*$_2$Ph); 5.36 (bs, 1H, η^3-NAr'-Si*H*Ph-H); 3.46 (bs, 1H, η^3-NAr'-SiHPh-*H*); 2.50 (s, 3H, *CH*$_3$, *Ar'*N); 2.46 (s, 3H, *CH*$_3$, *Ar'*N); 2.45 (s, 6H, 2 *CH*$_3$, *Ar'*N);1.63 (m, 2H, 2 *CH*, PMe^i*Pr*$_2$); resonances of methyl groups of PMe^{i}Pr$_2$ ligand in **III-66** are found in the range 0.83-1.05 and are obscured by the signals of free PMe^{i}Pr$_2$. ^{31}P{^{1}H}-NMR (121.5 MHz; C_6D_6; δ, ppm): 52.3 (s, *P*Me^{i}Pr$_2$).

NMR scale reaction of (ArN)$_2$W(PMe$_3$)$_3$ (III-23) with PhSiH$_3$ and BPh$_3$

A solution of BPh$_3$ (19.0 mg, 0.08 mmol) and PhSiH$_3$ (5.0 μl, 0.04 mmol) in 0.6 ml of C_6D_6 was added at room temperature to a solid (ArN)$_2$W(PMe$_3$)$_3$ (**III-23**) (30.0 mg, 0.04

mmol). The colour of the mixture turned brown immediately and formation of white precipitate was observed. The reaction mixture was transferred to an NMR tube and left at room temperature for 20 min. NMR analysis showed complete conversion of the starting material and selective formation of $(ArN)_2W(H)(SiH_2Ph)(PMe_3)$ (**III-68**). The product is not stable in solution and slowly decomposes to a mixture of unidentified compounds. All attempts to isolate the product were unsuccessful due to its instability.

$(ArN)_2W(H)(SiH_2Ph)(PMe_3)$ (**III-68**): ^{1}H-NMR (300 MHz; C_6D_6; δ, ppm): 10.45 (d, $^2J_{H-P}$ = 59.7 Hz, $^1J_{H-W}$ = 40.5 Hz, 1H, W*H*); 7.98 (d, $^3J_{H-H}$ = 6.9 Hz, 2H, *o*-H, Si*Ph*); 7.00-7.42 (m, 9H, *m*-H and *p*-H of Si*Ph*, *m*-H and *p*-H of *Ar*N); 6.45 (s+sat, $^1J_{H-Si}$ = 178.9 Hz, 2H, Si*H*$_2$Ph); 3.95 (sept, $^3J_{H-H}$ = 6.6 Hz. 4H, 4 *CH*, 2 *Ar*N); 1.21 (d, $^3J_{H-H}$ = 6.6 Hz. 24H, 8 *CH*$_3$, 2 *Ar*N); 1.17 (d, $^2J_{H-P}$ = 9.9 Hz, 9H, P*Me*$_3$). ^{31}P{^{1}H}-NMR (75.5 MHz; C_6D_6; δ, ppm): -0.4 (bs, *P*Me$_3$).

NMR scale reaction of $(Ar'N)_2Mo(PMe_3)_3$ (III-4) with $PhSiH_3$

$PhSiH_3$ (8.6 μl, 0.07 mmol) was added in one portion at room temperature to a solution of $(Ar'N)_2Mo(PMe_3)_3$ (**III-4**) (39 mg, 0.07 mmol) in 0.6 ml of C_6D_6 in an NMR tube. NMR analysis of the mixture after 10 min at room temperature established formation of $(Ar'N)Mo(SiH_2Ph)(NAr'\{SiH_2Ph\})(PMe_3)_2$ (**III-69**). The mixture was left at room temperature overnight. All volatiles were pumped off; the residue was dried in vacuum and redissolved in fresh C_6D_6. NMR spectra showed formation of a difficult-to-separate mixture of three main products, structures of which were suggested according to collected NMR data: $(Ar'N)MoH_4(PMe_3)_3$ (**III-70**, 27 %), [η^3-PhHSi-(Ar')N-SiHPh-H]$MoH_3(PMe_3)_3$ (**III-71**, 12 %), and $(Ar'N)Mo(\eta^2$-Ar'N=SiHPh$)(H)_2(PMe_3)_2$ (**III-72**, 61 %). $PhSiH_3$ (5.6 μl, 0.05 mmol) was added to the mixture in one portion at room temperature. The mixture was left overnight showing no further reaction with silane. Heating the mixture at 100 C° for one hour leads to a decomposition of **III-72**, disappearance of $PhSiH_3$, and formation of Ph_2SiH_2, Ph_3SiH, and SiH_4.[211] Formation of $(Ar'N\text{-}SiHPh)_2$ was also detected by NMR analysis.[15] Complexes **III-70** and **III-71** remained unreacted.

$(Ar'N)Mo(SiH_2Ph)(NAr'\{SiH_2Ph\})(PMe_3)_2$ (**III-69**): ^{1}H-NMR (600 MHz; toluene-d_8; - 2 °C; δ, ppm): 8.16 (d, $^3J_{H-H}$ = 7.2 Hz, 2H, *o-H*, Si*Ph*); 7.46 (d, $^3J_{H-H}$ = 7.4 Hz, 2H, *o-H*,

Si*Ph*); 6.83-7.22 (m, 12H, Si*Ph* and *Ar'*N signals overlapping with toluene signals); 5.93 (s, 2H, SiH_2Ph); 5.72 (s, 2H, SiH_2Ph); 2.66 (s, 3H, CH_3, *Ar'*N); 2.48 (s, 3H, CH_3, *Ar'*N); 2.38 (s, 3H, CH_3, *Ar'*N); 2.22 (s, 3H, CH_3, *Ar'*N); 1.31 (d, $^2J_{H\text{-}P}$ = 7.7 Hz, 18H, 2 PMe_3). ^{1}H-NMR (600 MHz; toluene-d_8; - 71 °C; δ, ppm): 8.21 (bs, 2H, *o-H*, Si*Ph*); 7.44 (bm, 8H, *o-H*, *m-H* and *p-H*, Si*Ph*); 6.98 (bm, 3H, *m-H* and *p-H*, *Ar'*N); 6.02 (bs, 1H, SiH_2Ph); 5.96 (bs, 1H, SiH_2Ph); 5.80 (bs, 1H, SiH_2Ph); 5.71 (bs, 1H, SiH_2Ph); 2.66 (bs, 3H, CH_3, *Ar'*N); 2.52 (bs, 3H, CH_3, *Ar'*N); 2.40 (bs, 3H, CH_3, *Ar'*N); 2.21 (bs, 3H, CH_3, *Ar'*N); 1.36 (bs, 9H, PMe_3); 0.78 (bs, 9H, PMe_3). ^{31}P{^{1}H}-NMR (121.5 MHz; C_6D_6; δ, ppm): -13.2 (bs, 2 *P*Me$_3$). ^{31}P{^{1}H}-NMR (243 MHz; toluene-d_8; 0 °C; δ, ppm): -12.8 (s, 2 *P*Me$_3$). ^{31}P{^{1}H}-NMR (243 MHz; toluene-d_8; - 71 °C; δ, ppm): -9.3 (d, $^2J_{P\text{-}P}$ = 199.2 Hz, *P*Me$_3$); -13.6 (d, $^2J_{P\text{-}P}$ = 199.2 Hz, *P*Me$_3$). ^{1}H-^{29}Si HSQC NMR (119.2 MHz; toluene-d_8; - 71 °C; *J* = 150 Hz; ^{29}Si projection; δ, ppm): 1.3 (Mo-*Si*H$_2$Ph); -32.1 (Ar'N-*Si*H$_2$Ph). ^{1}H-^{29}Si HSQC NMR (119.2 MHz; toluene-d_8; - 42 °C; *J* = 150 Hz; δ, ppm): 1.1 (Mo-*Si*H$_2$Ph); -31.7 (Ar'N-*Si*H$_2$Ph).

(Ar'N)MoH_4(PMe_3)$_3$ (**III-70**): ^{1}H-NMR (600 MHz; C_6D_6; δ, ppm): -5.31 (q, $^2J_{H\text{-}P}$ = 28.9 Hz, 4H, MoH_4); 1.23 (bs, 18H, 2 PMe_3); 2.82 (s, 3H, CH_3, *Ar'*N); 2.96 (s, 3H, CH_3, *Ar'*N); 7.02 (m, 3H, *m-H* and *p-H*, *Ar'*N). ^{31}P{^{1}H}-NMR (121.5 MHz; C_6D_6; δ, ppm): 6.2 (s, 3 *P*Me$_3$). ^{31}P{^{1}H}-NMR (121.5 MHz; C_6D_6; δ, ppm; selectively decoupled from methyl groups): 6.2 (pent, $^2J_{H\text{-}P}$ = 28.9 Hz, 3 *P*Me$_3$).

[η^3-PhHSi-(Ar')N-SiHPh-H]MoH_3(PMe_3)$_3$: (**III-71**) The NMR features are close to those for [η^3-PhHSi-(Ar)N-SiHPh-H]MoH_3(PMe_3)$_3$ (**III-64**). The characteristic signals are the following: ^{1}H-NMR (600 MHz; C_6D_6; δ, ppm): -7.08 (bs, MoH_3); 0.80 (bs, 18H, 3 PMe_3); 2.50 (bs, 6H, 2 CH_3, *Ar'*N); 5.55 (bs, 2H, 2 Si*H*Ph). ^{31}P{^{1}H}-NMR (121.5 MHz; C_6D_6; δ, ppm): -9.0 (bs, 3 *P*Me$_3$).

(Ar'N)Mo(η^2-Ar'N=SiHPh)$(H)_2$(PMe_3)$_2$ (**III-72**): ^{1}H-NMR (600 MHz; C_6D_6; δ, ppm): -4.76 (ddd, $^2J_{H\text{-}P}$ = 45.3 Hz, $^2J_{H\text{-}P}$ = 55.3 Hz, $^2J_{H\text{-}H}$ = 8.5 Hz, 1H, MoH_2); -2.46 (ddd, $^2J_{H\text{-}P}$ = 15.3 Hz, $^2J_{H\text{-}P}$ = 31.6 Hz, $^2J_{H\text{-}H}$ = 8.5 Hz, 1H, MoH_2); 0.85 (d, $^2J_{H\text{-}P}$ = 7.8 Hz, 9H, PMe_3); 1.35 (d, $^2J_{H\text{-}P}$ = 8.0 Hz, 9H, PMe_3); 1.80 (s, 3H, CH_3, *Ar'*N); 2.73 (s, 3H, CH_3, *Ar'*N); 2.83 (s, 3H, CH_3, *Ar'*N); 3.13 (s, 3H, CH_3, *Ar'*N); 6.36 (dd, $^3J_{H\text{-}P}$ = 2.3 Hz, $^3J_{H\text{-}P}$ = 15.0 Hz, 1H, Si*H*Ph); 7.08 (m, 3H, *m-H* and *p-H*, *Ar'*N); 7.34 (t, $^3J_{H\text{-}H}$ = 7.2 Hz, 1H, *p-H*, Si*Ph*) 7.42 (t, $^3J_{H\text{-}H}$ = 7.2 Hz, 2H, *m-H*, Si*Ph*); 8.25 (d, $^3J_{H\text{-}H}$ = 7.2 Hz, 2H, *o-H*, Si*Ph*).

$^{31}P\{^1H\}$-NMR (121.5 MHz; C_6D_6; δ, ppm): 4.2 (d, $^2J_{P\text{-}P}$ = 15.8 Hz, PMe_3); 8.4 (d, $^2J_{P\text{-}P}$ = 15.8 Hz, PMe_3). ^{29}Si-NMR (119.2 MHz; C_6D_6; δ, ppm): -12.1 (d, $^1J_{H\text{-}Si}$ = 218.8 Hz, *Si*HPh).

NMR scale reaction of $(Ar'N)_2Mo(PMe_3)_3$ (III-4) with $PhSiH_3$ and BPh_3

A solution of $PhSiH_3$ (19.6 µl, 0.16 mmol) and BPh_3 (7.7 mg, 0.032 mmol) in 0.6 ml of C_6D_6 was added in one portion at room temperature to $(Ar'N)_2Mo(PMe_3)_3$ (**III-4**) (17.9 mg, 0.032 mmol). The reaction mixture was immediately transferred to an NMR tube and the reaction was monitored by NMR spectroscopy for 24 h showing full conversion of the starting material and formation of a difficult-to-separate mixture of $(Ar'N)MoH_4(PMe_3)_3$ (**III-70**, 11 %), [η^3-PhHSi-(Ar')N-SiHPh-H]$MoH_3(PMe_3)_3$ (**III-71**, 14 %), and $(Ar'N)Mo(\eta^2$-Ar'N=SiHPh)$(H)_2(PMe_3)_2$ (**III-72**, 75 %).

NMR scale reaction of $(Ar'N)_2Mo(PMe_2Ph)_3$ (III-26) with $PhSiH_3$

$PhSiH_3$ (17.7 µl, 0.144 mmol) was added in one portion at room temperature to a solution of $(Ar'N)_2Mo(PMe_2Ph)_3$ (**III-26**) (36.0 mg, 0.048 mmol) in 0.6 ml of C_6D_6 in an NMR tube. Immediately after silane addition the colour of the solution changed to a different tint of green. The reaction mixture was left at room temperature for 10 min. NMR analysis showed the release of an equivalent of PMe_2Ph and selective formation of $(Ar'N)Mo(SiH_2Ph)(NAr'\{SiH_2Ph\})(PMe_2Ph)_2$ (**III-74**). The product is not stable at room temperature in solution and decomposes overnight to give a difficult-to-characterize mixture of compounds, one of the components of which was suggested to be $(Ar'N)Mo(H)(SiH_2Ph)(PMe_2Ph)_3$ (**III-75**). All attempts to isolate the product gave a difficult-to-separate mixture of **III-26**, **III-74**, and **III-75**.

$(Ar'N)Mo(SiH_2Ph)(NAr'\{SiH_2Ph\})(PMe_2Ph)_2$ (**III-74**): ^1H-NMR (300 MHz; C_6D_6; δ, ppm): 8.24 (d, $^3J_{H\text{-}H}$ = 6.9 Hz, 2H, *o*-H, Si*Ph*); 7.73 (m, 2H, *o*-H, Si*Ph*); 6.59-7.39 (m, 17H, *m*-H and *p*-H of 2 Si*Ph*, *m*-H and *p*-H of 2 *Ar*'N, *o*-H, *m*-H, and *p*-H of P*Ph*); 6.59 (bs, 2H, SiH_2Ph); 5.86 (bs, 2H, SiH_2Ph); 2.30 (s, 6H, 2 CH_3, *Ar*'N); 1.79 (s, 6H, 2 CH_3, *Ar*'N); 1.23 (bs, 6H, 2 CH_3, P*Me*$_2$Ph). $^{31}P\{^1H\}$-NMR (121.5 MHz; C_6D_6; δ, ppm): 5.4 (d, $^2J_{P\text{-}P}$ = 257.6 Hz, 1P, PMe_2Ph); -3.5 (d, $^2J_{P\text{-}P}$ = 257.6 Hz, 1P, PMe_2Ph).

$(Ar'N)Mo(H)(SiH_2Ph)(PMe_2Ph)_3$ (**III-75**): ^1H-NMR (300 MHz; C_6D_6; δ, ppm; selected signals): 5.99 (t, $^3J_{H\text{-}P}$ = 6.9 Hz, 2H, SiH_2Ph); -3.13 (dt, $^2J_{H\text{-}P}$ = 19.2 Hz and 63.0 Hz, 1H,

Mo*H*), other signals are obscured by the resonances of decomposition products. $^{31}P\{^{1}H\}$-NMR (121.5 MHz; C_6D_6; δ, ppm): 24.5 (t, $^{2}J_{P\text{-}P}$ = 23.1 Hz, 1P, *P*Me_2Ph); 12.5 (d, $^{2}J_{P\text{-}P}$ = 23.1 Hz, 2P, 2 *P*Me_2Ph).

NMR scale reaction of (^{t}BuN)$_2$Mo(PMe$_3$)$_2$ (III-27) with PhSiH$_3$

A: Low temperature reaction. $PhSiH_3$ (7.4 μl, 0.06 mmol) was added in one portion to a solution of (^{t}BuN)$_2$Mo(PMe$_3$)$_2$ (**III-27**) (23.4 mg, 0.06 mmol) in 0.6 ml of toluene-d_8 at -30 °C. The mixture was immediately frozen in liquid nitrogen and placed into the NMR machine precooled to -30 °C. Analysis of the reaction mixture at this temperature showed the formation of a mixture of the starting material **III-27** and (^{t}BuN)Mo(H)(η^3-PhHSi-N(^{t}Bu)-SiHPh-H)(PMe$_3$)$_2$ (**III-76**; two isomers in a 1:2 ratio). Addition of another equivalent of $PhSiH_3$ (7.4 μl, 0.06 mmol) and warming the reaction mixture up to 0 °C leads to the selective formation of the silyl derivative (^{t}BuN)Mo(H)(SiH$_2$Ph){(SiHPh)$_2$(μ-N^{t}Bu)}(PMe$_3$)$_2$ (**III-77**; see the preparation and characterization below).

(^{t}BuN)Mo(H)(η^3-PhHSi-N(^{t}Bu)-SiHPh-H)(PMe$_3$)$_2$ (**III-76**): ^{1}H-NMR (600 MHz; toluene-d_8; -31 °C; δ, ppm): -4.63 (dd, $^{2}J_{H\text{-}P}$ = 19.5 Hz and 54.9 Hz, Mo-*H*, minor isomer); - 4.40 (dd, $^{2}J_{H\text{-}P}$ = 15.8 Hz and 48.4 Hz, Mo-*H*, major isomer); 0.85 (m, overlapping signals of P*Me*$_3$ groups of two isomers); 1.41 (bs, overlapping signals of ^{t}*Bu*N group of two isomers); 6.82 (bs, Si*H*$_2$Ph, major isomer); 6.89 (bs, Si*H*$_2$Ph, minor isomer); 6.91 (bs, Si*H*Ph, major isomer); 7.22 (bs, Si*H*Ph, minor isomer); 7.25 (m, overlapping signals of *m-H* and *p-H* of Si*Ph* of two isomers); 8.25 (m, overlapping signals of *o-H* of Si*Ph* of two isomers). $^{31}P\{^{1}H\}$-NMR (243 MHz; toluene-d_8; -25 °C; δ, ppm): 2.4 (d, $^{2}J_{P\text{-}P}$ = 43.7 Hz, *P*Me$_3$, minor isomer); -0.8 (d, $^{2}J_{P\text{-}P}$ = 43.7 Hz, *P*Me$_3$, major isomer); -5.1 (d, $^{2}J_{P\text{-}P}$ = 43.7 Hz, *P*Me$_3$, minor isomer); -7.0 (d, $^{2}J_{P\text{-}P}$ = 43.7 Hz, *P*Me$_3$, major isomer). ^{29}Si INEPT+ NMR (119.2 MHz; toluene-d_8, -40 °C, δ, ppm): -19.5 (dd, $^{1}J_{H\text{-}Si}$ = 37.3 Hz, $^{1}J_{H\text{-}Si}$ = 199.8 Hz, *Si*H$_2$Ph, minor isomer); -16.2 (dd, $^{1}J_{H\text{-}Si}$ = 34.9 Hz, $^{1}J_{H\text{-}Si}$ = 195.6 Hz, *Si*H$_2$Ph, major isomer); 5.2 (d, $^{1}J_{H\text{-}Si}$ = 172.3 Hz, *Si*HPh, major isomer); 7.5 (d, $^{1}J_{H\text{-}Si}$ = 182.7 Hz, *Si*HPh, minor isomer).

B: Ambient temperature stoichiometric reaction. $PhSiH_3$ (16 μl, 0.13 mmol) and PMe_3 (13.5 μl, 0.13 mmol) were added in one portion at room temperature to a solution of (^{t}BuN)$_2$Mo(PMe$_3$)$_2$ (**III-27**) (51.3 mg, 0.13 mmol) in 0.6 ml of C_6D_6 in an NMR tube.

After 5 min. at room temperature, NMR analysis showed the formation of a difficult-to-separate mixture of (η^2-^{t}BuN=SiHPh)MoH$_4$(PMe$_3$)$_3$ (**III-78**; two isomers) and (^{t}BuN)Mo(H)(SiH$_2$Ph){(SiHPh)$_2$(μ-N^{t}Bu)}(PMe$_3$)$_2$ (**III-77**) in approximate ratio 1:1.

(η^2-^{t}BuN=SiHPh)MoH$_4$(PMe$_3$)$_3$ (**III-78**): ^{1}H-NMR (600.2 MHz; C$_6$D$_6$; δ, ppm): -5.82 (m, two overlapping quartets from two isomers, $^2J_{H-P}$ = 27.2 Hz, Mo-*H*); 1.90 (m, both isomers, *P*Me$_3$); 1.36 (s, both isomers, ^{t}*Bu*N); 6.60 (bs, Mo-Si*H*-(^{t}Bu)N, both isomers); 7.25 (m, both isomers, *p*-H, Si*Ph*); 7.33 (m, both isomers, *m*-H, Si*Ph*); 8.31 (m, both isomers, *o*-H, Si*Ph*). ^{1}H{^{31}P}-NMR (600.2 MHz; C$_6$D$_6$; δ, ppm): -5.87 (s, Mo*H*$_4$). ^{31}P{^{1}H}-NMR (121.5 MHz; C$_6$D$_6$; δ, ppm): -12.4 (bs, both isomers, 3 *P*Me$_3$); ^{31}P-NMR (243 MHz; C$_6$D$_6$; δ, ppm; selectively decoupled from methyl groups): -12.4 (pent, both isomers, $^2J_{H-P}$ = 27.2 Hz, 3 *P*Me$_3$); ^{29}Si{^{1}H}-NMR (119.2 MHz; C$_6$D$_6$; δ, ppm): 6.2 (m, two overlapping quartets from two isomers, $^2J_{Si-P}$ = 13.1 Hz, η^2-^{t}BuN=*Si*HPh).

C: Ambient temperature reaction with excess PhSiH$_3$. PhSiH$_3$ (31.6 μl, 0.256 mmol) and PMe$_3$ (5.3 μl, 0.051 mmol) were added at room temperature to a solution of (^{t}BuN)$_2$Mo(PMe$_3$)$_2$ (**III-27**) (20.0 mg, 0.051 mmol) in 0.6 ml of C$_6$D$_6$ in an NMR tube. After 5 min. at room temperature, NMR analysis showed quantitative formation of (^{t}BuN)Mo(H)(SiH$_2$Ph){(SiHPh)$_2$(μ-N^{t}Bu)}(PMe$_3$)$_2$ (**III-77**). Trimethylphosphine remained unreacted. All volatiles were pumped off; the residue was dried in vacuum and redissolved in fresh C$_6$D$_6$. NMR analysis of the solution showed the presence of two isomers of **III-77** in approximate ratio 1:1 (according to the ^{31}P{^{1}H}-NMR spectrum).

NMR scale reaction of (^{t}BuN)$_2$Mo(η^2-CH$_2$=CH$_2$)(PMe$_3$) (III-30) with PhSiH$_3$

A: Ambient temperature stoichiometric reaction. PMe$_3$ (11.3 μl, 2.01 mmol) and PhSiH$_3$ (6.8 μl, 0.06 mmol) were added in one portion at room temperature to a solution of (^{t}BuN)$_2$Mo(η^2-CH$_2$=CH$_2$)(PMe$_3$) (**III-30**) (18.7 mg, 0.06 mmol) in 0.6 ml of C$_6$D$_6$ in an NMR tube. The reaction mixture was left at room temperature for 10 min. NMR analysis showed the formation of (^{t}BuN)Mo(H)(SiH$_2$Ph){(SiHPh)$_2$(μ-N^{t}Bu)}(PMe$_3$)$_2$ (**III-77**) in a mixture with unidentified highly fluxional hydride complex (the ratio is 1:1, according to the ^{31}P{^{1}H}-NMR spectrum).

B: Low temperature stoichiometric reaction. PhSiH$_3$ (9.6 μl, 0.078 mmol) was added in one portion to a solution of (^{t}BuN)$_2$Mo(η^2-CH$_2$=CH$_2$)(PMe$_3$) (**III-30**) (26.7 mg, 0.078

mmol) in 0.6 ml of toluene-d_8 at – 30 °C in an NMR tube. The reaction mixture was immediately frozen in liquid nitrogen and the sample was placed into the NMR machine precooled to – 30 °C. Monitoring the reaction with NMR spectroscopy in the range -30 – 22 °C did not allow to observe any intermediates and only slow formation of (^{t}BuN)Mo(H)(SiH_2Ph){($SiHPh)_2$(μ-N^{t}Bu)}(PMe_3)$_2$ (**III-77**) was detected at -18 °C.

C: Ambient temperature reaction with excess $PhSiH_3$. $PhSiH_3$ (20.2 µl, 0.164 mmol) and PMe_3 (5.7 µl; 0.055 mmol) were added in one portion at room temperature to a solution of (^{t}BuN)$_2$Mo(η^2-CH_2=CH_2)(PMe_3) (**III-30**) (18.7 mg, 0.055 mmol) in 0.6 ml of C_6D_6 in an NMR tube. Immediately after addition the colour of the solution changed from dark-brown to yellow and then to yellowish green. The reaction mixture was left at room temperature for 10 min. NMR analysis showed complete conversion of the starting material, release of ethylene and the selective formation of (^{t}BuN)Mo(H)(SiH_2Ph){($SiHPh)_2$(μ-N^{t}Bu)}(PMe_3)$_2$ (**III-77**).

NMR scale reaction of (ArN)$_2$Mo(PMe_3)$_3$ (III-22) with $PhMeSiH_2$

$PhMeSiH_2$ (2.7 µl, 0.02 mmol) was added in one portion at room temperature to a solution of (ArN)$_2$Mo(PMe_3)$_3$ (**III-22**) (13.3 mg, 0.02 mmol) in 0.6 ml of C_6D_6 in an NMR tube. No visual changes were observed after silane addition and the reaction mixture was left at room temperature overnight. NMR analysis showed no reaction. Heating the reaction mixture at 100 °C for two hours leads to the decomposition to a mixture of unidentified products.

NMR scale reaction of (Ar'N)$_2$Mo(PMe_3)$_3$ (III-4) with $PhMeSiH_2$

$PhMeSiH_2$ (6.8 µl, 0.049 mmol) was added in one portion at room temperature to a solution of (Ar'N)$_2$Mo(PMe_3)$_3$ (**III-4**) (27.8 mg, 0.049 mmol) in 0.6 ml of C_6D_6 in an NMR tube. No visual changes were observed after silane addition and the reaction mixture was left at room temperature overnight. Similarly to the case of **III-22**, NMR analysis showed no reaction. Heating the reaction mixture at 50 °C for three days leads to a slow PMe_3 dissociation and decomposition to a mixture of unidentified products.

NMR scale reaction of $(ArN)_2Mo(PMe_2Ph)_2$ (III-24) with $PhMeSiH_2$

$PhMeSiH_2$ (12.2 μl, 0.104 mmol) was added in one portion at room temperature to a solution of $(ArN)_2Mo(PMe_2Ph)_2$ (**III-24**) (75.3 mg, 0.104 mmol) in 0.6 ml of C_6D_6 in an NMR tube. The reaction mixture was monitored with NMR spectroscopy for 30 min. at room temperature and 1 h at 50 °C. NMR analysis showed no reaction. BPh_3 (30.2 mg, 0.125 mmol) was added to the NMR tube and the colour of the solution changed from dark-green to brown immediately. The reaction mixture was left at room temperature for 5 min., then all volatiles were pumped off and the residue was extracted with hexanes (3.0 ml) to give a dark-brown oily substance, which was dried in vacuum (43.8 mg). NMR analysis showed the presence of a mixture of unidentified decomposition products.

NMR scale reaction of $(^tBuN)_2Mo(PMe_3)_2$ (III-27) with $PhMeSiH_2$

A. $PhMeSiH_2$ (5.3 μl, 0.038 mmol) was added at room temperature to a solution of $(^tBuN)_2Mo(PMe_3)_2$ (**III-27**) (15.0 mg, 0.038 mmol) in 0.6 ml of C_6D_6 in an NMR tube. No visual changes were observed after addition of silane. The reaction mixture was left at room temperature for 5 min. NMR spectra showed selective formation of the silylhydride derivative $(^tBuN)_2Mo(H)(SiHMePh)(PMe_3)$ (**III-85**; 55 %, according to $^{31}P\{^1H\}$-NMR analysis). The product is highly unstable in solution at room temperature and decomposes *via* PMe_3 dissociation within one hour. All attempts to isolate the product were unsuccessful due to its instability. A similar stoichiometric preparative scale reaction with N_2 purging through the reaction mixture afforded a difficult-to-characterize mixture of products, the main component of which was suggested to be $(^tBuN)Mo(H)(SiHMePh)(PMe_3)_3$ (**III-86**).

$(^tBuN)_2Mo(H)(SiHMePh)(PMe_3)$ (**III-85**): ^{1}H-NMR (300 MHz; C_6D_6; δ, ppm): 8.11 (d, $^3J_{H\text{-}H}$ = 7.2 Hz, 2H, *o-H*, Si*Ph*); 7.36 (t, $^3J_{H\text{-}H}$ = 7.2 Hz, 2H, *m-H*, Si*Ph*); 7.22 (t, $^3J_{H\text{-}H}$ = 7.2 Hz, 1H, *p-H*, Si*Ph*); 6.23 (bq + sat, $^3J_{H\text{-}H}$ = 3.8 Hz, $^1J_{H\text{-}Si}$ = 173.5 Hz, 1H, Si*H*MePh); 3.71 (d, $^2J_{H\text{-}P}$ = 57.6 Hz, 1H, Mo*H*); 1.31 (s, 9H, ^{t}*Bu*N); 1.11 (d, $^3J_{H\text{-}H}$ = 3.8 Hz, 3H, SiH*Me*Ph); 1.05 (d, $^2J_{H\text{-}P}$ = 9.6 Hz, 9H, P*Me*$_3$). $^{31}P\{^1H\}$-NMR (121.5 MHz; C_6D_6; δ, ppm): 14.2 (s, P*Me*$_3$).

$(^tBuN)Mo(H)(SiHMePh)(PMe_3)_3$ (**III-86**): ^{1}H-NMR (300 MHz; C_6D_6; δ, ppm): 8.13 (d, $^3J_{H\text{-}H}$ = 6.3 Hz, 2H, *o*-H, SiHMe*Ph*); 7.32-8.19 (m, 3H, *m*-H and *p*-H of SiHMe*Ph*); 5.59

(m, 1H, Si*H*MePh); 1.07-1.53 (m, overlapping signals ^{t}BuN and 3 P*Me$_3$*); 0.47 (bs, 3H, SiH*Me*Ph); -3.93 (dt, $^2J_{H\text{-}P}$ = 63.9 Hz and 20.7 Hz, 1H, Mo*H*). $^{31}P\{^1H\}$-NMR (121.5 MHz; C_6D_6; δ, ppm): 14.9 (dd, $^2J_{P\text{-}P}$ = 24.7 Hz and 23.1 Hz, 1P, *P*Me$_3$); 2.5 (two overlapping dd, $^2J_{P\text{-}P}$ = 23.1 and 24.7 Hz, 2P, 2 *P*Me$_3$).

B. The reaction was done analogously to **A** using 17.2 mg (0.044 mmol) of (^{t}BuN)$_2$Mo(PMe$_3$)$_2$ (**III-27**), 6.1 µl (0.044 mmol) of PhMeSiH$_2$, and 9.1 µl (0.088 mmol) of PMe$_3$. NMR analysis after overnight at room temperature showed the formation of a difficult-to-separate mixture of (^{t}BuN)$_2$Mo(H)(SiHMePh)(PMe$_3$) (**III-85**; 42 %) (^{t}BuN)Mo(H)(SiHMePh)(PMe$_3$)$_3$ (**III-86**, 8 %).

NMR scale reaction of (^{t}BuN)$_2$Mo(η^2-CH$_2$=CH$_2$)(PMe$_3$) (III-30) with PhMeSiH$_2$

PhMeSiH$_2$ (11.0 µl, 0.08 mmol) and PMe$_3$ (16.6 µl, 0.16 mmol) were added in one portion at room temperature to a solution of (^{t}BuN)$_2$Mo(η^2-CH$_2$=CH$_2$)(PMe$_3$) (**III-30**) (27.3 mg, 0.08 mmol) in 0.6 ml of C_6D_6 in an NMR tube. The colour of the solution changed from yellow to dark-brown almost immediately. NMR analysis after 30 min at room temperature showed 82 % conversion of **III-30** and the formation of a mixture of (^{t}BuN)$_2$Mo(H)(SiHMePh)(PMe$_3$) (**III-85**; 77 %) and (^{t}BuN)Mo(H)(SiHMePh)(PMe$_3$)$_3$ (**III-86**; 5 %). Leaving the sample overnight at room temperature leads to a decomposition to a mixture of unidentified products. A similar reaction in the presence of two equivalents of PMe$_3$ gives only traces of **III-86** in a mixture with unknown decomposition products.

NMR scale reaction of (^{t}BuN)$_2$Mo(PMe$_3$)$_2$ (III-27) with (EtO)$_3$SiH

(EtO)$_3$SiH (11.7 µl, 0.064 mmol) and PMe$_3$ (6.6 µl, 0.064 mmol) were added in one portion at room temperature to a solution of (^{t}BuN)$_2$Mo(PMe$_3$)$_2$ (**III-27**) (25.0 mg, 0.064 mmol) in 0.6 ml of C_6D_6 in an NMR tube. The mixture was left overnight at room temperature. NMR analysis showed complete conversion of the starting material and formation of a mixture of products, one of which was suggested to be (^{t}BuN)Mo(OEt)$_2$(PMe$_3$)$_3$ (**III-87**). $^{31}P\{^1H\}$-NMR (121.5 MHz; C_6D_6; δ, ppm): 14.8 (t, $^2J_{P\text{-}P}$ = 24.3 Hz, 1P, *P*Me$_3$); 3.4 (d, $^2J_{P\text{-}P}$ = 24.3 Hz, 2P, 2 *P*Me$_3$).

NMR scale reaction of $(ArN)_2Mo(PMe_3)_3$ (III-22) with $(EtO)_3SiH$

$(EtO)_3SiH$ (6.8 µl, 0.037 mmol) was added in one portion at room temperature to a solution of $(ArN)_2Mo(PMe_3)_3$ (**III-22**) (24.9 mg, 0.037 mmol) in 0.6 ml of C_6D_6 in an NMR tube. The mixture was monitored with NMR for one day at room temperature showing no reaction. Excess $(EtO)_3SiH$ (60.0 µl, 0.327 mmol) was added to the NMR tube and the reaction mixture was left under reduced pressure overnight at room temperature. NMR analysis showed complete conversion of the starting material forming two main products: $(ArN)Mo(OEt)_2(PMe_3)_3$ (**III-88**) and $(ArN)Mo(H)(OEt)(PMe_3)_3$ (**III-89**).

$(ArN)Mo(OEt)_2(PMe_3)_3$ (**III-88**): $^{31}P\{^1H\}$-NMR (121.5 MHz; C_6D_6; δ, ppm): 10.8 (t, $^2J_{P\text{-}P}$ = 24.3 Hz, 1P, PMe_3); -1.2 (d, $^2J_{P\text{-}P}$ = 24.3 Hz, 2P, 2 PMe_3).

$(ArN)Mo(H)(OEt)(PMe_3)_3$ (**III-88**): -1.5 (d, $^2J_{P\text{-}P}$ = 25.5 Hz, 2P, 2 PMe_3); -17.8 (t, $^2J_{P\text{-}P}$ = 25.5 Hz, 1P, PMe_3).

Preparation of silylamide molybdenum complexes

Preparation of $(ArN)Mo(Cl)(\eta^3\text{-}NAr\text{-}SiMeCl\text{-}H)(PMe_3)_2$ (III-44a)

$MeSiHCl_2$ (63.0 µl, 0.605 mmol) was added in one portion at room temperature to a solution of $(ArN)_2Mo(PMe_3)_3$ (**III-22**) (266 mg, 0.394 mmol) in 15 ml of hexanes. The colour of the solution turned from dark-green to brown almost immediately. The reaction mixture was stirred at room temperature with N_2 purging for 30 min. All volatiles were removed in vaccum to give brown oily residue. NMR analysis showed the presence of a 1:1 mixture of $(ArN)Mo(Cl)(\eta^3\text{-}NAr\text{-}SiMeCl\text{-}H)(PMe_3)_2$ (**III-44a**) and $(ArN)MoCl_2(PMe_3)_3$ (**III-47**). All attempts to isolate complex **III-44a** by recrystallization were unsuccessful. The only crystalline material isolated from different solvents and under different regimes was compound **III-47**.

Preparation of $(^tBuN)Mo(Cl)(\eta^3\text{-}N^tBu\text{-}SiMeCl\text{-}H)(PMe_3)_2$ (III-44c)

$MeSiHCl_2$ (50.0 µl, 0.48 mmol) was added in one portion at room temperature to a solution of $(^tBuN)_2Mo(PMe_3)_2$ (**III-27**) in Et_2O (6.0 ml, 0.384 mmol, C = 0.064 M). No visual changes were observed after addition and the mixture was stirred at room temperature for 10 min. All volatiles were pumped off to leave dark-brown oily substance

The yield is quantitative according to ^{1}H-NMR analysis. The product was extracted with 15 ml of hexanes, then concentrated and left at -80 °C overnight to afford a brown powder. Yield: 50.5 mg, 26 %. The product is not stable in solution and slowly decomposes to give (^{t}BuN)$MoCl_2(PMe_3)_3$ (**III-48**).

Preparation of (ArN)Mo(SiH_2Ph)(η^3-NAr-SiHPh-H)(PMe_3) (III-1)

$PhSiH_3$ (0.37 ml, 3.0 mmol) was added to a solution of $(ArN)_2Mo(PMe_3)_3$ (**III-22**) (1.01 g, 1.5 mmol) in 100 ml of hexane at room temperature. After the addition of $PhSiH_3$, the colour of reaction mixture turned from dark-green to brown immediately, and the formation of a brown precipitate was observed. The reaction mixture was stirred vigorously with N_2 purging at room temperature for 30 min., concentrated and left at -30°C overnight. More crystalline brown precipitate formed. The cold precipitate was filtered off, washed with cold hexanes (10 ml) and dried in vacuum to give a fine brown powder. Yield: 0.7 g, 77 %. The product is fluxional at room temperature. ^{1}H-NMR (300 MHz; C_6D_6; δ, ppm): 0.36 (bs, 3H, *CH*$_3$, ArN); 1.04 (d, $^2J_{H\text{-}P}$ = 8.4 Hz, 9H, P*Me*$_3$); 1.14 (d, $^3J_{H\text{-}H}$ = 6.6 Hz, 3H, *CH*$_3$, ArN); 1.18 (d, $^3J_{H\text{-}H}$ = 6.9 Hz, 6H, *2CH*$_3$, ArN); 1.23 (d, $^3J_{H\text{-}H}$ = 6.6 Hz, 3H, *CH*$_3$, ArN); 1.27 (d, $^3J_{H\text{-}H}$ = 6.9 Hz, 6H, *2CH*$_3$, ArN); 1.34 (d, $^3J_{H\text{-}H}$ = 6.9 Hz, 3H, *CH*$_3$, ArN); 2.71 (sept., $^3J_{H\text{-}H}$ = 6.6 Hz, 1H, *CH*, ArN); 3.46 (sept., $^3J_{H\text{-}H}$ = 6.9 Hz, 1H, *CH*, ArN); 4.04 (sept., $^3J_{H\text{-}H}$ = 6.6 Hz, 2H, *2CH*, ArN); 4.30 (bs, 1H, ArN-Si-*H*, agostic); 5.57 (s, 1H, Mo-Si-*H*); 5.78 (bs, 1H, ArN-Si-*H*, terminal); 5.94 (s, 1H, Mo-Si-*H*); 6.91 – 6.94 and 6.99 – 7.24 (overlapping multiplets, 8H, *m-H* and *p-H* of NAr, and *p-H* of Si-Ph aromatic protons); 6.96 (t, $^3J_{H\text{-}H}$ = 7.1 Hz, 2H, *m-H*, Si-Ph); 7.32 (t, $^3J_{H\text{-}H}$ = 7.2 Hz, 2H, *m-H*, Si-Ph); 7.43 (d, $^3J_{H\text{-}H}$ = 7.2 Hz, 2H, *o-H*, Si-Ph); 8.31 (d, $^3J_{H\text{-}H}$ = 7.2 Hz, 2H, *o-H*, Si-Ph). ^{1}H-NMR (600 MHz; toluene-d_8; δ, ppm): 0.30 (bs, 3H, *CH*$_3$, ArN); 1.05 (d, $^2J_{H\text{-}P}$ = 8.4 Hz, 9H, P*Me*$_3$); 1.12 (bs, 3H, *CH*$_3$, ArN); 1.17 (d, $^3J_{H\text{-}H}$ = 6.6 Hz, 6H, *2CH*$_3$, ArN); 1.20 (d, $^3J_{H\text{-}H}$ = 6.6 Hz, 3H, *CH*$_3$, ArN); 1.27 (d, $^3J_{H\text{-}H}$ = 6.6 Hz, 6H, *2CH*$_3$, ArN); 1.35 (d, $^3J_{H\text{-}H}$ = 6.6 Hz, 3H, *CH*$_3$, ArN); 2.68 (sept., $^3J_{H\text{-}H}$ = 6.6 Hz, 1H, *CH*, ArN); 3.47 (bs, 1H, *CH*, ArN); 4.01 (sept., $^3J_{H\text{-}H}$ = 6.6 Hz, 2H, *2CH*, ArN); 4.25 (bs, 1H, ArN-Si-*H*, agostic); 5.46 (s, 1H, Mo-Si-*H*); 5.75 (bs, 1H, ArN-Si-*H*, terminal); 5.84 (s, 1H, Mo-Si-*H*); 6.86 – 6.95 and 6.96 – 7.03 and 7.13 (overlapping multiplets, 6H, *m-H* and *p-H*, NAr); 6.95 (t, $^3J_{H\text{-}H}$ = 7.2 Hz, 2H, *m-H*, Si-Ph); 7.06 (t, $^3J_{H\text{-}H}$ = 7.2 Hz, 1H, *p-H*, Si-Ph);

7.22 (t, $^3J_{H-H}$ = 7.2 Hz, 1H, *p-H*, Si-Ph); 7.29 (t, $^3J_{H-H}$ = 7.2 Hz, 2H, *m-H*, Si-Ph); 7.40 (d, $^3J_{H-H}$ = 7.2 Hz, 2H, *o-H*, Si-Ph); 8.22 (d, $^3J_{H-H}$ = 7.2 Hz, 2H, *o-H*, Si-Ph). ^{1}H-NMR (600 MHz; toluene-d_8; - 50 °C; δ, ppm): 0.15 (bs, 3H, *CH*$_3$, ArN); 0.962 (d, $^2J_{H-P}$ = 8.4 Hz, 9H, P*Me*$_3$); 1.02 (bs, 3H, *CH*$_3$, ArN); 1.16 (bs, 3H, *CH*$_3$, ArN); 1.19 (bs, 6H, *2CH*$_3$, ArN); 1.28 (bs, 6H, *2CH*$_3$, ArN); 1.41 (bs, 3H, *CH*$_3$, ArN); 2.75 (bs, 1H, *CH*, ArN); 3.52 (bs, 1H, *CH*, ArN); 3.97 (bs, 2H, *2CH*, ArN); 4.35 (bm, $^2J_{H-H}$ = 5.4 Hz, 1H, ArN-Si-*H*, agostic); 5.68 (s, 1H, Mo-Si-*H*); 5.97 (s, 1H, Mo-Si-*H*); 6.03 (bd, $^2J_{H-H}$ = 5.4 Hz, ArN-Si-*H*, terminal); 6.80 – 7.02 and 7.06 – 7.16 (overlapping multiplets, 9H, *m-H* and *p-H*, NAr', and 1 *o-H* and 1 *p-H*, SiPh); 7.28 (bt, $^3J_{H-H}$ = 7.2 Hz, 1H, *p-H*, Si-Ph); 7.37 (bt, $^3J_{H-H}$ = 7.2 Hz, 2H, *o-H*, Si-Ph); 7.40 (bd, $^3J_{H-H}$ = 7.2 Hz, 2H, *m-H*, Si-Ph); 8.49 (bd, $^3J_{H-H}$ = 7.2 Hz, 2H, *m-H*, Si-Ph). ^{31}P{^{1}H} NMR (121.5 MHz; C_6D_6; δ, ppm): 10.4 (s, *P*Me$_3$). ^{31}P{^{1}H} NMR (121.5 MHz; toluene-d_8; δ, ppm): 10.6 (s, *P*Me$_3$). ^{31}P-NMR (selectively decoupled from methyl groups; 243 MHz; toluene-d_8; δ, ppm): 10.6 (d, $^2J_{H-P}$ = 9.3 Hz, *P*Me$_3$). ^{13}C{^{1}H}-NMR (150.9 MHz; toluene-d_8; δ, ppm): 17.8 (d, $^1J_{C-P}$ = 25.7 Hz, P*Me*$_3$); 22.5 (s, *CH*$_3$, ArN); 23.4 (s, *2CH*$_3$, ArN); 23.5 (s, *CH*$_3$, ArN); 24.1 (s, *2CH*$_3$, ArN); 26.3 (s, *CH*$_3$, ArN); 26.6 (s, *CH*$_3$, ArN); 26.9 (s, *CH*, ArN); 27.8 (s, *CH*, ArN); 28.9 (s, *2CH*, ArN); 122.2 (s, NAr); 122.9 (s, NAr); 123.0 (s, NAr); 123.1 (s, NAr); 125.0 (s, *o-C*, NAr); 126.1 (s, *p-C*, SiPh); 127.4 (s, *p-C*, SiPh); 127.6 (s, *m-C*, SiPh); 127.9 (s, *o-C*, NAr); 128.0 (s, *m-C*, SiPh); 128.2 (s, *o-C*, NAr); 128.8 (s, NAr); 130.6 (s, NAr); 136.0 (s, *o-C*, SiPh); 136.3 (s, *o-C*, SiPh); 136.9 (s, *o-C*, NAr); 140.2 (s, *i-C*, SiPh); 141.4 (s, *i-C*, SiPh); 144.5 (s, *i-C*, NAr); 153.6 (s, *i-C*, NAr). ^{29}Si{^{1}H}-NMR (119.2 MHz; toluene-d_8; - 50 °C; δ, ppm): -72.9 (dd, $^1J_{Si-H}$ = 113.0 Hz, $^1J_{Si-H}$ = 245.3 Hz, ArN-*Si*H$_2$Ph); 1.2 (t, $^1J_{Si-H}$ = 153.5 Hz, Mo-*Si*H$_2$Ph). IR (nujol): 1694 cm^{-1}, 2014 cm^{-1}, 2041 cm^{-1} and 2165 cm^{-1}. Elem. Anal. (%): calc. for $C_{39}H_{57}MoN_2PSi_2$ (736.968) C 63.56, H 7.80, N 3.80; found C 62.76, H 7.48, N 3.86.

Preparation of (ArN)Mo(SiD$_2$Ph)(η^3-NAr-SiDPh-D)(PMe$_3$) (III-1d$_4$)

The reaction was done analogously to the preparation of **III-1** described above, using 0.72 g (1.061 mmol) of (ArN)$_2$Mo(PMe$_3$)$_3$ (**III-22**), 0.27 ml (2.121 mmol) of PhSiD$_3$, and 30 ml of hexanes. Yield: 0.41 g, 68 %. The spectral data for **III-1d$_4$** are the same as those

for **III-1** except Si*H* resonances, which are not seen in the ^{1}H-NMR spectrum of **III-1d$_4$** due to full substitution with deuterium.

Preparation of (^{t}BuN)Mo(H)(SiH$_2$Ph){(SiHPh)$_2$(μ-N^{t}Bu)}(PMe$_3$)$_2$ (III-77)

$PhSiH_3$ (0.19 ml, 1.54 mmol) of was added in one portion to a solution of (^{t}BuN)$_2$Mo(PMe$_3$)$_2$ (**III-27**) in hexanes (12.0 ml, C = 0.064 M, 0.77 mmol) at -30 °C. The reaction mixture was stirred at -30 °C for 1 h 20 min. The reaction mixture was warmed up to 0/-5 °C and all volatiles were pumped off to leave a dark-brown solid, which was dried then in vacuum. Yield: 0.38 g, 82 %. The product is not stable in solution at room temperature and fully decomposes in a few hours to give a mixture of unidentified compounds. ^{1}H-NMR (600 MHz; toluene-d$_8$; - 28 °C; δ, ppm): 8.54 (d, $^3J_{H-H}$ = 6.7 Hz, 2H, *o*-H, Si*Ph*); 8.48 (d, $^3J_{H-H}$ = 6.6 Hz, 2H, *o*-H, Si*Ph*); 8.32 (bs, 2H, *o*-H, Si*Ph*); 7.49 (t, $^3J_{H-H}$ = 7.5 Hz, 2H, *m*-H, Si*Ph*); 7.46 (t, $^3J_{H-H}$ = 7.5 Hz, 2H, *m*-H, Si*Ph*); 7.40 (t, $^3J_{H-H}$ = 7.5 Hz, 2H, *m*-H, Si*Ph*); 7.32 (t, $^3J_{H-H}$ = 7.5 Hz, 1H, *p*-H, Si*Ph*); 7.26 (m, 2H, *p*-H, Si*Ph*); 6.67 (ddd, $^2J_{H-H}$ = 5.9 Hz, $^3J_{P-H}$ = 11.6 Hz, $^3J_{P-H}$ = 17.2 Hz, 1H, {(Si*H*Ph)$_2$(μ-N^{t}Bu)}); 6.03 (dd, $^3J_{P-H}$ = 9.6 Hz, $^3J_{P-H}$ = 3.7 Hz, 1H, {(Si*H*Ph)$_2$(μ-N^{t}Bu)}); 5.60 (dd, $^3J_{P-H}$ = 14.9 Hz, $^2J_{H-H}$ = 7.5 Hz, 1H, Si*H*$_2$Ph); 5.13 (bd, $^2J_{H-P}$ = 19.6 Hz, 1H, Si*H*$_2$Ph); 1.54 (dm, $^2J_{H-P}$ = 21.0 Hz, 1H, Mo*H*); 1.47 (s, 9H, ^{t}*Bu*N); 1.04 (d, $^2J_{P-H}$ = 7.5 Hz, 9H, P*Me*$_3$); 0.99 (d, $^2J_{P-H}$ = 6.0 Hz, 9H, P*Me*$_3$); 0.62 (s, 9H, ^{t}*Bu*N). ^{1}H-NMR (600 MHz; toluene-d$_8$; 22 °C; δ, ppm): 8.39 (d, $^3J_{H-H}$ = 7.3 Hz, 2H, *o*-H, Si*Ph*); 8.37 (d, $^3J_{H-H}$ = 7.3 Hz, 2H, *o*-H, Si*Ph*); 8.25 (d, $^3J_{H-H}$ = 7.0 Hz, 2H, *o*-H, Si*Ph*); 7.40 (t, $^3J_{H-H}$ = 7.0 Hz, 4H, Ph, *m-H*); 7.36 (t, $^3J_{H-H}$ = 7.3 Hz, 2H, *m*-H, Si*Ph*); 7.23 (m, 3H, *p*-H, Si*Ph*); 6.59 (ddd, $^2J_{H-H}$ = 5.8 Hz, $^3J_{P-H}$ = 11.6 Hz, $^3J_{P-H}$ = 17.5 Hz, 1H, {(Si*H*Ph)$_2$(μ-N^{t}Bu)}); 6.04 (dd, $^3J_{P-H}$ = 3.7 Hz, $^3J_{P-H}$ = 9.2 Hz, 1H, {(Si*H*Ph)$_2$(μ-N^{t}Bu)}); 5.50 (bddd, $^3J_{P-H}$ = 15.9 Hz, $^2J_{H-H}$ = 7.4 Hz, 1H, Si*H*$_2$Ph); 5.05 (d, $^3J_{H-p}$ = 19.4 Hz, 1H, Si*H*$_2$Ph); 1.50 (dm, $^2J_{H-P}$ = 21.0 Hz, 1H, Mo*H*); 1.39 (s, 9H, ^{t}*Bu*N); 1.14 (d, $^2J_{P-H}$ = 7.7 Hz, 9H, P*Me*$_3$); 1.05 (d, $^2J_{P-H}$ = 6.4 Hz, 9H, P*Me*$_3$); 0.61 (s, 9H, ^{t}*Bu*N). ^{1}H{^{31}P}-NMR (600 MHz; toluene-d$_8$; 22 °C; δ, ppm; selected signals): 6.59 (d, $^2J_{H-H}$ = 5.9 Hz, 1H, {(Si*H*Ph)$_2$(μ-N^{t}Bu)}); 6.04 (s, 1H, {(Si*H*Ph)$_2$(μ-N^{t}Bu)}); 5.49 (s, 1H, Si*H*$_2$Ph); 5.05 (s, 1H, Si*H*$_2$Ph); 1.55 (d, $^2J_{H-H}$ = 5.9 Hz, 1H, Mo*H*). ^{31}P{^{1}H}-NMR (243 MHz; toluene-d$_8$; - 28 °C; δ, ppm): - 40.2 (d, $^2J_{P-P}$ = 34.5 Hz, *P*Me$_3$); - 16.3 (d, $^2J_{P-P}$ = 34.5 Hz, *P*Me$_3$). ^{31}P{^{1}H}-NMR (121.5 MHz; toluene-d$_8$; 22 °C; δ, ppm): - 41.5 (d, $^2J_{P-P}$ =

32.0 Hz, PMe_3); - 17.2 (d, $^2J_{P\text{-}P}$ = 32.0 Hz, PMe_3). ^{29}Si-INEPT+ NMR (119.2 MHz; toluene-d_8; - 28 °C; J = 180 Hz, δ, ppm): - 14.3 (tdd, $^1J_{Si\text{-}H}$ = 154.5 Hz, $^2J_{Si\text{-}P}$ = 25.0 Hz, $^2J_{Si\text{-}P}$ = 28.6 Hz, SiH_2Ph); - 5.0 (d, $^1J_{Si\text{-}H}$ = 186.0 Hz, {$(SiHPh)_2(\mu\text{-}N^tBu)$}); 1.4 (ddd, $^1J_{Si\text{-}H}$ = 166.9 Hz, $^2J_{Si\text{-}P}$ = 25.0 Hz, $^2J_{Si\text{-}P}$ = 20.3 Hz, {$(SiHPh)_2(\mu\text{-}N^tBu)$}). ^{29}Si RF INEPT NMR (119.2 MHz; toluene-d_8; - 18 °C; J = 180 Hz; δ, ppm): 1.4 (dd, $^2J_{Si\text{-}P}$ = 16.7 Hz, $^2J_{Si\text{-}P}$ =28.6 Hz, {$(SiHPh)_2(\mu\text{-}N^tBu)$}, "up"); - 5.1 (d, $^2J_{Si\text{-}P}$ =10.7 Hz, {$(SiHPh)_2(\mu\text{-}N^tBu)$}, "up"); - 14.7 (t, $^2J_{Si\text{-}P}$ =23.8 Hz, SiH_2Ph, "down"). ^{1}H-^{31}P HSQC JC NMR (243.0 MHz; toluene-d_8; - 20 °C; J = 15 Hz; ^{1}H projection; δ, ppm): 1.6 (d, $^2J_{H\text{-}P}$ = 30.0 Hz, {$(SiHPh)_2(\mu\text{-}N^tBu)$}). ^{13}C{^{1}H}-NMR (151 MHz; toluene-d_8; - 28 °C; δ, ppm): 14.9 (d, $^1J_{C\text{-}P}$ = 18.1 Hz, PMe_3); 19.1 (d, $^1J_{C\text{-}P}$ = 24.1 Hz, PMe_3); 30.3 (s, CH_3, N^tBu); 31.7 (s, CH_3, N^tBu); 34.8 (s, *imido*-N^tBu); 54.7 (s, *amido*-N^tBu); 127.3 (s, *m*-C, Si*Ph*); 127.5 (s, *m*-C, Si*Ph*); 128.1 (s, *m*-C, Si*Ph*); 128.2 (s, *p*-C, Si*Ph*); 128.4 (s, *p*-C, Si*Ph*); 133.9 (s, *o*-C, Si*Ph*); 137.1 (s, *o*-C, Si*Ph*); 137.8 (s, *o*-C, Si*Ph*); 143.2 (s, *i*-C, Si*Ph*); 147.8 (s, *i*-C, Si*Ph*); 148.8 (s, *i*-C, Si*Ph*). IR (nujol): 1825 cm^{-1} (medium, Mo-H); 1890 cm^{-1} (strong, Si-H); 2037 cm^{-1} (strong, Si-H); 2142 cm^{-1} (strong, Si-H). Elem. Anal. (%): calc. for $C_{32}H_{56}MoN_2P_2Si_3$ (710.945) C 54.06, H 7.94, N 3.94; found C 53.99, H 7.87, N 4.22.

Stoichiometric reactions of (ArN)Mo(SiH_2Ph)(η^3-NAr-SiH_2Ph)(PMe_3) (III-1)

Preparation of (ArN)Mo(Et)(η^3-NAr-SiHPh-CH=CH_2)(PMe_3) (III-3)

A. Ethylene gas was added *via* vacuum transfer to a solution of (ArN)Mo(SiH_2Ph)(η^3-NAr-SiHPh-H)(PMe_3) (**III-1**) (502.6 mg, 0.682 mmol) in 100 ml of Et_2O at -80 °C. The reaction mixture was warmed up to ambient temperature and allowed to stir for 12 hours. All volatiles were pumped off and the residue was dried and extracted with 100 ml of hexanes. The solution was concentrated to 10 ml and left at -30 °C overnight to form a brown precipitate, which was filtered off, washed with 5 ml of cold hexanes, and dried in vacuum. Yield: 362.7 mg, 84 %.

B. $PhSiH_3$ (0.3 ml, 2.431 mmol) was added in one portion to a solution of $(Ar)_2Mo(\eta^2\text{-}CH_2{=}CH_2)(PMe_3)_2$ (**III-31**) (267 mg, 0.425 mmol) in 30 ml of Et_2O at -80 °C. The mixture was immediately frozen in liquid N_2 and excess ethylene was added *via* vacuum transfer. The reaction mixture was slowly warmed up to room temperature and allowed to stir for 3 days. During this time the colour of the mixture changed from purple to brown.

All volatiles were pumped off and the residue was extracted with 50 ml of hexanes. Hexanes solution was concentrated to 10 ml and left at -30 °C for two days to form a brown precipitate, which was filtered off and dried in vacuum. Yield: 139.7 mg, 48 %. ^{1}H-NMR (300 MHz; C_6D_6; δ, ppm): 7.67 (m, 2H, *o*-H, Si*Ph*); 6.85-7.10 (m, 9H, *m*-H and *p*-H of N*Ar* and Si*Ph*); 6.48 (s, 1H, Si*H*); 4.30 (dd, J_{H-H} = 3.9 Hz, 13.0 Hz, 1H, H_2C=CHSi); 4.09 (m, 2H, H_2C=CHSi and *CH* of N*Ar*); 3.83 (sept, $^3J_{H-H}$ = 6.6 Hz, 1H, *CH*, N*Ar*); 3.71 (sept, $^3J_{H-H}$ = 6.9 Hz, 1H, *CH*, N*Ar*); 2.95 (dd, $^3J_{H-H}$ = 13.0 Hz, 15.6 Hz, 1H, H_2C=*CH*Si); 2.70 (sept, $^3J_{H-H}$ = 6.9 Hz, 1H, *CH*, N*Ar*); 2.54 (m, 1H, CH_2, Mo*Et*); 2.04 (t, $^3J_{H-H}$ = 7.2 Hz, 3H, CH_3, Mo*Et*); 1.54 (m, 6H, 2CH_3, N*Ar*); 1.47 (m, 1H, CH_2, Mo*Et*); 1.40 (d, $^3J_{H-H}$ = 6.6 Hz, 6H, 2CH_3, N*Ar*); 1.15 (d, $^3J_{H-H}$ = 6.9 Hz, 3H, CH_3, N*Ar*); 1.10 (d, $^3J_{H-H}$ = 6.6 Hz, 6H, 2CH_3, N*Ar*); 0.70 (d, $^2J_{P-H}$ = 7.5 Hz, 9H, PMe_3); 0.31 (d, $^3J_{H-H}$ = 6.9 Hz, 3H, CH_3, N*Ar*). ^{31}P{^{1}H}-NMR (121.5 MHz; C_6D_6; δ, ppm): -17.2 (s, *P*me$_3$). ^{13}C{^{1}H}-NMR (75.5 MHz; C_6D_6; δ, ppm): 14.0 (d, $^1J_{C-P}$ = 19.6 Hz, PMe_3); 15.5 (s, CH_3, N*Ar*); 19.6 (d, $^3J_{C-P}$ = 5.9 Hz, CH_3, Mo*Et*); 22.1 (s, CH_3, N*Ar*); 24.2 (s, CH_3, N*Ar*); 24.3 (s, CH_3, N*Ar*); 25.5 (s, CH_3, N*Ar*); 27.2 (s, *CH*, N*Ar*); 27.6 (s, CH_3, N*Ar*); 27.9 (s, *CH*, N*Ar*); 29.7 (s, CH_3, N*Ar*); 30.2 (s, *CH*, N*Ar*); 31.6 (d, $^2J_{C-P}$ = 6.3 Hz, CH_2, Mo*Et*); 49.9 (d, J_{C-P} = 4.7 Hz, Si*CH*=CH_2); 75.4 (d, J_{C-P} = 13.2 Hz, SiCH=*C*H_2); 123.0 (s, *p*-C, Si*Ph*); 123.1 (s, *m*-C, N*Ar*); 123.7 (s, *p*-C, N*Ar*); 124.0 (s, *m*-C, N*Ar*); 127.0 (s, *m*-C, N*Ar*); 129.5 (s, *m*-C, Si*Ph*); 134.3 (s, *o*-C, Si*Ph*); 140.4 (s, *o*-C, N*Ar*), 141.3 (s, *o*-C, N*Ar*); 143.7 (s, *o*-C, N*Ar*); 144.2 (s, *o*-C, N*Ar*); 147.8 (s, *i*-C, Si*Ph*); 150.4 (s, *i*-C, N*Ar*); 152.0 (s, *i*-C, N*Ar*). ^{29}Si INEPT+ NMR (59.6 MHz; C_6D_6; J = 200 Hz; δ, ppm): -28.2 (d, $^1J_{Si-H}$ = 207.8 Hz, *Si*H). IR (nujol): 2105 cm^{-1} (Si-H). Elem. Anal. (%):calc. For $C_{37}H_{57}MoN_2Psi$ (684.861) C 64.89, H 8.39, N 4.09; found: C 64.48, H 8.30, N 3.74.

Preparation of (ArN)Mo(Et)(η^3-NAr-SiDPh-CH=CH$_2$)(PMe$_3$) (III-3$_D$)

The reaction was done analogously to the preparation of **III-3** (**A**), using 262.4 mg (0.461 mmol) of (ArN)Mo(SiD_2Ph)(η^3-NAr-SiDPh-D)(PMe$_3$) (**III-1d$_4$**) and 30 ml of Et_2O. The spectral data of **III-3$_D$** are the same except Si*H* resonances, which were not observed in the ^{1}H-NMR spectrum of **III-3$_D$** due to full substitution with deuterium. Yield: 92.2 mg, 29 %.

NMR scale generation of (ArN)Mo(H)(η^2-NAr-SiHPh-CH=CHPh)(PMe_3) (III-92)

Styrene (3.5 µl, 0.031 mmol) was added at room temperature to a solution of (ArN)Mo(SiH_2Ph)(η^3-NAr-SiHPh-H)(PMe_3) (**III-1**) (22.5 mg, 0.031 mmol) in 0.6 ml of C_6D_6 in an NMR tube. The reaction mixture was left at room temperature for 2.5 hours. NMR analysis showed a 100 % conversion of the starting material and selective formation (ArN)Mo(H)(η^2-NAr-SiHPh-CH=CHPh)(PMe_3) (**III-92**). ^{1}H-NMR (600 MHz; C_6D_6; δ, ppm): 8.00 (d, $^3J_{H-H}$ = 7.8 Hz, 2H, *o*-H, C*Ph*); 7.41 (d, $^3J_{H-H}$ = 7.8 Hz, 2H, *o*-H, Si*Ph*); 7.27 (m, 2H, *m*-H, C*Ph*); 7.06-6.88 (m, 10H, *p*-H of C*Ph*, *m*-H and *p*-H of Si*Ph*, m-H and *p*-H of N*Ar*); 6.22 (d, $^3J_{H-H}$ = 15.0 Hz, 1H, CH=CH); 6.15 (d, $^4J_{H-P}$ = 6.6 Hz, 1H, Si*H*); 3.56 (sept, $^3J_{H-H}$ = 6.6 Hz, 1H, *CH*, N*Ar*); 3.36 (sept, $^3J_{H-H}$ = 7.2 Hz, 1H, *CH*, N*Ar*); 3.30 (d, $^3J_{H-H}$ = 15.0 Hz, 1H, CH=CH); 3.05 (d, $^2J_{H-P}$ = 43.2 Hz, 1H, Mo-*H*); 2.63 (sept, $^3J_{H-H}$ = 7.2 Hz, 1H, *CH*, N*Ar*); 1.78 (sept, $^3J_{H-H}$ = 7.2 Hz, 1H, *CH*, N*Ar*); 1.39(d, $^3J_{H-H}$ = 7.2 Hz, 3H, CH_3, N*Ar*); 1.30 (d, $^3J_{H-H}$ = 7.2 Hz, 3H, CH_3, N*Ar*); 1.14 (d, $^3J_{H-H}$ = 6.6 Hz, 6H, $2CH_3$, N*Ar*); 1.12 (d, $^3J_{H-H}$ = 7.2 Hz, 3H, CH_3, N*Ar*); 1.10 (d, $^3J_{H-H}$ = 7.2 Hz, 3H, CH_3, N*Ar*); 0.95 (d, $^3J_{H-H}$ = 6.6 Hz, 3H, CH_3, N*Ar*); 0.75 (d, $^2J_{H-P}$ = 7.8 Hz, 9H, PMe_3); 0.47 (d, $^3J_{H-H}$ = 7.2 Hz, 3H, CH_3, N*Ar*). ^{31}P{^{1}H}-NMR (243 MHz; C_6D_6; δ, ppm): -19.2 (s, *P*Me_3). ^{31}P-NMR (selectively decoupled from methyl groups; 243 MHz; C_6D_6; δ, ppm): -19.2 (dd, $^2J_{H-P}$ = 43.7 Hz, $^4J_{H-P}$ = 7.3 Hz *P*Me_3). ^{29}Si INEPT+ NMR (119.2 MHz; C_6D_6; 200 Hz; δ, ppm): -8.2 (d, $^1J_{Si-H}$ = 197.9 Hz, *Si*H). ^{13}C{^{1}H}-NMR (75.5 MHz; C_6D_6; δ, ppm): 17.4 (d, $^1J_{C-P}$ = 21.1 Hz, P*Me*$_3$); 18.4 (s, CH_3, N*Ar*); 24.0 (s, CH_3, N*Ar*); 24.7 (s, CH_3, N*Ar*); 25.2 (s, CH_3, N*Ar*); 25.3 (s, CH_3, N*Ar*); 26.4 (s, CH_3, N*Ar*); 27.7 (s, CH_3, N*Ar*); 28.2 (s, *CH*, N*Ar*); 28.3 (s, *CH*, N*Ar*); 28.5 (s, *CH*, N*Ar*); 28.7 (s, *CH*, N*Ar*); 37.5 (d, $^4J_{C-P}$ = 6.8 Hz, Si-*CH*=CH_2); 83.4 (d, $^5J_{C-P}$ = 3.4 Hz, Si-CH=*CH*$_2$); 123.1, 123.2, 123.4, 123.8, 125.0, 126.6, 126.8, 127.1, 127.8, 128.1 (s, *p*-C of C*Ph*, *p*-C and *m*-C of Si*Ph* and N*Ar*); 128.2 (s, *m*-C, C*Ph*); 130.2 (s, *m*-C, C*Ph*); 135.5 (s, *o*-C, C*Ph*); 136.0, 136.1, 136.4, 136.8 (s, *o*-C, Si*Ph*); 138.5, 141.1, 141.4, 147.4, 147.6, 150.6, 150.7, 151.3 (s, aromatic quaternary carbons). IR (nujol): 1812 cm^{-1} (Mo-H); 2098 cm^{-1} (Si-H).

NMR scale generation of (ArN)Mo(SiH_2Ph)(η^3-NArSiH_2Ph)(η^2-CH_2=CHPh) (III-94)

A solution of BPh_3 (6.0 mg, 0.025 mmol) and styrene (2.9 µl, 0.025 mmol) in 0.6 ml of C_6D_6 was added in one portion at room temperature to solid (ArN)Mo(SiH_2Ph)(η^3-NAr-

SiHPh-H)(PMe_3) (**III-1**) (18.3 mg, 0.025 mmol). The mixture was immediately transferred to the NMR tube and the reaction was monitored by NMR analysis showing full conversion of **III-1** after 1.4 h to form selectively the $BPh_3 \cdot PMe_3$ adduct and the fluxional styrene complex (ArN)Mo(SiH_2Ph)(η^3-NAr-SiHPh-H)(η^2-CH_2=CHPh) (**III-94**). All volatiles were pumped off; the oily residue was dried in vacuum and redissolved in fresh C_6D_6 for analysis. The product is not thermally stable in solution and fully decomposes overnight at room temperature. After all NMR experiments, PMe_3 (2.6 µl, 0.025 mmol) was added to the sample. NMR analysis showed immediate quantitative substitution of the PhCH=CH_2 ligand with PMe_3, formation of (ArN)Mo(SiH_2Ph)(η^3-NAr-SiHPh-H)(PMe_3) (**III-1**) and slow reaction of the latter with styrene to give (ArN)Mo(H)(η^2-NAr-SiHPh-CH=CHPh)(PMe_3) (**III-92**).

(ArN)Mo(SiH_2Ph)(η^3-NAr-SiHPh-H)(η^2-CH_2=CHPh) (**III-94**): ^{1}H-NMR (300 MHz; C_6D_6; δ, ppm): 8.05 (d, $^3J_{H\text{-}H}$ = 6.3 Hz, 2H, *o*-H, SiH_2*Ph*); 6.75-7.29 (m, 19H, *m*-H and *p*-H of SiH_2*Ph*, *m*-H and *p*-H of N*Ar*, *m*-H, *p*-H, and *o*-H of η^3-NAr-SiH*Ph*-H and η^2-CH_2=CH*Ph*); 6.10 (s, 1H, Si*H*$_2$Ph); 5.70 (s, 1H, Si*H*$_2$Ph); 5.33 (bs, 1H, η^3-NAr-Si*H*Ph-H, found by ^{1}H-^{29}Si HSQC NMR with *J* = 200 Hz and 7 Hz); 4.56 (bs, 1H, η^3-NAr-SiHPh-*H*, ^{1}H-^{29}Si HSQC NMR with *J* = 7 Hz); 3.78 (sept, $^3J_{H\text{-}H}$ = 6.9 Hz, 2H, 2*CH*, N*Ar*); 3.64 (m, 2H, *CH* of N*Ar* and PhCH=*CH*$_2$, found by ^{1}H-^{1}H COSY and ^{1}H-^{13}C HSQC NMR); 3.54 (m, 1H, PhCH=*CH*$_2$); 3.39 (d, $^3J_{H\text{-}H}$ = 12.0 Hz, 1H, Ph*CH*=CH$_2$); 2.15 (bm, 1H, *CH*, NAr); 1.47 (d, $^3J_{H\text{-}H}$ = 6.9 Hz, 3H, *CH*$_3$, N*Ar*); 1.22 (d, $^3J_{H\text{-}H}$ = 6.9 Hz, 9H, 3*CH*$_3$, N*Ar*); 1.11 (d, $^3J_{H\text{-}H}$ = 6.9 Hz, 3H, *CH*$_3$, N*Ar*); 0.96 (d, $^3J_{H\text{-}H}$ = 6.9 Hz, 6H, 2*CH*$_3$, N*Ar*); 0.48 (d, $^3J_{H\text{-}H}$ = 6.9 Hz, 3H, *CH*$_3$, N*Ar*). ^{1}H-^{29}Si HSQC NMR (59.6 MHz; *J* = 200 Hz; C_6D_6, δ, ppm): -81.9 (η^3-NAr-*Si*HPh-H); 2.1 (SiH_2Ph). ^{13}C{^{1}H}-NMR (75.5 MHz; C_6D_6; δ, ppm): 152.9; 147.2; 146.5; 146.2 145.6; 142.2; 142.1 141.3; 136.6 (s, *o*-C, SiH_2*Ph*); 136.0 (s, *o*-C, η^3-NAr-SiH*Ph*-H); 128.1, 127.8; 125.4; 125.0; 124.9; 124.2; 123.8; 123.4; 122.6; 67.5 (bs, η^2-CH_2=*CH*Ph); 53.0 (s, η^2-*CH*$_2$=CHPh); 29.4 (s, *CH*, N*Ar*); 29.3 (s, *CH*, N*Ar*); 28.3 (s, *CH*, N*Ar*); 28.1 (s, *CH*, N*Ar*); 25.6 (s, *CH*$_3$, N*Ar*); 24.7 (s, *CH*$_3$, N*Ar*); 24.1 (s, *CH*$_3$, N*Ar*); 24.0 (s, *CH*$_3$, N*Ar*); 22.8 (s, *CH*$_3$, N*Ar*); 20.8 (s, *CH*$_3$, N*Ar*); 18.9 (s, *CH*$_3$, N*Ar*); 11.6 (s, *CH*$_3$, N*Ar*). ^{1}H-^{29}Si HSQC NMR (f1: 600 MHz; f2: 119.2 MHz; *J* = 200 Hz; toluene-d_8; ^{29}Si projection; δ, ppm): -82.4 (η^3-NAr-*Si*HPh-H); 1.9 (*Si*H$_2$Ph). ^{1}H-^{29}Si HSQC 1D JC NMR (f1: 600 MHz; f2: 119.2 Hz; *J* = 100 Hz, toluene-d_8; - 50 °C; ^{1}H

projection; δ, ppm): 4.68 (d, $^1J_{H\text{-}Si}$ = 112.4 Hz, 1H, η^3-NAr-SiHPh-*H*). ^{1}H-^{29}Si HSQC 1D JC NMR (f1: 600 MHz; f2: 119.2 Hz; *J* = 200 Hz, toluene-d_8; - 50 °C; ^{1}H projection; δ, ppm): 5.65 (d, $^1J_{H\text{-}Si}$ = 255.3 Hz, 1H, η^3-NAr-Si*H*Ph-H). ^{1}H-^{29}Si HSQC 1D JC NMR (f1: 600 MHz; f2: 119.2 Hz; *J* = 200 Hz; toluene-d_8; 22 °C; ^{1}H projection; δ, ppm): 6.05 (d, $^1J_{H\text{-}Si}$ = 186.1 Hz, 1H, SiH_2Ph); 5.65 (d, $^1J_{H\text{-}Si}$ = 168.1 Hz, 1H, SiH_2Ph). IR (nujol): 1571 cm^{-1} (weak, PhHC=CH_2); 1589 cm^{-1} (medium, PhHC=CH_2); 1771 cm^{-1} (weak, broad, η^3-NAr-SiHPh-*H*); 2080 cm^{-1} (strong, broad, SiH_2Ph); 2160 cm^{-1} (medium, broad, η^3-NAr-Si*H*Ph-H).

NMR scale generation of (ArN)Mo(SiH$_2$Ph)(η^3-NArSiH$_2$Ph)(η^2-CH$_2$=CH$_2$) (III-95)

A solution of BPh_3 (5.6 mg, 0.023 mmol) in 0.3 ml of C_6D_6 was added in one portion at -30 °C to a solution of complex (ArN)Mo(SiH_2Ph)(η^3-NAr-SiHPh-H)(PMe_3) (**III-1**) (17.1 mg, 0.023 mmol) in 0.3 ml of C_6D_6 in an NMR tube. The mixture was immediately frozen in liquid nitrogen and ethylene was added *via* vacuum transfer. The reaction mixture was slowly warmed up to room temperature and left for additional 5 min. NMR analysis showed quantitative formation of (ArN)Mo(SiH_2Ph)(η^3-NAr-SiHPh-H)(η^2-CH_2=CH_2) (**III-95**), accompanied by the production of BPh_3·PMe_3. The product is not stable at room temperature in solution and fully decomposes after 30 min. to give a difficult-to-characterize mixture of unidentified compounds. All attempts to isolate the product by extraction with hexanes led to the formation of a mixture of unidentified decomposition products. Instability of **III-95** also hampered its full spectroscopic characterization. ^{1}H-NMR (300 MHz; C_6D_6; δ, ppm): 7.79 (m, 2H, *o*-H, SiH_2*Ph*); 6.83-7.30 (overlapping with the residual solvent signal multiplet, 14H, *p*-H and *m*-H of SiH_2*Ph*, *o*-H, *m*-H, and *p*-H of η^3-NAr-SiH*Ph*-H, *m*-H and *p*-H of N*Ar*); 5.89 (d, $^2J_{H\text{-}H}$ = 3.3 Hz, 1H, SiH_2Ph); 5.80 (d, $^2J_{H\text{-}H}$ = 3.3 Hz, 1H, SiH_2Ph); 4.83 (d, $^2J_{H\text{-}H}$ = 5.1 Hz, 1H, η^3-NAr-Si*H*Ph-H); 3.60 (bs, 1H, η^3-NAr-SiHPh-*H*); 3.47 (sept, $^3J_{H\text{-}H}$ = 6.9 Hz, 1H, *CH*, N*Ar*); 3.32 (sept, $^3J_{H\text{-}H}$ = 6.9 Hz, 2H, 2*CH*, N*Ar*); 3.23 (sept, $^3J_{H\text{-}H}$ = 6.9 Hz, 1H, *CH*, N*Ar*); 3.03 (m, $J_{H\text{-}H}$ = 5.7 Hz and 12.3 Hz, 1H, η^2-C_2H_4); 2.82 (m, $J_{H\text{-}H}$ = 6.3 Hz and 13.5 Hz, 1H, η^2-C_2H_4); 2.61 (m, $J_{H\text{-}H}$ = 6.3 Hz and 12.3 Hz, 1H, η^2-C_2H_4); 1.37 (m, 1H, η^2-C_2H_4, found by ^{1}H-^{1}H COSY); 1.25 (d, $^3J_{H\text{-}H}$ = 6.9 Hz, 3H, CH_3, N*Ar*); 1.19 (d, $^3J_{H\text{-}H}$ = 6.9 Hz, 3H, CH_3, N*Ar*); 1.12 (d, $^3J_{H\text{-}H}$ = 6.9 Hz, 6H, 2CH_3, N*Ar*); 0.98 (d, $^3J_{H\text{-}H}$ = 6.9 Hz,

6H, 2*CH*$_3$, N*Ar*); 0.94 (d, $^3J_{H\text{-}H}$ = 6.9 Hz, 3H, *CH*$_3$, N*Ar*); 0.76 (d, $^3J_{H\text{-}H}$ = 6.9 Hz, 3H, *CH*$_3$, N*Ar*).

NMR scale reaction of (ArN)Mo(SiH$_2$Ph)(η^3-NAr-SiHPh-H)(PMe$_3$) (III-1) with acetone

Acetone (1.6 µl, 0.022 mmol) was added at room temperature to a solution of (ArN)Mo(SiH$_2$Ph)(η^3-NAr-SiHPh-H)(PMe$_3$) (**III-1**) (16.0 mg, 0.022 mmol) in 0.6 ml of C_6D_6 in an NMR tube. The reaction mixture was left at room temperature for 2 hours. During this time the reaction was monitored by NMR analysis, which showed a 100 % conversion of **III-1** and formation of (ArN)$_2$Mo(PMe$_3$)(η^2-O=CMe$_2$) (**III-96**) accompanied by the evolution of the molecule of PhSiH$_3$. Other silicon containing products were not detected. ^{1}H-NMR (300 MHz; C_6D_6; δ, ppm): 7.07-6.96 (m, 6H, *p*-H and *m*-H, N*Ar*); 3.98 (sept, $^3J_{H\text{-}H}$ = 6.9 Hz, 4H, *CH*, N*Ar*); 2.30 (s, 6H, η^2-O=C*Me*$_2$); 1.19 (m, 33H, *CH*$_3$ of N*Ar* and 9H of P*Me*$_3$). ^{31}P{^{1}H}-NMR (121.5 MHz; C_6D_6; δ, ppm): 7.3 (s, *P*Me$_3$). ^{13}C{^{1}H}-NMR (75.5 MHz; C_6D_6; δ, ppm): 13.3 (d, $^1J_{C\text{-}P}$ = 27.8 Hz, P*Me*$_3$); 24.0 (s, *CH*$_3$, N*Ar*); 24.1 (s, *CH*$_3$, N*Ar*); 28.0 (s, *CH*, N*Ar*); 32.3 (s, *CH*$_3$, η^2-O=C*Me*$_2$); 85.8 (s, η^2-O=C*Me*$_2$); 122.7 (s, *m*-C, N*Ar*); 123.9 (s, *p*-C, N*Ar*); 141.6 (s, *o*-C, N*Ar*); 153.9 (s, *i*-C, N*Ar*). IR (nujol): 1621 cm^{-1} (strong, O=C).

NMR scale reaction of (ArN)Mo(SiH$_2$Ph)(η^3-NAr-SiHPh-H)(PMe$_3$) (III-1) with acetophenone

Acetophenone (3.3 µl, 0.028 mmol) was added at room temperature to a solution of (ArN)Mo(SiH$_2$Ph)(η^3-NAr-SiHPh-H)(PMe$_3$) (**III-1**) (20.6 mg, 0.028 mmol) in 0.6 ml of C_6D_6 in an NMR tube. The reaction mixture was left at room temperature for 2 hours. During this time the reaction was monitored by NMR analysis showing a 100 % conversion of complex **III-1** and formation of the bis(imido) acetophenone adduct (ArN)$_2$Mo(PMe$_3$)(η^1-O=CMePh) (**III-97**) accompanied by the release of the molecule of PhSiH$_3$. Other silicon containing products were not detected. ^{1}H-NMR (300 MHz; C_6D_6; δ, ppm): 7.63 (d, $^3J_{H\text{-}H}$ = 7.2 Hz, 2H, *o*-H, C*Ph*); 7.24 (t, $^3J_{H\text{-}H}$ = 7.2 Hz, 2H, *m*-H, C*Ph*); 7.07-6.87 (m, 7H, *p*-H of C*Ph* and *m*-H and *p*-H of N*Ar*); 3.97 (sept, $^3J_{H\text{-}H}$ = 6.6 Hz, 2H, *CH*, N*Ar*); 3.27 (sept, $^3J_{H\text{-}H}$ = 6.6 Hz, 2H, *CH*, N*Ar*); 2.60 (s, 3H, C*Me*); 1.25 (d, $^2J_{H\text{-}P}$ = 9.9 Hz, 9H, P*Me*$_3$); 1.23 (d, $^3J_{H\text{-}H}$ = 6.6 Hz, 6H, 2*CH*$_3$, N*Ar*); 1.15 (d, $^3J_{H\text{-}H}$ = 6.6 Hz, 6H,

$2CH_3$, NAr); 0.98 (d, $^3J_{H-H}$ = 6.6 Hz, 12H, $4CH_3$, NAr). $^{31}P\{^1H\}$-NMR (121.5 MHz; C_6D_6; δ, ppm): 8.5 (s, PMe_3). $^{13}C\{^1H\}$-NMR (75.5 MHz; C_6D_6; δ, ppm): 13.3 (d, $^1J_{C-P}$ = 27.9 Hz, PMe_3); 23.8 (s, CH_3, NAr); 24.0 (s, CH_3, NAr); 24.1 (s, CH_3, NAr); 27.9 (s, CH, NAr); 28.1 (s, CH, NAr); 30.3 (s, CH_3, η^1-O=C*Me*Ph); 85.7 (s, η^1-O=*C*MePh); 122.4 (s, *m*-C, NAr); 122.7 (s, *m*-C, NAr); 124.0 (s, *p*-C, NAr); 124.1 (s, *p*-C, NAr); 125.3 (s, *o*-C, η^1-O=CMe*Ph*); 125.3 (s, *p*-C, η^1-O=CMe*Ph*); signal for the *m*-C of η^1-O=CMe*Ph* overlaps with the signal for C_6D_6; 141.3 (s, *o*-C, NAr); 141.9 (s, *o*-C, NAr); 151.6 (s, *i*-C, η^1-O=CMe*Ph*); 153.8 (s, *i*-C, NAr); 154.0 (s, *i*-C, NAr). IR (nujol): 2276 cm^{-1} (strong, O=C). Elem. Anal. (%): calc. for $C_{35}H_{51}MoN_2OP$ (642.706) C 65.41, H 8.00, N 4.36; found: C 64.96, H 8.12, N 4.28.

NMR scale reaction of (ArN)Mo(SiH_2Ph)(η^3-NAr-SiHPh-H)(PMe_3) (III-1) with benzaldehyde

Benzaldehyde (3.0 µl, 0.029 mmol) was added in one portion at -30 °C to a solution of (ArN)Mo(SiH_2Ph)(η^3-NAr-SiHPh-H)(PMe_3) (**III-1**) (21.0 mg, 0.029 mmol) in 0.6 ml of toluene-d_8 in an NMR tube. The sample was immediately frozen in liquid N_2 and placed into the NMR machine precooled to -30 °C. The reaction was monitored by low temperature VT NMR spectroscopy, showing at -10 °C the formation of a difficult-to-characterize mixture of products, one of which was suggested to be (ArN)Mo(η^2-ArN=SiHPh)(O=CHPh)(PMe_3) (**III-99**). Warming the sample up to room temperature leads to a decomposition to a mixture of unidentified products.

(ArN)Mo(η^2-ArN=SiHPh)(O=CHPh)(PMe_3) (**III-99**): 1H-NMR (600 MHz; toluene-d_8; -7 °C; selected resonances; δ, ppm): 13.28 (d, J_{H-P} = 6.9 Hz, 1H, PhC(O)*H*); 6.83 (bs, 1H, η^2-ArN=Si*H*Ph). $^{31}P\{^1H\}$-NMR (243 MHz; toluene-d_8; -50 °C; δ, ppm): 2.9 (s, PMe_3). ^1H-^{29}Si HSQC NMR (f1: 600 MHz; f2: 119.2 MHz; *J* = 200 Hz; toluene-d_8; -50 °C; ^{29}Si projection; δ, ppm): -49 (η^2-ArN=*Si*HPh). ^{29}Si INEPT+ NMR (119.2 MHz; *J* = 200 Hz; toluene-d_8; -50 °C; δ, ppm): -49.9 (d, $^1J_{Si-H}$ = 241.4Hz, η^2-ArN=*Si*HPh).

NMR scale reaction of (ArN)Mo(SiH_2Ph)(η^3-NAr-SiHPh-H)(PMe_3) (III-1) with acetonitrile

Acetonitrile (6.5 µl, 0.12 mmol) was added in one portion to frozen in liquid N_2 solution of (ArN)Mo(SiH_2Ph)(η^3-NAr-SiHPh-H)(PMe_3) (**III-1**) (30.4 mg, 0.04 mmol) in 0.6 ml of

toluene-d_8 in an NMR tube. The sample was placed into the precooled (-30 °C) NMR machine and the reaction was monitored by low temperature VT NMR spectroscopy. At -30 °C, the evolution of one equivalent of $PhSiH_3$ and formation of the initial product (ArN)Mo(η^2-ArN=SiHPh)(η^2-NCMe)(PMe_3) (**III-104**) was observed. Warming the sample up to room temperature gives (ArN)Mo(η^2-NAr-SiHPh-C(Me)=N)(PMe_3) (**III-108**) in a mixture with unidentified compounds.

(ArN)Mo(η^2-ArN=SiHPh)(η^2-NCMe)(PMe_3) (**III-104**): ^{1}H-NMR (600 MHz; toluene-d_8; -23 °C; δ, ppm): 7.95 (bs, 2H, *o*-H, Si*Ph*); 6.97-7.17 (m, 9H, *m*-H and *p*-H of 2 N*Ar* and Si*Ph*, overlapping with residual toluene-d_8 signals); 5.23 (s, 1H, Si*H*); 4.02 (bs, 1H, *CH*, N*Ar*); 3.76 (broad sept, $^3J_{H\text{-}H}$ = 5.4 Hz, 2H, 2 *CH*, N*Ar*); 3.64 (bs, 1H, *CH*, N*Ar*); 3.32 (s, 3H, η^2-NC*Me*); 1.42 (bd, $^3J_{H\text{-}H}$ = 6.0 Hz, 3H, CH_3, N*Ar*); 1.31 (bs, 3H, CH_3, N*Ar*); 1.24 (bs, 3H, CH_3, N*Ar*); 1.21 (bd, $^3J_{H\text{-}H}$ = 5.4 Hz, 6H, 2 CH_3, N*Ar*); 1.16 (bd, $^3J_{H\text{-}H}$ = 5.4 Hz, 6H, 2 CH_3, N*Ar*); 1.07 (bd, $^2J_{H\text{-}P}$ = 8.4 Hz, 9H, PMe_3); 0.54 (bs, 3H, CH_3, N*Ar*). ^{31}P{^{1}H}-NMR (243 MHz; toluene-d_8; -22 °C; δ, ppm): -1.8 (s, *P*Me_3). ^{13}C{^{1}H}-NMR (151 MHz; toluene-d_8; -20 °C; δ, ppm): 186.5 (s, η^2-N*C*Me); 155.32; 155.26; 153.5; 136.7; 122.3; other aromatic carbons are overlapping with the signals of toluene-d_8; 28.0 (s, CH); 27.89 (s, CH); 27, 85 (s, CH); 26.8 (s, CH_3, N*Ar*); 23.9 (s, CH_3, N*Ar*); 23.5(s, CH_3, N*Ar*); 23.1 (s, CH_3, N*Ar*); 22.8 (s, η^2-NC*Me*); 22.2 (s, CH_3, N*Ar*); 21.5 (s, CH_3, N*Ar*); 13.5 (d, $^1J_{C\text{-}P}$ = 22.6 Hz, PMe_3). ^{29}Si INEPT + NMR (119.2 MHz; toluene-d_8; J = 200 Hz; -20 °C; δ, ppm): -45.2 (d, $^1J_{Si\text{-}H}$ = 219.4 Hz, η^2-ArN=*Si*HPh).

(ArN)Mo(η^2-NAr-SiHPh-C(Me)=N)(PMe_3) (**III-108**): ^{1}H-NMR (600 MHz; toluene-d_8; -23 °C; selected resonances; δ, ppm): 7.45 (bd, $^3J_{H\text{-}H}$ = 6.0 Hz, 2H, *o*-H, Si*Ph*); 5.76 (bs, 1H, Si*H*); 3.03 (s, 3H, C(*Me*)=N); 1.12 (bs, 9H, PMe_3). ^{31}P{^{1}H}-NMR (243 MHz; toluene-d_8; -22 °C; δ, ppm): -1.7 (s, *P*Me_3). ^{29}Si INEPT + NMR (119.2 MHz; toluene-d_8; J = 200 Hz; -20 °C; δ, ppm): -47.6 (d, $^1J_{Si\text{-}H}$ = 228.9 Hz, N*Si*HPh).

NMR scale reaction of (ArN)Mo(SiH_2Ph)(η^3-NAr-SiHPh-H)(PMe_3) (III-1) with PhCN

Benzonitrile (3.8 µl, 0.037 mmol) was added at room temperature to a solution of (ArN)Mo(SiH_2Ph)(η^3-NAr-SiHPh-H)(PMe_3) (**III-1**) (27.2 mg, 0.037 mmol) in 0.6 ml of C_6D_6 in an NMR tube. The reaction was left at room temperature for one hour. NMR

analysis showed the formation an intermediate tentatively formulated as (ArN)Mo(η^2-NAr=SiHPh)(η^2-N≡CPh)(PMe_3) (**III-105**), which was unstable and rearranged slowly into another product. All volatiles were pumped off; the oily residue was dried in vacuum, redissolved in fresh C_6D_6 and left at room temperature overnight for complete rearrangement. NMR spectra showed the formation of only one compound, formulated as (ArN)Mo(η^2-NAr-SiHPh-CPh=N)(PMe_3) (**III-109**). Complex **III-109** is unstable at room temperature in solution and completely decomposes during one day.

(ArN)Mo(η^2-N(Ar)=SiHPh)(η^2-N≡CPh)(PMe_3) (**III-105**): $^{31}P\{^1H\}$-NMR (121.5 MHz; C_6D_6; δ, ppm): -6.4 (s, *P*Me_3).

(ArN)Mo(η^2-NAr-SiHPh-CPh=N)(PMe_3) (**III-109**): ^{1}H-NMR (300 MHz; C_6D_6; δ, ppm): 8.83 (d, $^3J_{H-H}$ = 6.9 Hz, 2H, *o*-H, C*Ph*); 8.06 (m, 2H, *o*-H, Si*Ph*); 7.75-6.96 (m, 12H, *p*-H and *m*-H of C*Ph*, Si*Ph* and N*Ar*); 5.34 (s, 1H, Si*H*); 3.75 (m, 4H, 4*CH*, N*Ar*); 1.41 (d, $^3J_{H-H}$ = 6.6 Hz, 3H, CH_3, N*Ar*); 1.25 (d, $^3J_{H-H}$ = 7.2 Hz, 3H, CH_3, N*Ar*); 1.14 (d, $^2J_{H-P}$ = 8.7 Hz, 9H, PMe_3); 1.05 (d, $^3J_{H-H}$ = 7.2 Hz, 6H, 2CH_3, N*Ar*); 0.98 (d, $^3J_{H-H}$ = 6.9 Hz, 6H, 2CH_3, N*Ar*); 0.89 (m, 3H, CH_3, N*Ar*); 0.61 (d, $^3J_{H-H}$ = 7.2 Hz, 3H, CH_3, N*Ar*). $^{31}P\{^1H\}$-NMR (121.5 MHz; C_6D_6; δ, ppm): - 3.5 (s, *P*Me_3). ^{29}Si INEPT+ NMR (59.6 MHz; C_6D_6; *J* = 200 Hz; δ, ppm): - 44.4 (d, $^1J_{Si-H}$ = 225.4 Hz, *Si*H). $^{13}C\{^1H\}$-NMR (75.5 MHz; C_6D_6; δ, ppm): 16.9 (d, $^1J_{C-P}$ = 22.6 Hz, PMe_3); 21.5 (s, CH_3, N*Ar*); 23.2 (s, CH_3, N*Ar*); 23.6 (s, CH_3, N*Ar*); 24.1 (s, CH_3, N*Ar*); 24.7 (s, CH_3, N*Ar*); 24.9 (s, CH_3, N*Ar*); 27.8 (s, *CH*, N*Ar*); 28.0 (s, *CH*, N*Ar*); 28.3 (s, *CH*, N*Ar*); 29.1 (s, *CH*, N*Ar*); 122.4 (s, *p*-C, N*Ar*); 122.7 (s, *p*-C, N*Ar*); 122.8 (s, *m*-C, N*Ar*); 123.3 (s, *m*-C, N*Ar*); 125.2 (s, *m*-C, N*Ar*); 126.8 (s, *m*-C, N*Ar*); 127.0 (s, *m*-C, Si*Ph*); *m*-C of C*Ph* signals are overlapping with benzene signal; 128.5 (s, *p*-C, Si*Ph*); 129.0 (s, *p*-C, C*Ph*); 133.4 (s, *o*-C, C*Ph*); 133.9 (s, *o*-C, C*Ph*); 135.5 (s, *o*-C, Si*Ph*); 136.9 (s, *o*-C, Si*Ph*); 141.5 (s, *o*-C, N*Ar*); 141.6 (s, *o*-C, N*Ar*); 143.5 (s, *o*-C, N*Ar*); 151.2, 153.6, 158.4 (all singlets, aromatic *i*-C); 192.4 (s, Ph*C*=N). IR (nujol): 2118 cm^{-1} (medium, Si-H).

NMR scale reaction of (ArN)Mo(SiH_2Ph)(η^3-NAr-SiHPh-H)(PMe_3) (III-1) with ^{i}PrCN

^{i}PrCN (1.9 μl, 0.021 mmol) was added at room temperature to a solution of (ArN)Mo(SiH_2Ph)(η^3-NAr-SiHPh-H)(PMe_3) (**III-1**) (15.3 mg, 0.021 mmol) in 0.6 ml of

C_6D_6 in an NMR tube. The reaction mixture was left at room temperature for 5 min. NMR analysis showed the formation of only one product, rationalized as nitrile adduct (ArN)Mo(η^2-N(Ar)=SiHPh)(η^2-N≡C^{i}Pr)(PMe_3) (**III-106**). This product was unstable and slowly rearranged into the compound (ArN)Mo(η^2-NAr-SiHPh-C(^{i}Pr)=N)(PMe_3) (**III-110**), most likely *via* intermolecular insertion of the nitrile into the Mo-Si bond of the silanimine moiety. After 1 hour 20 minutes at room temperature, the rearrangement was complete, all volatiles were pumped off; the oily residue was dried in vacuum and redissolved in fresh C_6D_6. Further NMR analysis showed the presence of only one product (ArN)Mo(η^2-NAr-SiHPh-C(^{i}Pr)=N)(PMe_3) (**III-110**) in solution.

(ArN)Mo(η^2-N(Ar)=SiHPh)(η^2-N≡C^{i}Pr)(PMe_3) (**III-106**): ^{1}H-NMR (300 MHz; C_6D_6; δ, ppm): 5.74 (d, $^3J_{H-P}$ = 3.9 Hz, 1H, Si*H*); 1.59 (d, $^3J_{H-H}$ = 6.9 Hz, 6H, 2*CH*$_3$, ^{i}*Pr*C≡N). ^{31}P{^{1}H}-NMR (121.5 MHz; C_6D_6; δ, ppm): - 4.4 (s, *P*Me$_3$).

(ArN)Mo(η^2-NAr-SiHPh-C(^{i}Pr)=N)(PMe_3) (**III-110**): ^{1}H-NMR (300 MHz; C_6D_6; δ, ppm): 7.94 (m, 2H, *o*-H, Si*Ph*); 7.09-6.89 (m, 3H, 9H, *m*-H and *p*-H of Si*Ph*, *m*-H and *p*-H of N*Ar*); 5.31 (s, 1H, Si*H*); 3.95 (m, 1H, *CH*, N*Ar*); 3.78 (sept, $^3J_{H-H}$ = 6.9 Hz, 1H, *CH*, ^{i}*Pr*C=N); 3.70 (sept, $^3J_{H-H}$ = 6.9 Hz, 2H, 2*CH*, N*Ar*); 3.63 (sept, $^3J_{H-H}$ = 7.5 Hz, 1H, *CH*, N*Ar*); 1.69 (d, $^3J_{H-H}$ = 6.9 Hz, 6H, 2*CH*$_3$, ^{i}*Pr*C=N); 1.36 (d, $^3J_{H-H}$ = 6.6 Hz, 3H, *CH*$_3$, N*Ar*); 1.30 (d, $^3J_{H-H}$ = 6.6 Hz, 3H, *CH*$_3$, N*Ar*); 1.22 (d, $^3J_{H-H}$ = 6.6 Hz, 3H, *CH*$_3$, N*Ar*); 1.18 (d, $^3J_{H-H}$ = 6.9 Hz, 6H, 2*CH*$_3$, N*Ar*); 1.12 (d, $^3J_{H-H}$ = 6.9 Hz, 6H, 2*CH*$_3$, N*Ar*); 1.05 (d, $^2J_{H-P}$ = 8.7 Hz, 9H, P*Me*$_3$); 0.60 (d, $^3J_{H-H}$ = 6.9 Hz, 3H, *CH*$_3$, N*Ar*). ^{31}P{^{1}H}-NMR (121.5 MHz; C_6D_6; δ, ppm): - 3.8 (s, *P*Me$_3$). ^{13}C{^{1}H}-NMR (75.5 MHz; C_6D_6; δ, ppm): 14.3 (d, $^1J_{C-P}$ = 21.9 Hz, P*Me*$_3$); 22.55 (s, *CH*$_3$, ^{i}*Pr*C=N); 22.60 (s, *CH*$_3$, N*Ar*); 23.76 (s, *CH*$_3$, N*Ar*); 23.83 (s, *CH*$_3$, N*Ar*); 24.2 (s, *CH*$_3$, N*Ar*); 26.8 (s, *CH*$_3$, N*Ar*); 28.0 (s, *CH*, N*Ar*); 28.1 (s, *CH*, N*Ar*); 28.2 (s, *CH*, N*Ar*); 28.6 (s, *CH*, ^{i}*Pr*C=N); 122.5 (s, *p*-C, N*Ar*); 122.6 (s, *p*-C, N*Ar*); 122.8 (s, *m*-C, N*Ar*); 123.0 (s, *m*-C, N*Ar*); 125.3 (s, *m*-C, N*Ar*); *m*-C of Si*Ph* signal is overlapping with the benzene signals; 129.7 (s, *p*-C, Si*Ph*); 136.9 (s, *o*-C, Si*Ph*); 141.3 (s, *o*-C, N*Ar*); 141.8 (s, *o*-C, N*Ar*); 143.7 (s, *o*-C, N*Ar*); 153.8, 155.6, 155.8 (all singlets, aromatic *i*-C); 195.9 (s, ^{i}Pr*C*=N). ^{29}Si INEPT+ NMR (59.6 MHz; C_6D_6; 200 Hz; δ, ppm): - 46.6 (d, $^1J_{Si-H}$ = 218.3 Hz, *Si*H). IR (nujol): 2103 cm^{-1} (medium, Si-H).

Preparation of (ArN)Mo(η^2-NAr-SiHPh-C(^{i}Pr)=N)(PMe_3) (III-110)

^{i}PrCN (37.7 µl, 0.42 mmol) was added at room temperature to a solution of (ArN)Mo(SiH_2Ph)(η^3-NAr-SiHPh-H)(PMe_3) (**III-1**) (281.3 mg, 0.38 mmol) in 15 ml of toluene. The reaction mixture was stirred at room temperature for 2 hours. Then all volatiles were pumped off; the residue was dried in vacuum, redissolved in fresh toluene and allowed to stir at room temperature overnight. All volatiles were removed under reduced pressure and the residue was extracted with hexanes. The solvent was pumped off to leave an oily substance, which was dissolved in 5 ml of Et_2O. The solution was left with stirring for 2 hours, and then ether was removed in vacuum to give a brown foam of (ArN)Mo(η^2-NAr-SiHPh-C(^{i}Pr)=N)(PMe_3) (**III-110**). Yield: 193.3 mg, 73 %. All attempts to recrystallize the product gave an oily substance. The product is not stable at room temperature in solution and after four days NMR analysis showed slow decomposition to a mixture of unidentified compounds. For spectral data see the procedure above.

NMR scale reaction of (ArN)Mo(η^2-NAr-SiHPh-C(^{i}Pr)=N)(PMe_3) (III-110) with $PhSiH_3$

$PhSiH_3$ (12.0 µl, 0.097 mmol) was added in one portion at room temperature to a solution of (ArN)Mo(η^2-NAr-SiHPh-C(^{i}Pr)=N)(PMe_3) (**III-110**) (21.5 mg, 0.031 mmol) in 0.6 ml of C_6D_6 in an NMR tube. No visual changes were observed after the addition of silane. The reaction mixture was left at room temperature for 4 days. NMR analysis showed selective formation of (ArN)Mo(SiH_2Ph)(η^3-NAr-SiHPh-H)(PMe_3) (**III-1**) in a mixture with unidentified silicon containing products.

NMR scale reaction of (ArN)Mo(SiH_2Ph)(η^3-NAr-SiHPh-H)(PMe_3) (III-1) with ^{t}BuCN

^{t}BuCN (3.7 µl, 0.034 mmol) was added at room temperature to a solution of (ArN)Mo(SiH_2Ph)(η^3-NAr-SiHPh-H)(PMe_3) (**III-1**) (24.8 mg, 0.034 mmol) in 0.6 ml of toluene-d_8 in an NMR tube. The reaction mixture was left at room temperature for 5 min. NMR analysis showed the formation of a single product (ArN)Mo(η^2-NAr=SiHPh)(η^2-N≡C^{t}Bu)(PMe_3) (**III-107**). This was confirmed by the observation of nitrile carbon signal at 204 ppm in the $^{13}C\{^1H\}$-NMR spectrum, suggesting the η^2-coordination of ^{t}BuCN

ligand. The ^{1}H-^{13}C HMBC NMR spectrum showed the absence of coupling between the Si*H* proton and nitrile carbon atom. Complex **III-107** decomposes slowly in solution affording a difficult-to-analyze mixture of compounds. One of the components of this mixture appears to be similar to the insertion product (ArN)Mo(η^2-NAr-SiHPh-C(^{i}Pr)=N)(PMe$_3$) (**III-110**) (see above) and was formulated as (ArN)Mo(η^2-NAr-SiHPh-C(^{t}Bu)=N)(PMe$_3$) (**III-111**). The product is not stable and decomposes completely in solution after one day at room temperature.

(ArN)Mo(η^2-NAr=SiHPh)(η^2-N≡C^{t}Bu)(PMe$_3$) (**III-107**): ^{1}H-NMR (600 MHz; toluene-d$_8$; δ, ppm): 7.98 (d, $^{3}J_{H\text{-}H}$ = 7.2 Hz, 2H, *o*-H, Si*Ph*); 6.87-7.10 (multiplet overlapping with residual toluene-d$_8$ signals, *p*-H and *m*-H of *Ar*N and Si*Ph*); 5.66 (d, $^{3}J_{H\text{-}P}$ = 3.6 Hz, 1H, Si*H*); 3.95 (m, 2H, 2*CH*, N*Ar*); 3.86 (sept, $^{3}J_{H\text{-}H}$ = 6.6 Hz, 1H, *CH*, N*Ar*); 2.50 (sept, $^{3}J_{H\text{-}H}$ = 6.6 Hz, 1H, *CH*, N*Ar*); 1.45 (d, $^{3}J_{H\text{-}H}$ = 6.6 Hz, 3H, *CH$_3$*, N*Ar*); 1.42 (d, $^{3}J_{H\text{-}H}$ = 6.6 Hz, 3H, *CH$_3$*, N*Ar*); 1.39 (s, 9H, ^{t}*Bu*C); 1.28 (d, $^{3}J_{H\text{-}H}$ = 6.6 Hz, 6H, 2*CH$_3$*, N*Ar*); 1.17 (m, 6H, 2*CH$_3$*, N*Ar*); 1.03 (d, $^{2}J_{H\text{-}P}$ = 9.0 Hz, 9H, P*Me$_3$*); 0.26 (d, $^{3}J_{H\text{-}H}$ = 6.6 Hz, 3H, *CH$_3$*, N*Ar*); 0.13 (d, $^{3}J_{H\text{-}H}$ = 6.6 Hz, 3H, *CH$_3$*, N*Ar*). ^{1}H{^{31}P}-NMR (600 MHz; toluene-d$_8$; δ, ppm): 5.66 (s, 1H, Si*H*); 1.03 (s, 9H, P*Me$_3$*). ^{31}P{^{1}H}-NMR (121.5 MHz; toluene-d$_8$; δ, ppm): -1.9 (s, *P*Me$_3$). ^{13}C{^{1}H}-NMR (151 MHz; toluene-d$_8$; - 30 °C; δ, ppm): 17.5 (d, $^{1}J_{C\text{-}P}$ = 27.2 Hz, P*Me$_3$*); 23.3 (s, *CH$_3$*, N*Ar*); 23.9 (s, *CH$_3$*, N*Ar*); 24.5 (s, *CH$_3$*, N*Ar*); 25.4 (s, *CH$_3$*, N*Ar*); 27.5 (s, *CH*, N*Ar*); 28.1 (s, *CH*, N*Ar*); 29.1 (s, *CH*, N*Ar*); 30.2 (s, *CH$_3$*, ^{t}*Bu*C); 35.0 (s, Me$_3$*C*C); 135.2 (s, *o*-C, Si*Ph*); 122.3 (s, *p*-C, Si*Ph*); 122.7 (s, *p*-C, N*Ar*); 123.3 (s, *p*-C, N*Ar*); 123.3 (s, *m*-C, N*Ar*); 123.9 (s, *m*-C, N*Ar*); 124.6 (s, *m*-C, N*Ar*); 126.4 (s, *m*-C, N*Ar*); 129.9 (s, *m*-C, Si*Ph*); 135.9 (s, *o*-C, Si*Ph*); 140.3 (s, *o*-C, N*Ar*); 141.2 (s, *o*-C, N*Ar*); 144.6 (s, *o*-C, N*Ar*); 145.6 (s, *o*-C, N*Ar*); 148.7 (s, *i*-C, Si*Ph*); 153.1 (s, *i*-C, N*Ar*); 153.4 (s, *i*-C, N*Ar*); 204.4 (s, ^{t}Bu*C*). ^{29}Si INEPT+ NMR (119.2 MHz; toluene-d$_8$; *J* = 200 Hz; - 30 °C; δ, ppm): -50.9 (d, $^{1}J_{Si\text{-}H}$ = 223.0 Hz, *Si*H).

(ArN)Mo(η^2-NAr-SiHPh-C(^{t}Bu)=N)(PMe$_3$) (**III-111**): ^{1}H-NMR (600 MHz; toluene-d$_8$; δ, ppm): 6.56 (s, 1H, Si*H*); 1.00 (d, $^{2}J_{H\text{-}P}$ = 7.2 Hz, 9H, P*Me$_3$*). ^{31}P{^{1}H}-NMR (121.5 MHz; toluene-d$_8$; δ, ppm): 3.3 (s, *P*Me$_3$). ^{29}Si INEPT+ NMR (119.2 MHz; toluene-d$_8$; *J* = 200 Hz; - 30 °C; δ, ppm): -20.6 (d, $^{1}J_{Si\text{-}H}$ = 224.2 Hz, *Si*H).

NMR scale reaction of (ArN)Mo(SiH_2Ph)(η^3-NAr-SiHPh-H)(PMe_3) (III-1) with $PhSiH_3$

$PhSiH_3$ (4.14 µl, 0.034 mmol) was added in one portion at room temperature to a solution of (ArN)Mo(SiH_2Ph)(η^3-NAr-SiHPh-H)(PMe_3) (**III-1**) (24.7 mg, 0.034 mmol) in 0.6 ml of C_6D_6 in an NMR tube. The ^1H-^1H EXSY NMR experiment established proton exchange between the silyl substituent in (ArN)Mo(SiH_2Ph)(η^3-NAr-SiHPh-H)(PMe_3) (**III-1**) and free silane. After overnight at room temperature, NMR analysis showed the formation of a mixture of $PhSiH_3$ (30 %), Ph_2SiH_2 (34 %), SiH_4 (34 %) and $PhSiH_2$-SiH_2Ph (2 %).[211] At 50 °C, an analogous overnigh reaction leads to full conversion of $PhSiH_3$ into Ph_2SiH_2 (47 %), SiH_4 (47 %) and $PhSiH_2$-SiH_2Ph (6 %).[211]

NMR scale reaction of (ArN)Mo(SiH_2Ph)(η^3-NAr-SiHPh-H)(PMe_3) (III-1) with $PhSiD_3$

(ArN)Mo(SiH_2Ph)(η^3-NAr-SiHPh-H)(PMe_3) (**III-1**) (23.0 mg, 0.031 mmol) was dissolved in 0.6 ml of toluene-d_8 to give a clear brown solution. The ^1H-NMR spectrum of **III-1**, acquired at -50 °C, was carefully integrated. $PhSiD_3$ (3.85 µl, 0.031 mmol) was added at room temperature to a solution, and the reaction mixture was left at for 5 min. The extent of deuterium incorporation into each position was calculated from the difference of integration of the residual protons in the ^1H-NMR spectra recorded at -50 °C.

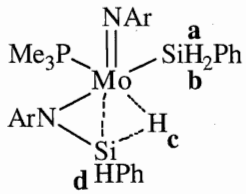

H position	H, %	D, %
A(b)	55	45
B(a)	55	45
c	54	46
d	58	42

NMR scale reaction of (ArN)Mo(SiH_2Ph)(η^3-NArSiH_2Ph)(PMe_3) (III-1) with (*m*-Tol)SiH_3

(*m*-Tol)SiH_3 (5.0 µl, 0.037 mmol) was added at room temperature to a solution of (ArN)Mo(SiH_2Ph)(η^3-NAr-SiHPh-H)(PMe_3) (**III-1**) (27.3 mg, 0.037 mmol) in 0.6 ml of C_6D_6 in an NMR tube. The reaction mixture was left at room temperature for 10 min. All volatiles were pumped off, and the residue was dried in vacuum and dissolved in toluene-

d_8. VT NMR spectra showed the formation of only one new product, (ArN)Mo{SiH_2(*m*-Tol)}(η^3-NAr-SiHPh-H)(PMe_3) (**III-1$_{tol}$**) (43 % by ^{1}H-NMR analysis), accompanied by the release of an equivalent of $PhSiH_3$, which was rationalized in terms of reversible silane addition to the electron deficient silanimine intermediate (ArN)Mo(η^2-NAr=SiHPh)(PMe_3) (**III-2**). No exchange with the agostic silicon centre was observed. *(ArN)Mo{SiH_2(m-Tol)}(η^3-NAr-SiHPh-H)(PMe_3)* (**III-1$_{tol}$**): ^{1}H-NMR (300 MHz; C_6D_6; δ, ppm): 8.14 (m, 2H, *o*-H, *m-Tol*SiH_2); 2.25 (s, 3H, *CH_3*, *m-Tol*SiH_2); all other signals are overlapping with those for starting material. $^{31}P\{^1H\}$-NMR (121.5 MHz; C_6D_6; δ, ppm): 10.5 (s, *P*Me_3). ^{1}H-NMR (600 MHz; C_6D_6; - 30 °C; δ, ppm): 8.45 (d, $^3J_{H\text{-}H}$ = 7.2 Hz, 2H, *o*-H, *m-Tol*SiH_2); 7.38 (d, $^3J_{H\text{-}H}$ = 7.8 Hz, 2H, *o*-H, *Ph*SiH); 6.12 (m, 1H, (Ar)NSi*H*Ph-H); 5.97 (bs, 1H, *m*-TolSi*H_2*); 5.64 (bs, 1H, *m*-TolSi*H_2*); 4.36 (m, 1H, (Ar)NSiHPh-*H*); 2.30 (s, 3H, *CH_3*, *m-Tol*SiH_2); all other signals are overlapping with those for starting material. $^{31}P\{^1H\}$-NMR (243 MHz; toluene-d_8; - 20 °C; δ, ppm): 12.2 (s, *P*Me_3).

NMR scale reaction of (ArN)Mo(SiH_2Ph)(η^3-$NArSiH_2Ph$)(PMe_3) (III-1) with H_2

Dihydrogen gas (~1.5 atm) was added *via* vacuum transfer to a solution of (ArN)Mo(SiH_2Ph)(η^3-$NArSiH_2Ph$)(PMe_3) (**III-1**) (15.7 mg, 0.021 mmol) in 0.6 ml of C_6D_6 in an NMR tube. No visual changes were observed after H_2 addition. The mixture was monitored with NMR spectroscopy for 24 h showing no reaction.

NMR scale reaction of (ArN)Mo(SiH_2Ph)(η^3-$NArSiH_2Ph$)(PMe_3) (III-1) with PMe_3

PMe_3 (2.3 µl, 0.022 mmol) was added in one portion at room temperature to a solution of (ArN)Mo(SiH_2Ph)(η^3-$NArSiH_2Ph$)(PMe_3) (**III-1**) (16.2 mg, 0.022 mmol) in 0.6 ml of C_6D_6 in an NMR tube. The reaction mixture was left at room temperature for 5 min. NMR analysis showed the formation of a mixture of the starting material and $(ArN)_2Mo(PMe_3)_3$ (**III-22**) (~ 1:1 ratio by $^{31}P\{^1H\}$-NMR analysis).

Reactions of $(RN)_2Mo(PMe_3)_{n\text{-}1}L$ with carbonyls

NMR scale generation of $(ArN)_2Mo(\eta^2\text{-}O{=}CMe_2)(PMe_3)$ (III-96)

Acetone (1.7 µl, 0.023 mmol) was added in one portion at room temperature to a solution of $(ArN)_2Mo(PMe_3)_3$ (**III-22**) (15.4 mg, 0.023 mmol) in 0.6 mL of C_6D_6 in an NMR tube.

The colour of the reaction mixture turned from dark-green to brown almost immediately. The mixture was left at room temperature for 5 min. NMR analysis showed the release of two equivalents of PMe_3 and formation of $(ArN)_2Mo(\eta^2\text{-}O{=}CMe_2)(PMe_3)$ (**III-93**). All volatiles were pumped off; the brown oily residue was dried in vacuum and redissolved in fresh C_6D_6. NMR spectra showed the presence of only $(ArN)_2Mo(\eta^2\text{-}O{=}CMe_2)(PMe_3)$ (**III-96**) in solution.

Preparation of $(ArN)_2Mo(\eta^1\text{-}O{=}CMePh)(PMe_3)$ (III-97)

A: NMR scale generation of III-97. Acetophenone (4.3 µl, 0.036 mmol) was added in one portion at room temperature to a solution of $(ArN)_2Mo(PMe_3)_3$ (**III-22**) (24.4 mg, 0.036 mmol) in 0.6 ml of C_6D_6 in an NMR tube. The colour of reaction mixture turned from dark-green to brown almost immediately. The reaction mixture was left at room temperature for 5 min. NMR spectra showed the formation of the only one product, $(ArN)_2Mo(\eta^1\text{-}O{=}CMePh)(PMe_3)$ (**III-97**), accompanied by the release of two equivalents of PMe_3. All volatiles were pumped off; the oily brown residue was dried in vacuum and redissolved in fresh C_6D_6. NMR spectra showed the presence of $(ArN)_2Mo(\eta^1\text{-}O{=}CMePh)(PMe_3)$ (**III-97**) only.

B: Preparative scale reaction. Acetophenone (90 µl, 0.76 mmol) was added in one portion at room temperature to a solution of $(ArN)_2Mo(PMe_3)_3$ (**III-22**) (515.2 mg, 0.76 mmol) in 40 ml of hexanes. The colour of the mixture changed from dark-green to brown almost immediately. The mixture was stirred at room temperature with N_2 purging for 20 min. All volatiles were pumped off to give an oily brown residue, which was dried in vacuum. The product was recrystallized from Hex/Et_2O (1/1) at -80 °C to give $(ArN)_2Mo(\eta^1\text{-}O{=}CMePh)(PMe_3)$ (**III-97**) as a brown solid. Yield: 201 mg, 41 %.

NMR scale reaction of $(ArN)_2Mo(\eta^1\text{-}O{=}CMePh)(PMe_3)$ (III-97) with $PhSiH_3$

A solution of $(ArN)_2Mo(\eta^1\text{-}O{=}CMePh)(PMe_3)$ (**III-97**) (21.9 mg, 0.034 mmol) in 0.5 ml of C_6D_6 was added at room temperature to a solution of $PhSiH_3$ (21.0 µl, 0.17 mmol) in 0.1 ml of C_6D_6 in an NMR tube. The reaction mixture was left at room temperature for 3 days. NMR analysis showed the release of the molecule of acetophenone and selective formation of the agostic complex $(ArN)Mo(SiH_2Ph)(\eta^3\text{-}NAr\text{-}SiHPh\text{-}H)(PMe_3)$ (**III-1**).

Formation of H_2, $PhSiH_2[OCH(Me)Ph]$,[215] and ethylbenzene was also observed by NMR spectroscopy.

NMR scale reaction of $(ArN)_2Mo(\eta^1$-O=CMePh)(PMe_3) (III-97) with acetophenone

Acetophenone (6.3 µl, 0.054 mmol) was added in one portion at room temperature to a solution of $(ArN)_2Mo(\eta^1$-O=CMePh)(PMe_3) (**III-97**) (6.9 mg, 0.011 mmol) in 0.6 ml of C_6D_6 in an NMR tube. The mixture was left at room temperature for 1 day showing no reaction. Heating the reaction mixture at 50 °C for 4 days leads to the stoichiometric transformation of the starting material (83 % conversion by $^{31}P\{^1H\}$-NMR analysis) to give $(ArN)_2Mo\{O$-C(Me)Ph-C(Me)Ph-O$\}(PMe_3)$ (**III-98**). ^{1}H-NMR (300 MHz; C_6D_6; δ, ppm): 7.89 (d, $^3J_{H-H}$ = 7.5 Hz, 2H, *o*-H, C*Ph*); 7.81 (d, $^3J_{H-H}$ = 7.5 Hz, 2H, *o*-H, C*Ph*); 7.34 (m, $^3J_{H-H}$ = 7.5 Hz, 4H, *m*-H, 2 C*Ph*); 6.88-7.24 (m, 8 H, *m*-H and *p*-H of 2 *Ar*N and *p*-H of 2 C*Ph*); 4.41 (sept, $^3J_{H-H}$ = 6.6 Hz, 2H, 2 *CH*, *Ar*N); 3.80 (sept, $^3J_{H-H}$ = 6.9 Hz, 2H, 2 *CH*, *Ar*N); 2.00 (s, 3H, C*Me*); 1.67 (s, 3H, C*Me*); 1.31 (d, $^3J_{H-H}$ = 6.6 Hz, 6H, 2 CH_3, *Ar*N); 1.25 (d, $^3J_{H-H}$ = 6.9 Hz, 6H, 2 CH_3, *Ar*N); 1.16 (m, 12H, 4 CH_3, *Ar*N); 1.05 (d, $^2J_{H-P}$ = 10.2 Hz, 9H, PMe_3). $^{31}P\{^1H\}$-NMR (121.5 MHz; C_6D_6; δ, ppm): 4.6 (s, *P*Me_3).

NMR scale generation of $(ArN)_2Mo(\eta^2$-O=CHPh)(PMe_3) (III-100)

Benzaldehyde (6.1 µl, 0.06 mmol) was added in one portion at room temperature to a solution of $(ArN)_2Mo(PMe_3)_3$ (**III-22**) (40.1 mg, 0.06 mmol) in 0.6 ml of C_6D_6 in an NMR tube. After addition of benzaldehyde, the colour of the reaction mixture turned from dark-green to brown almost immediately. The reaction mixture was left at room temperature for 10 min. NMR analysis showed the formation of only one complex, $(ArN)_2Mo(\eta^2$-O=CHPh)(PMe_3) (**III-100**), and release of two equivalents of PMe_3. All volatiles were pumped off; the oily brown residue was dried in vacuum and redissolved in fresh C_6D_6. NMR spectra showed the presence of only $(ArN)_2Mo(\eta^2$-O=CHPh)(PMe_3) (**III-100**) in solution. The same product can be also obtained by reaction of $(ArN)_2Mo(\eta^2$-CH_2=$CH_2)(PMe_3)$ (**III-31**) with benzaldehyde (15 min at room temperature). ^{1}H-NMR (300 MHz; C_6D_6; δ, ppm): 7.54 (d, $^3J_{H-H}$ = 7.5 Hz, 2H, *o*-H, η^2-O=CH*Ph*); 7.19 (t, $^3J_{H-H}$ = 7.8 Hz, 2H, *m*-H, η^2-O=CH*Ph*); 7.06 (m, 3H, *p*-H, η^2-O=CH*Ph* and N*Ar*); 6.89 (m, 4H, *m*-H, N*Ar*); 5.69 (s, 1H, η^2-O=C*H*Ph); 3.91 (sept, $^3J_{H-H}$ = 6.9 Hz, 2H, 2*CH*, N*Ar*); 3.45 (sept, $^3J_{H-H}$ = 6.9 Hz, 2H, 2*CH*, N*Ar*); 1.24 (m, $^3J_{H-H}$ = 6.9 Hz, 12H, 4CH_3, N*Ar*; $^2J_{H-P}$ =

6.6 Hz, 9H, P*Me*$_3$); 1.03 (d, $^3J_{H-H}$ = 6.9 Hz, 12H, N*Ar*). $^{31}P\{^1H\}$-NMR (121.5 MHz; C_6D_6; δ, ppm): 8.6 (s, *P*Me$_3$). $^{13}C\{^1H\}$-NMR (75.5 MHz; C_6D_6; δ, ppm): 13.3 (d, $^1J_{C-P}$ = 29.4 Hz, P*Me*$_3$); 23.3 (s); 23.5 (s); 23.8 (s); 24.0 (s); 79.0 (s, *CH*, η^2-O=C*H*Ph); 122.3 (s, *m*-C, N*Ar*); 122.5 (s, *m*-C, N*Ar*); 124.0 (s, *p*-C, N*Ar*); 124.3 (s, *o*-C, η^2-O=CH*Ph*); 125.6 (s, *p*-C, N*Ar*); 128.2 (s, *m*-C, η^2-O=CH*Ph*); 141.4 (s, *o*-C, N*Ar*); 141.8 (s, *o*-C, N*Ar*); 148.7 (s, *i*-C, η^2-O=CH*Ph*); 153.7 (s, *i*-C, N*Ar*); 153.9 (s, *i*-C, N*Ar*); *p*-C of η^2-O=CH*Ph* ligand is overlapping with signals from the solvent. IR (nujol): 1597 cm^{-1} (O=C).

NMR scale reaction of (ArN)$_2$Mo(η^2-O=CHPh)(PMe$_3$) (III-100) with PhSiH$_3$

PhSiH$_3$ (37.0 μl, 0.3 mmol) was added in one portion at room temperature to a solution of (ArN)$_2$Mo(η^2-O=CHPh)(PMe$_3$) (**III-100**) (37.3 mg, 0.06 mmol) in 0.6 ml of C_6D_6 in an NMR tube. The reaction was left at room temperature 2 days. NMR analysis showed selective formation of (ArN)Mo(SiH$_2$Ph)(η^3-NAr-SiHPh-H)(PMe$_3$) (**III-1**). Production of H_2, toluene, PhH$_2$Si(OBn), and PhHSi(OBn)$_2$[160, 214, 215b] was also observed by NMR spectroscopy.

NMR scale reaction of (ArN)$_2$Mo(η^1-O=CMePh)(PMe$_3$) (III-97) with benzaldehyde

Benzaldehyde (2.5 μl, 0.025 mmol) was added in one portion at room temperature to a solution of (ArN)$_2$Mo(η^1-O=CMePh)(PMe$_3$) (**III-97**) (15.9 mg, 0.025 mmol) in 0.6 ml of C_6D_6 in an NMR tube. The reaction mixture was left at room temperature for 2.5 weeks. NMR analysis showed full conversion of the acetophenone adduct **III-97** to (ArN)$_2$Mo(η^2-O=CHPh)(PMe$_3$) (**III-100**).

NMR scale reaction of (ArN)$_2$Mo(η^2-CH$_2$=CH$_2$)(PMe$_3$)$_2$ (III-31) with benzaldehyde

A solution of (ArN)$_2$Mo(η^2-CH$_2$=CH$_2$)(PMe$_3$)$_2$ (**III-31**) (32.2 mg, 0.051 mmol) in 0.6 ml of C_6D_6 was added at room temperature to solid BPh$_3$ (12.4 mg, 0.051 mmol). The colour of the solution changed from purple to yellow-orange almost immediately, and the mixture was transferred to an NMR tube and left at room temperature for additinoal 5 min. NMR analysis showed selective formation of Ph$_3$B·PMe$_3$ and (ArN)$_2$Mo(η^2-CH$_2$=CH$_2$)(PMe$_3$) (**III-101**). Benzaldehyde (6.5 μl, 0.064 mmol) was added in one portion at room temperature to the NMR tube. The colour of the solution turned to brown. The reaction mixture was left at room temperature for 1 day showing release of ethylene

and formation of a mixture of the starting material **III-101** and $(ArN)_2Mo(\eta^2$-O=C(Ph)OBn)(PMe_3) (**III-103**) (ratio is 1:3, respectively, according to the $^{31}P\{^1H\}$-NMR spectrum).

$(ArN)_2Mo(\eta^2$-CH_2=$CH_2)(PMe_3)$ (**III-101**): ^{1}H-NMR (300 MHz; C_6D_6; δ, ppm): 1.07 (d, $^2J_{H\text{-}P}$ = 9.0 Hz, 9H, P*Me*$_3$); 1.25 (dd, $^3J_{H\text{-}H}$ = 6.9 Hz, 24H, 8 *CH*$_3$, 2 N*Ar*); 1.70 (bq, $J_{H\text{-}H}$ = 9.6 Hz; $^3J_{H\text{-}P}$ = 21.6 Hz, 2H, η^1-*C*$_2$*H*$_4$); 2.60 (dd, $J_{H\text{-}H}$ = 12.0 Hz; $^3J_{H\text{-}P}$ = 24.0 Hz, 2H, η^1-*C*$_2$*H*$_4$); 3.90 (sept, $^3J_{H\text{-}H}$ = 6.9 Hz, 4H, 4 *CH*; 2 N*Ar*); 7.02 (m, 6H, *p*-H and *m*-H, 2 N*Ar*). $^{31}P\{^1H\}$-NMR (121.5 MHz; C_6D_6; δ, ppm): 20.3 (s, *P*Me$_3$).

$(ArN)_2Mo(\eta^2$-O=C(Ph)OCH_2Ph)(PMe$_3$) (**III-103**): ^{1}H-NMR (300 MHz; C_6D_6; δ, ppm): 7.98 (m, 2H, *o*-H, C*Ph*); 7.66 (m, 2H, *o*-H, C*Ph*); 6.77-7.35 (m, 12 H, *m*-H and *p*-H of 2 *Ar*N and *m*-H and *p*-H of 2 C*Ph*); 5.07 (dd, $^2J_{H\text{-}H}$ = 16.2 Hz, 2H, O*CH*$_2$Ph); 3.91 (sept, $^3J_{H\text{-}H}$ = 6.9 Hz, 2H, 2 *CH*, *Ar*N); 3.72 (sept, $^3J_{H\text{-}H}$ = 6.9 Hz, 2H, 2 *CH*, *Ar*N); 1.40 (d, $^3J_{H\text{-}H}$ = 6.9 Hz, 3H, *CH*$_3$, *Ar*N); 1.33 (d, $^3J_{H\text{-}H}$ = 6.9 Hz, 3H, *CH*$_3$, *Ar*N); 1.16 (d, $^2J_{H\text{-}P}$ = 8.7 Hz, 9H, P*Me*$_3$); 1.14 (obscured by PMe_3 signal; found by ^{1}H-^{1}H COSY, 3H, *CH*$_3$, *Ar*N); 1.01 (d, $^3J_{H\text{-}H}$ = 6.9 Hz, 3H, *CH*$_3$, *Ar*N); 0.97 (d, $^3J_{H\text{-}H}$ = 6.9 Hz, 3H, *CH*$_3$, *Ar*N); 0.88 (d, $^3J_{H\text{-}H}$ = 6.9 Hz, 3H, *CH*$_3$, *Ar*N); 0.84 (d, $^3J_{H\text{-}H}$ = 6.9 Hz, 3H, *CH*$_3$, *Ar*N); 0.73 (d, $^3J_{H\text{-}H}$ = 6.9 Hz, 3H, *CH*$_3$, *Ar*N). $^{31}P\{^1H\}$-NMR (121.5 MHz; C_6D_6; δ, ppm): 8.2 (s, *P*Me$_3$).

Stoichiometric reactivity of imido (vinylsilyl)amide complexes

Preparation of (ArN)Mo(H)(η^3-NAr-SiHPh-CH=CH_2)(PMe_3) (III-112)

A: NMR scale reaction of (ArN)Mo(Et)(η^3-NAr-SiHPh-CH=CH_2)(PMe_3) (III-3) with $PhSiH_3$. $PhSiH_3$ (39.6 µl, 0.321 mmol) was added in one portion at room temperature to a solution of (ArN)Mo(Et)(η^3-NAr-SiHPh-CH=CH_2)(PMe_3) (**III-3**) (11.0 mg, 0.016 mmol) in 0.6 ml of C_6D_6 in an NMR tube. The reaction mixture was left at room temperature for 2 days. NMR analysis showed only a 17 % conversion of the starting material to form (ArN)Mo(H)(η^3-NAr-SiHPh-CH=CH_2)(PMe_3) (**III-112**).

B: NMR scale reaction of III-3 with $PhSiH_3$ and PMe_3. $PhSiH_3$ (3.5 µl, 0.028 mmol) and PMe_3 (2.8 µl, 0.027 mmol) were added at room temperature to a solution of (ArN)Mo(Et)(η^3-NAr-SiHPh-CH=CH_2)(PMe_3) (**III-3**) (18.4 mg, 0.027 mmol) in 0.6 ml of C_6D_6 in an NMR tube. After 10 min at room temperature NMR analysis showed no reaction and the mixture was heated overnight at 50 °C. During this time the colour

turned to another tint of brown and NMR spectra showed the selective formation of the hydride derivative, (ArN)Mo(H)(η^3-NAr-SiHPh-CH=CH_2)(PMe_3) (**III-112**), and $PhEtSiH_2$.[202] Redistribution of $PhSiH_3$ to give Ph_2SiH_2 and SiH_4 was also observed.[211]

C: NMR scale reaction of III-3 with $PhMeSiH_2$ and PMe_3. $PhMeSiH_2$ (4.8 µl, 0.035 mmol) and PMe_3 (3.6 µl, 0.035 mmol) were added at room temperature to a solution of (ArN)Mo(Et)(η^3-NAr-SiHPh-CH=CH_2)(PMe_3) (**III-3**) (24.0 mg, 0.035 mmol) in 0.6 ml of C_6D_6 in an NMR tube. After 10 min at room temperature NMR analysis showed no reaction and the mixture was heated overnight at 50 °C. During this time the colour turned to another tint of brown and NMR spectra showed the selective formation of the hydride derivative, (ArN)Mo(H)(η^3-NAr-SiHPh-CH=CH_2)(PMe_3) (**III-112**), and PhMeEtSiH.

D: NMR scale reaction of III-3 with H_2. Hydrogen gas was added *via* vacuum transfer to a frozen solution of (ArN)Mo(Et)(η^3-NAr-SiHPh-CH=CH_2)(PMe_3) (**III-3**) (16.1 mg, 0.024 mmol) in 0.6 ml of C_6D_6 in an NMR tube. The mixture was warmed up to room temperature and left for 30 min. showing no reaction. The reaction mixture was heated at 50 °C for 36 hours. NMR analysis showed full conversion of the starting complex to form (ArN)Mo(H)(η^3-NAr-SiHPh-CH=CH_2)(PMe_3) (**III-112**) (67 % yield, according to $^{31}P\{^1H\}$-NMR), ethane and unidentified decomposition products. Traces of $ArNH_2$ were also observed by NMR spectroscopy.

E: Preparative scale reaction. PMe_3 (6.7 µl, 0.064 mmol) and $PhSiH_3$ (8.0 µl, 0.064 mmol) were added at room temperature to a solution of (ArN)Mo(Et)(η^3-NAr-SiHPh-CH=CH_2)(PMe_3) (**III-3**) (44.1 mg, 0.064 mmol) in 10 ml of toluene. The reaction mixture was left overnight at 50 °C. All volatiles were pumped off; the residue was dried and extracted with 15 ml of hexanes. The solvent was removed in vacuum to give an oily brown residue of (ArN)Mo(H)(η^3-NAr-SiHPh-CH=CH_2)(PMe_3) (**III-112**). Yield: 28.0 mg, 66 %. ^{1}H-NMR (300 MHz; C_6D_6; δ, ppm): 7.60 (m, 2H, *o*-H, Si*Ph*); 6.87-7.10 (m, 9H, *m*-H and *p*-H of N*Ar* and Si*Ph*); 6.62 (s, 1H, Si*H*); 4.53 (dd, $^3J_{H\text{-}H}$ = 5.1 Hz, 12.6 Hz, 1H, H_2C=CHSi); 4.43 (dd, $^3J_{H\text{-}H}$ = 5.1 Hz, 15.3 Hz, 1H, H_2C=CHSi); 4.08 (sept, $^3J_{H\text{-}H}$ = 6.6 Hz, 1H, *CH*, N*Ar*); 3.82 (sept, $^3J_{H\text{-}H}$ = 6.9 Hz, 2H, 2*CH*, N*Ar*); 2.69 (d, $^2J_{H\text{-}P}$ = 41.7 Hz, 1H, Mo-*H*); 2.50 (m, 1H, *CH*, N*Ar*); 2.49 (dd, $^3J_{H\text{-}H}$ = 12.6 Hz and 15.3 Hz, 1H, H_2C=*CH*Si); 1.57 (d, $^3J_{H\text{-}H}$ = 6.6 Hz, 3H, CH_3, N*Ar*); 1.43 (d, $^3J_{H\text{-}H}$ = 6.9 Hz, 3H, CH_3,

NAr); 1.31 (d, $^3J_{H-H}$ = 6.6 Hz, 12H, 4CH_3, NAr); 0.98 (d, $^3J_{H-H}$ = 6.9 Hz, 3H, CH_3, NAr); 0.80 (d, $^2J_{P-H}$ = 7.8 Hz, 9H, PMe_3); 0.41 (d, $^3J_{H-H}$ = 6.9 Hz, 3H, CH_3, NAr). $^{31}P\{^1H\}$-NMR (121.5 MHz; C_6D_6; δ, ppm): -15.6 (s, PMe_3). $^{13}C\{^1H\}$-NMR (75.5 MHz; C_6D_6; 297 K; δ, ppm): 17.8 (d, $^1J_{C-P}$ = 21.9 Hz, PMe_3); 23.7 (s, CH_3, NAr); 24.2 (s, CH_3, NAr); 25.5 (s, CH_3, NAr); 26.2 (s, CH_3, NAr); 27.3 (s, CH, NAr); 27.6 (s, CH, NAr); 28.2 (s, CH, NAr); 28.8 (s, CH_3, NAr); 39.7 (d, J_{C-P} = 6.8 Hz, SiCH=CH_2); 63.0 (d, J_{C-P} = 5.3 Hz, SiCH=CH_2); 123.2 (s, *p*-C, Si*Ph*); 123.3, 123.7, 123.6 (s, *m*-C and *p*-C, NAr); 127.4 (s, *m*-C, NAr); 129.7 (s, *m*-C, Si*Ph*); 140.65 (s, *o*-C, NAr); 140.7 (s, *o*-C, NAr), 140.9 (s, *o*-C, NAr); 141.0 (s, *o*-C, Si*Ph*); 142.5 (s, *o*-C, NAr); 151.0 (s, *i*-C, Si*Ph*); 151.8 (s, *i*-C, NAr); 156.1 (s, *i*-C, NAr). ^{29}Si INEPT+ NMR (59.6 MHz; C_6D_6; J = 200 Hz; δ, ppm): -27.7 (d, $^1J_{Si-H}$ = 204.9 Hz, *Si*H). IR (nujol): 2098 cm^{-1} (Si-H); 1796 cm^{-1} (Mo-H).

NMR scale reaction of (ArN)Mo(Et)(η^3-NAr-SiHPh-CH=CH_2)(PMe_3) (III-3) with $PhSiD_3$

$PhSiD_3$ (3.4 μl, 0.028 mmol) was added at room temperature to a solution of (ArN)Mo(Et)(η^3-NAr-SiHPh-CH=CH_2)(PMe_3) (**III-3**) (18.8 mg, 0.028 mmol) in 0.6 ml of C_6D_6 in an NMR tube. The reaction mixture was left at 50 °C overnight. All volatiles were pumped off; the residue was dried and redissolved in C_6D_6. NMR analysis showed the formation of (ArN)Mo(D)(η^3-NAr-SiHPh-CH=CH_2)(PMe_3) (**III-112$_D$**). The spectral data of the product are similar to those for **III-112** except the Mo*H* resonance, which was not observed in the ^{1}H-NMR spectrum of **III-112$_D$** due to full substitution with deuterium.

NMR scale reaction of (ArN)Mo(Et)(η^3-NAr-SiHPh-CH=CH_2)(PMe_3) (III-3) with $PhSiH_3$ and BPh_3

A solution of (ArN)Mo(Et)(η^3-NAr-SiHPh-CH=CH_2)(PMe_3) (**III-3**) (20.8 mg, 0.030 mmol) and $PhSiH_3$ (3.8 μl, 0.030 mmol) in 0.6 ml of toluene-d_8 was added in one portion at room temperature to solid BPh_3 (7.4 mg, 0.030 mmol). The mixture was immediately transferred to an NMR tube and was monitored by NMR spectroscopy at room temperature for 1 h until all starting material was consumed. NMR spectra showed the formation of $Ph_3B{\cdot}PMe_3$ adduct and the only one highly fluxional at room temperature molybdenum containing product, (ArN)Mo(SiH_2Ph)(η^3-NAr-Si(Et)Ph-H)(η^2-CH_2=CH_2)

(**III-113**). The structure of the product was suggested by NMR and IR analysis. All attempts to isolate **III-113** led to full decomposition presumably due to instability of the product in vacuum. In solution the product is stable at ambient temperature in inert gas atmosphere for a week. ^{1}H-NMR (300 MHz; toluene-d_8; δ, ppm): 7.82 (d, $^{3}J_{H\text{-}H}$ = 7.5 Hz, 2H, *o*-H, SiH_2*Ph*); 7.38 (d, $^{3}J_{H\text{-}H}$ = 7.8 Hz, 2H, *o*-H, η^3-NAr-Si(Et)*Ph*-H); 6.89-7.32 (overlapping with residual toulene-d_8 signals multiplet, 12H, *m*-H and *p*-H of N*Ar*, SiH_2*Ph* and η^3-NAr-Si(Et)*Ph*-H); 6.00 (s, 2H, SiH_2Ph, found by ^{1}H-^{29}Si HSQC with *J* = 200 Hz); 4.32 (bs, 1H, η^3-NAr-Si(Et)Ph-*H*, found by ^{1}H-^{29}Si HSQC with *J* = 7 Hz); 3.80 (sept, $^{3}J_{H\text{-}H}$ = 6.9 Hz, 2H, 2*CH*, N*Ar*); 3.16 (m, 1H, η^2-C_2H_4, found by ^{1}H-^{13}C HSQC); 3.05 (sept, $^{3}J_{H\text{-}H}$ = 6.9 Hz, 1H, *CH*, N*Ar*); 2.79 (m, 3H, 2H of η^2-C_2H_4 (found by ^{1}H-^{12}C HSQC) and 1*CH* of N*Ar*); 1.57 (m, 1H, η^2-C_2H_4, found by ^{1}H-^{13}C HSQC); 1.23 (m, 3H, CH_3, Si*Et*); 1.20 (d, $^{3}J_{H\text{-}H}$ = 6.9 Hz, 6H, 2CH_3, N*Ar*); 1.14 (d, $^{3}J_{H\text{-}H}$ = 6.9 Hz, 3H, CH_3, N*Ar*); 1.11 (d, $^{3}J_{H\text{-}H}$ = 6.9 Hz, 3H, CH_3, N*Ar*); 1.04 (d, $^{3}J_{H\text{-}H}$ = 6.9 Hz, 3H, 1CH_3, N*Ar*); 1.01 (d, $^{3}J_{H\text{-}H}$ = 6.9 Hz, 6H, 2CH_3, N*Ar*); 0.86 (m, 2H, CH_2, Si*Et*); 0.39 (d, $^{3}J_{H\text{-}H}$ = 6.9 Hz, 3H, CH_3, N*Ar*). ^{1}H-NMR (600 MHz; -53 °C; toluene-d_8; δ, ppm): 8.09 (broad signal, 2H, *o*-H, SiH_2*Ph*); 7.46 (d, $^{3}J_{H\text{-}H}$ = 7.2 Hz, 2H, *o*-H, η^3-NAr-Si(Et)*Ph*-H); 6.83-7.39 (overlapping with residual toulene-d_8 signals multiplet, 10H, *m*-H and *p*-H of N*Ar* and SiH_2*Ph*; *p*-H of η^3-NAr-Si(Et)*Ph*-H); 7.34 (t, $^{3}J_{H\text{-}H}$ = 7.2 Hz, 2H, *m*-H, η^3-NAr-Si(Et)*Ph*-H); 6.07 (s, 1H, SiH_2Ph); 5.75 (s, 1H, SiH_2Ph); 4.99 (s, 1H, SiH_2Ph); 4.21 (broad signal, 2H, 2*CH*, N*Ar*); 3.42 (bm, 1H, η^2-C_2H_4); 3.24 (m, 2H, 1H of η^2-C_2H_4 and *CH* of N*Ar*); 3.13 (bm, 1H, η^2-C_2H_4); 3.38 (bm, 1H, *CH*, N*Ar*); 1.84 (bm 1H, η^2-C_2H_4); 1.29 (bm, 8H, CH_2 of Si*Et* and 2CH_3 or N*Ar*); 1.20 (broad signal, 3H, CH_3, N*Ar*); 1.13 (broad signal, 3H, CH_3, N*Ar*); 1.07 (broad signal, 6H, 2CH_3, N*Ar*); 0.97 (t, $^{3}J_{H\text{-}H}$ = 7.2 Hz, 3H, CH_3, Si*Et*); 0.93 (bm, 3H, CH_3, N*Ar*); 0.35 (bd, $^{3}J_{H\text{-}H}$ = 6.9 Hz, 3H, CH_3, N*Ar*). ^{13}C{^{1}H}-NMR (75.5 MHz; C_6D_6; 298 K; δ, ppm): 153.6 (s, *i*-C, N*Ar*); 144.6 (s, *o*-C, N*Ar*); 143.3 (s, *i*-C, N*Ar*); 142.0 and 141.7 (singlets, *i*-C of SiH_2*Ph* and η^3-NAr-Si(Et)*Ph*-H); 138.6 (s, *o*-C, N*Ar*); 135.6 (s, *o*-C, SiH_2*Ph*); 135.4 (s, *o*-C, η^3-NAr-Si(Et)*Ph*-H); 131.1 (s, *m*-C, η^3-NAr-Si(Et)*Ph*-H); 130.7 (s, *m*-C, SiH_2*Ph*); 127.5, 126.4, 123.8, 123.7, 122.8 (singlets, *p*-C of SiH_2*Ph* and η^3-NAr-Si(Et)*Ph*-H; *m*-C and *p*-C of N*Ar*); 51.2 (s, η^2-C_2H_4); 44.0 (s, η^2-C_2H_4); 28.33 (bs, 2*CH*, N*Ar*); 28.28 (s, *CH*, N*Ar*); 27.5 (s, *CH*, N*Ar*); 25.0 (s, CH_3, N*Ar*); 24.8 (s, CH_3, N*Ar*); 24.6 (s, CH_3, N*Ar*); 24.1 (s, 2CH_3, N*Ar*); 23.5 (s, 2CH_3, N*Ar*); 22.7

(s, *CH*$_3$, NA*r*); 14.0 (s, *CH*$_3$, Si*Et*); 7.4 (s, *CH*$_2$, Si*Et*). ^{1}H-^{29}Si HSQC JC (600 MHz; -56 °C; toluene-d$_8$; ^{1}H projection; δ, ppm): 6.11 (d, $^1J_{Si-H}$ = 201.8 Hz, 1H, Si*H*$_2$Ph); 5.82 (d, $^1J_{Si-H}$ = 194.5 Hz, 1H, Si*H*$_2$Ph); 5.03 (d, $^1J_{Si-H}$ = 104.7 Hz, 1H, η^3-NAr-Si(Et)Ph-*H*). ^{29}Si INEPT+ NMR (119.2 MHz; -56 °C; toluene-d$_8$; *J* = 100 Hz; δ, ppm): -0.9 (t, $^1J_{Si-H}$ = 173.0 Hz, 163.4 Hz, *Si*H$_2$Ph); -64.4 (d, $^1J_{Si-H}$ = 107.3 Hz, η^3-NAr-*Si*(Et)Ph-H). IR (nujol): 2077 cm^{-1} (broad, intensive, Si-H of SiH$_2$Ph); 1772 cm^{-1} (broad, weak, Si-H of η^3-NAr-Si(Et)Ph-H).

NMR scale reaction of (ArN)Mo(Et)(η^3-NAr-SiHPh-CH=CH$_2$)(PMe$_3$) (III-3) with PhSiD$_3$ and BPh$_3$

The reaction was done analogously to the transformation with PhSiH$_3$ described above. Treatment of (ArN)Mo(Et)(η^3-NAr-SiHPh-CH=CH$_2$)(PMe$_3$) (**III-3**) (16.2 mg, 0.024 mmol) with PhSiD$_3$ (2.9 µl, 0.024 mmol) in the presence of one equivalent of BPh$_3$ (5.7 mg, 0.024 mmol) leads to the formation of the deuterated derivative (ArN)Mo(SiD$_2$Ph)(η^3-NAr-Si(Et$_d$)Ph-H)(η^2-CH$_2$=CH$_2$) (**III-113$_D$**). The presence of the proton in the agostic position was confirmed by the ^{1}H-NMR spectrum at -50 °C in toluene-d$_8$. ^{1}H-NMR analysis also showed ~30 % of H for both Si*H* signals in the silyl substituent (the ratio H/D was found by integration of Si*H* signals in the ^{1}H NMR spectrum). Apart from the Si*D* signal of the silyl Si*D*$_2$Ph ligand, the ^{2}D-NMR spectrum registered at room temperature in toluene-h$_8$ showed the presence of deuterium also in methylene and methyl positions of ethyl substituent at agostic silicon centre. ^{2}D-NMR (92.1 MHz; toluene-h$_8$, δ, ppm): 5.74 (bs, Si*D*$_2$Ph); 1.04 (bs, methyl of Si*Et*); 0.79 (bs, methylene of Si*Et*).

NMR scale reaction of (ArN)Mo(SiH$_2$Ph)(η^3-NAr-Si(Et)Ph-H)(η^2-CH$_2$=CH$_2$) (III-113) with PMe$_3$

PMe$_3$ (3.1 µl, 0.03 mmol) was added in one portion at room temperature to a solution of (ArN)Mo(SiH$_2$Ph)(η^3-NAr-Si(Et)Ph-H)(η^2-CH$_2$=CH$_2$) (**III-113**) (prepared *in situ* by the treatment of (ArN)Mo(Et)(η^3-NAr-SiHPh-CH=CH$_2$)(PMe$_3$) (**III-3**) (20.8 mg, 0.030 mmol) with PhSiH$_3$ (3.8 µl, 0.030 mmol) in the presence of BPh$_3$ (7.4 mg, 0.030 mmol)) in 0.6 ml of C$_6$D$_6$ in an NMR tube. The mixture was left at room temperature for 5 min. NMR analysis showed the release of ethylene and selective formation of

(ArN)Mo(SiH_2Ph)(η^3-NAr-Si(Et)Ph-H)(PMe_3) (**III-114**) as a mixture of two isomers (2:1 ratio, according to the $^{31}P\{^1H\}$-NMR spectrum), depending on the orientation of the Ph and Et substituents at the agostic silicon centre. ^{1}H-NMR (300 MHz; C_6D_6; δ, ppm): 8.39 (d, $^3J_{H\text{-}H}$ = 7.2 Hz, 2H, *o*-H, SiH_2*Ph*, major isomer); 8.24 (d, $^3J_{H\text{-}H}$ = 6.9 Hz, 2H, *o*-H, SiH_2*Ph*, minor isomer); 6.89-7.54 (m overlapping with the residual C_6D_6 signal, 14H for each isomer, *m*-H and *p*-H of N*Ar* ligands, *m*-H and *p*-H of SiH_2*Ph*, and *o*-H, *m*-H, *p*-H of η^3-NAr-Si(Et)*Ph*-H); 5.92 (bs, 1H, Si*H*$_2$Ph, major isomer); 5.88 (bs, 1H, Si*H*$_2$Ph, minor isomer); 5.62 (bs, 1H, Si*H*$_2$Ph, major isomer); 5.49 (bs, 1H, Si*H*$_2$Ph, minor isomer); 4.20 (m, 2H, 2*CH*, N*Ar*, minor isomer); 4.11 (sept, $^3J_{H\text{-}H}$ = 6.9 Hz, 2H, 2*CH*, N*Ar*, major isomer); 3.97 (broad dd, $^3J_{H\text{-}H}$ = 4.8 Hz, $^2J_{H\text{-}P}$ = 12.9 Hz, 1H, η^3-NAr-Si(Et)Ph-*H*, major isomer (found by ^{1}H-^{31}P HSQC NMR with *J* = 5 Hz and ^{1}H-^{29}Si HSQC NMR with *J* = 100 Hz)); 3.59 (m, overlapping signals of *CH*, N*Ar* of major isomer and η^3-NAr-Si(Et)Ph-*H* of minor isomer (found by ^{1}H-^{31}P HSQC NMR with *J* = 5 Hz and ^{1}H-^{29}Si HSQC NMR with *J* = 100 Hz)); 3.00 (m, 2H, 2*CH*, N*Ar*, minor isomer); 2.58 (sept, $^3J_{H\text{-}H}$ = 6.6 Hz, 1H, *CH*, N*Ar*, major isomer); 1.39 (d, $^3J_{H\text{-}H}$ = 6.9 Hz, 3H, CH_3, N*Ar*, major isomer); 1.34 (d, $^3J_{H\text{-}H}$ = 6.9 Hz, 3H, CH_3, N*Ar*, minor isomer); 1.26 (d, $^3J_{H\text{-}H}$ = 6.9 Hz, 6H, 2CH_3, N*Ar*, major isomer); 1.22 (d, $^3J_{H\text{-}H}$ = 6.9 Hz, 6H, 2CH_3, N*Ar*, minor isomer); 1.50 (m, overlapping signals for both isomers, 12H (4CH_3) of N*Ar* of major isomer, 3H (CH_3) of N*Ar* of minor isomer, 5H of Si*Et* for both major and minor isomers (found by ^{1}H-^{1}H COSY NMR)); 1.11 (d, $^3J_{H\text{-}H}$ = 8.4 Hz, 9H, PMe_3, minor isomer); 1.05 (d, $^3J_{H\text{-}H}$ = 8.7 Hz, 9H, PMe_3, major isomer); 1.01 (m, 3H, CH_3, N*Ar*, minor isomer); 0.30 (d, $^3J_{H\text{-}H}$ = 6.9 Hz, 3H, CH_3, N*Ar*, minor isomer); 0.08 (d, $^3J_{H\text{-}H}$ = 6.6 Hz, 3H, CH_3, N*Ar*, major isomer). $^1H\{^{31}P\}$-NMR (300 MHz; C_6D_6; δ, ppm; selected resonances): 5.92 (d, $^2J_{H\text{-}H}$ = 2.7 Hz, 1H, Si*H*$_2$Ph, major isomer); 5.88 (d, $^2J_{H\text{-}H}$ = 1.8 Hz, 1H, Si*H*$_2$Ph, minor isomer); 5.62 (d, $^2J_{H\text{-}H}$ = 2.7 Hz, 1H, Si*H*$_2$Ph, major isomer); 5.49 (d, $^2J_{H\text{-}H}$ = 1.8 Hz, 1H, Si*H*$_2$Ph, minor isomer); 3.97 (d, $^3J_{H\text{-}H}$ = 4.8 Hz, 1H, η^3-NAr-Si(Et)Ph-*H*, major isomer); 1.12 (s, 9H, PMe_3, minor isomer); 1.03 (s, 9H, PMe_3, major isomer). $^{31}P\{^1H\}$-NMR (121.5 MHz; C_6D_6; δ, ppm): 8.4 (s, PMe_3, minor isomer); 7.4 (s, PMe_3, major isomer). ^{1}H-^{29}Si HSQC NMR (119.2 MHz; *J* = 200 Hz; toluene-d_8; -50 °C; ^{29}Si projection; δ, ppm): 3.1 (*Si*H_2Ph, minor isomer); 4.0 (*Si*H_2Ph, major isomer). ^{1}H-^{29}Si HSQC NMR (119.2 MHz; *J* = 100 Hz; toluene-d_8; -50 °C; ^{29}Si projection; δ, ppm): -53.3 (η^3-NAr-

Si(Et)Ph-H, major isomer); -55.0 (η^3-NAr-*Si*(Et)Ph-H, minor isomer). ^{1}H-^{29}Si HSQC JC NMR (600 MHz; J = 100 Hz; toluene-d_8; -14 °C; ^{1}H projection; δ, ppm): 3.68 (dd, 1H, $^1J_{H\text{-}Si}$ = 107.1 Hz, $^2J_{H\text{-}P}$ = 10.7 Hz, η^3-NAr-Si(Et)Ph-*H*, minor isomer); 4.10 (dd, 1H, $^1J_{H\text{-}Si}$ = 105.4 Hz, $^2J_{H\text{-}P}$ = 11.6 Hz, η^3-NAr-Si(Et)Ph-*H*, major isomer); 5.48 (d, $^1J_{H\text{-}Si}$ = 156.1 Hz, 1H, Si*H*$_2$Ph, minor isomer); 5.66 (d, $^1J_{H\text{-}Si}$ = 150.1 Hz, 1H, Si*H*$_2$Ph, major isomer); 5.89 (d, $^1J_{H\text{-}Si}$ = 168.1 Hz, 1H, Si*H*$_2$Ph, minor isomer); 5.92 (d, $^1J_{H\text{-}Si}$ = 168.1 Hz, 1H, Si*H*$_2$Ph, major isomer). ^{13}C{^{1}H}-NMR (150.9 MHz; toluene-d_8; -12 °C δ, ppm; chemical shifts for both isomers): 153.5, 149.2, 144.9, 144.2, 143.8, 142.9, 141.7, 141.1, 141.0, 140.4 (s, aromatic quaternary carbons for both isomers); 137.0 (s, *o*-C, SiH$_2$*Ph*, major isomer); 136.0 (s, *o*-C, SiH$_2$*Ph*, minor isomer); 135.9 (s, *o*-C, η^3-NAr-Si(Et)*Ph*-H, major isomer); 135.8 (s, *o*-C, η^3-NAr-Si(Et)*Ph*-H, major isomer); 130.3 (s, *m*-H, SiH$_2$*Ph*, minor isomer); 129.9 (s, *m*-H, SiH$_2$*Ph*, major isomer); 129.0 (s, *m*-H, N*Ar*, major isomer); 128.3 (s, *m*-H, η^3-NAr-Si(Et)*Ph*-H, major isomer), 128.14, 128.11, 128.0, 127.4, 126.1 125.2, 124.5, 123.5, 123.2, 123.1, 122.9 (s, aromatic for both isomers); 28.5, 28.1, 27.9, 27.8, 27.7, 26.9 (s, *CH*, N*Ar*, both isomers); 26.3, 25.4, 24.4, 24.0, 23.9, 23.8, 23.6 (s, *CH*$_3$, N*Ar*, both isomers); 18.2 (d, $^1J_{C\text{-}P}$ = 25.7 Hz, P*Me*$_3$, minor isomer); 17.8 (d, $^1J_{C\text{-}P}$ = 27.2 Hz, P*Me*$_3$, major isomer); 8.8, 7.9, 7.11, 10.9 (s, Si*Et*, both isomers). IR (nujol): 2114 cm^{-1} (broad, intensive); 2033 cm^{-1} (broad, intensive); 1652 cm^{-1} (broad, weak).

NMR scale reaction of (ArN)Mo(SiH$_2$Ph)(η^3-NAr-Si(Et)Ph-H)(PMe$_3$) (III-114) with PhSiH$_3$

PhSiH$_3$ (18.5 μl, 0.15 mmol) was added in one portion at room temperature to a solution of (ArN)Mo(SiH$_2$Ph)(η^3-NAr-Si(Et)Ph-H)(PMe$_3$) (**III-114**) (generated in NMR tube by the reaction of (ArN)Mo(Et)(η^3-NAr-SiHPh-CH=CH$_2$)(PMe$_3$) (**III-3**) (20.5 mg, 0.03 mmol) with PhSiH$_3$ (3.7 μl, 0.03 mmol) and BPh$_3$ (7.2 mg, 0.03 mmol), followed by the addition of 3.1 μl (0.03 mmol) of PMe$_3$) in 0.6 ml of C$_6$H$_6$ in an NMR tube. The mixture was left at room temperature for one week. NMR analysis of the reaction mixture showed selective formation of PhEtSiH$_2$[202] and the agostic complex (ArN)Mo(SiH$_2$Ph)(η^3-NAr-SiHPh-H)(PMe$_3$) (**III-1**).

NMR scale reaction of (ArN)Mo(SiH_2Ph)(η^3-NAr-Si(Et)Ph-H)(PMe_3) (III-114) with $PhSiD_3$

$PhSiD_3$ (3.7 μl, 0.03 mmol) was added in one portion at room temperature to a solution of (ArN)Mo(SiH_2Ph)(η^3-NAr-Si(Et)Ph-H)(PMe_3) (**III-114**) (generated *in situ* by the reaction of (ArN)Mo(Et)(η^3-NAr-SiHPh-CH=CH_2)(PMe_3) (**III-3**) (20.5 mg, 0.03 mmol) with $PhSiH_3$ (3.7 μl, 0.03 mmol) and BPh_3 (7.2 mg, 0.03 mmol), followed by addition of 3.1 μl (0.03 mmol) of PMe_3) in 0.6 ml of C_6H_6 in an NMR tube. The mixture was left at room temperature for 24 h. NMR analysis of the reaction mixture after that showed the formation of Ph(Et)SiHD. Scrambling of deuterium was also observed for the agostic complex (ArN)Mo(SiX_2Ph)(η^3-NAr-Si(X)Ph-X)(PMe_3) (X = H, D). ^{2}D-NMR (92.1 MHz; benzene-h_6, δ, ppm): 4.65 (bs, Ph(Et)SiH*D*).

NMR scale reaction of (ArN)Mo(SiH_2Ph)(η^3-NAr-Si(Et)Ph-H)(PMe_3) (III-114) with (*m*-Tol)SiH_3

(*m*-Tol)SiH_3 (8.0 μl, 0.059 mmol) was added in one portion at room temperature to a solution of (ArN)Mo(SiH_2Ph)(η^3-NAr-Si(Et)Ph-H)(PMe_3) (**III-114**) (generated *in situ* by the reaction of (ArN)Mo(Et)(η^3-NAr-SiHPh-CH=CH_2)(PMe_3) (**III-3**) (20.1 mg, 0.0294 mmol) with $PhSiH_3$ (3.6 μl, 0.0294 mmol) and BPh_3 (7.1 mg, 0.0294 mmol), followed by addition of 3.0 μl (0.0294 mmol) of PMe_3) in 0.6 ml of C_6D_6 in an NMR tube. NMR analysis after 10 min. at room temperature revealed incorporation of the *m*-Tol group in the classical silyl position of **III-114**. The reaction mixture was left at room temperature for 2 weeks. NMR analysis showed the presence of $PhSiH_3$ and scrambling of *m*-Tol group (confirmed by the ^{1}H-^{13}C HMBC NMR spectrum) between two silicon positions of the agostic complex (ArN)Mo(SiH_2R)(η^3-NAr-Si(H)R-H)(PMe_3) (R = Ph, *m*-Tol).

NMR scale reaction of (ArN)Mo(H)(η^3-NAr-SiHPh-CH=CH_2)(PMe_3) (III-112) with $PhSiH_3$

$PhSiH_3$ (39.6 μl, 0.032 mmol) was added in one portion at room temperature to a solution of (ArN)Mo(H)(η^3-NAr-SiHPh-CH=CH_2)(PMe_3) (**III-112**) (10.5 mg, 0.016 mmol) in 0.6 ml of C_6D_6 in an NMR tube. The reaction mixture was left at room temperature for one week showing 63 % conversion of the starting material and formation of

(ArN)Mo(SiH_2Ph)(η^3-NAr-SiHPh-H)(PMe_3) (**III-1**). Formation of $PhEtSiH_2$[202] was also observed by NMR spectroscopy.

NMR scale reaction of (ArN)Mo(H)(η^3-NAr-SiHPh-CH=CH_2)(PMe_3) (III-112) with ethylene

Ethylene was added *via* vacuum transfer to a frozen in liquid N_2 solution of (ArN)Mo(H)(η^3-NAr-SiHPh-CH=CH_2)(PMe_3) (**III-112**) (19.0 mg, 0.029 mmol) in 0.6 ml of C_6D_6 in an NMR tube. The mixture was slowly warmed up to room temperature and left for 15 min. NMR analysis showed the selective formation of (ArN)Mo(Et)(η^3-NAr-SiHPh-CH=CH_2)(PMe_3) (**III-3**).

Preparation of (ArN)Mo(CH_2CH_2Ph)(η^3-NAr-SiHPh-CH=CH_2)(PMe_3) (III-115)

Styrene (3.6 µl, 0.032 mmol) was added in one portion at room temperature to a solution of (ArN)Mo(H)(η^3-NAr-SiHPh-CH=CH_2)(PMe_3) (**III-112**) (21.1 mg, 0.032 mmol) in 0.6 ml of C_6D_6 in an NMR tube. The reaction mixture was left at room temperature for 3 days until all starting material was consumed. NMR analysis showed quantitative formation of the product of styrene insertion into the Mo-H bond, (ArN)Mo(CH_2CH_2Ph)(η^3-NAr-SiHPh-CH=CH_2)(PMe_3) (**III-115**). All volatiles were pumped off; the residue was extracted with 2 ml of hexanes to give a dark-brown oil. Yield: 20.0 mg, 83 %. ^{1}H-NMR (300 MHz; C_6D_6; δ, ppm): 7.67 (m, 2H, *o*-H, Si*Ph*); 7.48 (d, $^3J_{H\text{-}H}$ = 7.2 Hz, 2H, *o*-H, CH_2CH_2*Ph*); 7.32 (t, $^3J_{H\text{-}H}$ = 7.2 Hz, 2H, *m*-H, CH_2CH_2*Ph*); 6.81-7.11 (m, 10H, *p*-H of CH_2CH_2*Ph*, *m*-H and *p*-H of Si*Ph*, and *m*-H and *p*-H or N*Ar*); 6.49 (s, 1H, Si*H*); 4.35 (dd, $^2J_{H\text{-}H}$ = 3.9 Hz, $^3J_{H\text{-}H}$ = 12.9 Hz, 1H, H_2C=CHSi); 4.17 (dd, $^2J_{H\text{-}H}$ = 3.9 Hz, $^3J_{H\text{-}H}$ = 15.6 Hz, 1H, H_2C=CHSi); 4.09 (sept, $^3J_{H\text{-}H}$ = 6.6 Hz 1H, *CH*, N*Ar*); 3.82 (sept, $^3J_{H\text{-}H}$ = 6.6 Hz, 2H, 2*CH*, N*Ar*); 3.66 (ddd, $^2J_{H\text{-}H}$ = 4.5 Hz, $^3J_{H\text{-}H}$ = 13.2 Hz, $^3J_{H\text{-}H}$ = 18.0 Hz, 1H, $MoCH_2CH_2$Ph); 3.24(ddd, $^2J_{H\text{-}H}$ = 3.6 Hz, $^3J_{H\text{-}H}$ = 13.2 Hz, $^3J_{H\text{-}H}$ = 18.0 Hz, 1H, $MoCH_2CH_2$Ph); 2.98 (dd, $^3J_{H\text{-}H}$ = 12.9 Hz and 15.6 Hz, 1H, H_2C=*CH*Si); 2.72 (m, 2H, $MoCH_2CH_2$Ph and *CH* from N*Ar*); 1.69 (m, 1H, $MoCH_2CH_2$Ph); 1.55 (d, $^3J_{H\text{-}H}$ = 6.6 Hz, 3H, CH_3, N*Ar*); 1.54 (d, $^3J_{H\text{-}H}$ = 6.6 Hz, 3H, CH_3, N*Ar*); 1.39 (m, 6H, 2CH_3, N*Ar*); 1.22 (d, $^3J_{H\text{-}H}$ = 6.6 Hz, 3H, CH_3, N*Ar*); 1.13 (m, 6H, 2CH_3, N*Ar*); 0.65 (d, $^2J_{H\text{-}P}$ = 7.5 Hz, 9H, PMe_3); 0.35 (d, $^3J_{H\text{-}H}$ = 6.6 Hz, 3H, CH_3, N*Ar*). ^{31}P{^{1}H}-NMR (121.5 MHz; C_6D_6; δ, ppm): -17.1 (s, *P*Me_3). ^{13}C{^{1}H}-NMR (75.5 MHz; C_6D_6; 297 K; δ, ppm):

13.9 (d, $^{1}J_{C\text{-}P}$ = 19.6 Hz, P*Me*$_3$); 22.3 (s, *C*H$_3$, N*Ar*); 24.1 (s, *C*H$_3$, N*Ar*); 24.2 (s, *C*H$_3$, N*Ar*); 24.6 (s, *C*H$_3$, N*Ar*); 25.5 (s, *C*H$_3$, N*Ar*); 25.7 (s, *C*H$_3$, N*Ar*); 27.3 (s, *C*H, N*Ar*); 27.8 (s, *C*H$_3$, N*Ar*); 28.3 (s, *C*H, N*Ar*); 28.4 (s, *C*H, N*Ar*); 29.5 (s, *C*H$_3$, N*Ar*); 30.1 (s, *C*H, N*Ar*); 41.0 (d, $^{2}J_{C\text{-}P}$ = 6.8 Hz, Mo*C*H$_2$CH$_2$Ph); 41.7 (d, $^{3}J_{C\text{-}P}$ = 5.3 Hz, MoCH$_2$*C*H$_2$Ph); 50.2 (d, $J_{C\text{-}P}$ = 4.5 Hz, Si*C*H=CH$_2$); 75.1 (d, $J_{C\text{-}P}$ = 12.8 Hz, SiCH=*C*H$_2$); 123.0 (s, N*Ar*); 123.2 (s, *p*-C, Si*Ph*); 123.9 (s, *p*-C, MoCH$_2$CH$_2$*Ph*); 125.4 (s, N*Ar*); 128.5 (s, *o*-C, MoCH$_2$CH$_2$*Ph*); 128.6 (s, *m*-C, Si*Ph*); 128.7 (s, *m*-C, MoCH$_2$CH$_2$*Ph*); 129.5 (s, N*Ar*); 134.2 (s, *o*-C, Si*Ph*); 141.1 (s, *o*-C, N*Ar*); 143.5 (s, *o*-C, N*Ar*); 147.7, 149.2, 150.2, 151.9 (s, i-C of N*Ar*, Si*Ph*, and MoCH$_2$CH$_2$*Ph*). ^{29}Si INEPT+ NMR (59.6 MHz; C_6D_6; *J* = 200 Hz; δ, ppm): -28.1 (d, $^{1}J_{Si\text{-}H}$ = 206.0 Hz, *Si*HPh).

NMR scale reaction of (ArN)Mo(CH$_2$CH$_2$Ph)(η^3-NAr-SiHPh-CH=CH$_2$)(PMe$_3$) (III-115) with PhSiH$_3$ and PMe$_3$

PhSiH$_3$ (3.9 μl, 0.032 mmol) and PMe$_3$ (3.3 μl, 0.032 mmol) were added in one portion at room temperature to a solution of (ArN)Mo(CH$_2$CH$_2$Ph)(η^3-NAr-SiHPh-CH=CH$_2$)(PMe$_3$) (**III-115**) (21.0 mg, 0.032 mmol) in 0.6 ml of C_6D_6 in an NMR tube. No reaction was observed after 10 min. at room temperature. The mixture was heated overnight at 50 °C showing full conversion of starting complex, formation of (PhCH$_2$CH$_2$)SiH$_2$Ph (proved by ^{1}H-^{1}H COSY and ^{1}H-^{13}C HMBC NMR experiments) and (ArN)Mo(H)(η^3-NAr-SiHPh-CH=CH$_2$)(PMe$_3$) (**III-112**). Decomposition side-process forming a difficult-to-characterize mixture of hydride compounds and traces of (ArN)Mo(H)(η^3-NAr-SiHPh-CH=CHPh)(PMe$_3$) (**III-92**) was also observed.

NMR scale reaction of (ArN)Mo(H)(η^3-NAr-SiHPh-CH=CHPh)(PMe$_3$) (III-92) with ethylene

Excess ethylene was added *via* vacuum transfer to a frozen in liquid N_2 solution of (ArN)Mo(H)(η^3-NAr-SiHPh-CH=CHPh)(PMe$_3$) (**III-92**) (17.0 mg, 0.023 mmol) in 0.6 ml of C_6D_6 in an NMR tube. The mixture was slowly warmed up to room temperature and left for additional 1 h 40 min. All volatiles were pumped off; the residue was dried in vacuum and redissolved in 0.6 ml of C_6D_6. NMR analysis showed the formation of (ArN)Mo(Et)(η^3-NAr-SiHPh-CH=CHPh)(PMe$_3$) (**III-93**; 36 % by ^{31}P{^{1}H}-NMR analysis) in a mixture with unidentified products. All attempts to purify **III-93** by

recrystallization from different solvents were unsuccessful. ^{1}H-NMR (300 MHz; C_6D_6; δ, ppm): 7.67 (d, $^3J_{H-H}$ = 6.3 Hz, *o*-H, Si*Ph*); 6.77-7.55 (m, 14H, aromatic protons of 2 N*Ar*, Si*Ph*, and C*Ph*); 5.97 (bs, 1H, Si*H*); 4.25 (m, 2H, CH=CHPh and *CH* from N*Ar*); 3.72 (m, 2H, CH=CHPh and *CH* from N*Ar*); 3.33 (sept, $^3J_{H-H}$ = 6.6 Hz, 1H, *CH*, N*Ar*); 2.64 (sept, $^3J_{H-H}$ = 6.9 Hz, 1H, *CH*, N*Ar*); 0.7-1.59 (broad agglomerate of signals of CH_3 groups of *Ar*N, Mo*Et*, and P*Me*$_3$ overlapping with each other and with signals of decomposition products); 0.40 (bs, 3H, CH_3, N*Ar*). ^{31}P{^{1}H}-NMR (121.5 MHz; C_6D_6; δ, ppm): -19.5 (s, *P*Me$_3$). ^{29}Si INEPT+ NMR (59.6 MHz; C_6D_6; *J* = 200 Hz; δ, ppm): -18.8 (d, $^1J_{Si-H}$ = 187.9 Hz, *Si*HPh).

NMR scale reaction of (ArN)Mo(Et)(η^3-NAr-SiHPh-CH=CHPh)(PMe$_3$) (III-93) with PhSiH$_3$ and PMe$_3$

PhSiH$_3$ (2.7 μl, 0.022 mmol) and PMe$_3$ (1.9 μl, 0.018 mmol) were added at room temperature to a solution of (ArN)Mo(Et)(η^3-NAr-SiHPh-CH=CHPh)(PMe$_3$) (**III-93**) (generated *in situ* using 17.0 mg (0.023 mmol) of (ArN)Mo(H)(η^3-NAr-SiHPh-CH=CHPh)(PMe$_3$) (**III-92**) and excess ethylene) in 0.6 ml of C_6D_6 in an NMR tube. No reaction was observed at room temperature and the mixture was left at 50 °C overnight. NMR analysis showed the formation of PhEtSiH$_2$,[202] (ArN)Mo(H)(η^3-NAr-SiHPh-CH=CHPh)(PMe$_3$) (**III-92**) and unidentified decomposition products. No formation of (PhCH$_2$CH$_2$)SiH$_2$Ph was observed by NMR spectroscopy.

Preparation of (ArN)Mo(N=CHPh)(η^3-NAr-SiHPh-CH=CH$_2$)(PMe$_3$) (III-117)

Benzonitrile (2.5 μl, 0.024 mmol) was added in one portion at room temperature to a solution of (ArN)Mo(H)(η^3-NAr-SiHPh-CH=CH$_2$)(PMe$_3$) (**III-112**) (15.9 mg, 0.024 mmol) in 0.6 ml of C_6D_6 in an NMR tube. Immediately after addition of PhCN the colour of the solution turned to a different tint of brown. The mixture was left at room temperature for 30 min. NMR analysis showed full conversion of the starting material and selective formation of the only one product, (ArN)Mo(N=CHPh)(η^3-NAr-SiHPh-CH=CH$_2$)(PMe$_3$) (**III-117**). All volatiles were pumped off leaving the brown residue, which was extracted with 2 ml of hexanes. The solvent was removed in vacuum to give a dark-brown oily material. Yield: 14.3 mg, 78 %. ^{1}H-NMR (300 MHz; C_6D_6; δ, ppm): 8.59 (bs, 1H, N=C*H*Ph, found with ^{1}H-^{13}C HSQC NMR and ^{1}H-^{31}P HSQC NMR); 7.59

(m, 4H, *o*-H of Si*Ph* and N=CH*Ph*); 7.30 (t, $^{3}J_{H-H}$ = 7.5 Hz, 2H, *m*-H, N=CH*Ph*); 6.72-7.19 (m, 10H, *m*-H and *p*-H of N*Ar*, *m*-H and *p*-H of Si*Ph*, and *p*-H of N=CH*Ph*); 6.23 (s, 1H, Si*H*); 4.56 (d, $^{3}J_{H-H}$ = 12.0 Hz, 1H, PhHSi-CH=CH_2); 4.06 (m, 2H, *CH* of N*Ar* and PhHSi-CH=CH_2); 3.94 (sept, $^{3}J_{H-H}$ = 6.6 Hz, 2H, 2*CH*, N*Ar*); 3.69 (m, 2H, *CH* of N*Ar* and PhHSi-*CH*=CH_2); 1.62 (d, $^{3}J_{H-H}$ = 6.6 Hz, 3H, CH_3, N*Ar*); 1.41 (dd, $^{3}J_{H-H}$ = 6.6 Hz, 6H, two overlapping CH_3 signals of N*Ar*); 1.15 (d, $^{3}J_{H-H}$ = 6.6 Hz, 6H, 2CH_3, N*Ar*); 1.14 (d, $^{3}J_{H-H}$ = 6.6 Hz, 6H, 2CH_3, N*Ar*); 0.63 (d, $^{3}J_{H-H}$ = 6.6 Hz, 3H, CH_3, N*Ar*); 0.61 (d, $^{2}J_{H-P}$ = 8.4 Hz, 9H, PMe_3). $^{31}P\{^{1}H\}$-NMR (121.5 MHz; C_6D_6; δ, ppm): -16.4 (s, *P*Me_3). $^{13}C\{^{1}H\}$-NMR (75.5 MHz; C_6D_6; 297 K; δ, ppm): 153.7 (bs, N=*C*HPh); 153.3 (d, J_{C-P} = 3.0 Hz, *i*-C, N*Ar*); 151.9 (d, J_{C-P} = 4.5 Hz, *i*-C, N*Ar*); 144.3 (s, *o*-C, N*Ar*); 142.0 144.3 (s, *o*-C, N*Ar*); 141.8 and 139.1 (s, *i*-C of Si*Ph* and N=CH*Ph*); 134.1 (s, *o*-C, Si*Ph*); 129.5 (s, *m*-C, N=CH*Ph*); 128.8 (s, *m*-C, Si*Ph*); 128.2 (s, *m*-C of N*Ar*); 127.9 (s, *m*-C of N*Ar*); 125.8 (s, *o*-C, N=CH*Ph*); 123.8, 123.6, 123.2, and 123.1 (s, *p*-C of N*Ar*, Si*Ph*, and N=CH*Ph*); 86.8 (d, J_{C-P} = 9.1 Hz, PhHSi-CH=*C*H_2); 66.3 (d, J_{C-P} = 5.3 Hz, PhHSi-*C*H=CH_2); 29.0 (s, CH_3, N*Ar*); 28.2 (s, *CH*, N*Ar*); 28.1 (s, *CH*, N*Ar*); 27.5 (s, *CH*, N*Ar*); 27.3 (s, *CH*, N*Ar*); 25.3 (s, CH_3, N*Ar*); 24.9 (s, CH_3, N*Ar*); 24.6 (s, CH_3, N*Ar*); 24.0 (s, CH_3, N*Ar*); 23.7 (s, CH_3, N*Ar*); 23.3 (s, CH_3, N*Ar*); 22.5 (s, CH_3, N*Ar*); 13.9 (d, J_{C-P} = 21.9 Hz, PMe_3). ^{29}Si INEPT+ NMR (59.6 MHz; C_6D_6; *J* = 200 Hz; δ, ppm): -30.2 (d, $^{1}J_{Si-H}$ = 206.2 Hz, *Si*HPh). IR (nujol): 1591 cm^{-1} (N=C); 2104 cm^{-1} (Si-H).

NMR scale reaction of (ArN)Mo(N=CHPh)(η^3-NAr-SiHPh-CH=CH_2)(PMe_3) (III-117) with $PhSiH_3$

$PhSiH_3$ (24.7µl, 0.2 mmol) was added in one portion at room temperature to a solution of (ArN)Mo(N=CHPh)(η^3-NAr-SiHPh-CH=CH_2)(PMe_3) (**III-117**) (15.2 mg, 0.02 mmol) in 0.6 ml of C_6D_6 in an NMR tube. The mixture was left at room temperature for 2 h showing no conversion of the starting material. Heating the reaction mixture at 50 °C overnight gives mainly decomposition and the formation of only traces of (PhCH=N)SiH_2Ph and (ArN)Mo(H)(η^3-NAr-SiHPh-CH=CH_2)(PMe_3) (**III-112**). Other products were not identified.

NMR scale reaction of (ArN)Mo(H)(η^3-NAr-SiHPh-CH=CH_2)(PMe_3) (III-112) with acetone

Acetone (1.2 µl, 0.016 mmol) was added in one portion at room temperature to a solution of (ArN)Mo(H)(η^3-NAr-SiHPh-CH=CH_2)(PMe_3) (**III-112**) (10.5 mg, 0.016 mmol) in 0.6 ml of C_6D_6 in an NMR tube. The reaction mixture was left at room temperature for 3 days. NMR analysis showed full conversion of the starting material and the formation of (ArN)Mo(O^{i}Pr)(η^3-NAr-SiHPh-CH=CH_2)(PMe_3) (**III-116**; ~60 % by NMR analysis) in a mixture with unidentified decomposition products. All attempts to isolate **III-116** by recristallyzation from different solvents were unsuccessful.

(ArN)Mo(O^{i}Pr)(η^3-NAr-SiHPh-CH=CH_2)(PMe_3) (**III-116**): NMR spectra are very busy and difficult-to-interpret due to the presence of many impurities, however, the ligation of Mo with O^{i}Pr is evident from the NMR spectra. ^{1}H NMR (300 MHz; C_6D_6; selected resonances; δ, ppm): 7.82 (m, 2H, *o*-H, Si*Ph*); 5.81 (bs, 1H, Si*H*); 5.93 (m, 1H, *CH*, O^{i}Pr, found by ^{1}H-^{31}P HSQC NMR with J = 5 Hz); 1.44 (m, 6H, 2 *CH$_3$*, O^{i}Pr, found by ^{1}H-^{1}H COSY NMR); 1.12 (d, $^2J_{H\text{-}P}$ = 7.0 Hz; 9H, P*Me$_3$*). ^{31}P{^{1}H}-NMR (121.5 MHz; C_6D_6; δ, ppm): -6.9 (s, *P*Me$_3$).

NMR scale reaction of (ArN)Mo(H)(η^3-NAr-SiHPh-CH=CH_2)(PMe_3) (III-112) with benzaldehyde

Benzaldehyde (2.4 µl, 0.024 mmol) was added in one portion at room temperature to a solution of (ArN)Mo(H)(η^3-NAr-SiHPh-CH=CH_2)(PMe_3) (**III-112**) (15.8 mg, 0.024 mmol) in 0.6 ml of C_6D_6 in an NMR tube. The reaction mixture was left at room temperatire for 30 min. During this time the coulour of the solution change to a different tint of brown. NMR analysis showed full conversion of the starting material and formation of (ArN)$_2$Mo(η^2-O=CHPh)(PMe_3) (**III-100**) and $PhH_2Si(CH{=}CH_2)$. The reaction of **III-112** with PhC(O)H was found to be poorly reprodusilbe often affording a mixture of unidentified decomposition products.

Preparation of (ArN)Mo(Et)(η^3-NAr-Si(OBn)Ph-CH=CH_2)(PMe_3) (III-118)

Benzaldehyde (2.5 µl, 0.024 mmol) was added in one portion at room temperature to a solution of (ArN)Mo(Et)(η^3-NAr-SiHPh-CH=CH_2)(PMe_3) (**III-3**) (16.7 mg, 0.024 mmol) in 0.6 ml of C_6D_6 in an NMR tube. The reaction mixture was left at room temperature

overnight. NMR analysis showed full conversion of the starting material and formation of (ArN)Mo(Et)(η^3-NAr-Si(OBn)Ph-CH=CH_2)(PMe_3) (**III-118**). All volatiles were pumped off leaving an oily brown residue, which was extracted with 2 ml of hexanes. The solvent was removed in vacuum to give a brown oily substance. Yield: 15.6 mg, 81 %. ^{1}H NMR (600 MHz; C_6D_6; δ, ppm): 7.80 (m, 2H, *o*-H, *Ph*); 7.71 (m, 2H, *o*-H, *Ph*); 6.90-7.47 (m, 12 H, m-H and p-H of 2 N*Ar* and *Ph* overlapping with residual C_6D_6 resonance); 4.86 (d, $J_{H\text{-}H}$ = 12.6 Hz, 1H, O*CH*$_2$Ph); 4.75 (d, $^2J_{H\text{-}H}$ = 12.6 Hz, 1H, O*CH*$_2$Ph); 4.36 (dd, $^2J_{H\text{-}H}$ = 4.2 Hz and 13.2 Hz, 1H, SiCH=*CH*$_2$); 4.20 (sept, $^3J_{H\text{-}H}$ = 6.6 Hz, 1H, *CH*, N*Ar*); 4.11 (dd, $J_{H\text{-}H}$ = 4.2 Hz and 15.6 Hz, 1H, SiCH=*CH*$_2$); 3.83 (bs, 1H, *CH*, N*Ar*); 3.75 (sept, $^3J_{H\text{-}H}$ = 6.6 Hz, 1H, *CH*, N*Ar*); 2.88 (dd, $J_{H\text{-}H}$ = 13.2 Hz and 15.6 Hz, 1H, Si*CH*=CH_2); 2.69 (m, 1H, *CH*$_2$, Mo*Et*); 2.62 (sept, $^3J_{H\text{-}H}$ = 6.6 Hz, 1H, *CH*, N*Ar*); 2.16 (t, $^3J_{H\text{-}H}$ = 7.2 Hz, 3H, *CH*$_3$, Mo*Et*); 1.60 (d, $^3J_{H\text{-}H}$ = 6.6 Hz, 3H, *CH*$_3$, N*Ar*); 1.56 (d, $^3J_{H\text{-}H}$ = 6.6 Hz, 3H, *CH*$_3$, N*Ar*); 1.47 (m, 1H, *CH*$_2$, Mo*Et*); 1.34 (d, $^3J_{H\text{-}H}$ = 6.6 Hz, 3H, *CH*$_3$, N*Ar*); 1.63 (d, $^3J_{H\text{-}H}$ = 6.6 Hz, 3H, *CH*$_3$, N*Ar*); 1.23 (d, $^3J_{H\text{-}H}$ = 6.6 Hz, 3H, *CH*$_3$, N*Ar*); 1.19 (d, $^3J_{H\text{-}H}$ = 6.6 Hz, 3H, *CH*$_3$, N*Ar*); 1.05 (d, $^3J_{H\text{-}H}$ = 6.6 Hz, 3H, *CH*$_3$, N*Ar*); 0.82 (d, $^2J_{H\text{-}H}$ = 7.8 Hz, 9H, P*Me*$_3$); 0.27 (d, $^3J_{H\text{-}H}$ = 6.6 Hz, 3H, *CH*$_3$, N*Ar*). ^{31}P{^{1}H}-NMR (243 MHz; C_6D_6; δ, ppm): -17.9 (s, *P*Me$_3$). ^{1}H-^{13}C HSQC NMR (f1: 600 MHz; f2: 151 MHz; J = 145 Hz; C_6D_6; ^{13}C projection; δ, ppm): 134.3 (*o*-C, *Ph*); 134.0 (*o*-C, *Ph*); 74.7 (SiCH=*CH*$_2$); 66.1 (O*CH*$_2$Ph); 50.6 (Si*CH*=CH$_2$); 33.0 (*CH*$_2$, Mo*Et*); 29.7 (*CH*$_3$, N*Ar*); 28.2 (*CH*, N*Ar*); 27.8 (*CH*, N*Ar*); 27.5 (*CH*, N*Ar*); 26.9 (*CH*, N*Ar*); 25.0 (*CH*$_3$, N*Ar*); 24.5 (*CH*$_3$, N*Ar*); 24.0 (*CH*$_3$, N*Ar*); 23.8 (*CH*$_3$, N*Ar*); 23.4 (*CH*$_3$, N*Ar*); 14.9 (*CH*$_3$, N*Ar*); 13.7 (P*Me*$_3$). ^{29}Si{^{1}H}-NMR (119.2 MHz; C_6D_6; δ, ppm): -28.1 (s, η^3-NAr-*Si*(OBn)(Ph)-CH=CH_2).

NMR scale reaction of (ArN)Mo(Et)(η^3-NAr-SiDPh-CH=CH_2)(PMe_3) (III-3$_D$) with benzaldehyde

Benzaldehyde (2.6 µl, 0.025 mmol) was added in one portion at roome temperature to a solution of (ArN)Mo(Et)(η^3-NAr-SiDPh-CH=CH_2)(PMe_3) (**III-3$_D$**) (17.4 mg, 0.025 mmol) in 0.6 ml of C_6D_6 in an NMR tube. The reaction mixture was left at room temperature overnight showing formation of a mixture of the starting material and (ArN)Mo(Et)(η^3-NAr-Si(OCH(D)Ph)Ph-CH=CH_2)(PMe_3) (**III-118$_D$**) (2:1 ratio,

according to the $^{31}P\{^{1}H\}$-NMR spectrum). ^{2}D-NMR (92.1 MHz; benzene-h_6, δ, ppm): 5.0 (bs, OCH(*D*)Ph).

NMR scale reaction of (ArN)Mo(Et)(η^3-NAr-Si(OBn)Ph-CH=CH_2)(PMe_3) (III-118) with $PhSiH_3$

$PhSiH_3$ (3.7 µl, 0.03 mmol) was added at room temperature to a solution of (ArN)Mo(Et)(η^3-NAr-Si(OBn)Ph-CH=CH_2)(PMe_3) (**III-118**) (15.6 mg, 0.02 mmol) in 0.6 ml of C_6D_6 in an NMR tube. The reaction mixture heated at 50 °C overnight, showing full conversion of the starting material and the formation of $PhEtSiH_2$,[202] and (ArN)Mo(H)(η^3-NAr-Si(OBn)Ph-CH=CH_2)(PMe_3) (**III-119**; 38 % by $^{31}P\{^{1}H\}$-NMR spectroscopy) in a mixture with unidentified decomposition products. Addition of excess $PhSiH_3$ (37.0 µl, 0.3 mmol) after 2 days at room temperature leads to a ~12 % conversion of **III-119** into (ArN)Mo(SiH_2Ph)(η^3-NAr-SiHPh-H)(PMe_3) (**III-1**). The silicon containing by-product was not identified due to its low abundance.

(ArN)Mo(H)(η^3-NAr-Si(OBn)Ph-CH=CH_2)(PMe_3) (**III-119**): ^{1}H NMR (600 MHz; C_6D_6; selected resonances; *δ*, ppm): 4.77 (d, $^{2}J_{H\text{-}H}$ = 12.6 Hz, 1H, O*CH*$_2$Ph); 4.71 (d, $^{2}J_{H\text{-}H}$ = 12.6 Hz, 1H, O*CH*$_2$Ph); 2.70 (d, $^{2}J_{H\text{-}P}$ = 43.2 Hz, 1H, Mo*H*); 2.28 (dd, $^{3}J_{H\text{-}H}$ = 13.2 Hz and 15.6 Hz, 1H, Si*CH*=CH_2); 0.81 (d, $^{2}J_{H\text{-}P}$ = 7.8 Hz, 9H, P*Me*$_3$); other signals are obscured by impurities. $^{31}P\{^{1}H\}$-NMR (121.5 MHz; C_6D_6; *δ*, ppm): -16.6 (s, *P*Me_3).

NMR scale reaction of (ArN)Mo(Et)(η^3-NAr-SiHPh-CH=CH_2)(PMe_3) (III-3) with acetone

Acetone (1.9 µl, 0.025 mmol) was added at room temperature to a solution of (ArN)Mo(Et)(η^3-NAr-SiHPh-CH=CH_2)(PMe_3) (**III-3**) (17.2 mg, 0.025 mmol) in 0.6 ml of C_6D_6 in an NMR tube. The mixture was left at room temperature for 4 days showing no reaction. Excess acetone (5.0 µl, 0.068 mmol) was added to the NMR tube and the mixture was left at room temperature overnight. NMR analysis showed no reaction. Heating the mixture for 1 h at 50 °C gives a mixture of unidentified decomposition products.

NMR scale reaction of (ArN)Mo(Et)(η^3-NAr-SiHPh-CH=CH_2)(PMe_3) (III-3) with phenylacetylene

Phenylacetylene (3.2 µl, 0.029 mmol) was added in one portion at room temperature to a solution of (ArN)Mo(Et)(η^3-NAr-SiHPh-CH=CH_2)(PMe_3) (**III-3**) (20.0 mg, 0.029 mmol) in 0.6 ml of C_6D_6 in NMR tube. The reaction mixture was left at room temperature for 15 min. NMR analysis showed the release of ethylene and formation of a mixture of the starting material, (ArN)Mo(Et)(η^3-NAr-SiHPh-CH=CH_2)(PMe_3) (**III-112**), the product of insertion of phenylacetylene into the Mo-H bond, (ArN)Mo(CH=CH_2Ph)(η^3-NAr-SiHPh-CH=CH_2)(PMe) (**III-124**; a mixture of *cis*- and *trans*- isomers was suggested), and unidentified decomposition products. NMR spectra are difficult-to-nterpret, however, the insertion of PhC≡CH into the Mo-H bond and formation of **III-124** was suggested on the basis of the ^{1}H-NMR spectrum (300 MHz; C_6D_6; RT), which showed new signals (5.60-6.65 ppm (m)) in typical olefinic region (also confirmed by the ^{1}H-^{13}C HSQC NMR spectrum).

Preparation and reactivity of mono(imido) complexes

Preparation of mono(imido) dichloride Mo(IV) complexes

Synthesis of (Ar'N)$MoCl_2(PMe_3)_3$ (III-5)[15]

PMe_3 (0.41 ml, 3.93 mmol) and $HSiCl_3$ (1.19 ml, 11.8 mmol) were added at room temperature to a solution of $(Ar'N)_2Mo(PMe_3)_3$ (**III-4**) (2.21 g, 3.93 mmol) in 150 ml of Et_2O. Within a minute the color changed from dark-green to yellow-brown. The reaction mixture was left overnight at room temperature, then concentrated to ~10 ml and filtered. The green residue of **III-5** was washed with 10 ml of cold hexanes and dried in vacuum. Yield: 1.65 g, 82 %. The combined fractions of mother liquor were evaporated slowly in vacuum at -30 °C to leave a yellow-brown oil, which mostly contained of $(Ar'N\text{-}SiClH)_2$ contaminated by **III-5**.

(Ar'N)$MoCl_2(PMe_3)_3$ (**III-5**): ^{1}H NMR (300 MHz; C_6D_6; δ, ppm): 6.84 (t, $^3J_{H\text{-}H}$ = 7.35 Hz, 1H, *p*-H, *Ar'*N); 6.70 (d, $^3J_{H\text{-}H}$ = 7.5 Hz, 2H, *m*-H, *Ar'*N); 2.42 (s, 6H, *Me*, *Ar'*N), 1.38 (vt, $^2J_{H\text{-}P}$ = 3.45 Hz, 18H, 2 *trans*-P*Me*$_3$); 1.24 (d, $^2J_{H\text{-}P}$ = 7.5 Hz, 9H, *cis*-P*Me*$_3$). ^{31}P{^{1}H}-

NMR (121.4 MHz; C_6D_6; δ, ppm): 3.69 (t, $^2J_{P\text{-}P}$ = 17.0, 1P, PMe_3); -7.9 (d, $^2J_{P\text{-}P}$ = 17.0 Hz, 2P, PMe_3). NMR parameters are identical to those reported earlier.[15]

(Ar'N-SiHCl)$_2$: ^{1}H-NMR (300 MHz; C_6D_6; δ, ppm): 6.82 (m, 3H, *m*-H and *p*-H, *Ar'*N); 5.44 (s+d, $^1J_{H\text{-}Si}$ = 337 Hz, 1H, Si-*H*); 2.19 (s, 6H, *Me*, *Ar'*N). ^{13}C{^{1}H}-NMR (75.4 MHz; C_6D_6; δ, ppm): 137.4 (s, *o*-C, *Ar'*N); 129.7 (s, *m*-C, *Ar'*N); 127.8 (s, *p*-C, *Ar'*N); 19.9 (s, *Me*). NMR parameters are identical to those reported earlier.[15]

Synthesis of (ArN)MoCl$_2$(PMe$_3$)$_3$ (III-47)

PMe_3 (0.25 ml, 2.45 mmol) and $HSiCl_3$ (0.74 ml, 7.29 mmol) were added at room temperature to a solution of $(ArN)_2Mo(PMe_3)_3$ (**III-22**) (1.64 g, 2.43 mmol) in Et_2O. After 20 min of stirring the formation of precipitate was observed. The reaction mixture was stirred overnight at room temperature. Then the mixture was concentrated and filtered. The residue was washed with pentane and dried in vacuum to give green solid of $(ArN)MoCl_2(PMe_3)_3$ (**III-47**). Yield: 1.08 g, 78 %. The combined fractions of mother liquor were evaporated slowly in vacuum at -30 °C to leave a yellow-brown oil, which according to NMR analysis mostly contained of $(ArN\text{-}SiClH)_2$.

(ArN)MoCl$_2$(PMe$_3$)$_3$ (**III-47**): ^{1}H-NMR (300 MHz; C_6D_6; δ, ppm): 7.01 (t, $^3J_{H\text{-}H}$ = 7.7 Hz, 1H, *p*-H, *Ar*N); 6.87 (d, $^3J_{H\text{-}H}$ = 7.7 Hz, 2H, *m*-H, *Ar*N); 4.12 (sept, $^3J_{H\text{-}H}$ = 6.8 Hz, 2H, 2 *CH*, *Ar*N); 1.40 (vt, $^2J_{H\text{-}P}$ = 2.4 Hz, 18H, 2 P*Me$_3$*); 1.27 (d, $^2J_{H\text{-}P}$ = 8.4 Hz, 9H, P*Me$_3$*); 1.17 (d, $^3J_{H\text{-}H}$ = 6.6 Hz, 12H, 4 *CH$_3$*, *Ar*N). ^{13}C{^{1}H}-NMR (75.4 MHz; toluene-d$_8$, -50 °C; δ, ppm): 146.8; 126.7 (*p*-C, *Ar*N); 123.9 (*m*-C, *Ar*N); 27.1 (s, *CH*, *Ar*N); 25.4 (s, *CH$_3$*, *Ar*N); 23.1 (d, $^1J_{C\text{-}P}$ = 23.0 Hz, P*Me$_3$*); 17.1 (vt, $^1J_{C\text{-}P}$ = 11.5 Hz, P*Me$_3$*). ^{31}P{^{1}H}-NMR (121.4 MHz; C_6D_6; δ, ppm): 3.6 (t, $^2J_{P\text{-}P}$ = 16.7 Hz, 1 PMe_3); -7.8 (d, $^2J_{P\text{-}P}$ = 16.7 Hz, 1 PMe_3). Elem. Anal. (%): calcd for $C_{21}H_{44}NMoP_3Cl_2$ (570.354): C 44.22, H 7.78, N 2.46; found: C 43.23, H 7.78, N 2.46.

(ArN-SiClH)$_2$: ^{1}H-NMR (300 MHz; C_6D_6; δ, ppm): 7.03-6.90 (m); 5.48 (s); 3.40 (sept, $^3J_{H\text{-}H}$ = 6.6 Hz, 2H, 2 *CH*, *Ar*N); 1.41 (d, $^3J_{H\text{-}H}$ = 6.6 Hz, 12H, 4 *CH$_3$*, *Ar*N). ^{1}H-^{29}Si HSQC NMR (59.6 MHz; C_6D_6; ^{29}Si projection; δ, ppm): 37.3.

Synthesis of (^{t}BuN)MoCl$_2$(PMe$_3$)$_3$ (III-48)[200]

To 25 ml of Et_2O solution of $(^tBuN)_2Mo(PMe_3)_2$ (**III-27**) (1.70 g, 4.35 mmol) was added an equivalent of PMe_3 followed by 0.7 ml of $HSiCl_3$ (6.94 mmol). Instantaneous reaction

occurs, resulting in the formation of a brown precipitate. The mixture was left at -30 °C overnight. The cold solution was filtered off, and the residue was washed with 3 ml of ether and dried to give 1.11 g (2.39 mmol, 55%) of a light-amber powder of (^{t}BuN)$MoCl_2(PMe_3)_3$ (**III-48**). Keeping the mother liquor at -30 °C over the period of 4 days afforded the second crop (0.225 g, 0.48 mmol, 11%) of the same compound. ^{1}H-NMR (300 MHz; C_6D_6; δ, ppm): 1.43 (vt, $^2J_{H\text{-}P}$ = 3.6 Hz, 18H, *trans*-P*Me*$_3$); 1.25 (d, $^2J_{H\text{-}P}$ = 7.6 Hz, 9H, *cis*-P*Me*$_3$); 1.01 (s, 9H, ^{t}*Bu*N). ^{31}P{^{1}H}-NMR (121.4 MHz; C_6D_6; δ, ppm): 7.3 (bs, 1P, *cis*-*P*Me_3); -5.9 (bs, *trans*-*P*Me_3).

Preparation and reactivity of molybdenum borohydride complexes

Synthesis of $(ArN)_2Mo(\eta^2\text{-}BH_4)(PMe_3)_2$ (III-125)

A solution of $(ArN)_2MoCl_2$(DME) (**III-11**) (0.364 g, 0.60 mmol) in THF (15 ml) was added to a mixture of $NaBH_4$ (0.35 g, 0.925 mmol) and PMe_3 (0.40 ml, 3.86 mmol). Upon addition of the reagents, the color turned dark brown due to the *in situ* formation of $(ArN)_2MoCl_2(PMe_3)_2$. The mixture was stirred for 2 h, during which time it became dark green. All volatiles were removed under reduced pressure, the residue was extracted into diethyl ether (20 ml), and the extract was filtered. The dark solid produced after evaporation of the volatiles is a mixture of **III-125** and an impurity, $(ArN)_2MoCl_2(PMe_3)_2$, according ^{1}H-NMR spectroscopy. Recrystallization from pentane (30 ml) at -30 °C afforded **III-125** as well-formed dark green crystals, which were collected by filtration, washed with the minimum amount of cold pentane, and dried in vacuum. Yield: 0.084 g. A second crop (0.050 g) was obtained in a similar fashion from the concentrated mother liquors. Combined yield: 0.134 g, 36 %. IR (selected bands): 2389, 2358, and 2102 cm^{-1}. ^{1}H-NMR (C_6D_6): two very broad, featureless resonances at ca. 4.6 and 3.7 ppm due to the paramagnetic nature of the compound. Elem. Anal. (%): found (calcd. for $C_{30}H_{56}BMoN_2P_2$): C, 58.24 (58.73); H, 9.07 (9.20); N, 4.38 (4.57). For EPR studies, complex **III-125** was dissolved in toluene in a glovebox. Immediately after preparation, samples were frozen in liquid N_2. The X-band EPR spectra of **III-125** were recorded at 120 and 295 K. Frozen solution spectra were measured first, and then the samples were allowed to thaw (still under an inert atmosphere) and fluid solution spectra measured at room temperature.

Preparation of (Ar'N)Mo(η^2-BH_4)$_2$(PMe_3)$_2$ (III-128)

A solution of $LiBH_4$ (2.5 ml, 2.0 M) in THF was added at room temperature to a solution of (Ar'N)Mo(Cl)$_2$(PMe_3)$_3$ (**III-5**) (300.0 mg, 0.58 mmol) and PMe_3 (0.12 ml, 1.17 mmol) in 50 ml of THF. After addition of $LiBH_4$ the colour of the reaction mixture turned from green to yellow-green and then, after 30 min of stirring, to yellow. The reaction mixture was stirred for additional 4 hours. All volatiles were pumped off and the residue was extracted with 50 ml of toluene. The solvent was removed under reduced pressure to give a yellow solid of (Ar'N)Mo(η^2-BH_4)$_2$(PMe_3)$_2$ (**III-128**), which was dried in vacuum and recrystallized at – 30°C from diethyl ether solution. Yield: 155.0 mg, 67 %. ^{1}H-NMR (600 MHz; toluene-d$_8$; 22 °C; δ, ppm): -0.01 (bs, η^2-B*H*$_4$); 1.27 (vt, $^2J_{H\text{-}P}$ = 7.5 Hz, 18H, 2 P*Me*$_3$); 2.23 (s, 6H, 2 *CH*$_3$, *Ar'*N); 6.71 (d, $^3J_{H\text{-}H}$ = 7.5 Hz, 2H, *m-H*, *Ar'*N); 6.80 (t, $^3J_{H\text{-}H}$ = 7.5 Hz, 1H, *p-H*, *Ar'*N). ^{1}H-NMR (600 MHz; toluene-d$_8$; -79 °C; δ, ppm): -5.38 (bs, 2H, η^2-B*H*$_4$, bridging); -1.10 (bs, 2H, η^2-B*H*$_4$, bridging); 1.16 (bs, 18H, 2 P*Me*$_3$); 2.30 (bs, 6H, 2 *CH*$_3$, *Ar'*N); 3.60 (bs, 2H, 2 B-*H*, terminal); 3.79 (bs, 2H, 2 B-*H*, terminal); 6.62 (m, 2H, *m-H*, *Ar'*N); 6.80 (m, 1H, *p-H*, *Ar'*N). ^{31}P{^{1}H}-NMR (243 MHz; toluene-d$_8$; 22 °C; δ, ppm): 2.1 (s, *PMe*$_3$). ^{11}B-NMR (96.3 MHz; C_6D_6; 22 °C; δ, ppm): -15.8 (bm, 2 η^2-*B*H$_4$). ^{11}B-NMR (96.3 MHz; toluene-d$_8$; -78 °C; δ, ppm): -16.4 (bs, 2 η^2-*B*H$_4$). ^{13}C{^{1}H}-NMR (75.5 MHz; toluene-d$_8$; 24 °C; δ, ppm): 16.2 (vt, $^1J_{C\text{-}P}$ = 24.2 Hz, 2P*Me*$_3$); 19.6 (s, 2*CH*$_3$, *Ar'*N); 126.0 (s, *p-C*, *Ar'*N); 128.8 (s, *m-C*, *Ar'*N); 136.1 (s, *o-C*, *Ar'*N); 156.0 (s, *i-C*, *Ar'*N). ^{13}C{^{1}H}-NMR (151 MHz; toluene-d$_8$; -80 °C; δ, ppm): 15.3 (vt, $^1J_{C\text{-}P}$ = 24.1 Hz, 2P*Me*$_3$); 20.1 (s, 2*CH*$_3$, *Ar'*N); 126.0 (s, *p-C*, *Ar'*N); 129.1 (s, *m-C*, *Ar'*N); 136.0 (s, *o-C*, *Ar'*N); 155.7 (s, *i-C*, *Ar'*N). IR (nujol, selected bands): B-H stretches appear at 2111 cm^{-1} (m), 2189 cm^{-1} (w), 2269 cm^{-1} (m), 2371 cm^{-1} (s) and 2395 cm^{-1} (s). Elem. Anal. (%): calc. for $C_{14}H_{35}B_2MoNP_2$ (396.944) C 42.36, H 8.89, N 3.53; found C 42.42, H 9.27, N 3.43.

Preparation of (ArN)Mo(η^2-BH_4)$_2$(PMe_3)$_2$ (III-8)

A solution of $LiBH_4$ in THF (2.0 M, 4.2 ml, 8.4 mmol) was added at room temperature to a solution of (ArN)Mo(Cl)$_2$(PMe_3)$_3$ (**III-47**) (2.38 g, 4.2 mmol) in 100 ml of THF. The reaction mixture was left with stirring overnight at room temperature. During this time the colour of the reaction mixture changed from green to brown. All volatiles were

pumped off; the residue was dried and extracted with 150 ml of hexanes. The solvent removed under reduced pressure to give fine yellow powder of (ArN)Mo(η^2-BH_4)$_2$(PMe_3)$_2$ (**III-8**), which was dried in vacuum. Yield: 1.07 g, 51 %. ^{1}H-NMR (300 MHz; toluene-d_8; 25 °C; δ, ppm): -0.02 (bs, η^2-B*H*$_4$); 1.16 (d, $^3J_{H-H}$ = 6.9 Hz, 12H, 4 *CH*$_3$, *Ar*N); 1.33 (vt, $^2J_{H-P}$ = 7.8 Hz, 18H, 2 P*Me*$_3$); 3.91 (sept, $^3J_{H-H}$ = 6.9 Hz, 2H, 2 *CH*, *Ar*N); 6.88 (d, $^3J_{H-H}$ = 7.8 Hz, 2H,*m-H*, *Ar*N); 7.00 (t, $^3J_{H-H}$ = 6.9 Hz, 1H, *p-H*, *Ar*N). ^{1}H-NMR (600 MHz; toluene-d_8; -44 °C; selected resonances; δ, ppm): -5.43 (bs, 2H, Mo-*H*-B); -1.16 (bs, 2H, Mo-*H*-B); 3.60 (bs, 4H, B*H*$_2$). ^{31}P{^{1}H}-NMR (121.5 MHz; toluene-d_8; 25 °C; δ, ppm): 1.1 (s, 2 *P*Me3). ^{13}C{^{1}H}-NMR (75.5 MHz; toluene-d_8; 25 °C; δ, ppm): 16.0 (vt, $^1J_{C-P}$ = 24.9 Hz, P*Me*$_3$); 23.4 (s, *CH*$_3$, *Ar*N); 27.8 (s, *CH*, *Ar*N); 123.7 (s, *m-C*, *Ar*N); 127.1 (s, *p-C*, *Ar*N); 146.4 (s, *o-C*, *Ar*N); 153.1 (s, *i-C*, *Ar*N). ^{11}B-NMR (192.6 MHz; toluene-d_8; 22 °C; δ, ppm): -15.84 (pent, $^1J_{B-H}$ = 80.9 Hz, 2 *BH*$_4$). IR (nujol, selected bands): B-H stretches appear at 1950 cm^{-1} (w), 1969 cm^{-1} (w), 2013 cm^{-1} (w), 2102 cm^{-1} (m), 2266 cm^{-1} (m), 2378 cm^{-1} (s), and 2405 cm^{-1} (s). Elem. Anal. (%): calc. for $C_{18}H_{43}B_2MoNP_2$ (453.050) C 47.72, H 9.57, N 3.09; found C 47.82, H 9.78, N 2.95.

NMR scale reaction of (Ar'N)Mo(η^2-BH_4)$_2$(PMe_3)$_2$ (III-128) with Me_2SiHCl and PMe_3

PMe_3 (17.0 µl, 0.17 mmol) and Me_2SiHCl (7.0 µl, 0.06 mmol) were added at room temperature to a solution of (Ar'N)Mo(η^2-BH_4)$_2$(PMe_3)$_2$ (**III-128**) (21.8 mg, 0.06 mmol) in 0.6 ml of C_6D_6 in an NMR tube. The reaction mixture was left at room temperature for 3 days until full conversion of the starting material was observed. NMR spectra showed selective formation of (Ar'N)Mo(H)(Cl)(PMe_3)$_3$ (**III-129**). After extraction with hexane and drying in vacuum the product was isolated in analytically pure form. Yield: 23.1 mg, 88 %. ^{1}H-NMR (300 MHz; C_6D_6; δ, ppm): 1.35 (d, $^2J_{H-P}$ = 5.7 Hz, 9H, P*Me*$_3$), 1.43 (vt, $^2J_{H-P}$ = 6.0 Hz, 18H, 2 P*Me*$_3$), 2.39 (s, 6H, 2 *CH*$_3$, *Ar'*N), 5.38 (dt, $^2J_{H-P}$ = 51.3 Hz, $^2J_{H-P}$ = 29.4 Hz, 1H, Mo*H*), 6.79 (m, 3H, *p*-H and *m*-H, *Ar'*N). ^{13}C{^{1}H}-NMR (75.5 MHz; C_6D_6; δ, ppm): 20.0 (s, *CH*$_3$, *Ar'*N), 21.1 (vt, $^1J_{C-P}$ = 11.1 Hz, P*Me*$_3$), 21.4 (d, $^1J_{C-P}$ = 15.1 Hz, P*Me*$_3$), 123.7 (s, *p*-C, *Ar'*N), 127.9 (s, *m*-C, *Ar'*N), 133.0 (s, o-C, *Ar'*N), 153.9 (s, *i*-C, *Ar'*N). ^{31}P{^{1}H}-NMR (121.5 MHz; C_6D_6; δ, ppm): -1.6 (d, $^2J_{P-P}$ = 14.6 Hz, 2 *P*Me$_3$), -17.1 (t, $^2J_{P-P}$ = 14.6 Hz, *P*Me$_3$). IR (nujol, selected bands): 1713 cm^{-1} (s, Mo-H).

Preparation of (Ar'N)Mo(H)(SiH_2Ph)(PMe_3)$_3$ (III-73)

$PhSiH_3$ (58.8 µl, 0.476 mmol) and PMe_3 (150.0 µl, 1.428 mmol) were added in one portion at room temperature to a solution of (Ar'N)Mo(η^2-BH_4)$_2$(PMe_3)$_2$ (**III-128**) (189.0 mg, 0.476 mmol) in 50 ml of toluene. No visual changes were observed and the mixture was left with stirring for two weeks at room temperature. All volatiles were pumped off, the residue was dried in vacuum and extracted with Et_2O (30 ml). Ether solution was concentrated to 5 ml, equal amount of hexane was added, and the mixture was left at -30 °C overnight to give a fine yellow powder of (Ar'N)Mo(H)(SiH_2Ph)(PMe_3)$_3$ (**III-73**), which was dried in vacuum. Yield: 125.5 mg, 48 %. ^{1}H-NMR (600 MHz; C_6D_6; δ, ppm): -3.56 (dt, 1H, $^2J_{P\text{-}H}$ = 18.5 Hz, $^2J_{P\text{-}H}$ = 65.4 Hz, Mo*H*); 1.12 (vt, $^2J_{H\text{-}P}$ = 6.5 Hz, 18H, 2 P*Me$_3$*); 1.20 (d, $^2J_{H\text{-}P}$ = 6.5 Hz, 9H, P*Me$_3$*); 2.49 (s, 6H, 2*CH$_3$*, *Ar'*N); 5.83 (t, $^3J_{H\text{-}P}$ = 7.8 Hz, 2H, Si*H$_2$*); 6.89 (t, $^3J_{H\text{-}H}$ = 7.5 Hz, 1H, *p*-H, *Ar'*N); 6.95 (d, $^3J_{H\text{-}H}$ = 7.5 Hz, 2H, *m*-H, *Ar'*N); 7.18 (t, $^3J_{H\text{-}H}$ = 7.5 Hz, 1H, *p*-H, *Ph*Si); 7.28 (t, $^3J_{H\text{-}H}$ = 7.5 Hz, 2H, *m*-H, *Ph*Si); 8.09 (d, $^3J_{H\text{-}H}$ = 7.5 Hz, 2H, *o*-H, *Ph*Si). ^{13}C{^{1}H}-NMR (75.5 MHz; C_6D_6; δ, ppm): 20.9 (s, *CH$_3$*, *Ar'*N); 21.6 (vt, $^1J_{C\text{-}P}$ = 21.9 Hz, P*Me$_3$*); 25.6 (d, $^1J_{C\text{-}P}$ = 21.9 Hz, P*Me$_3$*); 123.6 (s, *p*-C, *Ar'*N); 126.9 (s, *p*-C, *Ph*Si); 127.1 (s, *m*-C, *Ar'*N); 128.3 (s, *m*-C, *Ph*Si); 135.3 (s, *o*-C, *Ar'*N); 136.8 (s, *o*-C, *Ph*Si); 148.7 (s, *i*-C, *Ph*Si); 156.4 (s, *i*-C, *Ar'*N). ^{31}P{^{1}H}-NMR (121.5 MHz; C_6D_6; δ, ppm): -1.5 (d, $^2J_{P\text{-}P}$ = 23.1 Hz, 2*P*Me$_3$); 10.5 (t, $^2J_{P\text{-}P}$ = 23.1 Hz, *P*Me$_3$). ^{29}Si INEPT+ NMR (59.6 MHz; *J* = 200 Hz, C_6D_6; δ, ppm): 1.7 (t, $^1J_{Si\text{-}H}$ = 157.4 Hz, *Si*H$_2$Ph). IR (nujol, selected bands): 1647 cm^{-1} (s, Mo-H); 2152 cm^{-1} (s, Si-H). Elem. Anal. (%): calc. for $C_{23}H_{44}MoNP_3Si$ (551.549) C 50.09, H 8.04, N 2.54; found C 50.54, H 7.98, N 2.73.

Reaction of (ArN)Mo(η^2-BH_4)$_2$(PMe_3)$_2$ (III-8) with $PhSiH_3$ and PMe_3

$PhSiH_3$ (132.0 µl, 1.07 mmol) was added at room temperature to a solution of (ArN)Mo(η^2-BH_4)$_2$(PMe_3)$_2$ (**III-8**) (486.0 mg, 1.07 mmol) and PMe_3 (0.22 ml, 2.14 mmol) in 50 ml of toluene. The reaction mixture was stirred for 7 days at room temperature. Then all volatiles were pumped off, the residue was dried and extracted with 30 ml of Et_2O. Ether solution was concentrated and left at -78 °C overnight to give a yellow powder of (ArN)Mo(H)(SiH_2Ph)(PMe_3)$_3$ (**III-7**), which was dried in vacuum. Yield: 152.0 mg, 23 %. ^{1}H-NMR (600 MHz; C_6D_6; δ, ppm): -3.92 (dt, 1H, $^2J_{P\text{-}H}$ = 18.6

Hz, $^{2}J_{P\text{-}H}$ = 65.4 Hz, Mo-*H*), 1.17 (bs, 18H, 2 P*Me*$_3$), 1.21 (d, $^{2}J_{H\text{-}P}$ = 6.6 Hz, 9H, P*Me*$_3$), 1.31 (d, $^{3}J_{H\text{-}H}$ = 6.6 Hz, 12H, 4 *CH*$_3$, *Ar*N), 4.39 (sept, $^{3}J_{H\text{-}H}$ = 6.6 Hz, 2H. 2 *CH*, *Ar*N), 5.75 (t + sat, $^{3}J_{H\text{-}P}$ = 7.8 Hz, $^{1}J_{H\text{-}Si}$ = 147.0 Hz, 2H, PhSi*H*$_2$), 7.01 (d, $^{3}J_{H\text{-}H}$ = 7.2 Hz, 2H, *Ar*N, *m-H*), 7.05 (m, $^{3}J_{H\text{-}H}$ = 7.2 Hz, 1H, *Ar*N, *p-H*), 7.19 (t, $^{3}J_{H\text{-}H}$ = 7.2 Hz, 1H, *Ph*SiH$_2$, *p-H*), 7.28 (t, $^{3}J_{H\text{-}H}$ = 7.2 Hz, 2H, *Ph*SiH$_2$, *m-H*), 8.08 (d, $^{3}J_{H\text{-}H}$ = 7.2 Hz, 2H, *Ph*SiH$_2$, *o-H*). $^{13}C\{^{1}H\}$-NMR (151 MHz; C_6D_6; δ, ppm): 21.4 (vt, $^{1}J_{C\text{-}P}$ = 22.6 Hz, 2 P*Me*$_3$), 24.2 (s, *Ar*N, *CH*$_3$), 25.2 (d, $^{1}J_{C\text{-}P}$ = 22.6 Hz, P*Me*$_3$), 26.4 (s, *Ar*N, *CH*), 122.9 (s, *Ar*N, *p-C*), 123.3 (s, *Ar*N, *m-C*), 126.7 (s, *Ph*SiH$_2$, *p-C*), 127.1 (s, *Ph*SiH$_2$, *m-C*), 132.0 (s, *Ph*SiH$_2$, *i-C*), 136.6 (s, *Ph*SiH$_2$, *o-C*), 145.4 (s, *Ar*N, *o-C*), 146.6 (s, *Ar*N, *i-C*). $^{31}P\{^{1}H\}$-NMR (243 MHz; C_6D_6; δ, ppm): -1.9 (d, $^{2}J_{P\text{-}P}$ = 23.8 Hz, 2 *P*Me$_3$), 10.0 (t, $^{2}J_{P\text{-}P}$ = 23.8 Hz, *P*Me$_3$). ^{31}P-NMR (selectively decoupled from methyl groups; 243 MHz; C_6D_6; δ, ppm): -1.9 (bm, 2 *P*Me$_3$), 10.0 (dt, $^{2}J_{H\text{-}P}$ = 65.5 Hz, $^{2}J_{P\text{-}P}$ = 23.8 Hz, *P*Me$_3$). $^{29}Si\{^{1}H\}$-NMR (119.2 MHz; C_6D_6; δ, ppm): 0.2 (dd, $^{2}J_{Si\text{-}P}$ = 9.6 Hz, $^{2}J_{Si\text{-}P}$ = 21.7 Hz, *Si*H$_2$Ph). ^{29}Si INEPT+ NMR (119.2 MHz; *J* = 200 Hz; toluene-d$_8$; 22 °C; δ, ppm): -0.03 (t, $^{1}J_{Si\text{-}H}$ = 145.5 Hz, *Si*H$_2$Ph). IR (nujol, selected bands, selected bands): 1699 cm^{-1} (s, Mo-H); 1998 cm^{-1} (s, Si-H). Elem. Anal. (%): calc. for $C_{27}H_{52}MoNP_3Si$ (607.655) C 53.37, H 8.63, N 2.31; found C 53.76, H 8.53, N 2.21.

Reaction of (ArN)Mo(η^2-BH$_4$)$_2$(PMe$_3$)$_2$ (III-8) with (EtO)$_3$SiH and PMe$_3$

(EtO)$_3$SiH (0.24 ml, 1.28 mmol) and PMe$_3$ (0.33 ml, 3.21 mmol) were added in one portion at room temperature to a solution of (ArN)Mo(η^2-BH$_4$)$_2$(PMe$_3$)$_2$ (**III-8**) (0.15 g, 0.32 mmol) in 20 ml of Et$_2$O. The reaction mixture was left at room temperature with stirring for 5 days. All volatiles were pumped off to give as brown oil of (ArN)Mo(H)(Si(OEt)$_3$)(PMe$_3$)$_3$ (**III-130**), which was dried in vacuum. Yield: 72.2 mg, 34 %. The product is unstable at room temperature in solution and slowly (1 week) decomposes to form (ArN)Mo(OEt)$_2$(PMe$_3$)$_3$ (**III-88**) and a mixture of uncharacterized products. Increasing the temperature of the reaction of **III-8** with (EtO)$_3$SiH up to 50 °C leads to the decomposition process and formation of **III-88**.

(ArN)Mo(H)(Si(OEt)$_3$)(PMe$_3$)$_3$ (**III-130**). ^{1}H-NMR (300 MHz; C_6D_6; δ, ppm): -4.73 (dt, $^{2}J_{P\text{-}H}$ = 18.6 Hz, $^{2}J_{P\text{-}H}$ = 62.1 Hz, 1H, Mo-*H*); 1.20 (d, $^{2}J_{H\text{-}P}$ = 6.6 Hz, 9H, P*Me*$_3$); 1.31 (d, $^{3}J_{H\text{-}H}$ = 6.9 Hz, 12H, 4 *CH*$_3$, N*Ar*); 1.39 (t, $^{3}J_{H\text{-}H}$ = 6.9 Hz, 9H, 3 *CH*$_3$, Si(O*Et*)$_3$); 1.46 (vt,

$^{2}J_{H\text{-}P}$ = 6.6 Hz, 18H, 2 P*Me*$_3$); 4.02 (q, $^{3}J_{H\text{-}H}$ = 6.9 Hz, 6H, 3 *CH*$_2$, Si(O*Et*)$_3$); 4.43 (sept, $^{3}J_{H\text{-}H}$ = 6.9 Hz, 2H, 2 *CH*, N*Ar*); 6.95-6.97 (m, 3H, *m*-H and *p*-H of N*Ar*). ^{31}P{^{1}H}-NMR (121.5 MHz; C_6D_6; δ, ppm): 10.8 (t, $^{2}J_{P\text{-}P}$ = 24.3 Hz, 1P, *P*Me$_3$); -1.46 (d, $^{2}J_{P\text{-}P}$ = 24.3 Hz, 2P, 2 *P*Me$_3$). ^{13}C{^{1}H}-NMR (75.5 MHz; C_6D_6; δ, ppm): 146.1 (s, *i*-c, N*Ar*); 124.9 (s, *o*-C, N*Ar*); 123.6 (s, *m*-C, N*Ar*); 123.0 (s, *p*-C, N*Ar*); 58.1 (s, *C*H$_2$, Si(O*Et*)$_3$); 26.5 (s, *C*H, N*Ar*); 25.2 (d, $^{1}J_{C\text{-}P}$ = 23.4 Hz, P*Me*$_3$); 24.9 (s, *C*H$_3$, N*Ar*); 23.0 (vt, $^{1}J_{C\text{-}P}$ = 21.1 Hz, P*Me*$_3$); 19.7 (s, *C*H$_3$, Si(O*Et*)$_3$). ^{1}H-^{29}Si HSQC NMR (f1: 600 MHz; f2: 119.2 MHz; J = 7 Hz; C_6D_6; ^{29}Si projection; δ, ppm): 25.6 (*Si*(OEt)$_3$).

(ArN)Mo(OEt)$_2$(PMe$_3$)$_3$ (**III-88**). ^{1}H-NMR (300 MHz; C_6D_6; δ, ppm): 6.86-7.04 (m, 3H, *m*-H and *p*-H of N*Ar*); 4.00 (m, 6H, 2*CH* of N*Ar* and 2 *CH*$_2$ of Mo(O*Et*)$_2$); 1.39 (vt, $^{2}J_{H\text{-}P}$ = 7.2 Hz, 18H, 2 P*Me*$_3$); 1.27 (d, $^{2}J_{H\text{-}P}$ = 7.8 Hz, 9H, P*Me*$_3$); 1.21 (t, $^{3}J_{H\text{-}H}$ = 6.9 Hz, 6H, 2 *CH*$_3$, Mo(O*Et*)$_2$); 1.14 (d, $^{3}J_{H\text{-}H}$ = 6.9 Hz, 12H, 4 *CH*$_3$, N*Ar*). ^{31}P{^{1}H}-NMR (121.5 MHz; C_6D_6; δ, ppm): 2.6 (t, $^{2}J_{P\text{-}P}$ = 34.0 Hz, 1P, *P*Me$_3$); -8.84 (d, $^{2}J_{P\text{-}P}$ = 34.0 Hz, 2P, 2 *P*Me$_3$). ^{13}C{^{1}H}-NMR (75.5 MHz; C_6D_6; δ, ppm): 147.2 (s, *i*-c, N*Ar*); 132.6 (s, *o*-C, N*Ar*); 123.4 (s, *m*-C, N*Ar*); 119.2 (s, *p*-C, N*Ar*); 59.6 (s, *C*H$_2$, Mo(O*Et*)$_2$); 27.5 (s, *C*H, N*Ar*); 25.8 (s, *C*H$_3$, Mo(O*Et*)$_2$); 23.4 (d, $^{1}J_{C\text{-}P}$ = 24.9 Hz, P*Me*$_3$); 22.9 (s, *C*H$_3$, N*Ar*); 17.4 (vt, $^{1}J_{C\text{-}P}$ = 22.6 Hz, P*Me*$_3$).

Preparation of (ArN)Mo(H)(R)(PMe$_3$)$_3$ (R = H, SiR'$_3$)

Preparation of (ArN)Mo(H)(Cl)(PMe$_3$)$_3$ (III-6)

A solution of L-Selectride in THF (1.9 ml, 1.9 mmol, 1.0 M) was added at -30 °C to a solution of (ArN)MoCl$_2$(PMe$_3$)$_3$ (**III-47**) (1.05 g, 1.9 mmol) in 50 ml of toluene. The mixture was stirred at -30 °C for 15 min., then allowed to reach ambient temperature and stirred for additional two hours. Once the reaction reached room temperature the colour of the mixture changed from pale green to brown and formation of precipitate was observed. The mixture was filtered and the residue was extracted with 50 ml of toluene. All volatiles were removed in vacuum to give a fine brown solid of (ArN)Mo(H)(Cl)(PMe$_3$)$_3$ (**III-6**). Yield: 0.55 g, 65 %. ^{1}H-NMR (300 MHz; C_6D_6; 25 °C; δ, ppm): 1.19 (d, $^{3}J_{H\text{-}H}$ = 6.6 Hz, 4 *CH*$_3$, N*Ar*); 1.35 (d, $^{2}J_{H\text{-}P}$ = 5.7 Hz, 9H, P*Me*$_3$); 1.45 (vt, $^{2}J_{H\text{-}P}$ = 3 Hz, 18H, 2 P*Me*$_3$); 4.37 (sept, $^{3}J_{H\text{-}H}$ = 6.9 Hz, 2H, 2 *CH*, N*Ar*); 5.31 (dt, $^{1}J_{H\text{-}P}$ = 28.5 Hz, $^{1}J_{H\text{-}P}$ = 51.9 Hz, 1H, Mo-*H*); 6.86 (m, 3H, N*Ar*). ^{31}P{^{1}H}-NMR (121.5 MHz;

C_6D_6; 25 °C; δ, ppm): -17.75 (t, $^2J_{P\text{-}P}$ = 13.4 Hz, 1P, PMe_3); -1.10 (d, $^2J_{P\text{-}P}$ = 13.4 Hz, 2P, 2 PMe_3). $^{13}C\{^1H\}$-NMR (75.5 MHz; C_6D_6; 25 °C; δ, ppm): 21.1 (vt, $^1J_{C\text{-}P}$ = 11.3 Hz, P*Me*$_3$); 21.2 (d, $^1J_{C\text{-}P}$ = 15.9 Hz, P*Me*$_3$); 24.2 (s, *CH*$_3$, N*Ar*); 26.6 (s, *CH*, N*Ar*); 123.2, 124.9, 144.3 (all singlets, N*Ar* aromatic carbons). IR (nujol, selected bands): 1714 cm^{-1} (s, Mo-H). Elem. Anal. (%): calc. for $C_{21}H_{45}ClMoNP_3$ (535.903): C 47.07, H 8.46, N 2.61; found: C 46.47, H 8.14, N 2.77.

Preparation of (ArN)Mo(H)(SiH_2Ph)(PMe_3)$_3$ (III-7)

A. $PhSiH_3$ (128.0 µl, 1.04 mmol) and PMe_3 (108.0 µl, 1.04 mmol) were added at room temperature to a solution of (ArN)Mo(H)(Cl)(PMe_3)$_3$ (**III-6**) (111.0 mg, 0.21 mmol) in 10 ml of benzene. A solution of $LiBH_4$ in THF (2.0 M, 104.0 µl, 0.21 mmol; *Important*: no BH_3 should be present!!!) was added at room temperature and reaction mixture was allowed to stir for 30 minutes. Formation of white precipitate of LiCl was observed. The mixture was filtered; all volatiles were pumped off to give fine brown solid of (ArN)Mo(H)(SiH_2Ph)(PMe_3)$_3$ (**III-7**). Yield: 109.7 mg, 87 %.

B: NMR scale reaction. A solution of MeLi in Et_2O (1.6 M, 22.0 µl, 0.04 mmol) was added at room temperature to a mixture of $PhSiH_3$ (6.5 µl, 0.05 mmol) and (ArN)Mo(H)(Cl)(PMe_3)$_3$ (**III-6**) (19.0 mg, 0.04 mmol) in 0.6 ml of C_6D_6 in NMR tube. The reaction mixture was left at room temperature for 10 min. Formation of white precipitate of LiCl was observed. NMR analysis showed quantitative formation of (ArN)Mo(H)(SiH_2Ph)(PMe_3)$_3$ (**III-7**), which could be isolated *via* extraction with hexanes.

Preparation of (ArN)Mo(H)(SiHMePh)(PMe_3)$_3$ (III-133)

A solution of ^{n}BuLi in hexanes (1.6 M, 0.33 mmol) was added at room temperature to a mixture of $PhMeSiH_2$ (67.0 µl, 0.49 mmol) and (ArN)Mo(H)(Cl)(PMe_3)$_3$ (**III-6**) (174.0 mg, 0.33 mmol) in 10 ml of benzene. The reaction mixture was stirred at ambient temperature for 30 min. Formation of white precipitate of LiCl was observed. All volatiles were pumped off and the residue was extracted with 15 ml of hexanes. The solvent was removed under reduced pressure to give dark-brown oil. Recrystallization from hexanes solution at -80 °C yielded a dark-brown solid of (ArN)Mo(H)(SiHMePh)(PMe_3)$_3$ (**III-133**). Yield: 15.6 mg, 8 %. The product contains a

mixture of isomers due to chirality at the silicon centre). ^{1}H-NMR (300 MHz; C_6D_6; δ, ppm): 7.93 (d, $^{3}J_{H-H}$ = 6.9 Hz, 2H, *o*-H, Si*Ph*); 7.30 (t, $^{3}J_{H-H}$ = 7.2 Hz, 2H); 6.98-7.20 (m, 4H); 5.78 (bm, 1H, Si*H*); 4.27 (sept, $^{3}J_{H-H}$ = 6.9 Hz, 2H, 2 *CH*, N*Ar*); 1.27 (m, 21H, $^{3}J_{H-H}$ = 6.9 Hz, $^{2}J_{H-P}$ = 6.3 Hz, 12H from 4 *CH*$_3$, N*Ar* and 9H from P*Me*$_3$); 1.21 (d, $^{2}J_{H-P}$ = 6.6 Hz, 9H, P*Me*$_3$); 1.14 (d, $^{3}J_{H-H}$ = 4.5 Hz, 3H, Si*Me*); 1.04 (d, $^{2}J_{H-P}$ = 6.0 Hz, 9H, P*Me*$_3$); -3.38 (dtd, $^{2}J_{H-P}$ = 68.1 Hz and 20.1 Hz, Mo*H*). ^{13}C{^{1}H}-NMR (75.5 MHz; C_6D_6; δ, ppm): 21.8 (d, $^{1}J_{C-P}$ = 19.6 Hz, P*Me*$_3$); 23.1 (d, $^{1}J_{C-P}$ = 15.8 Hz, P*Me*$_3$); 24.80 (s, 4*CH*$_3$, N*Ar*); 24.83 (s, 4*CH*$_3$, N*Ar*); 26.65 (d, $^{1}J_{C-P}$ = 23.4 Hz, P*Me*$_3$); 26.73 (d, $^{1}J_{C-P}$ = 21.9 Hz, P*Me*$_3$); 27.3 (s, 2*CH*, N*Ar*); 123.9 (s, *m*-C, N*Ar*); 124.9 (s, *p*-C, N*Ar*); 126.8 (s, *p*-C, Si*Ph*); 127.5 (s, *m*-C, Si*Ph*); 129.9 (s, *i*-C, Si*Ph*); 135.0 (s, *o*-C, N*Ar*); 136.1 (s, *o*-C, Si*Ph*); 145.3 (s, *i*-C, N*Ar*). ^{31}P{^{1}H}-NMR (121.5 MHz; C_6D_6; δ, ppm): -2.6 (qd, $^{2}J_{P-P}$ = 29.2 Hz, 23.1 Hz, 21.9 Hz, 23.1 Hz, 2P, 2 *P*Me$_3$), 11.9 (dd, $^{2}J_{P-P}$ = 23.1 Hz and 21.9 Hz, 1P, *P*Me$_3$). ^{29}Si INEPT+ NMR (59.6 MHz; *J* = 200 Hz; C_6D_6; ^{29}Si projection; δ, ppm): 13.0 (d, $^{1}J_{Si-H}$ = 143.1 Hz, *Si*HMePh).

NMR scale generation of (ArN)Mo(H)(SiMe$_2$Ph)(PMe$_3$)$_3$ (III-134)

A solution of ^{n}BuLi in hexanes (1.6 M, 23.0 µl, 0.041 mmol) was added at room temperature to a solution of PhMe$_2$SiH (9.5 µl, 0.06 mmol) and (ArN)Mo(H)(Cl)(PMe$_3$)$_3$ (**III-6**) (22.0 mg, 0.041 mmol) in 0.6 ml of C_6D_6 in an NMR tube. The reaction mixture was left at ambient temperature for 10 min. Formation of white precipitate of LiCl was observed. NMR analysis showed full conversion of the starting material and formation of a difficult-to-characterize mixture of (ArN)Mo(H)(SiMe$_2$Ph)(PMe$_3$)$_3$ (**III-134**; < 10 %) and unidentified products.

(ArN)Mo(H)(SiMe$_2$Ph)(PMe$_3$)$_3$ (**III-134**): ^{1}H-NMR (300 MHz; C_6D_6; δ, ppm): -2.60 (dt, $^{2}J_{H-P}$ = 17.7 Hz and 69.3 Hz, 1H, Mo*H*); 0.20 (bs, 6H, Si*Me*$_2$Ph); 0.86-1.39 (m, *CH*$_3$ signals of N*Ar*, and P*Me*$_3$ obscured by the signals of impurities); 4.32 (bs 2H, 2 *CH*, N*Ar*); 7.00-7.30 (m, *m*-H and *p*-H of N*Ar* and Si*Ph* obscured by the signals of impurities); 7.81 (d, $^{3}J_{H-H}$ = 7.2 Hz, 2H, *o*-H, Si*Ph*). ^{31}P{^{1}H}-NMR (121.5 MHz; C_6D_6; δ, ppm): 12.9 (t, $^{2}J_{P-P}$ = 21.9 Hz, 1P, *P*Me$_3$); 6.1 (t, $^{2}J_{P-P}$ = 21.9 Hz, 1P, *P*Me$_3$).

Stoichiometric reactivity of (ArN)Mo(H)(Cl)(PMe_3)$_3$ (III-6)

Reaction of (ArN)Mo(H)(Cl)(PMe_3)$_3$ (III-6) with L-Selectride

A solution of L-Selectride (1.55 ml, 1.55 mmol, C = 1 M) in THF was added in one portion at -30 °C to a solution of complex (ArN)Mo(H)(Cl)(PMe_3)$_3$ (**III-6**) (0.88 g, 1.55 mmol) in 30 ml of toluene. The colour of the solution changed to a different tint of brown almost immediately. The mixture was slowly warmed up to room temperature and left with stirring for additional 10 min. The mixture was filtered and all volatiles were removed in vacuum to give a dark-brown oil of (ArN)Mo(H)$_2$(PMe_3)$_3$ (**III-131**). Yield: 0.63g, 77 %. The product is highly fluxional and unstable at room temperature and fully decomposes within 1 h to a mixture of unidentified compounds. ^{1}H-NMR (600 MHz; toluene-d$_8$; -29 °C; δ, ppm): -5.31 (dtd, $^2J_{H\text{-}P}$ = 60.6 Hz, $^2J_{H\text{-}P}$ = 46.2 Hz, $^2J_{H\text{-}H}$ = 7.2 Hz, 1H, Mo*H*); 1.35 (m, 21H, 4 *CH$_3$* of N*Ar* and P*Me$_3$*); 1.49 (bm, 18H, 2 P*Me$_3$*); 2.08 (m, overlapping with residual toluene-d$_8$ signal, $^2J_{H\text{-}P}$ = 43.2 Hz, $^2J_{H\text{-}H}$ = 7.2 Hz, 1H, Mo*H*, found by ^{1}H-^{1}H COSY and ^{1}H-^{31}P HSQC NMR); 4.43 (sept, $^3J_{H\text{-}H}$ = 6.6 Hz, 2H, 2 *CH*, N*Ar*); 6.91-7.32 (m, overlapping with residual toluene-d$_8$ resonances, 3H, *m*-H and *p*-H of N*Ar*). ^{1}H{^{31}P}-NMR (600 MHz; toluene-d$_8$; -30 °C; selected resonances; δ, ppm): -5.31 (d, $^2J_{H\text{-}H}$ = 7.2 Hz, 1H, Mo*H*); 1.38 (s, 9H, P*Me$_3$*); 1.50 (s, 18H, 2 P*Me$_3$*); 2.09 (d, $^2J_{H\text{-}H}$ = 7.2 Hz, 1H, Mo*H*). ^{31}P{^{1}H}-NMR (243 MHz; toluene-d$_8$; -26 °C; δ, ppm): 14 8 (d, $^2J_{P\text{-}P}$ = 19.4 Hz, 2P, 2 *P*Me$_3$); 13.1 (t, $^2J_{P\text{-}P}$ = 19.4 Hz, 1P, *P*Me$_3$). ^{1}H-^{13}C HSQC NMR (f1: 600 MHz; f2: 151 MHz; toluene-d$_8$; -30 °C; ^{13}C projection; δ, ppm): 124.9, 122.0, 121.9, (*m*-C and *p*-C, N*Ar*); 26.3 (*C*H, N*Ar*); 26.2 (*CH$_3$*, N*Ar*); 25.9 (PMe$_3$), 25.0 (*CH$_3$*, N*Ar*); 24.2 (P*Me$_3$*). IR (nujol): 1620 cm^{-1} (broad, medium, Mo-H).

Reaction of (ArN)Mo(H)(Cl)(PMe_3)$_3$ (III-6) with $LiBH_4$

A solution of $LiBH_4$ in THF (0.10 ml, 0.09 mmol, C = 2.0 M; *important*: BH_3 should not be present!!!) was added in one portion at romm temperature to a solution of (ArN)Mo(H)(Cl)(PMe_3)$_3$ (**III-6**) (50.0 mg, 0.09 mmol) in 10 ml of Et_2O. The reaction mixture was stirred at room temperature for 45 min. NMR analysis of the reaction mixture showed the formation of a mixture of (ArN)Mo(H)(η^2-BH_4)(PMe_3)$_2$ (**III-132**; highly fluxioanl at RT) and unidentified decomposition products. All attempts to isolate **III-132** in analytically pure form were unsuccessful. ^{1}H-NMR (300 MHz; C_6D_6; δ, ppm):

7.02 (t, $^3J_{H-H}$ = 7.8 Hz, 1H, *p*-H, N*Ar*); 6.89 (d, $^3J_{H-H}$ = 7.8 Hz, 2H, *m*-H, N*Ar*); 4.41 (sept, $^3J_{H-H}$ = 6.9 Hz, 2H, 2 *CH*, N*Ar*); 1.18 (d, $^3J_{H-H}$ = 6.9 Hz, 12H, 4 *CH*$_3$, N*Ar*); 0.90 (bs, 18H, P*Me*$_3$). $^{31}P\{^1H\}$-NMR (121.5 MHz; C_6D_6; δ, ppm): 3.3 (s, PMe_3).

VT NMR scale reaction of (ArN)Mo(H)(Cl)(PMe$_3$)$_3$ (III-6) with benzaldehyde

Benzaldehyde (5.2 µl, 0.051 mmol) was added at -80 °C to a solution of (ArN)Mo(H)(Cl)(PMe$_3$)$_3$ (**III-6**) (24.1 mg, 0.043 mmol) in 0.6 ml of toluene-d$_8$ in an NMR tube. The mixture was immediately frozen in liquid N_2 and the sample was placed into the NMR machine precooled to -30 °C. The temperature was dropped down to -50 °C and the reaction was monitored by VT NMR spectroscopy. NMR analysis showed the selective formation of *trans*-(ArN)Mo(H)(Cl)(η^2-PhC(O)H)(PMe$_3$)$_2$ (**III-136**) at -5 °C. All attempts to isolate **III-136** were unsuccessful and led to mixtures of **III-136**, (ArN)MoCl$_2$(PMe$_3$)$_3$ (**III-47**), (ArN)Mo(Cl)(OCH$_2$Ph)(PMe$_3$)$_3$ (**III-135**; see the NMR scale generation and characterization below), and unidentified decomposition products.

(ArN)Mo(H)(Cl)(η^2-PhC(O)H)(PMe$_3$)$_2$ (**III-136**): In solution exists as a mixture of two isomers ("up" and "down"), depending on the orientation of coordinated benzaldehyde (5:1 ratio, according to the $^{31}P\{^1H\}$-NMR spectrum). ^{1}H-NMR (600 MHz; toluene-d$_8$; 0 °C; *δ*, ppm): 7.71 (d, $^3J_{H-H}$ = 6.6 Hz, 2H, *o*-H, η^2-O=CH*Ph*, major isomer); 7.32 (dd, $^2J_{H-P}$ = 35.0 Hz, 1H, Mo*H*, major isomer); 7.29 (t, $^3J_{H-H}$ = 6.6 Hz, 2H, *m*-H, η^2-O=CH*Ph*, major isomer); 6.99 (m, 1H, *p*-H, η^2-O=CH*Ph*, major isomer); *o*-H, *m*-H and *p*-H signals of η^2-O=CH*Ph* of minor isomer are overlapping with the aromatic signals of η^2-O=CH*Ph* for major isomer; 7.08 (m, 2H, *m*-H of N*Ar*, overlapping signals of minor and major isomers); 6.85 (m, 1H, *p*-H of N*Ar*, overlapping signals of minor and major isomers); 6.59 (dd, $^2J_{H-P}$ = 41 Hz and 49 Hz, 1H, Mo*H*, minor isomer); 5.77 (s, 1H, η^2-O=C*H*Ph, major isomer); 5.17 (s, 1H, η^2-O=C*H*Ph, minor isomer); 4.37 (bs, 1H, *i*-Pr, N*Ar*, major isomer); 4.31 (bs, 1H, *i*-Pr, N*Ar*, major isomer); 4.12 (sept, $^3J_{H-H}$ = 6.9 Hz, 1H, *i*-Pr, N*Ar*, major isomer); 3.46 (bs, 1H, *i*-Pr, N*Ar*, major isomer); 1.49 (d, $^2J_{H-P}$ = 9.6 Hz (for major isomer), 9H, P*Me*$_3$, both isomers); 1.43 (bs, 6H, *i*-Pr, N*Ar*, both isomers); 1.28 (d, $^3J_{H-H}$ = 6.9 Hz, 3H, *i*-Pr, N*Ar*, major isomer); 1.26 (m, 3H, *i*-Pr, N*Ar*, minor isomer); 1.21 (m, 3H, *i*-Pr, N*Ar*, major isomer); 1.20 (d, $^2J_{H-P}$ = 7.8 Hz, 9H, P*Me*$_3$, minor isomer); 1.16 (d, $^2J_{H-P}$ = 9.6 Hz, 9H, P*Me*$_3$, major isomer); 1.03 (d, $^3J_{H-H}$ = 6.9 Hz, 3H, *i*-Pr, N*Ar*, minor

isomer). $^{31}P\{^1H\}$-NMR (243 MHz; toluene-d_8; -17 °C; δ, ppm): 1.43 (d, $^2J_{P\text{-}P}$ = 109.3 Hz, 1P, PMe_3, major isomer); 0.77 (d, $^2J_{P\text{-}P}$ = 114.2 Hz, 1P, PMe_3, minor isomer); -5.59 (d, $^2J_{P\text{-}P}$ = 109.3 Hz, 1P, PMe_3, major isomer); -5.56 (d, $^2J_{P\text{-}P}$ = 114.2 Hz, 1P, PMe_3, minor isomer). $^{13}C\{^1H\}$-NMR (151 MHz; toluene-d_8; -17 °C; δ, ppm): 150.5, 149.5, 148.2, 147.3, 146.8, 146.7, 144.7, 143.7 (*o*-C and *i*-C of N*Ar* and *i*-C of η^2-O=CH*Ph* for both isomers); 129.5 (s, η^2-O=CH*Ph*, *o*-C, minor isomer); 128.6 (s, η^2-O=CH*Ph*, *p*-C, major isomer); *m*-C and *p*-C signals of η^2-O=CH*Ph* of minor isomer are overlapping with PhMe-d_8 signals and corresponding signals of major isomer; 128.0 (s, η^2-O=CH*Ph*, *o*-C, major isomer); 126.7 (s, η^2-O=CH*Ph*, *m*-C, major isomer); 125.5 (s, *m*-C, N*Ar*, overlapping signals for both isomers); 123.1 and 123.0 (s, *p*-C, N*Ar* for two isomers); 86.8 (bs, η^2-O=*C*HPh, major isomer); 76.9 (s, η^2-O=*C*HPh, minor isomer); 27.0 (s, *i*-Pr, N*Ar*, both isomers); 26.9 (s, *i*-Pr, N*Ar*, major isomer); 25.9 (s, *i*-Pr, N*Ar*, both isomers); 23.4 (s, *i*-Pr, N*Ar*, minor isomer); 23.2 (s, *i*-Pr, N*Ar*, major isomer); 17.2 (d, $^1J_{C\text{-}P}$ = 27.5 Hz, P*Me*$_3$, major isomer); 16.9 (d, $^1J_{C\text{-}P}$ = 24.9 Hz, P*Me*$_3$, minor isomer); 16.8 (s, *i*-Pr, N*Ar*, minor isomer); 13.7 (d, $^1J_{C\text{-}P}$ = 24.9 Hz, P*Me*$_3$, minor isomer); 13.5 (d, $^1J_{C\text{-}P}$ = 27.5 Hz, P*Me*$_3$, major isomer). IR (nujol, selected bands): 1771 cm^{-1} (s, Mo-H); 1595 cm^{-1} (s, C=O)

RT NMR scale reaction of (ArN)Mo(H)(Cl)(PMe_3)$_3$ (III-6) with benzaldehyde

Benzaldehyde (5.2 µl, 0.051 mmol) was added at room temperature to a solution of (ArN)Mo(H)(Cl)(PMe_3)$_3$ (**III-6**) (24.1 mg, 0.043 mmol) in 0.6 ml of C_6D_6 in an NMR tube. NMR analysis after 10 min at room temperature showed the selective formation of (ArN)Mo(H)(Cl)(η^2-PhC(O)H)(PMe_3)$_2$ (**III-136**). The reaction mixture was left at room temperature for 5 h and was monitored by NMR spectroscopy, which during this time revealed the rearrangement of **III-136** into (ArN)Mo(Cl)(OCH_2Ph)(PMe_3)$_3$ (**III-135**).

An analogous room temperature reaction of **III-6** (27.9 mg, 0.049 mmol) with excess benzaldehyde (50.1 µl, 0.49 mmol) gives the formation of (ArN)Mo(Cl)(OCH_2Ph)(η^2-PhC(O)H)(PMe_3) (**III-137**). All attempts to isolate **III-137** gave difficult-to-separate mixtures of **III-137**, (ArN)$MoCl_2$(PMe_3)$_3$ (**III-47**), and (ArN)Mo(Cl)(OCH_2Ph)(PMe_3)$_3$ (**III-135**).

Room temperature addition of excess $PhSiH_3$ (10 equiv. to **III-6**) to both **III-135** and **III-137** releases, after 5 min., $PhH_2Si(OBn)$ and $PhHSi(OBn)_2$[160, 214, 215b] and recovers complex **III-6**.

Stoichiometric reaction of $(ArN)Mo(H)(Cl)(PMe_3)_3$ (**III-6**) with benzaldehyde and $PhSiD_3$ gives exclusively $(ArN)Mo(D)(Cl)(PMe_3)_3$ (**III-6$_D$**) (no Mo-bound hydride was observed in the ^{1}H-NMR spectrum).

(ArN)Mo(Cl)(OCH$_2$Ph)(PMe$_3$)$_3$ (**III-135**): ^{1}H-NMR (300 MHz; C_6D_6; δ, ppm): 7.40 (d, $^3J_{H\text{-}H}$ = 7.5 Hz, 2H, *o*-H, OCH_2*Ph*); 6.86-7.26 (m, 6H, *m*-H and *p*-H of N*Ar* and OCH_2*Ph*); 5.13 (s, 2H, O*CH*$_2$Ph); 4.32 (bm, 2H, 2 *CH*, N*Ar*); 1.58 (m, 6H, 2 *CH*$_3$, N*Ar*); 1.47 (d, $^3J_{H\text{-}H}$ = 6.3 Hz, *CH*$_3$, N*Ar*); 1.35 (bm, 27H, P*Me*$_3$); 1.26 (d, $^3J_{H\text{-}H}$ = 6.3 Hz, *CH*$_3$, N*Ar*). ^{31}P{^{1}H}-NMR (121.5 MHz; toluene-d$_8$; δ, ppm): 8.29 (t, $^2J_{P\text{-}P}$ = 15.8 Hz, 1P, *P*Me$_3$); 9.50 (d, $^2J_{P\text{-}P}$ = 15.8 Hz, 2P, 2 *P*Me$_3$). ^{13}C{^{1}H}-NMR (75.5 MHz; C_6D_6; δ, ppm): 151.4 (s, *i*-C, N*Ar*); 147.5 (s, *i*-C, OCH_2*Ph*); 144.7 (s, *o*-C, N*Ar*); 126.5, 125.3, 123.9 (*m*-C and *p*-C of N*Ar* and *p*-C of OCH_2*Ph*); *o*-C and *m*-C signals of OCH_2*Ph* are overlapping with signal of C_6D_6; 71.5 (s, O*CH*$_2$Ph); 27.2 (s, *i*-Pr, N*Ar*); 22.8 (s, *i*-Pr, N*Ar*); 21.9 (vt, $^1J_{C\text{-}P}$ = 21.2 Hz, P*Me*$_3$); 21.2 (s, *i*-Pr, N*Ar*); 20.9 (s, *i*-Pr, N*Ar*); 20.8 (s, *i*-Pr, N*Ar*); 16.6 (d, $^1J_{C\text{-}P}$ = 20.4 Hz, P*Me*$_3$).

$(ArN)Mo(Cl)(OCH_2Ph)(\eta^2\text{-}PhC(O)H)(PMe_3)$ (**III-137**): ^{1}H-NMR (300 MHz; C_6D_6; δ, ppm): 1.02 (d, $^2J_{H\text{-}P}$ = 7.2 Hz, 9H, P*Me*$_3$); 1.30 (d, $^2J_{H\text{-}P}$ = 7.8 Hz, 9H, P*Me*$_3$); 1.15-1.23 (m, 6H, 2 *CH*$_3$, N*Ar*); 1.28-1.31 (m, 3H, *CH*$_3$, N*Ar*); 1.41-1.44 (m, 3H, *CH*$_3$, N*Ar*); 3.45 (sept, $^3J_{H\text{-}H}$ = 6.7 Hz, 1H, *CH*, N*Ar*); 4.62 (d, $^2J_{H\text{-}H}$ = 12.2 Hz, 1H, O*CH*$_2$Ph); 4.88 (m, 1H, *CH*, N*Ar*); 5.14 (d, $^2J_{H\text{-}H}$ = 12.2 Hz, 1H, O*CH*$_2$Ph); 5.37 (d, $^3J_{H\text{-}P}$ = 3.9 Hz, 1H, η^2-PhC(O)*H*); 6.82-7.60 (m, 13 H, aromatic protons of N*Ar* and 2 C*Ph*).). ^{31}P{^{1}H}-NMR (121.5 MHz; C_6D_6; δ, ppm): -5.2 (d, $^2J_{P\text{-}P}$ = 289.8, 1P, *P*Me$_3$); -6.8 (d, $^2J_{P\text{-}P}$ = 289.8, 1P, *P*Me$_3$). ^{13}C{^{1}H}-NMR (75.5 MHz; C_6D_6; δ, ppm): 11.34 (dd, $^1J_{C\text{-}P}$ = 17.8 Hz, $J_{C\text{-}P}$ = 4.4 Hz, P*Me*$_3$); 13.3 (dd, $^1J_{C\text{-}P}$ = 18.7 Hz, $J_{C\text{-}P}$ = 5.0 Hz, P*Me*$_3$); 71.5 (s, O*CH*$_2$Ph); 90.7 (s, η^2-Ph*C*(O)H).

Preparation of (ArN)Mo(Cl)(OCy)(PMe$_3$)$_3$ (III-138)

Cyclohexanone (64.0 mg, 0.650 mmol) was added to a toluene solution of $(ArN)Mo(H)(Cl)(PMe_3)_3$ (**III-6**) (350.0 mg, 0.650 mmol). The reaction mixture was left

at room temperature fo 24 h. The product was crystallized at -78 °C, filtered off and dried in vacuum, affording a light-green crystalline solid of (ArN)Mo(Cl)(OCy)(PMe_3)$_3$ (**III-138**). Yield: 120 mg, 51 %. ^{1}H-NMR (300 MHz; C_6D_6; δ, ppm): 0.72-1.53 (m, 8H, O*Cy* and 12H, 4 *CH*$_3$, N*Ar*); 1.25 (d, $^2J_{H-P}$ = 7.3 Hz, 9H, P*Me*$_3$); 1.29 (vt, $^2J_{H-P}$ = 2.9 Hz, 18H, 2 P*Me*$_3$); 1.53-1.64 (m, 1H, O*Cy*); 1.67-1.80 (m, 2H, O*Cy*); 1.92-2.04 (m, 2H, O*Cy*); 3.1-4.3 (bm, 1H, *CH*, N*Ar*); 4.07 (m, 1H, *CH*-O, O*Cy*); 4.3-5.4 (bm, 1H, *CH*, N*Ar*); 6.85-7.08 (m, 3H, N*Ar*). ^{31}P{^{1}H}-NMR (121.5 MHz; C_6D_6; δ, ppm): -12.2 (d, $^2J_{P-P}$ = 14.8 Hz, 2P, 2 *P*Me$_3$); 7.0 (t, $^2J_{P-P}$ = 14.8 Hz, 1P, *P*Me$_3$). ^{13}C{^{1}H}-NMR (75.5 MHz; C_6D_6; δ, ppm): 17.3 (vt, $^1J_{C-P}$ = 9.4 Hz, P*Me*$_3$); 22.7 (d, $^1J_{C-P}$ = 20.7 Hz, P*Me*$_3$); 26.3 (s, *Cy*); 27.2 (s, *Cy*); 39.8 (s, *Cy*); 76.1 (s, *C*-O, *Cy*); 124.3 (s, N*Ar*); 128.7 (s, N*Ar*); 151.4 (s, *i*-C, N*Ar*); other signals were not found due to the fluxionality of the product.

NMR scale reaction of (ArN)Mo(H)(Cl)(PMe_3)$_3$ (III-6) with ethanol

EtOH (1.2 µl, 0.02 mmol) was added in one portion at room temperature to a solution of (ArN)Mo(H)(Cl)(PMe_3)$_3$ (**III-6**) (10.1 mg, 0.019 mmol) in 0.6 ml of C_6D_6 in an NMR tube. Release of the gas was observed almost immediately and the colour of the mixture slowly turned from brown to light green. The reaction mixture was monitored with NMR spectroscopy for 16 h at room temperature until all starting material was consumed. All volatiles were pumped off, the oily residue was dried in vacuum, redissolved in fresh C_6D_6 and checked with NMR analysis, which showed the presence of the only one product (ArN)Mo(Cl)(OEt)(PMe_3)$_3$ (**III-140**). Complex **III-140** is stable in solution at room temperature at least for a week. All attempts to crystallize **III-140** gave a greenish brown oily substance. Addition of excess $PhSiH_3$ to a solution of **III-40** in C_6D_6 at room temperature gives, after 5 min., the formation of $PhH_2Si(OEt)$ and recovers **III-6**.

(ArN)Mo(Cl)(OEt)(PMe$_3$)$_3$ (**III-140**): ^{1}H-NMR (300 MHz, C_6D_6 δ, ppm): 7.00 (m, 3H, *m*-H and *p*-H of N*Ar*); 4.31 (bs, 2H, 2*CH*, N*Ar*); 4.11 (q, $^3J_{H-H}$ = 6.9 Hz, 2H, O*CH*$_2$); 1.26 (m, 27H, 3P*Me*$_3$); 1.19 (d, $^3J_{H-H}$ = 6.9 Hz, 6H, 2*CH*$_3$, N*Ar*); 1.17 (d, $^3J_{H-H}$ = 6.9 Hz, 6H, 2*CH*$_3$, N*Ar*); 1.10 (t, $^3J_{H-H}$ = 6.9 Hz, 3H, OCH$_2$*CH*$_3$). ^{31}P{^{1}H}-NMR (121.5 MHz; C_6D_6; δ, ppm): 8.19 (t, $^2J_{P-P}$ = 15.8 Hz, *P*Me$_3$); -9.19 (d, $^2J_{P-P}$ = 15.8 Hz, 2*P*Me$_3$). ^{13}C{^{1}H}-NMR (75.5 Hz; C_6D_6; δ, ppm): 123.3 (s, N*Ar*); 123.2 (s, NAr); 64.4 (s, O*CH*$_2$); 26.1 (s,

CH, NA*r*); 25.6 (s, CH_3, NA*r*); 25.1 (s, CH_3, NA*r*); 21.4 (d, $^1J_{C\text{-}P}$ = 23.1 Hz, P*Me*$_3$); 20.7 (s, OCH_2CH_3); 16.8 (vt, $^1J_{C\text{-}P}$ = 11.6 Hz, P*Me*$_3$).

NMR scale reaction of (ArN)Mo(H)(Cl)(PMe_3)$_3$ (III-6) with benzyl alcohol

Benzyl alcohol (8.5 μl, 0.08 mmol) was added in one portion at room temperature to a solution of (ArN)Mo(H)(Cl)(PMe_3)$_3$ (**III-6**) (8.6 mg, 0.016 mmol) in 0.6 ml of C_6D_6 in an NMR tube. Immediate gas release and changing of the solution colour from brown to light green was observed. The mixture was left at room temperature for 5 h. NMR analysis after that showed full conversion of the starting material and the formation of a difficult-to-separate mixture of (ArN)Mo(Cl)(OCH_2Ph)(PMe_3)$_3$ (**III-135**) and (ArN)$MoCl_2$(PMe_3)$_3$ (**III-47**) (the ratio is 3:1, respectively, according to $^{31}P\{^1H\}$-NMR analysis). Lowering the temperature of the experiment does not improve selectivity of the reaction.

NMR scale reaction of (ArN)Mo(H)(Cl)(PMe_3)$_3$ (III-6) with acetonitrile

A. Acetonitrile (1.1 μl, 0.02 mmol) was added in one portion at room temperature to a solution of (ArN)Mo(H)(Cl)(PMe_3)$_3$ (**III-6**) (10.4 mg, 0.02 mmol) in 0.6 ml of C_6D_6 in an NMR tube. No visual changes were observed after CH_3CN addition. The mixture was left at room temperature for 5 min. and then the reaction was monitored by NMR analysis for 24 h, showing full conversion of the starting material to give (ArN)Mo(Cl)(N=CHMe)(PMe_3)$_2$ (**III-141**) as a mixture of *cis*- and *trans*- isomers (ratio 1:1.6, according to the $^{31}P\{^1H\}$-NMR spectrum).

B. A solution of (ArN)Mo(H)(Cl)(PMe_3)$_3$ (**III-6**) (22.7 mg, 0.04 mmol) and CH_3CN (5.0 μl, 0.1 mmol) in 0.6 ml of C_6D_6 was added in one portion at room temperature to a solid BPh_3 (9.7 mg, 0.04 mmol). Immediate formation of white precipitate of $Ph_3B{\cdot}PMe_3$ was observed. The mixture was transferred to an NMR tube and left at room temperature for 5 min. NMR analysis showed quantitative formation of (ArN)Mo(Cl)(N=CHMe)(PMe_3)$_2$ (**III-141**) (1:1.3 mixture isomers, according to the $^{31}P\{^1H\}$-NMR spectrum). The mixture was filtered, all volatiles were pumped off, and the residue was dried and extracted with 2.0 ml of hexanes. The solvent was removed in vacuum to give a brown oily substance. Yield: 13.7 mg, 68 %. ^{1}H-NMR (300 MHz; C_6D_6; δ, ppm): 7.70 (m, $^3J_{H\text{-}H}$ = 4.8 Hz, 1H, -N=C(*H*)CH_3, minor isomer, found through ^{1}H-^{13}C HMBC NMR); 6.86-7.13 (m, NA*r*

aromatic protons of both isomers); 6.15 (m, $^{3}J_{H\text{-}H}$ = 5.1 Hz, 1H, -N=C(*H*)CH_3, major isomer, found by ^{1}H-^{13}C HMBC NMR); 4.27 (sept, $^{3}J_{H\text{-}H}$ = 6.9 Hz, 2H, 2 *CH*, N*Ar*, minor isomer); 4.12 (sept, $^{3}J_{H\text{-}H}$ = 6.9 Hz, 2H, 2 *CH*, N*Ar*, major isomer); 2.37 (ddd, $^{3}J_{H\text{-}H}$ = 5.1 Hz, $J_{H\text{-}P}$ = 1.5 Hz and 2.7 Hz, 3H, -N=C(H)*CH_3*, major isomer, found by ^{1}H-^{13}C HMBC NMR); 2.26 (ddd, $^{3}J_{H\text{-}H}$ = 4.8 Hz, $J_{H\text{-}P}$ = 1.5 Hz and 3.6 Hz, 3H, -N=C(H)*CH_3*, minor isomer, found by ^{1}H-^{13}C HMBC NMR); 1.29 (d, $^{3}J_{H\text{-}H}$ = 6.9 Hz, 12H, 4 *CH_3*, N*Ar*, major isomer); 1.27 (d, $^{3}J_{H\text{-}H}$ = 6.9 Hz, 12H, 4 *CH_3*, N*Ar*, minor isomer); 1.16 (dd, $^{2}J_{H\text{-}P}$ = 7.2 Hz, $^{4}J_{H\text{-}P}$ = 3.6 Hz, 18H, 2 P*Me_3*, both isomers). $^{1}H\{^{31}P\}$-NMR (300 MHz; C_6D_6; δ, ppm; selected resonances): 7.70 (q, $^{3}J_{H\text{-}H}$ = 5.1 Hz, 1H, -N=C(*H*)CH_3, minor isomer); 6.15 (q, $^{3}J_{H\text{-}H}$ = 5.1 Hz, 1H, -N=C(*H*)CH_3, major isomer); 2.37 (d, $^{3}J_{H\text{-}H}$ = 5.1 Hz, 3H, -N=C(H)*CH_3*, major isomer); 2.26 (d, $^{3}J_{H\text{-}H}$ = 4.8 Hz, 3H, -N=C(H)*CH_3*, minor isomer); 1.16 (s, 18H, 2P*Me_3*, both isomers). $^{31}P\{^{1}H\}$-NMR (121.5 MHz; C_6D_6; δ, ppm): -0.1 (bs, 2*P*Me_3, minor isomer); -0.3 (s, 2*P*Me_3, major isomer). ^{31}P-NMR (121.5 MHz; C_6D_6; δ, ppm): -0.2 (bs, PMe_3, both isomers). $^{13}C\{^{1}H\}$-NMR (75.5 MHz, C_6D_6; δ, ppm): 154.1, 147.1 (s, aromatic N*Ar*); 146.6 (bs, -N=*C*(H)CH_3, minor isomer, found by ^{1}H-^{13}C HSQC NMR); 145.4 (d, $J_{C\text{-}P}$ = 11.3 Hz, -N=*C*(H)CH_3, major isomer, found by ^{1}H-^{13}C HSQC NMR); 125.7, 124.9, 123.6, 123.2, 115.9 (s, aromatic N*Ar*); 27.9 (s, *CH*, N*Ar*, major isomer); 27.7 (s, *CH*, N*Ar*, minor isomer); 23.72 (s, *CH_3*, N*Ar*, minor isomer); 23.67 (s, *CH_3*, N*Ar*, major isomer); 23.0 (s, -N=C(H)*CH_3*, major isomer); 19.1 (bs, -N=C(H)*CH_3*, minor isomer); 14.0 (dd, $^{3}J_{C\text{-}P}$ = 11.3 Hz, $^{1}J_{C\text{-}P}$ = 22.6 Hz, 2 P*Me_3*, minor isomer); 13.6 (dd, $^{3}J_{C\text{-}P}$ = 11.3 Hz, $^{1}J_{C\text{-}P}$ = 21.9 Hz, 2P*Me_3*, major isomer).

Reaction of (ArN)Mo(H)(Cl)(PMe_3)$_3$ (III-6) with benzonitrile

A: NMR scale generation of (ArN)Mo(Cl)(N=CHPh)(PMe_3)$_2$ (III-142). Benzonitrile (3.8 µl, 0.037 mmol) was added at room temperature in one portion to a solution of (ArN)Mo(H)(Cl)(PMe_3)$_3$ (**III-6**) (20.0 mg, 0.037 mmol) in 0.6 ml of C_6D_6 in an NMR tube. Immediate change of the colour from brown to greenish brown was observed. The mixture was left at room temperature for 5 min., and then the reaction was monitored by NMR analysis for 1.3 h at room temperature. The $^{31}P\{^{1}H\}$-NMR spectrum showed full conversion of the starting material, release of one equivalent of PMe_3, and quantitative formation of (ArN)Mo(Cl)(N=CHPh)(PMe_3)$_2$ (**III-142**). $PhSiH_3$ (4.6 µl, 0.037 mmol)

was added in one portion at room temperature to a mixture of **III-142** and PMe_3 in C_6D_6. The mixture was left at room temperature for 5 min., and then monitored by NMR spectroscopy. After 1 h at room temperature no reaction was observed and the mixture was left at 50 °C overnight. The ^{1}H-NMR analysis showed very slow formation of a mixture of $PhH_2Si(N{=}CHPh)$ (94 %) and $PhHSi(N{=}CHPh)_2$ (6 %) with only 5 % (according to the $^{31}P\{^1H\}$-NMR spectrum) conversion of **III-142** into the hydrido chloride **III-6**. Redistribution of $PhSiH_3$ to give Ph_2SiH_2 and SiH_4[211] was also observed. Addition of excess of $PhSiH_3$ and heating the reaction mixture at 50 °C for 14 days leads to the formation of $PhCH_2N(SiH_2Ph)_2$, and full conversion of **III-142** to give a 1:1 mixture of **III-6** and $(ArN)MoCl_2(PMe_3)_3$ (**III-47**).

B: NMR scale reaction of (ArN)Mo(Cl)(N=CHMe)(PMe_3)$_2$ (III-141) with PhCN. $(ArN)Mo(Cl)(N{=}CHMe)(PMe_3)_2$ (**III-141**) was generated in an NMR tube in 0.6 ml of C_6D_6 from $(ArN)Mo(H)(Cl)(PMe_3)_3$ (**III-6**) (10.4 mg, 0.02 mmol) and acetonitrile (1.1 µl, 0.02 mmol) (see procedure above). All volatiles were pumped off and the residue was dried in vacuum and redissovled in 0.6 ml of C_6D_6. Benzonitrile (10.0 µl, 0.098 mmol) was added in one portion to solution. The reaction mixture was left at room temperature for 24 h. NMR analysis showed full conversion of **III-141**, evolution of one equivalent of CH_3CN, and formation of $(ArN)Mo(Cl)(N{=}CHPh)(PMe_3)_2$ (**III-142**).

C: preparation of (ArN)Mo(Cl)(N=CHPh)(PMe_3)$_2$ (III-142). PhCN (36.0 µl, 0.352 mmol) was added in one portion at room temperature to a solution of $(ArN)Mo(H)(Cl)(PMe_3)_3$ (**III-6**) (188.9 mg, 0.352 mmol) in 15 ml of toluene. The mixture was stirred at room temperature for 50 min. All volatiles were pumped off, and the residue was extracted with 30 ml of diethyl ether. Et_2O solution was concentrated to 10 ml and left at -80 °C for a week affording a yellow powder of $(ArN)Mo(Cl)(N{=}CHPh)(PMe_3)_2$ (**III-142**), which was filtered off and dried in vacuum. Yield: 125.0 mg, 63 %. ^{1}H-NMR (300 MHz; C_6D_6; δ, ppm): 7.38 (d, $^3J_{H\text{-}H}$ = 7.6 Hz, 2H, *o*-H, -N=CH*Ph*); 7.27 (m, 2H, *m*-H, -N=CH*Ph*); 7.23 (t, $J_{H\text{-}P}$ = 6.0 Hz, 1H, -N=C*H*Ph, found by ^{1}H-^{31}P HSQC (J = 30 Hz) and ^{1}H-^{13}C HSQC NMR); 7.06 (m, 2H, *m*-H, N*Ar*); 6.85 (m, 1H, *p*-H, N*Ar*); 6.63 (t, $^3J_{H\text{-}H}$ = 7.6 Hz, 1H, *p*-H, -N=CH*Ph*); 4.21 (sept, $^3J_{H\text{-}H}$ = 7.0 Hz, 2H, 2 *CH*, N*Ar*); 1.32 (d, $^3J_{H\text{-}H}$ = 7.0 Hz, 12H, 4 *CH*$_3$, N*Ar*); 1.10 (dd, $^2J_{H\text{-}P}$ = 7.2 Hz, 18H, 2 P*Me*$_3$). $^1H\{^{31}P\}$-NMR (300 MHz; C_6D_6; selected resonances; δ, ppm): 7.22 (s,

1H, Mo-N=C*H*Ph); 1.10 (s, 18H, 2 P*Me*$_3$). ^{31}P{^{1}H}-NMR (121.6 MHz; C_6D_6; δ, ppm): -0.7 (s, 2 *P*Me$_3$). ^{1}H-^{13}C HSQC NMR (f1: 300 MHz; f2: 75.5 MHz, J = 145.0 Hz; C_6D_6; ^{13}C projection; δ, ppm): 150.2 (Mo-N=*C*HPh); 131.6, 128.7, 128.3, 123.5, 122.9, 122.3 (aromatic carbons of C*Ph* and N*Ar*); 27.6 (*C*H, N*Ar*); 23.5 (*C*H$_3$, N*Ar*); 13.0 (P*Me*$_3$). Elem. Anal. (%): calc. for $C_{25}H_{41}ClMoN_2P_2$ (562.947): C 53.34, H 7.34, N 4.98; found: C 53.04, H 7.30, N

PhCH$_2$*N(SiH*$_2$*Ph)*$_2$: ^{1}H-NMR (300 MHz; C_6D_6; δ, ppm): 5.19 (s, 4H, 2 Si*H*$_2$Ph); 4.00 (s, 2H, Ph*CH*$_2$).

NMR scale reaction of (ArN)Mo(Cl)(N=CHPh)(PMe$_3$)$_2$ (III-142) with benzaldehyde

Benzaldehyde (1.9 µl, 0.019 mmol) and was PMe$_3$ (2.0 µl, 0.019 mmol) were added at room temperature to a solution of (ArN)Mo(Cl)(N=CHPh)(PMe$_3$)$_2$ (**III-142**) (10.5 mg, 0.019 mmol) in 0.6 ml of C_6D_6 in an NMR tube. The reaction mixture was left at room temperature overnight. NMR analysis showed full conversion of the starting material and the formation of (ArN)Mo(Cl)(OCH$_2$Ph)(PMe$_3$)$_3$ (**III-135**), accompanied by the release of one equivalent of PhCN. Traces of (ArN)MoCl$_2$(PMe$_3$)$_3$ (**III-47**) were also observed in the NMR spectra.

NMR scale reaction of (ArN)Mo(Cl)(N=CHPh)(PMe$_3$)$_2$ (III-142) with L-Selectride

A solution of L-Selectride in THF (12.4 µl, 0.011 mmol, C = 0.85 M) was added in one portion at room temperature to a solution of (ArN)Mo(Cl)(N=CHPh)(PMe$_3$)$_2$ (**III-142**) (5.9 mg, 0.011 mmol) and PMe$_3$ (1.1 µl, 0.011 mmol) in 0.6 ml of C_6D_6 in an NMR tube. Immediately after addition of L-Selectride, the reaction mixture changed colour to a different tint of brown. NMR analysis after 10 min. at room temperature showed full conversion of the starting material and formation of a highly fluxional compound, which was assigned to (ArN)(PhCH$_2$N)Mo(PMe$_3$)$_3$ (**III-143**). ^{1}H-NMR (300 MHz; C_6D_6; δ, ppm): 7.00-7.71 (bm, 8H, N*Ar* and CH$_2$*Ph*); 3.67 (bm, 1H, CH, N*Ar*); 1.25-1.60 (bm, 4 *CH*$_3$, N*Ar* and *CH*$_2$); 1.01 (bm, 3 P*Me*$_3$). No signals were observed in the ^{31}P{^{1}H}-NMR spectrum due to the fluxionality of the product.

NMR scale reaction of (ArN)Mo(Cl)(N=CHPh)(PMe_3)$_2$ (III-142) with CatBH

CatBH (4.5 μl, 0.042 mmol) was added at room temperature in one portion to a solution of (ArN)Mo(Cl)(N=CHPh)(PMe_3)$_2$ (**III-142**) (22.5 mg, 0.042 mmol) in 0.6 ml of C_6D_6 in an NMR tube. Immediately after addition of CatBH, the colour of the mixture changed from yellowish brown to red. The reaction mixture was left at room temperature for 25 min. NMR analysis showed full conversion of the startion material and formation of (ArN)Mo(H)(Cl)(PMe_3)$_3$ (**III-6**) in a mixture with unidentified products. The reaction is also accompanied by the release of $PhCH_2N(BCat)_2$ (see the characterization below).

NMR scale reaction of (ArN)Mo(H)(Cl)(PMe_3)$_3$ (III-6) with styrene

Styrene (5.3 μl, 0.046 mmol) was added in one portion at room temperature to a solution of (ArN)Mo(H)(Cl)(PMe_3)$_3$ (**III-6**) (26.2 mg, 0.046 mmol) in 0.6 ml of C_6D_6 in an NMR tube. No visual changes were observed after $PhCH=CH_2$ addition. The mixture was left at room temperature for 5 min. and then the reaction was monitored by NMR analysis for 24 hours. Release of phosphine and the formation of styrene adduct *trans*-(ArN)Mo(H)(Cl)(PMe_3)$_2$(η^2-CH_2=CHPh) (**III-144**) in a mixture with the starting material was detected by NMR spectroscopy (**III-6/III-144** = 1.3 by the ^{31}P-NMR spectrum). No further conversion of the hydrido chloride **III-6** into **III-144** was observed in additional 24 hours. The mixture was added at room temperature to solid BPh_3 (11.2 mg, 0.046 mmol). Immediate formation of white precipitate of BPh_3·PMe_3 was observed. NMR analysis after 5 min. at room temperature showed full conversion of complex **III-6** and the quantitative formation of **III-144** as a mixture of two isomers (7:1 ratio, depending on the orientation of coordinated styrene). The mixture was filtered, all volatiles were pumped off, and the residue was extracted with 1 ml of hexane to give a brown oil. Yield: 13.2 mg, 51 %. The product is not stable in solution at room temperature and slowly (1 week) decomposes to give $PhCH_2CH_3$ and a difficult-to-characterize mixture of unidentified compounds.

trans-(ArN)Mo(H)(Cl)(PMe_3)$_2$(η^2-CH_2=CHPh) (**III-144**): ^{1}H-NMR (300 MHz; C_6D_6; δ, ppm): 7.61 (bd, $^3J_{H\text{-}H}$ = 6.9 Hz, 1H, *o*-H, CH_2=CH*Ph*); 7.43 (bd, $^3J_{H\text{-}H}$ = 6.9 Hz, 1H, *o*-H, CH_2=CH*Ph*); 7.27 (bm, 4H N*Ar* and *m*-H of CH_2=CH*Ph*); 7.02 (bm, 1H, *p*-H, CH_2=CH*Ph*); 6.84 (bm, 2H, N*Ar* and Mo-*H*, found by ^{1}H-^{31}P HSQC NMR, major

isomer); 5.97 (dd, $^{2}J_{H\text{-}P}$ = 51.3 Hz, $^{2}J_{H\text{-}P}$ = 31.8 Hz, 1H, Mo-*H*, minor isomer); 4.08 (bm, 1H, CH_2=CHPh, major isomer); 3.82 (m, 1H, CH_2=CHPh, minor isomer); 3.50 (bm, 1H, CH_2=CHPh, major isomer); 3.33 (bm, 2H, 2 *CH*, N*Ar*); 3.18 (m, 2H, CH_2=CHPh, minor isomer); 2.63 (broad dd, $J_{H\text{-}H}$ = 12.9 Hz, 1H, CH_2=CHPh, major isomer); 1.40 (bm, 9H, P*Me*$_3$, overlapping signals for both isomers); 1.20 (bd, $^{3}J_{H\text{-}H}$ = 6.6 Hz, 6H, 2 *CH*$_3$, N*Ar*); 1.12 (bm, 15H, 2 *CH*$_3$ of N*Ar* and P*Me*$_3$). ^{1}H{^{31}P}-NMR (300 MHz; C_6D_6; δ, ppm): 7.61 (d, $^{3}J_{H\text{-}H}$ = 6.9 Hz, 1H, *o*-H, CH_2=CH*Ph*); 7.43 (d, $^{3}J_{H\text{-}H}$ = 6.9 Hz, 1H, *o*-H, CH_2=CH*Ph*); 7.29 (m, 4H, N*Ar* and *m*-H of CH_2=CH*Ph*); 7.04 (m, 1H, *p*-H, CH_2=CH*Ph*); 6.84 (m, 2H, N*Ar* and Mo-*H*, found by ^{1}H-^{31}P HSQC NMR, major isomer); 5.97 (s, 1H, Mo-*H*, minor isomer); 4.08 (dd, $J_{H\text{-}H}$ = 13.7 Hz and 11.0 Hz, 1H, CH_2=CHPh, major isomer); 3.82 (dd, $J_{H\text{-}H}$ = 12.9 Hz, 1H, CH_2=CHPh, minor isomer); 3.50 (dd, $J_{H\text{-}H}$ = 11.0 Hz and 3.9 Hz, 1H, CH_2=CHPh, major isomer); 3.33 (sept, $^{3}J_{H\text{-}H}$ = 6.9 Hz, 2H, 2 *CH*, N*Ar*); 3.20 (m, 1H, CH_2=CHPh, minor isomer); 3.13 (dd, $J_{H\text{-}H}$ = 12.9 Hz and 3.6 Hz, 1H, CH_2=CHPh, minor isomer); 2.63 (dd, $J_{H\text{-}H}$ = 13.7 Hz and 3.9 Hz, 1H, CH_2=CHPh, major isomer); 1.40 (s, 9H, P*Me*$_3$, major isomer); 1.37 (s, 9H, P*Me*$_3$, minor isomer); 1.20 (d, $^{3}J_{H\text{-}H}$ = 6.9 Hz, 6H, 2 *CH*$_3$, N*Ar*); 1.15 (d, $^{3}J_{H\text{-}H}$ = 6.9 Hz, 6H, 2 *CH*$_3$, N*Ar*); 1.11 (s, 9H, P*Me*$_3$). ^{1}H-NMR (600 MHz; toluene-d_8; -15 °C; selected resonances; δ, ppm): 5.04 (bs, 1H, *CH*, N*Ar*, major isomer); 4.43 (m, 1H, *CH*, N*Ar*, minor isomer); 3.75 4.43 (m, 1H, *CH*, N*Ar*, minor isomer); 2.91 4.43 (bs, 1H, *CH*, N*Ar*, major isomer). ^{31}P{^{1}H}-NMR (243 MHz; toluene-d_8; δ, ppm): -2.7 (d, $^{2}J_{P\text{-}P}$ = 104.0, *P*Me$_3$, minor isomer); -0.05 (s, 2*P*Me$_3$, major isomer); 0.06 (d, $^{2}J_{P\text{-}P}$ = 104.0, *P*Me$_3$, minor isomer). ^{31}P-NMR (121.5 MHz; C_6D_6; δ, ppm): -0.05 (d, $^{2}J_{P\text{-}H}$ = 39.2 Hz, 2 *P*Me$_3$, major isomer). ^{31}P{^{1}H}-NMR (243 MHz; toluene-d_8; -18 °C; δ, ppm): -2.2 (d, $^{2}J_{P\text{-}P}$ = 103.7 Hz, *P*Me$_3$, minor isomer); 0.4 (d, $^{2}J_{P\text{-}P}$ = 111.0 Hz, *P*Me$_3$, major isomer); 0.8 (d, $^{2}J_{P\text{-}P}$ = 103.7 Hz, *P*Me$_3$, minor isomer); 1.0 (d, $^{2}J_{P\text{-}P}$ = 111.0 Hz, *P*Me$_3$, major isomer). ^{13}C{^{1}H}-NMR (75.5 MHz; C_6D_6; δ, ppm, major isomer): 149.0, 147.3, 146.6, 143.2 (s, quaternary C of N*Ar* and CH_2=CH*Ph*); 135.7 (s, *o*-C, CH_2=CH*Ph*); 128.4, 126.8, 125.7, 124.2, 123.4 (s, *m*-C and *p*-C of N*Ar* and CH_2=CH*Ph*); 60.5 (s, CH_2=*CH*Ph); 49.6 (bs, *CH*$_2$=CHPh); 28.4 (s, *CH*, N*Ar*); 24.9 (s, *CH*$_3$, N*Ar*); 23.9 (s, *CH*$_3$, N*Ar*); 17.9 (d, $^{1}J_{C\text{-}P}$ = 12.8 Hz, P*Me*$_3$); 17.5 (d, $^{1}J_{C\text{-}P}$ = 12.1 Hz, P*Me*$_3$). ^{1}H-^{13}C HSQC NMR (f1: 300 MHz; f2: 75.5 MHz; *J* = 145.0 Hz; C_6D_6; δ, ppm, selected

resonances for minor isomer): 72.2 (PhCH=CH_2); 51.7 (PhCH=CH_2). IR (nujol, selected bands): 1757 cm^{-1} (s, Mo-H).

Stoichiometric reactions of (ArN)Mo(H)(SiH_2Ph)(PMe_3)$_3$ (III-7)

NMR scale reaction of (ArN)Mo(H)(SiH_2Ph)(PMe_3)$_3$ (III-7) with $PhSiD_3$

$PhSiD_3$ (2.1 μl, 0.017 mmol) was added in one portion at room temperature to a solution of (ArN)Mo(H)(SiH_2Ph)(PMe_3)$_3$ (**III-7**) (10.3 mg, 0.017 mmol) and tetramethylsilane (1.0 μl, 0.007 mmol) in 0.6 ml of C_6D_6 in an NMR tube. The reaction mixture was left at room temperature for 10 min. NMR analysis showed scrambling of D between the silyl and the hydride positions: 59 % and 65 % of H/D exchange were observed for the hydride and silyl positions of **III-7**, respectively. The percentage of incorporated D was calculated *via* integration of the residual H resonances for the hydride and silyl substituents of the complex before and after $PhSiD_3$ additions. In both cases all the integrals were normalized in accordance with the integral of tetramethylsilane.

NMR scale reaction of (ArN)Mo(H)(SiH_2Ph)(PMe_3)$_3$ (III-7) with (*m*-Tol)SiH_3

(*m*-Tol)SiH_3 (2.5 μl, 0.017 mmol) was added in one portion at room temperature to a solution of (ArN)Mo(H)(SiH_2Ph)(PMe_3)$_3$ (**III-7**) (10.3 mg, 0.017 mmol) and tetramethylsilane (1.0 μl, 0.007 mmol) in 0.6 ml of C_6D_6 in an NMR tube. The reaction mixture was left at room temperature for 10 min. NMR analysis showed the formation of a mixture of **III-7** (73 %) and (ArN)Mo(H)[SiH_2(*m*-Tol)](PMe_3)$_3$ (**III-7$_{tol}$**, 27 %). The same ratio was found for the mixture of silanes (*m*-Tol)SiH_3 and $PhSiH_3$ in the ^{1}H-NMR spectrum. Percentages of **III-7** and **III-7$_{tol}$** in a mixture were calculated by the integration of the *ortho*-protons of the Si*Ph* and Si(*m-Tol*) groups (found by ^{1}H-^{13}C HMBC NMR spectroscopy by correlation of the Si*H* protons and *o*-H protons of Ph and *m*-Tol to the *i*-C of the Ph and *m*-Tol groups at Si) in complexes and was additionally verified by the normalization of these integrals in accordance with the integral intensity of tetramethylsilane resonance.

Preparation of (ArN)Mo(η^2-PhC(O)H)$_2$(PMe$_3$)$_2$ (III-145*PMe$_3$) and (ArN)Mo(η^2-PhC(O)H)$_2$(PMe$_3$) (III-145)

A: Room temperature NMR scale reaction of (ArN)Mo(H)(SiH$_2$Ph)(PMe$_3$)$_3$ (III-7) with benzaldehyde. PhC(O)H (11.6 μl, 0.114 mmol) was added in one portion at room temperature to a solution of (ArN)Mo(H)(SiH$_2$Ph)(PMe$_3$)$_3$ (**III-7**) (17.4 mg, 0.029 mmol) in 0.6 ml of C_6D_6 in an NMR tube. The reaction mixture was left at room temperature for 5 min. NMR analysis showed full conversion of the starting material and quantitative formation of (ArN)Mo(η^2-PhC(O)H)$_2$(PMe$_3$)$_2$ (**III-145*PMe$_3$**). Formation of PhHSi(OBn)$_2$[160, 214, 215b] and the release of PMe$_3$ were also detected by NMR spectroscopy. The product **III-145*PMe$_3$** is stable in solution at room temperature, however, decomposition was observed upon removal of volatiles in vacuum. ^{1}H-^{1}H EXSY NMR experiment for the mixture of **III-145*PMe$_3$** and PhC(O)H revealed no intermolecular, but showed slow intramolecular benzaldehyde exchange.

B: Low temperature VT NMR scale reaction of (ArN)Mo(H)(SiH$_2$Ph)(PMe$_3$)$_3$ (III-7) with benzaldehyde. PhC(O)H (13.7 μl, 0.135 mmol) was added in one portion to a frozen in liq. N_2 solution of (ArN)Mo(H)(SiH$_2$Ph)(PMe$_3$)$_3$ (**III-7**) (20.5 mg, 0.0337 mmol) in 0.6 ml of toluene-d$_8$ in an NMR tube. The mixture was slowly warmed up to -30 °C and placed into precooled to -30 °C NMR machine. The temperature was dropped down to -50 °C. At this temperature, NMR analysis showed the disappearance of **III-7** and formation of (ArN)Mo(η^2-PhC(O)H)$_2$(PMe$_3$)$_2$ (**III-145*PMe$_3$**) and PhHSi(OBn)$_2$.[160, 214, 215b] Warming the reaction mixture up to -40 °C leads to the dissociation of PMe$_3$ and formation of the mono(phosphine) complex (ArN)Mo(η^2-PhC(O)H)$_2$(PMe$_3$) (**III-145**), which, according to ^{31}P-^{31}P EXSY NMR spectroscopy, undergoes PMe$_3$ exchange with an external phosphine and PMe$_3$ ligands of **III-145*PMe$_3$**.

After full conversion of the starting material to complex **III-145** (2 hours at -20 °C) the reaction mixture was frozen in liq. N_2 and PhSiH$_3$ (12.5 μl, 0.1013 mmol) was added to the NMR tube. The sample was brought to -60 °C and the mixture was gradually warmed up with monitoring by NMR spectroscopy. At -15 °C, NMR analysis showed slow formation of (ArN)Mo(η^2-PhC(O)H)(PMe$_3$)$_3$ (**III-146**) and PhH$_2$Si(OBn).[160, 214, 215b] At 0 °C and higher, complex **III-146** reacts with PhSiH$_3$ to recover the starting compound **III-7** and form PhH$_2$Si(OBn). Addition of excess PhC(O)H to the mixture of

III-7, $PhH_2Si(OBn)$ and $PhHSi(OBn)_2$ leads, after overnight at room temperature, to the formation of $PhSi(OBn)_3$[160, 214, 215b]. All attempts to isolate complex **III-146** were unsuccessful due to its instability.

C: PhC(O)H (30.0 µl, 0.295 mmol) was added in one portion at room temperature to a solution of $(ArN)Mo(H)(SiH_2Ph)(PMe_3)_3$ (**III-7**) (43.7 mg, 0.072 mmol) in 2.5 ml of Et_2O. The reaction mixture was stirred at room temperature for 15 min. and then kept at -30 °C for a month, affording yellow-orange crystals of $(ArN)Mo(\eta^2\text{-}PhC(O)H)_2(PMe_3)$ (**III-145**), which were washed with cold (~ -30 °C) hexanes and dried in vacuum. Yield: 19.7 mg, 49 %. Exposing the solution of complex **III-145** to air at room temperature leads to surprisingly slow decomposition (~ 50 % overnight) to a mixture of unidentified products.

$(ArN)Mo(\eta^2\text{-}PhC(O)H)_2(PMe_3)_2$ (**III-145*PMe$_3$**): ^{1}H-NMR (600 MHz; toluene-d_8; - 55 °C; δ, ppm): 0.66 (bs, 9H, P*Me$_3$*); 1.15 (bs, 9H, P*Me$_3$*); 1.23 (bm, 6H, 2 *CH$_3$*, N*Ar*); 1.29 (bs, 3H, *CH$_3$*, N*Ar*); 1.45 (bs, 3H, *CH$_3$*, N*Ar*); 3.47 (bs, 1H, *CH*, N*Ar*); 4.36 (bs, 1H, *CH*, N*Ar*); 5.18 (d, $^3J_{H\text{-}P}$ = 9.6 Hz, 1H, η^2-O=C*H*Ph); 5.42 (bs, 1H, η^2-O=C*H*Ph); 6.83-7.32 (m, 5H, *m*-H and *p*-H of N*Ar*, *p*-H of two η^2-O=CH*Ph* ligands, resonances are obscured by the signals of C_6D_6, and $PhSiH(OBn)_2$); 7.40 (bs, 2H, *m*-H, η^2-O=CH*Ph*); 7.47 (bs, 2H, *m*-H, η^2-O=CH*Ph*); 7.71 (bd, $^3J_{H\text{-}H}$ = 6.0 Hz, 2H, *o*-H, η^2-O=CH*Ph*); 7.96 (bd, $^3J_{H\text{-}H}$ = 6.6 Hz, 2H, *o*-H, η^2-O=CH*Ph*). ^{31}P{^{1}H}-NMR (243 MHz; PhMe-d_8; - 27 °C; δ, ppm): -7.0 (d, $^2J_{P\text{-}P}$ = 218.7 Hz, *P*Me$_3$); 7.4 (d, $^2J_{P\text{-}P}$ = 218.7 Hz, *P*Me$_3$). ^{31}P{^{1}H}-NMR (243 MHz; toluene-d_8; - 55 °C; δ, ppm): -6.4 (d, $^2J_{P\text{-}P}$ = 219.5 Hz, *P*Me$_3$); 8.0 (d, $^2J_{P\text{-}P}$ = 219.5 Hz, *P*Me$_3$). ^{1}H-^{13}C HSQC NMR (f1: 600 MHz; F2: 151 MHz; toluene-d_8; - 30 °C; *J* = 145.0 Hz; ^{13}C projection; selected resonances; δ, ppm): 85.2 (η^2-O=*CH*Ph); 86.1 (η^2-O=*CH*Ph).

$(ArN)Mo(\eta^2\text{-}PhC(O)H)_2(PMe_3)$ (**III-145**): ^{1}H-NMR (600 MHz; C_6D_6; δ, ppm): 1.07 (d, $^3J_{H\text{-}H}$ = 6.6 Hz, 6H, 2 *CH$_3$*, N*Ar*); 1.12 (m, 15 H, 2 *CH$_3$* of N*Ar* and P*Me$_3$*); 3.43 (s, 1H, η^2-O=C*H*Ph); 3.43 (sept, $^3J_{H\text{-}H}$ = 6.6 Hz, 2H, 2 *CH*, N*Ar*); 5.86 (s, 1H, η^2-O=C*H*Ph); 6.80-6.88 (m, 5H, *o*-H and *p*-H of η^2-O=CH*Ph* and *m*-H of N*Ar*); 6.94 (t, $^3J_{H\text{-}H}$ = 8.4 Hz, 1H, *p*-H, N*Ar*); 6.99 (t, $^3J_{H\text{-}H}$ = 7.2 Hz, 1H, *p*-H, η^2-O=CH*Ph*); 7.08 (t, $^3J_{H\text{-}H}$ = 7.8 Hz, 2H, *m*-H, η^2-O=CH*Ph*); 7.27 (t, $^3J_{H\text{-}H}$ = 7.2 Hz, 2H, *m*-H, η^2-O=CH*Ph*); 7.50 (d, $^3J_{H\text{-}H}$ = 7.8 Hz, 2H, *o*-H, η^2-O=CH*Ph*). ^{31}P{^{1}H}-NMR (243 MHz; C_6D_6; δ, ppm): - 1.0 (s, *P*Me$_3$).

$^{13}C\{^1H\}$-NMR (151 MHz; C_6D_6; δ, ppm): 10.8 (d, $^2J_{C\text{-}P}$ = 22.6 Hz, P*Me*$_3$); 22.9 (s, 2 *CH*$_3$, N*Ar*); 24.2 (s, 2 *CH*$_3$, N*Ar*); 28.2 (s, 2 *CH*, N*Ar*); 75.1 (s, η^2-O=*C*HPh); 84.6 (s, η^2-O=*C*HPh); 122.4, 123.4, 125.1, 125.2, 125.3, 128.3, 128.4, 128.6, 143.4, 147.8, 147.9, 153.1 (all aromatic carbons of N*Ar* and two η^2-O=CH*Ph* ligands). IR (nujol, selected bands): 1596 cm^{-1} (strong, C=O); 1487 cm^{-1} (strong, C=O). Elem. Anal. (%): calc. for $C_{29}H_{38}MoNO_2P$ (559.530) C 62.25, H 6.85, N 2.50; found C 62.22, H 6.95, N 2.30.

(ArN)Mo(η^2-PhC(O)H)(PMe$_3$)$_3$ (**III-146**): ^{1}H-NMR (600 MHz; toluene-d_8; 0 °C; *δ*, ppm): 0.77 (d, $^2J_{H\text{-}P}$ = 6.0 Hz, 9H, P*Me*$_3$); 1.08 (d, $^2J_{H\text{-}P}$ = 7.2 Hz, 9H, P*Me*$_3$); all *CH*$_3$ signals of N*Ar* ligand are in the range 1.12-1.21 (found by ^{1}H-^{1}H COSY NMR) and are obscured by the aliphatic resonances of compounds **III-7** and **III-145** present in the mixture; 1.25 (bs, 9H, P*Me*$_3$); 3.71 (sept, $^3J_{H\text{-}H}$ = 7.2 Hz, 1H, *CH*, N*Ar*); 3.90 (sept, $^3J_{H\text{-}H}$ = 6.6 Hz, 1H, *CH*, N*Ar*); 5.59 (t, $^3J_{H\text{-}P}$ = 4.8 Hz, 1H, η^2-O=C*H*Ph); all aromatic signals of **III-146** are overlapping with the resonances of $PhHSi(OBn)_2$, **III-7**, **III-145**, and the residual C_6D_6 signal. $^{31}P\{^1H\}$-NMR (243 MHz; toluene-d_8; 0 °C; *δ*, ppm): -10.4 (d, $^2J_{P\text{-}P}$ = 255.1 Hz, 1P, *P*Me$_3$); -0.21 (dd, $^2J_{P\text{-}P}$ = 9.7 Hz and 255.1 Hz, 1P, *P*Me$_3$); 8.5 (vt, $^2J_{P\text{-}P}$ = 9.7 Hz, 1P, *P*Me$_3$). ^{1}H-^{13}C HSQC NMR (f1: 600 MHz; F2: 151 MHz; toluene-d_8; - 30 °C; *J* = 145.0 Hz; ^{13}C projection; selected resonances; *δ*, ppm): 73.0 (η^2-O=*CH*Ph).

NMR scale preparation of (ArN)Mo(SiH$_2$Ph)(O^{i}Pr)(PMe$_3$)$_2$ (III-147)

Acetone (3.5 µl, 0.048 mmol) was added in one portion to a frozen in liq. N_2 solution of (ArN)Mo(H)(SiH$_2$Ph)(PMe$_3$)$_3$ (**III-7**) (29.2 mg, 0.048 mmol) in 0.6 ml of toluene-d_8 in an NMR tube. The sample was immediately placed into precooled to -30 °C NMR machine. Upon increase of the temperature of the experiment the reaction was monitored by NMR analysis indicating at 0 °C very slow and selective transformation of **III-7** into (ArN)Mo(SiH$_2$Ph)(O^{i}Pr)(PMe$_3$)$_2$ (**III-147**). No intermediate compounds were observed below this temperature. Increase of the temperature of the experiment leads to a faster formation of **III-147** and full conversion was achieved after 1.3 h at room temperature. The 1D ^{1}H EXSY NMR spectra showed no exchange between free acetone and O^{i}Pr group, however, room temperature 1D ^{31}P EXSY NMR experiment revealed an intermolecular PMe_3 exchange. All volatiles were pumped off to give brown oil, which was dried in vacuum and redissolved in C_6D_6. NMR analysis showed the presence of only

complex **III-147** in solution. The product is fluxional at room temperature. The ^{1}H projection of the ^{1}H-^{13}C HSQC NMR spectrum registered at - 30 °C showed a normal $^{1}J_{H\text{-}C}$ of 138 Hz for CH in O^{i}Pr. All attempts to isolate the product gave mixtures of **III-147** with unidentified decomposition products.

(ArN)Mo(SiH$_2$Ph)(O^{i}Pr)(PMe$_3$)$_2$ (**III-147**): ^{1}H-NMR (600 MHz; toluene-d$_8$; -28 °C; δ, ppm): 1.11 (bs, 18H, 2 P*Me$_3$*); 1.27 (d, $^{3}J_{H\text{-}H}$ = 5.5 Hz, 6H, 2 *CH$_3$*, O^{i}*Pr*); 1.39 (d, $^{3}J_{H\text{-}H}$ = 6.6 Hz, 12H, 4 *CH$_3$*, N*Ar*); 3.84 (sept, $^{3}J_{H\text{-}H}$ = 6.6 Hz, 1H, *CH*, N*Ar*); 4.12 (sept, $^{3}J_{H\text{-}H}$ = 6.6 Hz, 1H, *CH*, N*Ar*); 4.24 (bs, 1H, *CH*, O^{i}*Pr*); 5.82 (bs, 2H, Si*H$_2$*Ph); 6.94 – 7.24 (m, 3H, *m*-H and *p*-H of N*Ar* overlapping with residual signals of toluene-d$_8$); 7.25 (t, $^{3}J_{H\text{-}H}$ = 6.9 Hz, 1H, *p*-H, SiH$_2$*Ph*); 7.34 (t, $^{3}J_{H\text{-}H}$ = 6.9 Hz, 2H, *m*-H, SiH$_2$*Ph*); 8.04 (d, $^{3}J_{H\text{-}H}$ = 6.9 Hz, 2H, *o*-H, SiH$_2$*Ph*). ^{31}P{^{1}H}-NMR (243 MHz; toluene-d$_8$; 22 °C; δ, ppm): -5.9 (s, 2 *P*Me$_3$). ^{13}C{^{1}H}-NMR (151 MHz; toluene-d$_8$; 0 °C; δ, ppm): 152.7; 148.3; 136.5 (s, *o*-C, Si*Ph*); 126.91; 126.87; 126.6; 123.5; 123.1 (all aromatic carbons of N*Ar* and Si*Ph*); 72.4 (s, O*C*H); 30.1 (bs, *CH*, N*Ar*); 27.2 (bs, *CH*, N*Ar*); 25. (s, *CH$_3$*, O^{i}Pr); 24.9 (s, *CH$_3$*, O^{i}Pr); 24.6 (bs, *CH$_3$*, N*Ar*); 23.7 (bs, *CH$_3$*, N*Ar*); 16.1 (d, $^{1}J_{C\text{-}P}$ = 13.6 Hz, P*Me$_3$*). ^{1}H-^{29}Si HSQC NMR (f1:300 MHz; f2: 59.6 MHz; *J* = 200 Hz; C$_6$D$_6$; ^{29}Si projection; δ, ppm): 4.9 (*Si*H$_2$Ph).

NMR scale reaction of (ArN)Mo(SiH$_2$Ph)(O^{i}Pr)(PMe$_3$)$_2$ (III-147) with acetone

Acetone (40.4 µl, 0.55 mmol) was added to a solution of (ArN)Mo(SiH$_2$Ph)(O^{i}Pr)(PMe$_3$)$_2$ (**III-147**) (generated *in situ* from 16.7 mg (0.028 mmol) of (ArN)Mo(H)(SiH$_2$Ph)(PMe$_3$)$_3$ (**III-7**) and 2.0 µl (0.028 mmol) of acetone) in 0.6 ml of C$_6$D$_6$ in an NMR tube. The reaction was monitored by NMR analysis overnight at room temperature showing slow (12 h) conversion of **III-147** into (ArN)Mo(SiH$_2$Ph)(η^2-O-C(Me)$_2$CH$_2$C(O)Me)(PMe$_3$) (**III-148**), accompanied by the release of an equivalent of PMe$_3$. ^{1}H-NMR (300 MHz; C$_6$D$_6$; δ, ppm): 1.01 (d, $^{2}J_{H\text{-}P}$ = 9.0 Hz, 9H, P*Me$_3$*); 1.26 (d, $^{3}J_{H\text{-}H}$ = 6.6 Hz, 6H, 2 *CH$_3$*, N*Ar*); 1.32 (m, 9H, 2 *CH$_3$* of N*Ar* and *CH$_3$* of η^2-OC*(Me)$_2$*CH$_2$C(O)Me); 1.42 (m, 3H, *CH$_3$*, η^2-OC*(Me)$_2$*CH$_2$C(O)Me); 2.16 (d, $^{2}J_{H\text{-}H}$ = 12.9 Hz, 1H, η^2-OC(Me)$_2$*CH$_2$*C(O)Me); 2.23 (s, 3H, η^2-OC(Me)$_2$CH$_2$C(O)*Me*); 2.59 (d, $^{2}J_{H\text{-}H}$ = 12.9 Hz, 1H, η^2-OC(Me)$_2$*CH$_2$*C(O)Me); 4.01 (sept, $^{3}J_{H\text{-}H}$ = 6.9 Hz, 1H, *CH*, N*Ar*); 4.07 (sept, $^{3}J_{H\text{-}H}$ = 6.6 Hz, 1H, *CH*, N*Ar*); 5.87 (m, 2H, Si*H$_2$*Ph); 6.98 (m, 3H, *m*-H and *p*-H, N*Ar*); 7.23 (m, 3H,

m-H and *p*-H, SiH_2Ph); 7.80 (m, 2H, *o*-H, SiH_2Ph). $^{31}P\{^1H\}$-NMR (121.5 MHz; C_6D_6; δ, ppm): -6.7 (s, PMe_3).

NMR scale reaction of (ArN)Mo(SiH_2Ph)(O^iPr)(PMe_3)$_2$ (III-147) with PMe_3

PMe_3 (46.8 µl, 0.615 mmol) was added in one portion at room temperature to a solution of complex (ArN)Mo(SiH_2Ph)(O^iPr)(PMe_3)$_2$ (**III-147**) (generated *in situ* from 24.9 mg (0.041 mmol) of (ArN)Mo(H)(SiH_2Ph)(PMe_3)$_3$ (**III-7**) and 3.0 µl (0.041 mmol) of acetone; PMe_3 released in the reaction was removed in vacuum) in 0.6 ml of C_6D_6 in an NMR tube. The reaction mixture was left at room temperature for 5 min. NMR analysis showed full conversion of **III-147** and the formation of **III-7** with the release of an equivalent of acetone.

NMR scale reaction of (ArN)Mo(SiH_2Ph)(O^iPr)(PMe_3)$_2$ (III-147) with benzaldehyde

Benzaldehyde (19.5 µl, 0.193 mmol) was added in one portion at room temperature to a solution of (ArN)Mo(SiH_2Ph)(O^iPr)(PMe_3)$_2$ (**III-147**) (generated *in situ* from 29.2 mg (0.048 mmol) of (ArN)Mo(H)(SiH_2Ph)(PMe_3)$_3$ (**III-7**) and 3.5 µl (0.048 mmol) of acetone) in 0.6 ml of C_6D_6 in NMR tube. The colour of the mixture changed to a different tint of brown almost immediately. NMR analysis after 10 min. at room temperature showed the release of acetone and selective formation of bis(benzaldehyde) adduct (ArN)Mo(η^2-PhC(O)H)$_2$(PMe_3)$_2$ (**III-145*PMe_3**) and $PhHSi(OBn)_2$.[160, 214, 215b]

NMR scale reaction of (ArN)Mo(SiH_2Ph)(O^iPr)(PMe_3)$_2$ (III-147) with cyclohexanone

Cyclohexanone (20.0 µl, 0.193 mmol) was added in one portion at room temperature to a solution of (ArN)Mo(SiH_2Ph)(O^iPr)(PMe_3)$_2$ (**III-147**) (generated *in situ* from 23.4 mg (0.039 mmol) of (ArN)Mo(H)(SiH_2Ph)(PMe_3)$_3$ (**III-7**) and 14.1 µl (0.193 mmol) of acetone; excess of $Me_2C(O)$ and released PMe_3 were removed in vacuum) in 0.6 ml of C_6D_6 in an NMR tube. The reaction mixture was left at room temperature overnight. NMR analysis showed the formation of a mixture of **III-147** and (ArN)Mo(SiH_2Ph)(OCy)(PMe_3)$_2$ (**III-149**) (1:1, according to the $^{31}P\{^1H\}$-NMR spectrum) and the release of acetone (see reparation and characterization of **III-149** below).

NMR scale reaction of (ArN)Mo(SiH_2Ph)(O^iPr)(PMe_3)$_2$ (III-147) with benzonitrile

Benzonitrile (3.2 μl, 0.028 mmol) was added in one portion at room temperature to a solution of (ArN)Mo(SiH_2Ph)(O^iPr)(PMe_3)$_2$ (**III-147**) (generated *in situ* from 16.7 mg (0.028 mmol) of (ArN)Mo(H)(SiH_2Ph)(PMe_3)$_3$ (**III-7**) and 2.0 μl (0.028 mmol) of acetone) in 0.6 ml of C_6D_6 in an NMR tube. No visual changes were observed after addition of PhCN, and the reaction mixture was left at room temperature for 2 hours. NMR analysis after that showed full conversion of complex **III-147** and the formation of (ArN)Mo(SiH_2Ph)(N=CHPh)(η^2-$Me_2C(O)$)(PMe_3)$_2$ (**III-150**; 70 % by $^{31}P\{^1H\}$-NMR spectroscopy; ~1:1 mixture of *cis-* and *trans-* isomers). ^{1}H-NMR (300 MHz; C_6D_6; mixture of isomers; δ, ppm): 1.09 (m, 2 P*Me$_3$* for each isomer, both isomers); 1.32 (d, $^3J_{H-H}$ = 6.9 Hz, 6H, 2 *CH$_3$*, N*Ar*, both isomers); 1.38 (d, $^3J_{H-H}$ = 6.9 Hz, 6H, 2 *CH$_3$*, N*Ar*, both isomers); 1.59 (m, 4 CH_3, η^2-*Me$_2$*C(O), both isomers); 4.18 (sept, $^3J_{H-H}$ = 6.9 Hz, 1H, *CH*, N*Ar*, one isomer); 4.36 (sept, $^3J_{H-H}$ = 6.9 Hz, 1H, *CH*, N*Ar*, one isomer); 5.50 (t, $^3J_{H-P}$ = 5.7 Hz, 2H, Si*H$_2$*Ph, one isomer); 5.61 (t, $^3J_{H-P}$ = 6.0 Hz, 2H, Si*H$_2$*Ph, one isomer); 6.80-7.55 (m, overlapping aromatic proton for both isomers); 7.83 (m, 2H, *o*-H, C*Ph*, one isomer); 7.96 (m, 1H, N=C*H*Ph, one isomer); 8.38 (m, 2H, *o*-C, *Ph*, one isomer). $^{31}P\{^1H\}$-NMR (121.5 MHz; C_6D_6; mixture of isomers; δ, ppm): 2.3 (s, 2 *P*Me_3, one isomer); 2.8 (s, 2 *P*Me_3, one isomer).

NMR scale reaction of (ArN)Mo(SiH_2Ph)(O^iPr)(PMe_3)$_2$ (III-147) with $PhSiH_3$

A: Room temperature reaction in the presence of PMe_3. $PhSiH_3$ (5.0 μl, 0.041 mmol) and PMe_3 (4.2 μl, 0.041 mmol) were added simultaneously in one portion at room temperature to a solution of complex (ArN)Mo(SiH_2Ph)(O^iPr)(PMe_3)$_2$ (**III-147**) (generated *in situ* from 24.9 mg (0.041 mmol) of (ArN)Mo(H)(SiH_2Ph)(PMe_3)$_3$ (**III-7**) and 3.0 μl (0.041 mmol) of acetone) in 0.6 ml of C_6D_6 in an NMR tube. The reaction mixture was left at room temperature for 5 min. NMR analysis showed full conversion of **III-147** and selective regeneration of complex **III-7**, accompanied by the release of $PhH_2Si(O^iPr)$.[160, 221]

B: Low temperature VT reaction. $PhSiH_3$ (7.6 μl, 0.062 mmol) was added in one portion to a frozen in liq. N_2 solution of complex (ArN)Mo(SiH_2Ph)(O^iPr)(PMe_3)$_2$ (**III-147**) (prepared *in situ* from 37.6 mg (0.062 mmol) of (ArN)Mo(H)(SiH_2Ph)(PMe_3)$_3$ (**III-**

7) and 22.7 μl (0.309 mmol) of acetone; excess acetone and released PMe_3 were removed in vacuum) in 0.6 ml of toluene-d_8 in an NMR tube. The mixture was immediately placed into precooled to – 30 °C NMR machine and the temperature was dropped down to – 50 °C. The temperature of the experiment was gradually increased and the reaction was monitored by NMR analysis, which at – 45 °C showed the release of $PhH_2Si(O^iPr)$ and $PhHSi(O^iPr)_2$[160, 221] and formation of $(ArN)Mo(H)_2(SiH_2Ph)_2(PMe_3)_2$ (**III-151**) (mixture of two isomers in a ratio 10:1, according to $^{31}P\{^1H\}$-NMR spectroscopy). An increase of the temperature of the experiment did not afford observation of other intermediates. Only formation of $(ArN)Mo(H)(SiH_2Ph)(PMe_3)_3$ (**III-7**) was observed upon warming the sample up to room temperature.

(ArN)Mo(H)$_2$(SiH$_2$Ph)$_2$(PMe$_3$)$_2$ (**III-151**): ^{1}H-NMR (600 MHz; toluene-d_8; - 45 °C; major isomer; δ, ppm): 0.77 (bs, 9H, P*Me$_3$*); 0.93 (bs, 6H, 2 *CH$_3$*, N*Ar*); 1.04 (bs, 6H, 2 *CH$_3$*, N*Ar*); 1.13 (bs, 6H, 2 *CH$_3$*, N*Ar*); 1.17 (bs, 9H, P*Me$_3$*); 1.23 (bs, 6H, 2 *CH$_3$*, N*Ar*); 2.53 (t, $^2J_{H\text{-}P}$ = 42.0 Hz, 1H, Mo*H*); 3.50 (d, $^2J_{H\text{-}P}$ = 25.7 Hz, 1H, Mo*H*); 4.10 (bs, 2H, 2 *CH*, N*Ar*); 5.06 (d, $^3J_{H\text{-}P}$ = 21.8 Hz, 1H Si*H$_2$*Ph); 5.51 (bs, 1H, Si*H$_2$*Ph); 5.78 (bd, $^3J_{H\text{-}P}$ = 15.8 Hz, 1H, Si*H$_2$*Ph); 6.04 (bs, 1H, Si*H$_2$*Ph); 6.73 (bs, 2H, overlapping signals of *p*-H for 2 SiH$_2$*Ph*); 6.86-7.40 (5 H, *m*-H of N*Ar* and SiH$_2$*Ph*, *p*-H of N*Ar*, signals overlapping with residual PhMe-d_8 resonances); 7.41 (bs 2H, *m*-H, SiH$_2$*Ph*); 7.96 (bs, 2H, *o*-H, SiH$_2$*Ph*); 8.45 (bs, 2H, *o*-H, SiH$_2$*Ph*). $^1H\{^{31}P\}$-NMR (600 MHz; toluene-d_8; - 45 °C; major isomer; selected resonances; δ, ppm): 2.53 (bs, 1H, Mo*H*); 3.50 (bs, 1H, Mo*H*); 5.05 (bs, 1H, Si*H$_2$*Ph); 5.51 (bs, 1H, Si*H$_2$*Ph); 5.78 (bs, 1H, Si*H$_2$*Ph); 6.04 (bs, 1H, Si*H$_2$*Ph). ^{1}H-NMR (selectively decoupled from one PMe_3 group at -32.9 ppm in the $^{31}P\{^1H\}$-NMR spectrum); 600 MHz; toluene-d_8; - 45 °C; major isomer; selected resonances; δ, ppm): 2.51 (bd, $^2J_{H\text{-}P}$ = 41.0 Hz, 1H, Mo*H*); 3.53 (d, $^2J_{H\text{-}P}$ = 25.7 Hz, 1H, Mo*H*); 5.03 (d, $^3J_{H\text{-}P}$ = 21.8 Hz, 1H Si*H$_2$*Ph); 5.50 (bs, 1H, Si*H$_2$*Ph); 5.79 (bt, $^3J_{H\text{-}P}$ = 7.0 Hz, 1H, Si*H$_2$*Ph); 5.99 (bs, 1H, Si*H$_2$*Ph). ^{1}H-NMR (selectively decoupled from one PMe_3 group at -12.5 ppm in the $^{31}P\{^1H\}$-NMR spectrum); 600 MHz; toluene-d_8; - 45 °C; major isomer; selected resonances; δ, ppm): 2.51 (bd, $^2J_{H\text{-}P}$ = 41.6 Hz, 1H, Mo*H*); 3.52 (bs, 1H, Mo*H*); 5.03 (bs, , 1H Si*H$_2$*Ph); 5.50 (d, $^3J_{H\text{-}P}$ = 10.6 Hz, 1H, Si*H$_2$*Ph); 5.8 (bt, $^3J_{H\text{-}P}$ = 6.9 Hz, 1H, Si*H$_2$*Ph); 5.99 (bs, 1H, Si*H$_2$*Ph). $^{31}P\{^1H\}$-NMR (243 MHz; toluene-d_8; - 45 °C; δ, ppm): - 37.6 (d, $^2J_{P\text{-}P}$ = 32.1 Hz, *P*Me$_3$, minor isomer); - 32.9 (d, $^2J_{P\text{-}P}$ = 32.7 Hz, *P*Me$_3$, major isomer); -

12.5 (d, $^2J_{P\text{-}P}$ = 32.7 Hz, PMe$_3$, major isomer); -6.4 (d, $^2J_{P\text{-}P}$ = 32.1 Hz, PMe$_3$, minor isomer). ^{31}P-NMR (selectively decoupled from Me groups at 1.17 ppm in the ^{1}H-NMR spectrum; 243 MHz; toluene-d$_8$; - 30 °C; major isomer; δ, ppm): -12.8 (t, $J_{P\text{-}H}$ = 34.9 Hz, P*Me$_3$*); -33.4 (bs, PMe$_3$). ^{31}P-NMR (selectively decoupled from Me groups at 0.77 ppm in the ^{1}H-NMR spectrum; 243 MHz; toluene-d$_8$; - 30 °C; major isomer; δ, ppm): - 12.8 (bs, P*Me$_3$*); - 33.3 (bs, PMe$_3$). ^{13}C{^{1}H}-NMR (151 MHz; toluene-d$_8$; - 50 °C; major isomer; δ, ppm): 17.0 (d, $^1J_{C\text{-}P}$ = 21.1 Hz, P*Me$_3$*); 19.6 (d, $^1J_{C\text{-}P}$ = 26.7 Hz, P*Me$_3$*); 23.3 (s, *CH$_3$*, N*Ar*); 24.5 (s, *CH$_3$*, N*Ar*); 25.0 (s, *CH$_3$*, N*Ar*); 25.6 (s, *CH$_3$*, N*Ar*); 27.1 (s, *CH*, N*Ar*); 122.9 (s, *p*-H, SiH$_2$*Ph*); 135.8 (s, *m*-C, SiH$_2$*Ph*); 136.0 (s, *o*-C, SiH$_2$*Ph*); 137.6 (s, *o*-C, SiH$_2$*Ph*). ^{29}Si INEPT+ NMR (119.2 MHz; toluene-d$_8$; - 50 °C; J = 200 Hz; major isomer; δ, ppm): - 12.1 (two doublets, $^1J_{Si\text{-}H}$ = 160.4 Hz and 171.7 Hz, overlapping resonances for two *Si*H$_2$Ph groups).

NMR scale reaction of (ArN)Mo(SiH$_2$Ph)(O^{i}Pr)(PMe$_3$)$_2$ (III-147) with (*m*-Tol)SiH$_3$

(*m*-Tol)SiH$_3$ (3.5 µl, 0.028 mmol) and PMe$_3$ (2.8 µl, 0.028 mmol) were added simultaneously in one portion at room temperature to a solution of (ArN)Mo(SiH$_2$Ph)(O^{i}Pr)(PMe$_3$)$_2$ (**III-147**) (generated *in situ* from 16.7 mg (0.028 mmol) of (ArN)Mo(H)(SiH$_2$Ph)(PMe$_3$)$_3$ (**III-7**) and 2.0 µl (0.028 mmol) of acetone) in 0.6 ml of C$_6$D$_6$ in an NMR tube. The reaction mixture was left for 15 min at room temperature. NMR analysis showed the formation of **III-7** exclusively and (*m*-Tol)H$_2$Si(O^{i}Pr). Formation of (*m*-Tol)H$_2$Si(O^{i}Pr) was suggested on the basis of a series of ^{1}H-^{13}C and ^{1}H-^{1}H correlation NMR experiments, however, busy NMR spectra prevented characterization of hydrosilation product. Exclusive formation of **III-7** was also observed in the NMR scale reactions of **III-147** with PhMeSiH$_2$ and PhMe$_2$SiH, which were done analogously to the reaction of **III-147** with PhSiH$_3$.

Preparation of (ArN)Mo(SiH$_2$Ph)(OCy)(PMe$_3$)$_2$ (III-149)

Cyclohexanone (7.0 µl, 0.067 mmol) was added in one portion at room temperature to a solution of (ArN)Mo(H)(SiH$_2$Ph)(PMe$_3$)$_3$ (**III-7**) (37.1 mg, 0.061 mmol) in 0.6 ml of C$_6$D$_6$ in an NMR tube. The reaction mixture was left at room temperature for 30 min. NMR analysis showed full conversion the starting material, release of one equivalent of PMe$_3$, and the selective formation of (ArN)Mo(SiH$_2$Ph)(OCy)(PMe$_3$)$_2$ (**III-149**). All

volatiles were pumped off; the residue was dried in vacuum and extracted with 4 ml of Et_2O. Ether solution was concentrated to ~2 ml and left at – 30 C° for two days affording precipitation of brown crystals, which were filtered off and dried in vacuum. Yield: 11.1 mg, 29 %. The product is fluxional at room temperature. ^{1}H-NMR (300 MHz; C_6D_6; δ, ppm): 7.99 (bd, $^3J_{H\text{-}H}$ = 6.9 Hz, 2H, *o*-H, Si*Ph*); 7.00-7.30 (m, 6H, *m*-H and *p*-H of N*Ar* and Si*Ph*); 5.75 (bs, 2H, SiH_2Ph); 4.06 (bs, 1H, *CH*, N*Ar*); 3.98 (bs, 1H, *CH*, N*Ar*); 3.88 (bs, 1H, O*CH*); 0.81-1.92 (m, 22H, 4 CH_3 of N*Ar* and 5 CH_2 of O*Cy*); 1.13 (bs, 18H, 2 PMe_3, found by ^{1}H-^{31}P HSQC NMR) ^{31}P{^{1}H}-NMR (121.5 MHz; C_6D_6; δ, ppm): - 5.8 (s, 2 *P*Me_3).

NMR scale reaction of (ArN)Mo(H)(SiH_2Ph)(PMe_3)$_3$ (III-7) with ethanol

EtOH (7.5 µl, 0.13 mmol) was added in one portion at room temperature to a solution of (ArN)Mo(H)(SiH_2Ph)(PMe_3)$_3$ (**III-7**) (15.7 mg, 0.026 mmol) in 0.6 ml of C_6D_6 in an NMR tube. The reaction mixture was left for at room temperature for 15 min. NMR analysis showed the formation of (Mo(H_4)(PMe_3)$_3$ (**III-155**)[253] and $ArNH_2$. The analogous stoichiometric reaction of **III-7** with ethanol gives a mixture of unidentified decomposition products. Only traces of **III-155** were observed.

NMR scale reaction of (ArN)Mo(H)(SiH_2Ph)(PMe_3)$_3$ (III-7) with benzonitrile

PhCN (6.4 µl, 0.055 mmol) was added in one portion at room temperature to a solution of (ArN)Mo(H)(SiH_2Ph)(PMe_3)$_3$ (**III-7**) (16.8 mg, 0.028 mmol) in 0.6 ml of C_6D_6 in an NMR tube. The reaction mixture was left for at room temperature for 1 h. NMR analysis showed the selective formation of (ArN)Mo(SiH_2Ph)(N=CHPh)(NCPh)(PMe_3)$_2$ (**III-156**; ~1:1 mixture of *cis*- and *trans*- isomers), accompanied by the release of an equivalent of PMe_3. The reaction mixture was monitored by NMR spectroscopy for additional 36 h at room temperature showing selective rearrangement of **III-156** into (ArN)Mo(SiH_2Ph)(η^3-N=C(Ph)-N=CHPh)(PMe_3) (**III-157**), which is accompanied by the release of another equivalent of PMe_3.

(ArN)Mo(SiH_2Ph)(N=CHPh)(NCPh)(PMe_3)$_2$ (**III-156**): ^{1}H-NMR (300 MHz; C_6D_6; δ, ppm; both isomers): 1.22 (m, 2 PMe_3 for each isomer, overlapping signals of both isomers, total 36H); 1.44 (d, $^3J_{H\text{-}H}$ = 6.9 Hz, 2 CH_3 of N*Ar* for each isomer, total 12H); 1.50 (d, $^3J_{H\text{-}H}$ = 6.9 Hz, 2 CH_3 of N*Ar* for each isomer, total 12H); 4.30 (sept, $^3J_{H\text{-}H}$ = 6.9

Hz, 2H, 2 *CH* of N*Ar* of one isomer); 4.48 (sept, $^{3}J_{H\text{-}H}$ = 6.9 Hz, 2H, 2 *CH* of N*Ar* of one isomer); 5.62 (t, $^{3}J_{H\text{-}P}$ = 5.7 Hz, 2H, SiH_2Ph of one isomer); 5.73 (t, $^{3}J_{H\text{-}P}$ = 6.3 Hz, 2H, SiH_2Ph of one isomer); 6.92-7.54 (m, overlapping aromatic signals of N*Ar*, Si*Ph*, and 2 C*Ph* for both isomers); 7.68 (d, $^{3}J_{H\text{-}H}$ = 7.5 Hz, 2H, *o*-H, C*Ph*, one isomer); 7.93 (t, $J_{H\text{-}P}$ = 6.6 Hz, 1H, N=C*H*Ph, one isomer); 7.96 (d, $^{3}J_{H\text{-}H}$ = 7.5 Hz, 2H, *o*-H, C*Ph*, one isomer); 8.08 (d, $^{3}J_{H\text{-}H}$ = 7.5 Hz, 2H, *o*-H, C*Ph*, one isomer); 8.50 (t, $J_{H\text{-}P}$ = 7.2 Hz, 1H, N=C*H*Ph, one isomer). $^{31}P\{^{1}H\}$-NMR (121.5 MHz; C_6D_6; δ, ppm; both isomers): 2.8 (s, 2 *P*Me$_3$, one isomer); 2.3 (s, 2 *P*Me$_3$, another isomer). ^{29}Si INEPT+ NMR (119.2 MHz; C_6D_6; *J* = 200 Hz; δ, ppm; both isomers): -12.6 (t, $^{1}J_{Si\text{-}H}$ = 151.4 Hz, *Si*H$_2$Ph, one isomer); -19.9 (t, $^{1}J_{Si\text{-}H}$ = 149.1 Hz, *Si*H$_2$Ph, one isomer). $^{13}C\{^{1}H\}$-NMR (151 MHz; C_6D_6; δ, ppm; both isomers; selected resonances): 197.1 (s, N=*C*HPh, one isomer); 153.0 (s, N=*C*HPh, one isomer); 136.4 (s, *o*-C, C*Ph*, one isomer); 134.9 (s, *o*-C, C*Ph*, one isomer); 28.1 (s, *CH*, N*Ar*, one isomer); 28.0 (s, *CH*, N*Ar*, one isomer); 23.9 (s, *CH$_3$*, N*Ar*, one isomer); 23.6 (s, *CH$_3$*, N*Ar*, one isomer); 16.6 (vt, $^{1}J_{C\text{-}P}$ = 24.2 Hz, P*Me$_3$*, one isomer), 15.1 (vt, $^{1}J_{C\text{-}P}$ = 24.2 Hz, P*Me$_3$*, one isomer)

(ArN)Mo(SiH$_2$Ph)(η^3-N=C(Ph)-N=CHPh)(PMe$_3$) (**III-157**): ^{1}H-NMR (300 MHz; C_6D_6; δ, ppm): 1.17 (d, $^{3}J_{H\text{-}H}$ = 6.6 Hz, 6H, 2 *CH$_3$*, N*Ar*); 1.21 (d, $^{3}J_{H\text{-}H}$ = 6.6 Hz, 6H, 2 *CH$_3$*, N*Ar*); 1.57 (d, $^{2}J_{H\text{-}P}$ = 9.0 Hz, 9H, P*Me$_3$*); 3.58 (sept, $^{3}J_{H\text{-}H}$ = 6.6 Hz, 2H, 2 *CH*, N*Ar*); 5.28 (s, 1H, η^3-N=C(Ph)-N=C*H*Ph); 5.84 (d, $^{2}J_{H\text{-}H}$ = 10.8 Hz, 1H, SiH_2Ph); 5.96 (d, $^{2}J_{H\text{-}H}$ = 10.8 Hz, 1H, SiH_2Ph); 6.64-7.32 (m, 14H, *m*-H and *p*-H of N*Ar* and 2 C*Ph*, *m*-, *p*-, and *o*-H of Si*Ph*); 7.86 (m, 2H, *o*-H, C*Ph*); 8.11 (m, 2H, *o*-H, C*Ph*). $^{31}P\{^{1}H\}$-NMR (121.5 MHz; C_6D_6; δ, ppm): 4.8 (s, *P*Me$_3$). $^{13}C\{^{1}H\}$-NMR (75.5 MHz; C_6D_6; δ, ppm): 197.1 (s, η^3-N=*C*(Ph)-N=CHPh); 153.0 (s, *i*-C); 150.3 (s, *i*-C); 144.7 (s); 135.8 (s, *i*-C); 134.9 (s, *o*-C, C*Ph*); 132.7 (s, *o*-C, C*Ph*); 131.7 (s, *o*-C, C*Ph*); 127.7; 123.9; 122.4; othe aromatic carbons are overlapping with the signal of C_6D_6; 54.7 (s, η^3-N=C(Ph)-N=*C*HPh); 28.2 (s, *CH*, N*Ar*); 23.3 (s, *CH$_3$*, N*Ar*); 23.2 (s, *CH$_3$*, N*Ar*); 14.1 (d, $^{1}J_{C\text{-}P}$ = 24.1 Hz, PMe$_3$). ^{29}Si INEPT+ NMR (119.2 MHz; C_6D_6; *J* = 200 Hz; δ, ppm): -25.4 (td, $^{1}J_{Si\text{-}H}$ = 203.9 Hz, $^{2}J_{Si\text{-}P}$ = 6.0 Hz, *Si*H$_2$Ph).

Catalytic studies

General procedure for catalytic hydrosilation using (ArN)Mo(SiH$_2$Ph)(η^3-NAr-SiHPh-H)(PMe$_3$) (III-1)

A solution of substrate, silane (when needed), and tetramethylsilane (5 mol. %) in 0.6 ml of C_6D_6 was added in one portion at room temperature to (ArN)Mo(SiH$_2$Ph)(η^3-NAr-SiHPh-H)(PMe$_3$) (**III-1**). The mixture was immediately transferred to an NMR tube and the reaction was monitored by NMR spectroscopy at appropriate temperature. Conversion of the substrate, yield and structure of products were determined by NMR analysis. Characteristic NMR signals of new hydrosilation products are presented below.

General procedure for catalytic hydrosilylation reactions using (ArN)Mo(Et)(η^3-NAr-SiHPh-CH=CH$_2$)(PMe$_3$) (III-3)

A solution of organic substrate, PhSiH$_3$ (1:1 mixture), and tetramethylsilane (5 mol. %) in C_6D_6 was added in one portion at room temperature to (ArN)Mo(Et)(η^3-NAr-SiHPh-CH=CH$_2$)(PMe$_3$) (**III-3**, 5 mol. %). The mixture was immediately transferred to an NMR tube and the reaction was monitored by NMR analysis. Depending on substrate, the reactions were performed either at room temperature or at 50 °C. The structures of all hydrosilylation products were determined by NMR spectroscopy. Conversion of organic substrates and yields of products were calculated by NMR analysis using tetramethylsilane as an internal standard. Characteristic NMR signals of new hydrosilation products are presented below.

General procedure for catalytic hydrogenation using (ArN)Mo(Et)(η^3-NAr-SiHPh-CH=CH$_2$)(PMe$_3$) (III-3)

Hydrogen gas (~ 1.5 atm) was added *via* vacuum transfer to a frozen in liquid nitrogen solution of organic substrate, (ArN)Mo(Et)(η^3-NAr-SiHPh-CH=CH$_2$)(PMe$_3$) (**III-3**; 5 mol. %), and tetramethylsilane (5 mol. %) in C_6D_6 in an NMR tube. The mixture was warmed up to room temperature showing (by NMR spectroscopy) no conversion of organic substrate. Depending on substrate, the reaction was monitored by NMR analysis at 50-60 °C. The structures of all products were determined by NMR spectroscopy.

Conversion of organic substrates and yields of products were calculated by NMR analysis using tetramethylsilane as an internal standard.

General procedure for hydrosilylation reactions using (ArN)Mo(H)(Cl)(PMe_3)$_3$ (III-6)

A solution of organic substrate and silane (1:1 ratio), and tetramethylsilane (5 mol. %) in 0.6 ml of C_6D_6 was added in one portion at room temperature to (ArN)Mo(H)(Cl)(PMe_3)$_3$ (**III-6**; 5 mol. %). The mixture was immediately transferred to an NMR tube. Depending on substrate, the reaction mixture was monitored by NMR analysis either at room temperature or at 50 °C. The structures of all products were determined by NMR spectroscopy. Conversion of organic substrates and yields of products were calculated by NMR analysis using tetramethylsilane as an internal standard. Characteristic NMR signals of new hydrosilation products are presented below.

Catalytic hydroboration of PhCN with CatBH using (ArN)Mo(H)(Cl)(PMe_3)$_3$ (III-6)

A solution of PhCN (27.2 µl, 0.235 mmol) and CatBH (25.0 µl, 0.235 mmol) was added in one portion at room temperature to (ArN)Mo(H)(Cl)(PMe_3)$_3$ (**III-6**) (6.3 mg, 0.011 mmol, 5 mol. %). The reaction mixture was immediately transferred to an NMR tube and the reaction was monitored by NMR spectroscopy for 12 h. NMR analysis showed complete conversion of CatBH and the formation of only $PhCH_2N(BCat)_2$. TON = 20. TOF = 1.7

$PhCH_2N(BCat)_2$: ^{1}H-NMR(300 MHz; $CDCl_3$; δ, ppm): 4.73 (s, 2H, *CH_2*N), 6.99-7.06 (m, 4H, B*Cat*), 7.18-7.24 (m, 4H, B*Cat*), 7.24-7.34 (m, 3H, *Ph*), 7.44-7.49 (m, 2H, *Ph*). ^{13}C{^{1}H}-NMR (75.5 MHz; $CDCl_3$; δ, ppm): 47.96 (*CH_2*N), 112.47 (*CH*, B*Cat*), 122.59 (*CH*, B*Cat*), 127.52 (*CH*, *Ph*), 127.88 (*CH*, *Ph*), 128.72 (*CH*, *Ph*), 140.32 (*i*-C, B*Cat*), 148.46 (*i*-C, B*Cat*). ^{11}B-NMR (96.3 MHz; C_6D_6; δ, ppm): 27.6 (bs).

General procedure for hydrosilation reactions using (ArN)Mo(H)(SiH_2Ph)(PMe_3)$_3$ (III-7)

A solution of organic substrate and silane (1:1 ratio), and tetramethylsilane (5 mol. %) in 0.6 ml of C_6D_6 were added in one portion at room temperature to (ArN)Mo(H)(SiH_2Ph)(PMe_3)$_3$ (**III-7**) (5 mol. %). The mixture was immediately

transferred to an NMR tube. Depending on the substrate, the reaction was monitored by NMR spectroscopy either at room temperature or at 50 °C. The structures of all products were determined by NMR analysis. Conversion of organic substrates and yields of products were calculated by NMR spectroscopy using tetramethylsilane as an internal standard. Characteristic NMR signals of new hydrosilation products are presented below.

Hydrosilation of PhC(O)H with $PhSiH_3$ using $(ArN)_2W(H)(SiH_2Ph)(PMe_3)$ (III-68)

A solution of $PhSiH_3$ (29.0 µl, 0.235 mmol) and benzaldehyde (23.9 µl, 0.235 mmol) was added in one portion at room temperature to $(ArN)_2W(H)(SiH_2Ph)(PMe_3)$ (**III-68**) (29.6 mg, 0.047 mmol). The mixture was immediately transferred to an NMR tube, and the reaction was monitored by NMR spectroscopy. After 5 min., the reaction leads to 100 % conversion of benzaldehyde to form a mixture of $PhH_2Si(OBn)$ and $PhHSi(OBn)_2$[160, 214, 215b] (1:1 ratio, respectively; TON = 5, TOF = 60.2).

Hydrosilation of PhC(O)Me with $PhSiH_3$ using $(ArN)_2Mo(\eta^1\text{-}O{=}CMePh)(PMe_3)$ (III-97)

A solution of $(ArN)_2Mo(\eta^1\text{-}O{=}CMePh)(PMe_3)$ (**III-97**) in C_6D_6 (33.3 µl, 0.002 mmol; C = 0.06 M; 1.0 mol %) was added at room temperature to a mixture of acetophenone (25.0 µl, 0.214 mmol) and $PhSiH_3$ (26.4 µl, 0.214 mmol) in 0.6 ml of C_6D_6 in an NMR tube. The reaction mixture was left at room temperature for 20 days. NMR analysis showed 35 % conversion of acetophenone and the formation of a mixture of $PhSiH_2[OCH(Me)Ph]$ (76 %) and $PhSi[OCH(Me)Ph]_3$ (24 %). TON: 38.

Characteristic NMR signals of new hydrosilation products

MePhHSi(OBn): ^{1}H-MNR (300 MHz; C_6D_6; δ, ppm): 0.34 (d, $^3J_{H\text{-}H}$ = 2.7 Hz, 3H, Si*Me*); 4.62 (s, 2H, CH_2, O*Bn*); 5.26 (q, $^3J_{H\text{-}H}$ = 2.7 Hz, 1H, *H*Si); 7.13 (m, 3H, *m-H* and *p-H*, *Ph*, O*Bn*); 7.23 (m, 3H, *m-H* and *p-H*, Si*Ph*); 7.43 (m, 2H, *o-H*, *Ph*, O*Bn*); 7.57 (m, 2H, *o-H*, Si*Ph*). ^{29}Si INEPT+ NMR (119.2 MHz; C_6D_6; J = 200 Hz; δ, ppm): - 0.9 (d, $^1J_{Si\text{-}H}$ = 209.9 Hz, PhMe*Si*H).

(EtO)$_3$Si(OBn):[216a] ^{1}H-MNR (300 MHz; C_6D_6; selected resonances; δ, ppm): 4.85 (s, 2H, CH_2, O*Bn*). ^{29}Si INEPT+ NMR (119.2 MHz; C_6D_6; J = 7 Hz; δ, ppm): - 81.6 (bm, signal is overlapping with other $(EtO)_nSi(OBn)_{4\text{-}n}$ products).

$(EtO)_2Si(OBn)_2$: ^{1}H-MNR (300 MHz; C_6D_6; selected resonances: δ, ppm): 4.88 (s, 4H, 2 *CH_2*, O*Bn*). ^{29}Si INEPT+ NMR (119.2 MHz; C_6D_6; J = 7 Hz; δ, ppm): - 81.6 (bm, signal is overlapping with other $(EtO)_nSi(OBn)_{4-n}$ products).

$(EtO)Si(OBn)_3$: ^{1}H-MNR (300 MHz; C_6D_6; selected resonances: δ, ppm): 4.91 (s, 6H, 3 *CH_2*, O*Bn*). ^{29}Si INEPT+ NMR (119.2 MHz; C_6D_6; J = 7 Hz; δ, ppm): - 81.6 (bm, signal is overlapping with other $(EtO)_nSi(OBn)_{4-n}$ products).

$Si(OBn)_4$: ^{1}H-MNR (300 MHz; C_6D_6; selected resonances: δ, ppm): 4.99 (s, 8H, 4 *CH_2*, O*Bn*). ^{29}Si INEPT+ NMR (119.2 MHz; C_6D_6; J = 7 Hz; δ, ppm): - 81.6 (bm, signal is overlapping with other $(EtO)_nSi(OBn)_{4-n}$ products).

$PhSiH_2[OCH(Me)Ph]$: ^{1}H-MNR (300 MHz; C_6D_6; selected resonances: δ, ppm): 1.38 (d, $^3J_{H\text{-}H}$ = 6.3 Hz, 3H, *CH_3*); 4.80 (q, $^3J_{H\text{-}H}$ = 6.3 Hz, 1H, *CH*); 5.20 (s, 2H, PhSi*H_2*). ^{29}Si-NMR (59.6 MHz; C_6D_6; δ, ppm): - 20.4 (t, $^1J_{Si\text{-}H}$ = 220.0 Hz, Ph*Si*H_2); ^{29}Si{^{1}H}-NMR (59.6 MHz; C_6D_6; δ, ppm): - 20.4 (s, Ph*Si*H_2).

$PhSiH[OCH(Me)Ph]_2$: ^{1}H-MNR (300 MHz; C_6D_6; selected resonances; δ, ppm): 1.42 (d, $^3J_{H\text{-}H}$ = 6.3 Hz, 3H, *CH_3*); 4.98 (m, $^3J_{H\text{-}H}$ = 6.0 Hz, 2H, *CH*); 5.30 (s, 1H, PhSi*H*). ^{29}Si-NMR (59.6 MHz; C_6D_6; δ, ppm): - 32.6 (d, $^1J_{Si\text{-}H}$ = 248.6 Hz, Ph*Si*H); ^{29}Si{^{1}H}-NMR (59.6 MHz; C_6D_6; δ, ppm): - 32.6 (s, Ph*Si*H).

$PhSi[OCH(Me)Ph]_3$: ^{1}H-MNR (300 MHz; C_6D_6; selected resonances; δ, ppm): 1.36 (d, $^3J_{H\text{-}H}$ = 6.0 Hz, 3H, *CH_3*); 5.03 (m, $^3J_{H\text{-}H}$ = 6.0 Hz, 3H, *CH*); ^{29}Si-NMR (59.6 MHz; C_6D_6; δ, ppm): -32.7 (s, Ph*Si*).

$PhH_2Si(OEt)$: ^{1}H-NMR (300 MHz, C_6D_6; selected resonances; δ, ppm): 5.19 (s, 2H, *H_2*Si). ^{29}Si INEPT+ NMR (119.2 MHz; C_6D_6; J = 200 Hz; δ, ppm): - 28.6 (t, $^1J_{Si\text{-}H}$ = 210.0 Hz, PhH_2*Si*).

$PhSiH(OEt)_2$: ^{1}H-NMR (300 MHz, C_6D_6; selected resonances; δ, ppm): 5.22 (s, 1H, *H*Si). ^{29}Si INEPT+ NMR (119.2 MHz; C_6D_6; J = 200 Hz; δ, ppm): - 30.8 (d, $^1J_{Si\text{-}H}$ = 241.3 Hz, PhH*Si*).

$PhH_2Si(O^iPr)$: ^{1}H-NMR (300 MHz, C_6D_6; δ, ppm): 7.61 (m, 2H, *o*-H, *Ph*Si); 7.10-7.20 (m, 3H, *m*-H and *p*-H, *Ph*Si); 5.23 (s, 2H, *H_2*Si); 3.91 (sept, $^3J_{H\text{-}H}$ = 6.1 Hz, 1H, *CH*,

SiO^i*Pr*); 1.08 (d, $^3J_{H\text{-}H}$ = 6.1 Hz, 6H, 2 *CH*$_3$, SiO^i*Pr*). ^{29}Si INEPT+ NMR (119.2 MHz; C_6D_6; *J* = 200 Hz; δ, ppm): - 22.5 (t, $^1J_{Si\text{-}H}$ = 213.4 Hz, Ph*Si*H$_2$).

PhSiH(O^{i}Pr)$_2$: ^{1}H-NMR (300 MHz, C_6D_6; δ, ppm): 7.79 (m, 2H, *o*-H, *Ph*Si); 7.20-7.10 (m, 3H, *m*-H and *p*-H, *Ph*Si); 5.28 (s, 1H, Si*H*); 4.20 (sept, $^3J_{H\text{-}H}$ = 6.1 Hz, 2H, 2 *CH*, Si(O^i*Pr*)$_2$); 1.16 (d, $^3J_{H\text{-}H}$ = 6.1 Hz, 12H, 4 *CH*$_3$, Si(O^i*Pr*)$_2$). ^{29}Si INEPT+ NMR (119.2 MHz; C_6D_6; *J* = 200 Hz; δ, ppm): - 34.8 (d, $^1J_{Si\text{-}H}$ = 239.7 Hz, Ph*Si*H).

EtN(SiH$_2$Ph)$_2$: ^{1}H-NMR (300 MHz, C_6D_6; selected resonances: δ, ppm): 5.19 (s, 2H, Si*H*$_2$Ph); 4.00 (s, 2H, C*H*$_2$Ph).

PhH$_2$Si(N=CHPh): ^{1}H-NMR (300 MHz, C_6D_6; selected resonances: δ, ppm): 8.90 (s, 1H, C*H*Ph); 7.70 (m, 2H, Ph); 7.63 (m, 2H, Ph); 5.42 (s, 2H, Si*H*$_2$Ph).

PhEtSiH$_2$:[202] ^{1}H-NMR (300 MHz; C_6D_6; δ, ppm): 0.73 (m, 2H, *CH*$_2$, Si*Et*); 0.95 (t, $^3J_{H\text{-}H}$ = 7.8 Hz, 3H, *CH*$_3$, Si*Et*); 4.46 (t+sat, $^3J_{H\text{-}H}$ = 7.2 Hz, $^1J_{H\text{-}Si}$ = 198.7 Hz, 2H, Si*H*$_2$); 7.47 (m, 2H, *o*-H, Si*Ph*); *m*-H and *p*-H resonances are overlapping with the residual C_6D_6 signal.

Kinetic studies using NMR spectroscopy

VT kinetic NMR studies of exchange between (ArN)Mo(SiH$_2$Ph)(η^3-NAr-SiHPh-H)(PMe$_3$) (III-1) and PhSiH$_3$

Mixtures of (ArN)Mo(SiH$_2$Ph)(η^3-NAr-SiHPh-H)(PMe$_3$) (**III-1**) (15.0 mg, 0.02 mmol) and PhSiH$_3$ (2.5 µl, 0.02 mmol) in 0.6 ml of C_6D_6 was immedially frozen after preparation. Samples were placed to an NMR machine at appropriate temperature (12 °C, 22 °C, 32 °C, and 42°C). A series of 1D ^{1}H EXSY NMR experiments (irradiation was applied for the resonance of one of the Si-bound protons of the classical Mo-SiH$_2$Ph group) with different mixing times (t_m = 0 - 0.6 s) were performed. Rate constants of the exchange process at different temperatures were calculated (Figure 49, chapt. VI) using the "Initial Rate Approximation" method, previously described in literature.[212, 251]

General procedure for kinetic NMR studies of the reaction of (ArN)Mo(Et)(η^3-NAr-SiHPh-CH=CHPh)(PMe_3) (III-3) with $PhSiH_3$

Reagents (either $PhSiH_3$ (variable concentration) or mixtures of 10 equiv. of $PhSiH_3$ and variable concentration of PMe_3) were added in one portion at room temperature to a solution of (ArN)Mo(Et)(η^3-NAr-SiHPh-CH=CHPh)(PMe_3) (**III-3**) (16.5 mg, 0.024 mmol) and either 5.0 mol. % of tetramethylsilane (for reactions with $PhSiH_3$) or 5.0 mol. % of P(*o*-Tol)$_3$ (for reactions with $PhSiH_3$ and PMe_3) in 0.6 ml of C_6D_6 in an NMR tube. No reaction was observed at room temperature. The NMR tube with the reaction mixture was placed into the NMR machine, the sample was warmed up to 50 °C, and the reaction was monitored by either ^{1}H- (for reactions with $PhSiH_3$) or $^{31}P\{^1H\}$-NMR analysis (for reactions with $PhSiH_3$ and PMe_3) overnight. The rate constants for each concentration of $PhSiH_3$ or PMe_3 were obtained from the integration of the Si*H* (^{1}H-NMR) or the *P*Me$_3$ ($^{31}P\{^1H\}$-NMR) resonances, respectively (integrals were normalized to the integral of the standartd: tetramethylsilane or P(*o*-Tol)$_3$). Data obtained from NMR analysis and corresponding concentrations were linearized in –ln[C(**III-3**)]/time coordinates.

General procedure for kinetic NMR studies with (ArN)Mo(H)(Cl)(PMe_3)$_3$ (III-6)

Reagents were added at -50 °C to a solution of (ArN)Mo(H)(Cl)(PMe_3)$_3$ (**III-6**) (16.5 mg, 0.031 mmol) and 5.0 mol. % of P(*o*-Tol)$_3$ in 0.6 ml of toluene-d_8 in an NMR tube. After addition the mixture was immediately frozen in liquid nitrogen and the NMR tube was placed into precooled (-30 °C) NMR machine. For benzaldehyde, depending on the experiment, the sample was slowly warmed up to a desired temperature (-5 °C for the reaction of **III-6** with PhC(O)H to produce *trans*-(ArN)Mo(H)(Cl)(η^2-PhC(O)H)(PMe_3)$_2$ (**III-136**), room temperature for the rearrangement of **III-136** into (ArN)Mo(Cl)(OCH_2Ph)(PMe_3)$_3$ (**III-135**) and the reaction of **III-135** with $PhSiH_3$ and PMe_3 to form **III-6**) and monitored by $^{31}P\{^1H\}$-NMR analysis. The rate constants were obtained from the integration of the ^{31}P-NMR signals of PMe_3 ligands (integrals were normatiled to the integral of the standartd, P(*o*-Tol)$_3$), resulting in the linear –ln[C]/time plots (see chapt. VI). An analogous procedure was used for kinetic NMR studies in the case of ethanol (see chapt. VI).

General procedure for VT kinetic NMR studies of the exchange processes in (ArN)Mo(H)(SiH_2Ph)(PMe_3)$_3$ (III-7)

One equivalent of PMe_3 or $PhSiH_3$, or a mixture of PMe_3 and $PhSiH_3$ (1:10 or 7:1, respectively) were added on one portion at room temperature to a solution of (ArN)Mo(H)(SiH_2Ph)(PMe_3)$_3$ (**III-7**) and 5.0 mol. % of either tetramethylsilane of P(*o*-Ph)$_3$ (used as standards) in 0.6 ml of C_6D_6 in an NMR tube. The sample was placed into NMR machine and, depending on the exchange process (either silane or phosphine), a series of ^{1}H-NMR or ^{31}P{^{1}H}-NMR and 1D ^{1}H EXSY NMR or 1D ^{31}P EXSY NMR spectra were obtained in the range 20 – 50 °C. 1D EXSY NMR spectra were acquired using different mixing times. Relaxation times of all components of the exchange process were measured independently and were taken into account in EXSY experiments. For PMe_3 exchange, all the data were taken into account, but the rate constants and activation parameters for the silyl/silane exchange between **III-7** and $PhSiH_3$ were calculated using the "Initial Rate Approximation"[212, 251](see chapt. VI).

General procedure for kinetic NMR studies of the reaction of (ArN)Mo(H)(SiH_2Ph)(PMe_3)$_3$ (III-7) with acetone

The dependence of the reaction rate on the concentration of acetone was detected by NMR studies of the reactions of (ArN)Mo(H)(SiH_2Ph)(PMe_3)$_3$ (**III-7**) with 1, 5, 7, 10, and 20 equivalents of acetone. Acetone was added in one portion at room temperature to a solution of complex (ArN)Mo(H)(SiH_2Ph)(PMe_3)$_3$ (**III-7**) (16.7 mg, 0.028 mmol) and tetramethylsilane (1.0 μl, 0.007 mmol) in 0.55 ml of C_6D_6 in an NMR tube. The sample was immediately placed into NMR machine, and the reactions were monitored by ^{1}H-NMR spectroscopy at room temperature until 50 % conversion of (ArN)Mo(H)(SiH_2Ph)(PMe_3)$_3$ (**III-7**). The concentration of the starting complex **III-7** in the reaction mixture was determined by the integration of the ^{1}H-NMR spectra and normalization of the integrals to the one for tetramethylsilane. The dependence of the reaction rate on the concentration of PMe_3 was detected in a pseudo-first order regime (**III-7**:acetone = 1:20) by addition of 0, 1, 3.8, and 7 equivalents of phosphine. Acetone (40.4 μl, 0.550 mmol) was added in one portion at room temperature to a solution of **III-7** (16.7 mg, 0.0275 mmol) and tetramethylsilane (1.0 μl, 0.007 mmol) in 0.55 ml of C_6D_6 in

NMR tube. The reactions were monitored by ^{1}H-NMR spectroscopy at room temperature until 50 % conversion of **III-7**. The concentration of **III-7** was calculated by integration of the ^{1}H-NMR spectra and normalization of the integrals to the one for tetramethylsilane signal. In both cases, obtained data were linearized in logarithmic coordinates (see chapt. VI), resulting in the calculation of the rate constants.

General procedure for VT kinetic NMR studies of the reaction of (ArN)Mo(H)(SiH_2Ph)(PMe_3)$_3$ (III-7) with acetone

VT kinetic NMR studies of the reaction of (ArN)Mo(H)(SiH_2Ph)(PMe_3)$_3$ (**III-7**) and acetone were performed in the pseudo-first order regime (**III-7**:acetone = 1:20). Acetone (36.5 µl, 0.497 mmol) was added in one portion at room temperature to a solution of **III-7** (15.1 mg, 0.0249 mmol) and tetramethylsilane (1.0 µl, 0.007mmol) in 0.5 ml of C_6D_6 in an NMR tube. The sample was immediately placed into preheated to desired temperature (12. °C,18 °C, 22 °C, 23.5 °C) NMR machine, and the reaction was monitored by ^{1}H-NMR analysis. For each ^{1}H-NMR spectrum, the concentration of **III-7** was determined by integration of its signals and normalization of these integrals to the one for tetramethylsilane. Obtained data were linearized in logarithmic coordinates (see chapt. VI), resulting in the calculation of the rate constants for each temperature.

Experimental details of EXSY NMR studies

The EXSY NMR spectra were acquired on a Bruker Avance AV600 spectrometer equipped with a BBO-Z grad probe and VT accessory. ^{31}P and ^{1}H 2D EXSY NMR spectra were recorded at different temperatures with a pulse sequence "noesygpph" (2D homonuclear correlation *via* dipolar coupling, dipolar coupling may be due to NOE or chemical exchange, phase sensitive, with gradient pulses in mixing time)[255] from Bruker pulse program library. A total of 2 scans per FID for ^{1}H and 4 scans for ^{31}P of 2K data points were used per time increment. A total of 256 time increments were collected for both ^{1}H and ^{31}P. The FIDs were Fourier transformed to generate and 1024 x 1024 data matrix. Two EXSY spectra were recorded at each temperature, one EXSY spectrum with a mixing time (t_m) of between 100 and 500 ms, which contains the exchange cross peaks and a reference EXSY spectrum with a mixing time 0 ms, which shows no exchange cross peaks. All spectra were processed and analyzed using Bruker Topspin 2.1 Pl4

software running on Windows XP. The peak volumes of the 2D spectra were determined by direct integration. The exchange rates were calculated using the Mestre Lab EXSY Calc 1.0 software (www.mestrelab.com).[256] The series of ^{1}H 1D EXSY NMR spectra were recorded at different temperatures using the "selnogp" (1D NOESY using selective refocussing with a shaped pulse, dipolar coupling may be due to NOE or chemical exchange)[257] pulse sequence from the Bruker library. Each spectrum was acquired using 16 scans and 32 K data points with a spectral width of 20 KHz. The offset frequency was always adjusted on resonance with the analyzed signal. The acquired FIDs were processed using a line broadening of 0.3 Hz and zero filled to 65 K points. At each temperature a series of 5 to 8 1D EXSY spectra were recorded with a mixing time ranging from 25 m to 2000 ms optimized for each exchange rate and a ^{1}H 1D spectrum used as a reference. The slopes of the buildup curves at 0 ms mixing time were determined by the initial rate approximation.[212, 251] More accurate measurements of the rates were also performed by employing the CIFIT2.0 software courtesy to Prof. Alex D. Bain from McMaster University (www.chemistry.mcmaster.ca/bain).[258] T1 relaxation times were measured by inversion recovery method using Bruker "t1ir" pulse program.

Crystal structure determinations

Crystallization conditions:

III-1 – hexanes, -30 °C

III-3 – cooling concentrated hexanes solution from ~35 °C to RT

III-6 – slow vaporization of diethyl ether solution into toluene at RT

III-7 – diethyl ether, -30 °C

III-8 – diethyl ether, -30 °C

III-47 – diethyl ether, -30 °C

III-77 – diethyl ether, -80 °C

III-125 – pentane, -30 °C

III-138 – concentrated C_6D_6 solution, RT

III-142 – diethyl ether, -30 °C

III-145 – directly from reaction mixture, diethyl ether, -30 °C

The crystals were mounted in a film of perfluoropolyether oil on a glass fibre and transferred to a Siemens three-circle diffractometer with a CCD detector (SMART system). The data were corrected for Lorentz and polarization effects. The structure was solved by direct methods and refined by full-matrix least squares procedures.[259] All non-hydrogen atoms were refined anisotropically; the hydrogen atoms except the hydride (which was located from Fourier difference synthesis and positionally refined isotropically) were placed in calculated positions and refined in a "riding" model.
For structure determination parameters, see Tables 25-35 in chapt. VI.

DFT calculations

The unconstrained geometry optimization was carried out for all the considered structures with the Gaussian 03 program package,[260] using DFT and applying Becke three parameter hybrid exchange functional in conjunction with gradient-corrected nonlocal correlation functional of Perdew and Wang (B3PW91).[261] The 6-31G(d,p) basis set was used for the H, C, N, Si, and P atoms. The Hay-Wadt effective core potentials (ECP) and the corresponding VDZ basis sets were used for the Mo atoms.[262] The same level of theory was used in the frequency calculations performed at the located stationary points. The thermodynamic parameters were calculated in the rigid rotor-harmonic oscillator approximation.

VI. Appendix

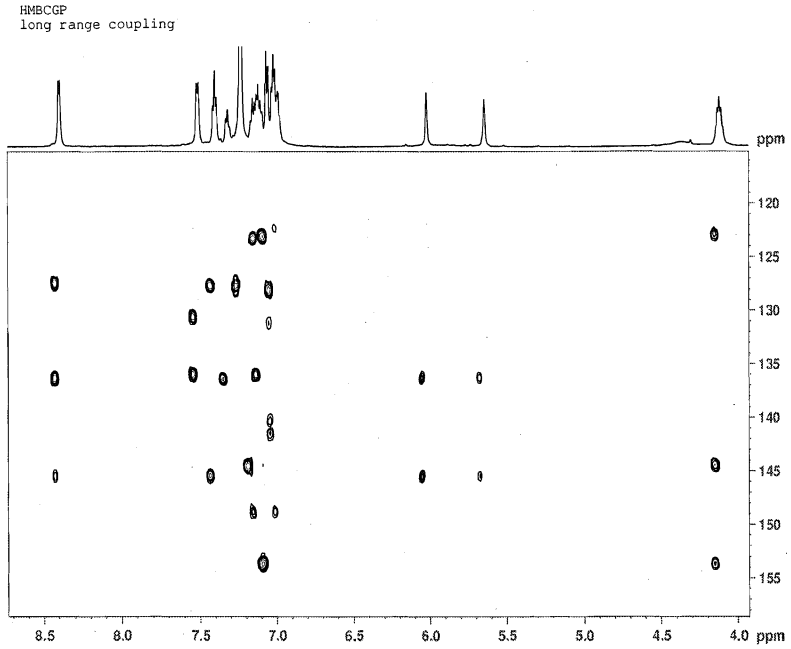

Figure 48. ^{1}H-^{13}C HMBC NMR of **III-1** (signals at ~8.43 and at ~7.55 ppm in ^{1}H-projection correspond to *o*-H of the agostic SiH_2Ph and Mo-bound SiH_2Ph substituents, respectively)

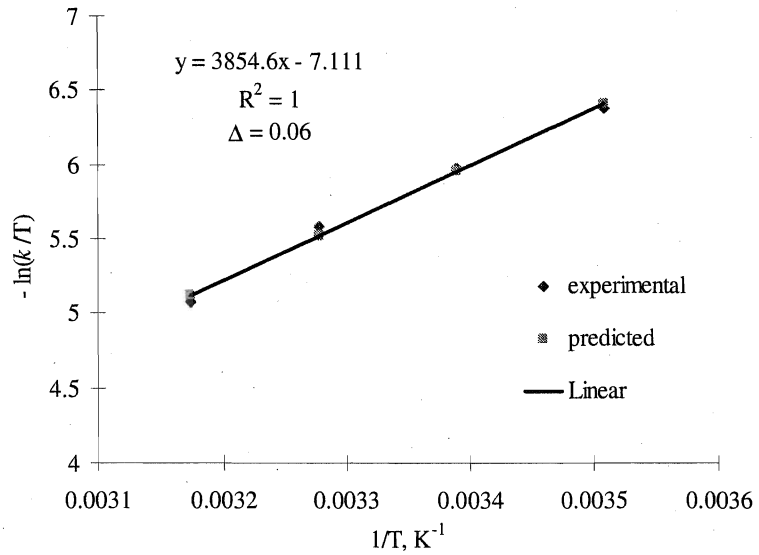

Figure 49. Eyring plot for exchange between **III-1** and $PhSiH_3$ (standard error: 0.06).

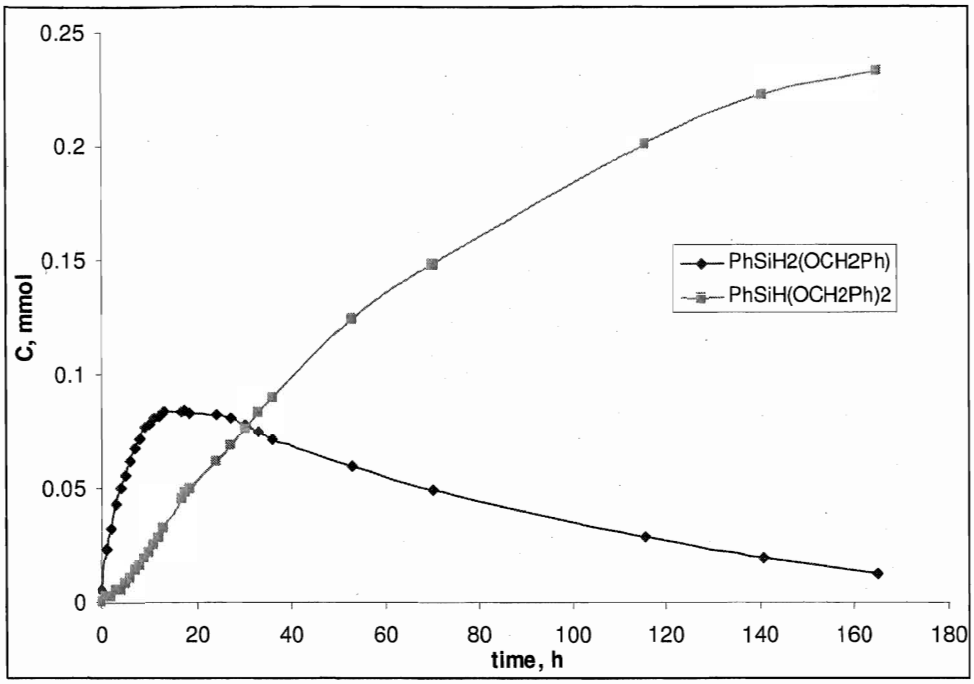

Figure 50. Kinetic profile of the hydrosilation of PhC(O)H with $PhSiH_3$ mediated by **III-1** (1.3 mol. %).

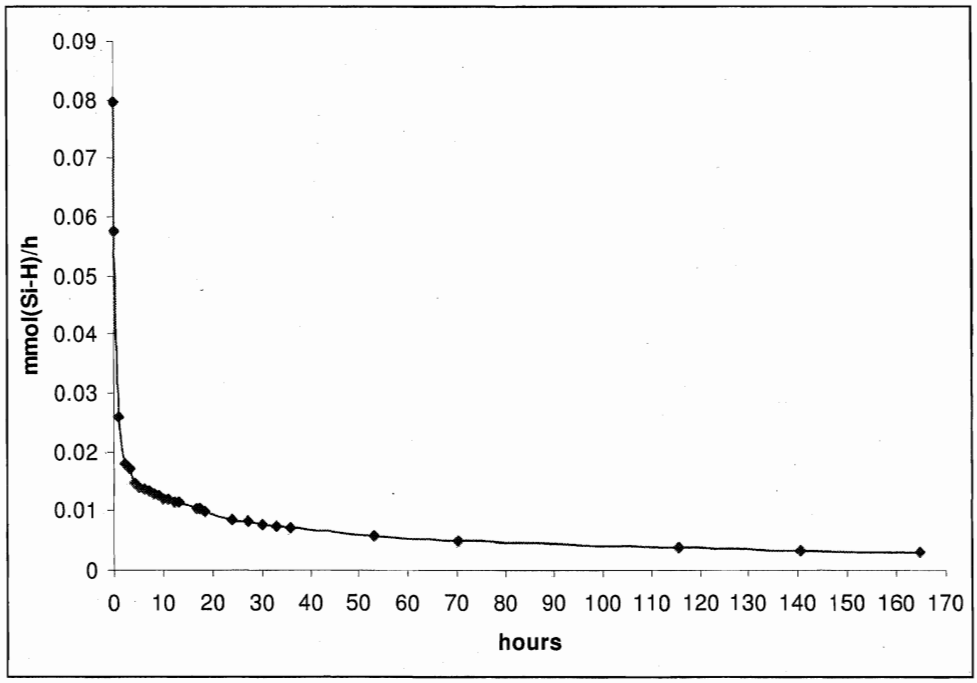

Figure 51. Deactivation of the catalyst **III-1** (TOF/time coordinates) in the hydrosilation of PhC(O)H with $PhSiH_3$ (1.3 mol. % load of **III-1**).

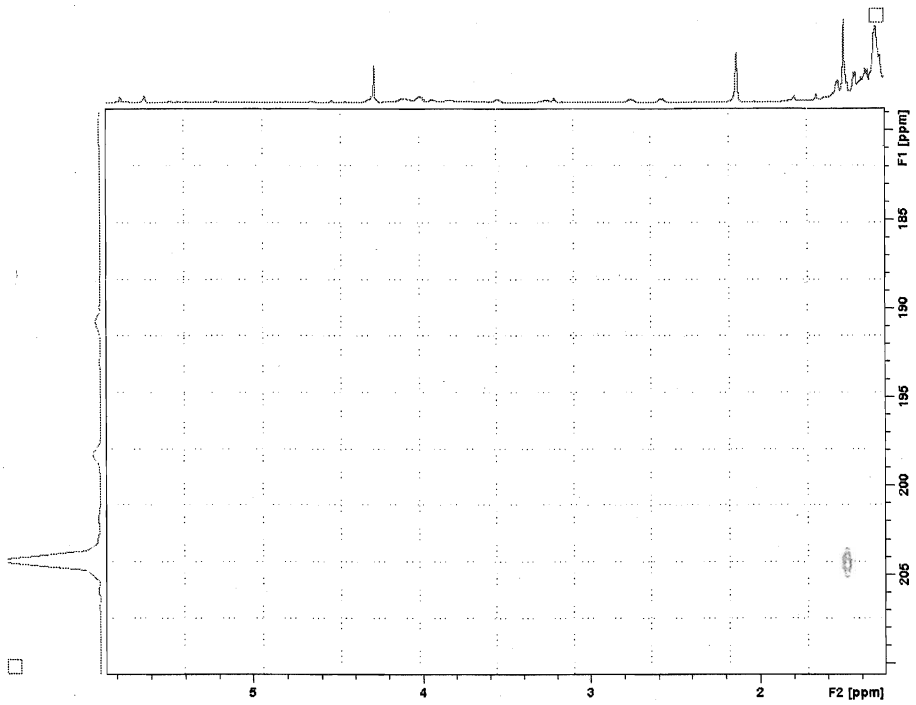

Figure 52. ^{1}H-^{13}C HMBC NMR spectrum (- 30 °C, toluene-d_8) of **III-107** (protons in ^{t}Bu group (at 1.39 ppm) are coupled to nitrile carbon at 204.4 ppm; no coupling between the Si*H* proton (at 5.66 ppm) and C≡N is observed).

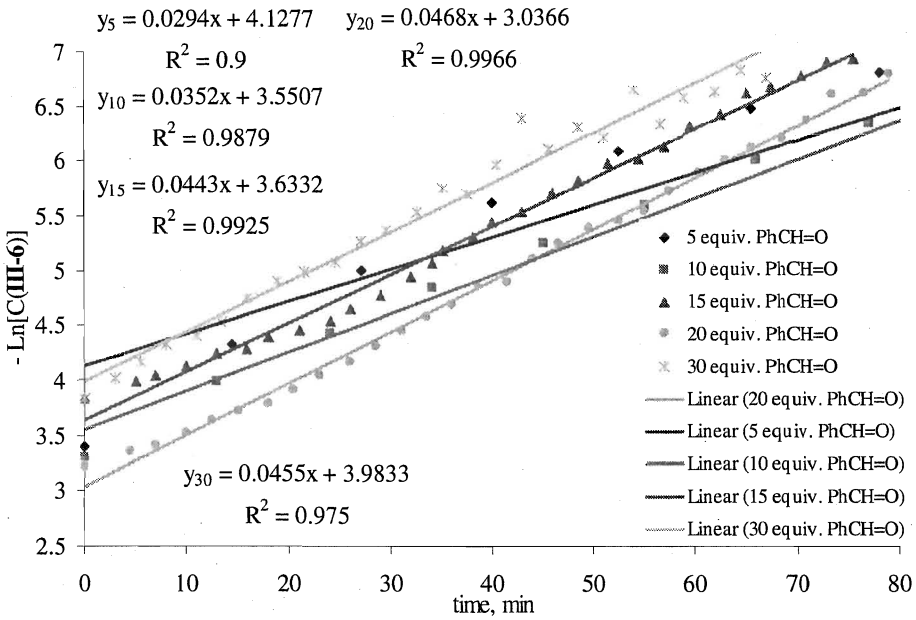

Figure 53. –Ln[C]/time dependence for reactions of **III-6** with benzaldehyde at -5 °C.

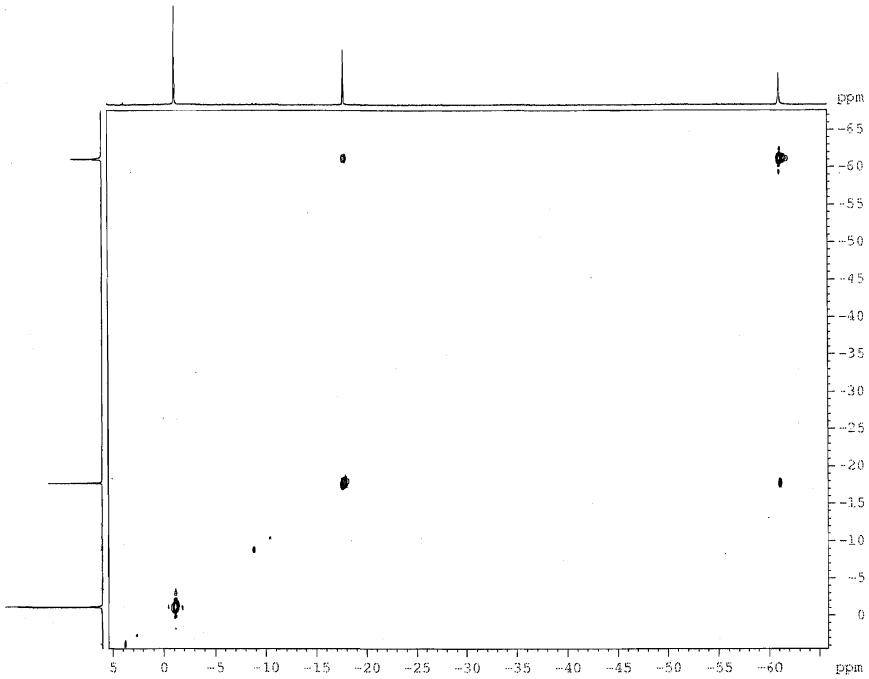

Figure 54. ^{1}H-^{1}H EXSY NMR spectrum (RT) of a mixture of **III-6** and PMe_3 showing exchange with *trans*-PMe_3 ligand.

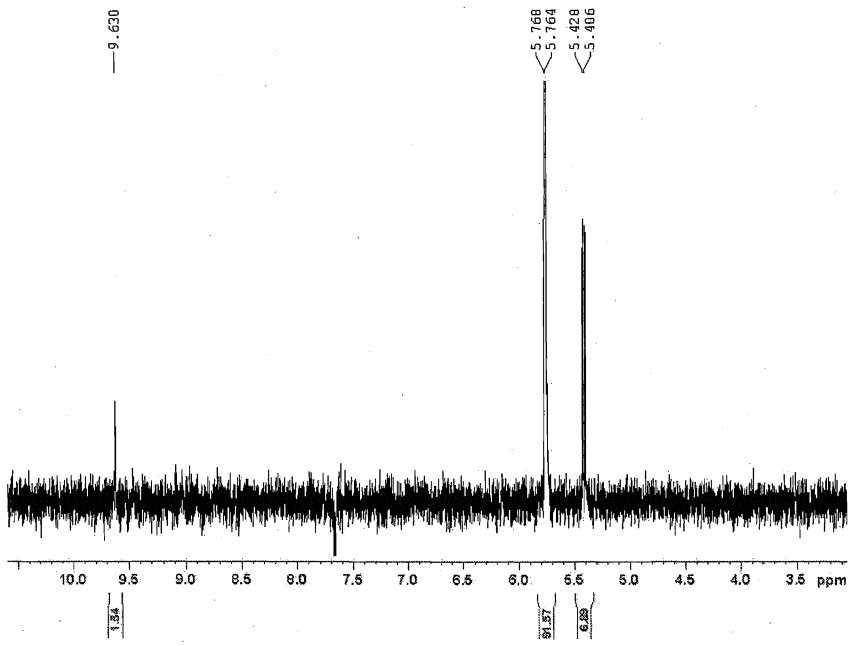

Figure 55. 1D ^{1}HEXSY NMR spectrum of a mixture of **III-136** and PhC(O)H (irradiation of the C(O)*H* proton in **III-136** at 5.763 ppm shows exchange with free PhC(O)H (9.63 ppm) and another isomer of **III-136** (5.42 ppm); t_m = 0.3 s).

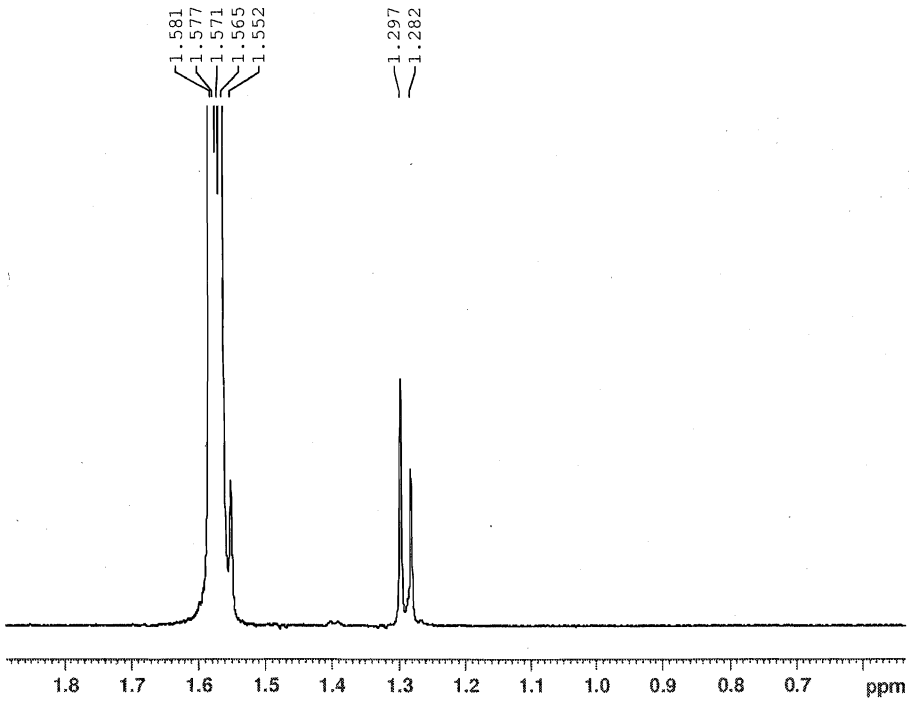

Figure 56. 1D ^{1}H EXSY NMR experiment of **III-136** (irradiation of the PMe_3 protons at 1.572 ppm shows exchange with another PMe_3 ligand (1.29 ppm); t_m = 1.0 s).

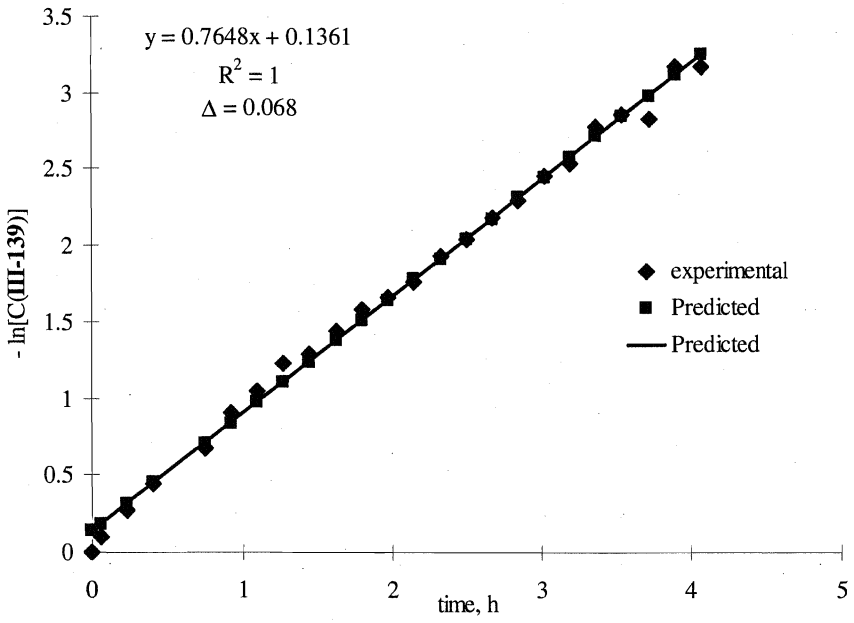

Figure 57. –Ln[C]/time plot for rearrangement of **III-136** into **III-135** at 22 °C (standard error: 0.068).

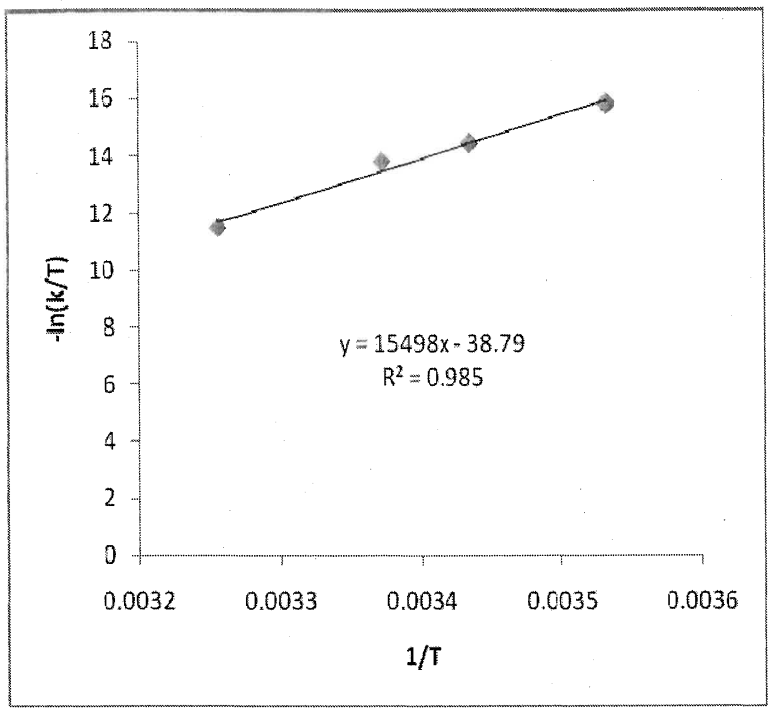

Figure 58. Eyring plot for the reaction of **III-136** with PhC(O)H (10 eq.).

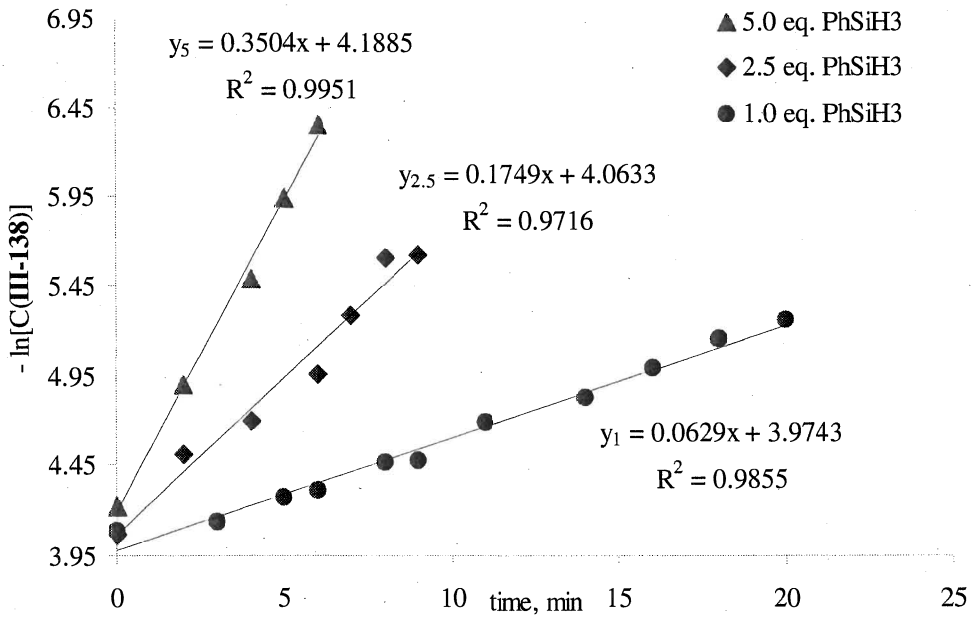

Figure 59. –Ln[C]/time dependence for reactions of **III-135** with $PhSiH_3$ at 22 °C in the presence of 20 equiv. of PMe_3.

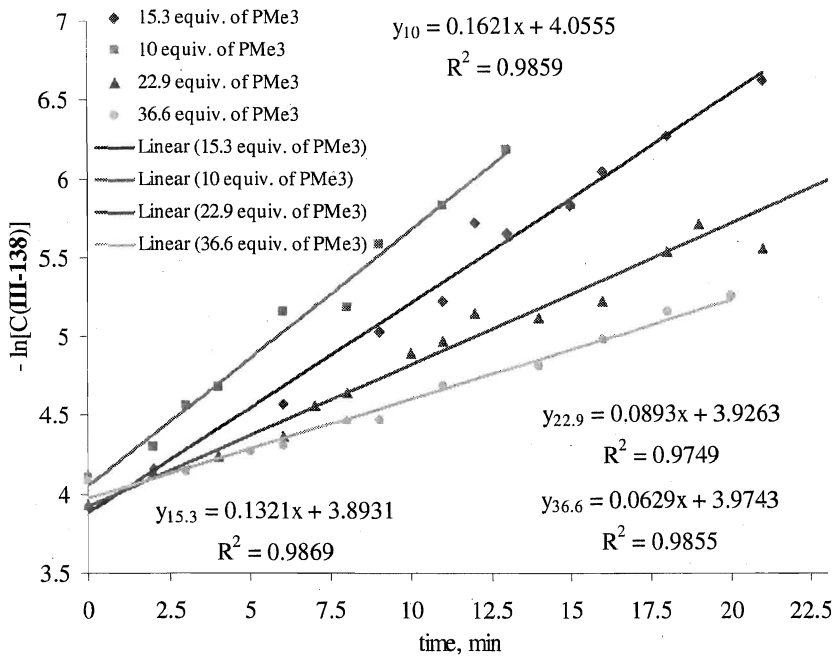

Figure 60. –Ln[C]/time dependence for reactions of **III-135** with $PhSiH_3$ at 22 °C in the presence of excess PMe_3.

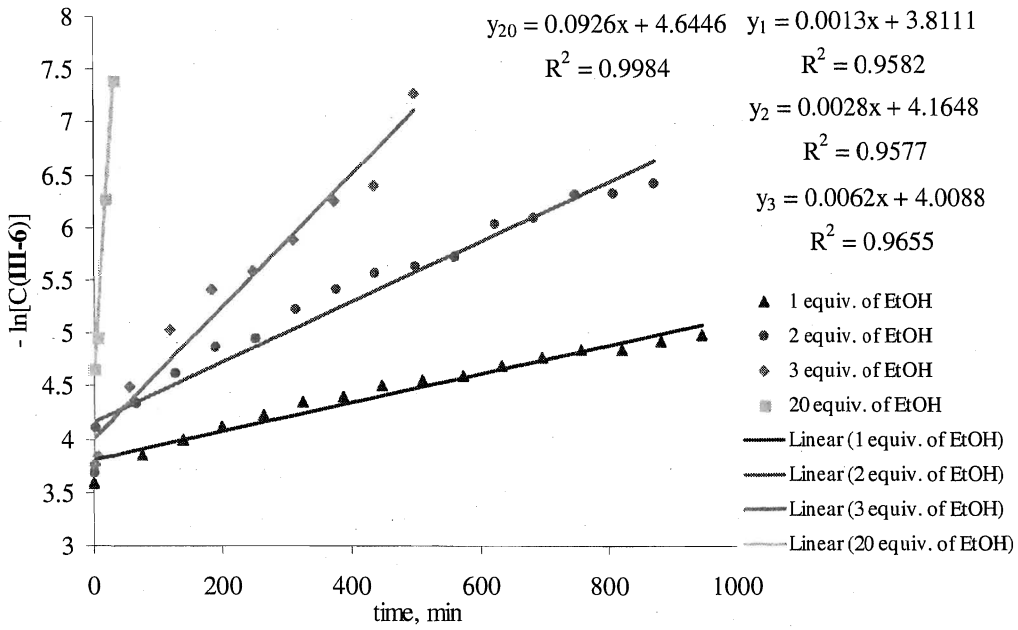

Figure 61. –Ln[C]/time dependence for reactions of **III-6** with EtOH at 22 °C.

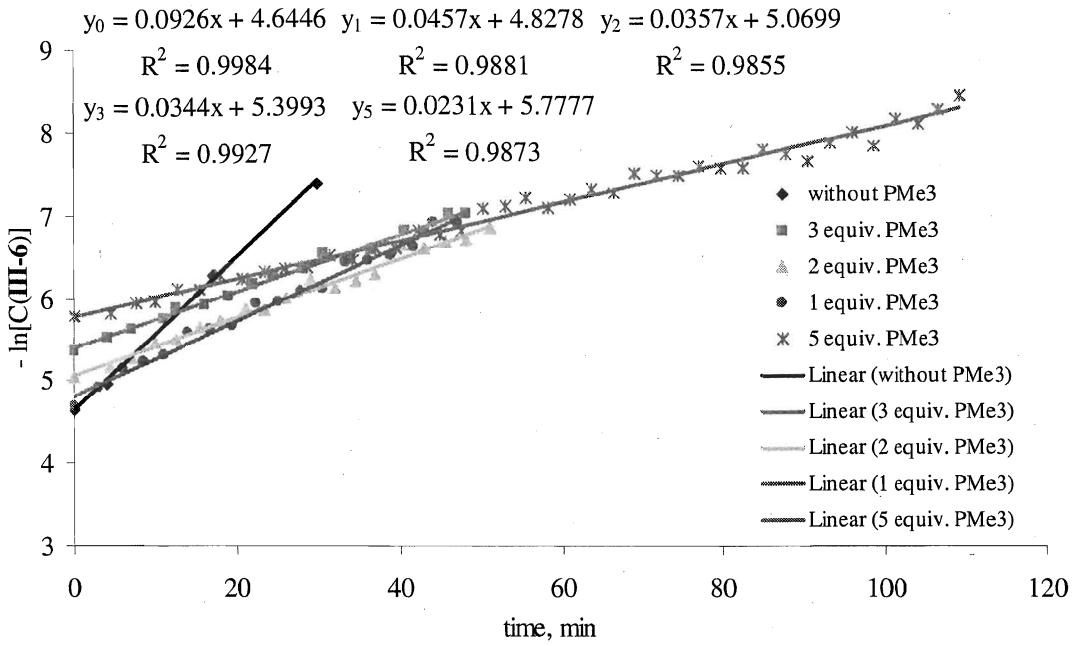

Figure 62. –Ln[C]/time dependence for reactions of **III-6** with EtOH at 22 °C in the presence of excess PMe_3.

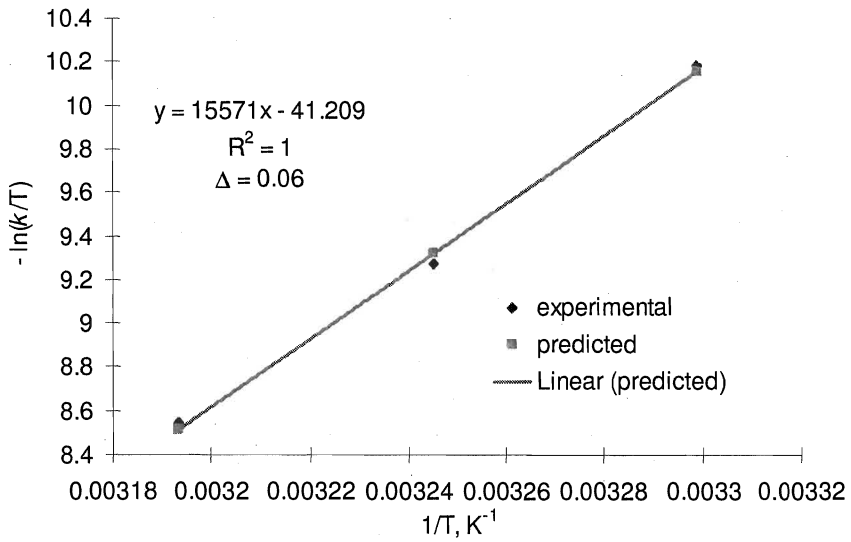

Figure 63. Eyring plot for exchange between SiH_2Ph substituent in **III-7** and free $PhSiH_3$ (standard error 0.06).

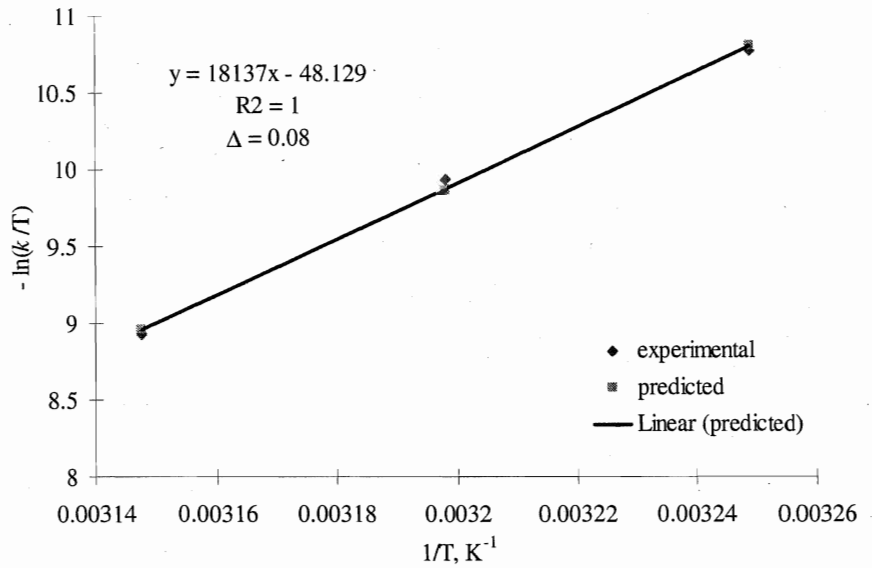

Figure 64. Eyring plot for exchange between SiH_2Ph substituent in **III-7** and free $PhSiH_3$ in the presence of 7 equiv. of PMe_3 (standard error 0.08).

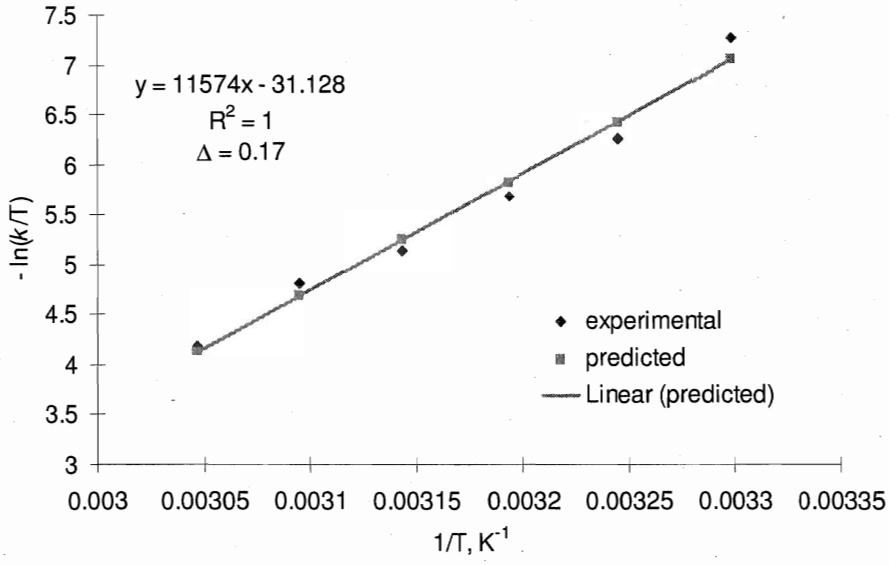

Figure 65. Eyring plot for intramolecular phosphine exchange in **III-7** (standard error 0.17).

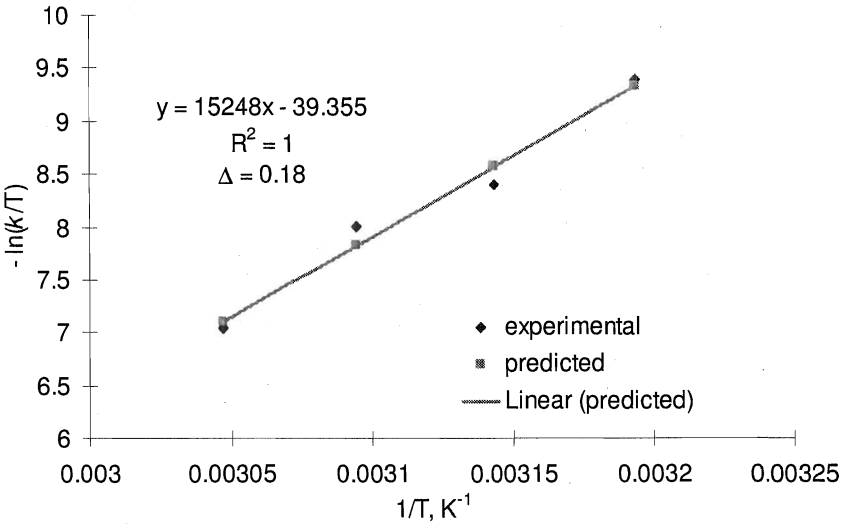

Figure 66. Eyring plot for intermolecular phosphine exchange between **III-7** and free PMe_3 (standard error 0.18).

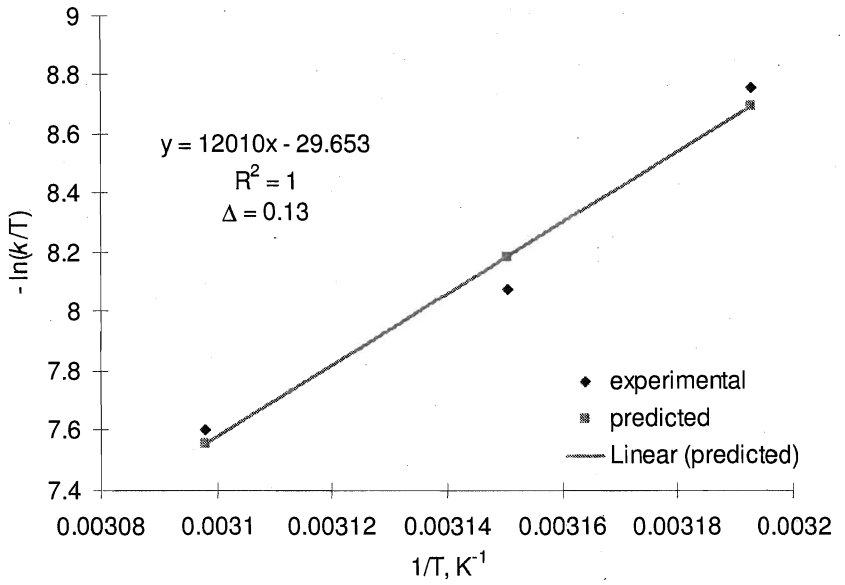

Figure 67. Eyring plot for intermolecular phosphine exchange between **III-7** and free PMe_3 in the presence of 10 equiv. of $PhSiH_3$ (standard error 0.13).

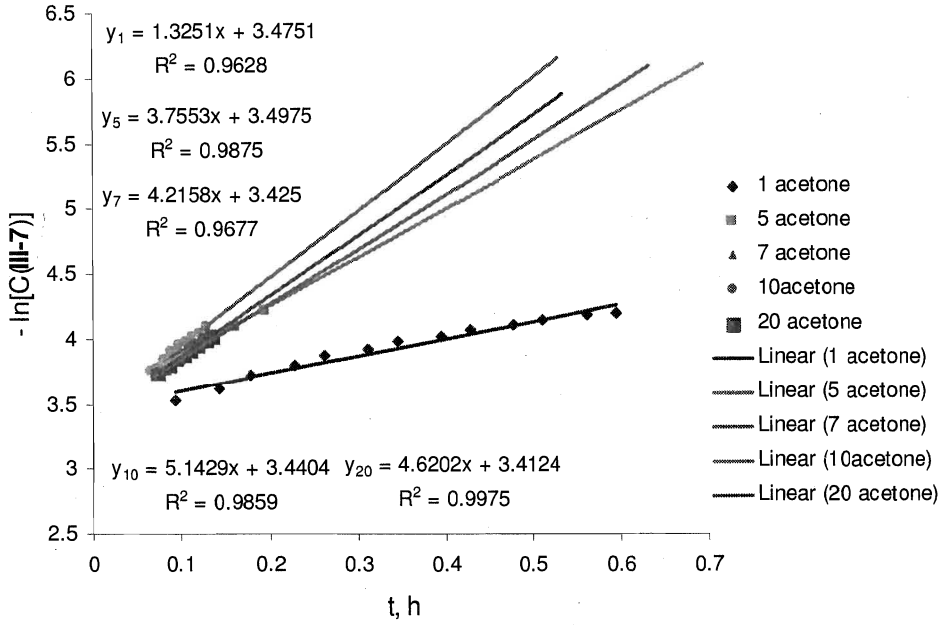

Figure 68. –Ln[C]/time dependence for reactions of **III-7** with acetone at 22 °C (50 % conversion).

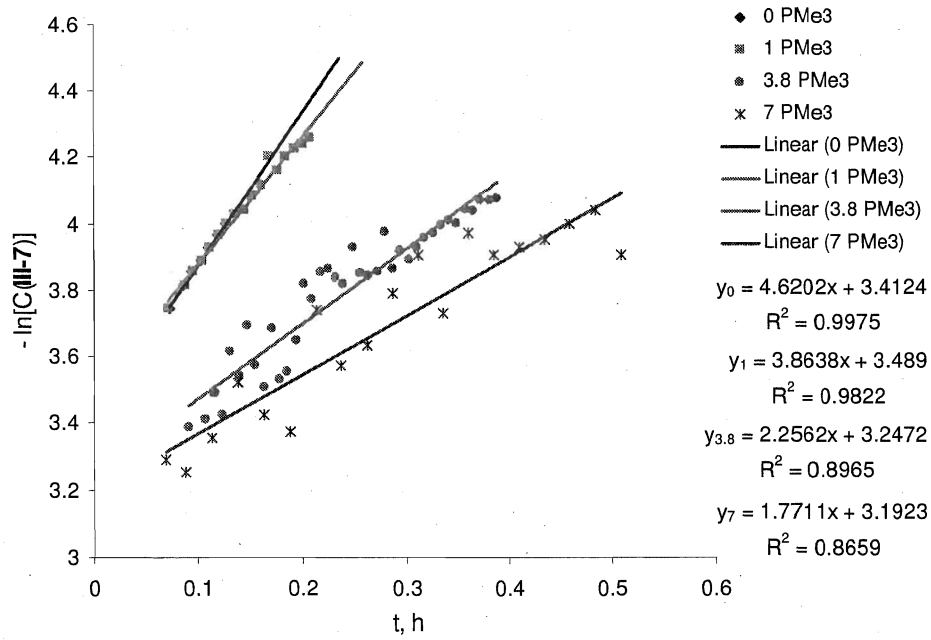

Figure 69. –Ln[C]/time dependence for reactions of **III-7** with acetone at 22 °C (50 % conversion) in the presence of PMe_3.

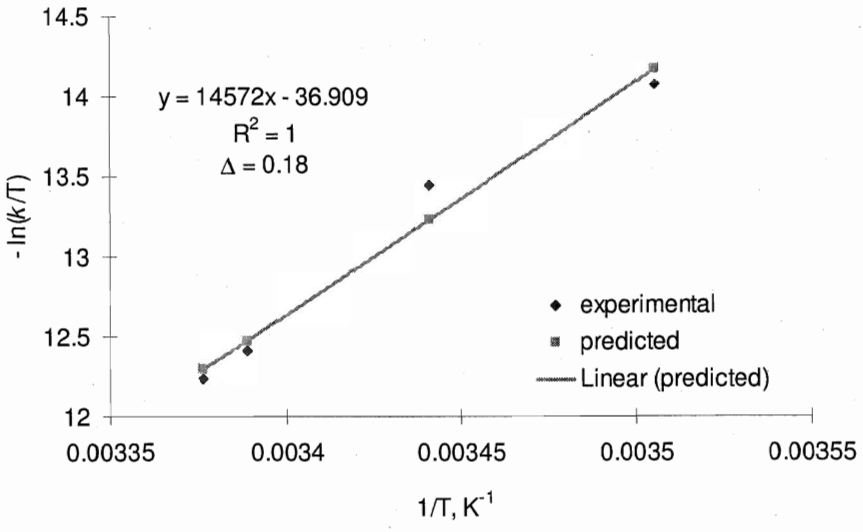

Figure 70. Eyring plot for the reaction of **III-7** with 20 equiv, of acetone (50 % conversion; standard error 0.18).

Table 25. Crystal structure determination parameters for **III-47**.

Empirical formula / weight	$C_{21}H_{44}Cl_2MoNP_3$ / 570.32		
Color, habit	dark-brown plate		
Crystal size, mm	0.40 x 0.25 x 0.06		
Crystal system, space group	Monoclinic, P 2(1)/c		
Unit cell dimensions:			
a, Å	17.819(2)	α, °	90
b, Å	9.5317(11)	β, °	97.754(2)
c, Å	16.9762(19)	γ, °	90
Volume, $Å^3$	2857.0(6)		
Z	4		
Calculated density, g/cm^3	1.326		
Absorption coefficient, mm^{-1}	0.822		
F(000)	1192		
Diffractometer	Bruker-SMART-APEX-2		
Temperature, K	150(2)		
Radiation, (lambda, A)	graphite monochromatized MoK\a (0.71073)		
Theta range, deg	2.31 to 29.00		
Limiting indices	-24<=h<=24, -13<=k<=12, -23<=l<=23		
Reflections collected / unique	29747 / 7564 [R(int) = 0.0771]		
Completeness to theta = 29.00	99.7 %		
Reflections with I>2sigma(I)	5361		
Min. and Max. transmission	0.7344 and 0.9523		
Refinement method	Full-matrix least-squares on F^2 (SHELXL-97)		
Hydrogen treatment	All H atoms were found from diff. Fourier synthesis and refined isotropically.		
Data / restraints / parameters	7564 / 0 / 253		
Goodness-of-fit on F^2	1.149		
Final R indices [I>2sigma(I)]	R1 = 0.0689, wR2 = 0.1210		
R indices (all data)	R1 = 0.1078, wR2 = 0.1291		
Largest diff. peak and hole, e/A^3	0.802 and -1.563		

Table 26. Crystal structure determination parameters for **III-1**.

Empirical formula	$C_{44}H_{69}MoN_2PSi_2$[a]		
Formula weight	809.10		
Color	dark-orange		
Crystal size, mm	0.35 x 0.18 x 0.12		
Crystal system, space group	Monoclinic, P 2(1)/c		
Unit cell dimensions:			
a, Å	8.5536(12)	α, °	90.00
b, Å	22.691(3)	β, °	97.423(3)
c, Å	23.379(3)	γ, °	90.00
Volume, $Å^3$	4499.6(11)		
Z	4		
Calculated density, g/cm^3	1.194		
Absorption coefficient, mm^{-1}	0.411		
F(000)	1728		
Diffractometer	Bruker-SMART-APEX-2		
Temperature, K	153(2)		
Radiation, (lambda, Å)	graphite monochromatized MoK\a (0.71073)		
Theta range, deg	1.79 to 29.00		
Limiting indices	-11<=h<=11, -30<=k<=30, -31<=l<=31		
Reflections collected / unique	11725 / 7701		
Absorption correction type	Semi-empirical from equivalents		
Solution method	Direct methods (SHELXS-97)		
Refinement method	Full-matrix least-squares on F^2 (SHELXL-97)		
Data / restraints / parameters	11725 / 0 / 459		
Goodness-of-fit on F^2	1.054		
Final R indices [I>2sigma(I)]	R1 = 0.0718, wR2 = 0.1749		
R indices (all data)	R1 = 0.1195, wR2 = 0.1600		
Largest diff. peak and hole, e/A^3	1.018 and -0.828		

[a] Molecular formula and molecular weight were calculated for a mixture of **III-1** and a molecule of co-crystallized hexane.

Table 27. Crystal structure determination parameters for **III-7**.

Empirical formula	$C_{27}H_{52}MoNP_3Si$	
Formula weight	607.64	
Temperature, K	120(2)	
Wavelength, Å	0.71073	
Crystal system	Triclinic	
Space group	P-1	
Unit cell dimensions	a = 8.9866(2) Å	α = 90.6070(10) °
	b = 10.0238(2) Å	β = 99.7140(10) °
	c = 20.0398(5) Å	γ = 112.5150(10) °
Volume, $Å^3$	1638.06(6)	
Z	2	
Density (calculated), mg/m^3	1.232	
Absorption coefficient, mm^{-1}	0.599	
F(000)	644	
Crystal size, mm^3	0.38 x 0.22 x 0.14	
Theta range for data collection, °	1.03 to 29.95	
Index ranges	-12<=h<=12, -13<=k<=13, -25<=l<=28	
Reflections collected	12426	
Independent reflections	8391 [R(int) = 0.0184]	
Completeness to theta = 29.95°	88.3 %	
Absorption correction	Semi-empirical from equivalents	
Max. and min. transmission	0.9209 and 0.8045	
Refinement method	Full-matrix least-squares on F^2	
Data / restraints / parameters	8391 / 0 / 306	
Goodness-of-fit on F^2	1.021	
Final R indices [I>2sigma(I)]	R1 = 0.0320, wR2 = 0.0732	
R indices (all data)	R1 = 0.0403, wR2 = 0.0761	
Largest diff. peak and hole, $e/Å^3$	1.332 and -0.415	

Table 28. Crystal structure determination parameters for **III-77**.

Empirical formula	$C_{32}H_{55}MoN_2P_2Si_3$		
Formula weight	709.93		
Crystal size, mm	0.22 x 0.10 x 0.08		
Space group	P21/n		
Unit cell dimensions:			
a, Å	10.893(3)	α, °	90.00
b, Å	22.132(7)	β, °	100.687(14)
c, Å	15.524(5)	γ, °	90.00
Volume, $Å^3$	3678(2)		
Z	4		
Calculated density, g/cm^3	1.282		
Absorption coefficient, mm^{-1}	0.565		
F(000)	1500		
Diffractometer	Bruker-SMART-APEX-2		
Temperature, K	123(2)		
Radiation, (lambda, A)	graphite monochromatized MoK\a (0.71073)		
Theta range, deg	1.62 to 28.50		
Limiting indices	-14<=h<=14, -29<=k<=29, -20<=l<=20		
Reflections collected / unique	9186 / 2281		
Absorption correction type	Semi-empirical from equivalents		
Solution method	Direct methods (SHELXS-97)		
Refinement method	Full-matrix least-squares on F^2 (SHELXL-97)		
Data / restraints / parameters	9186 / 0 / 377		
Goodness-of-fit on F^2	0.711		
Final R indices [I>2sigma(I)]	R1 = 0.0994, wR2 = 0.2698		
R indices (all data)	R1 = 0.2074, wR2 = 0.3381		
Largest diff. peak and hole, e/A^3	1.059 and -0.893		

Table 29. Crystal structure determination parameters for **III-3**.

Empirical formula	$C_{74}H_{112}Mo_2N_4P_2Si_2$[a]	
Formula weight	1367.68	
Temperature, K	123(2)	
Wavelength, Å	0.71073	
Crystal system	Monoclinic	
Space group	P2(1)/c	
Unit cell dimensions	a = 20.7264(11) Å	α = 90 °
	b = 17.4162(10) Å	β = 110.163(3) °
	c = 22.0696(12) Å	γ = 90 °
Volume, $Å^3$	7478.4(7)	
Z	4	
Density (calculated), mg/m^3	1.215	
Absorption coefficient, mm^{-1}	0.451	
F(000)	2904	
Crystal size, mm	0.28 x 0.16 x 0.08	
Theta range for data collection, °	1.05 to 30.00	
Index ranges	-29<=h<=29, -24<=k<=24, -29<=l<=31	
Reflections collected	83082	
Independent reflections	20834 [R(int) = 0.0721]	
Completeness to theta = 30.00°	95.5 %	
Absorption correction	Semi-empirical from equivalents	
Max. and min. transmission	0.9648 and 0.8840	
Refinement method	Full-matrix least-squares on F^2	
Data / restraints / parameters	20834 / 0 / 755	
Goodness-of-fit on F^2	1.029	
Final R indices [I>2sigma(I)]	R1 = 0.0537, wR2 = 0.0987	
R indices (all data)	R1 = 0.0986, wR2 = 0.1090	
Largest diff. peak and hole, $e/Å^3$	1.261 and -0.810	

[a] The crystal data, empirical formula, and molecular weight were calculated for the fragment containing two molecules of **III-3**.

Table 30. Crystal structure determination parameters for **III-125**.

Empirical formula	$C_{30}H_{56}BMoN_2P_2$	
Formula weight	613.49	
Temperature, K	150	
Wavelength, Å	0.71073	
Space group	P1	
Unit cell dimensions	a = 11.2581(3) Å	α = 102.8021(14) °
	b = 12.8096(4) Å	β = 93.3190(14) °
	c = 13.0998(4) Å	γ = 107.7986(11) °
Volume, $Å^3$	1737.88(9)	
Z	2	
Density (calculated), mg/m^3	1.172	
Absorption coefficient, mm^{-1}	0.489	
R1	0.0452 [I>2sigma(I)]	
wR2	0.1077 (all data)	

Table 31. Crystal structure determination parameters for **III-8**.

Empirical formula	$C_{18}H_{43}B_2MoNP_2$	
Formula weight	453.03	
Temperature, K	123(2)	
Wavelength, Å	0.71073	
Crystal system	Orthorhombic	
Space group	Pna2(1)	
Unit cell dimensions	a = 19.0671(5) Å	α = 90 °
	b = 9.5190(3) Å	β = 90 °
	c = 14.0089(4) Å	γ = 90 °
Volume, $Å^3$	2542.61(13)	
Z	4	
Density (calculated), mg/m^3	1.183	
Absorption coefficient, mm^{-1}	0.643	
F(000)	960	
Crystal size, mm	0.28 x 0.26 x 0.22	
Theta range for data collection, °	2.14 to 29.50	
Index ranges	-26<=h<=25, -13<=k<=13, -14<=l<=19	
Reflections collected	18750	
Independent reflections	5977 [R(int) = 0.0399]	
Completeness to theta = 29.50°	98.0 %	
Absorption correction	Semi-empirical from equivalents	
Max. and min. transmission	0.8715 and 0.8405	
Refinement method	Full-matrix least-squares on F^2	
Data / restraints / parameters	5977 / 1 / 262	
Goodness-of-fit on F^2	1.007	
Final R indices [I>2sigma(I)]	R1 = 0.0334, wR2 = 0.0663	
R indices (all data)	R1 = 0.0565, wR2 = 0.0716	
Absolute structure parameter	0.43(10)	
Largest diff. peak and hole, $e/Å^3$	0.343 and -0.366	

Table 32. Crystal structure determination parameters for **III-6**.

Empirical formula	$C_{21}H_{45}ClMoNP_3$
Formula weight	535.88
Temperature, K	120(2)
Wavelength, Å	0.71073
Crystal system	Monoclinic
Space group	P21/c
Unit cell dimensions:	
	a = 21.8377(8) Å β = 114.664(1) °
	b = 15.3687(6) Å
	c = 18.3470(7) Å
Volume, $Å^3$	5595.8(4)
Z	8
Density (calculated), mg/m^3	1.272
Absorption coefficient, mm^{-1}	0.743
F(000)	2256
Crystal size, mm	0.18 x 0.10 x 0.08
Theta range for data collection, °	1.03 to 27.00
Index ranges	-27<=h<=27, -19<=k<=19, -20<=l<=20
Reflections collected	34830
Independent reflections	12198 [R(int) = 0.0621]
Completeness to theta = 27.00°	99.9 %
Max. and min. transmission	0.8779 and 0.9429
Refinement method	Full-matrix least-squares on F^2
Data / restraints / parameters	8935/ 0 / 522
Goodness-of-fit on F^2	1.02
Final R indices [I>2sigma(I)]	R1 = 0.0456, wR2 = 0.1023
R indices (all data)	R1 = 0.0758, wR2 = 0.1133

Table 33. Crystal structure determination parameters for **III-138**.

Empirical formula	$C_{27}H_{55}ClMoNOP_3$
Formula weight	634.02
Crystal size, mm	0.30 x 0.28 x 0.04
Unit cell dimensions:	
	a, Å 12.6249(11) α, ° 90
	b, Å 19.6456(17) β, ° 102.5750(10)
	c, Å 13.7219(12) γ, ° 90
Volume, $Å^3$	3321.7(5)
Z	4
Calculated density, g/cm^3	1.268
Absorption coefficient, mm^{-1}	0.639
F(000)	1344
Temperature, K	153(2)
Radiation, (lambda, Å)	graphite monochromatized MoK\a (0.71073)
Theta range, deg	1.65 to 30.00
Limiting indices	-17<=h<=17, -27<=k<=27, -19<=l<=19
Reflections collected / unique	38454 / 9652 [R(int) = 0.0355]
Completeness to theta = 30.00 °	99.7 %
Reflections with I>2sigma(I)	8215
Min. and Max. transmission	0.8315 and 0.9749
Solution method	Direct methods (SHELXS-97)
Refinement method	Full-matrix least-squares on F^2 (SHELXL-97)
Hydrogen treatment	All H atoms were found from diff. Fourier synthesis and refined isotropically.
Data / restraints / parameters	9652 / 0 / 307
Goodness-of-fit on F^2	1.149
Final R indices [I>2sigma(I)]	R1 = 0.0444, wR2 = 0.1258
R indices (all data)	R1 = 0.0537, wR2 = 0.1289
Largest diff. peak and hole, $e/Å^3$	2.881 and -0.447

Table 34. Crystal structure determination parameters for **III-142**.

Empirical formula	$C_{25}H_{41}ClMoN_2P_2$	
Formula weight	562.93	
Temperature, K	153(2)	
Wavelength, Å	0.71073	
Crystal system	Monoclinic	
Space group	P2(1)/c	
Unit cell dimensions:		
	a = 22.805(4) Å	α = 90.00 °
	b = 16.318(3) Å	β = 110.478(3) °
	c = 16.590(3) Å	γ = 90.00 °
Volume, $Å^3$	5783.4(19)	
Z	8	
Density (calculated), mg/m^3	1.293	
Absorption coefficient, mm^{-1}	0.671	
F(000)	2352	
Crystal size, mm	0.19 x 0.12 x 0.06	
Theta range for data collection, °	0.95 to 28.00	
Index ranges	-30<=h<=30, -21<=k<=21, -21<=l<=21	
Reflections collected	13937	
Independent reflections	7310	
Completeness to theta = 28.00°	99.9 %	
Refinement method	Full-matrix least-squares on F^2	
Data / restraints / parameters	13937/ 0 / 559	
Goodness-of-fit on F^2	0.863	
Final R indices [I>2sigma(I)]	R1 = 0.0610, wR2 = 0.1332	
R indices (all data)	R1 = 0.1480, wR2 = 0.1109	

Table 35. Crystal structure determination parameters for **III-145**.

Empirical formula	$C_{29}H_{38}MoNO_2P$	
Formula weight	559.51	
Temperature, K	123(2)	
Wavelength, Å	0.71073	
Crystal system	Monoclinic	
Space group	P2(1)/n	
Unit cell dimensions	a = 10.9983(4) Å	α = 90 °
	b = 18.5204(6) Å	β = 93.261(2) °
	c = 13.6935(4) Å	γ = 90 °
Volume, $Å^3$	2784.75(16)	
Z	4	
Density (calculated), mg/m^3	1.335	
Absorption coefficient, mm^{-1}	0.553	
F(000)	1168	
Crystal size, mm	0.34 x 0.26 x 0.22	
Theta range for data collection, °	1.85 to 30.00.	
Index ranges	-15<=h<=15, -26<=k<=25, -19<=l<=17	
Reflections collected	24780	
Independent reflections	8084 [R(int) = 0.0596]	
Completeness to theta = 30.00 °	99.5 %	
Absorption correction	Semi-empirical from equivalents	
Max. and min. transmission	0.8880 and 0.8342	
Refinement method	Full-matrix least-squares on F^2	
Data / restraints / parameters	8084 / 0 / 307	
Goodness-of-fit on F^2	0.949	
Final R indices [I>2sigma(I)]	R1 = 0.0440, wR2 = 0.1007	
R indices (all data)	R1 = 0.0752, wR2 = 0.1110	
Largest diff. peak and hole, $e/Å^3$	1.324 and -0.499	

VII. References

[1] Hegedus, L. S. *Transition Metals in the Synthesis of Complex Organic Molecules*, 2nd ed., University Science Books, Sausalito, **1999**, pp. 39-53.

[2] (a) Carey, F. A.; Sundberg, R. J. *Advanced Organic Chemistry. Part B: Reactions and Synthesis*, 5th ed., Springer, New York, **2007**, pp. 367-462. (b) Brown, H. C. *Boranes in Organic Chemistry*, Cornell University Press, Ithaca, **1972**. (c) Brown, H. C. *Organic Synthesis via Boranes*, Wiley, New York, **1975**, (d) Brown, H. C.; Zaidlewicz, M. *Organic Synthesis via Boranes Vol. 2: Recent Developments*, Aldrich Chemical Company, Milwaukee, **2001**. (e) Midland, M. M. *Chem. Rev.* **1989**, *89*, 1553.

[3] *Modern Reduction Methods*, Andersson, P. G.; Munslow, I. J. (Eds.), Wiley-VCH, Weinheim, **2008**.

[4] For example, see following reviews and references therein: (a) Harmon, R. E.; Gupta, S. K.; Brown, D. J. *Chem. Rev.* **1973**, *73*, 21. (b) Noyori, R.; Kitamura, M.; Ohkuma, T. *PNAS* **2004**, *101*, 15, 5356. (c) Knowles, W. S.; Noyori, R. *Acc. Chem. Res.* **2007**, *40*, 1238.

[5] For example, see following reviews and references therein: (a) Brinkman, J. A.; Sowa, J. R. in *Catalysis of Organic Reactions*, Herkes, F. E. (Ed.), Marcel Dekker, Inc., New York, **1998**, pp. 543-549. (b)

[6] For example, see following reviews and references therein: (a) Seayad, J.; Tillack, A.; Hartung, C. G.; Beller, M. *Adv. Synth. Catal.* **2002**, *8*, 344. (b) Pohlki, F.; Doye, S. *Chem. Soc. Rev.*, **2003**, *32*, 104. (c) Alonso, F.; Beletskaya, I. P.; Yus, M. *Chem. Rev.* **2004**, *104*, 3079. (d) Severin, R.; Doye, S. *Chem. Soc. Rev.* **2007**, *36*, 1407. (e) Muller, T. E.; Hultzsch, K. C.; Yus, M.; Foubelo, F.; Tada, M. *Chem. Rev.* **2008**, *108*, 3795.

[7] (a) Marciniec, B.; Gulinski, J.; Urbaniak, W.; Kornetka, Z. W. *Comprehensive Handbook on Hydrosilylation*, Marciniec, B. (Ed.), Pergamon Press: Oxford, **1992**. (b) Marciniec, B.; Maciejewski, H.; Pietraszuk, C.; Pawluć, P. *Hydrosylilation: A Comprehensive Review on Recent Advances*, Marciniec, B. (Ed.), Springer: London, **2008**.

[8] (a) Barry, J. T.; Chacon, S. T.; Chisholm, M. H.; Huffman, J. C.; Streib, W. E. *J. Am. Chem. Soc.* **1995**, *117*, 1974. (b) Leboeuf, J. F.; Leblanc, J. C.; Moise, C. *C. R. Acad. Sci., Ser. II* **1988**, *307*, 1757. (c) Green, M. L. H.; Knowles, P. J. *J. Chem. Soc., Perkin Trans. 1* **1973**, 989.

[9] For example, see: (a) Halterman, R. L.; Ramsey, T. M.; Chen, Z. *J. Org. Chem.* **1994**, *59*, 2642. (b) Harrod, J. F.; Xin, S. *Can. J. Chem.* **1995**, *73*, 999. (c) Broene, R. D.; Buchwald, S. L. *J. Am. Chem. Soc.* **1993**, *115*, 12569. (d) Carter, M. B.; Schiøtt, B.; Gutiérrez, A.; Buchwald, S. L. *J. Am. Chem. Soc.* **1994**, *116*, 11667. (e) Yun, J.; Buchwald, S. L. *J. Am. Chem. Soc.* **1999**, *121*, 5640. (f) Yun, S. S.; Yong, S. Y.; Lee, S. *Bull. Korean Chem. Soc.* **1997**, *18*, 1058.

[10] (a) Chalk, A. J.; Harrod, J. F. *J. Am. Chem. Soc.* **1965**, *87*, 16. (b) Ojima, I.; Kogure, T.; Kumagai, M.; Horiuchi, S.; Sato, T. *J. Organomet. Chem.* **1976**, *122*, 83. (c) Peyronel, J. F.; Kagan, H. B. *Nouv. J. Chem.* **1978**, *2*, 211. (d) Reyers, C.; Prock, A.; Giering, W. P. *Organometallics* **2002**, *21*, 546 and references therein.

[11] (a) Nolin, K. A.; Krumper, J. R.; Pluth, M. D.; Bergman, R. G.; Toste, F. D. *J. Am. Chem. Soc.* **2007**, *129*, 14684. (b) Chung, L. W.; Lee, H. G.; Lin, Z.; Wu, Y.-D. *J. Org. Chem.* **2006**, *71*, 6000. (c) Thiel, W. *Angew. Chem., Int. Ed.* **2003**, *42*, 5390.

[12] (a) Royo, B.; Romão, C. C. *J. Mol. Catal. A: Chem.* **2005**, *236*, 107. (b) Reis, P. M.; Romão, C. C.; Royo, B. *Dalton Trans.* **2006**, 1842. (c) Costa, P. J.; Romão, C. C.; Fernandens, A. C.; Royo, B.; Reis, P.; Calhorda, M. J. *Chem. Eur. J.* **2007**, *13*, 3934.

[13] (a) Ison, E. A.; Trivedi, E. R.; Corbin, R. A.; Abu-Omar, M. M. *J. Am. Chem. Soc.* **2005**, *127*, 15374. (b) Du, G. D.; Abu-Omar, M. M. *Organometallics* **2006**, *25*, 4920. (c) Du, G. D.; Fanwick, P. E.; Abu-Omar, M. M. *J. Am. Chem. Soc.* **2007**, *129*, 5180. (d) Du, G.; Fanwick, P. E.; Abu-Omar, M. M. *Inorganica Chimica Acta* **2008**, *361*, 3184. (e) Du, G.; Abu-Omar, M. M. *Curr. Org. Chem.* **2008**, *12*, 1185.

[14] (a) Nikonov, G. I.; Mountford, P.; Ignatov, S. K.; Green, J. C.; Cooke, P. A.; Leech, M. A.; Kuzmina, L. G.; Razuvaev, A. G.; Rees, N. H.; Blake, A. J.; Howard, J. A. K.; Lemenovskii, D. A. *J. Chem. Soc., Dalton Trans.*, **2001**, 2903. (b) Nikonov, G. I.; Mountford, P.; Green, J. C.; Cooke, P. A.; Leech, M. A.; Blake, A. J.; Howard, J. A. K.; Lemenovskii, D. A. *Eur. J. Inorg. Chem.* **2000**, 1917. (c) Nikonov, G. I.; Mountford, P.;

Kuzmina, L. G.; Howard, J. A. K.; Lemenovskii, D. A.; Roitershtein, D. M. *J. Organomet. Chem.* **2001**, *628*, 25. (d) Nikonov, G, I,; Mountford, P.; Dubberley, S. R. *Inorg. Chem.* **2003**, *42*, 258. (e) Ignatov, S. K.; Rees, N. H.; Merkoulov, A. A.; Dubberley, S. R.; Razuvaev, A. G.; Mountford, P.; Nikonov, G. I. *Chem. Eur. J.* **2008**, *14*, 296. (f) Ignatov, S. K.; Rees, N. H.; Merkoulov, A. A.; Dubberley, S. R.; Razuvaev, A. G.; Mountford, P.; Nikonov, G. I. *Organometallics* **2008**, *27*, 5968. (g) Nikonov, G. I. *J. Organomet. Chem.* **2001**, *635*, 24. (h) Dubberley, S. R.; Ignatov, S. K.; Rees, N. H.; Razuvaev, A. G.; Mountford, P.; Nikonov, G. I. *J. Am. Chem. Soc.* **2003**, *125*, 642.

[15] Ignatov, S. K.; Rees, N. H.; Dubberley, S. R.; Razuvaev, A. G.; Mountford P.; Nikonov, G. I. *Chem. Comm.*, **2004**, 952.

[16] Gountchev, T. I.; Tilley, T. D.; *J. Am. Chem. Soc.* **1997**, *119*, 12831.

[17] Nikonov G. I. *Adv. Organomet. Chem.*, **2005**, *53*, pp. 217-309 and references therein.

[18] (a) Piers, W. E. *Chem. Eur. J.* **1998**, *4*, 13. (b) Jordan, R. F. *Adv. Organomet. Chem.* **1991**, *32*, 325. (c) Hoveyda, A. J.; Morken, J. P. *Angew. Chem. Int. Ed. Engl.* **1996**, *35*, 1262. (d) Antinolo, A.; Carrillo-Hermosilla, F.; Fajardo, M.; Fernandez-Baeza, J.; Garsia-Yuste, S.; Otero, A. *Coord. Chem. Rev.* **1999**, *193-195*, 43. (e) Chakraborty, S.; Krause, J. A.; Guan, H. *Organometallics* **2009**, *28*, 582.

[19] (a) Abdur-Rashid, K.; Faatz, M.; Lough, A. J.; Morris, R. H. *J. Am. Chem. Soc.* **2001**, *123*, 7473. (b) Brintzinger, H. H.; Fischer, D.; Mulhaupt, R.; Rieger, B.; Waymouth, R. M. *Angew. Chem., Int. Ed. Engl.* **1995**, *34*, 1143. (c) Marciniec, B. *Appl. Organomet. Chem.* **2000**, *14*, 527. (d) Duckett, S. B.; Perutz, R. N. *Organometallics* **1992**, *11*, 90. (e) Bergens, S. H.; Noheda, P.; Whelan, J.; Bosnich, B. *J. Am. Chem. Soc.* **1992**, *114*, 2128. (f) Shu, R.; Harrod, J. F.; Lebuis, A.-M. *Can. J. Chem.* **2002**, *80*, 489. (g) Harrod, J. F.; Shu, R.; Woo, H.-G.; Samuel, E. *Can. J. Chem.* **2001**, *79*, 1075.

[20] See, for example: (a) Britovsek, G. J. P.; Gibson, V. C.; Wass, D. F. *Angew. Chem., Int. Ed.* **1999**, *38*, 428. (b) Gibson, V. C.; Spitzmesser, S. K. *Chem. Rev.* **2003**, *103*, 283. (c) Bolton, P. D.; Mountford, P. *Adv. Synth. Catal.* **2005**, *347*, 355.

[21] Ma, K.; Piers, W. E.; Gao, Y.; Parvez, M. *J. Am. Chem. Soc.* **2004**, *126*, 5668.

[22] Kubas, G. J.; Ryan, R. R.; Swanson, B. I.; Vergamini, P. J.; Wasserman, H. J. *J. Am. Chem. Soc.* **1984**, *100*, 451.

[23] Kubas, G. J. *Metal Dihydrogen and σ-Bond Complexes*, Kluwer Academic/Plenum: New York, **2001**.

[24] (a) Crabtree, R. H. Hamilton, D. G. *Adv. Organomet. Chem.*, **1988**, *28*, 299. (b) Crabtree, R. H. *Angew. Chem. Int. Ed. Engl.* **1993**, *32*, 789.

[25] (a) Brookhardt, M.; Green, M. L. H. *J. Organomet. Chem.* **1983**, *250*, 395. (b) Brookhardt, M.; Green, M. L. H.; Wong, L. L. *Prog. Inorg. Chem.* **1988**, *36*, 1.

[26] (a) Schneider, J. *Angew. Chem. Int. Ed. Engl.* **1996**, *35*, 1068. (b) Hall, C.; Perutz, R. N. *Chem. Rev.* **1996**, *96*, 3125.

[27] Hoyano, J. K.; Elder, M.; Graham, W. A. G. *J. Am. Chem. Soc.* **1969**, *91*, 4568.

[28] Graham, W. A. G. *J. Organomet. Chem.* **1986**, *300*, 81.

[29] Corey, J. Y.; Braddock-Wilking, J. *Chem. Rev.* **1999**, *99*, 175.

[30] Andrews, M. A.; Kirtley, S. W.; Kaez H. D. In *Transition Metal Hydrides*, R. Bau (Ed.) Washington, **1978**, p.215.

[31] Bennett, M. J.; Simpson, K. A. *J. Am. Chem. Soc.* **1971**, *93*, 7156.

[32] Colomer, E.; Corriu, R. J. P.; Marzin, C.; Vioux, A. *Inorg. Chem.* **1982**, *21*, 368.

[33] Schubert, U.; Ackermann, K.; Wörle, B. *J. Am. Chem. Soc.* **1982**, *104*, 7378.

[34] Kubas, G. J. *J. Organomet. Chem.* **2001**, *635*, 37.

[35] For instance, see: (a) Salomon, R. G.; Kochi, J. K. *J. Organomet. Chem.* **1974**, *64*, 135. (b) Nelson, J. H.; Wheelock, K. S.; Cusachs, L. C.; Jonassen, H. B. *J. Am. Chem. Soc.* **1969**, *91*, 7005. (c) Pidun, U.; Frenking, G. *J. Organomet. Chem.* **1996**, *525*, 269. (d) Arber, J. M.; Urch, D. S.; Mingos, D. M. P.; Royse, S. J. *J. Chem. Soc., Chem. Commun.* **1982**, 1241. (e) Nelson, J. H.; Wheelock, K. S.; Cusachs, L. C.; Jonassen, H. B. *Chem. Commun.* **1969**, 1019.

[36] Albright, T. A.; Burdett, J. K.; Whangbo, M.-H. *Orbital Interactions in Chemistry*, Wiley: New York, **1985**, p.36.

[37] Burkey, T. J. *J. Am. Chem. Soc.* **1990**, *112*, 8329.

[38] Schubert, U. *Adv. Organomet. Chem.*, **1990**, *30*, 151.

[39] Lin, Z. *Chem. Soc. Rev.* **2002**, *31*, 239.

[40] (a) Michalczyk, M. J.; Kink, M. J.; Haller, K. J.; West, R.; Michl, J. *Organometallics* **1986**, *5*, 531. (b) Kapp, J.; Remko, M.; Schleyer, P. *Inorg. Chem.* **1997**, *36*, 4241.

[41] (a) Wiberg, N.; Schuster, H.; Simon A.; Peters, K. *Angew. Chem., Int. Ed. Engl.*, **1986**, *25*, 79. (b) Watanabe, H.; Kato, M.; Okawa, T.; Nagai, Y.; Goto, M. *J. Organomet. Chem.,* **1984**, *271*, 225. (c) Weidenbruch, M. *Comm. Inorg. Chem.* **1986**, *5*, 247.

[42] Choi, S.-H.; Feng, J.; Lin, Z. *Organometallics*, **2000**, *19*, 2051.

[43] (a) Heinekey, D. M.; Lledós, A.; Lluch, J. M. *Chem. Soc. Rev.,* **2004**, *33*, 175. (b) Maseras, F.; Lledós, A.; Clot, E.; Eisenstein, O. *Chem. Rev.*, **2000**, *100*, 601.

[44] Bau, R.; Drabnis, M. H. *Inirg. Chim. Acta* **1997**, *259*, 27.

[45] (a) Schubert, U.; Schwartz, M.; Möller, F. *Organometallics* **1994**, *13*, 1554. (b) Yin, J.; Klozin, J.; Abboud, K.; Jones, W. M. *J. Am. Chem. Soc.* **1995**, *117*, 3298. (c) Freeman, W.; Tilley, T.D.; Rheingold, A. L. *J. Am. Chem. Soc.* **1994**, *116*, 8428. (d) Herrmann, W. A.; Huber, N. W.; Behm, J. *Chem. Ber.* **1992**, *125*, 1405. (e) Procopio, L. J.; Carroll, P. J.; Berry, D. H. *J. Am. Chem. Soc.* **1994**, *116*, 177. (f) Herrmann, W. A.; Eppinger, J.; Spiegler, M.; Runte, O.; Anwander, R. *Organometallics* **1997**, *16*, 1813. (g) Nagl, I.; Scherer, W.; Tafipolsky, M.; Anwander, R. *Eur. J. Inorg. Chem.*, **1999**, 1405. (h) Eppinger, J.; Spiegler, M.; Hieringer, W.; Herrmann, W. A.; Anwander, R. *J. Am. Chem. Soc.* **2000**, *122*, 3080. (i) Klimpel, M. G.; Görlitzer, H. W.; Tafipolsky, M.; Spiegler, M.; Scherer, W.; Anwander, R. *J. Organomet. Chem.* **2002**, *647*, 236. (j) Rees, W.S.; Just, O.; Schumann, H.; Weimann, R. *Angew. Chem., Int. Ed. Engl.* **1996**, *35*, 419.

[46] (a) Lichtenberger, D.L.; Rai-Chaudhuri, A.; *Organometallics* **1990**, *9*, 1686. (b) Lichtenberger, D.L.; Rai-Chaudhuri, A.; *J. Am. Chem. Soc.* **1990**, *112*, 2492. (c) Lichtenberger, D.L.; Rai-Chaudhuri, A.; *J. Am. Chem. Soc.* **1989**, *111*, 3583. (d) Lichtenberger, D.L.; Rai-Chaudhuri, A. *Inorg. Chem.* **1990**, *29*, 975. (e) Lichtenberger, D.L. *Organometallics* **2003**, *22*, 1599.

[47] (a) Rabaa, H.; Saillard, J.-Y.; Schubert. U. *J. Organomet. Chem.* **1987**, *330*, 397. (b) Schubert. U.; Scholz, G.; Müller, J.; Ackermann, K.; Wörle, B.; *J. Organomet. Chem.* **1986**, *306*, 303. (c) Bader, R. F. W.; Matta, C. F.; Cortés-Guzmán, F. *Organometallics* **2004**, *23*, 66253.

[48] Bent, H. A. *Chem. Rev.* **1961**, *61*, 275.

[49] Huheey, J. E.; Keiter, E. A.; Keiter, R. R. *Inorganic Chemistry: Principles of Structure and Reactivity*. 4th Ed., HarperCollins College Publishers: New York, **1993**, pp. 225-229.

[50] Nikonov, G. I. *Organometallics* **2003**, *22*, 1597.

[51] Harris, R. K.; Mann, B. E. Eds., *NMR and the Periodic Table*. Academic Press, London, **1978**.

[52] Alkorta, I.; Elguero, J.; Mó, O.; Yáñez, M.; Del Bene, J. E. *J. Phys. Chem. A* **2002**, *106*, 9325.

[53] Normally, $\nu_{Si\text{-}H}$ for hydrosilanes are found at energies greater than 2100 cm^{-1}: Smith, A. L. *Specrochim. Acta* **1960**, *16,* 87.

[54] Williams, E. A.; Cargioli, J. D. In *Annual Reports on NMR Spectroscopy;* Webb, G. A., Ed.; Academic Press: New York, **1979**; *Vol. 9*, p 221.

[55] Butler, I. S.; Harrod, J. F. *Inorganic Chemistry;* Benjamin Cummings: New York, **1989**; p 110.

[56] Fryzuk, M. D.; MacKay, B. A.; Patrick, B. O. *J. Am. Chem. Soc.* **2003**, *125*, 3234.

[57] Sommer, L. H.; Pietrusza, E. W.; Whitmore, F. C. *J. Am. Chem. Soc.* **1947**, *69*, 188.

[58] Spiers, J. L.; Webster, J. A.; Barnes, G. H. *J. Am. Chem. Soc.* **1957**, *79*, 974.

[59] Marko, I. E.; Sterin, S.; Buisine, O.; Mignani, G.; Branlard, P.; Tinant, B.; Declercq, J.-P. *Science* **2002**, *298*, 204.

[60] For example, see the following manuscripts and references therein: (a) Sakaki, S.; Mizoe, N.; Sugimoto, M. *Organometallics* **1998**, *17*, 2510. (b) Sakaki, S.; Ogawa, M.; Musashi, Y.; Arei, T. *J. Am. Chem. Soc.* **1994**, *116*, 7258. (c) Sakaki, S.; Mizoe, N.; musashi, Y.; Biswas, B.; Sugimoto, M. *J. Phys. Chem., A.* **1998**, *102*, 8027. (d) Sakaki, S.; Mizoe, N.; Sugimoto, M.; Musashi, Y. *Coord. Chem. Rev.* **1999**, *190-192*, 933. (e) Sakaki, S.; Mizoe, N.; Musashi, Y.; Biswas, B.; Sugimoto, M. *J. Mol. Struct., (Theochem)* **1999**, *461-462*, 533. (f) Giorgi, G.; De Angelis, F.; Re, N.; Sgamellotti, A. *J. Mol. Struct.* **2003**, *623*, 277.

[61] Ryan, J. W.; Speier, J. L. *J Am. Chem. Soc.* **1964**, *86*, 895.

[62] Oro, L. A.; Fernandez, M. J. Esteruelas, M. A.; Jimenez, M. S. *J. Mol. Catal.* **1986**, *37*, 151.

[63] Selin, T. G.; West, R. *J. Am. Chem. Soc.* **1962**, *84*, 1863.

[64] Eaborn, C.; Hitchcock, P. B.; Tune, D. J.; Walton, D. R. M. *J. Organomet. Chem.* **1973**, *54*, C1.

[65] (a) Sommer, L. H.; Michael, K. W.; Fujimoto, H. *J. Am. Chem. Soc.* **1967**, *89*, 1519. (b) Sommer, L. H.; Lyons, J. E.; Fujimoto, H. *J. Am. Chem. Soc.* **1969**, *91*, 7051.

[66] (a) Blakeney, A. J.; Gladysz, J. A. *Inorg. Chim. Acta.* **1980**, *53,* L25. (b) Brinkman, K. C.; Blakeney, A. J.; Krone-Schmidt, W.; Gladysz, J. A. *Organometallics* **1984**, *3,* 1325.

[67] Schroeder, M. A.; Wrighton, M. S. *J. Organomet. Chem.* **1977**, *128*, 345.

[68] For catalytic reduction of alkenes into alkanes with hydrosilanes see, for instance: (a) Doyle, M. P.; McOsker, C. C. *J. Org. Chem.* **1978**, *43*, 693. (b) Carey, F. A.; Tremper, H. S. *J. Org. Chem.* **1969**, *34*, 4. (c) Onopchenko, A.; Sabourin, E. T.; Beach, D. L. *J. Org. Chem.* **1984**, *49*, 3389.

[69] Randolph, C. L.; Wrington, M. S. *J. Am. Chem. Soc.* **1986**, *108*, 3366.

[70] See, for example: Wakatauki, Y.; Yamazaki, H.; Nakano, M.; Yamamoto, Y. *J. Chem. Soc. Chem. Commun.* **1991**, 703.

[71] Curtis, M. D.; Epstein, P. S. *Adv. Organomet. Chem.* **1981**, *19*, 213.

[72] Speier, J. L. *Adv. Organomet. Chem.* **1979**, *17*, 407.

[73] Marciniec, B.; Gulinski, J. *J. Organomet. Chem.* **1984**, *266*, C19.

[74] Seitz, F.; Wrighton, M. S. *Angew. Chem., Int. Ed. Engl.* **1988**, *27*, 289.

[75] (a) Haddleton, D. M.; Perutz, R. N. *J. Chem. Soc., Chem. Commun.* **1985**, 1372. (b) Duckett, S. B.; Haddleton, D. M.; Jackson, S. A.; Perutz, R. N.; Poliakoff, M.; Upmacis, R. K. *Organometallics* **1988**, *7*, 1526.

[76] (a) Bentz, P. O.; Ruiz, J.; Mann, B.; Spencer, C. M.; Maitlis, P. M. *J. Chem. Soc., Chem. Commun.* **1985**, 1374. (b) Ruiz, J.; Bentz, P. O.; Mann, B. E.; Spencer, C. M.; Taylor, B. F.; Maitlis, P. M. *J. Chem. Soc., Dalton Trans.* **1987**, 2709. (c) Tanke, R. S.; Crabtree, R. H. *J. Chem. Soc., Chem. Commun.* **1990**, 1057. (d) Tanke, R. S.; Crabtree, R. H. *J. Am. Chem. Soc.* **1990**, *112*, 7984.

[77] Duckett, S. B.; Perutz, R. N. *J. Chem. Soc., Chem. Commun.* **1991**, 28.

[78] (a) LaPointe, A. M.; Rix, F. C.; Brookhart, M. *J. Am. Chem. Soc.* **1997**, *119*, 906. (b) Uozumi, Y.; Tsuji, H.; Hayashi, T. *J. Org. Chem.* **1998**, *63*, 6137. (c) Marciniec, B.; Maciejewski, H.; Kownacki, I. *J. Organomet. Chem.* **2000**, *597*, 175. (d) Skvortsov, N. K.; Bel'skii, V. K.; Maciejewski, H.; Gulinski, J. *Russ. J. Gen. Chem.* **2003**, *73,* 66. (e) Tillack, A.; Pulst, S.; Baumann, W.; Baudisch, H.; Kortus, K.; Rosendahl, U. *J.*

Organomet. Chem. **1997**, *532*, 117. (f) Fontaine, F.-G.; Nguyen, R.-V.; Zargarian, D. *Can. J. Chem.* **2003**, *81*, 1299. (g) Hyder, I.; Jimenez-Tenorio, M.; Puerta, M. C.; Valerga, P. *J. Chem. Soc. Dalton Trans.* **2007**, 3000. (h) Chen, Y.; Sui-Seng, C.; Boucher, S.; Zargarian, D. *Organometallics* **2005**, *24*, 149.

[79] (a) Widenhoefer, R. A. *Acc. Chem. Res.* **2002**, *35*, 905. (b) Wang, X.; Stankovich, S. Z.; Widenhoefer, R. A. *Organometallics* **2002**, *21*, 901. (c) Wang, X.; Chakrapani, H.; Stengone, C. N.; Widenhoefer, R. A. *J. Org. Chem.* **2001**, *66*, 1755. (d) Perch, N. S.; Widenhoefer, R. A. *J. Am. Chem. Soc.* **2004**, *126*, 6332. (e) Stengone, C. N.; Widenhoefer, R. A. *Tetrahedron Lett.* **1999**, *40*, 1451. (f) Widenhoefer, R. A.; DeCarli, M. A *J. Am. Chem. Soc.* **1998**, *120*, 805.

[80] (a) Marciniec, B.; Walczuk, E.; Blazejewska-Chadyniak, P.; Kujawa-Welten, M.; Krompiec, S. *Catalytic activity of rhodium-siloxide complexes in Hydrosilylation of allyl ethers and allyl esters*, in: N. Auner, J. Weis (Eds), *Organosilicon Chemistry V – From Molecules to Materials*, Verlag Chemie, **2003,** 363–374. (b) Marciniec, B.; Blazejewska-Chadyniak, P.; Kubicki, M. *Can. J. Chem.* **2003**, *81*, 1292. (c) Marciniec, B.; Maciejewski, H.; Szubert, K.; Kurdykowska, M. *Chem. Month.* **2006**, *137*, 605.

[81] (a) Tanke, R. S.; Crabtree, R. H. *Organometallics* **1991**, *10*, 415. (b) Brookhart, M.; Grant, B. E. *J. Am. Chem. Soc.* **1993**, *115*, 2151. (c) Tuttle, T.; Wang, D.; Thiel, W.; Kohler, J.; Hofmann, M.; Weis, J. *J. Organomet. Chem.* **2007**, *692*, 2282.

[82] Hostetler, M. J.; Butts, M. D.; Bergman, R. G. *Organometallics* **1993**, *12*, 65.

[83] (a) Stradiotto, M.; Cipot, J.; McDonald, R. *J. Am. Chem. Soc.* **2003**, *125*, 5618. (b) Cipot, J.; McDonald, R.; Ferguson, M. J.; Schatte, G.; Stradiotto, M. *Organomrtallics* **2007**, *26*, 594. (c) Hesp, K. D.; McDonald, R.; Ferguson, M. J.; Stradiotto, M. *J. Am. Chem. Soc.* **2008**, *130*, 16394. (d) Stradiotto, M.; Hesp, K. D.; Lungren, R. J. *Angew. Chem. Int. Ed.* **2010**, *49*, 494.

[84] Glaser, P. B.; Tilley, T. D. *J. Am. Chem. Soc.* **2003**, *125*, 13640.

[85] (a) Beddie, C.; Hall, M. B. *J. Am. Chem. Soc.* **2004**, *126*, 13564. (b) Beddie, C.; Hall, M. B. *J. Phys. Chem.* **2006**, *110*, 1416.

[86] Bohme, U. *J. Organomet. Chem.* **2006**, *691*, 4400.

[87] Rankin, M. A.; MacLean, D. F.; Schatte, G.; McDonald, R.; Stradiotto, M. *J. Am. Chem. Soc.* **2007**, *129*, 15855.

[88] (a) Tamao, K.; Ishida, N.; Tanaka, T.; Kumada, M. *Organometallics*, **1983**, *2*, 1695. (b) Fleming, I.; Henning, R.; Plaut, H. *J. Chem. Soc. Chem. Commun.* **1984**, 29.

[89] Brook, M. A. *Silicon in Organic, Organometallic and Polymer Chemistry,* Wiley: New York, **2000**.

[90] (a) Takahashi, K.; Minami, T.; Ohara, Y.; Hiyama, T. *Bull. Chem. Soc. Jpn.* **1995**, *68*, 2649. (b) Takahashi, K.; Minami, T.; Ohara, Y.; Hiyama, T. *Tetrahedron Lett.* **1993**, *34*, 8263. (c) Tamao, K.; Kobayashi, K.; Ito, Y. *Tetrahedron Lett.* **1989**, *30*, 6051. (d) Denmark, S. E.; Sweis, R. F. *Acc. Chem. Res.* **2002**, *35*, 835.

[91] (a) Lee, H. M.; Nolan, S. P. *Org. Lett.* **2000**, *2*, 2053. (b) Mowery, E. E.; DeShong, P. *J. Org. Chem.* **1999**, *64*, 1684. (c) Denmark, S. E.; Sweis, R. F. *J. Am. Chem. Soc.* **2001**, *123*, 6439.

[92] (a) Jun, C. H.; Crabtree, R. H. *J. Organomet. Chem.* **1993**, *447*, 177. (b) Ojima, I.; Clos, N.; Donovan, R. J.; Ingallina, P. *Organometallics* **1990**, *9*, 3127.

[93] (a) Takeuchi, R.; Tanouchi, N. *J. Chem. Soc., Chem. Commun.* **1993**, 1319. (b) Takeuchi, R.; Tanouchi, N. *J. Chem. Soc., Perkin Trans.* **1994**, *1*, 2909. (c) Takeuchi, R.; Nitta, S.; Watanabe, D. *J. Org. Chem.* **1995**, *60*, 3045. (d) Takeuchi, R.; Nitta, S.; Watanabe, D. *J. Chem. Soc., Chem. Commun.* **1994**, 1777. (e) Takeuchi, R.; Ebata, I. *Organometallics* **1997**, *16*, 3707.

[94] Ojima, I.; Kumagai, M.; Nagai, Y. *J. Organomet. Chem.* **1974**, *66*, C14.

[95] (a) Bennett, M. A.; Wilkinson, G. *J. Chem. Soc. A* **1961**, 1418. (b) Vrieze, K.; Volger, H. C.; Praat, A. P. *J. Organomet. Chem.* **1968**, *14*, 185.

[96] Schrock, R. R.; Osborn, J. A. *J. Am. Chem. Soc.* **1971**, *93*, 2397.

[97] For applications of $[Rh(cod)(NCMe)_2][BF_4]$ in catalysis see, for instance: (a) Nambo, M.; Noyori, R.; Itami, K. *J. Am. Chem. Soc.* **2007**, *129*, 8080. (b) Murata, M.; Yamasaki, H.; Ueta, T.; Nagata, M.; Ishikura, M.; Watanabe, S.; Masuda, Y. *Tetrahedron* **2007**, *63*, 4087. (c) Oi, S.; Taira, A.; Honna, Y.; Sato, T.; Inoue, Y. *Tetrahedron: Asymmetry* **2006**, *17*, 598.

[98] Denmark, S. E.; Pan, W. *Org. Lett.* **2002**, *4*, 4163.

[99] Trost, B. M.; Ball, Z. T. *J. Am.Chem. Soc.* **2003**, *125*, 30.

[100] Martin, M.; Sola, E.; Lahoz, F. J.; Oro, L. A. *Organometallics* **2002**, *21*, 4027.

[101] (a) Na, Y.; Chang, S. *Org. Lett.* **2000**, *2*, 1887. (b) Trost, B. M.; Ball, Z. T. *J. Am. Chem. Soc.* **2001**, *123*, 12726.

[102] (a) Chung, L. W.; Wu, Y.-D.; Trost, B. M.; Ball, Z. T. *J. Am. Chem. Soc.* **2003**, *125*, 11578. (b) Trost, B. M.; Ball, Z. T. *J. Am. Chem. Soc.* **2005**, *127*, 17644.

[103] (a) Ojima, I.; Nihonyanagi, M.; Nagai, Y. *J. Chem. Soc., Chem. Commun.* **1972**, 938. (b) Ojima, I.; Kogure, T.; Nihonyanagi, M.; Nagai, Y. *Bull. Chem. Soc. Jpn.* **1972**, *45*, 3506.

[104] (a) Glushkova, N. E.; Kharitonov, N. P. *Izv. Akad. Nauk SSSR Ser. Khim.* **1967**, 88. (b) Calas, R.; Frainnet, E.; Bonastre, J. *C.R. Acad. Sci. Paris.* **1960**, *251*, 2987. (c) Sadykh-Zade, S. I.; Petrov, A. D. *Zh. Obshch. Khim.* **1959**, *29*, 3194. (d) Sadykh-Zade, S. I.; Petrov, A. D. *Dok. Acad. Nauk SSSR* **1958**, *121*, 119.

[105] (a) Ojima, I.; Nihonyanagi, M.; Kogure, T.; Kumagai, M.; Horiushi, S.; Nakatsugawa, K. *J. Organomet. Chem.* **1975**, *94*, 449. (b) Ojima, I.; Kogure, T. *Organometallics* **1982**, *1*, 1390.

[106] Dumont, W.; Poulin, J.-C.; Dang, T. P.; Kagan, H. B. *J. Am. Chem. Soc.* **1973**, *95*, 8295.

[107] See the following reviews and references therein: (a) Brunner, H. *Angew. Chem.* **1983**, *95*, 921. (b) Ojima, I.; Hirai, K. In *Asymmetric Synthesis*; Morrison, J. D. Ed.; Academic Press: London, **1985**, *5*, p. 103. (c) Ojima, I. In *The Chemistry of Silicon Compounds*; Patai, S. Ed.; Wiley: New York, **1989**, Chap. 25, p. 1479. (d) Brunner, H.; Nishiyama, H.; Itoh, K. In *Catalytic Asymmetric Synthesis*, Ojima, I. Ed.; VCH: New York, **2000**, pp. 111–145. (e) Noyori, R. *Asymmetric Catalysis in Organic Synthesis*; Wiley: New York, **1994**, p. 124. (f) Brunner, H. In *Transition Met. Org. Synth.*, Beller, M.; Bolm, C. Ed.; **1998**, *2*, p. 131. (g) Nishiyama, H. In *Comprehensive Asymmetric Catalysis I-III*, Jacobsen, E.; Pfaltz, A.; Yamamoto, H. Eds.; Springer-Verlag: Berlin, **1999**, *1*, pp. 267-287. (h) Schneider, N.; Finger, M.; Haferkemper, C.; Bellemin-Laponnaz, S.; Hofmann, P.; Gade, L. H. *Chem. Eur. J.* **2009**, *15*, 11515. (i) Diez-Gonzalez, S. Nolan, S. P. *Org. Prep. Proc. Int.* **2007**, *39*, 523.

[108] (a) Carpentier, J.F.; Bette, V. *Curr. Org. Chem.* **2002**, *6*, 913. (b) Riant, O.; Mostefai, N.; Courmarcel, J. *Synthesis* **2004**, 2943.

[109] Compare to the modified Chalk-Harrod mechanism for hydrosilation of alkenes (Scheme 13) as well as the Crabtree-Ojima catalytic cycle for addition of silanes to alkynes (Scheme 25, **B**).

[110] Zheng, G. Z.; Chan, T. H. *Organometallics* **1995**, *14*, 70.

[111] Kolb, I.; Hetflejs, *J. Collect. Czech. Chem. Commun.* **1980**, *45*, 2224.

[112] (a) Schneider, N.; Finger, M.; Haferkemper, C.; Bellemin-Laponnaz, S.; Hofmann, P.; Gade, L. H. *Angew. Chem. Int. Ed.* **2009**, *48*, 1609. (b) Schneider, N.; Finger, M.; Haferkemper, C.; Bellemin-Laponnaz, S.; Hofmann, P.; Gade, L. H. *Chem. Eur. J.* **2009**, *15*, 11515.

[113] (a) Cesar, V.; Bellemin-Lapponaz, S.; Gade, L. H. *Angew. Chem. Int. Ed.* **2004**, *43*, 1014. (b) Cesar, V.; Bellemin-Lapponaz, S.; Wadepohl, H.; Gade, L. H. *Chem. Eur. J.* **2005**, *11*, 2862.

[114] Fujita, M.; Hiyama, T. *J. Org. Chem.* **1988**, *53*, 5405.

[115] Mimoun, H.; De Saint Laumer, J. Y.; Giannini, L.; Scopelliti, R.; Floriani, C. *J. Am. Chem. Soc.* **1999**, *121*, 6158.

[116] Kennedy-Smith, J. J.; Nolin, K. A.; Gunterman, H. P.; Toste, F. D. *J. Am. Chem. Soc.* **2003**, *125*, 4056.

[117] (a) Sweeney, Z. K.; Polse, J. L.; Andersen, R. A.; Bergman, R. G.; Kubinec, M. G. *J. Am. Chem. Soc.* **1997**, *119*, 4543. (b) Sweeney, Z. K.; Polse, J. L.; Bergman, R. G.; Andersen, R. A. *Organometallics* **1999**, *18*, 5502. (c) Gountchev, T. I.; Tilley, T. D. *J. Am. Chem. Soc.* **1997**, *117*, 112831.

[118] Dress, M.; Strassner, T. *Inorg. Chem.* **2007**, *46*, 10850.

[119] Thiel, W. R.; *Angew. Chem. Int. Ed.* **2003**, *42*, 5390.

[120] Ziegler, J. E.; Du, G.; Fanwick, P. E.; Abu-Omar, M. M. *Inorg. Chem.* **2009**, *48*, 11290.

[121] (a) Bullock, R. M.; Voges, M. H. *J. Am. Chem. Soc.* **2000**, *122*, 12594. (b) Voges, M. H.; Bullock, R. M. *J. Chem. Soc., Dalton Trans.* **2002**, 759. (c) Bullock, R. M. *Chem. Eur. J.* **2004**, *10*, 2366.

[122] Dong, H.; Berke, H. *Adv. Synth. Catal.* **2009**, *351*, 1783.

[123] Tran, B. L.; Pink, M.; Mindiola, D. J. *Organometallics* **2009**, *28*, 2234.

[124] (a) Deutsch, C.; Krause, N.; Lipshutz, B. H. *Chem. Rev.* **2008**, *108*, 2916. (b) Lipshutz, B. H.; Lower, A.; Noson, K. *Org. Lett.* **2002**, *4*, 4045. (c) Lipshutz, B. H.; Frieman, B. A. *Angew. Chem. Int. Ed.* **2005**, *44*, 6345. (d) Lipshutz, B. H.; Noson, K.; Chrisman, W.; Lower, A. *J. Am. Chem. Soc.* **2003**, *125*, 8779. (e) Diez-Gonzalez, S.; Scott, N. M.; Nolan, S. P. *Organometallics* **2006**, *25*, 2355. (f) Diez-Gonzalez, S.; Nolan, S. P. *Acc. Chem. Res.* **2008**, *41*, 349. (g) Kaur, H.; Zinn, F. K.; Stevens, E. D.; Nolan, S. P. *Organometallics* **2004**, *23*, 1157. (h) Shaikh, N. S.; Enthaler, S.; Junge, K.; Beller, M. *Angew. Chem. Int. Ed.* **2008**, *47*, 2497. (f) Mankad, N. P.; Laitar, D. S.; Sadighi, J. P. *Organometallics* **2004**, *23*, 3369. (j) Diez-Gonzalez, S.; Kaur, H.; Zinn, F. K.; Stevens, E. D.; Nolan, S. P. *J. Org. Chem.* **2005**, *70*, 4784. (i) Render, S.; Oestreich, M. *Angew. Chem. Int. Ed.* **2007**, *46*, 498.

[125] Calimano, E.; Tilley, T. D. *Organometallics* **2010**, *29*, 1680.

[126] Feldman, J. D.; Peters, J. C.; Tilley, T. D. *Organometallics* **2002**, *21*, 4065.

[127] (a) Watanabe, T.; Hashimoto, H.; Tobita, H. *J. Am. Chem. Soc.* **2007**, *129*, 11338. (b) Watanabe, T.; Hashimoto, H.; Tobita, H. *Angew. Chem. Int. Ed.* **2004**, *43*, 218. (c) Ochiai, M.; Hashimoto, H.; Tobita, H. *Dalton Trans.* **2009**, 1812.

[128] Klei, S. R.; Tilley, T. D.; Bergman, R. G. *Organometallics* **2002**, *21*, 4648.

[129] Mitchell, G. P.; Tilley, T. D. *J. Am. Chem. Soc.* **1997**, *119*, 11236.

[130] Zhang, X.-H.; Chung, L.-W.; Lin, Z.; Wu, Y.-D. *J. Org. Chem.* **2008**, *73*, 820.

[131] (a) Verdaguer, X.; Lange, U. E. W.; Reding, M. T.; Buchwald, S. L. *J. Am. Chem. Soc.* **1996**, *118*, 6784. (b) Verdaguer, X.; Lange, U. E. W.; Buchwald, S. L. *Angew. Chem. Int. Ed.* **1998**, *37*, 1103. (c) Willoughby, C. A.; Buchwald, S. L. *J. Am. Chem. Soc.* **1994**, *116*, 11703.

[132] (a) Takaki, K.; Kamata, T.; Miura, Y.; Shishido, T.; Takehira, K. *J. Org. Chem.* **1999**, *64*, 3891. (b) Takaki, K.; Komeyama, K.; Takehira, K. *Tetrahedron* **2003**, *59*, 10381.

[133] Hashimoto, H.; Aratani, I.; Kabuto, C.; Kira, M. *Organometallics* **2003**, *22*, 2199.

[134] For example, see: Lachaize, S.; Sabo-Etienne, S.; Donnadieu, B.; Chaudret, B. *Chem. Commun.* **2003**, 214.

[135] For application of silylated imines in organic synthesis see, for example: (a) Buonora, P.; Olsen, J.-C.; Oh, T. *Tetrahedron* **2001**, *57*, 6099. (b) Panunzio, M.; Zarantonello, P. *Org. Proc. Res. Dev.* **1998**, *2*, 49. (c) Ghosez, L.; Bayard, P.; Nshimyumukiza, P.; Gouverneur, V.; Sainte, F.; Bcaudegnics, R.; Rivera, M.; Frisquc-Hesbain, A.-M.; Wynats, C. *Tetrahedron* **1995**, *51*, 11021. (d) Andreoli, P.; Billi, L.; Cainelli, G.; Panunzio, M.; Bandini, E.; Martelli, G.; Spunta, G. *Tetrahedron* **1991**, *47*, 9061. (e) Andreoli, Cainelli, G.; Panunzio, M.; Bandini, E.; Martelli, G.; Spunta, G. *J. Org. Chem.* **1991**, *56*, 5984. (f) Fu, N.; Tidwell, T. T. *Tetrahedron* **2008**, *64*, 10465. (g) Ha, D.-C.; Hart, D. J.; Yang, T.-K. *J. Am. Chem. Soc.* **1984**, *106*, 4819.

[136] Chalk, A. J. *J. Organomet. Chem.* **1970**, *21*, 207.

[137] (a) Murai, T.; Sakane, T.; Kato, S. *Tetrahedron Lett.* **1985**, *26*, 5145. (b) Murai, T.; Sakane, T.; Kato, S. *J. Org. Chem.* **1990**, *55*, 449.

[138] (a) Fry, J. L. *J. Chem. Soc., Chem. Commun.* **1974**, 45. (b) Fry, J. L.; Ott, R. A. *J. Org. Chem.* **1981**, *46*, 602.

[139] (a) Corriu, R. J. P.; Moreau, J. J. E.; Pataud-Sat, M. *J. Organomet. Chem.* **1982**, *228*, 301. (b) Caporusso, A. M.; Panziera, N.; Petrici, P.; Pitzalis, E.; Salvadori, P.; Vitulli, G.; Martra, G. *J. Mol. Catal. A: Chem.* **1999**, *150*, 275. (c) Reddy, N. P.; Uchimaru, Y.; Lautenschlager, H.-J.; Tanaka, M. *Chem. Lett.* **1992**, 45.

[140] Tanabe, M.; Osakada, K. *Organometallics* **2001**, *20*, 2118.

[141] Kim, J.; Kang, Y.; Lee, J.; Kong, Y. K.; Gong, M. S.; Kang, S. O.; Ko, J. *Organometallics* **2001**, *20*, 937.

[142] (a) Procopio, L. J.; Caroll, P. J.; Berry, D. H. *J. Am. Chem. Soc.* **1991**, *113*, 1870. (b) Procopio, L. J.; Caroll, P. J.; Berry, D. H. *Organometallics* **1993**, *12*, 3087. (c) Procopio, L. J.; Caroll, P. J.; Berry, D. H. *Polyhedron* **1995**, *14*, 45.

[143] Arnold, J.; Tilley, T. D. *J. Am. Chem. Soc.* **1987**, *109*, 3318.

[144] Watanabe, T.; Hashimoto, H.; Tobita, H. *J. Am. Chem. Soc.* **2006**, *128*, 2176.

[145] (a) Taw, F. L.; White, P. S.; Bergman, R. G.; Brookhart, M. *J. Am. Chem. Soc.* **2002**, *124*, 4192. (b) Taw, F. L.; Mueller, A. H.; Bergman, R. G.; Brookhart, M. *J. Am. Chem. Soc.* **2003**, *125*, 9808. (c) Nakazawa, H.; Kawasaki, T.; Miyoshi, K.; Suresh, C. H.; Koga,

N. *Organometallics* **2004**, *23*, 117. (d) Nakazawa, H.; Kamata, K.; Itazaki, M. *Chem. Commun.* **2005**, 4004.

[146] Deglmann, P.; Ember, E.; Hofmann, P.; Pitter, S.; Walter, O. *Chem. Eur. J.* **2007**, *13*, 2864.

[147] Colvin, E. W.; McGarry, D. G. *J. Chem. Soc., Chem. Commun.* **1985**, 539.

[148] Kocienski, P. J. *Protecting Groups*, Thieme: Stuttgart **1994**, pp. 28-42.

[149] (a) Ojima, I.; Li, Z.; Zhu, J. *The Chemistry of Organic Silicon Compounds*, Rappoport, S.; Apeloig, Y. (Eds.), Wiley, New York **1998**, chap. 29. (b) Lickiss, P. D. *Adv. Inorg. Chem.* **1995**, *42*, 147. (c) Schubert, U.; Lorenz, C. *Chem. Ber.* **1995**, *128*, 1267.

[150] (a) Pillot, J.-P.; Roux, P.; Richard, C.; Birot, M.; Dunogues, J. in *Progress in Organosilicon Chemistry*, Marciniec, B.; Chojnowski, J. (Eds.), Gordon and Breach Publishers, Basel, **1995**, p. 465 and refs. therein. (b) Blum, Y.; McDermott, G. A. in *Inorganic and Organometallic Polymers and Oligomers*, Harrod, J. F.; Laine, R. M. (Eds.), Kluwer, Dordrecht, The Netherlands, **1991** and refs therein.

[151] (a) Fessenden, R.; Fessenden, J. S. *Chem. Rev.* **1960**, *61*, 361. (b) Kannengiesser, G.; Damm, F. *Bull. Soc. Chim. Fr.* **1969**, *3*, 891.

[152] (a) Baay, Y. L.; Mac.Diarmid, A. G. *Inorg. Chem.* **1969**, *8*, 986. (b) Kubas, G. J. *Heterolytic Splitting of H-H, S-H and other σ-Bonds on Electrophilic Metal Centers*. In *Advances in Inorganic Chemistry*. Vol. 56, Van Eldik, R. (Ed.), pp.127-177.

[153] Chalk, A. J. *J. Chem. Soc. D: Chem. Commun.* **1970**, 847.

[154] Archer, N. J.; Haszeldine, R. N.; Parish, R. V. *J. Chem. Soc. D: Chem. Commun.* **1971**, 524.

[155] (a) Ojima, I.; Kogure, T.; Nihonyanagi, M.; Kono, H.; Inaba, S. *Chem. Lett.* **1973**, 501. (b) Corriu, R. J. P.; Moreau, J. J. E. *J. Organomet. Chem.* **1976**, *114*, 135.

[156] Dwyer, J.; Hilal, H. S.; Parish, R. V. *J. Organomet. Chem.* **1982**, *228*, 191.

[157] (a) Oehmichen, U; Singer, H. *J. Organomet. Chem.* **1983**, *243*, 199. (b) Lou, X.-L.; Crabtree, R. H. *J. Am. Chem. Soc.* **1989**, *111*, 2527. (c) Doyle, M. P.; High, K. G.; Bagheri, V.; Pieters, R. J.; Lewis, P. J.; Pearson, M. M. *J. Org. Chem.* **1990**, *55*, 6082. (d) Barber, D. E.; Lu, Z.; Richardson, T.; Crabtree, R. H. *Inorg. Chem.* **1992**, *31*, 4709. (e) Barton, D. H.; Kelly, M. J. *Tetrahedron Lett.* **1992**, *33*, 5041. (f) Gregg, B. T.; Cutler, A.

R. *Organometallics* **1994**, *13*, 1039. (g) Scharrer, E.; Chang, S.; Brookhart, M. *Organometallics* **1995**, *14*, 5686. (h) Chang, S.; Scharrer, E.; Brookhart, M. *J. Mol. Catal. A: Chem.* **1998**, *130*, 107. (i) Matarasso-Tchiroukhine, E. *J. Chem. Soc., Chem. Commun.* **1990**, 681.

[158] Bühl, M.; Mauschick, F. T. *Organometallics* **2003**, *22*, 1422.

[159] Fang, X.; Huhmann-Vincent, J.; Scott, B. L.; Kubas, G. J. *J. Organomet. Chem.* **2000**, *609*, 95.

[160] Yun, S. S.; Lee, J.; Lee, S. *Bull. Korean. Chem. Soc.* **2001**, *22*, 623.

[161] Ito, H.; Takagi, K.; Miyahara, T.; Sawamura, M. *Org. Lett.* **2005**, *7*, 3001.

[162] For example, see: Wang,W.-D.; Eisenberg, R. *Organometallics* **1991**, *10*, 2222 and references therein.

[163] Wang, J. X.; Dash, A. K.; Berthet, J. C.; Ephritikhine, M.; Eisen, M. S. *J. Organomet. Chem.* **2000**, *610,* 49.

[164] For example, see: (a) Liu, X.; Wu, Z.; Peng, Z.; Wu, Y.-D.; Xue, Z. *J. Am. Chem. Soc.* **1999**, *121*, 5350. (b) Hays, D. S.; Fu, G. S. *J. Org. Chem.* **1997**, *62*, 7070.

[165] Corbin, R. A.; Ison, E. A.; Abu-Omar, M. M. *Dalton Trans.* **2009**, 2850.

[166] Takahashi, T.; Hasegawa, M.; Suzuki, N.; Saburi, M.; Rousset, C. J.; Fanwick, P. E.; Negishi, E. *J. Am. Chem. Soc.* **1991**, *113*, 8564.

[167] Ura, Y.; Gao, G.; Bao, F.; Ogasawara, M.; Takahashi, T. *Organometallics* **2004**, *23*, 4804.

[168] (a) Kesti, M. R.; Waymouth, R. M. *Organometallics* **1992**, *11*, 1095. (b) Kesti, M. R.; Abdurahman, M.; Waymouth, R. M. *J. Organomet. Chem.* **1991**, *417*, C12. (c) Corey, J. Y.; Zhu, X.-H. *Organometallics* **1992**, *11*, 672.

[169] Ura, Y.; Hara, R.; Takahashi, T. *Chem. Lett.* **1998**, 195.

[170] Sakaki, S.; Takayama, T.; Sumimoto, M.; Sugimoto, M. *J. Am. Chem. Soc.* **2004**, *126*, 3332.

[171] Bode, B. M.; Day, P. N.; Gordon, M. S. *J. Am. Chem. Soc.* **1998**, *120*, 1552.

[172] Bareille, L.; Becht, S.; Cui, J. L.; Le Gendre, P.; Moïse, C. *Organometallics* **2005**, *24*, 5802.

[173] (a) Molandre, G. A.; Retsch, W. H. *Organometallics* **1995**, *14*, 4570. (b) Molandre, G. A.; Knight, E. E. *J. Org. Chem.* **1998**, *63*, 7009. (c) Schumann, H.; Keitsch, M. R.; Winterfeld, J.; Mühle, S.; Molander, G. A. *J. Organomet. Chem.* **1998**, *559*, 181. (d) Dash, A. K.; Wang, J. Q.; Eisen, M. S. *Organometallics* **1999**, *18*, 4724. (e) Dash, A. K.; Wang, J. X.; Berthet, J. C.; Ephritikhine, M.; Eisen, M. S. *J. Organomet. Chem.* **2000**, *604*, 83. (f) Dash, A. K.; Gourevich, I.; Wang, J. Q.; Wang, J.; Kapon, M.; Eisen, M. S. *Organometallics* **2001**, *20*, 5084. (g) Molandre, G. A.; Romeo, J. A. C. *Chem. Rev.* **2002**, *102*, 2161. (h) Rastätter, M.; Zulys, A.; Roesky, P. W. *Chem Commun.* **2006**, 874. (i) Barnea, E.; Eisen, M. S. *Coord. Chem. Rev.* **2006**, *250*, 855.

[174] (a) Asao, N.; Sudo, T.; Yamamoto, Y. *J. Org. Chem.* **1996**, *61*, 7654. (b) Sudo, T.; Asao, N.; Yamamoto, Y. *J. Org. Chem.* **1999**, *64*, 2494. (c) Sudo, T.; Asao, N.; Yamamoto, Y. *J. Org. Chem.* **2000**, *65*, 8919.

[175] Takahashi, T.; Bao, F.; Gao, G.; Ogasawara, M. *Org. Lett.* **2003**, *5*, 3479.

[176] Nakano, T.; Nagai, Y. *Chem. Lett.* **1988**, 481.

[177] Sato, F.; Jinbo, T.; Sato, M. *Tetrahedron Lett.* **1980**, *21*, 2171.

[178] Berk, S. C.; Kreutzer, K. A.; Buchwald, S. L. *J. Am. Chem. Soc.* **1991**, *113*, 5093.

[179] Barr, K. J.; Berk, S. C.; Buchwald, S. L. *J. Org. Chem.* **1994**, *59*, 4323.

[180] (a) Verdaguer, X.; Berk, S. C.; Buchwald, S. L. *J. Am. Chem. Soc.* **1995**, *117*, 12641. (b) Verdaguer, X.; Hansen, M. C.; Berk, S. C.; Buchwald, S. L. *J. Org. Chem.* **1997**, *62*, 8522. (c) Elend, D. M.; Fray, J.; Pryde, D. *Arkivoc* **2006**, 114. (d) Willoughby, C. A.; Duff Jr., R. R.; Davis, W. M.; Buchwald, S. L. *Organometallics* **1996**, *15*, 472. (e) Tillack, A.; Lefeber, C.; Peulecke, N.; Thomas, D.; Rosenthal, U. *Tetrahedron Lett.* **1997**, *38*, 1533. (f) Heutling, A.; Pohlki, F.; Bytschkov, I.; Doye, S. *Angew. Chem. Int. Ed.* **2005**, *44*, 2951.

[181] Berk, S. C.; Buchwald, S. L. *J. Org. Chem.* **1992**, *57*, 3751.

[182] Breeden, S. W.; Lawrence, N. J. *Synlett* **1994**, 833.

[183] Hao, L.; Harrod, J. F.; Lebuis, A. M.; Mu, Y.; Shu, R.; Samuel, E.; Woo, H. G. *Angew. Chem. Int. Ed.* **1998**, *37*, 3126.

[184] (a) Fuchikami, T.; Ubukata, Y.; Tanaka, Y. *Tetrahedron Lett.* **1991**, *32*, 1199. (b) Schmidt, T. *Tetrahedron Lett.* **1994**, *35*, 3513. (c) Frost, C. G.; Hartley, B. C. *Org. Lett.*

2007, *9*, 4259. (d) Dioumaev, V.; Bullock, R. M. *Nature* **2000**, *424*, 530. (e) Gadek, A.; Szymanska-Buzar, T. *Polyhedron* **2006**, *25*, 1441.

[185] (a) Fernandes, A. C.; Fernandes, R.; Romao, C. C.; Royo, B. *Chem. Commun.* **2005**, 213. (b) Fernandes, A. C.; Romao, C. C. *J. Mol. Catal. A: Chem.* **2006**, *253*, 96. (c) Fernandes, A. C.; Romao, C. C. *J. Mol. Catal. A: Chem.* **2007**, *272*, 60.

[186] Matsuo, T.; Kawaguchi, H. *J. Am. Chem. Soc.* **2006**, *128*, 12362.

[187] Fernandes, A. C.; Romao, C. C. *Tetrahedron* **2006**, *62*, 9650.

[188] (a) Nakano, T.; Nagai, Y. *Chem. Express* **1990**, *5*, 21. (b) Bedard, T. C.; Corey, J. C. *J. Organomet. Chem.* **1992**, *428*, 315.

[189] Xin, S.; Harrod, J. F. *J. Organomet. Chem.* **1995**, *499*, 181.

[190] For example, see: (a) Shubina, E. S.; Belkova, N. V.; Krylov, A. N.; Vorontsov, E. V.; Epstein, L. M.; Gusev, D. G.; Niedermann, M.; Berke, H. *J. Am. Chem. Soc.* **1996**, *118*, 1105. (b) Epstein, L.; Shubina, E. S. *Coord. Chem. Rev.* **2002**, *231*, 165 and references therein. (c) Bakhmutova, E. V.; Bakhmutov, V. I.; Belkova, N. V.; Besora, M.; Epstein, L. M.; Lledos, A.; Nikonov, G. I.; Shubina, E. S. *Chem. Eur. J.* **2004**, *10*, 661.

[191] Bryan, J. C.; Mayer, J. M. *J. Am. Chem. Soc.* **1990**, *112*, 2298.

[192] Wigley, D. E. In *Progress in Inorganic Chemistry*, Karlin, K, D. (Ed.); Wiley-Interscience: New York, **1994**, *42*, pp. 239-482.

[193] (a) Schrock, R. R.; Murdzek, J. S.; Bazan, G. C.; Robbins, J.; DiMare, M.; O'Regan, M. *J. Am. Chem. Soc.* **1990**, *112*, 3875. (b) Fox, H. H.; Yap, K. B.; Robbins, J.; Cai, S.; Schrock, R. R. *Inorg. Chem.* **1992**, *31*, 2287.

[194] Schrock, R. R.; DePue, R. T.; Feldman, J.; Yap, K. B.; Yang, D. C.; Davis, W. M.; Park, L.; DiMare, M.; Schofield, M.; Anhaus, J.; Walborsky, E.; Evitt, E.; Krüger, C.; Betz, P. *Organometallics* **1990**, *9*, 2262.

[195] Williams, D. S.; Schofield, M. H.; Schrock, R. R. *Organometallics* **1993**, *12*, 4560.

[196] Dyer, P. W.; Gibson, V. C.; Howard, J. A. K.; Wilson, C. *J. Organomet. Chem.* **1993**, *462*, C15.

[197] Radius, U.; Sundermeyer, J.; Pritzkow, H. *Chem. Ber.* **1994**, *127*, 1827.

[198] Dyer, P. W.; Gibson, V. C.; Clegg, W. *J. Chem. Soc., Dalton Trans.* **1995**, 3313.

[199] Dyer, P. W.; Gibson, V. C.; Howard, J. A. K.; Whittle, B.; Wilson, C. *Polyhedron* **1995**, *14*, 103.

[200] Compound (^{t}BuN)$MoCl_2(PMe_3)_3$ has been previously prepared by another route: Green, M. L. H.; Konidaris, P. C.; Mountford, P.; Simpos, S. J. *Chem. Commun.* **1992**, 256.

[201] Burckhardt, U.; Casty, G. L.; Tilley, T. D.; Woo, T. W.; Rothlisberger, U. *Organometallics* **2000**, *19*, 3830.

[202] Bissinger, P.; Paul, M.; Jurgen, R.; Schmidbaur, H. *Chem. Ber.* **1993**, *79*, 1075.

[203] (a) Spencer, M. D.; Shelby, Q. D.; Girolami, G. S. *J. Am. Chem. Soc.* **2007**, *129*, 1860. (b) Heyn, R. H.; Tilley, T. D. *J. Am. Chem. Soc.* **1992**, *114*, 1917. (c) Chen, W.; Shimada, S.; Tanaka, M. *Science* **2002**, *295*, 308.

[204] (a) Wiberg, N.; Schuster, H.; Simon, A.; Peters, K. *Angew. Chem., Int. Ed. Engl.* **1986**, *25*, 79. (b) Watanabe, H, Kato, M.; Okawa, T.; Nagai, Y.; Goto, M. *J. Organomet. Chem.* **1984**, *271*, 225. (c) Weidenburch, M. *Comments Inorg. Chem.* **1986**, *5*, 247.

[205] Hong, P.; Damrauer, N. H.; Carroll, P. J.; Berry, D. H. *Organometallics* **1993**, *12*, 3698.

[206] Nikonov, G. I.; Vyboishchikov, S. F.; Kuzmina, L. G.; Howard, J. A. K. *Chem. Commun.* **2002**, 568.

[207] See, for example: (a) Petri, S. H. A.; Neumann, B.; Tammler, H.-G.; Jutzi, P. *J. Organomet. Chem.* **1998**, *553*, 317. (b) Minato, M.; Zhou, D.-Y.; Zhang, L.-B.; Hirabayashi, R.; Kakeya, M.; Matsumoto, T.; Harakawa, A.; Kikutsuji, G.; Ito, T. *Organometallics* **2005**, *24*, 3434.

[208] Berry, D. H.; Chey, J.; Zipin, H. S.; Carroll, P. J. *Polyhedron* **1991**, *10*, 1189.

[209] Ueno, K.; Masuko, A.; Ogino, H. *Organometallics* **1999**, *18*, 2694.

[210] Appleton, T. G.; Clark, H. C.; Manzer, L. E. *Coord. Chem. Rev.* **1973**, *10*, 335.

[211] (a) Sadow, A. D.; Tilley, T. D. *Organometallics* **2001**, *20*, 4457. (b) Kim, B. H.; Woo, H.-G. *Adv. Organomet. Chem.* **2004**, *52*, 143.

[212] Naumann, C.; Patrick, B. O.; Sherman, J. C. *Tetrahedron* **2002**, *58*, 787.

[213] Marciniec, B.; Gulinski, J. *J. Organomet. Chem.* **1993**, *446*, 15.

[214] Yun, S. S.; Kim, T. S.; Kim, C. H. *Bull. Korean Chem. Soc.* **1994**, *15*, 522.

[215] (a) Gutsulyak, D. V.; Kuzmina, L. G.; Howard, J. A. K.; Vyboischikov, S. F.; Nikonov, G. I. *J. Am. Chem. Soc.* **2008**, *130*, 3732. (b) Leelasubcharoen, S.; Zhizhko, P. A.; Kuzmina, L. G.; Churakov, A. V.; Howard, J. A. K.; Nikonov, G. I. *Organometallics* **2009**, *28*, 4500.

[216] (a) Onaka, M.; Higuchi, K.; Nanami, H.; Izumi, Y. *Bull. Chem. Soc. Jpn.* **1993**, *66*, 2638. (b) Baba, T.; Kawanami, Y.; Yuasa, H.; Yoshida, S. *Catal. Lett.* **2003**, *91*, 31.

[217] For reduction of carbonyl compounds to alkanes, see: (a) West, C. T.; Donnelly, S. J.; Kooistra, D. A.; Doyle, M. P. *J. Org. Chem.* **1973**, *38*, 2675. (b) Barclay, L. R. C.; Sonawane, H. R.; MacDonald, M. C. *Can. J. Chem.* **1972**, *50*, 281. (c) Fry, J. L.; Orfanopoulos, M.; Adlington, M. G.; Dittman, W. R.; Silverman, S. B. *J. Org. Chem.* **1978**, *43*, 374.

[218] For example: (a) Yue, C. J.; Liu, Y.; He, R. *J. Mol. Catal. A* **2006**, *259*, 17. (b) Stapleton, R. L.; Chai, J.; Taylor, N. J.; Collins, S. *Organometallics* **2006**, *25*, 2514.

[219] Fu, P.-F.; Brard, L.; Li, Y.; Marks, T. J. *J. Am. Chem. Soc.* **1995**, *117*, 7151.

[220] Ejfler, J.; Kobulka, M.; Hojniak, M.; Sobota, P. *J. Mol. Catal. A* **2004**, *224*, 93.

[221] Gunji, Y.; Yamashita, Y.; Ikeno, T.; Yamada, T. *Chem. Lett.* **2006**, *35*, 714.

[222] (a) Calas, R.; Frainnet, E.; Bazouin, A.; Hebd, C. R. *Seances Acad. Sci.* **1961**, *252*, 420. (b) Caporusso, A. M.; Panziera, N.; Petrici, P.; Pitzalis, E.; Salvadori, P.; Vitulli, G.; Martra, G. *J. Mol. Catal. A* **1999**, *150*, 275. (c) Ochiai, M.; Hashimoto, H.; Tobita, H. *Angew. Chem.* **2007**, *119*, 8340; *Angew. Chem. Int. Ed.* **2007**, *46*, 8192. (d) Mitzel, N. W.; Riede, J.; Schier, A.; Paul, M.; Schmidbaur, H. *Chem. Ber.* **1993**, *126*, 2027.

[223] For an example of η^2-coordination, see: Blackmore, I. J.; Emiao, C. J. S.; Buschhaus, M. S. A.; Patric, B. O.; Legzdins, P. *Organometallics* **2007**, *26*, 4881.

[224] For examples of η^1-coordination, see: (a) Yang, J.; Brookhart, M. *J. Am. Chem. Soc.* **2007**, *129*, 12656. (b) Weinert, C. S. *Organometallics* **2005**, *24*, 5759. (c) Müller, B.; Vahrenkamp, H. *Eur. J. Inorg. Chem.* **1999**, 117. (d) Song, J. S.; Szalda, D. J.; Bullock, R. M. *Inorg. Chim. Acta* **1997**, *259*, 161. (e) Bochmann, M.; Webb, K. J.; Hursthouse, M. B.; Mazid, M. *J. Chem. Soc., Chem. Commun.* **1991**, 1735.

[225] See, for example: Onozawa, S.; Sakakura, T.; Tanaka, M.; Shiro, M. *Tetrahedron* **1996**, *52*, 4291 and references therein.

[226] Jackson, A. B.; Schauer, C. K.; Wite, P. S.; Templeton, J. L. *J. Am. Chem. Soc.* **2007**, *129*, 10628.

[227] For C-H bond activation in nitriles, see: (a) Takaya, H.; Murahashi, S.-I. *Synlett* **2001**, 991. (b) Heeres, H. J.; Mettsma, A.; Teuben, J. H. *Angew. Chem.* **1990**, *102*, 449; *Angew. Chem. Int. Ed. Engl.* **1990**, *29*, 420. (c) Naota, T.; Tannna, A.; Murahashi, S.-I. *Chem. Commun.* **2001**, 63. (d) Murahashi, S.-I.; Takaya, H.; Naota, T. *Pure Appl. Chem.* **2002**, *74*, 19. (e) Atesin, T. A.; Li, T.; Lachaize, S.; Brennessel, W. W.; Garcia, J. J.; Jones, W. D. *J. Am. Chem. Soc.* **2007**, *129*, 7562. (f) Fujita, E.; Creytz, C. *Inorg. Chem.* **1994**, *33*, 1729.

[228] (a) Ura, Y.; Gao, G.; Bao, F.; Ogasawara, M.; Takahashi, T. *Organometallics* **2004**, *23*, 4808. (b) Zhao, W.-G.; Hua, R. *Eur. J. Org. Chem.* **2006**, 5495. (c) Sprengers, J. W.; De Greef, M.; Duin, M. A.; Elsevier, C. J. *Eur. J. Inorg. Chem.* **2003**, 3811. (d) Burgos, F.; Chavez, I.; Manriquez, J. M.; Valderrama, M.; Lago, E.; Molins, E.; Delpech, F.; Castel, A.; Riviere, P. *Organometallics* **2001**, *20*, 1287. (e) Sakakura, T.; Lautenschlager, H.-J.; Tanaka, M. *J. Chem. Soc., Chem. Commun.* **1991**, 40.

[229] Nagashima, H.; Suzuki, A.; Iura, T.; Ryu, K.; Matsubara, K. *Organometallics* **2000**, *19*, 3579.

[230] For the insertion of nitriles into the M-H bond of TM complexes, see: (a) Frömberg, W.; Erker, G. *J. Organomet. Chem.* **1985**, *280*, 343. (b) Frömberg, W.; Erker, G. *J. Organomet. Chem.* **1985**, *280*, 355. (c) Bercaw, J. E.; Davies, D. L.; Wolczanski, P. T. *Organometallics* **1986**, *5*, 443. (d) Kreutzer, K. A.; Fisher, R. A.; Davis, W. M.; Spaltenstein, E.; Buchwald, S. L. *Organometallics* **1991**, *10*, 4031. (e) Luinstra, G. A.; Rief, U.; Prosenc, M. H. *Organometallics* **1995**, *14*, 1551. (f) Ossola, F.; Brianese, N.; Porchia, M.; Rossetto, G.; Zanella, P. *J. Chem. Soc., Datlon Trans.* **1990**, 877. (g) Figueroa, J. S.; Cummins, C. C. *J. Am. Chem. Soc.* **2003**, *125*, 4020. (h) Yu, Y.; Sadique, A. R.; Smith, J. M.; Dugan, T. R.; Cowley, R. E.; Brennessel, W. W.; Flashenriem, C. J.; Bill, E.; Cundari, T. R.; Holland, P. L. *J. Am. Chem. Soc.* **2008**, *130*, 6624. (i) Debad, J. D.; Legzdins, P.; Lumb, S. A.; Batchelor, R. J., Einstein, F. W. D. *Organometallics* **1995**, *14*, 2543. (j) Temprado, M.; McDonough, J. E.; Mendiratta, A.; Tsai, Y.; Fortman, G. C.; Cummins, C. C.; Rybak-Akimova, E. V.; Hoff, C. D. *Inorg. Chem.* **2008**, *47*, 9380. (k)

Evans, W. J.; Montalvo, E.; Foster, S. E.; Harada, K. A.; Ziller, J. W. O*rganometallics* **2007**, *26*, 2904. (l) Pozmik, G.; Carroll, P. G.; Wayland, B. B. *Organometallics* **1993**, *12*, 3410. (m) Sauvageot P.; Sadorge, A.; Nuber, B.; Kubicki, M. M.; Leblanc, J.-C.; Moise, C. *Organometallics* **1999**, *18*, 2133.

[231] (a) Erker, G.; Fromberg, W.; Atwood, J. L.; Hunter, W. E. *Angew. Chem.* **1984**, *96*, 72. (b) Chatt, J.; Richards, R. L.; King, F.; Leigh, J. *J. Chem. Soc., Dalton Trans.* **1976**, 2435.

[232] (a) Nikonov, G. I.; Mountford, P.; Dubberley, S. R. *Inorg. Chem.* **2003**, *42*, 58. (b) Ignatov, S. K.; Rees, N. H.; Dubberley, S. R.; Razuvaev, A. G.; Mountford, P.; Nikonov, G. I. *Chem. Commun.* **2004**, 952.

[233] Boncella, J. M.; Wang, S. Y. S.; Vanderlende, D. D. *J. Electroanal. Chem.* **1999**, *591*, 8.

[234] (a) Crabtree, R. H. *The Organometallic Chemistry of the Transition Metals*, 4th ed.; Wiley: New York, 2005. (b) Crabtree, R. H. Hydrogen and Hydrides as Ligands. In *Comprehensive Inorganic Chemistry*; Wilkinson, G., Ed.; Pergamon: London, Chapter 19.

[235] For example, see: (a) Poli, R. In *Recent Advances in Hydride Chemistry*; Poli, R., Peruzzini, M., Eds.; Elsevier: Amsterdam, 2001; Chapter 6. (b) Marks, T. J.; Kolb, J. R. *Chem. Rev.* **1977**, *77*, 263. (c) Kandiah, M.; McGrady, G. S.; Decken, A.; Sirsch, P. *Inorg. Chem.* **2005**, *44*, 8650. (d) Jensen, J. A.; Girolami, G. S. *Inorg. Chem.* **1989**, *28*, 2107.

[236] Baya, M.; Houghton, J.; Daran, J.-C.; Poli, R. *Angew. Chem., Int. Ed.* **2006**, *46*, 429.

[237] Brandts, J. A. M.; van Leur, M.; Gossage, R. A.; Boersma, J.; Spek, A. L.; Van Koten, G. *Organometallics* **1999**, *18*, 2633.

[238] (a) Kirtley, S. W.; Andrews, M. A.; Bau, R.; Grynkewich, G. W.; Marks, T. J.; Tipton, D. L.; Whittlesey, B. R. *J. Am. Chem. Soc.* **1977**, *99*, 7154. (b) Atwood, J. L.; Hunter, W. E.; Carmona-Guzman, E.; Wilkinson, G. *J. Chem. Soc., Dalton Trans.* **1980**, 467. (c) Tamm, M.; Dressel, B.; Lugger, T.; Frohlich, R.; Grimme, S. *Eur. J. Inorg. Chem.* **2003**, 1088. (d) Tamm, M.; Dressel, B.; Bannenberg, T.; Grunenberg, J.; Herdtweck, E. *Z. Natuforsch.* **2006**, *61*, 896.

[239] Xu, Z.; Lin, Z. *Coord. Chem. Rev.* **1996**, *156*, 139.

[240] (a) Eikey, R. A.; Abu-Omar, M. M. *Coord. Chem. Rev.* **2003**, *243*, 83. (b) Duncan, A. P.; Bergman, R. G. *Chem. Rec.* **2002**, *2*, 431. (c) Hazari, N.; Mountford, P. *Acc. Chem. Res.* **2005**, *38*, 839.

[241] Basuli, F.; Bailey, B. C.; Watson, L. A.; Tomaszewski, J.; Huffman, J. C.; Mindiola, D. J. *Organometallics* **2005**, *24*, 1886.

[242] (a) Fletcher, D. A.; McMeeking, R. F.; Parkin, D. *J. Chem. Inf. Comput. Sci.* **1996**, *36*, 746 (The United Kingdom Chemical Database Service). (b) Allen, F. H.; Kennard, O. *Chem. Des. Autom. News* **1993**, *8*, 31.

[243] Radius, U.; Hoffmann, R. *Chem. Ber.* **1996**, *129*, 1345.

[244] See, for example: (a) Castro, A.; Galakhov, M. V.; Gomez, M.; Gomez-Sal, P.; Martin, A.; Sanchez, F. *J. Organomet. Chem.* **2000**, *595*, 36. (b) Cundari, T. R. *J. Am. Chem. Soc.* **1992**, *114*, 7879.

[245] Shaikh, N. S.; Junge, K.; Bellerm M. *Org. Lett.* **2007**, *9*, 5429 and references therein.

[246] Bette, V.; Mortreux, A.; Savoia D.; Carpentier, J. F. *Tetrahedron* **2004**, *60*, 2837.

[247] (a) Ito, H.; Kato, T.; Sawamura, M. *Chem. Lett.* **2006**, *35*, 1038. (b) Ojima, I.; Donovan, R. J.; Clos, N. *Organometallics* **1991**, *10*, 2606. (c) Cavanaugh, D. M.; Gregg, B. T.; Cutler, A. R. *Organometallics* **1996**, *15*, 2764.

[248] Yamashita, H.; Uchimaru, Y. *Chem. Commun. 1999*, 1763.

[249] See, for example: (a) Belkova, N. V.; Shubina, E. S.; Epstein, L. M. *Acc. Chem. Res.* **2005**, *38*, 624. (b) Belkova, N. V.; Dub, P. V.; Baya, M.; Houghton, J. *Inorg. Chim. Acta* **2007**, *360*, 149.

[250] Guedes da Silva, M. F. C.; Frausto da Silva, J. J. R.; Pombeiro, A. J. L. *Inorg. Chem.* **2002**, *41*, 219.

[251] Hu, H.; Krishnamurthy, K. *J. Magn. Reson.* **2006**, *182*, 173.

[252] Jordan, R. B. *Reaction Mechanisms of Inorganic and Organometallic Systems*. Oxford University Press: New York, **1991**.

[253] Brookhart, M.; Cox, K.; Cloke, F. G. N.; Green, J. C.; Green, M. L. H.; Hare, P. M.; Bashkin, J.; Derome, A. E.; Grebenik, P. D. *J. Chem. Soc., Dalton Trans.* **1985**, 423.

[254] Elem. Anal. for chloro-substituted agostic complexes of molybdenum were obtained and generously donated by Dr. Nikonov.

[255] (a) Jeener, J.; Meier, B. H.; Bachmann, P; Ernst, R. R. *J. Chem. Phys.* **1979**, *71*, 4546. (b) Wagner, R.; Berger, J. *J. Magn. Reson.* **1996**, *123 A*, 119.

[256] (a) Lu, J.; Ma, D.; Hu, J.; Tang, W.; Zhu, D. *J. Chem. Soc., Dalton Trans.* **1998**, 2267. (b) Zolnai, Z.; Juranic, N.; Vikic-Topic, D.; Macura, S. *J. Chem. Inf. Comput. Sci.* **2000**, *40*, 611.

[257] Kessler, H.; Oschkinat, H.; Griesinger, C.; Bermel, W. *J. Magn. Reson.* **1986**, *70*, 106. (b) Stonehouse, J.; Adell, P.; Keeler, J.; Shaka, A. J. *J. Am. Chem. Soc.* **1994**, *116*, 6037. (c) Stott, K.; Stonehouse, J.; Keeler, J.; Hwang, T. L.; Shaka, A. J. *J. Am. Chem. Soc.* **1995**, *117*, 4199.

[258] (a) Bain, A. D.; Cramer, J. A. *J. Magn. Reson.* **1996**, *118 A*, 21. (b) Bain, A. D.; Cramer, J. A. *J. Magn. Reson.* **1993**, *103 A*, 217. (c) Bain, A. D.; Cramer, J. A. *J. Phys. Chem.* **1993**, *97*, 2884. (d) Bain, A. D.; Fletcher, D. A. *Mol. Phys.* **1998**, *95*, 1091.

[259] SHELXTL-Plus, Release 5.10; Bruker AXS Inc.: Madison, WI, 1997.

[260] Frisch, M. J.; Trucks, G. W.; Schlegel, H. B.; Scuseria, G. E.; Robb, M. A.; Cheeseman, J. R.; Zakrzewski, V. G.; Montgomery (Jr), J. A.; Stratmann, R. E.; Burant, J. C.; Dapprich, S.; Millam, J. M.; Daniels, A. D.; Kudin, K. N.; Strain, M. C.; Farkas, O.; Tomasi, J.; Barone, V.; Cossi, M.; Cammi, R.; Mennucci, B.; Pomelli, C.; Adamo, C.; Clifford, S.; Ochterski, J.; Petersson, G. A.; Ayala, P. Y.; Cui, Q.; Morokuma, K.; Malick, D. K.; Rabuck, A. D.; Raghavachari, K.; Foresman, J. B.; Cioslowski, J.; Ortiz, J. V.; Stefanov, B. B.; Liu, G.; Liashenko, A.; Piskorz, P.; Komaromi, I.; Gomperts, R.; Martin, R. L.; Fox, D. J.; Keith, T.; Al-Laham, M. A.; Peng, C. Y.; Nanayakkara, A.; Gonzalez, C.; Challacombe, M.; Gill, P. M. W.; Johnson, B.; Chen, W.; Wong, M. W.; Andres, J. L.; Gonzalez, C.; Head-Gordon, M.; Replogle, E. S.; Pople, J. A. *Gaussian 03*; Gaussian, Inc.: Wallingford, CT, 2004.

[261] (a) Becke, A. D. *J. Chem. Phys.* **1993**, *98*, 5648. (b) Perdew, J. P.; Burke, K.; Wang, Y. *Phys. Rev. B* **1996**, *54*, 16533.

[262] Hayand, P. J.; Wadt, W. R. *J. Chem. Phys.* **1985**, *82*, 299.